

---

# **FRONTIERS IN CATALYSIS: ADVANCED SYNTHESIS, CHARACTERIZATION, MODELING**

**Meeting of the Catalysis Science Program  
Chemical Sciences, Geosciences and Biosciences Division  
Office of Basic Energy Sciences  
U.S. Department of Energy  
Annapolis, Maryland  
May 31-June 3, 2009**



**The Summary of Discussions Held by the Meeting Participants  
is located at the end of this book of abstracts, starting at page 341.**

This document was produced under contract number DE-AC05-06OR23100 between the U.S. Department of Energy and Oak Ridge Associated Universities.

## FOREWORD

The 2009 Catalysis Science Program Meeting is sponsored by the Division of Chemical Sciences, Geosciences and Biosciences, Office of Basic Energy Sciences (OBES), U.S. Department of Energy. It is being held on May 31 through June 3, 2009, at the Westin Annapolis Hotel, Annapolis, MD. The purposes of this meeting are to discuss the recent advances in the interdisciplinary areas conforming catalysis science, to foster exchange of ideas and cooperation among participants, and to discuss the new opportunities for catalysis and chemical transformations with energy technologies.

Catalysis activities within OBES emphasize fundamental research aimed at understanding and controlling the chemical reactivity of fluid and condensed matter. The long-term goal of this research is to discover the fundamental principles and develop the techniques to predict structure-reactivity relations. Such knowledge, integrated with advances in synthesis, instrumentation, characterization, and theory, will help us to control chemical reactions along desired pathways. Ultimately, this new knowledge will result in chemical and materials processes to efficiently convert fossil and renewable resources, or to generate, convert and store energy, with minimum impact to our environment.

Special thanks go to our invited speakers, who will expose us to recent advances in their fields, to the program investigators and their students, postdocs, and collaborators, for their dedication to the continuous success and visibility of the OBES Catalysis Science Program, and to the session moderators, for their invaluable help. We also thank the Oak Ridge Institute of Science and Education staff, Ms. Margaret Lyday and other contributing staff members of ORISE for the logistical and web support and the compilation of this volume.

Susannah Scott<sup>1</sup>, David Dixon<sup>2</sup> and Raul Miranda<sup>3</sup>

<sup>1</sup> University of California–Santa Barbara

<sup>2</sup> University of Alabama–Tuscaloosa

<sup>3</sup> Office of Basic Energy Sciences  
U.S. Department of Energy

**MEETING OVERVIEW**  
**2009 DOE/BES Catalysis Sciences Meeting**  
**May 31 – June 3, 2009 Annapolis, MD**

<b>Time</b>	<b>Sunday, May 31</b>	<b>Monday, June 1</b>	<b>Tuesday, June 2</b>	<b>Wednesday, June 3</b>
7:30 AM				<b>Continental breakfast</b> Outside Capitol AB
8:00		<b>Continental breakfast</b> Outside Capitol AB	<b>Continental breakfast</b> Outside Capitol AB	<b>Wednesday morning session</b> Capitol A
8:30		<b>Monday morning session</b> Capitol A	<b>Tuesday morning session</b> Capitol A	
11:30				
<b>noon</b>		<b>Lunch buffet</b>		<b>Lunch buffet</b>
12:20 PM			<b>Lunch buffet</b>	
1:00		<b>Networking/Poster Setup</b>	<b>Networking</b>	<b>Poster Take-down</b> <b>Meeting Adjourns</b>
3:00	<b>Registration/Poster Setup</b> Outside Capitol AB	<b>Monday afternoon session</b> Capitol A	<b>Tuesday afternoon session</b> Capitol A	
7:00	<b>Sunday evening session</b> Capitol A	<b>Dinner/Posters</b>	<b>Dinner/Posters</b>	

## Agenda

### Sunday Evening, May 31, 2009

- 7:00 – 7:10 p.m. Welcome: David Dixon and Susannah Scott
- 7:10 – 8:10 p.m. **Plenary:** David Avnir, The Hebrew University of Jerusalem  
*Organically doped metals - a new family of materials: Catalysis and more*
- 8:10 – 8:50 p.m. Frances Arnold, California Institute of Technology, Chemistry and Chemical Engineering  
*Directed evolution of cytochrome P450: C-H hydroxylation on demand*
- 8:50 – 9:30 p.m. Eric Rohlving, Division Director  
*New and Upcoming Activities at the Office of Basic Energy Sciences*

### Monday Morning, June 1, 2009 Characterization

#### Session Chair: Ludwig Bartels

- 8:30 – 9:30 a.m. **Plenary:** Jeroen Anton van Bokhoven, ETH Zürich, Chemistry and Bioengineering  
*Shining light on catalysts*
- 9:30 – 10:10 a.m. Zdenek Dohnalek, Pacific Northwest National Laboratory  
*Alcohol Chemistry on  $\text{TiO}_2(110)$  and  $(\text{WO}_3)_3/\text{TiO}_2(110)$  Model Catalysts*
- 10:10 – 10:40 a.m. Break

#### Session Chair: Ulrike Diebold

- 10:40 – 11:20 a.m. Stewart Parker, ISIS Facility, Rutherford Appleton Laboratory  
*Catalysts studied with neutron vibrational spectroscopy*
- 11:20 – 12:00 p.m. Robert Hamers, University of Wisconsin, Chemistry  
*Ultra-stable molecular interfaces for renewable energy applications*
- 12:00 p.m. Lunch

## Monday Afternoon, June 1, 2009    Synthesis

### Session Chair: Don Tilley

- 3:00 – 4:00 p.m.    **Plenary:** Ryong Ryoo, Korea Advanced Institute of Science and Technology  
*Hierarchically porous zeolites for catalytic applications*
- 4:00 – 4:40 p.m.    Steve Suib, University of Connecticut, Chemistry  
*Synthesis of Catalysts for Selective Oxidations and Activation of CO<sub>2</sub>*
- 4:40 – 4:55 p.m.    Break

### Session Chair: Marcus Weck

- 4:55 – 5:35 p.m.    Craig Barnes, University of Tennessee, Chemistry  
*New Approaches to Nanostructured Metal Oxide Catalysts*
- 5:35 – 6:15 p.m.    Rick Finke, Colorado State University, Chemistry  
*An Ockham's Razor-Based Nucleation and Growth Kinetic Model with Applications to Nanocluster, Organometallic, Solid-State and Neurological Protein Aggregation Chemistries and Catalysis*
- 6:15 – 7:00 p.m.    Discussion of future research areas  
Moderators: Tobin Marks and Susannah Scott
- 7:00 – 10:00 p.m.    Dinner followed by Poster Session

## Tuesday Morning, June 2, 2009    Applications

### Session Chair: Andrew Gellman

- 8:30 – 9:30 a.m.    **Plenary:** Robert Grubbs, Caltech, Chemistry  
*Reactions of organometallic carbene complexes-homogeneous and heterogeneous*
- 9:30 – 10:30 a.m.    Jens Norskov, Technical University of Denmark, Physics  
*Tailoring surface chemical properties using electronic structure theory*
- 10:30 – 11:00 a.m.    Break
- Session Chair: Francisco Zaera**
- 11:00 – 11:40 a.m.    Radoslav Adzic, Brookhaven National Laboratory, Chemistry and Materials Science  
*Enhancing the Reaction Kinetics of O<sub>2</sub> Reduction and Ethanol Oxidation with Pt Monolayer and PtRhSnO<sub>2</sub> Electrocatalysts - the Main Remaining Challenges of Fuel Cell Electrocatalysis*

11:40 – 12:20 p.m. Stefan Vajda, Argonne National Laboratory, Chemistry and Chemical Engineering  
*Selective Bond Breaking and Making on Size Selected Clusters: Role of Size, Composition and Support*

12:20 p.m. Lunch

**Tuesday Afternoon, June 2, 2009                      Theory**

**Session Chair: William Schneider**

3:00 – 4:00 p.m. **Plenary:** Weitao Yang, Duke University, Chemistry  
*Developments in Density Functional Theory and ab initio QM/MM Methods for Catalysis*

4:00 – 4:40 p.m. Manos Mavrikakis, University of Wisconsin, Chemical Engineering  
*Near-surface alloys for improved heterogeneous catalysis*

4:40 – 4:55 p.m. Break

**Session Chair: David Sherrill**

4:55 – 5:35 p.m. Andrew Rappe, University of Pennsylvania, Chemistry  
*Using ferroelectric oxides to control surface chemistry*

5:35 – 6:00 p.m. Graeme Henkelman, University of Texas-Austin, Chemistry and Biochemistry  
*First principles dynamics over long time scales*

6:00 – 6:25 p.m. Suljo Linic, University of Michigan, Chemical Engineering  
*Well-defined highly uniform targeted metallic nano-structures as highly selective heterogeneous catalysts, photo-electro-catalysts, and platforms for chemical characterization*

6:25 – 7:00 p.m. Discussion of future research areas  
Moderators: Matt Neurock and David Dixon

7:00 p.m. Dinner followed by Poster Session

**Wednesday Morning, June 3, 2009**

**Session Chair: Peter Stair**

8:00 – 9:00 am. **Plenary:** Andreas Stierle, Max-Planck-Institut für Metallforschung  
*In-situ study of nanoparticle shape changes under reaction conditions*



- 9:00 – 9:30 a.m.      Beatriz Roldán Cuenya, University of Central Florida, Physics  
*Catalytic decomposition and oxidation of alcohols over supported, size-selected, Pt and Pt-M nanoparticles: oxidation state effects*
- 9:30 – 10:00 a.m.      Break
- 10:00– 10:30 a.m.      Umit Ozkan, Ohio State University, Chemical Engineering  
*Investigation of the oxygen reduction reaction activity of heteroatom-containing carbon nano-structures*
- 10:30 a.m.              Discussion of future research areas  
Moderators: David Dixon and Susannah Scott
- 11:30 a.m.              Lunch

## Table of Contents

Foreword.....	i
Meeting Overview .....	ii
Agenda.....	iii
Table of Contents .....	vii

### Sunday Evening Sessions

<b>Plenary:</b> David Avnir - <i>Organically Doped Metals - A New Family of Materials: Catalysis and More</i> .....	1
---	---

Frances Arnold – <i>In Darwin’s Honor: Laboratory Evolution of a Cytochrome P450 Monooxygenase</i> .....	2
--	---

### Monday Morning Sessions

<b>Plenary:</b> Jeroen Anton van Bokhoven - <i>Shining Light on Catalysts</i> .....	3
---	---

Zdenek Dohnálek - <i>Alcohol Chemistry on TiO<sub>2</sub>(110) and (WO<sub>3</sub>)<sub>3</sub>/TiO<sub>2</sub>(110) Model Catalysts</i> .....	4
--	---

Stewart Parker - <i>Catalysts Studied with Neutron Vibrational Spectroscopy</i> .....	5
---	---

Robert Hamers - <i>Ultra-Stable “Smart” Molecular Interfaces for Renewable Energy</i> .....	6
---	---

### Monday Afternoon Sessions

<b>Plenary:</b> Ryong Ryoo - <i>Hierarchically Porous Zeolites for Catalytic Applications</i> ....	7
--	---

Steven Suib - <i>Microporous and Mesoporous Nano-Size Transition Metal Oxides: Preparation, Characterization, and Applications</i> .....	8
--	---

Craig Barnes - <i>New Approaches to Nanostructured Metal Oxide Catalysts</i> .....	11
--	----

Richard Finke - <i>Nanocluster Catalysts Formation and Stabilization Fundamental Studies</i> .....	14
--	----

### Tuesday Morning Sessions

<b>Plenary:</b> Robert Grubbs - <i>Olefin Metathesis Catalysts for the Synthesis of Large and Small Molecules</i> .....	18
---	----

Jens Nørskov - <i>Tailoring of Surface Chemical Properties Using Electronic Structure Theory</i> .....	19
--	----

Radoslav Adzic - *Metal and Metal Oxide-Supported Platinum Monolayer Electro catalysts for Oxygen Reduction*..... 20

Stefan Vajda - *Selective Bond Breaking and Making on Size-Selected Catalysts: The Role of Size, Composition and Support*..... 26

## **Tuesday Afternoon Sessions**

**Plenary:** Weitao Yang - *Developments in Density Functional Theory and ab initio QM/MM Methods for Catalysis* ..... 27

Manos Mavrikakis - *Near-Surface Alloys for Improved Heterogeneous Catalysis*... 29

Andrew Rappe - *Using Ferroelectric Oxides to Control Surface Chemistry* ..... 30

Graeme Henkelman - *First Principles Dynamics Over Long Time Scales*..... 31

Suljo Linic - *Experimental and Theoretical Studies of Adsorbate/Adsorbate/Substrate Interactions: Towards Predictive Catalysis*..... 32

## **Wednesday Morning Sessions**

**Plenary:** Andreas Stierle - *In-Situ Study of Nanoparticle Shape Changes Under Reaction Conditions*..... 35

Beatriz Roldán Cuenya - *Influence of the Oxidation State of Supported Size-Selected Pt Nanoparticles on Catalytic Decomposition and Oxidation of High-Order Alcohols: Activity, Selectivity, and Lifetime*..... 36

Umit Ozkan - *Investigation of the Oxygen Reduction Reaction Activity of Heteroatom-Containing Carbon Nano-Structures* ..... 39

## **Poster Presentations**

Eric Altman - *Structure-Reactivity Relationships in Multi-Component Transition Metal Oxide Catalysts*..... 42

Aravind Asthagiri - *First-Principles Studies of the Initial Oxidation of Transition Metal Surfaces*..... 45

Perla Balbuena - *Theory-Guided Design of Nanoscale Multi-Metallic Catalysts for Fuel Cells*..... 46

Perla Balbuena - *Modeling Catalyzed Growth of Single-Wall Carbon Nanotubes* ... 49

Ludwig Bartels - *Controlling Adsorbate Motion*..... 52

Alexis Bell - *Catalysis for the Selective Synthesis of Fuels and Chemical*..... 53

Janet Blumel - *Catalysts Immobilized on Oxide Supports: New Insights by Solid-State NMR Spectroscopy* ..... 56

Suzanne Blum - <i>Single-Molecule Fluorescence Imaging for Studying Organic, Organometallic, and Inorganic Reaction Mechanisms</i> .....	57
Jeff Brinker - <i>Catalytic and Transport Behaviors of Model Porous and Composite Nanostructures</i> .....	59
Richard Brutchey - <i>Catalytic Oxidation of Olefins by Osmium Tetraoxide on Carbonaceous Supports</i> .....	62
Uwe Burghaus - <i>Characterization of Fundamental Catalytic Properties of MoS<sub>2</sub>/WS<sub>2</sub> Nanotubes and Nanoclusters for Desulfurization Catalysis – A Surface Chemistry Study</i> .....	63
Nicholas Camillone - <i>Ultrafast and Chemically Specific Microscopy for Atomic Scale Imaging of Nano-Photocatalysis</i> .....	66
Charles Campbell - <i>Oxide-Supported Metal Nanoparticles: Correlating Catalytic Kinetics, Energetics and Surface Structure</i> .....	69
Jingguang Chen - <i>Structure-Property Relationship in Metal Carbides and Bimetallic Alloys</i> .....	72
Jingguang Chen - <i>Dedicated Beamline Facilities for Catalytic Research – Synchrotron Catalysis Consortium (SCC)</i> .....	75
Peng Chen - <i>Real-Time In-Situ Optical Imaging of Nanocatalysis at the Single-Molecule Level</i> .....	78
William Curtis Conner - <i>Nitrogen-Substituted Zeolite Catalysts for Base-Catalyzed Reactions: Where is the Nitrogen?</i> .....	79
David Cox - <i>Hydrocarbon Dehydrogenation and Oxidation over Model Metal Oxide Surfaces</i> .....	82
Richard Crooks - <i>Understanding Multimetallic Catalysts using Dendrimer-Encapsulated Nanoparticles</i> .....	85
Larry Curtiss - <i>Density Functional Studies of Methanol Decomposition on Sub-Nanometer Clusters</i> .....	86
Abhaya Datye - <i>Nanostructured Catalysts for Hydrogen Generation from Renewable Feedstocks</i> .....	87
Robert Davis - <i>Structure and Function of Supported Base Catalysts</i> .....	93
W. Nicholas Delgass - <i>Catalysis Science Initiative: Catalyst Design by Discovery Informatics</i> .....	96
Ulrike Diebold - <i>Towards a Molecular Scale Understanding of Surface Chemistry and Photocatalysis on Metal Oxides: Surface Science Experiments and First Principles Theory</i> .....	102

David Dixon - <i>Early Transition Metal Oxides as Catalysts: Crossing Scales from Clusters to Single Crystals to Functioning Materials</i> (C. Peden (PNNL) – PI) .....	105
James Dumesic - <i>Fundamental Studies of the Reforming of Oxygenated Compounds over Supported Metal Catalysts</i> .....	110
Jonah Erlebacher - <i>Engineering Catalytic Nanoporous Metals for Reactions Important to the Hydrogen Economy</i> .....	113
Maria Flytzani-Stephanopoulos - <i>Nanostructured, Metal-Ion Modified Ceria and Zirconia Catalysis</i> .....	116
Heinz Frei - <i>Mechanistic Study of Ethylene Hydroformylation over Supported Rh Nanoparticles under Reaction Conditions by Time Resolved FTIR Spectroscopy</i> ..	122
Anatoly Frenkel - <i>Mesoscopic Behavior of Supported Metal Clusters: Pt/<math>\gamma</math>-Al<sub>2</sub>O<sub>3</sub></i> ..	123
Cynthia Friend - <i>Exploiting Metastable Oxygen on Gold Surfaces for the Selective Functionalization of Olefins</i> .....	124
Bruce Gates - <i>Dynamic Characterization of Structure and Bonding in Supported Molecular Catalysts</i> .....	127
Andrew Gellman - <i>Enantioselective Explosions on Chiral Surfaces</i> .....	130
D. Wayne Goodman - <i>The Physical and Chemical Properties of Nanostructured Metal and Mixed-Metal Catalysts</i> .....	131
Raymond Gorte - <i>Thermodynamic Properties of Supported Catalysts</i> .....	136
Vadim Guliants - <i>Surface Termination of M1 Phase and Rational Design of Propane Ammoxidation Catalysts</i> .....	139
Gary Haller - <i>Nanoporous Structured Silica (MCM-41 and SBA-15) Catalysts and Catalyst Supports</i> .....	142
Jonathan Hanson - <i>In Situ Measurement of Metal Oxide and Metal Rearrangement of CuFe<sub>2</sub>O<sub>4</sub> Spinel During Catalyst Activation for Water Gas Shift (WGS) Reaction Catalysis</i> .....	145
James Haw - <i>Supported Molecular Catalysts: Synthesis, In-Situ Characterization and Performance</i> .....	146
Tony Heinz - <i>Controlling Structural, Electronic, and Energy Flow Dynamics of Catalytic Processes through Tailored Nanostructures</i> .....	150
Michael Henderson - <i>Fundamental Studies of Heterogeneous Photocatalysis on Model TiO<sub>2</sub> Surfaces</i> .....	156
Jan Hrbek - <i>Catalysis: Reactivity and Structure (FWP CO-009)</i> .....	162
Thomas Jaramillo - <i>Designing New Electrocatalysts: A Case Study of the Hydrogen Evolution Reaction (HER)</i> .....	168

Christopher Jones - <i>Developing the Science of Immobilized Molecular Catalysts</i> .....	169
Alexander Katz - <i>Controlling Heterogeneous Ti-Epoxidation Activity via Support Effects</i> .....	179
John Kitchin - <i>Modeling Coverage Dependence in Surface Reaction Networks</i> .....	182
Harold Kung - <i>Nanostructure Catalytic Materials: An Investigation of Effect of Active Site Environment</i> .....	184
Victor Lin - <i>Selective and Efficient Catalysis in 3-D Controlled Environments</i> .....	187
Meilin Liu - <i>Understanding the Interfacial Structures-Chemistry Relationships in Solid Oxide Fuel Cells (SOFCs)</i> .....	193
Ping Liu - <i>Water-Gas-Shift Reaction on Metal-Oxide Catalysts: A Density Functional Study</i> .....	196
Raul Lobo - <i>Novel Photocatalysts with One-Dimensional and Two-Dimensional Nanostructures</i> .....	197
Tobin Marks - <i>Supported Organometallic Complexes: Surface Chemistry, Spectroscopy, Catalysis and Homogeneous Models</i> .....	200
Christopher Marshall - <i>Structure/Composition/Function Relationships in Supported Nanoscale Catalysts for Oxidative Hydrolysis Cellulose to Monosaccharide Sugars and their Derivatives</i> .....	205
Eric McFarland - <i>Investigations of Electronic Promotion of C-x Bond Transformations</i> .....	208
Michael McKittrick - <i>Exploring Visible-Light Photocatalysts via the Dye-Sensitization of Titanium Dioxide Materials</i> .....	211
Charles Mullins - <i>Surface Chemistry of Gold Model Catalysts</i> .....	212
Djamaladdin Musaev - <i>Principles of Selective O<sub>2</sub>-Based Oxidation by Optimal (Multinuclear) Catalytic Sites</i> .....	215
Matthew Neurock - <i>Theory Aided Design of Active and Durable Nanoscale Cathode Catalysts</i> .....	221
Justin Notestein - <i>Novel Structures of Supported Metal Oxide Catalysts Using Calixarene and Macrocyclic Amine Complexes on Hybrid Organic-Inorganic Surfaces</i> .....	224
Ralph Nuzzo - <i>The Reactivity and Structural Dynamics of Supported Metal Nanoclusters Using Electron Microscopy, in situ X-Ray Spectroscopy, Electronic Structure Theories, and Molecular Dynamics Simulations</i> .....	225

Steve Overbury - <i>Fundamentals of Heterogeneous Catalysis on Surfaces and Nanostructures</i> .....	231
Charles Peden - <i>Early Transition Metal Oxides as Catalysts: Crossing Scales from Clusters to Single Crystals to Functioning Materials</i> .....	237
Baron Peters - <i>Methylrhenumtrioxide Activation on Amorphous Silica-Alumina: Benchmark Test of DFT Model, an Aluminum Site Model, and Preliminary Results on Initiation Pathways</i> .....	246
Talat Rahman - <i>Enhanced Reactivity and Selectivity of Oxide Nanostructures</i> ....	247
Fabio Ribeiro - <i>Fundamental Studies on the Kinetics of Oxidation Reactions</i> .....	248
Robert Rioux - <i>Thermal, X-Ray and Electrical Probes of the Liquid-Solid Interface during the Synthesis of Heterogeneous Catalysts</i> .....	251
Jose Rodriguez - <i>Active Sites and Mechanisms for the Water-Gas Shift Reaction on Metal and on Metal and Metal/Oxide Catalysts (BNL FWP CO-027)</i> .....	252
Aaron Sadow - <i>Ligand-Based Approaches for Preparation and Characterization of Surface Supported Transition Metal Centers for Catalytic Applications</i> .....	258
Lanny Schmidt - <i>Biofuels from Biomass by Catalytic Autothermal Reforming</i> .....	259
William Schneider - <i>Towards Realistic Models of Heterogeneous Catalysis: Simulations of Redox Catalysis from First Principles</i> .....	262
Udo Schwarz - <i>Atomic Resolution Imaging and Quantification of Chemical Functionality of Surfaces</i> .....	265
Susannah Scott - <i>Catalysis Science Initiative: Hierarchical Design of Heterogeneous Catalysts for Hydrocarbon Transformations</i> .....	268
Jorge Seminario - <i>Analysis of Events in Oxygen Reduction Using GENIP</i> .....	271
Gabor Somorjai - <i>Nanoscience and Nanoparticles for 100% Selective Catalytic Reactions</i> .....	272
Gabor Somorjai - <i>The Influence of Electron Flow at Oxide-Metal Interfaces on the Selectivity and Turnover Rates of Catalytic Reactions</i> .....	278
Peter Stair - <i>Synthesis and Understanding of Novel Catalysts</i> .....	281
Peter Stair - <i>Institute for Catalysis in Energy Processes (ICEP)</i> .....	284
Peter Stair - <i>Structure/Composition/Function Relationship in Supported Nanoscale Catalysts for Hydrogen</i> .....	290
Ceren Susut - <i>An In Situ Electrode-Potential-Controlled Nuclear Magnetic Resonance Investigation of Sulfur-Poisoning Effect on Pt-Based Mono- and Bi-metallic Nanoscale Electrocatalysts</i> .....	296

Janos Szanyi - <i>Surface Chemistry on Base-Metal Oxide Nanostructures: A Model System Approach</i> .....	299
Don Tilley - <i>Transformations of Organic Compounds via Homogeneous Catalysis &amp; Heterogeneous Catalysis with Well-Defined Single Sites</i> .....	302
Dion Vlachos - <i>An Integrated Approach Toward Rational Nanocatalyst Design for Hydrogen Production</i> .....	305
John Vohs - <i>Fundamental Studies of the Steam Reforming of Alcohols on Pd/ZnO and Co/ZnO Catalysts</i> .....	307
Israel Wachs - <i>Photooxidation of H<sub>2</sub>O and C<sub>3</sub> Hydrocarbons to H<sub>2</sub> Fuel and C<sub>3</sub>-Oxygenates with Molecular Designed Heterogeneous Nano-Photocatalysts</i> .....	310
Jason Weaver - <i>Growth and Reactivity of Oxide Phases on Crystalline Pd and Pt Surfaces</i> .....	314
Michael White - <i>Catalysis on the Nanoscale: Preparation, Characterization and Reactivity of Metal-Based Nanostructures</i> .....	317
Francisco Zaera - <i>Catalysis Science Initiative: Molecular Level Design of Chiral Heterogeneous Catalysts</i> .....	323
<b>Participant List</b> .....	<b>329</b>
<b>Author Index</b> .....	<b>333</b>



# Sunday Evening Sessions

Organically doped metals - a new family of materials:  
Catalysis and more

David Avnir

*Institute of Chemistry, The Hebrew University of Jerusalem*  
*Jerusalem 91904, Israel*  
[david@chem.ch.huji.ac.il](mailto:david@chem.ch.huji.ac.il)

We describe a new materials technology, which enables the incorporation of organic molecules within metals [*Chem. Mater.*, **14**, 1736 (2002)]. A new family of hybrid materials is thus obtained, which, to the best of our knowledge, has been unknown. The entrapment methodologies proved versatile for different types of molecules - small, polymers, and enzymes - and for various metals, including Ag, Au, Cu, Pd and Co. The motivation has been based on the fact that organic and bioorganic molecules represent a very rich library of properties that metals are devoid of. One can only imagine the huge potential which can be opened by the ability to tailor metals with any of the properties of organic molecules. Likewise one expects that the incorporation of a molecule within the sea of electrons of a metal, will affect its physical and chemical properties. Indeed, successful studies have demonstrated the feasibility and potential of this idea. Examples include metals with enzymatic activities (see below), chiral metals, metals with unorthodox functionalities (see below), alteration of conductivity, superior antibacterial Ag, new polymeric/metallic composites, and more.

As metals play a key role in catalysis, this direction has been a main focus in our studies. We have explored so far five different directions:

1. The first of these directions was to render a metal either acidic or basic by the entrapment of a suitable polymer. When the polyacid Nafion was successfully entrapped in Ag, "acidic" silver resulted, which is of course an unorthodox property of this metal. Nafion@Ag was then tested as a heterogeneous acidic catalyst for the pinacol-pinacolone rearrangement, and was found very efficient [*Adv. Functional Mater.*, **15**, 1141 (2005)]. With this we have demonstrated that a metal can serve as a support for homogeneous catalysts. (Ceramics and polymers have been used so far). One can envisage the use of such a matrix, for instance, entrapment in (magnetic) cobalt can yield easily separable catalysts.

2. The second direction focuses on the metal itself - can its catalytic properties be affected by the dopant? Encouraging results were obtained for Ag [*Adv. Functional Mater.* **17**, 913 (2007)]: Doping of Ag with Congo Red (CR@Ag) followed by thermal activation of the hybrid material, significantly improves the performance of Ag as a catalyst for methanol oxidation to formaldehyde (a high industrial volume process), outperforming both pure Ag and CR-coated Ag in terms of lowering the temperature needed for maximal conversion by 100 °C, lowering the temperature by 200 °C to reach the maximal selectivity (aldehyde formation), and increasing the maximal space velocity by a factor of two.

3. Inducing chirality in a catalytic metal was our next goal. Very recently we were able to achieve it [*Nature-Chemistry*, **1**(2), xx, (2009)] by entrapping within palladium several (chiral) cinchona alkaloids, resulting in cinchonine@Pd, cinchonidine@Pd, quinidine@Pd and quinine@Pd. With these hybrids enantioselective catalytic hydrogenations of acetophenone and isophorone were affected although with moderate ee's.

4. The fourth direction [*JACS.*, **130**, 11880 (2008); *C&EN*, **86** (51), 13, Dec. 22, 2008.] explores yet another new concept: The entrapment of an organometallic catalytic complex within a catalytic metal. The feasibility of this idea was proven with (RhCl(COD)(Ph<sub>2</sub>P(C<sub>6</sub>H<sub>4</sub>SO<sub>3</sub>Na))), ([Rh]), entrapped within silver, ([Rh]@Ag). Several aspects were demonstrated with the development of this heterogeneous catalyst: again, a metal can be used as a support for heterogenizing a homogeneous catalyst; the homogeneous catalyst is stabilized by the entrapment within the metal; the products of the composite catalyst are different compared to those obtained from the homogeneous one; and the adsorption of [Rh] on the surface of Ag and its entrapment are very different processes - only the latter provided appreciable catalytic activity. A direction we explore now is bi-functional catalysis, in which both the dopant and the metal will act as different catalysts for consecutive reaction steps.

5. Last but not least, a natural extension is into biocatalysis. Here too we have a proof of feasibility at hand [*Biomaterials*, **30** 1263 (2009)]: We have been able to immobilize successfully two enzymes, acid phosphatase and alkaline phosphatase in either silver or gold. The entrapped enzymes retained their catalytic activity in the resulting metal powder and kinetic investigation revealed Michaelis-Menten behavior. Protectability of the entrapped enzyme against harsh conditions was shown: The acidic enzyme is kept alive under basic conditions.

## **In Darwin's honor: laboratory evolution of a cytochrome P450 monooxygenase**

Prof. Frances H. Arnold

Division of Chemistry and Chemical Engineering  
California Institute of Technology 210-41  
Pasadena CA 91125

When making his case for the key role of natural selection in evolution, Darwin pointed to the enormous phenotypic variation that could be achieved in relatively few generations of artificial selection. Today, artificial selection (or 'directed evolution') applied to proteins allows us to observe how readily the functional molecules of life adapt in the face of defined selection pressures. Circumventing our profound ignorance of how sequence encodes function, directed evolution is a powerful approach to generating useful new biological molecules. Here I will describe our efforts to direct the evolution of the cytochrome P450 BM3 (CYP102A1) from *Bacillus megaterium*. Properties such as catalytic activity or stability can frequently be enhanced by single amino acid substitutions, and accumulating relatively few beneficial mutations (as little as 1-2% of the sequence) can make very significant changes to enzyme function. I will show how a P450 fatty acid hydroxylase has been converted into a whole family of catalysts for oxidation of small alkanes to carbohydrate synthesis and drug lead diversification. Where natural evolution has gone (e.g. impressive diversification of function in the P450 enzyme superfamily), directed evolution can follow. Even more interesting are the catalysts nature may not care about, but chemists dream of. While yielding useful biocatalysts for chemical synthesis, these studies provide new insights into the mechanisms underlying evolution of natural enzymes.

# Monday Morning Sessions

## Shining Light on Catalysts

Jeroen A. van Bokhoven  
ETH Zurich  
Institute for Chemical and Bioengineering  
HCI, E 127, 8093 Zurich  
[jeroen.vanbokhoven@chem.ethz.ch](mailto:jeroen.vanbokhoven@chem.ethz.ch)

Understanding the functioning of a heterogeneous catalyst is essential to the design and control of the structure of the catalyst of the future. There is close interplay between the reactant and the catalytically active site, which determines the ultimate performance of the latter. There are exciting new opportunities in the field of X-ray absorption spectroscopy. Space- and time-resolved spectra of high quality can be measured, which makes it possible to determine the structure inside a catalytic reactor space and time resolved. Moreover, secondary emission spectroscopy enables determining the electronic and geometric structure of a catalyst under actual catalytic conditions. I will present actual examples that illustrate the state of the art in situ characterization of catalysts using X-ray absorption.

## Alcohol Chemistry on TiO<sub>2</sub>(110) and (WO<sub>3</sub>)<sub>3</sub>/TiO<sub>2</sub>(110) Model Catalysts

**Zdenek Dohnálek**

Pacific Northwest National Laboratory, Fundamental and Computational Sciences  
Directorate, Chemical and Materials Sciences Division, , Richland, Washington 99352  
e-mail: [Zdenek.Dohnalek@pnl.gov](mailto:Zdenek.Dohnalek@pnl.gov)

Well defined, monodispersed clusters supported on single crystalline surfaces provide an excellent platform for model catalytic studies. Our work in this area focuses on the catalytic reactions of alcohols with rutile TiO<sub>2</sub>(110) and monodispersed cyclic (WO<sub>3</sub>)<sub>3</sub> clusters supported on TiO<sub>2</sub>(110). A combined experimental and theoretical approach is used to provide a detailed understanding of the site-specific reactivity and to yield structure-reactivity relationships. On TiO<sub>2</sub>(110) *in-situ* scanning tunneling microscopy (STM) studies show that the adsorption and dissociation of alcohols proceeds on bridge-bonded oxygen vacancies (O<sub>v</sub>'s). Studies of the rotational dynamics of alkoxy groups show that at room temperature alkyl chains rapidly rotate between structurally equivalent orientations. At elevated temperature, isothermal STM scanning is employed to study the diffusion dynamics of the O<sub>v</sub>'s and alcohol dissociation products. Kinetic parameters controlling the diffusion are extracted and compared to the theoretical DFT calculations. In the reactivity studies, two distinct dehydration channels are observed on TiO<sub>2</sub>(110), one related to reactions on the Ti<sup>4+</sup> rows and the other on O<sub>v</sub> sites. The (WO<sub>3</sub>)<sub>3</sub>/TiO<sub>2</sub>(110) model catalyst is prepared via direct sublimation of WO<sub>3</sub> and characterized using STM. In the reactivity studies, we find a dramatic lowering of the alcohol dehydration barrier relative to that on TiO<sub>2</sub>(110). Our results show that (WO<sub>3</sub>)<sub>3</sub> clusters provide an extremely efficient dehydration reaction channel for alcohols, which utilizes both strong Lewis acid W(VI) sites and doubly-bonded oxygen tungstyl (W=O) groups. Comparison of all C1 to C4 aliphatic alcohols shows that all alcohols readily react with (WO<sub>3</sub>)<sub>3</sub> clusters by heterolytic cleavage of the RO-H bond to give alkoxy (RO-) bound to W(VI) centers and a proton (H<sup>+</sup>) attached to terminal oxygen atom of a tungstyl group. Competing dehydration, dehydrogenation, and condensation channels are also observed. The trends observed for primary, secondary, and tertiary alcohols are determined from temperature programmed desorption (TPD) and used to infer details about the reaction mechanisms. A quantitative correlation between the coverage of (WO<sub>3</sub>)<sub>3</sub> clusters and the product yield indicates that the W=O groups are the primary reaction sites. DFT theory provides reaction mechanisms for all three channels demonstrating that they can occur on W(VI) Lewis acid sites with energy barriers of 30-40 kcal/mol, with dehydration being favored over the others.

# Catalysts Studied With Neutron Vibrational Spectroscopy

Stewart F. Parker

ISIS Facility, STFC Rutherford Appleton Laboratory, Chilton Didcot, Oxon, OX11 0QX, UK.

e-mail: [stewart.parker@stfc.ac.uk](mailto:stewart.parker@stfc.ac.uk)

In this talk I will highlight the uses of inelastic neutron scattering (INS) spectroscopy [1] as applied to the study of adsorbed species on catalysts. The advantages of INS spectroscopy for such studies are that neutrons are highly penetrating so windows in cells are unnecessary and aluminium or steel are usable. There are no selection rules so all modes are allowed. INS intensities are straightforwardly related to the atomic displacements of the atoms in the mode so are can be readily calculated from any method that provides frequencies and displacements, these include most ab initio packages, normal coordinate analysis and molecular dynamics. The disadvantages are that the technique is insensitive so a large surface area to bulk is essential (thus single crystal studies are not currently feasible) and only hydrogen ( $^1\text{H}$ ) has a sufficiently large scattering cross section to make surface studies feasible [2] I will demonstrate the use of INS with three examples:

(1) In a fuel cell a catalyst is essential for the dissociation of hydrogen at the anode. The best materials are Pt/C with a Pt content in the 40-60 wt% range. Such materials are opaque to visible and infrared electromagnetic radiation but are largely transparent to neutrons and it is possible to observe the high coordination sites of hydrogen on these materials [3] By combining studies from different types of INS spectrometer it is also possible to observe both the stretch and bend modes of the on-top hydrogen [4]. Comparison with CO tolerant Pt(40%)/Ru(20%)/C catalysts reveals a surprising difference between the two materials [5].

(2) 1200000 tonnes of  $\text{CH}_3\text{Cl}$  are made annually at the INEOS plant in the northwest UK. This is made by the reaction of  $\text{CH}_3\text{OH}$  and  $\text{HCl}$  over  $\eta\text{-Al}_2\text{O}_3$ . This also produces an unwanted by-product of  $\text{CH}_3\text{OCH}_3$ . Infrared studies of the reaction showed the presence of the expected adsorbed methoxy intermediate plus an unassigned band that may have been due to a second intermediate. INS studies of the system showed unambiguously that the unassigned band was due to a combination band of the adsorbed methoxy, proving that this was the only surface species [6,7].

(3) Raney nickel is widely used as a hydrogenation catalyst on both a laboratory and an industrial scale. The material is supplied as a slurry in water, drying the catalyst under flowing hydrogen produces a hydrogen saturated surface. A combination of INS, neutron diffraction and periodic density functional theory has been used to characterise both the structure and dynamics of the adsorbed hydrogen [8].

I will conclude with a brief look at the prospects for INS spectroscopy of catalysts.

## References

1. *Vibrational spectroscopy with neutrons, with applications in chemistry, biology, materials science and catalysis*, P.C.H. Mitchell, S.F. Parker, A.J. Ramirez-Cuesta and J. Tomkinson, World Scientific, Singapore, 2005.
2. P.W. Albers and S.F. Parker, *Advances in Catalysis*, 51 (2007) 99.
3. P.W. Albers, M. Lopez, G. Sextl, G. Jeske and S.F. Parker, *J. Cat.*, 22 (2004) 44.
4. S.F. Parker, C.D. Frost, P. Albers, M. Lopez and K. Seitz, *Catal. Today*, 114 (2006) 418.
5. P.W. Albers, M. Lopez and S.F. Parker, *Surf. Sci.*, 602 (2008) 3611.
6. A.R. McNroy, D.T. Lundie, J.M. Winfield, C. Dudman, P. Jones, S.F. Parker, J.W. Taylor and D. Lennon, *Phys. Chem. Chem. Phys.*, 7 (2005) 3093.
7. A.R. McNroy, D.T. Lundie, J.M. Winfield, C.C. Dudman, P. Jones, S.F. Parker and D. Lennon, *Catal. Today*, 114 (2006) 403.
8. S.F. Parker, D. Bowron. S. Imberti, A.K. Soper, K. Refson and P. Albers, *Nature Chemistry*, submitted for publication.

## Ultra-stable “smart” molecular interfaces for renewable energy

R.J. Hamers

University of Wisconsin, Department of Chemistry, Madison, WI 53706

Email: rjhamers@wisc.edu

Emerging applications in catalysis and photovoltaic energy are placing increasing emphasis on the need for ultra-stable molecular interfaces in order to achieve high stability and a high degree of functionality. Materials such as carbon and metal oxides are oxidatively stable and are useful supports, but have little selectivity. By linking these materials to molecular systems with novel types of functionality it is possible to produce molecular interfaces having a high degree of functionality. Our work has focused on the fabrication and characterization of ultra-stable, functional molecular interfaces to these materials, and understanding how the chemistry impacts the electronic structure.

Vertically aligned carbon nanofibers are of interested because this novel form of carbon presents large amounts of edge-plane graphite, leading to high electrochemical electron-transfer rates along the nanofiber sidewalls. Measurements of the electron-transfer to redox-active groups tethered to the surface via photochemical grafting or via a surface “click” reaction show a nearly electron-transfer constant rate, suggesting that the mechanism of electron transfer is not simple through-bond tunneling.[1,2] Similar methods have recently been applied to TiO<sub>2</sub> and other metal oxides; in this case we have developed molecular layers that are exhibit extraordinarily high stability, able to withstand pH=1 and 65°C for more than 2 months. [3,4] I will discuss recent results on new methods for fabricating ultra-stable interfaces and resulting electronic properties relevant for electrocatalysis and photovoltaic energy conversion.

[1] E.C. Landis, R.J. Hamers, *Journal of Physical Chemistry C*, **2008**, *112*, 16910-16918.

[2] E.C. Landis, Robert J. Hamers, *Chemistry of Materials*, **2009**, *21*, 724-730

[3] B. Li, R. Franking, E.C. Landis, H.Kim, and R. J. Hamers, *ACS Applied Surfaces and Interfaces* **2009**, accepted.

[4] R. Franking, E.C. Landis, B. Li, and R.J. Hamers, *Langmuir*, submitted.



# Monday Afternoon Sessions

## Hierarchically Porous Zeolites for Catalytic Applications

**Ryong Ryoo**

Center for Functional Nanomaterials, Department of Chemistry, and Graduate School of Nanoscience and Nanotechnology (WCU), KAIST, Daejeon, 305-701, Korea. rryoo@kaist.ac.kr

Hierarchical pore systems (HPS) are defined by the different porosity levels in two or multiple length scales. HPS can be found ubiquitously in nature and human artworks, such as the circularly systems of plants and animals, the cellular shells of diatoms, animal nerve systems, man-made architectures, and traffic systems in modern cities. HPS are naturally or artificially designed for accommodation of maximum functions in a limited volume or area, and also achievement of their maximum efficiencies (e.g., mass transfer or transportation). Here, we present various routes to hierarchically mesoporous/microporous zeolite materials, such as agglomeration of zeolite nanoparticles, delamination of layered zeolite precursors, post-synthetic demetallation treatment, generation of mesopores by hard nanotemplates, or by surfactants. Particular emphasis is given to the recent synthesis method which uses organosilane surfactants as the mesopore-directing agent, while the microporous zeolite frameworks are formed through the structure-direction by ordinary  $\text{Na}^+$  ions or small organic amines. Another strategy of particular interest is to use bifunctional surfactants that can direct porous structures in the meso- and micro-length scales simultaneously. In this case, both pore systems are generated by a single kind of surfactant, without other zeolite structure-directing agents such as  $\text{Na}^+$  and tetrapropylammonium. The zeolite structure is directed by functional groups in the surfactants. These methods are demonstrated as a means of decreasing zeolite framework thickness and hence achieving minimal diffusion path lengths. It has been confirmed that such zeolites are suitable for catalytic applications involving bulky species, due to catalytic activities at the mesopore walls. In addition, the hierarchical zeolites exhibit a significantly prolonged catalytic lifetime in a number of small molecular reactions taking place inside micropores, as compared with bulk crystalline zeolite. This effect is attributed to facile diffusion to/from micropores via mesopores. The hierarchical zeolite synthesis, structure determination, and characterization of catalytic properties are discussed in this lecture.

## MICROPOROUS AND MESOPOROUS NANO-SIZE TRANSITION METAL OXIDES: PREPARATION, CHARACTERIZATION, AND APPLICATIONS

**Postdocs:** W. S. Willis.

**Students:** C. Chen, T. Coons, V. Crisostomo; Y. Ding, J. Durand, A. Espinal, S. Frueh, B. Hu, A. Iyer, L. Jin, J. Kona, W. Li, A. Morey, N. Opembe, S. Sithambaram, Y. Xing, L. Xu., Y. Zhang.

**Collaborators:** M. Aindow; A. Doble; A. Frenkel; J. Hanson; D. Mullins.

**Contacts:** Department of Chemistry, Unit 3060, University of Connecticut, Storrs, CT 06269-3060.

[Steven.Suib@Uconn.edu](mailto:Steven.Suib@Uconn.edu)

### Goal

To synthesize and characterize nano-size wires, helices, lines, patterns, powders, and other morphologies of porous transition metal oxides for selective catalytic oxidations; and activation of CO<sub>2</sub>.

### DOE Interest

Fundamental understanding of the mechanisms of selective catalytic oxidations is important in the areas of energy and catalysis. Porous nano-size metal oxides<sup>1-35</sup> are useful in environmentally friendly applications such as adsorption,<sup>14,22</sup> catalysis,<sup>1-35</sup> sensors, batteries,<sup>2,3,16</sup> environmental remediation, and other areas. Electron and energy transfer, mixed valency, redox cycling, mechanistic studies, and detailed knowledge of structure are significant in catalysis for energy purposes. Characterization of molecular transformations and design and control of structure and composition are routes being used to reach these goals.

### Recent Progress

*Synthesis of Nanomaterials.*

The focus of our synthetic work involves novel syntheses and phases, new morphologies, and framework substitutions.<sup>1-35</sup> Metal oxides of manganese, titanium, copper, zinc, iron, and mixed metal systems have been the focus of this work. Unique pillared materials,<sup>24,33</sup> controlled morphologies<sup>1-3,6-10,13,15,17-19</sup> of various nano-size metal oxides, and control of particle sizes<sup>1-3,6,9-10,15,17</sup> have been realized.

*Characterization Studies.*

*In situ* X-ray powder diffraction (XRD), *In situ* synchrotron XRD,<sup>11</sup> adsorption, electron microscopy, X-ray absorption, infrared, Raman, thermal, chemical analysis, and other methods have been used to study the above materials after preparation, in certain cases *in situ* during catalytic reactions, and after reaction. Synchrotron work has been done at Brookhaven National Labs.

*Catalysis.*

All materials described above have been studied in various catalytic reactions. Selective oxidations<sup>14,18,20-25</sup> of alcohols with O<sub>2</sub> or with peroxides; kinetic isotope effects,<sup>23</sup> oxidations of aromatics,<sup>35</sup> production of imines,<sup>28</sup> epoxidations,<sup>12</sup> ring openings,<sup>34</sup> tandem production of quinoxalines,<sup>28,32</sup> photocatalytic degradations of phenol, catalytic degradation of organic dyes,<sup>30</sup> selective oxidation of hydrocarbons like cyclohexanol<sup>31</sup> and other reactions have been studied. Evidence of catalytic redox cycling, multifunctional catalysis, morphological effects in catalysis, catalytic intermediates, and other phenomena have been observed with these systems.

### Future Plans

Future plans include studies of the role of hydrophobicity in these and other catalytic reactions, activation of CO<sub>2</sub>, control of pore sizes, and understanding the role of morphology in selective catalytic oxidations.

### Publications (2006-2008)

1. Durand, J. P.; Villegas, J. C.; Gomez-Mower, S.; Giraldo, O.; Suib, S. L. Colloidal Manganese Oxide Precursor to Octahedral layered OL-3 Materials, *J. Inorg. & Organomet. and Polym. Materials*, 2007, **17**, 459-467.
2. Ngala, K.; Doble, A.; Suib, S. L., Characterization and Electro-catalytic Behavior of Layered Li<sub>2</sub>MnO<sub>3</sub> and its Acid-Treated form, *Chem. Mat.*, 2007, **19**, 229-234.
3. Crisostomo, V.; Ngala, K.; Suib, S. L., New Synthetic Route, Characterization, and Electrocatalytic Activity of Nano-sized Manganite, *Chem. Mat.*, 2007, **19**, 1832-1839.
4. Suib, S. L.; Hu, N.; Rusling, J. F. Layer-by-Layer Assemblies of Thin Films on Electrodes, in *Encyclopedia of Electrochemistry*, Bard, Stratman, Wiley, 2007, 375-396.
5. Li, W.; Crisostomo, V.; Nyutu, E.; Ding, Y.; Suib, S. L.; Transition Metal Oxide (TMO) Nanorods: Synthesis, Characterization, Properties, and Applications, in *Nanorod Research Developments*, Nova Science Publishers, 2007.
6. Ding, Y.; Shen, X. F.; Gomez, S.; Luo, H.; Aindow, M.; Suib, S. L. Hydrothermal Growth of Manganese Dioxide Into Novel 3D Hierarchical Nano-architectures, *Adv. Funct. Mater.*, 2006, **16**, 549-555.
7. Li, W.; Yuan, J.; Shen, X. F.; Gomez-Mower, S.; Xu, L. P.; Sithambaram, S.; Aindow, M.; Suib, S. L. Hydrothermal Synthesis of Structure and Shape Controlled Manganese Oxide Octahedral Molecular Sieve (OMS) Nano-materials, *Adv. Funct. Mat.*, 2006, **16**, 1247-1253.
8. Li, W.; Yuan, J.; Gomez-Mower, S.; Sithambaram, S. Synthesis of Single Crystal Manganese Oxide Octahedral Molecular Sieve (OMS) Nanostructures with Tunable Tunnels and Shapes, *J. Phys. Chem.*, 2006, **110**, 3066-3070.
9. Li, W.; Zhang, L.; Sithambaram, S.; Aindow, M. A.; Suib, S. L., Shape Evolution of Single-crystalline Mn<sub>2</sub>O<sub>3</sub> Using a Solvothermal Approach, *J. Phys. Chem. B*, 2007, **111**, 14694-14697.
10. Xing, Y.; Suib, S. L., Inorganic Synthesis for the Stabilization of Nanoparticles, *Chem. Mater.*, 2007, **19**, 4820-4826.
11. Shen, X.; Hanson, J.; Suib, S. L., *In-situ* Synthesis of Mixed-Valent Manganese Oxide Nanocrystals: An *in-situ* Synchrotron X-ray Diffraction Study, *J. Am. Chem. Soc.*, 2006, **128**, 4570-4571.
12. Ghosh, R.; Shen, X.; Villegas, J. C.; Ding, Y.; Malinger, K.; Suib, S. L., Role of Manganese Oxide Octahedral Molecular Sieves in Styrene Epoxidation, *J. Phys. Chem.*, 2006, **110**, 7592-7599.
13. Karunanithi, A. T.; Aquah, C.; Achenie, L.; Sithambaram, S.; Suib, S. L.; Gani, R. An Experimental Verification of morphology of ibuprofen crystals from CAMD designed solvent, *Chem. Eng. Sci.*, 2007, **62**, 3276-3281.
14. Luo, J.; Zhang, Q.; Garcia-Martinez, J.; Suib, S. L. Adsorptive and Acidic Properties, Reversible Lattice Oxygen Evolution, and Catalytic Mechanism of Cryptomelane-Type Manganese Oxides as Oxidation Catalysts, *J. Am. Chem. Soc.*, 2008, **130**, 3198-3207.
15. Chen, C.; Abbas, S.; Morey, A.; Sithambaram, S.; Xu, L. X.; Garces, H. F.; Hines, W. A.; Suib, S. L. Controlled synthesis of Self-Assembled Metal oxide Hollow Spheres Via Tuning Redox Potentials: Versatile Nanostructured Cobalt Oxides, *Adv. Mat.*, 2008, **20**, 1205-1209.
16. Liu, Z.; Xing, Y.; Chen, C.; Zhao, L. L.; Suib, S. L.; Framework doping of indium in manganese oxide materials: Synthesis, characterization and electrocatalytic reduction of oxygen, *Chem. Mater.*, 2008, **20**, 2069-2071.

17. Nyutu, E.; Chen, C. H.; Crisostomo, V.; Sithambaram, S.; Suib, S. L., Systematic Control of Particle Size in Rapid Open-Vessel Microwave Synthesis of K-OMS-2 Nanofibers, *J. Phys. Chem.*, 2008, **112**, 6786-6793.
18. Ding, Y.; Xu, L.; Chen, C.; Shen, X.; Suib, S. L., Syntheses of Nano-Structures of Cobalt Hydrotalcite-Like Compounds and  $\text{Co}_3\text{O}_4$  via Microwave-Assisted-Reflux Method, *J. Phys. Chem.*, 2008, **112**, 8177-8183
19. Nyutu, E.; Chen, C. H.; Dutta, P.; Suib, S. L., Effect of Microwave Frequency on Hydrothermal Synthesis of Nanocrystalline Tetragonal Barium Titanate, *J. Phys. C*, 2008, **112**(26), 9659-9667.
20. Calvert, C.; Morey, A.; Joesten, R.; Ngala, K.; Villegas, J.; Shen, X.; Suib, S. L., Synthesis, Characterization, and Rietveld Refinement of Tungsten Framework Doped Porous Manganese Oxide (K-OMS-2) Material, *Chem. Mater.*, 2008, in press.
21. Sithambaram, S.; Nyutu, E. K.; Suib, S. L., OMS-2 Catalyzed Oxidation of Tetralin: a Comparative study of Microwave and Conventional Heating under Open Vessel Conditions Corresponding, *Appl. Catal.*, 2008, in press.
22. Yuan, J.; Liu, X.; Akbulut, O.; Hu, J.; Suib, S. L.; Kong, J.; Stellacci, F., Superwetting nanowire membranes for selective absorption, *Nature Nanotechnology*, 2008, **3**(6), 332-336.
23. Opembe, N. N.; Son, Y. C.; Sriskandakumar, T.; Suib, S. L., Kinetics and mechanism of 9H-fluorene oxidation catalyzed by manganese oxide octahedral molecular sieves, *Chem. Sus. Chem*, 2008, **1**(3), 182-185.
24. Suib, S. L., Porous Manganese Oxide Octahedral Molecular Sieves and Octahedral Layered Materials, *Acc. Chem. Res.*, 2008, **41**(4), 479-487.
25. Suib, S. L., Structure, porosity, and redox in porous manganese oxide octahedral layer and molecular sieve materials, *J. Mat. Chem.*, 2008, **18**(14), 1623-1631.
26. Shen, X.; Garces, L. J.; Ding, Y.; Laubernds, K.; Zerger, R. P.; Aindow, M.; Neth, E. J.; Suib, S. L., Behavior of  $\text{H}_2$  chemisorption on Ru/ $\text{TiO}_2$  surface and its application in evaluation of Ru particle sizes compared with TEM and XRD analyses, *Appl. Catal., A: General*, 2008, **335**(2), 187-195.
27. Xing, Y.; Liu, Z.; Gomez, S.; Suib, S. L., Tuning of Texture and Structure of Copper-Containing Nanocomposite Oxide Materials, *J. Phys. Chem. C*, 2008, **112**(5), 1446-1454.
28. Sithambaram, S.; Kumar, R.; Son, Y. C.; Suib, S. L., Tandem catalysis: Direct catalytic synthesis of imines from alcohols using manganese octahedral molecular sieves, *J. Catal.*, 2008, **253**(2), 269-277.
29. Haji, S.; Malinger, K. A.; Suib, S. L.; Erkey, C., Fuels and fuel processing, *Fuel Cell Tech.*, 2006, 165-211.
30. Sriskandakumar, T.; Opembe, N.; Chen, C.; Morey, A.; King'onde, C., Suib, S. L., Green Decomposition of Organic Dyes using Octahedral Molecular Sieves Manganese Oxide Catalysts, *J. Phys. Chem. A*, 2009, **113**, 1523-1530.
31. Kumar, R.; Sithambaram, S.; Suib, S. L., Cyclohexane Oxidation Catalyzed by Manganese Oxide Octahedral Molecular Sieves - Effect of Acidity of the Catalyst, *J. Catal.*, 2009, **262**, 304-313.
32. Sithambaram, S.; Suib, S. L., Manganese Octahedral Molecular Sieves Catalyzed Tandem Process for Synthesis of Quinoxalines, *Green Chem.*, 2008, **10**, 1029 - 1032.
33. Chen, C. H.; Crisostomo, V. M.; Li, W. N.; Xu, L.; Suib, S. L., A Designed Single-step Method for Synthesis and Structural Study of Organic-Inorganic Hybrid Materials: Well-ordered Layered Manganese Oxide Nanocomposites, *J. Am. Chem. Soc.*, 2008, **130**, 14390-14391.
34. Sithambaram; Xu; Chen; Ding, Kumar; Calvert; Suib, S. L., Manganese Octahedral Molecular Sieve Catalysts for Selective Oxide Ring Opening, *Catal. Today*, 2009, **140**, 162-168.
35. Jin, L.; Chen, C.; Crisostomo, V. M. B.; Xu, L.; Son, Y. C.; Suib, S. L., gamma- $\text{MnO}_2$  Octahedral Molecular Sieve: Preparation, Characterization, and Catalytic activity in the Atmospheric Oxidation of Toluene, *J. Appl. Catal.*, 2009, **355**, 169-175.

## New Approaches to Nanostructured Metal Oxide Catalysts

Students: Richard Mayes, Geoff Eldrich, Michael Peretich, Josh Abbott, Nan Chen  
 Collaborators: Edward Hagaman<sup>1</sup>, Jian Jiao<sup>1</sup>, Zili Wu<sup>2</sup>, Chendu Liang<sup>2</sup> (<sup>1</sup>Oak Ridge National Laboratory; <sup>2</sup>Center for Nanophase Materials Science, Oak Ridge TN)  
 Contact: Department of Chemistry; University of Tennessee, Knoxville, TN 37996-1600  
[cebarnes@utk.edu](mailto:cebarnes@utk.edu)  
 Web page: <http://www.chem.utk.edu/faculty/barnes.html>

### Goal

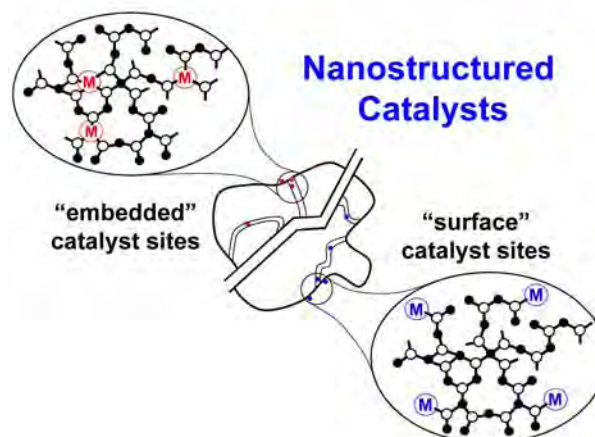
Our research program is focused on developing a general methodology for preparing targeted, nanostructured, single site catalysts. We have addressed these goals from a ground up approach which involves three key components: a rigid building block that is the major component of the support matrix as well as a structure directing agent and two types of chemical linkers: one that will eventually become the site where reaction occurs and a second type that is not directly involved in catalysis but shores up the matrix by forming chemically and thermally robust links between building blocks. Finally, we have chosen a linking reaction involving complementary functionality on the building block and linkers such that self condensation is prevented.

### DOE Interest

The preparation of next generation, heterogeneous catalysts will require a new set of synthetic methodologies to arrive at the goal of obtaining robust, selective catalysts that can be tailored to a desired reaction and feedstock. Achieving the level of selectivity desired of such “ultraselective” catalysts will require entirely new approaches to nanostructured heterogeneous catalysts than are currently available. This level of structural control requires that the synthesis of the final metal-support ensemble be critically linked to the initial steps involved in the formation of the support matrix itself. A scientific goal of this research project is to develop a general methodology with which to prepare nanostructured mixed metal oxide catalysts. Nanostructuring in this context involves tailoring the local environments of catalyst sites on a support such that all are identical (single site catalysts). Control of the atomic level structure around the catalyst site as well as at the meso- and macroscopic scales (e.g. porosity and surface area) are design criteria in the development of new synthetic methodologies for these heterogeneous catalysts.

### Recent Progress

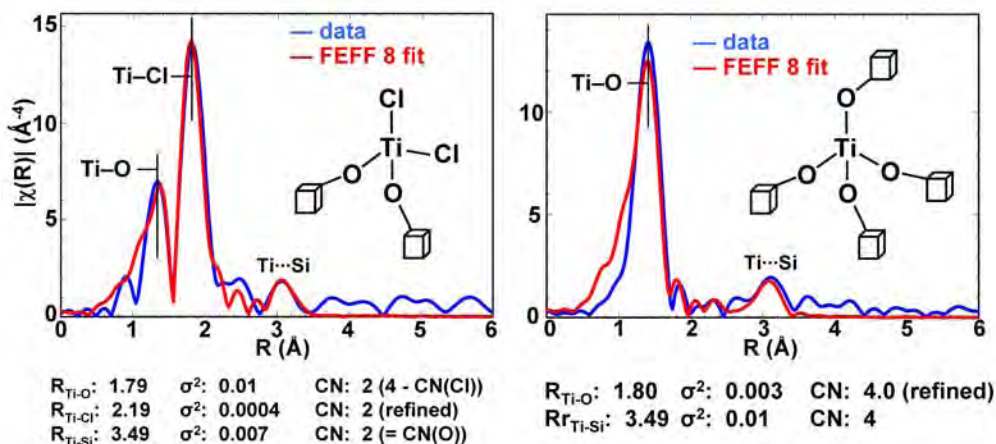
To understand our strategy toward preparing nanostructured catalysts, it is important to know exactly how we define nanostructuring in this context. Nanostructured heterogeneous catalysts are materials in which the form and structure of the catalyst-support matrix are designed and simultaneously controlled at several different length scales. At the level of the active site itself, nanostructuring requires that we be able to identify and target specific arrangements of metals and ligands such that a desired catalyst “ensemble” is obtained and all other potential metal species excluded (the definition of a single site catalyst). In the context of metals on the surfaces of metal oxide supports, some tailoring of the surface functionality that both holds them in place and contributes to the sphere of coordinating ligands must take place as



the catalyst ensemble is developed. Catalytic activity is directly proportional to the number of accessible sites in the system. Therefore, a second goal in developing nanostructured catalysts is to achieve the highest density of sites possible within the support matrix while maintaining site isolation. Finally, all sites must be accessible and mass transfer rates should be as high as possible. An operational target satisfying this goal is to achieve a distribution of meso- and microporosity throughout the solid.

For the past year our work has focused in four areas: 1) concluding spectroscopic characterization of atomically dispersed high valent titanium and vanadium in  $\text{Si}_8\text{O}_{20}$  building block (bb) matrices; 2) developing new precursors for incorporating polynuclear titanium catalyst ensembles in similar bb matrices; 3) investigating the incorporation of atomically dispersed aluminum centers into  $\text{Si}_8\text{O}_{20}$  matrices and, 4) beginning to build the bridge between the nanostructuring that we engineer into these materials and their activities as catalysts in oxidation and solid acid chemistries.

*Characterization of atomically dispersed Ti and V systems:* Titanium(IV) and vanadium(IV, V) systems are now considered fully characterized: IR, Raman UV/vis, surface area, metal content and metal site structure (EXAFS). The EXAFS data shown below illustrate how we are able to vary the “embeddedness” of a tetrahedral Ti center into our silicate bb lattice simply by following the ratio of the coordination numbers of the Ti-O and Ti-Cl features. In the two plots below, the target species were 2- and 4-connected Ti centers. It should be noted that the 2-connected sample represents an average of a distribution of titanium centers in the sample while the 4-connected sample may be described as a single site catalyst.

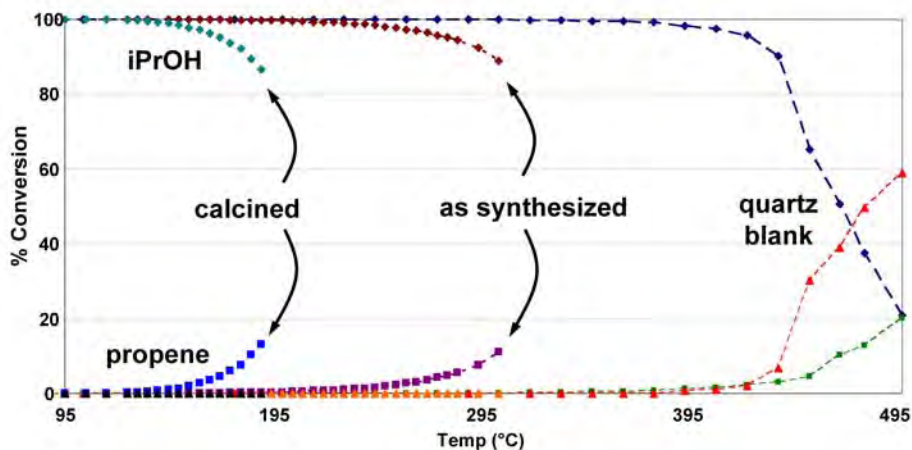


*Characterization of atomically dispersed Al systems:* While  $\text{AlCl}_3$  appears to react similar to other metal chloride linking reagents we have tested, the coordinative unsaturation predicted for a neutral  $\text{AlO}_3$  center lead us to investigate what types of center would develop. While gravimetric studies are consistent with the loss of all chloride ligands from around aluminum  $^{27}\text{Al}$  SSNMR studies (data obtained by Dr. Jian Jiao) indicates that a mixture of 4-, 5- coordinate aluminum atoms are present in the matrix. At the same time, IR studies of the pyridine adduct clearly indicate that, as predicted only Lewis acid sites are present in the matrix. Finally, catalysis studies in a flow reactor (differential mode) clearly show that aluminum (as well as all other atomically dispersed metal catalysts) behaves exclusively as solid acid catalysts cleanly dehydrating isopropanol to propene at low temperatures.

## Future Plans

Work will continue with all of the metals described above. We have purchased an *in situ* UV/vis (DRUV), IR (DRIFTS) and Raman spectroscopy cell (Harrick) to correlate spectroscopic changes with observed catalytic activity measured in our atmospheric flow cell. Titanium and

*Lightoff Curves iPrOH dehydration to propene:  
Overlay Aluminum silicate catalysts*



vanadium will be investigated in the context of both oxidation and solid acid reactions. Aluminum will be investigated as a solid acid catalyst.

### **Publications (2006 – 2009)**

1. *Building Block Approaches to Single Site, Site Isolated Heterogeneous Catalysts*, C. E. Barnes invited contribution in, *Recent Advancements in Surface Organometallic Chemistry*, J.-M. Basset, R. Psaro, D. Roberto and R. Ugo, eds., Elsevier, 2009 (in press).
2. *Solid-state  $^{119}\text{Sn}$  MAS NMR of  $\text{Si}_8\text{O}_{20}(\text{SnMe}_3)_8$  in related lattices*, Jian Jiao, Ming-Yung Lee, C. E. Barnes, E. W. Hagaman, *Magn. Reson. Chem.* **2008**, 46, 690–692.
3. *Nanostructured Catalysts: Controlling Single-Site Composition*, C E. Barnes R. Mayes, (2008), in *Nanomaterials: Inorganic and Bioinorganic Perspectives*, edited by Charles M. Lukehart and Robert A. Scott. Chichester, UK: John Wiley & Sons, Ltd, pp 673-686, 2008.
4. *Building Block Approaches to Single Site, Site Isolated Heterogeneous Catalysts, Reaction of the  $\text{Si}_8\text{O}_{20}(\text{SnMe}_3)_8$  Building Block with Silyl Chlorides: A New Synthetic Methodology for Preparing Nanostructured Building Block Solid*, J. C. Clark and C. E. Barnes, *Chem. Mater.*, **2007**, 19, 3212-3218.
5. *Synthesis and structure of functionalized spherosilicate building block molecules for materials synthesis*, J. C. Clark; S. Saengkerdsub; G. T. Eldridge; C. Campana; C. E. Barnes, *J. Organomet. Chem.* **2006**, 691, 3213-22.



**Nanocluster Catalysts Formation and Stabilization Fundamental Studies**

Postdocs: Prof. Saim Özkar, Dr. Murielle A. Watzky  
Students: Lisa S. Ott, L.; Eric E. Finney, Clarie Besson, Chris Graham, Joe E. Mondloch  
Collaborators: Prof. Robert Bergman (UC Berkeley)  
Contacts: Department of Chemistry, Colorado State University,  
Ft. Collins, CO 80523  
phone: (970)-491-2541; Email: [rfinke@lamar.colostate.edu](mailto:rfinke@lamar.colostate.edu)  
web page: <http://www.chm.colostate.edu/rgf/index.html>

**Goals**

Three primary goals define our DOE-funded program: one goal is to determine which stabilizers and other factors are best for the formation, stabilization and catalytic activity of transition-metal nanocluster catalysts; a second goal is to continue our mechanistic studies of the nucleation, growth and agglomeration of transition-metal nanocluster catalysts; and a third goal is to exploit custom-made nanoclusters in interesting catalytic reactions.

**DOE Interest**

Nanoclusters are metal particle catalysts closely analogous to the supported-metal particles in commonly used commercial heterogeneous catalysts. However, nanoclusters have the advantage of being soluble; *hence, they can be made and studied by powerful solution synthesis, spectroscopic characterization and kinetic methods.* Well-defined nanoparticle catalysts promise to be important in the development of the concepts and technical advances en route to achieving the “Holy Grail” of heterogeneous catalysis, namely single-size, single type of active site, high selectivity, and high activity metal-particle catalysts. Nanoparticles are also expected to have their own, unique catalytic reactivity as well, especially if their surface composition and associated stabilizing ligands can be understood and controlled.

**Recent Progress**

(1) *Nanocluster Stabilization Fundamental Studies.* We published 4 papers in 2007-early 2009 in the previously little investigated area of the factors that allow nanocluster stabilization, while still permitting high catalytic activity.<sup>1,2,3,4</sup> Our publications included the first review in the area<sup>3</sup> as well as one paper that updated the synthesis of a classic polyoxometalate<sup>5</sup>  $P_2W_{18}O_{62}^{6-}$  that was needed to make and study the nanocluster stabilizer,  $P_2W_{17}O_{61}^{10-}$ .<sup>4</sup> Highlights of our discoveries include: (i) that the potentially tetradentate  $P_2W_{17}O_{61}^{10-}$  is quite a good nanocluster stabilizer, albeit slightly less efficacious than the current “gold standard”  $P_2W_{15}Nb_3O_{62}^{9-}$  polyoxoanion stabilizer;<sup>4</sup> (ii) that ionic liquids do

provide excellent nanoparticle stabilization as others had implied, but that the imidazolium component of the ionic liquid can also lead to oxidative addition to, and thus poisoning of, the surface of the nanoparticles in at least some cases;<sup>2</sup> and (iii) that halides are reasonable anionic-stabilizers of nanoparticles as typically believed, although not too much better than traditionally weakly coordinating anions such as  $\text{BF}_4^-$ .<sup>1</sup>

(2) *Fundamental Studies of Nanocluster Nucleation, Growth and Agglomerations in Nature.* Our studies in this area allowed us: (i) to publish only the third paper on the more general, 4-step mechanism for nucleation, growth and two types of agglomeration that we discovered in 2005, a paper which shows that primary variable turning on this mechanism is a large concentrations of coordinating ligand<sup>6</sup>; (ii) to understand an interesting supersensitivity we observed to the concentration of nanocluster precursor and the reaction temperature, effects that are likely important—but previously unrecognized—in many other nanocluster syntheses<sup>7</sup>; and (iii) to publish the first paper showing that there are two rate constants for bimolecular and novel autocatalytic agglomeration that one needs to measure as the preferred way to quantitate nanocluster stability in the future.<sup>8</sup> We were also able: (iv) to publish an invited, feature review of nanoparticle nucleation and growth.<sup>9</sup>

(3) *The First Mechanism-Based Nanocluster Size Control Treatment and Associated Equation.* In an important paper, we were able to use the 2-step nucleation and growth mechanism, and its two rate constants ( $k_1$  and  $k_2$ , respectively), along with the initial concentration of nanocluster precursor,  $[A]_0$ , and final nanocluster size,  $D_f$ , to develop an equation that accounts for nanocluster size vs time.<sup>10</sup> This advance towards the “Holy Grail” of size control in nanocluster synthesis should allow better, rational, mechanism-based control of nanoparticle size at least for nanoparticles that grow by the nucleation and autocatalytic growth pathway noted below.

(4) *Initial Investigations of the Broader Applicability of the Finke-Watzky (F-W) 2-Step Mechanism of Nucleation and Autocatalytic Growth in Other Parts of Nature.* In what promises to be one of the largest and broadest impacts of our DOE funded mechanistic studies of nanoparticle nucleation and growth, we discovered that our DOE-funded, 2-step, F-W mechanism of slow, continuous nucleation ( $A \rightarrow B$ ), followed by typically fast, autocatalytic growth ( $A + B \rightarrow 2B$ ), applies to other, seemingly disparate areas of science. The first is: (i) an interesting organometallic catalyst formation reaction under study in Bob Bergman’s group in which an Ir-Cl bond is replaced by a Me group from  $\text{SnMe}_4$  to form an Ir-Me complex plus  $\text{SnMe}_3\text{Cl}$ . Together with Prof. Bergman and his postdoc Stuart Smith, we showed that a poor, inefficient  $\text{Pt}(\text{P}^t\text{Bu}_3)_2$  precatalyst (A) chemically “evolves” to a much faster, effectively “smarter”  $\text{Pt}(\text{SnMe}_3)(\text{P}^t\text{Bu}_3)(\text{Cl})$

catalyst (B) according to the generalized 2-step F-W mechanism of nucleation and growth.<sup>11</sup>

In a second, expected to be far reaching study, we showed that (ii) the F-W 2-step mechanism is the only kinetic treatment presently available able to deconvolute nucleation from growth rate constants for the 41 usable (non-prion) protein aggregation kinetic data sets we could find in the literature.<sup>12</sup> Moreover, we recently extended the applicability of the F-W 2-step mechanism to prion-protein aggregation relevant to prion-based neurological diseases.<sup>13</sup> Such protein aggregation is thought to be key underlying step in Alzheimer's, Parkinson's, Huntington's and prion-based neurological diseases—presently the most feared among all diseases. Learning how to control nucleation or growth are two promising therapeutic strategies one can envision. While these studies were funded with other monies (since they fall outside the specific scope of our current DOE grant), these papers<sup>12,13</sup> do acknowledge our DOE grant since it was that long-term DOE support that led to the original discovery of the F-W 2-step mechanism.

### **Future Plans**

In the coming year we plan to finish up one final paper resulting from Eric Finney's Ph.D. thesis on using the F-W 2-step mechanism to analyze solid-state kinetic data. We then will focus on very promising studies initiated by Joe Mondloch using the F-W 2-step mechanism to understand the surprisingly little investigated kinetics and mechanism of supported heterogeneous catalyst formation—little investigated since it is hard to follow the kinetics of supported metal particle formation.<sup>14</sup> That exciting work promises to help bring better, mechanism-based synthesis, size control and stabilizing ligand control to the very important area of catalysis by supported metal particles.

### **Publications (2007-2009)**

---

1. L. Starkey-Ott, S. Campbell, K. R. Seddon, R. G. Finke, "Transition-metal Nanocluster Formation and Stabilization Fundamental Studies: Ranking the Nanocluster Stabilizing Ability of Halides", *J. Nanoscience and Nanotechnology* **7** (2007) 2400-2410.
2. L. Starkey-Ott, R. G. Finke, "Evidence That Imidazolium-Based Ionic Liquids Can be Metal(0)/Nanocluster Catalyst Poisons in at Least the Test Case of Iridium(0)-Catalyzed Acetone Hydrogenation", *Inorg. Chem.* **46(24)** (2007) 10335-10344.
3. L. Starkey-Ott, R. G. Finke, "Transition-Metal Nanocluster Stabilization for Catalysis: A Critical Review of Ranking Methods and Putative Stabilizers", *Coord. Chem. Rev.* **251** (2007) 1075-1100.

- 
4. “Ranking the Lacunary,  $(\text{Bu}_4\text{N})_9\{\text{H}[\alpha_2\text{-P}_2\text{W}_{17}\text{O}_{61}]\}$  Polyoxometalate’s Stabilizing Ability for  $\text{Ir}(0)_n$  Nanocluster Formation and Stabilization Using the 5 Criteria Method Plus Necessary Control Experiments”, Graham, C. R.; Ott, L. S.; Finke, R. G., *Langmuir.*, **2009**, *25*, 1327-1336.
  5. “The Classic Wells-Dawson Polyoxometalate,  $\text{K}_6[\alpha\text{-P}_2\text{W}_{18}\text{O}_{62}]\cdot 14\text{H}_2\text{O}$ : Answering the 88 Year-Old Question of What is Its Preferred, Optimum Synthesis?”, Graham, C. R.; Finke, R. G. *Inorg. Chem.* **2008**, *47*, 3679-3686.
  6. E. E. Finney, R. G. Finke, “The Four-Step, Double-Autocatalytic Mechanism for Transition-Metal Nanocluster Nucleation, Growth and Then Agglomeration: Metal, Ligand, Concentration, Temperature, and Solvent Dependency Studies”, *Chem. Mater.* **20** (2008) 1956-1970.
  7. L. Starkey-Ott, R. G. Finke, “Supersensitivity of  $\text{Ir}(0)_n$  Transition-Metal Nanoparticle Formation to Initial Ir Precursor Concentration and Reaction Temperature. Understanding Its Origins”, *J. Nanoscience and Nanotechnology*, **8**, (2008) 1551–1556.
  8. L. Starkey-Ott, R. G. Finke, “Transition-Metal Nanocluster Stabilization vs Agglomeration Fundamental Studies: A Quantitative Measurement of the Two Rate Constants for Agglomeration and Their Informative Temperature Dependence”, *Chem. Mater.*, **20** (2008), 2592-2601.
  9. E. E. Finney, R. G. Finke, “Nanocluster nucleation and growth kinetic and mechanistic studies: A review emphasizing transition-metal nanoclusters.” *J. Colloid and Interface Science*, **317(2)** (2008) 351-374.
  10. “Transition-Metal Nanocluster Size vs. Formation Time and the Catalytically Effective Nucleus Number: A Mechanism-Based Treatment”, Watzky, M. A.; Finney, E. E.; Finke, R. G., *J. Am. Chem. Soc.* **2008**, *47*, 10790-10800.
  11. S. E. Smith, J. M. Sasaki, R. G. Bergman, J. E. Mondloch, R. G. Finke, “Platinum Catalyzed Phenyl and Methyl Group Transfer from Tin to Iridium: Evidence for an Autocatalytic Reaction Pathway with an Unusual Preference for Methyl Transfer”, *J. Am. Chem. Soc.*, **130** (2008) 1839-1841.
  12. A. M. Morris, M. A. Watzky, J. N. Agar, R. G. Finke, “Fitting Neurological Protein Aggregation Kinetic Data via a 2-Step, Minimal / Ockham’s Razor” Model: the Finke-Watzky Mechanism of Nucleation Followed by Autocatalytic Surface Growth“, *Biochem.* **47** (2008) 2413-2427.
  13. “Fitting yeast and mammalian prion aggregation kinetic data with the Finke-Watzky 2-step model of nucleation and autocatalytic growth”, Watzky, M. A.; Morris, A. M.; Ross, E. D.; Finke, R. G. *Biochem.*, **2008**, *47*, 10790-10800.
  14. “Monitoring  $\text{Pt}(0)_n$  Nanocluster Heterogeneous Catalyst Formation on  $\text{Al}_2\text{O}_3$  and  $\text{TiO}_2$ : Product and Kinetic Evidence for a 2-Step, Nucleation and Autocatalytic Growth Mechanism”, Mondloch, J. E., Finke, R. G., *J. Am. Chem. Soc.* **2009**, accepted for publication.

# Tuesday Morning Sessions

**Olefin Metathesis Catalysts for the Synthesis of Large and Small Molecules**

Lead PI: Robert H. Grubbs  
Contact: California Institute of Technology, Div. of Chemistry and Chem. Eng.,  
Pasadena, CA 91125, [rhg@caltech.edu](mailto:rhg@caltech.edu)

Ruthenium based olefin metathesis catalysts have provided new routes to olefins that appear in a variety of structures. Their functional group tolerance and ease of use allow their application in the synthesis of multifunctional bioactive molecules. The same systems are also useful for the synthesis of an array of new materials from multifunctional polymers to supramolecular systems. Underlying these developments has been the discovery of active catalysts with controlled selectivity through the synthesis of new ligands that control the geometry of the intermediate carbene and metallacycle complexes. To increase catalyst lifetimes and efficiencies, strategies for the support of the homogeneous catalysts and catalyst reactivation are being developed.

## **Tailoring of surface chemical properties using electronic structure theory**

J. K. Nørskov

Center for Atomic-scale Materials Design

Department of Physics, Technical University of Denmark

norskov@fysik.dtu.dk

Electronic structure methods based on density functional theory have reached a level of sophistication where they can be used to describe complete catalytic reactions on transition metal surfaces. This opens the possibility that computational methods can be used to tailor surfaces with desired chemical properties. Recent progress in this direction for transition metal catalysts will be discussed. First, it will be shown that certain catalytic reactions can be described in semi-quantitative detail on the basis of calculations. The accuracy of present theoretical methods will be discussed on this basis. Next a number of developments that are necessary in order to be able to treat complex reactions on a large number of different catalysts are treated. Correlations between activation energies and reaction energies (BEP relations) and between adsorption energies of different species (scaling relations) are introduced and explained in terms of the d-band model. The d-band model is also used to explain trends in adsorption energies and activation energies for alloys. These methods allow the understanding of the trends in reactivity of complete catalytic reactions. Finally, it is shown how these concepts can be used to identify the factors determining the catalytic activity of a given transition metal surface, and how this can form the basis for screening of a large number of metals and alloys for catalytic properties.

**Metal and Metal Oxide-Supported Platinum Monolayer Electrocatalysts for Oxygen Reduction**

Additional PIs: Jia Wang, Kotaro Sasaki, Miomir Vukmirovic, Ping Liu (BNL), Jai Prakash (Illinois Institute of Technology)

Post-docs: Wei-Ping Zhou, Kuanping Gong, Yun Cai

Graduate students: Meng Li, Kurian Kuttiyiel (U. Stony Brook)

Gests (own support): Yuji Ando (Nat'l Institute Adv. Indus. Sci. and Tech., Japan), Wei-Fu Chen (National Science Council, Taiwan), Yangchuan Xing (sabbatical leave Missouri U. Sci. Tech.) Hiroko Karan (sabbatical leave, The City University NY)

Collaborators: Manos Mavrikakis (U. Wisconsin at Madison), Eli Sutter, Yimei Zhu (Center for Functional Nanomaterials, BNL), A. Kowal, Institute of Surface Chemistry and Catalysis, Krakow, Poland, Talat Rahman (Florida State U.) Bruce Koel (Lehigh U), Francis DiSalvo, Héctor Abruña (Cornell U.)

Contact: Radoslav Adzic ([adzic@bnl.gov](mailto:adzic@bnl.gov))

**Goals**

This program involves studies of platinum monolayer electrocatalysts for the O<sub>2</sub> reduction reaction aiming at producing ultimately low Pt content electrocatalysts with high activity and good stability, supported by stable, inexpensive alloy-, metal- or metal-alloy-core-shell-, oxide-, carbide- or nitride-nanoparticles. Moreover, studies using well-defined surfaces are carried out to gain understanding of the atomic-scale phenomena involved in the interactions of Pt monolayers with supporting surfaces. By kinetic modeling and theoretical calculations a deeper insight into the kinetics of the O<sub>2</sub> reduction reaction, the role of proton transfer, and the bonding of O<sub>2</sub>, O, and OH is sought. Establishing Pd as an alternative for Pt is also addressed, as well as improving the catalysts for methanol oxidation and developing new efficient catalysts for ethanol oxidation.

**DOE Interest**

Our research directly addresses the DOE program goals. The outcome from our work will provide original approaches to designing improved fuel-cell catalysts, thus increasing efficiency of chemical energy conversion in electrical energy, which are critical for practical automotive fuel cells to impact transportation energy systems. The project is focused at developing several Pt ML catalysts that are likely to have the highest Pt mass activity, and excellent potential to overcome the obstacles hindering the broad application of fuel cells. The results will enhance our understanding of the metal monolayer-support



interactions, thereby allowing us to develop a viable approach for controlling chemical reactivity in the top atomic layer for energy-conversion applications.

## Recent Progress

### *\*Pt MLs on metal and alloy single crystal extended surfaces and core-shell nanoparticle electrocatalysts:*

The studies the ORR on Pd<sub>3</sub>Fe(111) and Pt monolayer-covered Pd<sub>3</sub>Fe(111) surfaces, using combined UHV, DFT and electrochemical methods, showed a complete Pd layer to form on a Pd<sub>3</sub>Fe(111). LEIS and LEED studies show that a segregated Pd layer, having the same structure as bulk termination, is formed on the high temperature annealed Pd<sub>3</sub>Fe(111) surface. The Pd surface-segregated layer shows quite different electronic, electrochemical and electrocatalytic properties compared to a Pd(111) and the Pd open-structures. With a full Pd layer formed, the Pd<sub>3</sub>Fe(111) electrode has the ORR activity comparable to Pt(111) (Figure 1). The enhanced ORR activity of Pd segregated surface on Pd<sub>3</sub>Fe(111) appears to be due to the large down-shift of the d-band center of Pd, which decreases the BE<sub>Pd-O</sub> and facilities the O or OH hydrogenation rate in the ORR. A monolayer of Pt placed on Pd skin-like surface not only increases the surface ORR activity (by a factor more than 2 vs Pt in terms of specific surface area activity at 0.9 V) but also suppresses completely the H<sub>2</sub>O<sub>2</sub> formation.

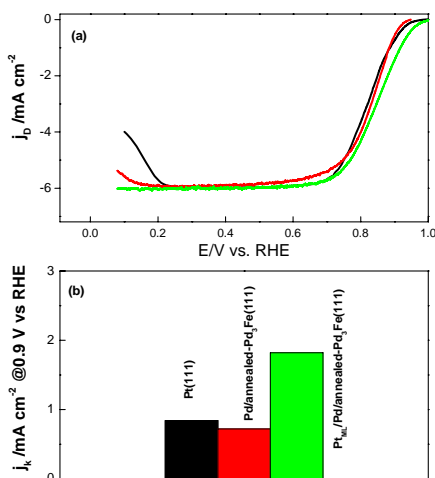


Figure 1: (a) Polarization curves for the ORR on an annealed-Pd<sub>3</sub>Fe(111) covered with (green) or without (red) Pt monolayer and a Pt(111) surfaces (black) at 1600 rpm in oxygen-saturated 0.1 M HClO<sub>4</sub> at room temperature; scan rate: 20 mV/s.

(b) The bar plot showing a comparison of the ORR specific surface activities of the corresponding three surfaces at 0.9 V<sub>RHE</sub>.

### *\*Metal interlayer concept for fine-tuning a Pt<sub>ML</sub>-core interaction*

This concept was further refined, and for several systems a considerable enhancements of the ORR rates were observed. Placing of a Pd monolayer on a number of surfaces that are not suitable as a core for Pt made them quite suitable. This approach opens up numerous possibilities for: i) Screening off the effect of cores, ii) Modifying nanoparticle structure and shape, iii) Facilitates use of various cores.

Pd interlayer was found to screen-off the adverse effect of Re and Ru on the ORR, and makes the nanoparticles as active as those of Pt. Large enhancements were obtained with PdIr alloys of different compositions. The selection of the metals constituting the shell and the core was based upon considering the segregation properties of the two metals, and their electronic—and strain-inducing effects on a Pt overlayer. The effect of thickness of Pt and Pd layers on the activity for ORR was determined. These catalysts showed higher activity for ORR than Pt.

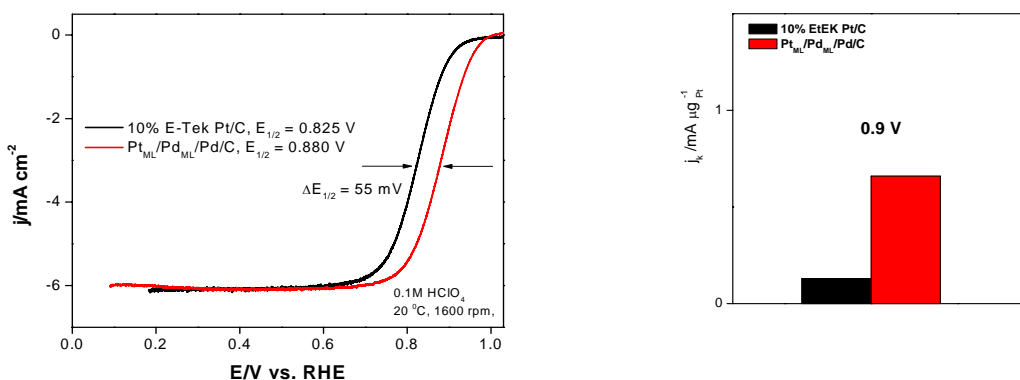


Fig. 2 Placing an interlayer of Pd on Pd/C nanoparticle causes a shift of 55 mV in  $E_{1/2}$  (left panel); Pt mass activity enhanced by 6 times in comparison with a commercial catalyst (right panel).

#### ***\*Cu-UPD-mediated Pt deposition on metal nanoparticles***

The well-defined core-shell nanoparticles were synthesized using the underpotential deposited Cu for a UPD-mediated layer-by-layer in situ “annealing” method that enhances the interlayer diffusion during kinetically controlled Pt deposition at room temperature. The thickness and uniformity of the Pt shells are unambiguously confirmed via Z-contrast scanning transmission electron microscopy coupled with element-sensitive electron energy loss spectroscopy (Figure 3). The monolayer thick Pt shell on 5-nm Pd core exhibits the Pt mass activity 3 times of the best value for Pt nanoparticles, illustrating the virtue of monolayer approach in maximizing Pt utilization. The observed structure sensitivity and experimental ability to control at atomic level led to our DFT calculations using a nanoparticle model, instead of the commonly used slab model, for the first time, to study the structural behavior of metal nanoparticles and its influence on the ORR activity. Pronounced effects of nanoparticle structures on catalytic activity were found in both DFT calculations and experiments.

#### ***\*Electrocatalysts for ethanol and methanol oxidation***

Ethanol is an ideal fuel for automotive fuel cells applications, but its slow and complex, oxidation-reaction kinetics even on the best available catalysts are a major obstacle for it. This reaction generates several reaction intermediates and, furthermore, the oxidation of

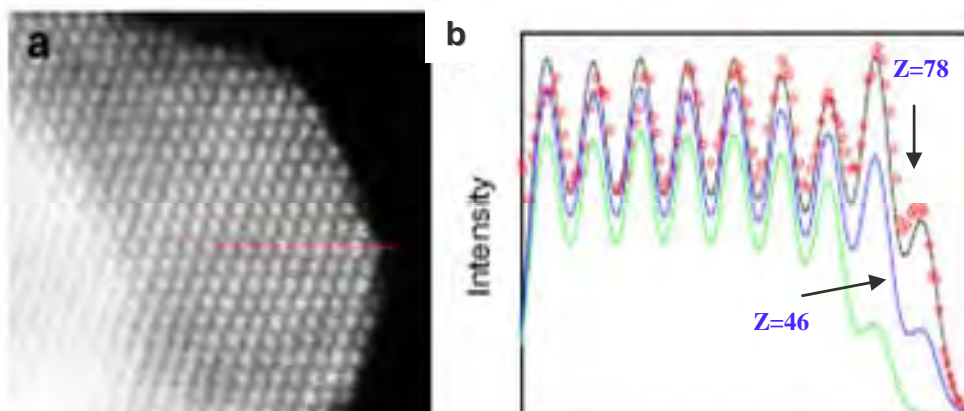


**Figure 3. Verifying a Pt ML shell on a Pd core nanoparticle structure. HAADF - STEM image with (3D) atomic structure modeling.**

(a) Intensity profiles from scans;

(b) best fits to structure models (points experiment; black with Pt ML, pink with Pd ML, green core only).

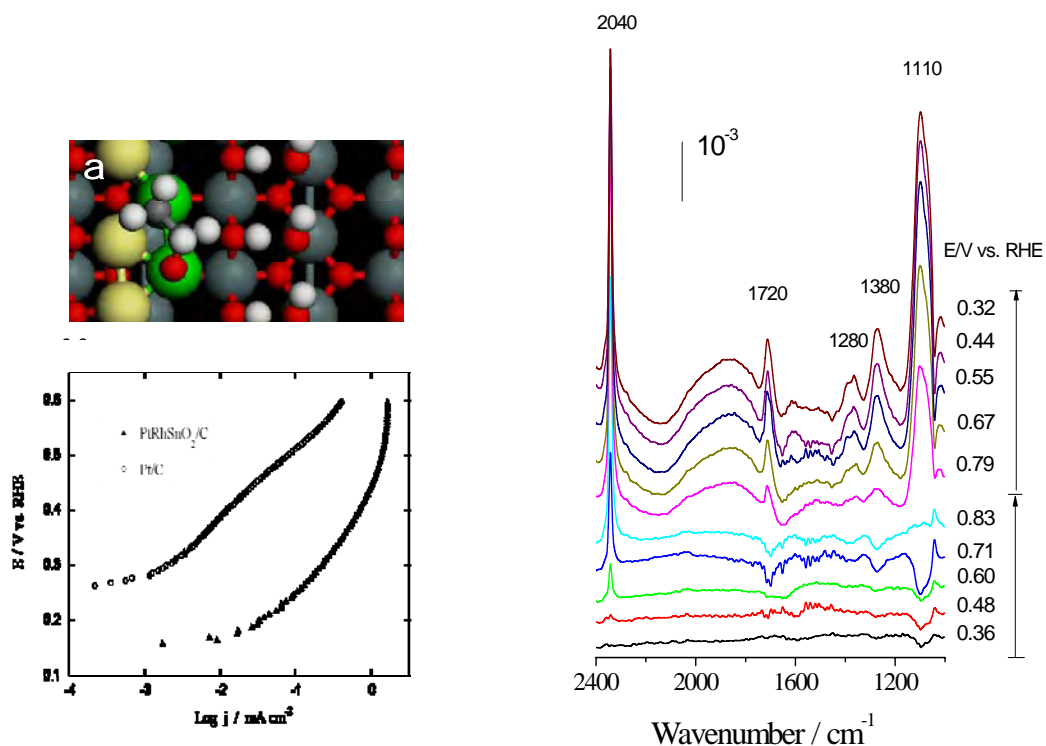


Figure 4 Optimized geometry of  $\text{CH}_2\text{CH}_2\text{O}$  adsorption on a  $\text{RhPt}/\text{SnO}_2(110)$  surface. Sn: large grey; Pt: large yellow; Rh: large green; C: small grey; O: small red; H: small white from DFT calculations. (upper left); Quasi-steady-state polarization curves for the oxidation of ethanol on  $\text{PtRhSnO}_2/\text{C}$  and  $\text{Pt}/\text{C}$  electrocatalysts containing  $\sim 30\text{nmol Pt}$ ,  $8\text{nmol Rh}$  and  $60\text{nmol SnO}_2$ , and  $25\text{nmol Pt}$ , respectively.  $0.1\text{M HClO}_4$ ;  $0.2\text{M ethanol}$  (left); *In situ* IRRAS spectra of ethanol oxidation on  $\text{PtRhSnO}_2/\text{C}$  (right).

ethanol to CO<sub>2</sub> is not fully completed, i.e., the C-C bond is not broken except at extreme positive potentials that are useless for energy conversion. Using a novel composite nanoparticle catalyst consisting of Pt, SnO<sub>2</sub> and Rh, we recently demonstrated that ethanol can be oxidized to CO<sub>2</sub> at room temperature and at low overpotentials. We verified, by *in situ* FTIR spectroscopy with SnO<sub>2</sub>/Rh/Pt(111) that catalyst splits the C-C bond only if both Pt and Rh are its components. The DFT calculations indicate that the ethanol oxidation on RhPt/SnO<sub>2</sub>(110) occurs *via* an oxametallacyclic conformation (CH<sub>2</sub>CH<sub>2</sub>O).

## Future Work

### ***\*Atomic level designing of the ORR catalysts having high-activity and stability***

We plan to explore the interaction of Pt monolayers with smooth surfaces of Pd nanorods, nanowires, and nanotubes. This will help in developing of Pt ML catalysts with predominantly high-coordination atoms deposited on smooth cores of: i) Pd or its alloy nanorods, nanowires or nanotubes cores; ii) Pd or Ir alloy nanoparticles with refractory metals that preclude core dissolution in acid environment. The concept of the metal monolayer (Pd) will be further explored with low-filled d-band metal cores. We will explore depositing uniform metal layers on carbon nanotubes and placing contiguous Pt monolayers on them.

### **\*Ethanol oxidation catalysts**

We will continue studies of the ternary catalysts for ethanol oxidation.

### ***\*Metal-metal oxide electrocatalysts***

We will study selected Magnelli phases because they are conductive and stable in acids. Our new method of depositing metal on oxide surfaces will be employed to place a metal adlayer whose role will be to prevent too strong an effect of oxide on Pt. Pt will be precisely deposited on those metal sites by the Cu displacement method.

## Publications 2006-2008

1. K. Sasaki, J. Zhang, J. Wang, F. Uribe, R. Adzic\*, Platinum submonolayer-monolayer electrocatalysts – an electrochemical and x-ray absorption spectroscopy study, *Res. Chem. Intermed.* (special issue) 32 (2006) 543-559.
2. M.H. Shao, P. Liu, R.R. Adzic\*, Superoxide is the intermediate in the oxygen reduction reaction on platinum electrode. *J. Am. Chem. Soc.* 128 (2006) 7408-7409.
3. M.H. Shao, K. Sasaki, R.R. Adzic\*, Pd-Fe nanoparticles as electrocatalysts for oxygen reduction. *J. Am. Chem. Soc.* 128 (2006) 3526-3527.
4. P. Liu\*, J. T. Muckerman, R. R. Adzic, Adsorption of Platinum on the stoichiometric RuO<sub>2</sub>(110) surface, *J. Chem. Phys.* 124 (2006) 141101.
5. J. X. Wang\*, T. E. Springer, R. R. Adzic, Dual-Pathway Kinetic Equation for the Hydrogen Oxidation Reaction on Pt Electrodes, *J. Electrochem. Soc.* 153, (2006) A1732-1740.
6. M.H. Shao, T. Huang, P. Liu, J. Zhang, K. Sasaki, V.B. Vukmirovic, R. R. Adzic\*, Palladium Monolayer- and Palladium Alloy- Electrocatalysts for Oxygen Reduction, *Langmuir* (Electrochemistry special issue) 22 (2006) 10409.
7. F.H.B. Lima, J. Zhang, M. H. Shao, K. Sasaki, M. B. Vukmirovic, E. A. Ticianelli, R. R. Adzic\*, Catalytic

- Activity - *d*-band Center Correlation for the O<sub>2</sub> Reduction Reaction on Pt in Alkaline Solutions, *J. Phys. Chem. C*, 111(2007) 404-410.
8. J. Zhang, K. Sasaki, E. Sutter, R. R. Adzic\*, Stabilization of Platinum Oxygen Reduction Electrocatalysts Using Gold Clusters, *Science*, 315 (2007) 220.
  9. M. Shao, P. Liu, J. Zhang, R. R. Adzic\*, Origin of Enhanced Activity in Palladium Alloy Electrocatalysts for Oxygen Reduction Reaction, *J. Phys. Chem., B* 2007, 111, 6772-6775.
  10. R. R. Adzic\*, J. Zhang, K. Sasaki, M. B. Vukmirovic, M. Shao, J.X. Wang, A.U. Nilekar, Mavrikakis, J. A. Valerio, F. Uribe, Platinum Monolayer Fuel Cell Electrocatalysts, *Topics in Catalysis*, 46 (2007) 249-262.
  11. A.U. Nilekar, Y. Xe, J. Zhang, M. B. Vukmirovic, K. Sasaki, R. R. Adzic, M. Mavrikakis\*, Bimetallic and Ternary Alloys for Improved Oxygen Reduction, *Topics in Catalysis*, 46 (2007) 276-284.
  12. M. Shao, K. Sasaki, N. S. Marinkovic, L. Zhang, R. R. Adzic\*, Synthesis and Characterization of Platinum Monolayer Oxygen-Reduction Electrocatalysts with Co-Pd Core-Shell Nanoparticle Supports, *Electrochem. Comm.*, 9 (2007) 2848-2853.
  13. J. X. Wang\*, J. Zhang, R. R. Adzic, Dual-Trap Kinetic Equation for the Oxygen Reduction Oxidation Reaction on Pt(111) in Acidic Media, *J. Phys. Chem. A*, 111 (2007) 12702-12710.
  14. B. Vukmirovic J. Zhang, K. Sasaki, F. Uribe, M. Mavrikakis, R. R. Adzic. Platinum Monolayer Electrocatalysts for Oxygen Reduction, *Electrochim. Acta*, 52 (2007) 2257
  15. M. H. Shao, K. Sasaki, P. Liu, R.R. Adzic, Pd<sub>3</sub>Fe and Pt Monolayer-Modified Pd<sub>3</sub>Fe Electrocatalysts for Oxygen Reduction, *Z. Phys. Chem.* 221 (2007) 1175-1190.
  16. M. B. Vukmirovic\*, P. Liu, J. T. Muckerman, and R. R. Adzic, Electrodeposition of Pt onto RuO<sub>2</sub>(110) Single-Crystal Surface, *J. Phys. Chem. C.*, 111 (2007) 15306.
  17. F. H. B. Lima, J. Zhang, M. H. Shao, K. Sasaki, M. B. Vukmirovic, E. A. Ticianelli, and R. R. Adzic, Pt monolayer electrocatalysts for O<sub>2</sub> reduction: PdCo/C substrate-induced activity in alkaline media, *J Solid State Electrochem.*, 12 (2008) 399-407.
  18. K. Sasaki, L. Zhang, R. R. Adzic, Niobium oxide-supported platinum ultra-low amount electrocatalysts for oxygen reduction, *Phys. Chem. Chem. Phys.*, 10 (2008), 159-167.
  19. K. Sasaki, R. R. Adzic, Monolayer-level Ru- and NbO<sub>2</sub>-Supported Platinum Electrocatalysts for Methanol Oxidation, *J. Electrochem. Soc.*, 155 (2008) B180- B186.
  20. J. X. Wang, F. Uribe, T. E. Springer, J. Zhang, R. R. Adzic, Intrinsic kinetic equation for oxygen reduction reaction in acidic media: The double Tafel slope and fuel cell applications”, *Faraday Discuss.* 140 347-362 (2009).
  21. Peter A. Ferrin, Shampa Kandoi, Junliang Zhang, Radoslav Adzic, Manos Mavrikakis, Molecular and Atomic Hydrogen Interactions with Au-Ir Near-Surface Alloys, *J. Phys. Chem.C* 2009,113, 1411–1417
  22. K. Sasaki, R.R. Adzic, XAS of Platinum Monolayer Fuel Cell Electrocatalysts – Unambiguous, Direct Correlation of Spectroscopy Data with Catalytic Properties, *Synchrotron Radiation News*, 22(1) (2009) 17-21.
  23. A. Kowal, M. Li, M. Shao, K. Sasaki, M.B. Vukmirovic, J. Zhang, N. S. Marinkovic, P. Liu, A.I. Frenkel, R. R. Adzic, Ternary Pt/Rh/SnO<sub>2</sub> Electrocatalysts for Oxidizing Ethanol to CO<sub>2</sub>, *Nature Materials*, 8 (2009) 325.

#### Book Chapters

24. N.S. Marinkovic, M.B. Vukmirovic and R.R. Adzic\*, Some Recent Studies in Ruthenium Electrochemistry and Electrocatalysis, *Modern Aspects of Electrochemistry*, C. Vayenas, R. White, M. Gamboa-Adelco, Editors, Vol. 42, Springer 2007 (New York)
25. F. Lima, R. R. Adzic: Platinum Monolayer Electrocatalysts for Fuel Cells, in *Handbook of Fuel Cells–Advances in Electrocatalysis, Materials, Diagnostics and Durability*, Eds. W. Vielstich, H. A. Gasteiger, H. Yokokawa Volume5: J. Wiley&Sons, in press.
26. Ye Xu, Minhua Shao, Manos Mavrikakis, Radoslav R. Adzic: Recent Developments in the Electrocatalysis of the O<sub>2</sub> Reduction Reaction, in *Fuel Cell Catalysis: a Surface Science Approach*, Ed. M. Kopper, J. Wiley and Sons, in press.
27. K. Sasaki, M. Shao, R.R. Adzic, Dissolution and Stability of Platinum in Oxygen Cathodes, *Polymer Electrolyte Fuel Cell Durability*, T.J. Schmidt et al (Eds), Springer Science, in press.

## Selective Bond Breaking and Making on Size-Selected Catalysts: The Role of Size, Composition and Support

\*S. Vajda<sup>a,b</sup>, L. Curtiss<sup>a</sup>, J. Elam<sup>a</sup>, J. Greeley<sup>a</sup>, B. Lee<sup>a</sup>, S. Lee<sup>a</sup>, C. Marshall<sup>a</sup>, F. Mehmood<sup>a</sup>, S. Mucherie<sup>a</sup>, M. Pellin<sup>a</sup>, P. Redfern<sup>a</sup>, S. Seifert<sup>a</sup>, R. Winans<sup>a</sup>, P. Zapol<sup>a</sup>, I. Barke<sup>c</sup>, K.-H. Meiwes-Broer<sup>c</sup>, A. Kleibert<sup>c,d</sup>, K. Sell<sup>c</sup>, V. von Oeynhausen<sup>c</sup>, A. Fraile-Rodríguez<sup>d</sup>, Y. Lei<sup>e</sup>, R. Meyer<sup>e</sup>, J. Alonso<sup>f</sup>, M. López<sup>f</sup>, L. Molina<sup>f</sup>, B. Hammer<sup>g</sup>, <sup>h</sup>D. Teschner, <sup>h</sup>R. Schlögl  
<sup>a</sup>Argonne National Laboratory, USA, <sup>b</sup>Yale University, USA, <sup>c</sup>Universität Rostock, Germany, <sup>d</sup>Paul-Scherrer Institut, Switzerland, <sup>e</sup>University of Illinois at Chicago, USA, <sup>f</sup>Universidad Valladolid, Spain, <sup>g</sup>Aarhus Universitet, Denmark, <sup>h</sup>Fritz-Haber-Institut, Germany  
e-mail: [vajda@anl.gov](mailto:vajda@anl.gov)

The elucidation of the size/composition/shape/structure and function correlation, the effect of support along with the determination of the nature of the nanocatalyst under reaction conditions are instrumental for addressing fundamental aspects of catalysis which may lead to the development of new classes of catalysts. Uniform particles on technologically relevant supports are prerequisites for such studies<sup>1</sup>, making size-selected clusters of few atoms to several nm in size as ideal model systems. The experimental studies are based on 1) chemically uniform support fabrication, 2) size-selected cluster deposition, 3) electron microscopy of nanoclusters, 4) synchrotron X-ray characterization of clusters under working conditions, combined with mass spectroscopy analysis of reaction products. Density functional theory calculations are used to understand the activity of clusters and the underlying reaction mechanisms.

This contribution focuses on the following reactions:

1) Selective activation of the C=C bond in propene to form propylene oxide on alumina supported Ag nanoparticles<sup>2</sup> and clusters<sup>3</sup>. Scanning electron microscopy is used to image the nanoparticles before and after the catalytic reaction. Grazing incidence X-ray scattering reveals a change in the shape of the catalysts upon the inlet of the reactants at room temperature and a further evolution with temperature.<sup>2</sup> The size-dependent activity and selectivity of Ag nanocatalysts (between 9 and 25 nm in diameter) will be discussed and compared with the performance of Ag<sub>3</sub> clusters and stabilized Au<sub>6-10</sub> clusters. The gold catalyst works without the commonly used TiO<sub>2</sub> support and with water vapour replacing hydrogen.<sup>4</sup>

2) Selective dehydrogenation of propane on Pt<sub>8-10</sub> clusters. Pt clusters on mesoporous membranes identify the first viable Pt-based catalyst composition which, while the most selective under oxidative conditions, outperforms by a factor of 40 to 100 the activity of the best reported Pt-based and VOx-based catalysts, respectively.<sup>5</sup>

3) Methanation & Fischer-Tropsch on nickel and cobalt clusters. It is chosen to illustrate the recent addition of X-ray absorption to the temperature-programmed reaction / X-ray scattering capabilities. The first reactivity studies show size/composition and support effects in catalytic performance; X-ray absorption data allow for simultaneous monitoring of the oxidation state of the particles as a function of temperature and support.<sup>6</sup>

1. A.T. Bell, *Science* **299**, 1688 (2003)

2. S. Vajda, S. Lee, K. Sell, I. Barke, A. Kleibert, V. von Oeynhausen, K.-H. Meiwes-Broer, A. Fraile-Rodríguez, J. W. Elam, M. J. Pellin, B. Lee, S. Seifert, R. E. Winans, *J. Chem. Phys.*, *submitted*

3. Y. Lei, S. Lee, R. J. Meyer, B. Lee, S. Seifert, R. E. Winans, J. W. Elam, M. J. Pellin, D. Teschner, R. Schlögl, J. P. Greeley, P. C. Redfern, L. C. Curtiss, and S. Vajda, *to be submitted*

4. S. Lee, L. M. Molina, M. L. María J. López, J. A. Alonso, B. Hammer, B. Lee, S. Seifert, R. E. Winans, J. W. Elam, M. J. Pellin, and S. Vajda, *Angew. Chemie. Int. Ed.* **48**, 1467 (2009)

5. S. Vajda, M. Pellin, J. Greeley, C. Marshall, L. Curtiss, G. Ballentine, J. Elam, S. Catillon-Mucherie, P. Redfern, F. Mehmood, and P. Zapol, *Nat. Mater.* **8**, 213 (2009)

6. in progress

# Tuesday Afternoon Sessions

## Developments in Density Functional Theory and ab initio QM/MM Methods for Catalysis

Weitao Yang

Department of Chemistry, Duke University

Email: weitao.yang@duke.edu

Combined QM/MM methods provide an accurate and efficient energetic description of complex chemical and biological systems, leading to significant advances in the understanding of chemical reactions in solution and in enzymes. Ab initio QM/MM methods capitalize on the accuracy and reliability of the associated quantum mechanical approaches, however at a much higher computational cost compared with semiempirical quantum mechanical approaches. Thus reaction path and activation free energy calculations encounter unique challenges in simulation timescales and phase space sampling. Recent developments of the QM/MM minimum free energy path method overcome these challenges and enable accurate free energy determination for reaction processes in solution and enzymes. Applications to several solution and enzyme reactions, including the OMP decarboxylation in orotidine 5'-monophosphate decarboxylase, will be featured.

Central to catalysis modeling is density functional theory (DFT) of electronic structure, which is widely and successfully applied in simulations throughout engineering and sciences. However, there are spectacular failures for many predicted properties, which can be traced to the delocalization error and static correlation error of commonly used approximations. These errors include significant underestimation of the barriers of chemical reactions, the band gaps of materials, the energies of dissociating molecular ions and charge transfer excitation energies. Typical DFT calculations also fail to describe degenerate or near degenerate systems, as arise in the breaking of chemical bonds, and strongly correlated materials. These can all be characterized and understood through the perspective of fractional charges and fractional spins introduced recently. The failure to describe the bandgaps in Mott insulators can also be traced to the violation of the combined condition for fractional charges and fractional spins. Understanding the errors of functionals in the simplest way possible --- as violations of exact conditions for fractional charges and fractional spins -- opens the path forward for reduction of the errors and for applications of density functional theory in new frontiers.

### References

H. Hu and W. T. Yang, "Free energies of chemical reactions in solution and in enzymes with ab initio QM/MM methods," *Ann Rev of Phys Chem*, 59:573, 2008.

H. Hu, Z. Y. Lu, J. M. Parks, S. K. Burger, and W. T. Yang, "Quantum mechanics/molecular mechanics minimum free-energy path for accurate reaction energetics in solution and enzymes: Sequential sampling and optimization on the potential of mean force surface", *J. Chem. Phys.*, 128:034105, 2008.



H. Hu, A. Boone, and W. T. Yang, "Mechanism of OMP decarboxylation in orotidine 5'-monophosphate decarboxylase", *J. Am. Chem. Soc.*, 130:14493, 2008

P. Mori-Sanchez, A. J. Cohen, and W. T. Yang, "Self-interaction-free exchange -correlation functional for thermochemistry and kinetics," *J. Chem. Phys.* 124:91102, 2006.

A. J. Cohen, P. Mori-Sanchez, and W. T. Yang, "Insights into current limitations of density functional theory," *Science*, vol. 321, pp. 792–794, Aug 2008.

P. Mori-Sanchez, A. J. Cohen, and W. T. Yang, "Localization and delocalization errors in density functional theory and implications for band-gap prediction," *Phys. Rev. Lett.* 100:146401, 2008.

P. Mori-Sanchez, A. J. Cohen, and W. T. Yang, "Discontinuous nature of the exchange-correlation functional in strongly correlated systems," *Phys. Rev. Lett.* 102:066403, 2009.

**Near-surface alloys for improved heterogeneous catalysis**

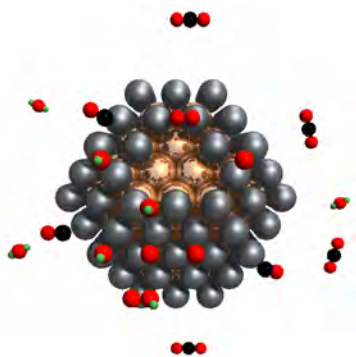
Lead PI's: M. Mavrikakis, M. Barteau, R. Crooks

Co-PI's: J. A. Dumesic; D. Buttrey, J. Chen, R. Lobo, J. Lauterbach, D. Vlachos

Collaborators: R. Adzic, B. Eichhorn

Students: A. Nilekar, P. Ferrin, R. West, J. Herron (Wisconsin); D. Hansgen, W. Huang, J. Dellamorte, W. Pyrz (Delaware); M. Weir, E. Carino (Texas)

Contact: Department of Chemical & Biological Engineering, University of Wisconsin-Madison, Madison, WI 53706; [manos@engr.wisc.edu](mailto:manos@engr.wisc.edu)



Most of the world's hydrogen supply is currently obtained by reforming hydrocarbons. 'Reformate' hydrogen contains significant quantities of CO that poison current hydrogen fuel-cell devices. Catalysts are needed to remove CO from hydrogen through selective oxidation. Here, we report a first-principles-based screening, identification, and synthesis of a nanoparticle catalyst comprising a Ru core covered with an approximately 1–2-monolayer-thick shell of Pt atoms.

The distinct catalytic properties of these well-characterized core–shell nanoparticles were demonstrated for preferential CO oxidation in hydrogen feeds and subsequent hydrogen light-off. For H<sub>2</sub> streams containing 1,000 p.p.m. CO, H<sub>2</sub> light-off is complete by 30 °C, which is significantly better than for traditional PtRu nano-alloys (85 °C), monometallic mixtures of nanoparticles (93 °C) and pure Pt particles (170 °C). Density functional theory studies suggest that the enhanced catalytic activity for the core–shell nanoparticle originates from a combination of an increased availability of CO-free Pt surface sites on the Ru@Pt nanoparticles and a hydrogen-mediated low-temperature CO oxidation process that is clearly distinct from the traditional bifunctional CO oxidation mechanism<sup>1</sup>.

**References:**

1. S. Alayoglu, A. U. Nilekar, M. Mavrikakis, B. Eichhorn, "Ru@Pt Core-Shell Nanocatalysts For Enhanced CO-Tolerant Catalytic Hydrogen Activation", *Nature Mater.* **2008**, 7, 333.

**Using Ferroelectric Oxides to Control Surface Chemistry**

Lead PI: Andrew M. Rappe  
Contact: University of Pennsylvania, Dept. of Chemistry and  
Dept. of Materials Science and Engineering  
231 S. 34<sup>th</sup> St, Philadelphia, PA 19104,  
Email: [rappe@sas.upenn.edu](mailto:rappe@sas.upenn.edu)

In this talk, I will explain how the polar dipole of a ferroelectric oxide can provide great surface chemical flexibility, opening up new opportunities for tunable catalysis. I will describe how the substrate material can be selected and then patterned to affect the surface properties. The influence of the polar dipole and annealing conditions on surface stoichiometry will also be illustrated, leading to a wide variety of surfaces that can be controllably obtained from a single material. I will then report results on how poled ferroelectric surfaces can influence molecular events and surfaces, and conversely how chemical atmospheres can dramatically affect ferroelectric surfaces. In all cases, contributions to computational methodology that underpin the surface chemical research will be discussed, as will collaborations with experimental researchers.

## First Principles Dynamics Over Long Time Scales

Graeme Henkelman

University of Texas at Austin, Department of Chemistry & Biochemistry

1 University Station A5300 Austin, TX 78712-0165

email: henkelman@mail.utexas.edu

A computational method for simulating the dynamics of atomic systems on time scales much longer than can be accessed with classical dynamics will be presented. Possible reaction mechanisms available to the system are found by exploring the potential energy surface from minima to find nearby saddle points. Reaction rates are then calculated using harmonic transition state theory, and the system is propagated in time according to the kinetic Monte Carlo algorithm. Our algorithm is efficient enough to model the evolution of systems with ab-initio forces. A few examples will be shown, including metal cluster formation on oxides and catalytic reactions on metal surfaces.

### Selected Recent Publications

W. Tang, E. Sanville, and G. Henkelman, A grid-based Bader analysis algorithm without lattice bias, *J. Phys.: Condens. Matter* **21**, 084204 (2009).

L. Xu and G. Henkelman, Adaptive kinetic Monte Carlo for first-principles accelerated dynamics, *J. Chem. Phys.* **129**, 114104 (2008).

R. A. Ojifinni, J. Gong, N. S. Froemming, D. W. Flaherty, M. Pan, G. Henkelman, and C. B. Mullins, Carbonate formation and decomposition on atomic oxygen pre-covered Au(111), *J. Am. Chem. Soc.* **130**, 11250-11251 (2008).

D. Mei, L. Xu, and G. Henkelman, Dimer saddle point searches to determine the reactivity of formate on Cu(111), *J. Catal.* **258**, 44-51 (2008).

S.-C. Li, Z. Zhang, D. Sheppard, B. D. Kay, J. M. White, Y. Du, I. Lyubinetsky, G. Henkelman, and Z. Dohnalek, Intrinsic diffusion of hydrogen on rutile TiO<sub>2</sub>(110), *J. Am. Chem. Soc.* **130**, 9080-9888 (2008).

R. A. Ojifinni, N. S. Froemming, J. Gong, M. Pan, T. Kim, J. M. White, G. Henkelman, and C. B. Mullins, Water enhanced low temperature CO oxidation and isotope effects on atomic oxygen covered Au(111), *J. Am. Chem. Soc.* **130**, 6801-6812 (2008).

D. Sheppard, R. Terrell, and G. Henkelman, Optimization methods for finding minimum energy paths, *J. Chem. Phys.* **128**, 134106 (2008).

E. Sanville, S. D. Kenny, R. Smith, and G. Henkelman, Improved grid-based algorithm for Bader charge allocation, *J. Comp. Chem.* **28**, 899-908 (2007).

## **Experimental and Theoretical Studies of Adsorbate/adsorbate/substrate Interactions: Towards Predictive catalysis**

PI: Suljo Linic

Students: Hongliang Xin, Phillip Christopher

Contacts: University of Michigan, 2300 Hayward Street, Ann Arbor, MI 48109,  
[linic@umich.edu](mailto:linic@umich.edu)

### **Goal and Background**

The central objective of our research effort is to employ combined experimental/theoretical approaches to develop predictive theories of heterogeneous catalysis and to apply these theories to formulate energy-efficient, selective, and stable catalysts. We are motivated by a realization that recent scientific advancements, mainly in the area of molecular science, have potential to bring a revolutionary transformation to the field of discovery in heterogeneous catalysis. The landscape-changing advances driving the transformation are:

1. **Development of powerful spectroscopy and microscopy techniques** which allow us to study underlying chemical transformations that govern the performance of catalysts, including reaction mechanisms and the evolution of catalyst structure, with high spatial and temporal resolutions and at relevant conditions.
2. **Development of quantum computational methodologies** (for example, Density Functional Theory (DFT)), which can be utilized to study chemical transformations at the elementary step level with reasonable accuracy and efficiency. These tools are allowing us to make reasonable quantitative predictions about the outcome of a chemical process.
3. **Development of novel synthetic chemistry approaches** designed to synthesize targeted nano-structured materials with almost atomic precision and with a high degree of uniformity. These well-defined and uniform nano-structured materials are not only attractive heterogeneous catalysts, but they also represent an ideal platform to study heterogeneous catalysis on molecular scale.

### **DOE Interest**

Development of energy efficient, selective and stable heterogeneous catalysts is predicated on our ability to: (i) relate the electronic and geometric structure of materials to their catalytic performance, (ii) develop reliable predictive models which would guide the process of discovery, and (iii) establish mechanisms to control the synthesis of the desired materials. This project aims to advance the field of catalysis by formulating reliable structure/performance relationships and utilizing these relationships to identify novel catalytic materials.

### **Recent Progress**

#### ***DFT and Ab initio Thermodynamic Studies of Critical Parameters Affecting Adsorbate/Adsorbate/Substrate Interactions***

DFT calculations showed that interactions between adsorbates and metal substrate can only be perturbed by changing the one-electron spectra of the adsorbate/substrate system or affecting the electro-static interactions between adsorbates on the metal surface. These conclusions were validated in two case studies; one focusing on the adsorption of various adsorbates on different metal alloys and the other addressing the interactions between alkali promoters and the adsorbates on metal surfaces. The studies showed that adsorption on metals is affected by alloying since the one-electron energy of the metal changes in response to alloying. On the other hand, adsorption on metal surfaces is affected by alkali promoters due to long-range electrostatic interactions between the alkali promoter and the adsorbate.

#### ***Experimental Development of Relationships Between Geometric Structure of Alloy Catalysts, their Electronic Features, and their Performance.***

Various experimental studies showed that there exists a universal relationship between the electronic structure of alloy materials, their chemical activity (defined in terms of the adsorption energy of organic molecules, CO, oxygen, sulfur compounds, etc.) and catalytic performance. In these studies we employed electron energy loss near edge spectroscopy (ELNES), x-ray absorption near edge spectroscopy (XANES), and Auger electron spectroscopy (AES) to measure the electronic fingerprint (in the vicinity of the Fermi level) of multiple Ni and Pt alloys. Our analysis showed that the measured electronic structure of alloys can be conclusively related to their catalytic performance. These studies validated a simple and physically transparent model, which allows us to a priori predict the general effect of alloying on the electronic structure of a material and therefore on its chemical performance.

### ***Targeted Metallic Nano-structures as Highly Selective Partial Oxidation Catalysts***

We have also been exploring potential utilization of highly uniform, targeted nano-structured materials as selective heterogeneous catalysts. The advantage of these materials compared to conventional catalytic materials is that their structure can be controlled with almost atomic precision, and that it is possible to synthesize highly homogeneous structures. We demonstrated some of these advantages recently when we showed that well-defined, tailored Ag nano-structures are much more selective in heterogeneous epoxidation of ethylene to form ethylene oxide (EO) ( $\text{ethylene} + \frac{1}{2} \text{O}_2 \rightarrow \text{EO}$ ) than conventional industrial catalysts.

We showed using quantum chemical Density Functional Theory (DFT) calculations, where we studied critical elementary chemical steps that govern the selectivity to EO in the process, that the Ag(100) surface should be inherently more selective than the Ag(111) surface. We note that catalytic particles, synthesized using conventional synthesis procedure and currently used in commercial ethylene epoxidation process, are dominated by the (111) surface. To synthesize Ag nano-structures which are dominated with the Ag(100) faces, we employed a synthesis procedure which uses organic stabilizer molecules to direct the growth of the nano-structure in a particular direction and to control the surface facets that terminate the nano-structure. This synthetic strategy allowed us to synthesize well-defined and highly uniform Ag nano-wires and nano-cubes which are dominated by the (100) facet, see Figure 1.

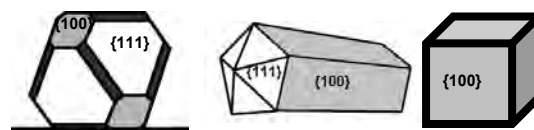


**Figure 1** Surface termination of different nanostructures

Subsequent experiments showed that Ag nano-wires and nano-cube catalysts can achieve selectivity to EO greater than 80 %. Figure 2 shows the measured selectivity to EO on conventional (spherical), nano-wires, and nano-cube catalysts. Figure 2 illustrates that the well-defined nano-structured materials, dominated by the (100) facet, are inherently more selective than conventional catalysts.

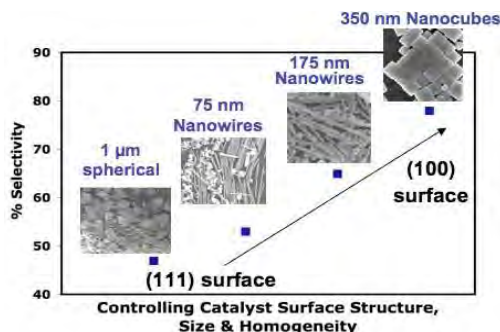


**Figure 2:** Selectivity to EO measured for different shape of nanostructured particles at identical conditions.

### ***Well-defined Nano-structures as Excellent Platform for Chemical Characterization***

We have also recently started exploring these metallic nano-structures as possible platforms for chemical characterization. The features of these nano-structures that are particularly appealing are: (i) the nanostructures are well defined on atomic level, and their surface to volume ratio is fairly high, which makes these structures inherently better suited for the studies of surface

chemical processes compared to traditional single crystal model systems, which are while very well defined, characterized by low surface to volume ratio. (ii) we can synthesize these nanostructures with high degree of uniformity in size and shape, which rules out possible effects due to diversity in size and shape, i.e. these, (iii) the nanostructures are effective scatterers of electromagnetic radiation which make them suitable as platforms for a number of chemical characterization techniques including surface enhanced Raman (SERS) or IR spectroscopies.

To illustrate the potential utility of these nanostructures as an effective platform for chemical characterization, we have performed in-situ SERS measurements during catalytic ethylene epoxidation on Ag nano-wires. These studies allowed us for the first time to spectroscopically identify in-situ the critical surface intermediate that governs the selectivity in the process. The Raman vibrational fingerprint of the critical intermediate is shown in Figure 3. Based on comparing this vibrational fingerprint to calculated normal modes, we have identified this intermediate to be surface oxametallacycle, with the molecular structure shown in Figure 3.

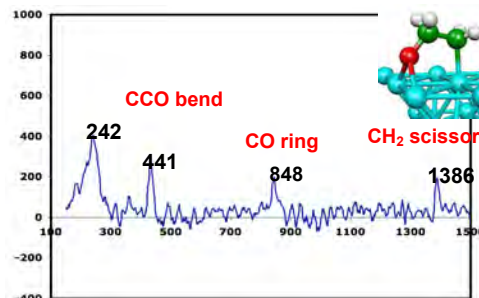


**Figure 3.** Vibrational fingerprint of the critical surface intermediate measured in-situ using SERS.

#### Peer-reviewed publications:

1. Laursen S, Linic S, “Strong chemical interactions between Au and off-stoichiometric defects on oxides as a possible source of chemical activity of nano-sized Au adsorbed on the oxide”, **Journal of Physical Chemistry C, in press DOI: 10.1021/jp810603u**
2. Eranda Nikolla, Johannes Schwank and Suljo Linic, Measuring and Relating the Electronic Structures of Nonmodel Supported Catalytic Materials to Their Performance, **J. Am. Chem. Soc., 2009, 131 (7)**, pp 2747–2754
3. Eranda Nikolla, Johannes W. Schwank, and Suljo Linic, “Comparative study of the kinetics of methane steam reforming on supported Ni and Sn/Ni alloy catalysts: the impact of the formation of Ni alloy on chemistry”, **Journal of Catalysis(in press)** doi:10.1016/j.jcat.2009.02.006
4. Phillip Christopher and Suljo Linic, “Engineering Selectivity in Heterogeneous Catalysis: Ag Nanowires as Selective Ethylene Epoxidation Catalysts”, **Journal of the American Chemical Society, 2008, 130, 34, 11264**
5. Eranda Nikolla, Johannes W. Schwank, and Suljo Linic, “Hydrocarbon steam reforming on Ni alloys at solid oxide fuel cell operating conditions”, **Catalysis Today 136(3-4): 243-248, 2008**
6. E.Nikolla, J. Schwank, S. Linic, Promotion of the long-term stability of reforming Ni catalysts by surface alloying, **Journal of Catalysis, 250(1), 85-93, 2007**
7. J. Mukherjee, S. Linic, “First principles investigations of electrochemical oxidation of hydrogen at solid oxide fuel cell operating conditions”, **Journal of the Electrochemical Society, 154(9), B919-B924, 2007**
8. E.Nikolla, A. Holewinski, J. Schwank, S. Linic; “Controlling Carbon Surface Chemistry by Alloying: Carbon Tolerant Reforming Catalyst”, **Journal of the American Chemical Society, 2006; 128(35); 11354-11355.**
9. Laursen S, Linic S, “Oxidation catalysis by oxide-supported Au nanostructures: The role of supports and the effect of external conditions” **Physical Review Letters, 2006, 97 (2), 026101**

# Wednesday Morning Sessions



## In-situ Study of Nanoparticle Shape Changes under Reaction Conditions

Andreas Stierle,\*

Max-Planck-Institut für Metallforschung, D-70569 Stuttgart, Germany

e-mail: [stierle@mf.mpg.de](mailto:stierle@mf.mpg.de)

Substantial effort has been made within the past few decades to understand the fundamentals of catalytic reactions using pioneering-type experiments under highly idealized conditions, such as very low oxygen pressures ( $10^{-6}$  mbar), and very idealized model systems (single crystal surfaces). However, understanding chemical reactions on single crystal surfaces in vacuum very often does not allow prediction of the performance of devices composed of nanoparticles operating at ambient gas pressure, such as catalysts or gas sensors. In my talk I will highlight the size dependent oxidation mechanism of Pd nanoparticles on MgO, which was unraveled using high energy x-ray diffraction together with a combinatorial sample preparation approach [1]. Further on, I will discuss Rh nanoparticle shape changes under oxygen and CO exposure, based on a quantitative analysis of x-ray reciprocal space maps [2]. In the last part of my presentation I will address carbon incorporation taking place during CO oxidation over a Pd/MgO(100) model catalyst at near atmospheric pressures [3].

### References:

1. P. Nolte, A. Stierle, N. Kasper, N. Y. Jin-Phillipp, H. Reichert, A. Rühm, J. Okasinski, H. Dosch, S. Schöder, *Phys. Rev. B* **77**, 115444 (2008).
2. P. Nolte, A. Stierle, N. Y. Jin-Phillip, N. Kasper, T. U. Schulli, H. Dosch, *Science* **321**, 1654 (2008).
3. P. Nolte, A. Stierle, O. Balmes, V. Srot, P. A. van Aken, L. P. H. Jeurgens, H. Dosch, *Catalysis Today* (2009), in press. DOI:10.1016/j.cattod.2008.12.002

**Influence of the oxidation state of supported size-selected Pt nanoparticles on catalytic decomposition and oxidation of high-order alcohols: activity, selectivity and lifetime**

Students: Jason R. Croy, Simon Mostafa, Farzad Behafarid

Contacts: University of Central Florida, Department of Physics, 4000 Central Florida Blvd., MAP310, Orlando, FL 32816-2385; [roldan@physics.ucf.edu](mailto:roldan@physics.ucf.edu)

### Goal

Obtain a qualitative and quantitative understanding of the effect of two factors on nanocatalyst reactivity: i) oxidation state of the nanocatalysts (that might be tuned by changing the nanoparticle size, composition, and oxide support), ii) nature of the oxide support and its interface with the nanoparticles.

### DOE Interest

Chemical reactions of significant interest in the field of energy generation (fuel cells) are being targeted, namely, the oxidation and decomposition of high-order alcohols such as 2-propanol and 2-butanol. Some byproducts from the latter reactions such as acetone and butanone are also valuable to the chemical synthesis industry. Catalytic reforming of gasoline additives, e.g. methanol, ethanol, and potentially butanol, may serve as an on-board source of hydrogen. Additionally, efficient catalysts for the dehydrogenation of higher order alcohols may also contribute to improvements in chemical heat pumps, such as those based on the 2-propanol/acetone/hydrogen cycle.

### Recent Progress

The next generation of nanocatalysts requires detailed knowledge of the correlation between their structure, chemical composition, and reactivity. To study these effects, large quantities of homogeneous, size-selected nanoparticles are needed. We have synthesized size- and shape-selected Pt and Pt-M (M = Au, Fe, Ru and Pd) nanoparticles with well defined interparticle distances by means of diblock copolymer encapsulation. The enhanced thermal stability (up to 1060°C) against coarsening and/or desorption of our self-assembled Pt nanoparticles deposited on TiO<sub>2</sub>(110) was demonstrated [1]. Furthermore, following our synthesis approach, TiO<sub>2</sub> nanostripes with tunable width, orientation, and uniform arrangement over large surface areas, were produced, Fig. 1. Our study revealed the existence of strong nanoparticle/support interactions in novel micellar nanoparticle systems that can be utilized to pattern catalytic oxide surfaces at the nanoscale.

The influence of the oxidation state of noble metal nanocatalysts on their chemical reactivity is currently a subject of debate. We have investigated how the particle size, oxide support (nanocrystalline SiO<sub>2</sub>, Al<sub>2</sub>O<sub>3</sub>, TiO<sub>2</sub>, CeO<sub>2</sub> and ZrO<sub>2</sub> powders), and cluster composition (Pt-Metal nanoalloys) affected the stability of Pt oxide species in size-selected clusters. In all of these systems, PtO was found to be the most stable Pt oxide

species, and reducible oxide supports ( $\text{TiO}_2$ ) were found to facilitate the thermal decomposition of Pt oxides, possibly by oxygen spill-over to vacancies in the support.

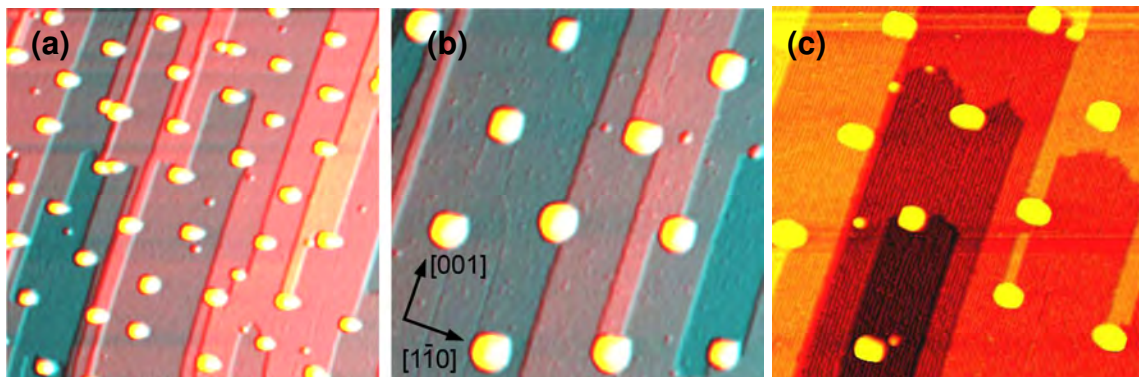


Fig. 1: STM images (200 x 200 nm) (a) and (100 x 100 nm) (b),(c) of Pt nanoparticles synthesized by micelle encapsulation and deposited on  $\text{TiO}_2(110)$ . The images were acquired after annealing in UHV at 1040°C for 10 min (a, b) and at 1060°C for 10 min (c). [1]

Our synthesis method led to morphologically stable nanoparticles, preserving their initial size and substrate dispersion after prolonged annealing pre-treatments in oxygen (up to 8 hours at 500°C). However, the presence of  $\text{O}_2$  during these thermal pre-treatments was found to strongly influence the surface segregation of metal M in our bimetallic Pt-M particles [2] as well as the degree of oxidation of the Pt component, Fig. 2. This directly affected the nanoparticle's catalytic activity for methanol decomposition by way of metal M's occupation of surface sites available for reaction with methanol.

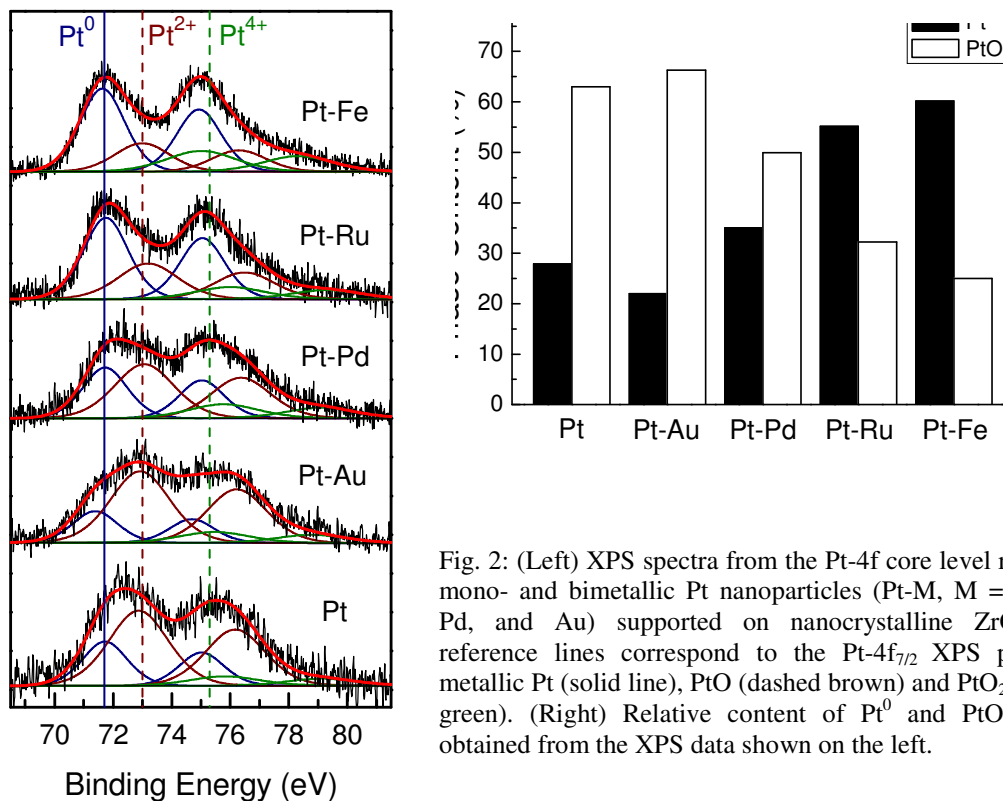


Fig. 2: (Left) XPS spectra from the Pt-4f core level region of mono- and bimetallic Pt nanoparticles (Pt-M, M = Fe, Ru, Pd, and Au) supported on nanocrystalline  $\text{ZrO}_2$ . The reference lines correspond to the Pt-4f<sub>7/2</sub> XPS peaks of metallic Pt (solid line), PtO (dashed brown) and PtO<sub>2</sub> (dashed green). (Right) Relative content of Pt<sup>0</sup> and PtO species obtained from the XPS data shown on the left.

The activity and selectivity of micellar Pt nanoparticles supported on ZrO<sub>2</sub> for ethanol, 2-propanol and 2-butanol decomposition and oxidation is being studied, with emphasis on the role played by surface Pt oxides in their reactivity. Attention is being paid to changes in the oxidation state of nanosized catalysts during the above chemical reactions.

### **Future Plans**

Improve the stability and selectivity of fuel-cell nanocatalysts through: (i) the optimization of the nanocatalyst size and oxide supports, and (ii) the addition of secondary metals (Ru, Ir, Pd, Rh, Sn, Au) to Pt nanoparticles to take advantage of bi-functional synergistic effects. Since all of these aspects influence the oxidation state of the nanoparticle catalysts, the proposed investigations will continue to shed light into the relationship between catalytic performance and oxidation state of the active metal species. Future work will also include Pd catalysts.

### **Publications (2008-2009)**

1. A. Naitabdi, F. Behafarid, B. Roldan Cuenya, "Enhanced Thermal Stability and Nanoparticle-mediated Surface Patterning: Pt/TiO<sub>2</sub>(110)", *Appl. Phys. Lett.* **94** (2009) 083102.
2. J.R. Croy, S. Mostafa, L. Hickman, H. Heinrich, B. Roldan Cuenya, Bimetallic Pt/Metal catalysts for the decomposition of methanol: Effect of secondary metal on the oxidation state, activity, and selectivity of Pt, *Appl. Catal. A* **350** (2008) 207-216.

## Investigation of the Oxygen Reduction Reaction Activity of Heteroatom-containing Carbon Nano-structures

Postdoc: Xiaoguang Bao  
 Students: Elizabeth J. Biddinger, Dieter von Deak, Douglas S. Knapke, Katie Luthman  
 Collaborators: Christopher Hadad (Ohio State University, Dept. of Chemistry)  
 Contacts: The Ohio State University, 333A Koffolt Lab, 140 W 19th Avenue  
 Columbus, Ohio 43210; [ozkan.1@osu.edu](mailto:ozkan.1@osu.edu)

### Goal

To enhance the fundamental understanding of the electrocatalyzed oxygen reduction reaction over heteroatom-doped graphitic nanostructured carbon materials that would help in the development of precious-metal free ORR catalysts for PEM and DMFC fuel cells.

### DOE Interest

A fundamental understanding of the oxygen reduction reaction over heteroatom-containing nanostructured carbon catalysts is important for the development of precious-metal-free electrocatalysts for PEM and Direct Methanol Fuel Cells. Through an understanding of the nature of active sites and the ORR mechanism on these nano-structured materials, carbon-based catalysts can be modified for enhanced ORR activity. Additionally, any insight to be gained into the role of hetero-atoms in graphitic carbon and the techniques to be developed for synthesis, characterization and electrochemical testing of these materials can be extended to tailor unique nanoscale catalysts and electrocatalysts for a variety of reactions.

### Recent Progress

*Sulfur used as a carbon nanostructure growth promoter.* Sulfur can be used as a carbon nanofiber growth promoter. From the literature, it is unclear if sulfur becomes incorporated into the carbon nanostructure. When we introduced sulfur, in the form of thiophene, into the acetonitrile pyrolysis feed used to produce nitrogen containing carbon nanostructure ( $CN_x$ ) catalysts, the  $CN_x$  yield increased. Through X-Ray Photoelectron Spectroscopy (XPS), temperature programmed desorption (TPD) and temperature programmed oxidation (TPO) experiments, it was found that sulfur was both adsorbed to the  $CN_x$  surface and incorporated into the graphitic matrix. As long as acetonitrile was still in the fiber growth feed, ORR activity was unaffected by the growth promoter concentration or the amount of sulfur incorporated into the  $CN_x$ . These results also indicate that sulfur, as incorporated in this study, does not play a role in ORR activity.

*Exploring ORR activity on high surface area nanoarchitectures.* Techniques are being developed to fabricate carbon nanostructures, (Figure 1), with varying orientations of the graphitic planes in order to study the effect of edge plane exposure on ORR activity. These nanostructures are doped with nitrogen and other promising heteroatoms to investigate the effect

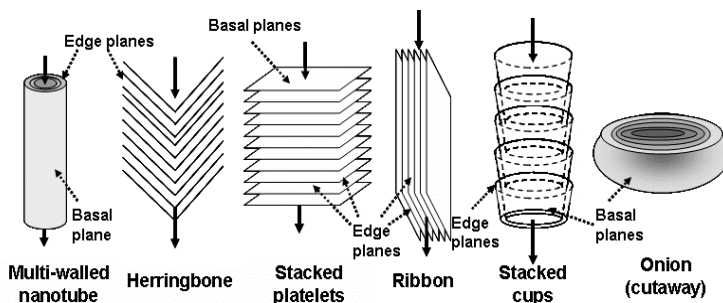


Figure 1. Differences in edge vs basal plane exposure in different carbon nano-structures

of heteroatom placement in the nanostructure on ORR activity and selectivity.

**Electrochemically Accelerated Carbon Corrosion.** By accelerating the degradation of graphitic carbon catalysts in a simulated fuel cell environment, carbon corrosion testing can be quantified separately from other effects. VC and  $CN_x$  catalysts were compared in accelerated aging conditions by examining the growth of the hydroquinone/quinone peak in cyclic voltammetry after extended potential holds. It was found that graphitic  $CN_x$  catalysts are considerably more stable than Vulcan carbon supports which are presently used in PEM fuel cells. Figure 2 shows a comparison of the changes in current for these two materials. Cyclic voltammograms for VC after accelerated aging at 1.2V vs. NHE for various time periods in 0.5M  $H_2SO_4$  are also included to demonstrate the experiment that led to the data in part (a).

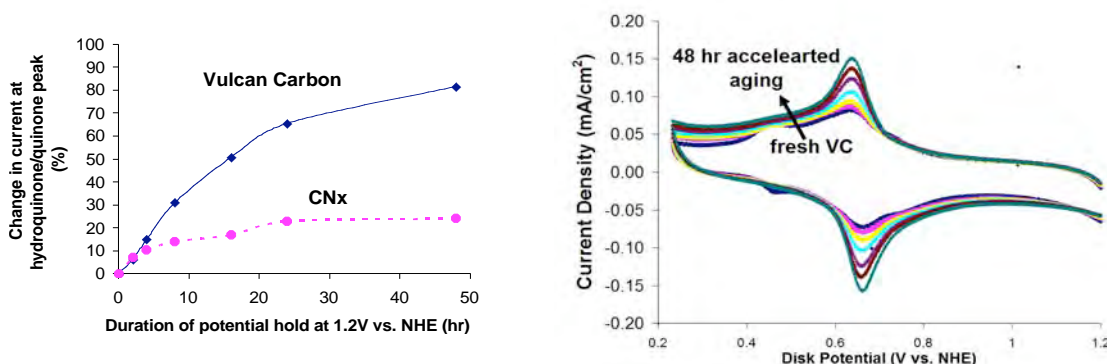


Figure 2. (a) Change in current at the hydroquinone/quinone cyclic voltammogram (CV) peak, an indicator of carbon corrosion, for VC and  $CN_x$ . (b) Cyclic voltammograms on VC after accelerated aging at 1.2V vs. NHE for 2, 4, 8, 16, 24, and 48 hours in 0.5M  $H_2SO_4$ . Experiment conditions: 1000 rpm, 426  $\mu g/cm^2$  loading, 10 mV/sec CV scan rate

**Full PEM fuel cell testing of heteroatom doped carbon materials.** Procedures for fabricating membrane electrode assemblies (MEAs) have been modified from the decal method reported by Los Alamos National Laboratories for our  $CN_x$  catalysts. Optimization of the method for the  $CN_x$  catalysts is ongoing. With the addition of an Arbin 50W hydrogen/direct methanol fuel cell test stand,  $CN_x$  catalyst MEA performance and electrocatalytic conditioning are being explored.

**Initial computational chemistry studies: Computational exploration of heteroatoms in graphite materials.** As a collaborative effort, density functional theory (DFT) calculations have been performed for nitrogen 1s orbital energies in small polycyclic aromatic hydrocarbons (PAHs), which have a similar electronic structure to carbon-nitride catalyst materials, and compared to the experimental XPS nitrogen 1s spectra. A strong correlation between DFT B3LYP method N 1s energies and experimental XPS N 1s energies was established for the PAHs studied (Figure 3). Additionally, experimental ionization potentials trended strongly with the DFT adiabatic ionization potentials. This calibration will be extended to larger and more complex molecules that are more like  $CN_x$  catalysts.

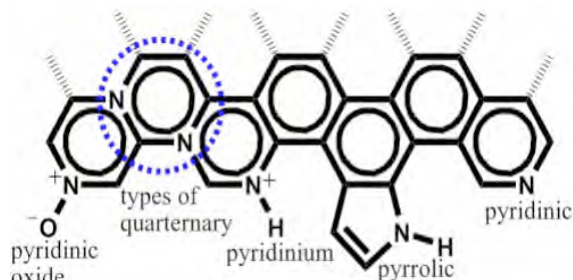


Figure 3. Possible N species found in nitrated graphene

## **Future Plans**

*Incorporation of other heteroatoms into carbon-nitrogen nanostructures:* Boron and phosphorous both have potential to impact the electrocatalytic ORR activity when incorporated into  $CN_x$ . Studies involving the effect of these heteroatoms on the  $CN_x$  yield, physical and chemical characteristics, ORR activity and selectivity, as well as, stability will be studied.

*Selective site blocking of heteroatom carbon ORR catalysts:* Graphitic edge planes and functional groups on carbon can be chemically blocked to study the nature of ORR activity more closely. Several methods of blocking will be studied to better understand the nature of activity for the  $CN_x$  catalysts.

*Computational chemistry studies to complement the experimental work.* A collaborative effort is in progress to gain insight into the ORR mechanism over the nitrogen-doped carbon catalysts combining experimental and computational work. It is planned to use both cluster models and periodic boundary models to explore the possible ORR mechanism over the nitrogen-doped carbon catalysts in acidic solution. Different nitrogen species such as quaternary and pyridinic N will be considered to address the potentially different role played in the ORR process.

### **Publications (August 2007-2009)**

1. Biddinger, E. J.; von Deak, D.; Ozkan, U. S., "Nitrogen-containing carbon nanostructures as oxygen-reduction catalysts." *Topics in Catalysis*, 2009, accepted.
2. Biddinger, E. J.; Knapke, D. S.; von Deak, D.; Ozkan, U. S., "Effect of Sulfur as a Growth Promoter for  $CN_x$  Nanostructures as PEM and DMFC ORR Catalysts," 2009, to be submitted.

### **Oral Presentations (August 2007-2009)**

1. E.J. Biddinger, P.H. Matter, U.S. Ozkan, "Nanostructured  $CN_x$  Cathode Catalysts for PEMFCs & DMFCs," 3<sup>rd</sup> MEA Manufacturing Symposium, Dayton, Ohio, August 2007.
2. E.J. Biddinger, D. von Deak, U.S. Ozkan, "Active Site Investigation of  $CN_x$  Cathode Catalysts for use in PEM and Direct Methanol Fuel Cells," American Chemical Society Spring Meeting, New Orleans, Louisiana, April 2008.
3. Biddinger, E.J., von Deak, D., Ozkan, U.S., "Investigation of the ORR Active Sites in Nano-structured  $CN_x$  Catalysts for PEM and Direct Methanol Fuel Cells, " *14th International Congress on Catalysis*, Seoul, Korea, July 2008.
4. E.J. Biddinger, D.S. Knapke, D. von Deak, U.S. Ozkan, "Feasibility of Using Sulfur as a Growth Promoter for  $CN_x$  Nanostructures as PEM and DMFC ORR Catalysts," American Chemical Society Spring Meeting, Salt Lake City, Utah, March 2009.

### **Invited Lectures by the P.I. (August 2007-2009)**

1. "Role of Catalysis in Fuel Cells," Universite Claude Bernard, Lyon, France, Sep. 2007.
2. "Catalysis for Fuel Cells," Politecnico di Milano Dipartimento di Chimica, Materiali e Ingegneria Chimica, Milan, Italy, October 2007.
3. "Nanostructured  $CN_x$  Catalysts for Oxygen Reduction Reaction in PEM Fuel Cells " Tri-state Catalysis Society, Lexington, KY, November 2007.
4. "Pt-free Oxygen Reduction Catalysts for PEM Fuel Cells" Gordon Research Conference, Ventura, California, January 2008.
5. "CN<sub>x</sub> ORR catalysts" Chicago Catalysis Club, Chicago, IL, January 2008.
6. "Catalysis Research and Its Impact on Energy, Environment and Economics: Fuel Cells and Catalysis" Ohio University, Athens., OH, February 2008.
7. "Energy, Catalysis, and the Future" Kent State University, Kent, OH September 2008.

# Poster Presentations



**Structure-Reactivity Relationships in Multi-Component Transition Metal Oxide Catalysts**

Postdocs, Researchers: Dr. Min Li, Dr. Todd Schwendemann

Students:

Collaborators: A. Boothroyd (Oxford University), R.F. Klie (Univ. Illinois, Chicago), C.H. Ahn (Yale), V.E. Henrich (Yale), C.A.F. Vaz (Yale).

Contact: Prof. Eric I. Altman, Department of Chemical Engineering, Yale University, PO Box 208260, New Haven, CT 06520; Phone (203) 432-4375; E-mail [eric.altman@yale.edu](mailto:eric.altman@yale.edu)

**Goal**

Interactions between metal cations in oxides can lead to catalysts that are vastly more reactive and selective than any of the constituent binary oxides. This effect has variously been attributed to modification of the geometry of the catalytic site around the active metal cation and to modification of the electron density around the active metal cation; however, it has not been possible to separate these two effects since compositional changes have generally been accompanied by structural changes. The goal of this project is to determine the relative importance of these two effects by characterizing the reactivity of epitaxial transition metal oxides where the electron density and geometry around the active cation can be varied independently.

**DOE Interest**

Transition metal oxides are widely used as catalysts in the chemical and energy industries. In the chemical industry, oxides are used for a wide range of selective partial oxidation reactions such as the oxidation of o-xylene to phthalic anhydride which employs a titania-supported vanadium oxide catalyst. In the energy sector, a combination of vanadium, tungsten, and titanium oxides are used to catalytically reduce nitrogen oxides emitted from power plants. The fundamental research in this project aims to put design of new catalysts that are more selective, more active, and that enable new, more catalytic efficient pathways on a more systematic, rational basis. Advances in these areas will enable more efficient use of scarce resources while also potentially reducing the environmental impact of power generation and chemical transformations.

**Recent Progress**

Over the last two years our work has focused on separating structural and electronic effects in multi-component transition metal oxides. We have been pursuing two approaches in tackling this problem: 1) comparing epitaxial vanadia layers grown on a range of supports where the structure and interfacial chemistry can be varied independently; 2) comparing the surfaces of tungstates and vanadates where a variety of secondary cations can be substituted into the material without otherwise appreciably changing the structure.

We have been taking advantage of our previous finding that vanadia tends to grow epitaxially on transition metal oxides by comparing the surface chemistry of supported vanadia layers where the interfacial chemistry is held constant but the structure is changed, and where the structure is held constant but the interfacial chemistry is changed. For the former, we have been comparing epitaxial vanadia layers grown on TiO<sub>2</sub> rutile (110) and anatase (001). Although the vanadia in the bulk of thick epitaxial films is VO<sub>2</sub>, we demonstrated with ion scattering

spectroscopy (ISS) that the surface layer can be capped with oxygen, yielding a  $V_2O_5$  surface as illustrated in Fig. 1. The surface chemical properties of these  $V_2O_5$  surfaces were characterized using 1-propanol temperature programmed desorption (TPD). For vanadia on the rutile (110) support, we observed two reaction channels for dehydrogenation to propionaldehyde, at 400 K and above 500 K. Despite previous reports that multilayer vanadia films are inactive for alcohol dehydrogenation, propionaldehyde desorption at 400 K was observed even for epitaxial films more than 15 nm thick where there is no interaction with the substrate. The peak at 500 K, however, vanished as the film was thickened, suggesting that it is associated with adsorbates interacting with V sites neighboring surface Ti. While thick films with no *chemical* interaction with the support remained active for dehydrogenation, the fraction of the alcohol that desorbed unreacted increased nearly ten-fold. It was, therefore, concluded that the interaction with the Ti promoted the deprotonation of the alcohol to form an alkoxide which then dehydrogenates with nearly the same activation energy, independent of the chemical interaction of the vanadia with the rutile support. Further, since the structure of the vanadia film was held constant as the surface was moved away from the vanadia/titania interface, the results show that a direct chemical interaction with the support is not required for dehydrogenation activity, rather the support can impart activity by maintaining the vanadia in a structurally active form. The results for epitaxial vanadia on anatase (001) indicate that the structure can influence the energetics of the dehydrogenation reaction. In the monolayer regime, propionaldehyde desorption peaked at 350 K with no secondary channel above 500 K. Thicker vanadia films remained active for dehydrogenation, but the propionaldehyde peak shifted towards 400 K. Thus, vanadia in a non-bulk  $V_2O_5$  structure again remains active in the absence of a direct chemical interaction with support, and the structure influences the chemical interactions with the support. We are now working on supports that have the same surface structure as anatase (001) but are chemically different, including  $WO_3$  and  $LaCoO_3$ . For the latter, we have also been characterizing the surface structure of different crystal planes, which is of broader interest in catalysis and materials science.

We have started work on  $CaWO_4$  (100) surfaces. Calcium tungstate is the base member of the scheelite family of materials which includes a wide array catalytically important tungstates and molybdates, most notably bismuth molybdate which is a propene ammoxidation catalyst and is also a promising material for demanding partial oxidation reactions, including oxidative dehydrogenation of propane. The W (or Mo) cations are coordinated in isolated  $WO_4$  and other cations can be substituted for Ca. Thus it is an interesting material for looking at the effects of the secondary cation, the coordination geometry (in comparison to  $WO_3$  which is octahedral), and the separation of the W cations on surface catalytic properties. We have completed spectroscopic characterization of the surface by ISS and XPS, and by electron diffraction (RHEED and LEED) which show that the surface is (1x1), fully oxidized, and does not reconstruct. We will be starting to characterize the surface chemical properties in detail using TPD and the surface structure in more detail with STM shortly.

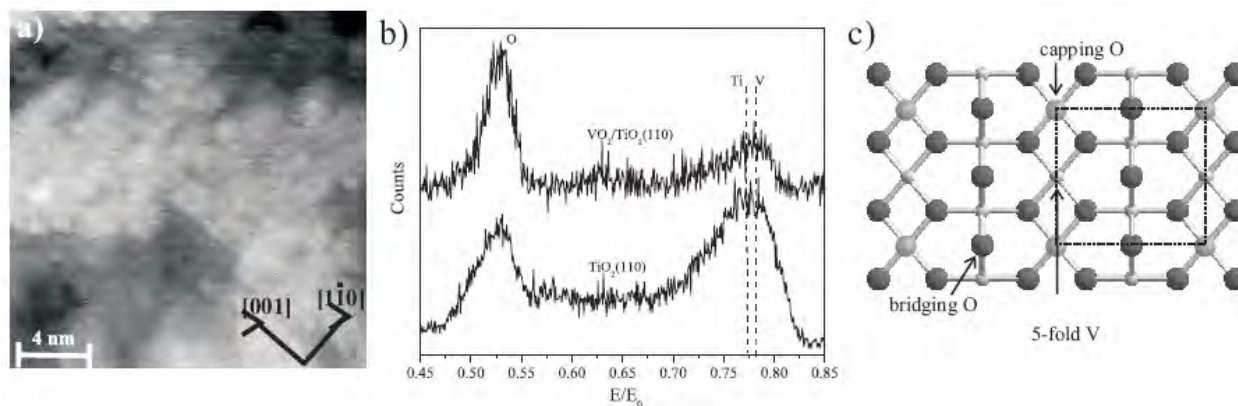


**Figure 1.** a) STM image of an epitaxial vanadia thin film grown on TiO<sub>2</sub> rutile (110) showing the atomic rows characteristic of the rutile structure. (b) Comparison of ISS spectra for bare TiO<sub>2</sub>(110) and an epitaxial vanadia film grown on the same surface. (c) Model of the epitaxial vanadia surface capped by 1/2 layer of O. The decrease in the metal/O ISS peak in the vanadia layer compared to the TiO<sub>2</sub> surface can be quantitatively explained by the capping oxygen atoms. In the model the small white balls represent Ti, the large dark balls structural surface O, and the light gray large balls capping O atoms.

### Future Plans

Over the next several months we will be wrapping up the work on the chemical properties of epitaxial vanadia layers on different substrates. When that work is completed we will focus on CaWO<sub>4</sub> and related materials, as well as LaCoO<sub>3</sub> which can be used as a model for understanding the surface structures of III-III perovskites.

### Recent Publications

M. Li and E.I. Altman, "Reactivity of Epitaxial Vanadia on TiO<sub>2</sub>: Are Support Interactions Required for Reactivity?" *Journal of Physical Chemistry C* **113** (2009) 2798.

C.A.F. Vaz, C.H. Ahn, V.E. Henrich and E.I. Altman, "Growth and Characterization of Thin Epitaxial Co<sub>3</sub>O<sub>4</sub>(111) Thin Films," *Journal of Crystal Growth*, doi:10.1016/j.jcrysgr.2009.03.006.

## First-principles studies of the initial oxidation of transition metal surfaces

Aravind R. Asthagiri\*, Jeffery M. Hawkins, Jason F. Weaver

University of Florida, Department of Chemical Engineering

Email: aasthagiri@che.ufl.edu

Scanning Tunneling Microscopy (STM) studies of the oxidation of a range of transition metal (TM) surfaces have shown the development of a rich range of oxide phases in between the transition from chemisorbed oxygen and bulk oxide formation. We have performed density functional theory (DFT) calculations to probe the atomic-level mechanisms for the initiation of oxidation on the Pt(111) and Pd(111) surfaces. We have examined the energetic and kinetics of possible mechanisms (subsurface O and metal-O exchange) involved in the initial transition from the chemisorbed surface oxygen phase to the 2D oxide phases. For Pt(111) we find that subsurface oxygen is not the precursor to the oxidation of the surface. Instead, we predict a strong preference for the formation and growth of one-dimensional Pt oxide chains at oxygen coverages greater than 0.5 ML [1]. Beyond 0.5 ML additional O atoms prefer to cluster along the oxygen rows formed by the  $p(2\times 1)$  structure and induce a large buckling ( $\sim 1.8$  Å) of the Pt atoms. The buckled structures result in large charge transfer and the oxide chains formed have similar charge distribution to bulk PtO<sub>2</sub>. Our DFT results qualitatively match the recent STM images obtained of the oxidation of the Pt(111) surface. We will also present our ongoing work to model the growth and stability of the 1D oxide chains on Pt(111) to more complex Y-structures observed experimentally [2] and a comparative study of the oxidation of the Pd(111) surface.

### References

1. J.M. Hawkins, J.F. Weaver, and A. Asthagiri, *Phys. Rev. B* **79**, 125434 (2009).
2. S.P. Devarajan, J.A. Hinojosa Jr., J.F. Weaver, *Surf. Sci.* **602**, 3116 (2008).

**Theory-guided design of nanoscale multi-metallic catalysts for fuel cells**

Additional PI: Jorge M. Seminario  
Post-docs: Yuguang Ma and Juan Sotelo  
Graduate students: Rafael Callejas-Tovar, Pussana Hirunsit, Gustavo Ramírez-Caballero  
Undergraduate students: Julibeth Martínez de la Hoz, Santosh Koirala, Birendra Adhikari  
Contacts: Texas A&M University, 3122 TAMU, College Station, TX 77843, phone 979-845-3375, [balbuena@tamu.edu](mailto:balbuena@tamu.edu)

**Goals**

Characterization of thermodynamic and kinetic surface segregation trends in Pt-based alloys on clean surfaces and in presence of oxygenated adsorbates, including effects of low-coordination sites. Connection of segregation to dissolution trends of the metal atoms in acid medium. Size effect on the thermodynamic phase diagrams of nanoalloys. Analysis of the hydration effect on the coupled electron-proton transfer for O<sub>2</sub> reduction on supported bimetallic clusters.

**DOE Interest**

This research will allow design of catalysts for the oxygen reduction reaction with much better activities and durabilities; simultaneously advancing the fundamental and applied aspects of catalytic reactions such as the physics, the chemistry, methods, and development of accurate guidelines for rational design.

**Recent Progress**

*Surface segregation effects in alloy nanoparticles:* Analysis of core-shell and ordered alloys showed segregation trends to be dependent on three main factors: atomic size, surface energies, and heat of formation of the alloy. Formation of subsurface alloys was observed in some core-shell structures having more than one layer of Pt on the shell. However, the segregation trend in most cases changes substantially when oxygen is adsorbed on the surface, and is then dominated by the tendency of the most oxyphilic species to migrate to the surface. Low coordination sites such as steps and kinks usually enhance the segregation trend; however, one interesting exception is the case of Ir cores covered by one monolayer of Pt, where Ir (in spite of its oxyphilicity) does not segregate to the surface even in the presence of up to 0.5 monolayer of oxygen. To complement our thermodynamic analysis, we developed a new model to investigate the kinetics of metal segregation for an infinitely diluted solute in bimetallic alloys (Figure 1).

*Surface activity and metal dissolution in acid medium:* We found that Pt atoms forming skin monolayers have enhanced stability against dissolution with respect to those on pure Pt surfaces. Such stability enhancement follows the opposite order of the oxygen adsorption strengths in Pt<sub>3</sub>M alloys (M = Ni, Co, Fe), indicating the protective role of the subsurface atoms determined by their strong binding to the surface layer.

*Reactivity of low-coordinated sites in acid medium.* Using a combined density functional theory and Green's function approach we studied the reduction of oxygen on small supported clusters in aqueous acid medium, modeled by hydronium and dihydrated hydronium (H<sub>7</sub>O<sub>3</sub><sup>+</sup>). In particular,

we showed that a locally neutral neighborhood of an active site in the bimetallic cluster assists in the protonation reaction (Figure 2). Equally effective to that end is the hydronium hydration.

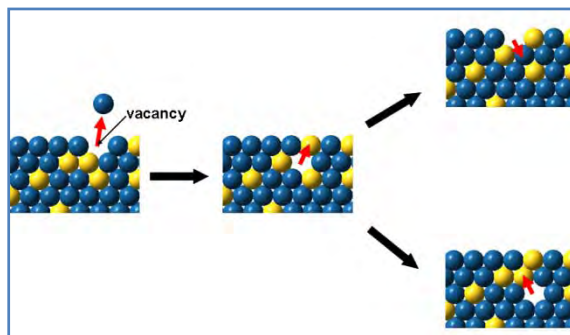


**Figure 1.** Plausible mechanism of surface segregation through vacancies.

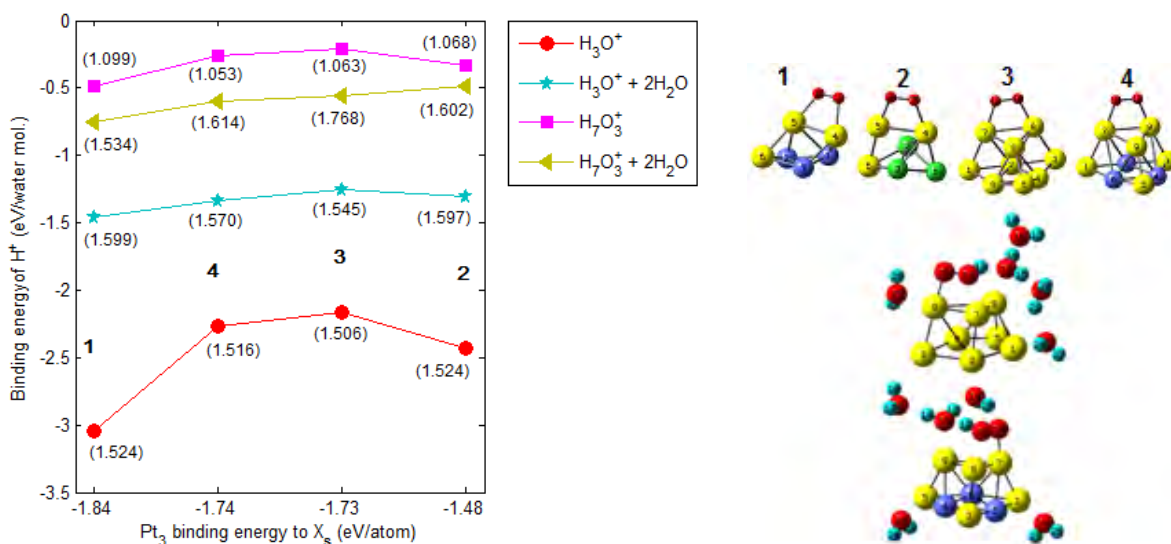


**Figure 2.** Proton binding energy versus binding energy (per atom) of the Pt<sub>3</sub> island to substrate atoms X<sub>s</sub> in protonation of 1-4. The distances cation-core-proton (O<sup>(c)</sup>-H<sup>+</sup>, in Å) are given in parenthesis. The lines are drawn as guide to the eye. Right, from top to bottom, the four nanoclusters used in this work, and complexes 3 and 4 dihydrated and protonated by H<sub>7</sub>O<sub>3</sub><sup>+</sup>.

## Future Plans

*Metal dissolution trends:* We are extending our analysis of metal dissolution trends to include other elements accompanying platinum in dispersed alloys or forming the core in core-shell structures. The application of this technique, along with the evaluation of the surface segregation trends provides useful information regarding surface composition, activity, and durability of a given alloy.

*Kinetic Monte Carlo analysis:* We are developing a kinetic Monte Carlo (KMC) technique to evaluate the evolution of the surface as a function of time, under reaction, and under applied potential. The KMC program requires as input the rates of the diffusion and migration processes

from the subsurface and on the surface that we have already obtained in our previous and current DFT analysis. We will also complete the evaluation of phase diagrams for nanoalloys started this period.

*Surface evolution analysis:* We are studying the reactivity of Au(322) and Pt(322) stepped surfaces and Co(322) kinked surfaces. Our main goal in this project is to study the metal-atom – oxygen interaction on different locations on the surfaces to determine the role of the local strain produced by the adsorbate on surface reconstruction or faceting (when present).

### **Publications (2007-2009)**

1. Gustavo Ramirez-Caballero and Perla B. Balbuena, “Effect of confinement on oxygen adsorbed between Pt(111) surfaces,” *J. Phys. Chem. C*, in press.
2. J. Martinez de la Hoz, R. Callejas-Tovar, and P. B. Balbuena, “Size effect on the stability of Cu-Ag nanoalloys,” *Mol. Sim.*, in press.
3. Y. Ma and P. B. Balbuena, “Surface segregation in bimetallic Pt<sub>3</sub>M (M=Fe, Co, Ni) alloys with adsorbed oxygen,” *Surf. Sci.*, 603, 349-353, (2009).
4. P. Hirunsit and P. B. Balbuena, “Surface atomic distribution and water adsorption on PtCo alloys,” *Surf. Sci.*, 603, 911-919, (2009).
5. Y. Ma and P. B. Balbuena, “A kinetic model of surface segregation in Pt-based alloys,” *J. Chem. Theory and Computation*, 4, 1991-1995, (2008).
6. Z. Gu and P. B. Balbuena, “Atomic oxygen absorption into Pt-based alloy subsurfaces,” *J. Phys. Chem. C*, 112, 5057-5065, (2008).
7. Y. Ma and P. B. Balbuena, “Pt-surface segregation in bimetallic Pt<sub>3</sub>M alloys,” *Surf. Sci.*, 602, 107-113, (2008).
8. F. Tarazona-Vasquez and P. B. Balbuena, “Pt(II) uptake by dendrimer outer pockets: 2. Solvent-mediated complexation,” *J. Phys. Chem. B*, 112, 4182-4193, (2008).
9. F. Tarazona-Vasquez and P. B. Balbuena, “Pt(II) uptake by dendrimer outer pockets: 1. Solventless ligand exchange reaction,” *J. Phys. Chem. B*, 112, 4172-4181, (2008).
10. R. Callejas-Tovar and P. B. Balbuena, “Oxygen adsorption and surface segregation in (211) surfaces of Pt(shell)/M(core) and Pt<sub>3</sub>M (M=Co, Ir) alloys,” *Surf. Sci.*, 602, 3531-3539, (2008).
11. Y. Ma and P. B. Balbuena, “Surface properties and dissolution trends of Pt<sub>3</sub>M alloys in the presence of adsorbates,” *J. Phys. Chem. C*, 112, 14520-14528, (2008).
12. G. Ramirez-Caballero and P. B. Balbuena, “Surface segregation of core atoms in core-shell structures,” *Chem. Phys. Lett.*, 456, 54-57, (2008).
13. J. Sotelo and J. M. Seminario, “Local reactivity of O<sub>2</sub> to Pt<sub>3</sub> on Co<sub>3</sub>Pt and related backgrounds,” *J. Chem. Phys.* 128, 204701, (2008).
14. P. F. Salazar and J. M. Seminario, “Identifying Receptor-Ligand Interactions through an ab Initio Approach,” *J. Phys. Chem. B*, 112, 1290-1292, (2008).

**Modeling catalyzed growth of single-wall carbon nanotubes**

Graduate students: Jin Zhao and Diego Gómez-Gualdrón  
Undergraduate students: Juan Carlos Burgos  
Collaborators: Daniel E. Resasco (U. of Oklahoma)  
Contacts: Texas A&M University, 3122 TAMU, College Station, TX 77843,  
phone 979-845-3375, [balbuena@tamu.edu](mailto:balbuena@tamu.edu)

**Goal**

Computational characterization of: a) role of morphology, size, and chemical composition of the supported catalyst on the precursor decomposition and initial stages of C deposition and reaction; b) effect of the surface morphology and chemical composition on the selectivity towards growing caps of different chiralities.

**DOE Interest**

Single-wall carbon nanotubes offer high potential as components of micro and nanoelectronic devices, in biomedical applications, and as catalytic supports. These properties are strongly related to the nanotube diameter and chirality. We expect that our studies may contribute to the understanding of the nanotube growth and therefore, to provide guidance for synthesis methods to become able of controlling the production of nanotubes of specific types. In addition, understanding catalyzed growth of carbon nanotubes may provide new insights for the design of other catalytic processes involving desired or undesired growth of carbon structures.

**Recent Progress**

*Thermodynamics and kinetics of C<sub>2</sub> addition as a function of nanotube chirality:* Examination of the C<sub>2</sub> addition to the edge of minimal growing nanotube caps of several chiralities indicates that thermodynamics and kinetics may favor the growth of arm-chair or near arm-chair tubes for this reaction. In the presence of the metal cluster, we detect oxidation of the metal atoms and reorganization of the cluster geometry both dependent on the nascent nanotube chirality. The root growth reaction is shown to occur by displacement of a cobalt atom initially interacting with the armchair site while the added carbon atoms bond each other forming a new hexagonal ring, whereas the carbon dissolution process shows formation of dimers inside the cluster only for the (6,5) near-arm-chair system. The energetic of both steps reveals that the dissolution stage is likely controlling the overall nanotube growth rate. Figure 1 illustrates the interplay between the carbon and metal atoms during the growth reaction.

*Effect of a stepped surface on the growth of carbon structures:* Density functional theory analyses of the adsorption of carbon on stepped Co (211) surfaces reveals a variety of surface phenomena including surface reconstruction (Figure 2) and formation of carbon structures depending on the location of the adsorbed carbon atoms (Figure 3). We have found the formation of graphene planes following the orientation of the (100) plane as shown in Figure 3, but also in other cases we have found the formation of horizontally aligned semi-nanotubes.

**Future Plans**

*Analysis of carbon structures growth on chiral surfaces:* We want to determine how the surface chirality may affect the formation of specific carbon structures perhaps favoring growth of



specific chiralities. To that end we are testing carbon adsorption in a variety of chiral surfaces (defined by their three  $hkl$  indexes).

*Effect of surface composition on the formation of carbon structures:* We have started investigating  $\text{Fe}_3\text{Al}$  surfaces because these are known to be alternative steel formulations. We expect to understand how the role of other atoms (in this case Al) that do not have a high affinity to carbon, may be used to tune the formation of carbon nanostructures.

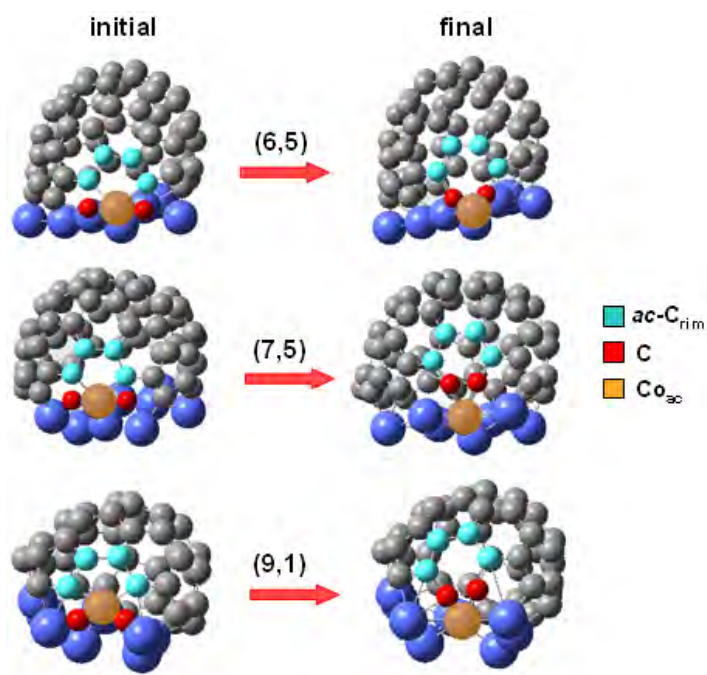


**Figure 1.** Initial and final geometries of the systems investigated. The atoms of the *arm-chair* active site are highlighted in light blue, the C atoms added to the system in red and the Co atom initially interacting with the *arm-chair* site in orange. The other C atoms are grey and the other Co atoms are blue. The highlighted atoms lay on a common plane, except for (9,1) where the highlighted Co is out-of-plane toward the center of the cap interior.

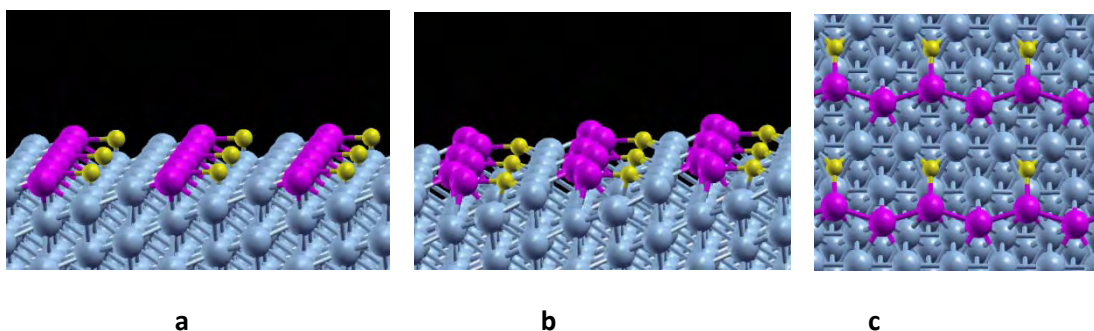


**Figure 2.** Surface reconstruction of a Co (2 1 1) surface by addition of a single carbon at a top (terrace) site. a) Side view of the initial state. b) Side view of the system after relaxation. c) Top view of the relaxed system. Note that the formation of zig-zag chains on the step edge.

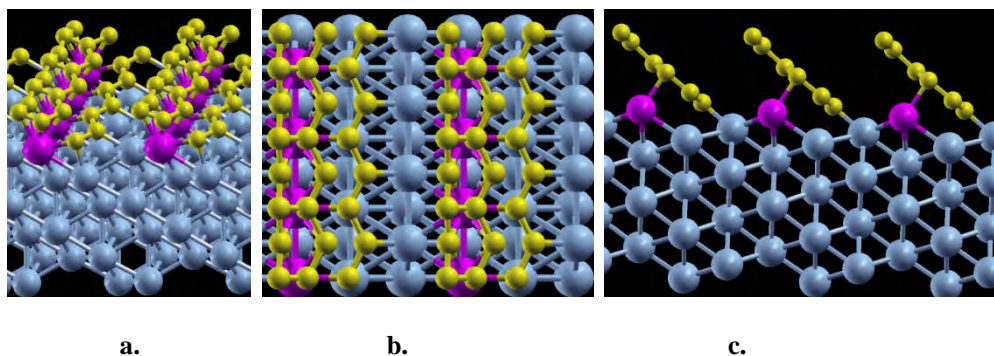


**Figure 3.** Evolution of higher C pressures on (211) Co surfaces. Each unit cell contains twelve carbon atoms. a and b are the side and top view respectively of the initial structure to which new C atoms are initially added at both sides of the chain, in the terraces next and previous to the step. c is a side view after relaxation, two of the atoms bond to one of the terraces, but the other two stand out of the metal surface, all of them forming a graphene surface that follows the orientation of the (1 0 0) lattice plane of the metal.

### Publications (2007-2009)

1. A. Martinez-Limia, J. Zhao, and P. B. Balbuena, "Molecular dynamics study of the initial stages of catalyzed single-wall carbon nanotubes growth: Force field development," *J. Mol. Modeling*, 13, 595-600 (2007).
2. J. Zhao and P. B. Balbuena, "Effect of nanotube length on the aromaticity of single-wall carbon nanotubes," *J. Phys. Chem. C*, 112, 3482-3488, (2008).
3. Jin Zhao and P. B. Balbuena, "Effect of nanotube cap on the aromaticity of single-wall carbon nanotubes," *J. Phys. Chem. C*, 112, 13175-13180, (2008).
4. Diego A. Gómez-Gualdrón and Perla B. Balbuena, "The role of cap chirality on the mechanism of growth of single-wall carbon nanotubes," *Nanotechnology*, 19, 485604 (2008).
5. Diego A. Gómez-Gualdrón and Perla B. Balbuena, "Effect of metal cluster-cap interactions on the catalyzed growth of single-wall carbon nanotubes," *J. Phys. Chem. C*, 113, 698-709, (2009).
6. Diego A. Gómez-Gualdrón and Perla B. Balbuena, "Growth of chiral single-walled carbon nanotubes in the presence of a cobalt cluster," *Nanotechnology*, in press.

### Controlling Adsorbate Motion

Lead PI: T.F. Heinz (Columbia University)

Postdoc: Zhihai Cheng (UCR), Christophe Huchon (UCR), Sampyo Hong (UCF)

Students: Greg Pawin (UCR), Daeho Kim (UCR), Dezheng Sun (UCR), MiaoMiao Luo (UCR), Jon Wyrick (UCR), Duy Tran Le (UCF)

Contact: Pierce Hall, University of California, Riverside, CA 92506 ([Ludwig.Bartels@ucr.edu](mailto:Ludwig.Bartels@ucr.edu)) /  
Dept. of Physics, Univ. of Central Florida, Orlando, FL 32816 ([talat@physics.ucf.edu](mailto:talat@physics.ucf.edu))

This collaboration devises methods for controlling the flow of reactants at catalyst surfaces with the ultimate goal of providing selective transport towards and occupation at sites of greater activity (e.g., step-edges, other surface irregularities, and regions of different composition).

Adsorbates generally diffuse in an isotropic fashion on metal surfaces, i.e. in all possible surface directions. Our investigations have shown that 1-dimensional guidance can arise from the detailed molecule/substrate interaction. We initially demonstrated this effect using a molecule, 9,10-diacetylthioanthracene (DTA), that we designed for this purpose. We found that when deposited on a Cu(111) substrate, DTA diffuses exclusively along the direction in which it is initially aligned. This behavior violates the substrate symmetry. It converts a 2D random walk into a 1D phenomenon. Extension of this concept to transport of cargo molecules was successful with a combination of anthraquinone as a carrier and CO<sub>2</sub> as cargo. We could also use these systems to study the strength of hydrogen bonds at surfaces and the extent to which structural anisotropy in the reaction potential can lead to temporal asymmetry in reaction rates (Principle of Microscopic Reversibility / Detailed Balance).

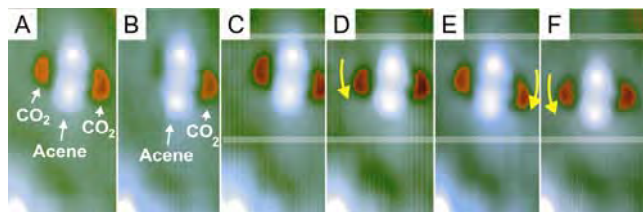


Fig. 1 A-C) detachment and reattachment of a CO<sub>2</sub> molecule (depression, red) on the left side of an AQ (protrusion, blue/white). (C-F) diffusion of AQ with two CO<sub>2</sub> molecules by means of individual steps of its oxygen atoms (see Fig. 3). All images V = -35 mV, I = 60 pA, T = 50K, A = 20 x 40 Å. Note the edge of a cluster of AQ molecules in the bottom left serving as a marker and the Cu(111) surface state oscillations.

Typically small nanoparticle facets rather than large crystals are employed in heterogeneous catalysis. This begs the question, how diffusion of reactants proceeds within the confinement of their small surface facets. In this research program, we developed a model system that allows us the study of adsorbates in confined facets of predetermined and uniform size. To this end we employ pores of anthraquinone honeycomb structures. This has proven to be very rich in unexpected phenomena. For instance, CO molecules diffuse inside the pores of anthraquinone molecular honeycombs on top of a Cu(111) surface much more rapidly than on the bare surface, suggesting a lowering of the diffusion barrier as a consequence of finite facet size. Moreover, we find that the molecules prefer sites at the center of the pore. By placing a number of molecules inside a pore and studying the occupancy of every single underlying substrate atom over time, we find the following plots, which attest to the formation of a shell structure.

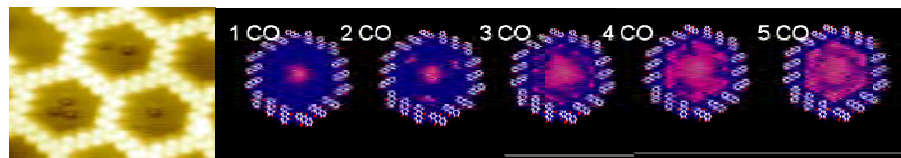


Fig. 2 Anthraquinone Honeycomb on Cu(111) with one, two and three molecules in the pores. Relative occupancy of the substrate sites inside the pores with CO molecules as a function of molecules inside a pore.

#### References:

1. Wong K.L., Pawin G., Kwon K.-Y., Lin X., Jiao T., Solanki U., Fawcett R.H.J., Bartels L., Stolbov S., Rahman T.S., *A Molecule Carrier*, **Science** 315, 1391 (2007)
2. Pawin G., Solanki U., Kwon K.-Y., Wong K.L., Lin X., Jiao T., Bartels L., *A quantitative approach to hydrogen bonding at a metal surface*, **J. Am. Chem. Soc. Comm.** 129, 12056 (2007)
3. Pawin G., Wong K.L., Kwon K.-Y., Frisbee R., Rahman T.S., Bartels L., *Surface Diffusive Motion in a Periodic and Asymmetric Potential*, **J. Am. Chem. Soc. Comm.** 130, 15244 (2008)

### Catalysis for the Selective Synthesis of Fuels and Chemical

Postdoc: Jennifer Strunk  
Students: Jason Bronkema, Andrew Getsoian, Ned Stephenson, Will Vining  
Collaborators: Martin Head-Gordon (UC Berkeley)  
Contacts: Department of Chemical Engineering, University of California, Berkeley,  
CA 94720-1462; [bell@cchem.berkeley.edu](mailto:bell@cchem.berkeley.edu)

#### Goal

The goal of this program is to develop a molecular understanding of catalytically active centers and to use this knowledge to in order to synthesize unusual chemical and physical environments at such centers. The program involves a synergistic combination of efforts in the areas of catalyst synthesis, characterization, and evaluation. Quantum chemical simulations of catalytically active centers are used guide the interpretation of experimental findings and suggest novel structures to be attempted synthetically.

#### DOE Interest

Understanding the fundamental relationships between catalyst composition and structure and catalyst activity and selectivity is one of the primary goals of the DOE Chemical Energy program. Work done on this project contributes to an atomic and molecular understanding of catalysis, and in particular to the definition of the structure of a catalytically active site, the mechanism by which chemical transformations occur at such sites, and the means by the activity and selectivity of a site can increased.

#### Recent Progress

*Olefin epoxidation at Fe(III) Porphyrin Centers:* The role of pophyrin composition on the rate parameters for each of the elementary processes involved in the epoxidation of olefins with H<sub>2</sub>O<sub>2</sub> was established. This effort has contributed to a comprehensive understanding all of the factors governing the activity and selectivity of such catalysts for olefin epoxidation.

*Methanol Oxidation at Isolated Vanadate Centers:* The structure and properties of isolated vanadate centers deposited on SiO<sub>2</sub>, TiO<sub>2</sub>, and monolayer deposits of TiO<sub>x</sub> deposited on SiO<sub>2</sub> have been characterized both experimentally and theoretically and investigated for the oxidation of methanol. The catalyst activity increased by nearly two orders of magnitude for titania coverages well under a monolayer. The strong effect of titania on the rate of methanol oxidation to formaldehyde is attributed to the formation of oxygen defects in titania-containing catalysts. Evidence for such defects obtained by EPR and DFT calculations has shown that the occurrence of defects adjacent to isolated vanadates can explain the strong enhancement in the rate of methanol oxidation observed for titania-containing catalysts.

*Preparation and Characterization of 2-D Model Catalyst Systems:* Work has been initiated on preparation and characterization of two-dimensional models of supported

VO<sub>x</sub> catalysts. Isolated vanadate species and vanadate oligomers have been deposited onto nanometer-thick layers of silica grown on a Si wafer and then characterized by XPS and SIMS.

### **Future Plans**

*Catalysis by Vanadate Species on Tailored Supports:* Work will continue on the synthesis and characterization of monolayer and bilayer coatings of titania, zirconia, and other oxides on silica, as part of an effort to prepare tailored supports. These model structures will be compared with those proposed on the basis of quantum mechanical calculations. Isolated metal oxo species, e.g., vanadates and molybdates will then be deposited onto these tailored supports and investigated with the aim of identifying the role of the deposited layer on the activity and selectivity of the oxo species for a variety of test reactions. The importance of the interlayer on processes such as oxygen transport and reactant adsorption will be explored.

*Preparation and Characterization of 2-D Model Catalyst Systems:* Work will continue on the preparation and characterization of two-dimensional, models of supported metal oxides. The aim of this work is to identify and characterize the spatial distribution of metal oxo species such as vanadates and molybdates. A recently installed confocal Raman microscope that is coupled to an atomic force microscope will be used to identify oxo clusters and to acquire tip-enhanced Raman spectra of individual metal oxo species. The catalytic performance of such 2-D model catalysts will be investigated using a newly developed reactor system.

### **Publications (2006-2008)**

1. Ruddy, D.; Ohler, N.; Bell, A. T.; Tilley, T. D., "Thermolytic Molecular Precursor Route to Site-Isolated Vanadia-Silica Materials and their Catalytic Performance in Methane Selective Oxidation," *Journal of Catalysis* (2006), 238 (2) 277.
2. Stephenson, N.; Bell, A. T., "Influence of Solvent Composition on the Kinetics of Cyclooctene Epoxidation by Hydrogen Peroxide Catalyzed by Iron(III) [tetrakis(pentafluorophenyl)] porphyrin, chloride [(F<sub>20</sub>TPP)FeCl]," *Inorganic Chemistry* (2006), 45 (6) 2758
3. Karshtedt, D.; McBee, J.; Bell, A. T.; Tilley, T. D., "Stoichiometric and Catalytic Arene Activations by Platinum Complexes Containing Bidentate Monoanionic Nitrogen-based Ligands," *Organometallics* (2006), 25 (7) 1801
4. Stephenson, N.; Bell, A. T., "Effects of Methanol on the Thermodynamics of Iron(III) [Tetrakis(pentafluorophenyl)] Porphyrin Chloride Dissociation and the Creation of Catalytically Active Species for the Epoxidation of Cyclooctene," *Inorganic Chemistry* (2006), 45 (14) 5591.
5. Pokrovski, K. A.; Bell, A. T., "An Investigation of the Factors Influencing the Activity of Cu/Ce<sub>x</sub>Zr<sub>1-x</sub>O<sub>2</sub> for Methanol Synthesis via CO Hydrogenation," *Journal of Catalysis* (2006), 241 (2) 276.
6. Stephenson, N. A.; Bell, A. T., "The Influence of Substrate Composition on the Kinetics of Olefin Epoxidation by Hydrogen Peroxide Catalyzed by Iron(III) [Tetrakis(pentafluorophenyl)] Porphyrin," *Journal of Molecular Catalysis A: Chemical* (2006), 258 231.
7. Pokrovski, K. A.; Bell, A. T., "Effect of Dopants on the Activity of Cu/M<sub>0.3</sub>Zr<sub>0.7</sub>O<sub>2</sub> (M = Ce, Mn, and Pr) for CO Hydrogenation to Methanol," *Journal of Catalysis* (2006), 244, 43-51.
8. Stephenson, N. A.; Bell, A. T., "Mechanistic Study of Iron(III)[Tetrakis(pentafluorophenyl)] Porphyrin Triflate (F<sub>20</sub>TPP)Fe(OTf) Catalyzed Cyclooctene Epoxidation by Hydrogen Peroxide," *Inorganic Chemistry* (2007), 46, 2278-2285.

9. Stephenson, N. A.; Bell, A. T., "Effects of Porphyrin Composition on the Activity and Selectivity of the Iron(III) Porphyrin Catalysts for the Epoxidation of Cyclooctene by Hydrogen Peroxide," *Journal of Molecular Catalysis A: Chemical* (2007), 272, 108-117.
10. Stephenson, N. A.; Bell, A. T., "Mechanistic Insights into Iron Porphyrin-Catalyzed Olefin Epoxidation by Hydrogen Peroxide: Factors Controlling Activity and Selectivity," *Journal of Molecular Catalysis A: Chemical* (2007), 275 54-62.
11. Bronkema, J.; Bell, A. T., "Mechanistic Studies of Methanol Oxidation to Formaldehyde on Isolated Vanadate Sites Supported on MCM-48," *Journal of Physical Chemistry C* (2007), 111, 420-430.
12. Khaliullin, R. Z. ; Head-Gordon, M. ; Bell, A. T., "Theoretical Study of Solvent Effects on the Thermodynamics of Iron(III) [Tetrakis(pentafluorophenyl)] Porphyrin Chloride Dissociation," *Journal of Physical Chemistry B* (2007), 111, 10992-10998.
13. Bronkema, J.; Leo, D. C.; Bell, A. T., "Mechanistic Studies of Methanol Oxidation to Formaldehyde on Isolated Vanadate Sites Supported on High-Surface-Area Anatase," *Journal of Physical Chemistry C* (2007), 111, 14530-14540.
14. Bronkema, J.; Bell, A. T., "Mechanistic Studies of Methanol Oxidation to Formaldehyde on Isolated Vanadate Sites Supported on High-Surface-Area Zirconia," *Journal of Physical Chemistry C* (2008), 112, 6404-6412.
15. Bronkema, J.; Bell, A. T., "An Investigation of the Reduction and Reoxidation of Isolated Vanadate Sites Supported on MCM-48," *Catalysis Letters* (2008), 122, 1-8.
16. Goodrow, A.; Bell A. T., "A Theoretical Investigation of the Selective Oxidation of Methanol to Formaldehyde on Isolated Vanadate Species Supported on Silica," *Journal of Physical Chemistry C* (2007), 111 (40) 14753-14761.
17. Goodrow, A.; Bell, A. T., "A Theoretical Investigation of the Selective Oxidation of Methanol to Formaldehyde on Isolated Vanadate Species Supported on Titania," *Journal of Physical Chemistry C* (2008), 112 (34) 13204-13214 (2008).

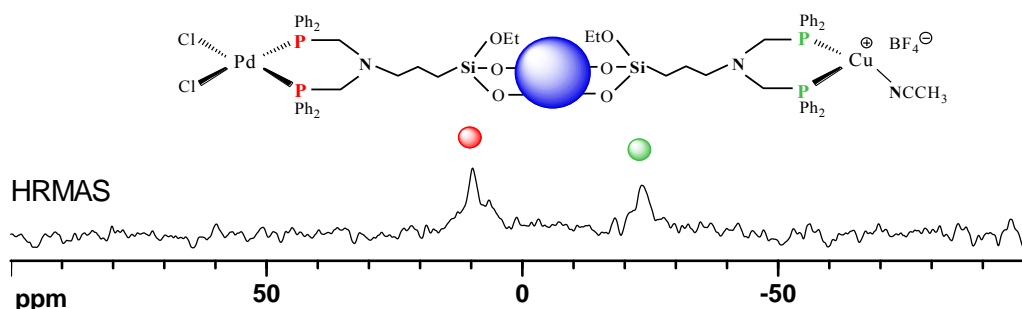
## Catalysts Immobilized on Oxide Supports: New Insights by Solid-State NMR Spectroscopy

M. Perera, C. Hilliard, J. Guenther, A. Naghipour, J. Blümel\*  
Texas A&M University, Department of Chemistry, College Station, TX, 77842-3012  
e-mail: [bluemel@tamu.edu](mailto:bluemel@tamu.edu)

Molecular catalysts immobilized on oxide supports are easy to design, and they are as selective and active as their homogeneous analogues. Furthermore, they can easily be separated from the reaction mixture and recycled many times.<sup>1</sup> These features make immobilized catalysts attractive not only for academic, but also for industrial purposes. Homogeneous catalysts can be bound to oxide supports by phosphine linkers, as shown in the Figure below.<sup>2,3</sup> Silica is the most favorable support, both from an analytical, and preparative point of view. For the analysis of the resulting amorphous solid materials we optimized classical solid-state and suspension NMR spectroscopy.<sup>4,5</sup> Both can be employed for probing the nature and mobility of surface-bound species.

In the first part of our poster, the HRMAS method, which we have implemented for immobilized catalysts, and the kind of information it provides, will briefly be described. This section should be of interest to many participants of the Catalysis Sciences Meeting, because our new technique can be applied to a wide variety of systems in chemistry and related disciplines.

Next, new insights concerning the syntheses, immobilization, characterization, activities, and lifetimes of mononuclear catalysts,<sup>1</sup> as well as intrinsic problems therewith will be displayed. New perspectives that have been obtained with the heterodimetallic Pd(0)/Cu(I) Sonogashira catalyst system using <sup>31</sup>P HRMAS,<sup>2</sup> will be presented:



The most fascinating aspect of the Sonogashira catalyst system concerns the mobility of the Pd fragment on the surface, which can be found in case of sub-monolayer surface coverages by HRMAS NMR.

Finally, a new generation of successful linker systems for immobilized catalysts will be presented, only one of which has been communicated briefly so far.<sup>6</sup> These new linkers finally solve two of the most persistent problems of immobilized catalysts, (a) destruction of the catalyst by contact with the reactive support surface, and (b) deactivation by dimerization or agglomeration with neighboring catalyst molecules.

### References

1. (a) J. Blümel, *Coord. Chem. Rev.* **2008**, 252, 2410.  
(b) C. Merckle, J. Blümel, *Topics Catal.* **2005**, 34, 5.
2. T. Posset, J. Blümel, *J. Am. Chem. Soc.* **2006**, 128, 8394.
3. M. Bogza, T. Oeser, J. Blümel, *J. Organomet. Chem.* **2005**, 690, 3383.
4. T. Posset, F. Rominger, J. Blümel, *Chem. Mater.* **2005**, 17, 586.
5. S. Brenna, T. Posset, J. Furrer, J. Blümel, *Chem. Eur. J.* **2006**, 12, 2880.
6. Y. Yang, B. Beele, J. Blümel, *J. Am. Chem. Soc.* **2008**, 130, 3771.

## Single-Molecule Fluorescence Imaging for Studying Organic, Organometallic, and Inorganic Reaction Mechanisms

Postdoc: Sung-Gon Lim  
Students: Yong Wang  
Contacts: University of California, Irvine, Chemistry Department NSII 1102, Irvine, CA 92697-2025; blums@uci.edu

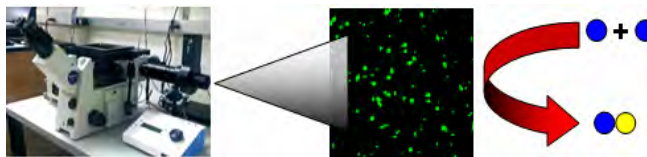
### Goal

Image individual steps in organic, organometallic, and inorganic reaction mechanisms using single-molecule fluorescence microscopy and use this increased understanding to develop new catalytic reactions.

### DOE Interest

The reactive behavior of individual molecules is seldom observed, because we usually measure the average properties of billions of molecules. What we miss is important: The catalytic activity of less than 1% of the molecules under observation can dominate the outcome of a chemical reaction seen at a macroscopic level. Currently available techniques to examine reaction mechanisms (such as nuclear magnetic resonance spectroscopy and mass spectrometry) study molecules as an averaged ensemble. These ensemble techniques are unable to detect minor components (under ~1%) in mixtures or determine which components in the mixture are responsible for *reactivity* and *catalysis*. In the field of mechanistic chemistry, there is a resulting dogma that if an intermediate is very reactive, it often cannot be observed (termed “Halpern’s Rule”). Ultimately, the development of single-molecule imaging technology could be a powerful tool to observe these “unobservable” intermediates and active catalysts (Figure 1). Single-molecule techniques have already transformed biology and the understanding of biochemical processes. This transformative imaging technique has broad, multidisciplinary impact with the potential to change the way the chemical community studies reaction mechanisms, especially in the core area of catalysis.

**Figure 1.** Real-time imaging of individual catalytic turnovers, project schematic.



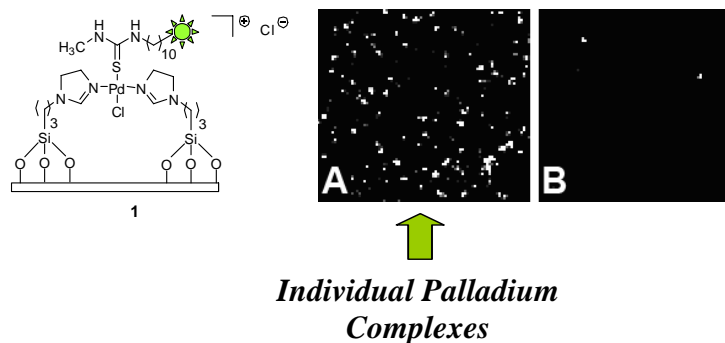
### Recent Progress

The single-molecule imaging of individual palladium(II) complexes tagged with spectator fluorophores has been achieved and will be described (Figure 2A, compared to control 2B). The camera detects and quantifies single molecules based on the photons given off by the spectator fluorophore. This method for attaching spectator fluorophores to metal complexes and subsequently imaging the complexes at the single-molecule level has the potential to be highly general. The requisite high-quantum-yield BODIPY fluorophores are synthesized and shown to act as spectators when bound to metal complexes. These combined experimental results lay the fundamental groundwork for studying organometallic reaction chemistry at the single-molecule level using



fluorophore tags. We are currently employing these tagged ligands for imaging live reactions at metal centers on the single molecule level.

**Figure 2.**



### **Future Plans**

*Imaging of Individual Reactions:* Develop techniques for first real-time imaging of individual binding events between metal and ligands.

*Determine Kinetics at Single-Molecule Level:* What is heterogeneity of reaction at surface over small surface areas?

**Catalytic and Transport Behaviors of Model Porous and Composite Nanostructures**

Postdocs: Jiebin Pang  
Students: Shisheng Xiong, Adam Wise  
Collaborators: Ying-Bing Jiang (UNM), Darren Dunphy (UNM)  
Contacts: 1001 University Blvd SE Suite 100, Albuquerque, NM 87106;  
[cjbrink@sandia.gov](mailto:cjbrink@sandia.gov)

**Goal**

Combine self-assembly, interfacial assembly and atomic layer deposition to create model, highly ordered porous or composite thin film nanostructures. Systematically control pore size, shape, and chemistry to reveal new nanoscale transport phenomena in gas and liquid media. Prepare ordered nanoparticle/polymer or oxide composites with controlled nanoparticle spacing and arrangement and interfacial chemistries to test collective catalytic and charge-transfer characteristics of 2D and 3D systems.

**DOE Interest**

Improved membrane technologies are needed for many energy-related applications, including (but not limited to) CO<sub>2</sub> sequestration, biofuel purification, controlled oxidation, and hydrogen purification and separation. Also, new processing methods are required for producing robust 2D and 3D NP arrays on arbitrary substrates to investigate collective behavior between NPs for charge-transfer and catalytic applications (e.g. solar cells, solid-state lighting, electrocatalysis).

**Recent Progress**

*Sub-10 nm Thick Membranes Made by Plasma-Defined Atomic Layer Deposition* - Using our newly developed plasma-assisted ALD and extending it to the deposition of a bridged polysilsesquioxane, we fabricated ultrathin microporous membranes with an unprecedented combination of flux and selectivity. Passivation of internal pores of an ordered mesoporous support (Fig. 1) with trimethylsilyl groups followed by remote oxygen plasma activation of the immediate surface allowed deposition of a <5-nm thick film from the hybrid precursor, (C<sub>2</sub>H<sub>5</sub>O)<sub>3</sub>-Si-C<sub>2</sub>H<sub>4</sub>-Si-(OC<sub>2</sub>H<sub>5</sub>)<sub>3</sub>) (see Fig. 1). ALD is avoided within the internal volume of the film by capping of all free reactive silanol groups with non-reactive trimethyl silane groups; subsequent remote oxygen plasma exposure converts only surface trimethylsilyl groups to ALD-reactive silanols. By this process, ALD takes place on the surface of the substrate, while internal, hydrophobic -Si(CH<sub>3</sub>)<sub>3</sub> groups remain unhydrolyzed and do not undergo condensation reactions with ALD precursors. A further oxygen plasma step was used to remove the C<sub>2</sub> organic bridge to create templated micropores.

We evaluated the transport properties of our membrane and compared membrane permeance and selectivity to the highest performance membranes produced through conventional sol-gel processes as well as CVD (Fig. 2). The combined flux and selectivity of our membrane are well-above the existing so-called 'upper bound' of other the membranes systems. Note also that the He permeability for CVD and sol-gel membranes were measured at >673K, while the ALD membrane was measured at room temperature. The high flux and selectivity are attributed to the ultra-thinness and precise control of pore size.

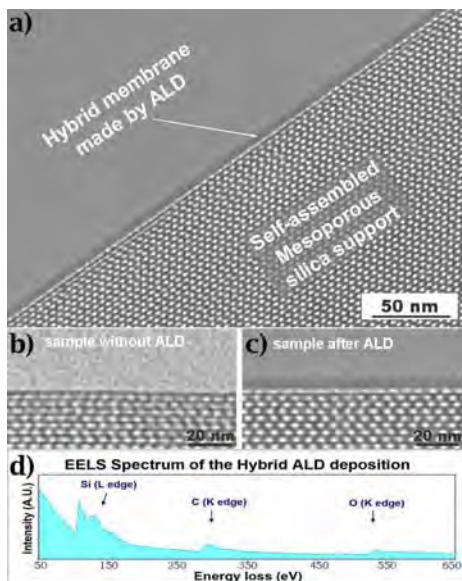


**Figure 1.** a) Cross-sectional TEM image of the hybrid membrane supported on mesoporous silica; b) original mesoporous silica support; c) support coated with ALD membrane; d) EELS spectrum of the membrane.

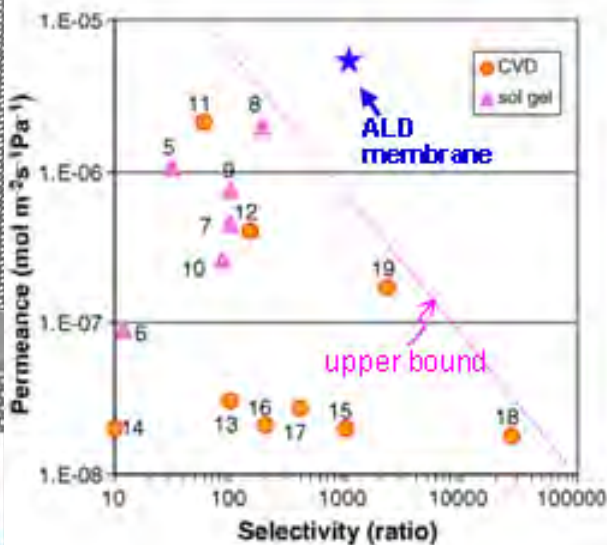


**Figure 2.** Comparison of ALD silica membrane with representative silica membranes made by CVD and sol-gel approaches. Permeance is He permeance; selectivity is He to N<sub>2</sub> selectivity.

*Free Standing, Patternable Nanoparticle/Polymer Monolayer Arrays* - Recently we reported a general, facile and robust method to prepare free-standing, patternable nanoparticle/polymer monolayer arrays by evaporation induced self-assembly at a fluid interface (C.J.B et. al., JACS 2008). The ultra-thin monolayer nanoparticle/polymer arrays are sufficiently robust for transfer to arbitrary substrates and can be suspended as a free-standing membrane over cm-sized holes, even with free edges (see Fig. 3a). These ultra-thin nanoparticle/polymer monolayer arrays are of interest for fundamental investigations of electronic, magnetic and optical properties in 2D artificial solids, as well as for integration into micro- and macro-scale devices for use in energy/charge transfer and catalytic applications.

Recently, we have extended our interfacial self-assembly process to NP/semiconducting polymer composites and have developed patterning strategies whereby the polymer layer serves as a resist for e-beam lithography. Also, by transferring NP/semiconducting polymer films onto the DOE SNL/LANL Center for Integrated Nanotechnology (CINT) Discovery Platforms® fabricated with pre-deposited interdigitated electrodes, electron transfer at the metallic NP/polymer interfaces as well as electron transport across the composite films have been studied by current voltage and confocal Raman microscopy under applied bias.

## Future Plans

We will synthesize NP/polymer arrays for use in fuel cell and electrocatalytic applications, and characterize these using standard electrochemical methodologies. Specifically, we will address the issues of increasing Pt utilization in fuel cell membranes, the effect of collective behavior in NP arrays, as well as create multifunctional NP arrays for multistep electrocatalytic reactions. Simultaneously, we will vary NP size, shape, and chemistry and characterize the NP/polymer self-assembly process to gain insight into how to control NP symmetry and organization both in plane and through thickness. We will study assembly of binary NP systems to develop superlattices. We will also combine supported NP/polymer arrays with ultrathin ALD-derived membranes to control transport to and from the electrochemically active NP arrays (for example, reducing CO<sub>2</sub> transport in alkaline fuel cell structures).

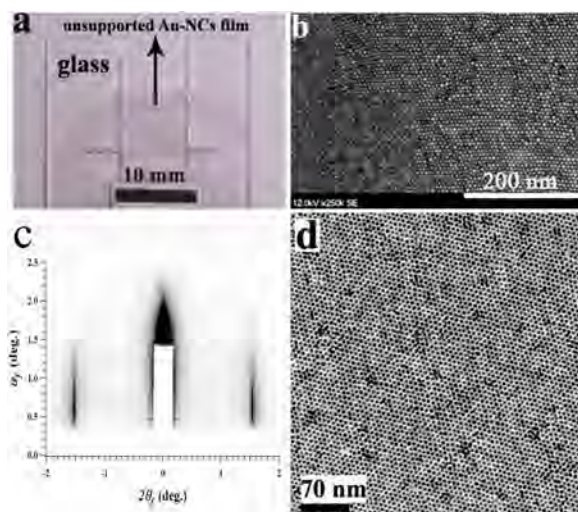


**Figure 3.** An optical image (a) of a large area NP/PMMA supported and unsupported monolayer; SEM (b) and TEM (d) images and a GISAXS pattern (c) of the NP/PMMA thin film nanocomposite.

## Publications (2007-2009)

“Porous Nanoparticle Supported Lipid Bilayers (Protocells) as Delivery Vehicles”, Liu, J; Stace-Naughton, A; Jiang, X; Brinker CJ., *J. Am. Chem. Soc.*, **January 2009**, *131* (4), 1354-1355.

“Dynamic Investigation of Gold Nanocrystal Assembly using *in situ* Grazing-Incidence Small-Angle X-ray Scattering”, Dunphy D; Fan HY; Li XF; Wang J; Brinker CJ., *Langmuir*, **October 2008**, *24* (19), 10575-1057.

“Free-Standing, Patternable Nanoparticle/Polymer Monolayer Arrays Formed by Evaporation Induced Self-Assembly at a Fluid Interface”, Pang, J.; Xiong, S.; Jaeckel, F.; Sun, Z.; Dunphy, D.; Brinker, C. J., *J. Am. Chem. Soc.*; **March 2008**, *130* (11) 3284-3285.

“Sub-10 nm thick microporous membranes made by plasma-defined atomic layer bridged silsesquioxane precursor”, YB Jiang, G. Xomeritakis, Z. Chen, C. Dunphy, DJ Kissel, JL Cecchi, and CJ Brinker, *J. Am. Chem. Soc.*, **November 2007**, *129* (50), 15446-15447.

## Catalytic Oxidation of Olefins by Osmium Tetraoxide on Carbonaceous Supports

Laura L. Lazarus and Richard L. Brutchey\*

Department of Chemistry, University of Southern California, Los Angeles, CA 90089  
email: brutchey@usc.edu

Osmium tetraoxide ( $\text{OsO}_4$ ) is the most successful homogeneous catalyst for the dihydroxylation of olefins; however, a major drawback of this system is that osmium compounds are toxic and expensive. This makes  $\text{OsO}_4$  a perfect candidate for translation into a heterogeneous analog whereby metal waste and costs can be minimized via catalyst recovery. As such, we are developing new heterogeneous catalysts by immobilizing  $\text{OsO}_4$  directly onto carbonaceous supports. We can react  $\text{OsO}_4$  with  $\pi$ -bonds in  $\text{C}_{60}$  and carbon nanotubes (CNTs) via [3+2] cycloadditions, which serve to covalently attach the osmium center directly onto the carbon surface and give a base-stabilized  $\text{Os(VI)O}_2(\text{diolate})$  catalyst precursor. These  $\text{Os(VI)O}_2(\text{diolate})$  sites can be reoxidized to  $\text{Os(VIII)}$  to produce catalytically active sites for the dihydroxylation of olefins that are impervious to leaching because tetrasubstituted osmium diolates do not hydrolyze under normal catalytic conditions. The supported catalysts are being characterized by FT-IR, XPS, and UV-vis spectroscopies to verify the presence of osmium and its oxidation state. Using cyclohexene as a model olefin with *N*-methylmorpholine *N*-oxide as the oxidant, we are screening the effects of solvent and support type on catalytic activity and selectivity.

**Characterization of fundamental catalytic properties of MoS<sub>2</sub>/WS<sub>2</sub> nanotubes and nanoclusters for desulfurization catalysis – a surface chemistry study****Additional PIs:** none**Postdoc:** Evgueni Kadossov**Collaborators:** L. Ming (Argonne National Laboratory, Chicago, USA – SEM sample characterization); B.W. Arey (Pacific Northwest National Laboratory, Richland, USA – SEM sample characterization); R. Tenne (Weizmann Institute of Science, Israel – nanomaterials fabrication)**Contacts:** Department of Chemistry and Molecular Biology, NDSU Dept. 2735, PO Box 6050, Fargo, ND 58108-6050; Phone 701-231-9742; Email Uwe.Burghaus@ndsu.edu URL <http://www.chem.ndsu.nodak.edu>**Goal**

This project has two main goals. First, the catalytic activity of novel nanomaterials (MoS<sub>2</sub> and WS<sub>2</sub> nanoparticles and nanotubes) for hydrodesulfurization (HDS) catalysis will be characterized. In doing so, realistic supports (sapphire, silica) and materials which may constitute the next generation of HDS catalysts have been chosen. Thus, quite complex systems are analyzed with ultra-high vacuum surface science tools (AES, TDS, molecular beam scattering, etc.). Second, more traditional model systems for HDS such as vapor-deposited Mo and MoS<sub>2</sub> clusters will be studied in order to gain mechanistic insights. In this first project year we focused our attention on the first goal, namely the study of novel nanomaterials towards HDS catalysis.

**DOE Interest**

Desulfurization catalysis is important for currently used energy related applications as well as it will remain pertinent for possible future technology in the energy and transportation sector. In this project we explore the application of new nanomaterials for hydrodesulfurization catalysis.

**Recent Progress**

The results obtained so far could be published in two contributions in *Catalysis Letters*. In total, eight peer-refereed publications acknowledge this grant during this first project year.

*WS<sub>2</sub> nanoparticles supported on silica as novel hydrodesulfurization catalysts:* The reactive and non-reactive adsorption kinetics of thiophene (C<sub>4</sub>H<sub>4</sub>S) on WS<sub>2</sub> nanoparticles with fullerene-like (onion-like) structures (IF inorganic fullerenes) has been studied under ultra-high vacuum (UHV) conditions. Sample temperature ramping techniques (*adsorption kinetics*) were applied. At low temperatures, thiophene adsorbs molecularly. At higher temperatures, the formation of H<sub>2</sub>S and alkanes in a hydrogen/thiophene ambient is evident on fully sulfided as well as reduced and oxidized WS<sub>2</sub> nanoparticles (*surface reactions*).

Although some of the nanomaterials used in this project have become commercially available, powders consisting of nanoparticles and nanotubes have been provided by R. Tenne (Israel). The nanoparticles/nanotubes (NP/NT) have been deposited on silica and sapphire supports (see below) using the drop-and-dry technique. The sample morphology has been characterized by SEM/TEM (scanning electron microscopy / transmission electron microscopy) at Argonne National Laboratory by L. Ming.

The following results have been obtained:

- In collaboration with Argonne National Laboratory, the morphology and chemical composition of IF-WS<sub>2</sub> were characterized using energy-dispersive X-ray spectroscopy (EDX) and scanning electron microscopy (SEM), both before and after UHV kinetics experiments. No significant changes in morphology or chemical composition were found.
- Thiophene adsorbed molecularly on pristine (fully sulfided) IF-WS<sub>2</sub> samples at low temperatures, as verified by multi-mass thermal desorption spectroscopy (TDS).
- Thiophene binding energies are in the range of (43–60) kJ/mol, depending on coverage.
- Reactivity screening of pristine IF-WS<sub>2</sub> as well as reduced and oxidized IF-WS<sub>2</sub> have been conducted.
- The hydrodesulfurization (HDS) activity of pristine IF-WS<sub>2</sub> at UHV conditions was close to the detection limit of the mass spectrometer used. (This is in contrast to IF-MoS<sub>2</sub>; see below.) Nevertheless, H<sub>2</sub>S and alkane fragments were detected.
- Partially reduced and oxidized samples are also catalytically active (towards HDS), but with small reaction rates, similar to those detected for fully sulfided IF-WS<sub>2</sub>.
- The IF-WS<sub>2</sub> appears to be very stable under reducing conditions.

*MoS<sub>2</sub> nanoparticles supported on silica and sapphire:* The catalytic activity of the rather new nanomaterial, IF-MoS<sub>2</sub> (inorganic fullerene-like nanoparticles), towards HDS activity has been characterized under UHV conditions. Thiophene TDS as well as quasi steady-state kinetics experiments have been conducted. The IF-MoS<sub>2</sub> nanoparticles were supported on sapphire and silica.

- Thiophene adsorbed molecularly on IF-MoS<sub>2</sub> at low adsorption temperatures. In addition to a condensation peak, two TDS features were observed, corresponding to binding energies of 46 and 52 kJ/mol (1x10<sup>13</sup>/sec pre-exponential) respectively.
- Kinetics experiments with reduced and sulfided samples as well as spectroscopic data (Auger electron spectroscopy) suggest assigning the TDS peaks to sulfur- and Mo/MoO<sub>x</sub>-like adsorption sites. Thus we could identify the active sites on the catalyst, which is a significant result.
- HDS activity was present in both reduced and sulfided samples, but the largest HDS activity was seen in reduced samples.

*KMCS:* As we regularly use kinetics techniques such as TDS, it seems appropriate to work on a more sophisticated modeling of TDS data. As commercial software is unavailable, the PI's group has developed computer codes over the years. In this subproject, a kinetic Monte Carlo simulation (KMCS) algorithm for simulating experimental TDS data has been developed. The KMCS is based on the master equation approach, and applies a first-passage time analysis, i.e., the time dependence of the

kinetics is correctly matched. The KMCS-TDS scheme used here includes multiple kinetically distinct adsorption sites in order to model experimental data realistically. Furthermore, the effect of lateral interactions is included. After discussing the results of extensive tests of the algorithm by means of synthetic data (obtained by analytically integrating the Polanyi-Wigner equation), experimental TDS curves were then reproduced by the KMCS. Two applications were demonstrated: iso-butane adsorption on ZnO(0001)-Zn and n-pentane adsorption on nanotubes. We used prior experimental data of the PI group for testing the KMCS scheme. The postdoctoral associate under my mentorship, E. Kadossov, is currently working on a KMCS code of the capture zone model. He will publish the results independently.

### **Future Plans**

We started kinetics experiments on Mo clusters vapor-deposited on silica. The first sample is mounted in the kinetics apparatus. We will shortly start related molecular beam-scattering work (simultaneous with the kinetics experiments) by means of the 2<sup>nd</sup> UHV system in our group.

### **Publications acknowledging this grant**

- 1) “Adsorption of thiophene on inorganic MoS<sub>2</sub> fullerene-like nanoparticles”, *Catalysis Letters* (in press), by M. Komarneni, A. Sand, U. Burghaus
- 2) “Reactive and non-reactive interactions of thiophene with WS<sub>2</sub> fullerene-like nanoparticles: an ultra-high vacuum surface science study”, *Catalysis Letters* 125 (2008) 236–242, by J. Goering, U. Burghaus (NDSU), B.W. Arey (PNNL), O. Eidelman, A. Zak, R. Tenne (Weizmann Inst.)
- 3) “Multi-site Kinetic Monte Carlo Simulations of Thermal Desorption Spectroscopy Data”, *submitted*, by E. Kadossov and U. Burghaus
- 4) “Adsorption kinetics of small organic molecules on thick and thinner layers of carbon nanotubes”, *Chemical Physics Letters* (in press), by M. Komarneni, A. Sand, M. Lu, U. Burghaus
- 5) “Possible effect of carbon nanotube crystal structure on gas-surface interactions – the case of benzene, water, and n-pentane adsorption on SWCNTs at ultra-high vacuum conditions”, *submitted*, by M. Komarneni, A. Sand, J. Goering, U. Burghaus, (at NDSU) M. Lu, (at Argonne Nat. Lab.) L. Monica Veca, Ya-Ping Sun (at Clemson Uni.)
- 6) “Adsorption kinetics of methanol on carbon nanotubes revisited – solvent effects and pitfalls in ultra-high vacuum surface science experiments”, *submitted*, by J. Goering, M. Komarneni, A. Sand, U. Burghaus
- 7) “Gas-Carbon Nanotubes Interactions: A Review of Surface Science Studies on CNTs”, by U. Burghaus, chapter 1 (pages 1–58) in: *Carbon Nanotubes: New Research*, Avery P. Ottenhouse (ed.), Nova Science, Inc. (NY), 2008, ISBN 978-1-60692-236-1 (*in press*)
- 8) “Adsorption kinetics and dynamics of CO<sub>2</sub> on metal and metal oxide single crystals – an ultra-high vacuum surface chemistry study”, Mini review (25 pages draft) request from *Catalysis Today*, 10th international conference on CO<sub>2</sub> utilization, ICCDU-X, this time in Tianjin, China, May 2009, will be peer reviewed, by U. Burghaus



### **Ultrafast and Chemically Specific Microscopy for Atomic Scale Imaging of Nano-Photocatalysis**

Contacts: P. Sutter, Nanoscience Department and Center for Functional Nanomaterials  
Brookhaven National Laboratory, Upton, NY 11973  
Phone: (631) 344-4412; Email: [psutter@bnl.gov](mailto:psutter@bnl.gov)  
N. Camillone, Chemistry Department  
Brookhaven National Laboratory, Upton, NY 11973  
Phone: (631) 344-4412; Email: [nicholas@bnl.gov](mailto:nicholas@bnl.gov)

#### **Goal**

The objective of this program is to develop and apply novel techniques to understand photocatalytic reactions at the level of single electrons and individual molecules. Our work focuses on combining sub-nanometer spatial resolution, sub-picosecond temporal resolution and chemical specificity, to study in unprecedented detail the links between optical and electronic excitation, charge and energy transfer, and the resulting reactions that underlie heterogeneous photocatalysis.

#### **DOE Interest**

This effort addresses the long-standing challenge of characterizing chemical transformations with simultaneous temporal, spatial and chemical resolution at the molecular level. We are working to understand photoinduced processes on nanostructures and model catalyst surfaces by (1) mapping the dynamics of nonequilibrium charge populations (“hot carriers”) and the chemical reactions they drive, and (2) identifying chemical species on photocatalysts and investigating the mechanisms of their non-thermal, electron-mediated chemistry. Because photoinduced heterogeneous catalysis depends on the transfer of charge or energy from the photoexcited catalyst to an adsorbate molecule, its efficiency depends on the hot-carrier relaxation rate near the binding site, the cross section for electron (or hole) capture into adsorbate affinity levels, and the lifetime of the electronic excitation of the adsorbate. Our effort is aimed at breaking new ground in probing these fundamental mechanistic steps to contribute to the rational design of next-generation materials for solar photocatalytic chemistries.

#### **Recent Progress**

##### **1. Ultrafast Scanning Tunneling Microscopy**

To probe hot-carrier dynamics with near-atomic resolution, we are developing a new approach to time-resolved scanning tunneling microscopy (STM). Since the invention of STM, the idea of observing laser-stimulated phenomena with atomic resolution has been pursued; recent work has suggested that femtosecond laser excitation of the tip–surface junction may enable probing ultrafast dynamic phenomena. However, to date, truly simultaneous sub-picosecond- and sub-nanometer-resolved measurements have proved elusive. We have recently completed construction of a novel experimental setup that is designed to meet this challenge. Our system (Fig. 1) is capable of two-color femtosecond pulse-pair excited STM. We employ high repetition rate, sub-100 fs pulse, Ti:Sapphire laser excitation combined with a modulated-delay cross-correlation lock-in amplified detection scheme and a cryogenic ultra-high vacuum STM. The

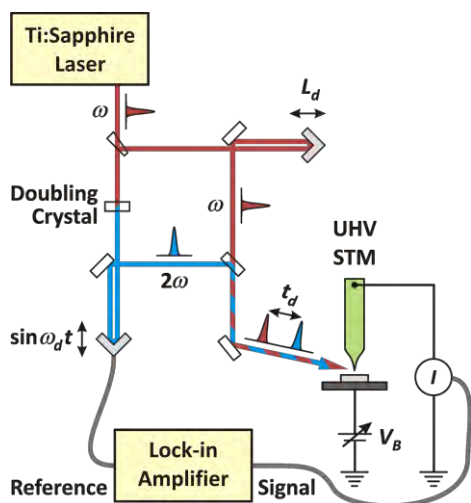


**FIG. 1.** Simplified schematic of our two-color cross-correlation setup. The femtosecond Ti:Sapphire oscillator output is split, frequency doubled, recombined, and focused onto the tip-sample junction.

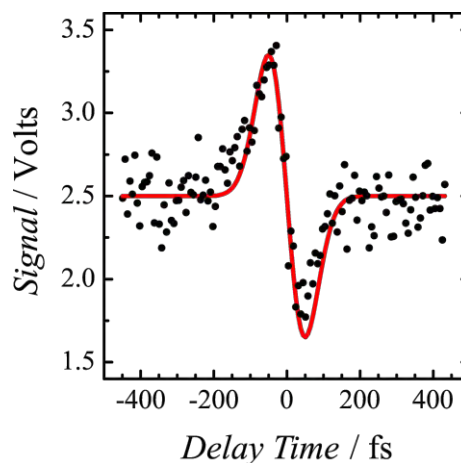


**FIG. 2.** Two-color cross-correlation measurement made with femtosecond pulses incident on the tip-sample junction [W tip, Ag(111) sample]. The signal has the form of a derivative as expected for the modulated-delay acquisition scheme. The solid line is a guide to the eye.

system is specifically designed to address the key issues that have historically hampered progress: thermal expansion and drift, vibration and optical interference.

We have recently observed the first signals that are due to photoexcited tunneling electrons (Fig. 2); this, therefore, potentially represents the first sub-ps-resolved measurement of the *local* (nm-scale) hot-carrier dynamics on a surface. The photoinduced current with the tip in tunneling range of the surface is markedly enhanced compared to that with the tip retracted and evidences distinct dynamics consistent with the slower relaxation of electrons near the Fermi level. Systematic measurements aimed at deconvolving the contributions of photoemitted and tunneling electrons to the observed signal and understanding these exciting results are underway.

## 2. Reactions Induced by Atomically-Precise Hot-Carrier Injection

Vacuum tunneling in STM can be used to inject charge carriers with a well-defined energy distribution into individual atoms or molecular bonds. This local charge injection is a versatile tool for studying reactions driven by charge and/or energy transfer from a population of hot carriers as found in photocatalysis. When coupled to *ab-initio* theory, such measurements can provide information on the nature of the molecule-electron interaction, energetic thresholds for the onset of different reaction branches, and channels for (re-)distribution of energy within a single molecule. While such experiments have been performed on metals and on selected semiconductor surfaces, they have not been attempted on materials relevant to photocatalysis.

We have successfully developed the capability of injecting charge carriers into individual surface sites and bonds of adsorbed molecules on rutile  $\text{TiO}_2(110)$  at temperatures between 50 and 100 K. The enhanced stability in cryogenic STM has allowed us to perform unique, detailed spectroscopic studies on single adsorbed molecules on this model photocatalyst surface. We have used local carrier injection to drive and characterize a variety of surface processes.

First, we have demonstrated that the injection of tunneling electrons into surface sites along the bridging oxygen atom ( $\text{O}_{\text{br}}$ ) row near a single O-atom vacancy on  $\text{TiO}_2(110)$  can be used to trigger the controlled hopping of the vacancy along the  $\text{O}_{\text{br}}$  row. We have thus manipulated vacancies to create geometric structures such as lines, dimers, and multi-vacancy clusters

(Fig. 3). By analyzing the dependence of the vacancy hopping rate on the tunneling current, we have investigated the carrier-mediated hopping mechanism. Our results demonstrate the possibility of constructing larger complexes of reactive sites, such as O-vacancies, to probe their unique stability, electronic structure and chemical reactivity.

We have also examined in detail the non-thermal desorption of hydrogen atoms from bridging hydroxyls (*i.e.*, H chemisorbed on  $O_{br}$ ) on  $TiO_2(110)$ . By desorbing H-atoms with single-atom precision (Fig. 4), we have obtained detailed information on the mechanism. Our data clearly show H-desorption to be a two-electron process. Concurrent *ab-initio* calculations show that the underlying mechanism involves charge transfer into the antibonding orbital of the hydroxyl complex: addition of a single electron leaves the O–H bond nearly unchanged, but adding a second electron increases the equilibrium bond length by over 1 Å, breaking the bond and desorbing the H.

Finally, we have investigated the structure and electron-initiated diffusion and dissociation of molecularly adsorbed water on  $TiO_2$ . We have found that: (1)  $H_2O$  exhibits multiple adsorption geometries; (2) electron injection into single molecules shows adsorption-geometry-dependent energy re-distribution pathways (*e.g.*, dissociation vs. diffusion); (3) atomically precise electron injection can be used to cleave individual O–H bonds in  $H_2O$  one-by-one, to produce first a  $Ti_{5f}$ -bound OH species and finally leave behind a strongly chemisorbed O-atom; and (4) bias-dependent STM can readily map low-lying *unoccupied* orbitals of *individual* adsorbed water molecules providing information that is inaccessible by other techniques.

### Future Plans

We are working toward sub-ps local-probe investigations of size-dependent hot-carrier dynamics in supported metal nanoparticles and spatially-resolved photocatalysis on oxide-supported metal nanoparticles. We will investigate water splitting and related chemistries on metal oxides and oxide-supported metal nanoparticles. Combining ultrafast laser excitation, local electronic excitation probing, local charge injection and STM imaging, we will be uniquely positioned to study reaction dynamics relevant to a fundamental understanding of the electron/hole and molecular dynamics at regular lattice sites, defect sites, and on supported nanoparticles. Ultimately we aim to understand the fundamental connections relating photocatalyst structure, thermal and non-thermal excitation, carrier dynamics and reaction efficiency and selectivity.

### Publications

Danda P. Acharya, Cristian V. Ciobanu, Peter W. Sutter, “Manipulation of Single Oxygen Vacancy Defects on  $TiO_2(110)$ ,” *Phys. Rev. Lett.*, **in review** (2009).

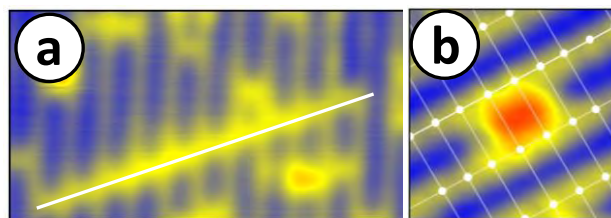


FIG. 3. STM-current induced oxygen vacancy formations: (a) a diagonal line of oxygen vacancies, (b) an oxygen vacancy dimer.

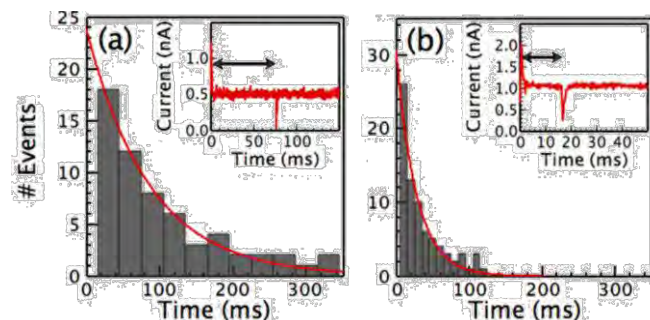


FIG. 4. Insets: Tunneling current vs. time for single H-atom desorption from  $O_{br}$  sites on  $TiO_2(110)$ . Analysis of desorption times for many (>100) individual atoms reveals the per-electron desorption yield. Tunneling current setpoint: (a) 0.5 nA; (b) 1.0 nA.

**Oxide-Supported Metal Nanoparticles:  
Correlating Catalytic Kinetics, Energetics and Surface Structure**

Postdoc: Junfa Zhu  
Students: Lucas Cameron, Jason Farmer, Matthew Thibodaux, Jason Sellers, Eric Karp  
Collaborators: Prof. Hajo Freund and Dr. Svetlana Schauermaun, Fritz Haber Institute, Berlin;  
Prof. Graeme Henkelman, University of Texas at Austin;  
Prof. Vladimir Matolin, Charles University, Prague, Czech Republic;  
Drs. Carsten Stegelmann and Anders Andreasen, Aalborg University and Danish  
National Laboratory for Sustainable Energy, Denmark;  
Dr. Chuck Peden, PNNL, Prof. Chuck Mims, University of Toronto; and  
Prof. Manos Mavrikakis, University of Wisconsin.  
Contacts: Chemistry Department, Box 351700, University of Washington,  
Seattle, WA 98195-1700, [campbell@chem.washington.edu](mailto:campbell@chem.washington.edu)

**Goals**

To provide the basic understanding of surface structure / function relationships needed to develop new and improved catalyst materials, involving metal nanoparticles supported on oxide surfaces, for reactions of importance in energy conversion and environmental protection. To clarify the geometric, energetic and dynamic factors which control the atomic-level structure of certain metal / oxide interfaces, and the interplay between this structure and the chemical / catalytic reactivity of metal-on-oxide surfaces.

**DOE Interest**

More efficient processes for a variety of chemical conversions must be developed if we are to have the energy needed for sustained industrial and economic development using alternate feedstreams and avoid serious environmental problems for human health. Solid catalysts hold great promise for many of these new processes, and some of the most promising involve nanoparticles of late transition metals supported on oxides. We are pursuing an experimental research program aimed to provide the basic understanding needed to improve such catalysts for these important reactions.

**Recent Progress**

We have prepared model catalysts consisting of metal nanoparticles supported on single-crystalline oxide surfaces, and structurally characterized them using a variety of ultrahigh vacuum surface science techniques. Interactions at the interface between the metal and the oxide dictate the metal particle morphology, which in turn controls catalytic activity and selectivity in many cases. We have measured the strengths of these interactions, and try to correlate these bonding energetics with catalyst performance (chemisorption and catalytic reactivity, resistance to sintering, etc.). We have also developed new calorimetric techniques for measuring adsorption / surface reaction energies of well-defined surface species which is broadly important to all of surface chemistry. By knowing these energies for catalytic intermediates and nanostructures on well-chosen model catalysts, we position ourselves to better understand the relationship between the nanoscopic details of catalyst structure and the industrially-important parameters of catalyst performance (activity, selectivity, resistance to sintering, etc.).

### *Metal Adsorption Energetics*

We performed calorimetric measurements of Ca and Li adsorption energies on MgO(100) and ion-damaged MgO(100) surfaces as a detailed function of coverage. In collaboration with Graeme Henkelman's group at the University of Texas, we showed that these energies provide a powerful way to assess the nature of the defect sites on oxide surfaces and even their lateral distributions, when combined with Henkelman's DFT calculations and kinetic modeling. We have started measurements of metal adsorption energies on CeO<sub>2</sub>(111). We also are measuring the chemical and high-pressure catalytic reactivity and sintering kinetics of supported nanoparticles, and will correlate these with the lateral diameter, thickness and composition of the metal nanoparticles and the structure and stoichiometry of the oxide support surface upon which they sit, using the measured energetics to provide fundamental understanding of these correlations. The energetics of metal atoms on nanoparticle catalysts, and the strength with which they bond adsorbed intermediates, provide the key thermodynamic underpinnings to the structure – function relationships we strive to understand.

### *Molecule Adsorption Energetics on Size-selected Metal Nanoparticles*

In an ongoing collaboration with Prof. Hajo Freund at the Fritz Haber Institute in Berlin, we have designed, built and tested a new single crystal adsorption calorimeter apparatus in Prof. Freund's lab in Berlin. We used it to make the first-ever direct measurements of adsorption heats of a small molecule (CO) on size-controlled metal nanoparticles on a single-crystal oxide surface. We hope to correlate these size effects with the effect of size on metal atom stability. That our calorimeter design has been employed by such a well-respected group suggests that it will soon have an even broader impact.

### *Studies of Catalytic Reaction Kinetics and Mechanisms*

Identifying the “rate-determining step” has been of central importance in understanding chemical kinetics in multi-step reaction mechanisms for decades. An even more useful concept is to identify the rate-controlling transition states and the rate-controlling intermediates. We have found a rigorous method for identifying these for cases where a microkinetic model of the mechanism exists. Since these key species are the ones whose relative energies most strongly influence the net reaction rate, they also identify the species whose energetics must be most accurately measured or calculated to achieve an accurate kinetic model for any reaction mechanism. These few distinct chemical species are also the ones whose relative energies one could adjust to achieve a faster or slower net reaction rate. Thus, it is very important to identify these rate-controlling transition states and rate-controlling intermediates for both applied and basic research, whether in catalysis or any other field of chemistry.

We also performed kinetic measurements on supported Pt catalysts which show that the reverse water gas shift reaction does *not* proceed mainly through dissociative CO<sub>2</sub> adsorption (as typically assumed), since the rate is 1000-fold faster than the maximum possible rate of CO<sub>2</sub> dissociation. In collaboration with Manos Mavrikakis, we showed that the absolute rates and reaction orders are consistent with the rate being dominated by a mechanism he found by DFT calculations that involves instead a key adsorbed COOH intermediate produced from CO<sub>2</sub> reacting with adsorbed H. We also collaborated at PNNL's EMSL with Dr. Chuck Peden (PNNL) and Prof. Chuck Mims (University of Toronto) to perform transient kinetics measurements which elucidate the mechanism methanol synthesis over Cu catalysts, using powerful *in situ fast-scan FTIR* and mass spectroscopy.

## Future plans

To clarify the unique role of ceria as a support, we will continue to measure metal adsorption energies on CeO<sub>2</sub>(111) thin films with different defect densities and extents of surface reduction. The most difficult part of this work is preparing a pulsed metal atom beam of sufficient intensity and stability to measure metal adsorption energies. We are building a new ultrahigh vacuum calorimeter chamber with a geometry that will make this much easier.

## Publications acknowledging this grant's support (2007-9)

1. A Kinetic Model for Sintering of Supported Metal Particles with Improved Size-dependent Energetics, and Applications to Au on TiO<sub>2</sub>(110), S. C. Parker and C. T. Campbell, *Physical Review B* 75, Art. No. 035430, 15 pages (2007).
2. Reactivity and Sintering Kinetics of Au / TiO<sub>2</sub>(110) Model Catalysts: Particle Size Effects, S. C. Parker and C. T. Campbell, *Topics in Catalysis*, 44, 3-13 (2007).
3. Catalyst Sintering Kinetics and its Effect on Particle Size Distributions, with Examples for Gold Supported on TiO<sub>2</sub>, C. T. Campbell and S. C. Parker, *Proceedings of the 2007 Meeting of the North American Catalysis Society* (Houston).
4. Kinetic Monte Carlo simulations of Pd deposition and island growth on MgO(100), L. Xu; G. Henkelman\*; C. T. Campbell; H. Jonsson, *Surface Sci.* 601, 3133-42 (2007).
5. Growing Pt Nanowires as a Densely Packed Array on Metal Gauze, E. P. Lee, Z. Peng, D. M. Cate, Ho. Yang, C. T. Campbell and Y. Xia\*, *Journal of the American Chemical Society* (Rapid Communication), 129, 10634-5 (2007).
6. SPR Microscopy and Its Applications to High-Throughput Analyses of Biomolecular Binding Events and Their Kinetics, C. T. Campbell and G. Kim, *J. Biomaterials* 28, 2380–2392 (2007).
7. Ca Adsorption on MgO(100): Energetics, Structure and Role of Defects, J. F. Zhu, J. A. Farmer, N. Ruzicky, L. Xu; C. T. Campbell\* and G. Henkelman, *Journal of the American Chemical Society* 130, 2314-22 (2008). (This DOE plus Other Grants of Co-Authors.)
8. Catalytic Reaction Energetics by Single Crystal Adsorption Calorimetry: Hydrocarbons on Pt(111), O. Lytken, W. Lew and C. T. Campbell\*, *Chemical Society Reviews* (invited paper for special issue in honor of Ertl's Nobel Prize) 37, 2172 – 2179 (2008).
9. Isotope effects in methanol synthesis and the reactivity of copper formate on a Cu/SiO<sub>2</sub> catalyst, Y. Yang, C. Mims\*, R. Disselkamp, D. Mei, J.-H. Kwak, J. Szanyi, C. H. F. Peden and C. T. Campbell, *Catalysis Letters* 125, 201-8 (2008).
10. Experimental measurements of the energetics of surface reactions, C. T. Campbell and O. Lytken, *Surface Science* (invited paper for special issue in honor of Ertl's Nobel Prize, in press).
11. Defect sites and their distributions on MgO(100) by Li and Ca adsorption calorimetry, J. A. Farmer, C. T. Campbell, L. Xu; and G. Henkelman, *Journal of the American Chemical Society* 131, 3098-3103 (2009).
12. The degree of rate control: how much the energies of intermediates and transition states control rates, C. Stegelmann, A. Andreasen, C. T. Campbell, *Journal of the American Chemical Society* (in press).
13. Lithium Adsorption on MgO(100): Calorimetric Energies and Structure, J. A. Farmer, N. Ruzicky, J. F. Zhu and C. T. Campbell, *Physical Review B* (submitted).

**Structure-Property Relationship in Metal Carbides and Bimetallic Alloys**

Graduate Students: Michael Humbert, Carl Menning, Thomas Kelly  
Collaborators: M.A. Barteau (Univ. Delaware), J.A. Dumesic (Univ. Wisconsin), P. Liu (Brookhaven National Lab), M. Neurock (Univ. Virginia)  
Contact: J.G. Chen, Department of Chemical Engineering, University of Delaware, jgchen@udel.edu

**Research Goals:**

It is well known that the electronic and catalytic properties of transition metals can be modified by alloying with carbon to form carbides or with another metal to produce bimetallic alloys. The carbides and bimetallic alloys often demonstrate properties that are distinctively different from those of the pure parent metals. The objective of the current project is to use selected carbides and bimetallic alloys as model systems to unravel the relationship between the electronic/geometric structures and the chemical/catalytic properties to assist the rational design of catalytic materials. Furthermore, it is becoming apparent of the critical needs to identify alternative catalysts that can either replace Platinum (Pt) or substantially reduce the amount of Pt. Metal carbides and bimetallic alloys are potential materials to achieve such objective.

**Research Approaches:**

The current research project involves three parallel approaches: (1) Fundamental surface science investigations of the reaction mechanisms of several carefully-chosen probe reactions on carbide and bimetallic surfaces. (2) Correlation of chemical activities of these surfaces with their electronic properties using a combination of experimental measurements and DFT modeling. (3) Reactor or electrochemical evaluation of relevant carbide and bimetallic powders/thin films to bridge the “materials gap” and “pressure gap” between model surface science studies and heterogeneous catalysis/electrocatalysis.

**Recent Progress:****A. Designing Bimetallic Surfaces for Selective Hydrogenation**

Our studies of the low-temperature hydrogenation of C=C and C=O bonds of unsaturated hydrocarbons on the subsurface Pt-Ni-Pt(111) structure were one of the earliest examples that clearly demonstrated the novel reaction pathways that were not present on parent metals. In the past year we extended these hydrogenation studies to other Pt-3d-Pt(111) surfaces to correlate the general trend between surface d-band center, binding energy, and hydrogenation activity and selectivity. For example, by correlating the DFT calculations of the binding energy of cyclohexene on the Pt-Ni-Pt(111), Pt-Co-Pt(111), Pt-Fe-Pt(111) and Pt-Cu-Pt(111) subsurface structures with experimental data, a volcano relationship was observed for the hydrogenation activity as the d-band center moves further away from the Fermi level, i.e, when the adsorption of cyclohexene is too weak for the hydrogenation to occur.

**B. Extending Model Surfaces to Polycrystalline Films and Supported Catalysts**

One of the main objectives in the past year is to perform surface science and catalytic studies on polycrystalline films and supported catalysts, whose chemical compositions were

identified from the corresponding single crystal carbide and bimetallic surfaces. For example, we have performed extensive investigation of the synthesis and characterization of polycrystalline, phase-pure WC (tungsten monocarbide) thin films using Physical Vapor Deposition. The surface chemistry of the polycrystalline WC film was investigated using surface science techniques, such as TPD and HREELS. The comparative studies showed strong similarities between polycrystalline WC with WC/W(110) using several probe molecules. Another example is the synthesis and catalytic evaluation of supported Ni-Pt and Co-Pt catalysts, which showed the unique low-temperature hydrogenation pathway that was initially identified on the Ni/Pt(111) and Co/Pt(111) surfaces. We utilized a wide range of characterization techniques, including TEM and EXAFS to confirm the formation of the bimetallic structures in the supported catalysts. The hydrogenation activities were then evaluated using both batch and flow reactors, which confirmed a correlation between model surfaces and supported catalysts.

### **C. Anchoring Bimetallic Structures on Carbides to enhance Activity and Stability**

Our DFT and experimental results have revealed that the subsurface Pt-Ni-Pt structure, which is desired for enhanced hydrogenation activity and selectivity, is not thermodynamically stable in the presence of adsorbed oxygen. The subsurface Pt-Ni-Pt structure is also attributed for the enhanced Oxygen Reduction Reaction (ORR) activity at the cathode of PEM fuel cells. The objective for this part of the research is to enhance the stability by anchoring the subsurface Ni on a carbide substrate, such as tungsten monocarbide (WC). Another potential advantage of the Pt-Ni-WC structure is to replace the bulk Pt with WC, which should lead to a significant reduction of Pt in the catalyst formulation. Our preliminary results confirmed both advantages by anchoring the bimetallic structures on the WC substrate.

#### **Future Plans:**

In the next year we will use several probe reactions to further investigate the activity, selectivity and stability of carbides and bimetallic alloys in heterogeneous catalysis: (1) We will investigate the hydrogenation activity, selectivity and stability of alkenes and unsaturated aldehyde on the Pt-Ni-WC surfaces, to further unravel the correlation between the selective hydrogenation activity with the d-band center of these surfaces. (2) We will continue studies of Pt-based bimetallic catalysts as cathode electrocatalysts for the reduction of oxygen; our main focus in these studies will be to determine the stability of the Pt-3d bimetallic structures under *in-situ* fuel cell conditions and to identify ways to improve their electrochemical stability using a combination of UHV surface science, DFT modeling, and *in-situ* electrochemical measurements.

#### **DOE Interest:**

The overall goal of the current research is to demonstrate the possibility to predict and design materials with desirable catalytic properties. We believe that carbides and bimetallic alloys are excellent model systems to directly correlate the relationship between electronic/geometric structures and chemical/catalytic properties. Such structure-property relationship, to be determined using a combination of surface science experiments, DFT modeling, and catalytic studies, should help in predicting and controlling the catalytic and electrocatalytic properties of transition metals in general and carbide/bimetallic catalysts in particular.



### Publications Sponsored by Current DOE Grant (2007-2008):

- L.E. Murillo, A.M. Goda and J.G. Chen, "Selective Hydrogenation of C=O Bond in Acrolein through Architecture of Bimetallic Surface Structures", *J. Am. Chem. Soc.* 129 (2007) 7101.
- E.C. Weigert, M.B. Zellner, A.L. Stottlemeyer and J.G. Chen, "A Combined Surface Science and Electrochemical Study of Tungsten Carbides as Anode Electrocatalysts", *Topics in Catal.* 46 (2007) 349-357.
- O. Skoplyak, C.A. Menning, M.A. Barteau and J.G. Chen, "An experimental and theoretical study of the trend in the reactivity of methanol on Co/Pt(111) and Ni/Pt(111) bimetallic surfaces", *J. Chem. Phys.* 127 (2007) 114707.
- J.G. Chen, C.A. Menning and, M.B. Zellner, "Monolayer Bimetallic Surfaces: Experimental and Theoretical Studies of General Trends in the Electronic and Chemical Properties", (*Invited Review*), *Surf. Sci. Reports*, 63 (2008) 201–254.
- C.A. Menning, and J.G. Chen, "Thermodynamics and Kinetics of Oxygen-Induced Segregation of 3d Metals in Pt-3d-Pt(111) and Pt-3d-Pt(100) Bimetallic Structures", *J. Chem. Phys.* 128 (2008) 164703.
- L.E. Murillo and J.G. Chen, "A Comparative Study of the Adsorption and Hydrogenation of Acrolein on Pt(111), Ni(111) Film and Pt-Ni-Pt(111) Bimetallic Surfaces", *Surf. Sci.* 602 (2008) 919-931.
- W. Chen, T.E. Madey, A.L. Stottlemeyer, J.G. Chen, P. Kaghazchi, and T. Jacob, "Structure Sensitivity in Adsorption and Decomposition of NO on Ir", *J. Phys. Chem. C*, 112 (2008) 19113-19120.
- O. Skoplyak, C.A. Menning, M.A. Barteau and J.G. Chen, "Reforming of oxygenates for H<sub>2</sub> production on 3d/Pt(111) bimetallic surfaces", *Topics in Catal.* 51 (2008) 49-59.
- M.P. Humbert and J.G. Chen, "Correlating Hydrogenation Activity with Binding Energies of Hydrogen and Cyclohexene on M/Pt(111) (M = Fe, Co, Ni, Cu) Bimetallic Surfaces", *J. Catal.* 257 (2008) 297-306.
- Y. Shu, L.E. Murillo, J.P. Bosco, W. Huang, A.I. Frenkel, and J.G. Chen, "The Effect of Impregnation Sequence on the Hydrogenation Activity and Selectivity of Supported PtNi Bimetallic Catalysts", *Appl. Catal. A*, 339 (2008) 169-179.
- S. Lu, W.W. Lonergan, J.P. Bosco, S. Wang, Y. Zhu, Y. Xie, and J.G. Chen, "Low Temperature Hydrogenation of Benzene and Cyclohexene: A Comparative Study between  $\gamma$ -Al<sub>2</sub>O<sub>3</sub> Supported PtCo and PtNi Bimetallic Catalysts", *J. Catal.* 259 (2008) 260-268.
- L.E. Murillo and J.G. Chen, "Adsorption and Reaction of Propanal, 2-Propenol and 1-Propanol on Ni/Pt(111) Bimetallic Surfaces", *Surf. Sci.* 602 (2008), 2412-2420.
- M.P. Humbert, L.E. Murillo, and J.G. Chen, "Rational Design of Pt-Based Bimetallic Catalysts with Enhanced Hydrogenation Activity", *ChemPhysChem*, 9 (2008) 1262-1264.
- N. Ji, T. Zhang, M. Zheng, A. Wang, H. Wang, X. Wang, J.G. Chen, "Direct catalytic conversion of cellulose into ethylene glycol using Ni-promoted tungsten carbide catalysts", *Angew. Chem. Int. Ed.* 47 (2008) 8510-8513 (*Journal Cover; Featured in Angewandte Press Release in Sept. 2008*).

**Dedicated Beamline Facilities for Catalytic Research –  
Synchrotron Catalysis Consortium (SCC)**

Research Staff: Nebojsa Marinkovic, University of Delaware  
Collaborators/co-PIs: Chi-Chang Kao, Brookhaven National Laboratory  
Steve L. Hulbert, Brookhaven National Laboratory  
Jan Hrbek, Brookhaven National Laboratory  
David R. Mullins, Oak Ridge National Laboratory  
Steve Overbury, Oak Ridge National Laboratory  
Jose A. Rodriguez, Brookhaven National Laboratory  
Jonathan Hanson, Brookhaven National Laboratory  
Simon R. Bare, UOP LLC  
Undergraduate interns: J. Bosco, J. Quigley (U. Delaware), E. Horowitz (Yeshiva U.), E. Frenkel (Binghamton U.), Rebecca Segal (Yeshiva U.)  
Contact: J.G. Chen, Dept. of Chemical Engineering, Univ. of Delaware, jgchen@udel.edu

**Goals:** The mission of the Synchrotron Catalysis Consortium (SCC), which is the first of its kind in the US, is to promote the utilization of synchrotron techniques for cutting-edge catalytic research under in-situ conditions. The consortium PIs and co-PIs are from academic, national, and industrial laboratories and have extensive experience in the areas of catalysis, electrocatalysis, advanced materials, and synchrotron spectroscopies. The beamlines and supporting facilities that SCC members acquired and built are located in the National Synchrotron Light Source (NSLS) at Brookhaven National Laboratories. A primary goal of the SCC team is to provide assistance and to develop new sciences/techniques to the catalysis community through the following concerted efforts:

1. Dedicated beamtime on two X-ray Absorption Fine Structure (XAFS) beamlines, and, and combined X-ray diffraction (XRD) / XAFS measurements on a recently-acquired beamline
2. Dedicated facilities, including state-of-the-art *in-situ* reaction cells, gas-handling systems, and advanced detectors
3. A dedicated research staff to assist the experimental set-up and safety training
4. Training courses for graduate students and postdoctoral fellows on XAFS techniques and data analysis
5. Assistance in idea development and proposal-writing for potential XAFS users from the catalysis community
6. Development and test of new hardware/software for catalytic and electrocatalytic research

**Recent Progress:**

**A. Dedicated Beamlines and Infrastructure:** The SCC members have continued to make significant progress in setting up dedicated facilities for the catalysis community on three beamlines, X18A, X18B and X19A. The X18B and X19A were the first two beamlines that were established by the consortium during the first three-year of the grant. The access of SCC users to beamline X18A was provided last year by the National Synchrotron Light Source due to overwhelming

demands by the catalysis communities to the two existing SCC beamlines. The dedicated SCC beamline staff, Dr. Ned Marinkovic, provided assistance to the catalysis user groups in many ways, including training the users on beamline operation and safety, setting up dedicated reactors and gas-handling systems, and providing experimental assistance when needed.

**B. Workshop and Training Courses:** In order to promote the utilization of synchrotron facilities in the catalysis and electrocatalysis communities, it is critical to train graduate students, postdoctoral fellows, and research staff on planning their future research program, data collection and data analysis. The SCC PIs and staff have provided training to new catalysis users. A. Frenkel gave on-site help 2-3 days a week, and consulted visiting groups on issues ranging from data analysis to planning XAFS experiments. SCC members have organized several training courses and workshops in the past year.

**C. New instrumentation for catalysis research:** We have made significant progress in the development of new synchrotron capabilities to catalysis studies:

- *An instrument for synchronous DRIFTS/XAFS/MS measurements (X19A and X18A)*
- *Combined QEXAFS/XRD instrument (X18A)*
- *Multi-sample reactor for projects with faster screening (X19A and X18A)*

**DRIFTS/XAFS/MS measurements:** Together with the researchers from Harrick Scientific, we are in the process of designing a Diffuse Reflectance Infrared Fourier Transform Spectroscopy (DRIFTS) cell for transmission XAFS. The cell can be used for *in situ* measurement at the following conditions: temperatures up to 800 °C, gaseous environment.

**Combined QEXAFS/XRD instrument:** XAFS and XRD techniques give complementary information about the structure of catalytic materials. The SCC and NSLS teams are currently building the first in the US instrument for combined, time-resolved Quick XRD/XAFS experiments at beamline X18A. Such a combination will allow the measurement of changes in the actual structure (in the short, medium and long range order), electronic properties and chemical activity of heterogeneous catalysts simultaneously. First experiments of the combined capability were successful, upgrades to QEXAFS are in progress.

**Multi-sample reactor for projects with faster screening:** With the help of Drs. Marshall and Kropf of the Argonne National Lab, we have fabricated a multi-sample reactor to assist catalysis users who plan to characterize multiple catalysts under the same *in situ* conditions. First experiments of the visiting group from Tufts University, utilizing this reactor were successful.

**DOE Interest:** The availability of well-maintained, user-friendly and state-of-the-art synchrotron facilities, as provided by SCC, should help a large number of catalysis and electrocatalysis groups in their efforts to perform cutting-edge beamline research. The SCC also provides a new model for operating synchrotron facilities; such model demonstrates a closer interaction between funding agencies, beamline scientists and external researchers. The closer interaction should lead to the more efficient utilization of the synchrotron facilities, which ultimately benefits the nation as a whole by increasing the return on the investments made in our national laboratory system. Similar types of synchrotron consortium for catalysis currently exist in Europe and Japan. *The current consortium represents a critical first step for the catalysis community in the United States to remain competitive in catalytic and electrocatalytic research using synchrotron techniques.*

## Publications Acknowledged Current DOE Grant (2007-2008):

**Overall there are over 70 publications. Below is a selected list of publications:**

- C Johnson, B Long, J Nguyen, V Day, A Borovik, B Subramaniam, J Guzman, Correlation between Active Center Structure and Enhanced Dioxygen Binding in Co(salen) Nanoparticles: Characterization by In Situ Infrared, Raman, and X-ray Absorption Spectroscopies, *J. Phys. Chem. C*, **112**, 12272-12281 (2008).
- W Shen, F Huggins, N Shah, G Jacobs, Y Wang, X Shi, G Huffman, Novel Fe–Ni Nanoparticle Catalyst for the Production of CO- and CO<sub>2</sub>-free H<sub>2</sub>, *Appl. Catal. A*, **351**, 102-110 (2008).
- D Kim, J Kwak, J Szanyi, S Cho, C Peden, Roles of Pt and BaO in the Sulfation of Pt/BaO/Al<sub>2</sub>O<sub>3</sub> Lean NO<sub>x</sub> Trap Materials: Sulfur K-edge XANES and Pt LIII XAFS Studies, *J. Phys. Chem. C*, **112**, 2981-2987 (2008).
- S Ma, K Nam, W Yoon, X Yang, K Ahn, K Oh, K Kim, Electrochemical Properties of Manganese Oxide Coated onto Carbon Nanotubes for Energy-Storage Applications, *J. Power Sources*, **178**(1), 483-489 (2008).
- C Lu, J Raitano, S Khalid, L Zhang, S Chan, Cubic Phase Stabilization in Nanoparticles of Hafnia-Zirconia Oxides: Particle-Size and Annealing Environment Effects, *J. Appl. Phys.*, **103**, 124303 (2008).
- G. Jacobs, M. Milling, Y. Ji, Patterson, P.M., Sparks, D.E., and Davis, B.H., “Characterizing Hf<sub>x</sub>Zr<sub>1-x</sub>O<sub>2</sub> by EXAFS: Relationship Between Bulk and Surface Composition, and Impact on Catalytic Selectivity for Alcohol Conversion,” *Catalysis Letters* **127** (2009) 248-259.
- X. Teng, Q Wang, P Liu, W Han, A Frenkel, W Wen, N Marinkovic, J Hanson, J Rodriguez, Formation of Pd/Au Nanostructures from Pd Nanowires via Galvanic Replacement Reaction, *J. Am. Chem. Soc.*, **130**(3), 1093-1101 (2008).
- M. Knecht, M Weir, A Frenkel, R Crooks, Structural Rearrangement of Bimetallic Alloy PdAu Nanoparticles Within Dendrimer Templates to Yield Core/Shell Configurations, *Chem. Mater.*, **20**, 1019-1028 (2008).
- S. Oyama, Y Lee, The Active Site of Nickel Phosphide Catalysts for the Hydrodesulfurization of 4,6-DMDBT, *J. Catal.*, **258**, 393–400 (2008).
- Y. Shu, L Murillo, J Bosco, W Huang, A Frenkel, J Chen, The Effect of Impregnation Sequence on the Hydrogenation Activity and Selectivity of Supported Pt/Ni Bimetallic Catalysts, *Appl. Catal. A*, **339**, 169-179 (2008).
- K. Suriye, R Lobo-Lapidus, G Yeagle, P Praserthdam, R Britt, B Gates, Probing Defect Sites on TiO<sub>2</sub> with H<sub>3</sub>Re<sub>3</sub>(CO)<sub>12</sub>: Spectroscopic Characterization of the Surface Species, *Chem. Eur. J.*, **14**, 1402 (2008).
- W. Deng, A Frenkel, R Si, M Flytzani-Stephanopoulos, Reaction-Relevant Gold Structures in the Low Temperature Water-Gas Shift Reaction on Au-CeO<sub>2</sub>, *J. Phys. Chem. C*, **112**(33), 12834-12840 (2008).
- S. Lu, W Lonergan, J Bosco, S Wang, Y Zhu, Y Xie, J Chen, Low Temperature Hydrogenation of Benzene and Cyclohexene: A Comparative Study Between gamma-Al<sub>2</sub>O<sub>3</sub> Supported PtCo and PtNi Bimetallic Catalysts, *J. Catal.*, **259**, 260-268 (2008).
- E. Kunkes, D Simonetti, J Dumesic, W Pyrz, J Chen, The Role of Rhenium in the Conversion of Glycerol to Synthesis Gas Over Carbon Supported Platinum-Rhenium Catalysts, *J. Catal.*, **260**, 164-177 (2008).
- Q. Wang, J Hanson, A Frenkel, Solving the Structure of Reaction Intermediates by Time-Resolved Synchrotron X-ray Absorption Spectroscopy, *J. Chem. Phys.*, **129**, 234502 (2008).
- E. Poverenov, I Efremenko, A Frenkel, Y Ben-David, L Shimon, G Leitens, J Marin, D Milstein, A Terminal Pt(IV)-oxo Complex Bearing no Stabilizing Electron Withdrawing Ligands and Exhibiting Diverse Reactivity, *Nature*, **455**, 1093-1096 (2008).

## Real-Time In-Situ Optical Imaging of Nanocatalysis at the Single-Molecule Level

Peng Chen

Department of Chemistry and Chemical Biology, Cornell University, Ithaca, NY 14853  
Email: pc252@cornell.edu

Nanoparticles are important catalysts for many chemical transformations, ranging from petroleum processing to energy production. Understanding nanoparticle activity is essential, but hampered by their static and dynamic structural heterogeneity. Using single-molecule fluorescence microscopy, we imaged the real-time catalysis by Au-nanoparticles in aqueous environments at the single-particle level.<sup>1-4</sup> We find that for product generation, all Au-nanoparticles follow a Langmuir-Hinshelwood mechanism but with heterogeneous reactivity; and for product dissociation, subpopulations are present that show differential selectivity between parallel reaction pathways with distinct kinetics. Individual Au-nanoparticles show large temporal activity fluctuations, attributable to both catalysis-induced and spontaneous dynamic surface restructuring whose timescales at the surface catalytic and product docking sites can be quantified. Individual nanoparticles also show reactant-concentration dependent surface switching behaviors, and the switching concentration differs largely from one particle to another. These studies reveal the intricate interplay of catalysis, heterogeneous reactivity, surface restructuring dynamics, and variable surface sites in nanocatalysis.

### References

1. W. Xu, J. S. Kong, Y.-T. E. Yeh & P. Chen. Single-molecule nanocatalysis reveals heterogeneous reaction pathways and catalytic dynamics. *Nature Mater.* **7**, 992-996 (2008).
2. W. Xu, J. S. Kong & P. Chen. Single-molecule kinetic theory of heterogeneous and enzyme catalysis. *J. Phys. Chem. C* **113**, 2393-2404 (2009).
3. W. Xu, J. S. Kong & P. Chen. Probing the catalytic activity and heterogeneity of au-nanoparticles at the single-molecule level. *Phys. Chem. Chem. Phys.*, DOI:10.1039/B820052A (2009).
4. P. Chen, W. Xu, X. Zhou, D. Panda & A. Kalininskiy. Single-nanoparticle catalysis at single-turnover resolution. *Chem. Phys. Lett.* **470**, 151-157 (2009).

**Nitrogen-Substituted Zeolite Catalysts for Base-Catalyzed Reactions: Where is the Nitrogen?**

Additional PIs: Scott M. Auerbach, George W. Huber  
Postdoc: Geoffrey A. Tompsett  
Students: Karl D. Hammond, Murad Gharibeh, Vishal Agarwal  
Collaborators: Clare P. Grey (Stony Brook University)  
Contacts: University of Massachusetts, Department of Chemical Engineering, 159 Goessmann Laboratory, Amherst, MA 01003; [wconner@ecs.umass.edu](mailto:wconner@ecs.umass.edu)

**Goals**

Development of basic catalysts within controlled pores for the production of fuels from renewable feedstocks, as examples mesoporous or microporous (zeolites); Production of nitrogen-substituted zeolites with high crystallinity and microporosity for investigation as alkaline catalysts; Provide a definitive spectroscopic signature that unambiguously confirms highly nitrogen-substituted zeolite Y and ascertain the likely location of nitrogen substitutions.

**DOE Interest**

Zeolites acting as acids have largely replaced homogeneous acid catalysts in many petrochemical processes. The microporous nature of zeolites provides a unique, confined reaction environment for catalytic reactions, increasing selectivity. Extending the abilities of zeolites to include catalyzing base-catalyzed reactions has been an active area of research for over forty years, and is especially important in light of recent interest in biomass energy. Preparing zeolites that act as strong bases has proven to be difficult, however, and characterizing the resulting materials is a relatively new field. Most published spectral assignments rely on intuitive assignments of NMR or IR spectra, for example. We seek to provide a definitive spectroscopic signature that corresponds to highly nitrogen-substituted zeolite Y, a material that should act as a strong base under appropriate conditions. We do this via a combination of synthetic techniques, physical adsorption, infrared spectroscopy, Raman spectroscopy, X-ray diffraction, and  $^{29}\text{Si}$  nuclear magnetic resonance spectroscopy.

**Recent Progress**

*Synthesis and characterization:* High-temperature ammonia treatment of Y zeolite generates new peaks in the silicon NMR spectrum in the  $-45$  to  $-90$  ppm range [1–4], consistent with nitrogen substitution of oxygen near silicon. The substitution reaction is highly dependent on the reaction conditions, especially temperature, flow rate, and Si/Al ratio of the starting material [2,3]. Flow rate is particularly important, as higher flow rates ( $500$ – $2000$   $\text{cm}^3/\text{min}$ ) remove water from the vicinity of the zeolite, preventing dealumination and the reversal of the substitution reaction [3]. The effects of flow rate and temperature are shown in *Fig. 1*

*Simulation:* Calculations of chemical shifts and the corresponding intensities for various possible silicon environments confirm that the experimentally observed peaks in the NMR spectrum correspond to nitrogen substitutions *in the zeolite framework*. In particular, the calculated chemical shifts for surface substitutions (Si–NH<sub>2</sub> for Si–OH) are too close to TMS to explain the new peaks [1]. Fits of the spectrum indicate substitution is biased toward Brønsted–Lowry acid sites at relatively low temperatures, but at higher temperatures the resulting spectra are consistent with random substitution [2].

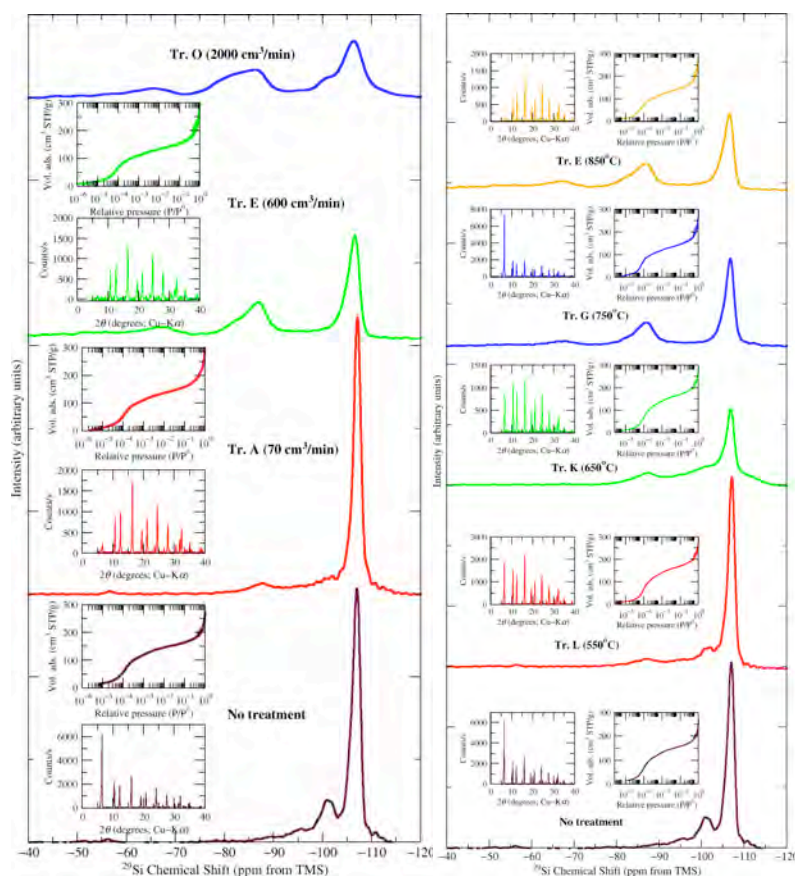


Fig. 1. Effects of flow rate (left) and temperature (right) on the NMR spectrum (indicating degree of substitution). Insets: X-ray pattern and adsorption isotherm showing changes in crystallinity with only minor changes in porosity. Image adapted from Ref. 3.

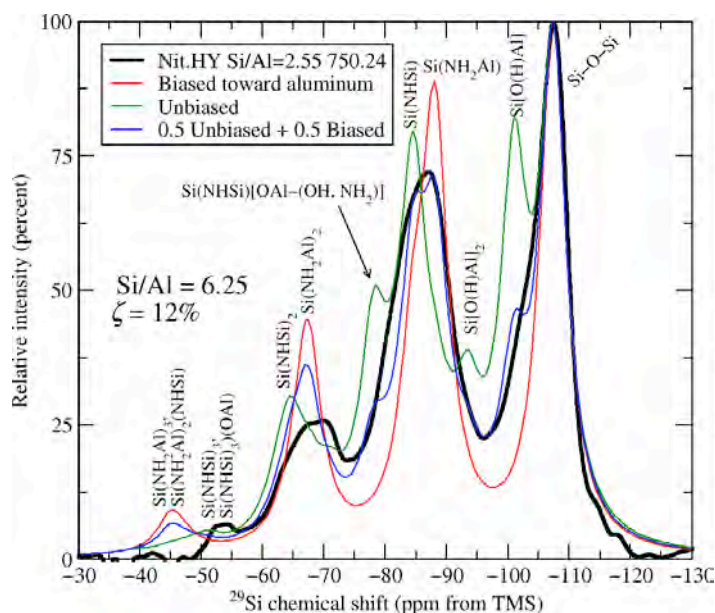


Fig. 2. Simulated (colors) and measured (black)  $^{29}\text{Si}$  NMR spectra of zeolite Y treated under 2000  $\text{cm}^3/\text{min}$  flowing ammonia for 24 h at 750  $^\circ\text{C}$ . The blue spectrum represents a 1:1 addition of the biased and unbiased spectra, indicating that at least the first substitution is biased toward acid sites. Image from Ref. 2.

## Future Plans

*Stability:* Verify that the materials are stable with respect to the presence of water and alcohols and provide an estimate of the temperature ranges at which they can be used without severe damage to the catalyst.

*Activity:* Test nitrogen-substituted Y zeolites prepared to have reasonable substitution with no measurable changes in crystallinity or microporosity as well as alkaline earth mesoporous molecular sieves for activity in the aldol condensation of furfural and other biomass-derived compounds. Use of nitrogenated zeolites in the synthesis of biodiesel from waste oil.

*Simulation:* Kinetic study of the mechanism and rate of nitrogen-substitution reactions.

## Publications (2008–2009)

1. K. D. Hammond, F. Dogan, G. A. Tompsett, V. Agarwal, C. P. Grey, W. C. Conner, and S. M. Auerbach, "Spectroscopic Signatures of Nitrogen-Substituted Zeolites," *J. Am. Chem. Soc.* **130** (2008) 14912–14913.
2. F. Dogan, K. D. Hammond, G. A. Tompsett, H. Huo, W. C. Conner, S. M. Auerbach, and C. P. Grey, *J. Am. Chem. Soc.*, submitted April 2009.
3. K. D. Hammond, M. Gharibeh, G. A. Tompsett, F. Dogan, C. P. Grey, S. M. Auerbach, and W. C. Conner, *Chem. Mater.*, in preparation (intended for submission April–May 2009).
4. K. D. Hammond and S. M. Auerbach, "Modeling and Spectroscopy of Basic Zeolites," to appear in *Silica and Silicates in Modern Catalysis*, to be published by Research Signpost.
5. V. Agarwal, W. C. Conner, G. W. Huber, and S. M. Auerbach, "First Principles Calculations of Nitrogen-Substituted Zeolites: Effects of Ion Exchange and Aluminum Content on Base Strength," *J. Phys. Chem. C*, in preparation (intended for submission April–May 2009).
6. V. Agarwal, W. C. Conner, G. W. Huber, and S. M. Auerbach, "First Principles Calculations of the Substitution Mechanism and Catalyst Stability of Nitrogen-Substituted Zeolites," *J. Catal.*, in preparation (intended for submission April–May 2009).
7. Kris R. Payer, L. Krogh, Geoffrey A. Tompsett and W. Curt. Conner, "The Effects of Thermal and Mechanical Perturbation on Mesoporous Isotherm Hysteresis Stability", *J. Porous Materials* (2009), 16-1, 91-99 DOI 10.1007/s10934-007-9172-9
8. Torren R. Carlson, Geoffrey A. Tompsett, W. C. Conner and George W. Huber, *Aromatic Production from Catalytic Fast Pyrolysis of Biomass-Derived Feedstocks*, *Topics in Catalysis*, 52, 241-252, DOI 10.1007/s11244-008-9160-6
9. Karl Hammond, Geoffrey A. Tompsett, Scott Auerbach, J. Falconer, and W. Curtis Conner, High-Resolution Physical Adsorption on Supported Borosilicate MFI Zeolite Membranes: Comparison With Powdered Samples *Journal of Membrane Science* 325 (2008), pp. 413-419
10. E. You, G. Tompsett, W.C. Conner, *Pre-adsorption on SBA-15*, In Preparation for *Langmuir*, 2009.
11. E You, G. Tompsett and W.C. Conner, *Preparation and Characterization of SBA-15 Materials*, In Preparation for *J. Porous Materials*, 2009.
12. G. Tompsett, E. You, E. Trivella, L. Krogh, E. Maglara, Stacy Zones and W.C. Conner, *Adsorption of Microporous Materials: Empirical Model for the Low Pressure Isotherm* In Preparation for *Langmuir*, 2009.
13. Carlson, T. R.; Jae, J.; and Huber, G. W.; Mechanistic Insights from Isotopic Studies of Glucose Conversion to Aromatics Over ZSM-5, *Angewandte Chemie*, (submitted).
14. Tompsett, G. A.; Li, N.; and Huber, G. W.; Catalytic Conversion of Sugars to Fuels, Book Chapter in *Thermochemical Conversion of Biomass*, edited by Robert Brown, publisher Wiley, in-press.
15. Olcay, H.; Xu, Y. and Huber, G. W.; Aqueous-phase hydrogenation of acetic acid over transition metal catalysts: The role of the acetyl species; *Angewandte Chemie* (submitted).
16. Yu-Chuan, George W. Huber.; The critical role of heterogeneous catalysis in lignocellulosic biomass conversion, *Energy and Environmental Science* **2**, 68-80 (2009).
17. Corma, A.; Huber, G. W.; Sauvanaud, L.; and O'Conner, P.; Biomass to chemicals: Catalytic conversion of glycerol/water mixtures into acrolein, reaction network. *Journal of Catalysis*, **257**, 163-171 (2008).
18. Carlson, T.R.; Vispute, T.P.; and Huber, G.W.; Green Gasoline by Catalytic Fast Pyrolysis of Solid Biomass-derived Compounds, *ChemSusChem*, **1**, 397-400 (2008).
19. Gates, B.C.; Huber, G.W.; Marshall, C.L.; Ross, P.N.; Siirola, J.; and Wang, Y.; Catalysts for Emerging Energy Applications, *MRS Bulletin*, **33**, 1-7 (2008).
20. Vispute, T.P.; and Huber, G.W.; Breaking the Chemical and Engineering Barriers to Lignocellulosic Biofuels, *International Sugar Journal*, **110**, 138, 140, 142, 146, 148-149 (2008).



**Hydrocarbon Dehydrogenation and Oxidation over Model Metal Oxide Surfaces**

Students: John D. Brooks, Yujung Dong  
Collaborators: G.V. Gibbs, VPI&SU Geosciences  
Contacts: Department of Chemical Engineering, Virginia Polytechnic Institute & State University, Blacksburg, VA 24061; dfcox@vt.edu

**Goal**

Develop an understanding of structure/function relationships determining selectivity in metal oxide catalytic surface chemistry related to alkane oxidation and dehydrogenation.

**DOE Interest**

Process chemistries for the conversion of alkanes to alkenes or selectively-oxygenated products can utilize lower-cost feedstocks and offer a more versatile usage of petrochemical resources. Industrial reaction processes for ethane dehydrogenation are driven by nonselective free-radical gas-phase reactions which could be improved with the development of selective heterogeneous catalysts. Studies of the reaction of C<sub>2</sub> hydrocarbon fragments on materials like chromia which are useful for dehydrogenation of larger alkanes provide insight into fundamental chemical processes effecting selectivity in these catalytic systems.

**Recent Progress**

*C<sub>2</sub> Alkyl Reactions on  $\alpha$ -Cr<sub>2</sub>O<sub>3</sub>(0001)*: The examination of ethyl, ethylidene and ethylidyne on the (0001) surface has clearly demonstrated structure sensitivity in the reaction of alkyl fragments on chromia surfaces. The stoichiometric (0001) surface exposes cations with a larger number of coordination vacancies (three) than the previously studied (10 $\bar{1}$ 2) surface where the cations expose a single coordination vacancy. The chemistry for the (0001) surface is richer, showing more coupling (C-C bond making) chemistry attributable to the presence of multiple coordination vacancies, but the majority products are the same on both surfaces. The primary difference is the existence of multiple reaction channels for ethyl and ethylidene on (0001) when only one is observed on (10 $\bar{1}$ 2). The multiple reaction channels are attributed to surface cation reaction sites of different coordination numbers caused by the deposition of halogen atoms from the halogenated molecules used to generate the fragments.

*Computational Studies of Methylene Diffusion and Reaction on  $\alpha$ -Cr<sub>2</sub>O<sub>3</sub>(10 $\bar{1}$ 2):* Experimental photoemission and thermal desorption studies have shown that methylene binds at surface Cr centers, and reacts by both dehydrogenation to surface carbon and coupling to ethylene. The coupling process involves diffusion of methylene between neighboring cation sites, and two reaction channels to ethylene are observed. DFT explains the two reaction channels in terms of a low and high barrier route to surface diffusion – (1) a low barrier route between neighboring cations across troughs in the surface, and (2) a high barrier route through a bidentate (Cr–CH<sub>2</sub>–O) surface intermediate characterized by a local (but not global) minimum in the potential energy surface.

### **Future Plans**

*Probe Molecules for  $\alpha$ -Cr<sub>2</sub>O<sub>3</sub>(0001) Surface Characterization:* Find probe molecules capable of distinguishing between cations of different coordination. These probes are necessary for interpretation of the previously-observed alkyl chemistry.

*Reaction of C<sub>1</sub> Fragments and C<sub>2</sub> Alkenyl Fragments on  $\alpha$ -Cr<sub>2</sub>O<sub>3</sub>(0001):* To provide a complete understanding of the reaction network of small (C<sub>1</sub> and C<sub>2</sub>) reaction intermediates and their likely roles in determining selectivity during ethane dehydrogenation.

*Computational Studies of Carbene Isomerization on  $\alpha$ -Cr<sub>2</sub>O<sub>3</sub>(10 $\bar{1}$ 2):* To provide a fundamental understanding of the mechanistic reasons for the experimentally observed preference to isomerization rather than dehydrogenation in the reaction of carbenes.

*Reaction of C<sub>1</sub> Fragments on  $\alpha$ -Fe<sub>2</sub>O<sub>3</sub>(10 $\bar{1}$ 2):* To provide experimental data on a purely electronic effect in surface chemistry by comparison to available reaction data for C<sub>1</sub> fragments on  $\alpha$ -Cr<sub>2</sub>O<sub>3</sub>(10 $\bar{1}$ 2). Because of the common bulk crystal structures, the two surfaces differ primarily in terms of the d electron count on Fe<sup>3+</sup> (d<sup>5</sup>) and Cr<sup>3+</sup> (d<sup>3</sup>) cations.

### Publications (2007-2009)

1. J.D. Brooks, Q. Ma and D.F. Cox, Reactions of ethyl groups on a model chromia surface: ethyl chloride on stoichiometric  $\alpha\text{-Cr}_2\text{O}_3$  ( $10\bar{1}2$ ), *Surface Science*, **603** (2009) 523-528.
2. M.A. McKee, Q. Ma, D.R. Mullins, M. Neurock and D.F. Cox, Reactions of vinyl groups on a model chromia surface: vinyl chloride on stoichiometric  $\alpha\text{-Cr}_2\text{O}_3$  ( $10\bar{1}2$ ), *Surface Science*, **603** (2009) 265-272.
3. G.V. Gibbs, A.F. Wallace, D.F. Cox, P.M. Dove, R.T. Downs, N.L. Ross and K.M. Rosso, The role of directed van der Waals bonded interactions in the determination of the structures of molecular arsenate solids, *The Journal of Physical Chemistry A*, **113** (2009) 736-749.
4. G.V. Gibbs, R.T. Downs, D.F. Cox, K.M. Rosso, N.L. Ross, A. Kirfel, T. Lippmann, W. Morgenroth and T.D. Crawford, Experimental bond critical point and local energy density properties determined for Mn-O, Fe-O and Co-O bonded interactions for tephroite,  $\text{Mn}_2\text{SiO}_4$ , fayalite,  $\text{Fe}_2\text{SiO}_4$  and  $\text{Co}_2\text{SiO}_4$  olivine and selected organic metal complexes: Comparison with properties calculated for non-transition and transition metal M-O bonded interactions for silicates and oxides, *The Journal of Physical Chemistry A*, **112** (2008) 8811-8823.
5. G.V. Gibbs, R.T. Downs, D.F. Cox, N.L. Ross, M.B. Boisen, Jr. and K.M. Rosso, Shared and closed-shell O-O interactions in silicates, *The Journal of Physical Chemistry A*, **112** (2008) 3693-3699.
6. G.V. Gibbs, R.T. Downs, D.F. Cox, N.L. Ross, C.T. Prewitt, K.M. Rosso, T. Lippmann and A. Kirfel, Connections Between Bonded Interactions and the Crystal Chemistry of Minerals: A Review, *Zeitschrift fur Kristallographie*, **223** (2008) 1-40.
7. G.V. Gibbs, D.F. Cox, K.M. Rosso, N.L. Ross, R.T. Downs, and M.A. Spackman, Theoretical electron density distributions for Fe and Cu sulfide Earth materials: a connection between bond length, bond critical point properties, local energy densities and bonded interactions, *The Journal of Physical Chemistry B*, **111** (2007) 1923-1931.

## Understanding Multimetallic Catalysts using Dendrimer-Encapsulated Nanoparticles

Lead PI: Richard M. Crooks

Students: Sue V. Myers and Michael G. Weir

Contact: Department of Chemistry and Biochemistry, The University of Texas at Austin,  
1 University Station, A5300, Austin, TX 78712-0165; crooks@cm.utexas.edu

Nanoscale materials often exhibit more interesting physical and catalytic properties than their bulk counterparts. A prerequisite for understanding these properties is the synthesis of well-defined nanoparticles. For studies of homogeneous catalysis particularly, standard synthetic methods typically produce particles with a distribution of sizes, compositions, and structures that make it difficult to correlate structure to function. In contrast, the dendrimer templating technique developed in our lab can be used to synthesize well-defined, catalytically active nanoparticles consisting of 30 to 250 atoms. Our long-term goal, therefore, is to correlate nanoparticle structure to catalytic function using a combination of synthesis, advanced characterization methods, and theory. Moreover, a key component of our project is to perform characterization studies during catalytic reactions.

We have recently been carrying out *in-situ* EXAFS analysis of dendrimer-encapsulated nanoparticles (DENs) under catalytic conditions. Initial studies involve Pt monometallic DENs consisting of an average of 240 atoms. A custom-built cell is used to measure changes in the local structure of these nanoparticles during electrochemical CO adsorption and stripping. EXAFS analysis of the DENs prior to electrochemical CO oxidation is consistent with our earlier studies. Preliminary analysis of the CO adsorption process reveals changes to the nanoparticles that could arise from increased crystallinity or chemical reduction. After removal of CO, permanent changes in structure are observed.

A second aspect of this project focuses on comparison of the measured rates of electrochemical reactions catalyzed by DENs with theoretical studies. For example, theory predicts that PdCu bimetallic particles will be better catalysts for the oxygen reduction reaction (ORR) than monometallic Pd. Accordingly, we synthesized PdCu DENs containing an average of 64 atoms at five different metal ratios. Particle sizes are 1.2-1.3 ( $\pm$  0.4) nm in diameter as measured by TEM. EXAFS analysis indicates that these materials have an alloy structure. Electrocatalytic analysis of these materials is underway.

### References

1. M. R. Knecht; M. G. Weir; V. S. Myers; W. D. Pyrz; H. Ye; V. Petkov; D. J. Buttrey; A. I. Frenkel; R. M. Crooks "Synthesis and Characterization of Pt Dendrimer-Encapsulated Nanoparticles: Effect of the Template on Nanoparticle Formation" *Chem. Mater.* **2008**, *20*, 5218-5228.
2. V. Petkov; N. Bedford; M. R. Knecht; M. G. Weir; R. M. Crooks; W. Tang; G. Henkelman; A. Frenkel "Periodicity and Atomic Ordering in Nanosized Particles of Crystals" *J. Phys. Chem. C* **2008**, *112*, 8907-8911.
3. M. R. Knecht; M. G. Weir; A. I. Frenkel; R. M. Crooks "Structural Rearrangement of Bimetallic Alloy PdAu Nanoparticles within Dendrimer Templates to Yield Core/Shell Configurations" *Chem. Mater.* **2008**, *20*, 1019-1028.
4. H. Ye; J. A. Crooks; R. M. Crooks "The Effect of Particle Size on the Kinetics of the Electrocatalytic Oxygen Reduction Reaction Catalyzed by Pt Dendrimer-Encapsulated Nanoparticles" *Langmuir* **2007**, *23*, 11901-11906.

## Density Functional Studies of Methanol Decomposition on Sub-nanometer Clusters

Lead PI: Peter C. Stair  
Additional PIs: Stefan Vajda, Jeff Elam, Chris Marshall,  
Postdocs: Faisal Mehmood  
Collaborators: Peter Zapol, Jeffrey Greeley  
Contact: L. Curtiss, CSE/MSD/CNM Divisions, Argonne National  
Laboratory, 9700 S. Cass Ave., Argonne, IL 60439;  
[curtiss@anl.gov](mailto:curtiss@anl.gov)

Extensive experimental and theoretical work has been done to understand the decomposition of methanol on various metal and metal oxide nanoparticles for hydrogen production. The activity of sub-nanometer sized particles  $< 1\text{nm}$  however is not very well known, primarily because of technical challenges involved in preparation and stabilization of the clusters. As part of a joint experimental/theoretical study on the properties of small Pd clusters, we have carried out density functional calculations for the methanol decomposition reaction on Pd<sub>4</sub> and Pd<sub>8</sub> clusters. The thermodynamics and kinetics of three decomposition routes involving C-O, C-H and O-H scission were investigated; activation energy barriers were determined with the nudged elastic band method. A detailed analysis of the PES for methanol decomposition shows C-O activation to be the least favorable step. In addition, all possible reaction paths for the Pd<sub>4</sub> cluster are lower in comparison to single crystal surface and large nanoparticles. We will discuss the implication of a linear correlation between the transition state and final state energies that is followed for all elementary reaction steps on Pd<sub>4</sub> and Pd<sub>8</sub> clusters. We also present results that include the effects of an aluminum oxide support as well as results on other clusters such as Co<sub>n</sub>.

**Nanostructured Catalysts for Hydrogen Generation from Renewable Feedstocks**

Additional PIs: Yong Wang (Pacific Northwest National Lab), John Vohs (Univ. of Pennsylvania)

Post-docs: Vanessa Lebarbier (UNM and PNNL), Barr Halevi (UNM)

Graduate Students: Travis Conant, Eric Petersen, Patrick Burton (UNM), Ese Jerrero (UPenn).

Undergrad Students: Jonathan Paiz, Ehren Baca, Loren Baca (UNM).

Collaborator: Robert Schloegl, Fritz Haber Institute, Berlin, Germany.

Contacts: Abhaya Datye, University of New Mexico, Dept. of Chemical & Nuclear Engineering, MSC 01 1120, Albuquerque, NM, 87131-0001; [datye@unm.edu](mailto:datye@unm.edu)  
Yong Wang, Pacific Northwest National Laboratory, 902 Battelle Boulevard, P.O. Box 999, Richland, WA 99352; [yongwang@pnl.gov](mailto:yongwang@pnl.gov)  
John Vohs, Department of Chemical and Biomolecular Eng., Univ. of Pennsylvania, Philadelphia, PA 19104; [vohs@seas.upenn.edu](mailto:vohs@seas.upenn.edu)

**Goal**

This is a collaborative effort involving the research groups at the University of New Mexico (Datye), Pacific Northwest National Labs (Wang) and University of Pennsylvania (Vohs). The research program is directed towards the development of highly active and selective catalysts for the production of hydrogen from renewable alcohols. The initial work has focused on the fundamental understanding of methanol conversion to hydrogen, and on associated reactions such as the water gas shift, with the ultimate goal of designing advanced catalysts for converting renewable feedstocks such as bioethanol to hydrogen.

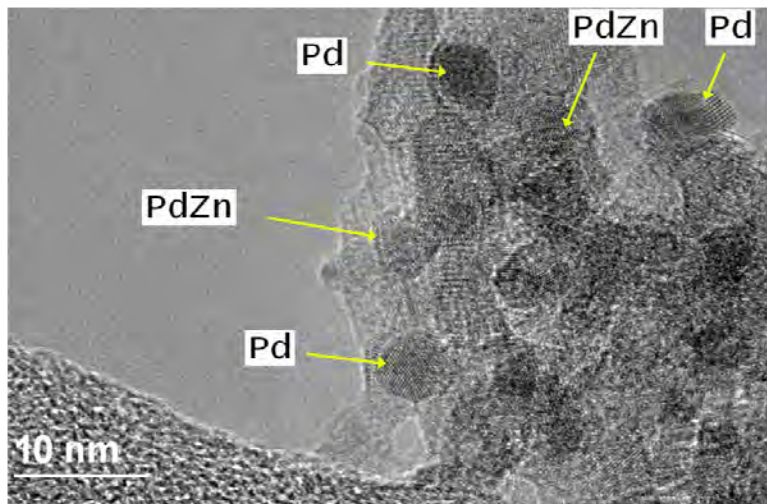
**DOE Interest**

The proposed project directly addresses one of the BES long-term program measures, namely to demonstrate progress in understanding, modeling, and controlling chemical reactivity and energy transfer processes in the gas phase, at interfaces, and on surfaces for energy-related applications. The robust and integrated approaches developed will lead to new discoveries in catalyst synthesis, characterization, mechanistic understanding of reforming reactions and control of surface sites, all of which will have a broad impact on the design of catalysts at the nanoscale. The results of the proposed work will impact chemical reactivity at the level of elementary surface reactions for a wide range of bimetallic catalyzed chemical transformations. The applications of the tools will lead to new fundamental understanding of the science underlying hydrogen fuels and to discovery of principles for rational design of new processes relevant to a Hydrogen Economy. The project addresses basic research needs to assure a secure energy future.

**Recent Progress****Pd/ZnO reactivity**

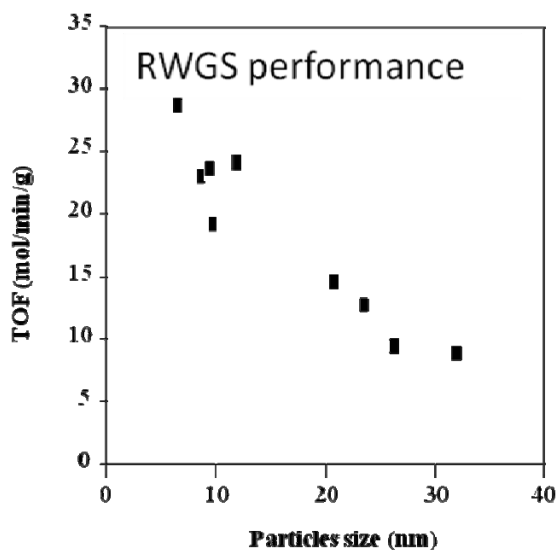
Pd/ZnO/Al<sub>2</sub>O<sub>3</sub> catalysts were studied for methanol steam reforming, water-gas-shift (WGS), and reverse-water-gas-shift (RWGS) reactions. WGS activity was found to be comparable to that of commercial Pt-based catalysts with stable performance demonstrated for 100 hours time-on-stream at a temperature of 360°C without evidence of metal sintering. WGS activity was found to be dependent on the Pd:Zn ratio with a maximum activity obtained at approximately 1:1 Pd:Zn. WGS reaction rates were found to follow first order kinetics with

$r_{WGS} = 1.02 \times 10^6 s^{-1} e^{\left(\frac{-58.3 kJ mol^{-1}}{RT}\right)} [CO]$ . During methanol steam reforming, CO selectivities were observed to be lower than the calculated equilibrium values over a range of temperatures and steam/carbon ratios studied while the reaction rate constants were approximately of the same magnitude for both WGS and methanol steam reforming. These results indicate that although Pd/ZnO/Al<sub>2</sub>O<sub>3</sub> are active WGS catalysts, WGS is not involved in methanol steam reforming. In addition, RWGS rate constants were found to be on the order of about 20 times lower than that of methanol steam reforming, suggesting that RWGS reaction could be one of the sources for small amount of CO formation in methanol steam reforming.



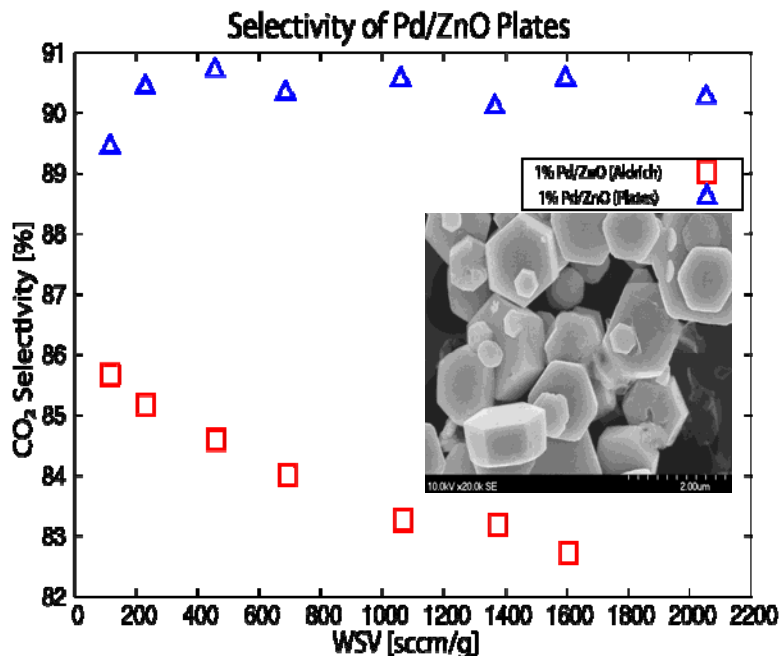
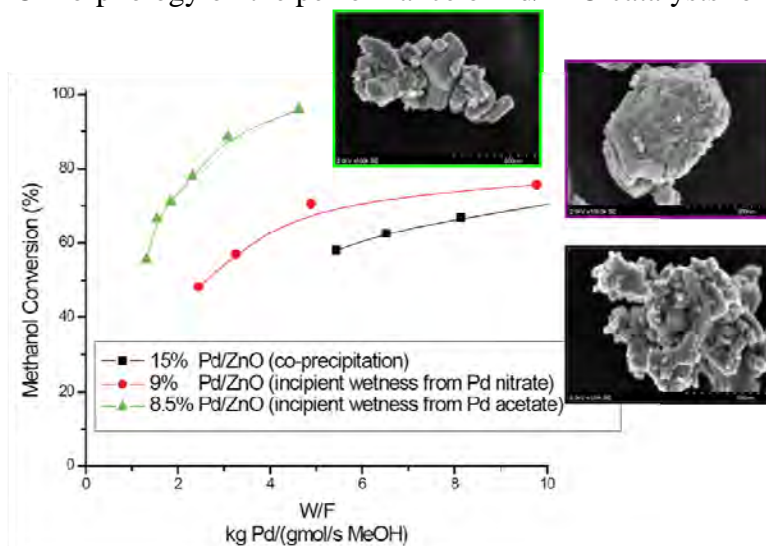
### PdZn particle size effect

The effect of PdZn particle size on the catalytic activity of Pd/ZnO catalysts for the reverse-water-gas-shift (RWGS) reaction was subsequently studied using supported catalysts prepared by incipient wetness impregnation of Palladium acetate on commercial ZnO powder (Aldrich). The PdZn particle size was varied by adjusting Pd loading and reducing the catalysts at different temperatures. Reactivity measurements indicated that the turnover frequency for the RWGS reaction increases as the PdZn crystallite size decreases. This observation is consistent with previously observed trends for PdZn particle size effects for the steam reforming of methanol, where higher CO selectivity correlated with smaller PdZn particles. Thus, RWGS has been identified as a potential reaction pathway to undesired CO formation in methanol steam reforming on Pd/ZnO catalysts for hydrogen production.



### ZnO morphology

To investigate the effect of ZnO morphology on the performance of Pd/ZnO catalysts for alcohol steam reforming a set of catalysts was made by modifying a faceted commercial high purity ZnO powder. These included ZnO powder (Aldrich) impregnated with Palladium acetate and or nitrate as well as ZnO powder (Aldrich) and Palladium nitrate co-dissolved in 15.7 M nitric acid then co-precipitated. The morphology and catalytic performance of these powders demonstrates that the more faceted powders made from ZnO powder impregnated with Palladium acetate are more active.



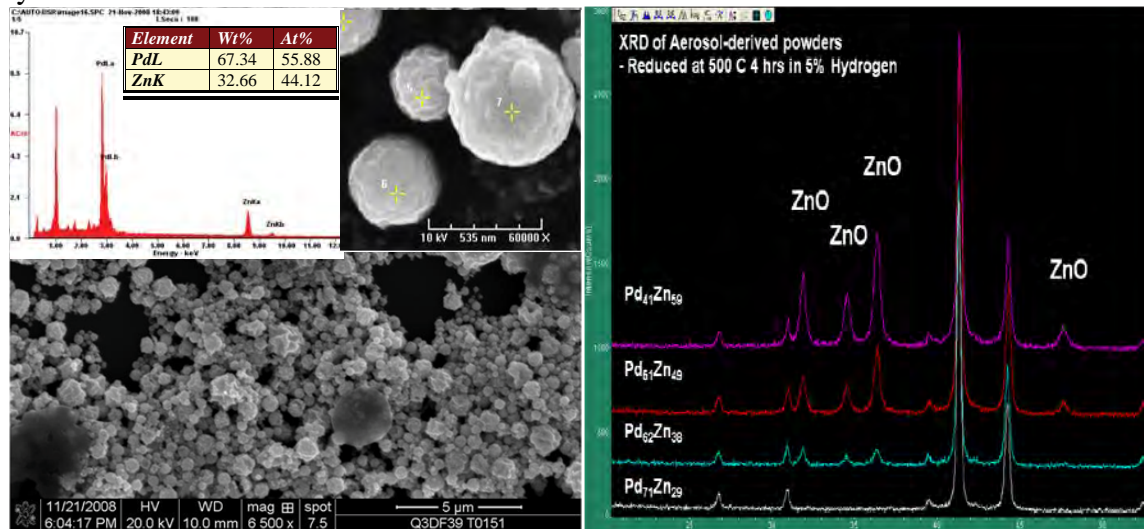
To further understand to role of ZnO facing highly faceted model ZnO powders we synthesized. These highly faceted powders preferentially expose the ZnO(0001) plane which is thought to be the most active crystal plane, as seen in the model catalysts studies of Vohs et al. These plates were impregnated with Palladium acetate and compared to similarly prepared samples made using the commercial ZnO powders (Aldrich) used in the previous tests. Methanol steam reforming reactivity tests demonstrated that the ZnO powders preferentially exposing the ZnO(0001) plane were more selective to CO<sub>2</sub> production

### PdZn alloy powders from aerosol decomposition

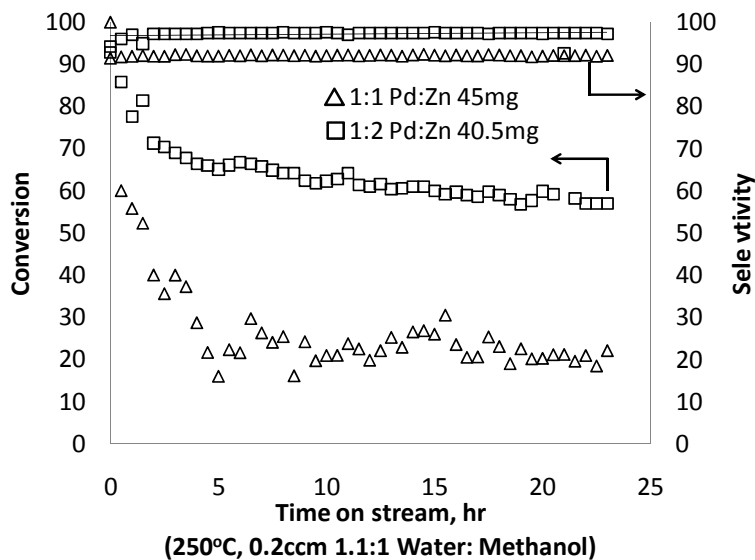
In an effort to better understand the role of PdZn in steam reforming of alcohols a range of compositions of bulk PdZn alloys were synthesized using a technique which forms particles by drying aerosols generated from metal solutions. These particles are spherical, range from 50-500nm in diameter, and energy dispersive analysis proved these particles have homogenous compositions, corresponding to the bulk compositions demonstrated by the analysis. The initially small size of previous batches severely restricted the ability to properly characterize and test aerosol-powders. We have now successfully scaled up the synthesis process so that production of 2 grams of powder per batch is now possible. The larger size of these more recent batches of



PdZn powders has allowed for extensive characterization to confirm the samples are truly homogenous and have confirmed the ability to make phase-pure PdZn bulk alloys using aerosol-synthesis methods.



Methanol steam reforming activity tests conducted on the aerosol-derived powders demonstrated that 1:2 PdZn ( a mixture of PdZn and ZnO) is more stable than 1:1 PdZn(PdZn only). This result indicates that the presence of ZnO in the catalysts corresponds to a reduction in the deactivation of PdZn catalyst. The presence of ZnO in the synthesized powders also demonstrated that PdZn+Zno will form under reaction conditions, just as PdZn will from Pd+ZnO as was shown previously.

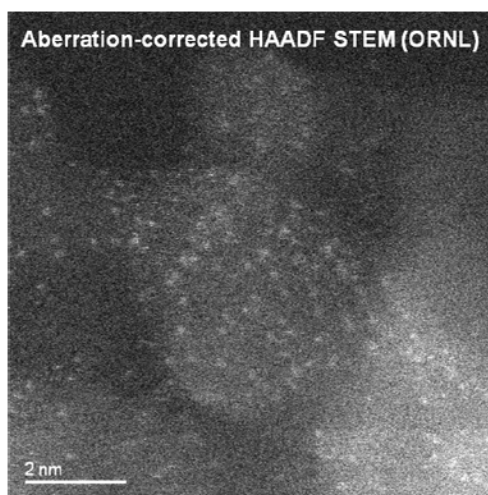
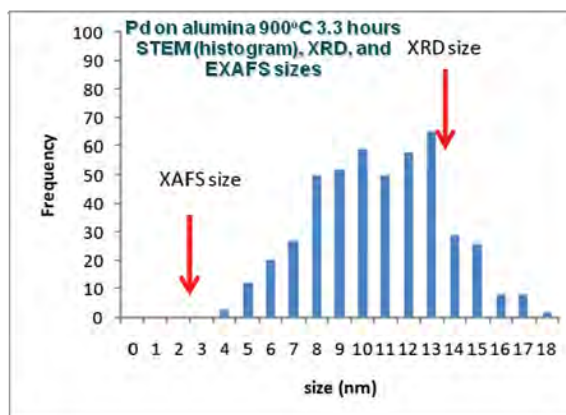


### Pd/Al<sub>2</sub>O<sub>3</sub> particle size

To better understand the observed effect of PdZn particle size on catalyst performance we began to study the simpler Pd/alumina system. Alumina-supported Pd was produced using Pd-nitrate and the incipient wetness method to produce powder with a 2.5% Pd loading on gamma alumina. The sample was calcined and then treated in flowing N<sub>2</sub>/H<sub>2</sub> at temperatures ranging from 300-900 °C, producing a series of samples having a range of Pd crystallite sizes. These samples were characterized by several techniques that overlap in their ability to resolve sizes. The techniques include Extended X-ray Absorption Fine Structure (EXAFS), X-ray Diffraction (XRD), and high-angle annular dark-field imaging in a Scanning Transmission Electron

Microscope (HAADF-STEM). Some of the samples were also examined using the newly available technique of Aberration-Corrected Electron Microscopy (ACEM).

Average crystallite sizes obtained from the EXAFS data were found to be significantly smaller than those obtained from XRD and STEM. This suggests that the presence of particles in the 0-1 nanometer size range is weighting the EXAFS-obtained average size to smaller values than those obtained from XRD and STEM. For the EXAFS average size to be brought into line with the TEM and XRD average sizes, these samples must have 0-1 nm size fractions comprising 10-20% of the Pd present. Further examination of these samples



by ACEM confirmed the presence of an abundance of single atoms and small clusters of atoms on the support. The weight fraction of this highly dispersed phase was estimated from the ACEM images and was found to be in excellent agreement with the predictions of EXAFS/STEM. These results demonstrate that alumina can stabilize a dispersed Pd phase even after sintering to temperatures as high as 900 °C. These isolated palladium atom anchoring sites may help explain the relative sinter-resistance of alumina-supported catalysts and may further help explain some why in some cases sintering and reduction of Pd/ZnO catalyst surface area during catalyst activation did not correspond to decreased catalytic activity.

## Future Work

The results of our studies of model catalysts already provide considerable insight into how Zn, PdZn particle size, and the ZnO substrate affect the reactivity of Pd/ZnO catalysts towards methanol. The role of ZnO on the reactivity of the Pd will be further explored through the bimetallic alloy particles prepared by aerosol routes. These alloy particles allow us to investigate the role of the metal phase independent of the support, which is difficult to do in conventional supported catalysts. Future work will also include in-situ IR studies under reaction conditions. In-situ EXAFS will be used to improve our understanding of the small Pd and PdZn particles formed on these catalysts, as well as to ensure that the aerosol PdZn particles are homogenous on all size scales. During the next year, we will also commence work on ethanol reactivity on these bimetallic catalysts.

In addition to expansion of previous studies of methanol steam reforming reactivity to ethanol steam reforming, the highly faceted low-surface area ZnO powders made this past year will be used to bridge previous studies on single crystal and high-surface ZnO powder. The importance of the ZnO support and ability to apply knowledge gained in this study will be further explored through testing of Pd/ZnO catalysts made from several commercially available ZnO powders that have been obtained. The attempt to bridge model and more-realistic supports

will also include extension of our studies of Palladium dispersed on alumina to include alcohol reactivity measurements as well as moving on to study Palladium dispersed on Zinc Oxide.

### Publications (2007-2009)

1. Bera, P. and J.M. Vohs, *Reaction of CH<sub>3</sub>OH on Pd/ZnO(0001) and PdZn/ZnO(0001) model catalysts*. Journal of Physical Chemistry C, 2007. 111(19): p. 7049-7057.
2. Burton, P.D., D. Lavenson, M. Johnson, D. Gorm, A.M. Karim, T. Conant, A.K. Datye, B.A. Hernandez-Sanchez, and T.J. Boyle, *Synthesis and activity of heterogeneous Pd/Al<sub>2</sub>O<sub>3</sub> and Pd/ZnO catalysts prepared from colloidal palladium nanoparticles*. Topics in Catalysis, 2008. 49(3-4): p. 227-232.
3. Conant, T., A. Karim, and A. Datye, *Coating of steam reforming catalysts in non-porous multi-channeled microreactors*. Catalysis Today, 2007. 125(1-2): p. 11-15.
4. Conant, T., A.M. Karim, V. Lebarbier, Y. Wang, F. Girgsdies, R. Schlögl, and A. Datye, *Stability of bimetallic Pd-Zn catalysts for the steam reforming of methanol*. Journal of Catalysis, 2008. 257(1): p. 64-70.
5. Dagle, R.A., Y.H. Chin, and Y. Wang, *The effects of PdZn crystallite size on methanol steam reforming*. Topics in Catalysis, 2007. 46(3-4): p. 358-362.
6. Dagle, R.A., A. Platon, D.R. Palo, A.K. Datye, J.M. Vohs, and Y. Wang, *PdZnAl catalysts for the reactions of water-gas-shift, methanol steam reforming, and reverse-water-gas-shift*. Applied Catalysis A: General, 2008. 342(1-2): p. 63-68.
7. Datye, A.K., P.L. Hansen, and S. Helveg, *Electron microscopy techniques*. Handbook of Heterogeneous Catalysis (2nd Edition), 2008. 2: p. 803-833.
8. Jeroro, E., V. Lebarbier, A. Datye, Y. Wang, and J.M. Vohs, *Interaction of CO with surface PdZn alloys*. Surface Science, 2007. 601(23): p. 5546-5554.
9. Jeroro, E. and J.M. Vohs, *Zn modification of the reactivity of Pd(111) toward methanol and formaldehyde*. Journal of the American Chemical Society, 2008. 130(31): p. 10199-10207.
10. Jeroro, E. and J.M. Vohs, *Exploring the role of Zn in PdZn reforming catalysts: Adsorption and reaction of ethanol and acetaldehyde on two-dimensional PdZn alloys*. Journal of Physical Chemistry C, 2009. 113(4): p. 1486-1494.
11. Karim, A.M., T. Conant, and A.K. Datye, *Controlling ZnO morphology for improved methanol steam reforming reactivity*. Physical Chemistry Chemical Physics, 2008. 10(36): p. 5584-5590.
12. Lebarbier, V., R. Dagle, T. Conant, J.M. Vohs, A.K. Datye, and Y. Wang, *CO/FTIR spectroscopic characterization of Pd/ZnO/Al<sub>2</sub>O<sub>3</sub> catalysts for methanol steam reforming*. Catalysis Letters, 2008. 122(3-4): p. 223-227.

**Structure and Function of Supported Base Catalysts**

Postdoc: Daniel Lahr (no longer at UVa)  
Graduate Students: Jianren Tai (graduated), Yuanzhou Xi, Joseph Kozlowski  
Undergrad Student: Matthew Aronson  
Contact: Chemical Engineering, University of Virginia, 102 Engineers Way,  
Charlottesville, VA 22911; [rjd4f@virginia.edu](mailto:rjd4f@virginia.edu)

**Goal**

Solid bases are heterogeneous catalysts that have not been broadly exploited compared to solid acids. Thus, we have focused our efforts on understanding how a variety of solid bases, including metal oxides, mixed metal oxides and zeolites, function in catalytic transformations. Our most recent objective involved probing the reactivity of layered double hydroxides for transesterification reactions that are important for conversion of biorenewable resources to fuels and chemicals. The synthesis of biodiesel fuel from plant oils (triglycerides) and methanol currently employs homogeneous base catalysts to facilitate transesterification although these liquid base catalysts need to be removed and neutralized in the process. Our work involves the investigation of solid base catalysts that can be easily recovered from reacting systems. In particular, the role of water in the transesterification of tributyrin (a model triglyceride) with methanol over the hydroxyl form of hydrotalcite was explored.

**DOE Interest**

Solid base catalysts exhibit high activities and selectivities for many kinds of reactions important for fuels and chemicals production, including transesterifications, condensations, alkylations, cyclizations, and isomerizations; however, many of these processes are carried out industrially using liquid bases as catalysts. These applications can require nearly stoichiometric amounts of the liquid base for conversion to the desired product. Replacement of liquid bases with solid base catalysts allows for easier separation from the product as well as possible regeneration and reuse. Basic solids also have the added advantages of being non-corrosive and environmentally friendly, which allows for easier disposal.

A molecular-level understanding of solid basicity is required before structure/function properties of new materials can be effectively predicted. A significant fraction of previous research on solid bases therefore involves the correlation of base strength to catalyst composition. However, since strong bases are also poisoned by carbon dioxide and water, common side products in catalytic reactions, new base catalysts that are more resistant to deactivation by these molecules need to be developed. The search for novel solid bases that catalyze transformations with high product selectivity, high reaction rate, and low deactivation rate is an ongoing process.

Research in this program addresses at least two long term measures relevant to the BES. For example our project involves designing, modeling, fabricating, characterizing, analyzing, assembling and using new materials and structures, particularly at the nanoscale, for

energy-related applications. Moreover, the project will advance the understanding, modeling, and controlling of chemical reactions on surfaces for energy-related applications, employing lessons from inorganic, organic and self-assembling systems.

### Recent Progress

Hydrotalcites (Mg-Al double layered hydroxides) were prepared by coprecipitation or by hydrothermal synthesis involving urea hydrolysis (see Figure 1a). The synthetic Mg-Al HTs were activated by either thermal decomposition (Figure 1b) or thermal decomposition followed by reconstruction with water (Figure 1c). The transesterification reaction was performed in a batch reactor with methanol to tributyrin molar ratio of 30:1 at 333 K.

The reconstructed HTs were significantly more active than the decomposed HTs on a surface area basis because the presence of Brønsted base sites on the former. The areal reaction rate and CO<sub>2</sub> adsorption capacity of a reconstructed sample decreased significantly as the interlayer water was removed by thermal treatment. Interestingly, the catalytic activity of reconstructed HTs was inversely correlated to the crystallite size, suggesting the importance of crystal edges and defects in catalysis. Both the decomposed and reconstructed HT samples deactivated during the transesterification reaction. The crystal structure of decomposed HT was stable under reaction condition as shown in Figure 1(b) and (d). However, the Brønsted base sites of the reconstructed HT were deactivated by the product of the hydrolysis side reaction, resulting in the intercalation of butyric anions and expansion of the interlayer distance, as illustrated by the diffraction patterns in Figure 1(c) and (e).

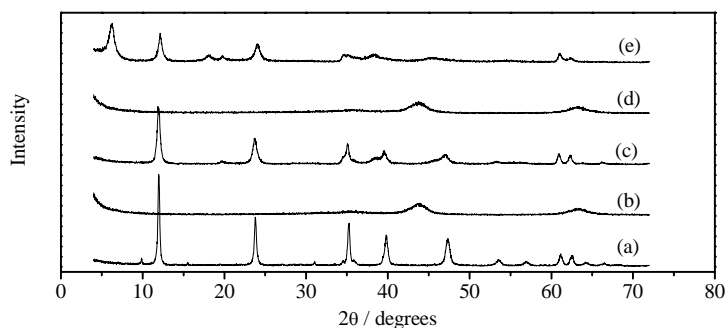


**Figure 1.** XRD patterns of (a) HT prepared by urea hydrolysis, (b) thermally decomposed HT to form mixed oxide, (c) sample in (b) reconstructed to form layered HT, (d) recycled mixed oxide in (b) after 2 runs, (e) recycled HT from (c) after 2 runs.

### Future Plans

We propose to minimize the negative role of interlayer water and hydroxyl, which can lead to severe deactivation during transesterification, by intercalating other basic anions in the interlayer spaces. We have achieved some success intercalating ethylene glycol into the interlayer gallery of the rare earth layered crystalline hydroxide compounds based on yttrium. This will be the basis of our future work.

### List of Publications Funded Solely by this Grant (2006-2009)

1. J. Li, J. Tai and R.J. Davis, "Hydrocarbon Oxidation and Aldol Condensation over Basic Zeolite Catalysts," *Catal. Today* **116** (2006) 226-233.
2. J. Tai and R.J. Davis, "Synthesis of Methacrylic Acid by Aldol Condensation of Propionic Acid with Formaldehyde over Acid-Base Bifunctional Catalysts," *Catal. Today* **123** (2007) 42-49.
3. D.G. Lahr, J. Li and R.J. Davis, "Oxidation of H<sub>2</sub> and CO over Ion Exchanged X and Y Zeolites," *J. Am. Chem. Soc.* **129** (2007) 3420-3425.
4. Y. Xi and R.J. Davis, "Influence of Water on the Activity and Stability of Activated Mg-Al Hydrotalcites for the Transesterification of Tributyrin with Methanol" *J. Catal.* **254** (2008) 190-197.
5. M.A. Haider, M.R. Gogate and R.J. Davis, "Fe-Promotion of Supported Rh Catalysts for Direct Conversion of Syngas to Ethanol" *J. Catal.* **216** (2009) 9-16.

### Publications That Acknowledge This Grant Together with Other Sources (2006-2009)

6. W.C. Ketchie, M. Murayama and R.J. Davis, "Promotional Effect of Hydroxyl on the Aqueous Phase Oxidation of Carbon Monoxide and Glycerol over Supported Au Catalysts" *Topics in Catalysis*, **44** (2007) 307-317.
7. W.C. Ketchie, E.P. Maris and R.J. Davis, "In-situ X-ray Absorption Spectroscopy of Supported Ru Catalysts in the Aqueous Phase," *Chem. Mater.* **19** (2007) 3406-3411.
8. E.P. Maris and R.J. Davis, "Hydrogenolysis of Glycerol over Carbon-Supported Ru and Pt Catalysts," *J. Catal.*, **249** (2007) 328-337.
9. W.C. Ketchie, Y.-L. Fang, M.S. Wong, M. Murayama and R.J. Davis, "Influence of Gold Particle Size on the Aqueous-phase Oxidation of Carbon Monoxide and Glycerol," *J. Catal.* **250** (2007) 94-101.
10. W.C. Ketchie, M. Murayama and R.J. Davis, "Selective Oxidation of Glycerol over Carbon-Supported AuPd Catalysts," *J. Catal.*, **250** (2007) 264-273.
11. E.P. Maris, W.C. Ketchie, M. Murayama and R.J. Davis, "Glycerol Hydrogenolysis on Carbon-Supported PtRu and AuRu Bimetallic Catalysts," *J. Catal.* **251** (2007) 281-294.

**CATALYSIS SCIENCE INITIATIVE: Catalyst Design by Discovery Informatics**

Co-PIs: J. M. Caruthers, M. Abu-Omar (Chemistry), F. H. Ribeiro, K. T. Thomson,  
Research Associates: G. Medvedev, T. Malik (Cyber Center)  
Students: L. Bollman, J. Cao (ECE), M. Jones (Chemistry), B. Kromer, B. Krishnamurthy, G. Krishnamurthy, T. Manz, K. Novstrup, J. Ratts, C. Shaffer, A. Shehab (CS), S. Stamatis, J. Switzer, N. Travia (Chemistry), H. Wang (IE), D. Williams, M. Shekhar  
Collaborators: V. Venkatasubramanian; Energy Center at Purdue; S. P. Midkiff, School of Electrical and Computer Engineering; S. Dunlop, Information Technology at Purdue (ITaP); G.E. Blau, S. Orcun, , e-Enterprise Center  
Contact: W. Nicholas Delgass, Forney Hall of Chemical Engineering, 480 Stadium Mall Drive, Purdue University, West Lafayette, IN 47907-2100, (765) 494 4059, FAX (765) 494 0805, [Delgass@ecn.purdue.edu](mailto:Delgass@ecn.purdue.edu)

**Goal**

Develop and apply an informatics-intensive, model-based approach that extracts knowledge from data for the design of catalysts, focusing first on single-site olefin polymerization catalysts and water gas shift catalysts for the production of hydrogen.

**DOE Interest**

Validation of this new design concept has the potential to change the catalysis research landscape by dramatically shortening hypothesis testing and new discovery cycles for virtually any catalyst system, heterogeneous or homogeneous. Applications with energy impact include generation of hydrogen for fuel, production of fuels and chemicals from coal or biomass, removal of sulfur from transportation fuels, engine NO<sub>x</sub> after-treatment and the development of more environmentally friendly chemical processes.

**Recent Progress**

- *Kinetics and Mechanism of 1-Hexene Polymerization Catalyzed by [rac-(C<sub>2</sub>H<sub>4</sub>(1-indenyl)<sub>2</sub>)ZrMe<sub>2</sub>], Brintzinger's Catalyst.*

While we have continued to develop our detailed quantitative modeling of the mixed metallocene/aryloxide system with further understanding of effects solvent and catalyst structure on rate constants for propagation and initiation, we focus here on polymerization of 1-hexene catalyzed by (EBI)ZrMe<sub>2</sub> activated with B(C<sub>6</sub>F<sub>5</sub>)<sub>3</sub> as investigated by following monomer consumption, evolution of the molecular weight distribution (MWD), the vinylidene/vinylene formation and the active state of the catalyst. These experimental studies were done to extend the current set of literature data from a max conversion of 10% to over 90%; thus creating the most inclusive multi-response data set available for single-site polymerization. Comprehensive kinetic

modeling of the extensive data set was carried out beginning with the current kinetic model proposed in the literature [Liu, Z. X., E. Somsook, C. B. White, K. A. Rosaen, and C. R. Landis, *JACS*, 123, 11193 (2001)], where the mechanism includes traditional initiation, propagation and chain transfer via  $\beta$ -hydride elimination reactions. The literature model was able to describe the first order monomer decay as shown in Fig. 1a; however, this traditional model is unable to describe the evolution of the MWD (Fig. 1b), the development of vinylidene/vinylene groups (Figs. 2a and 2b) and the  $\text{CH}_3\text{OD}$

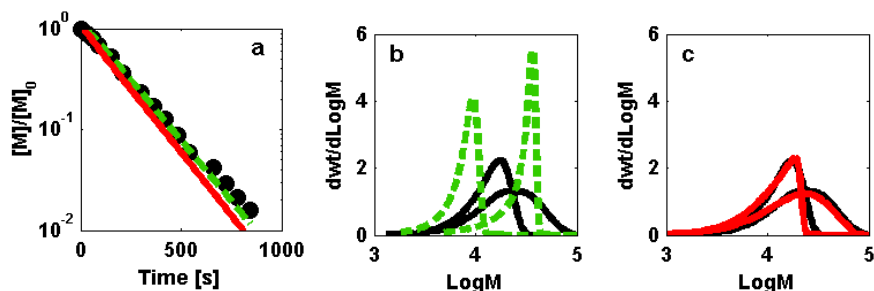


**Figure 1** Monomer consumption (A) and time evolution of the molecular weight distribution (B and C) for the data (●), the literature model (- - -) and the punctuated chain transfer model (- - -). The molecular weight distribution is given at times corresponding to 60s (19% monomer conversion) and 840s (98% monomer conversion).

quenching experiment which revealed less than 50% of the catalyst is attached to polymer chains of 4-mers or greater at the time of quench (Fig. 2c).

The inability of a kinetic model composed of traditional mechanisms to quantitatively predict the multi-response data required us to develop alternative mechanisms. A number of kinetic models were considered and rejected, including a two-site mechanism, initially dead catalyst and catalyst deactivation. The best improvement to

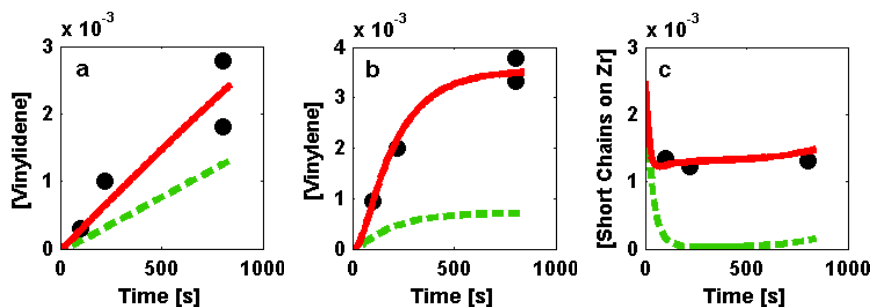
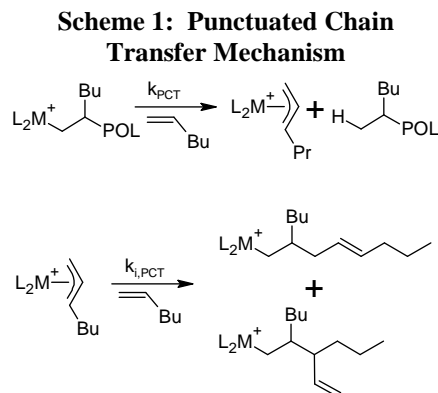


**Figure 2** Vinylidene (a) and vinylene (b) evolution and concentration of Zr with an attached “short” polymer chain (i.e. 0 to 3 mers) (c) for the data (●), the literature model (- - -) and the punctuated chain transfer model (- - -).

the kinetic model includes initiation plus propagation with punctuated chain transfer (PCT), where the metal species remains inactive to new chain growth for a period of time following chain termination. The clear improvement in the model’s ability to predict the data can be seen in Figs. 1 and 2, where the new model does a markedly improved job of fitting the MWD with unquestionable improvements seen in fitting the additional data types. The addition of PCT to the model resulted in a doubling of the propagation rate



constant, hence illustrating that even the seemingly straightforward analysis of *apparent* first order monomer consumption can be in considerable error in the absence of quantitative analysis of multi-response data. Kinetic analysis, using the informatics tools developed in our group, unequivocally shows that PCT is first order in monomer allowing us to hypothesize and test for possible mechanisms such as the one shown in Scheme 1 based on literature observations of similar allylic species.



The quantitative analysis of the rich multi-response kinetic data for the (EBI)ZrMe<sub>2</sub> system should affect a paradigm change in investigation of single-site polymerization catalysts. Hitherto even the best kinetic analysis did not include quantitative analysis of the evolution of the MWD, which, as shown in Fig. 1, results in a seriously incomplete picture of the polymerization mechanism. Moreover, the inclusion of other multi-response data also further constrains potential kinetic mechanisms. Quantitative analysis provides the researcher with a tool that is at least as significant as any modern spectroscopic methods for the determination of mechanism.

- **Synthesis, Characterization and Preliminary Polymerization Studies with New Catalyst Families**

Now that we have working catalyst chemistry models for the aryloxide catalyst system and a kinetic model for the Britzinger catalyst, we are eager to expand the chemical diversity of our catalyst library in order to facilitate further development of quantitative catalyst chemistry models. An important

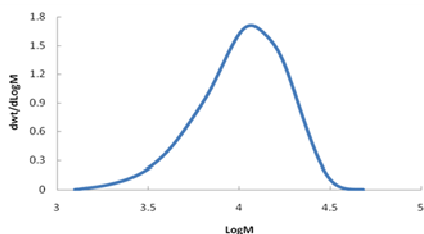


Figure 4. Representative MWD obtained from GPC for polymerization of 1-hexene in hexane by the octahedral [ONNO]ZrBn<sub>2</sub> catalyst. 74% monomer conversion.

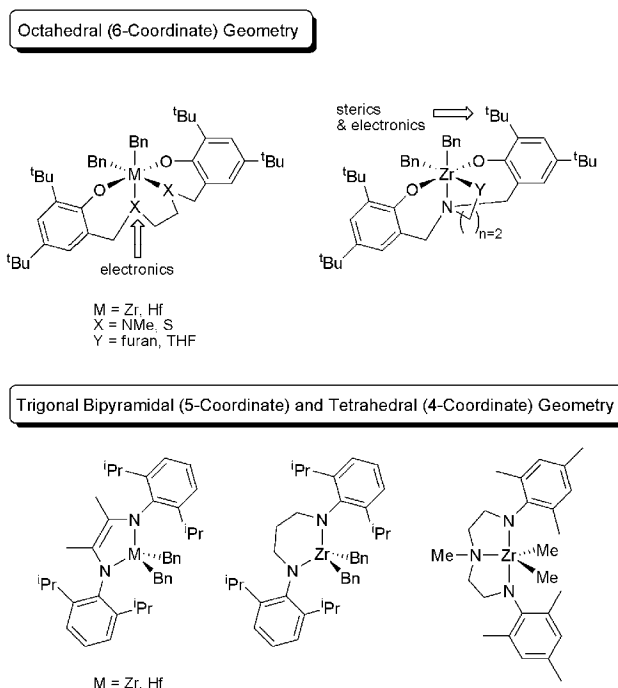


Figure 3. Known catalysts we have already obtained.

addition to our growing library of new and known Group IV molecules is inclusion of non metallocene (or mixed aryloxide) systems. Fig. 3 shows some of the literature

catalysts we have chosen. We hypothesize that  $k_i$  and  $k_p$  are largely dependent on  $E_{IPS}$  and either steric crowding or bond-breaking/reforming energies depending on which step is rate-determining:  $\pi$ -complex formation or insertion. Based on observations found in the literature for a wide range of catalysts, we believe that there is a strong hard/soft effect of the ligand on the rate of chain transfer. We have observed similar effects moving between NMe and S donation. Early studies, e.g Fig. 4, show that these catalysts are widely active as catalysts for polymerization or in a few cases oligomerization of  $\alpha$ -olefins. Full kinetic analysis including monomer consumption, end group analysis, and kinetic modeling of the MWD is underway.

In addition, we have synthesized a series of second-generation mixed-Cp catalysts with greater variations in donation at the metal center (Fig. 5). These changes are observed to have large effects on monomer consumption and molecular weight, especially in the case of S, where only oligomerization occurs.

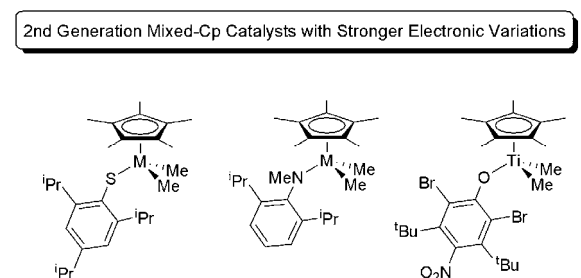
- ***Designing Catalysts for the Water Gas Shift Reaction***

From a data base of more than 220 catalysts for which we have orders of reaction and activation energies as well as detailed chemical characterization, we have been able to enhance the rate substantially and to draw a number of conclusions about the behavior of the catalysts:

- The WGS reaction is product inhibited. Literature data that does not account for this fact is not quantitatively reliable.
- TORs (turnover rates) on Pt and Pd are independent of metal particle size, but strongly dependent on support. On a given support, Pt is roughly an order of magnitude more active than Pd when both metals are unpromoted.
- On alumina, alloying Pd with Zn and Pd or Pt with Fe can enhance the rate by more than an order of magnitude.
- Over a wide variety of metals and supports, all catalysts have similar orders of reaction. Nanoparticles of gold on  $TiO_2$ , however, give the highest rates we have measured (~10 times more active per metal atom than the commercial  $CuO/ZnO/Al_2O_3$  catalyst, see Fig. 6) and show substantially different orders of reaction than others we have measured.

Now that the iron promoted catalysts, and particularly supported nanogold catalysts have brought us to a rate comparable to that of Cu, we are eager to model these systems in detail in order to facilitate design of even more active members of these catalyst families. For the kinetic modeling, we are building a package written in C with MPI (the standard Message Passing Interface for parallel programming), for use on massively parallel computers to perform Bayesian analysis via Markov Chain Monte Carlo sampling of posterior distributions. Catalyst characterization data, as well as the fact that PdFe and PtFe are equally active, suggest that the source of high activity of the Fe

Figure 5. These catalysts have been developed and fully characterized



promoted catalysts is Fe that can be reduced to  $\text{Fe}^0$  in the presence of the noble metal. For the gold catalysts, both EXAFS and TEM confirm the small Au particle size. The intensity of the XANES for the Au  $L_3$ -edge for supported Au catalysts was smaller than for Au foil, suggesting an electron deficient nature of the nano-sized Au clusters.

**Future plans:** *Water Gas Shift Reaction* - With the computing tools now in place we will begin detailed kinetic modeling of the data in our broad WGS data base. We expect to be able to separate the catalysts into classes based on their kinetic parameters (and perhaps computed

variables such as coverage). These efforts and subsequent testing of hypothesis formulated to explain the chemical origins of the catalytic behavior will be aided by collaboration with Bill Schneider at Notre Dame, with whom we have been collaborating on NOx reactions on Pt. Through a combination of this kinetic characterization and *operando* EXAFS (done in collaboration with Jeff Miller at Argonne National Laboratories), *in situ* DRIFTS, and XPS of samples before and after reaction, we will further pursue identification of the active components of the promoted catalysts and identification of the chemical descriptors that control the WGS reaction. The role of the redox properties of the support or promoter phase in activating water, the higher CO order and therefore weaker CO metal interaction in the most active catalysts (Au), and the stabilization of promoters in unusual chemical states at WGS reaction conditions are some of the key questions that will drive this work.

*Single Site Olefin Polymerization* – Building on our successful model for aryloxide catalysts, we will quantitatively determine mechanisms for propagation, initiation, chain transfer and catalyst degradation for our growing library of group IV metal catalysts in order to test the following hypotheses concerning mechanisms for olefin polymerization:

- $k_p$  and  $k_i$  are primarily controlled by ion pair separation energy,  $E_{\text{IPS}}$ , and steric crowding at the catalytic site if  $\pi$ -complex formation is the rate-determining step (rds).
- When insertion is the rate determining step (rds) both bond breaking/reformation and  $E_{\text{IPS}}$  contribute to  $k_p$  and  $k_i$ .
- The presence of opportunistic coordination can significantly alter  $E_{\text{IPS}}$  affecting both the rate determining step (rds) and ratio of  $k_i$  to  $k_p$ .
- Strong  $\pi$ -donating ligands such as amides weaken the coordinated carbon-carbon double bond, affecting  $k_i$  and  $k_p$ .
- Chain transfer via  $\beta$ -hydride elimination is controlled by sterics; however, there is an additional contribution from the hardness of the ligand.

The resulting models will provide a complete description of the olefin polymerization process and a set of rational design tools for the development of new catalysts.

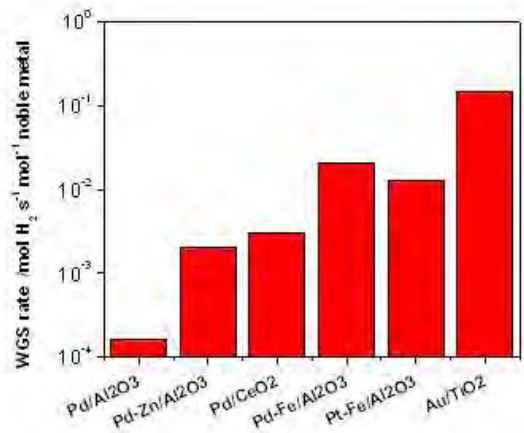


Figure 6. Comparison of WGS rates for monometallic and bimetallic catalysts at 240°C and 1 atm (7% CO, 22% H<sub>2</sub>O, 8% CO<sub>2</sub>, 37% H<sub>2</sub>, balance Ar).

### Publications (2007-2009)

1. Manz, Thomas A., Khamphree Phomphrai, Grigori Medvedev, Balachandra B. Krishnamurthy, Shalini Sharma, Jesmin Haq, Krista A. Novstrup, Kendall T. Thomson, W.N. Delgass, James M. Caruthers, and Mahdi M. Abu-Omar, "Structure-Activity Correlation in Titanium Single-Site Olefin Polymerization Catalysts Containing Mixed Cyclopentadienyl/Aryloxide Ligation," *J. Am. Chem. Soc.*, 129(13), 3776-3777 (2007).
2. Blau, Gary E., Michael Lasinski, Seza Orcun, Shuo-Huan Hsu, James, M. Caruthers, W.N. Delgass, Venkat Venkatasubramanian, " High Fidelity Mathematical Model Building with High Throughput Experimentation: A Bayesian Approach," *Computers in Chemical Engineering*, 32, 971-989 (2008).
3. Bhan, Aditya and W.Nicholas Delgass, "'Propane Aromatization on HZSM-5 and Ga/HZSM-5". *Catalysis Reviews*, 50, 19-151 (2008).
4. Phatak, A. A., N. Koryabkina, S. Rai, J. L. Ratts, W. F. Ruettinger, R. J. Farrauto, G. E. Blau, W. N. Delgass and F. H. Ribeiro, "Kinetics of the water-gas shift reaction on Pt catalysts supported on alumina and ceria," *Catalysis Today*, 123, 224-234 (2007).
5. Bollmann, Luis, Joshua L. Ratts, Ajay M. Joshi, W. Damion Williams, Jorge Pazmino, Yogesh V. Joshi, Jeffrey T. Miller, A. Jeremy Kropf, W. Nicholas Delgass, Fabio H. Ribeiro, "Effect of Zn addition on the water-gas shift reaction over supported palladium catalysts," *J. Catal*, 257, 43-54 (2008).
6. Manz, T. A., S. Sharma, K. Phomphrai, K. A. Novstrup, A. E. Fenwick, P.E. Fanwick, G. A. Medvedev, M. M. Abu-Omar, W. N. Delgass, K. T. Thomson, and J. M. Caruthers, "Quantitative Effects of Ion Pairing and Sterics on Chain Propagation Kinetics for 1-hexene Polymerization Catalyzed by Mixed Cp'/ARO Complexes," *Organometallics*, 27, 5504-5520 (2008).
7. Hsu, Shuo-Huan, Stephen D. Stamatis, James M. Caruthers, W. Nicholas Delgass, Venkat Venkatasubramanian, Gary E. Blau, Michael Lasinski, Seza Orcun, "A Bayesian Framework for Building Kinetic Models of Catalytic Systems," *Industrial and Engineering Chemistry Research*, accepted.
8. Phatak, Abhijit A., W. Nicholas Delgass, Fabio H. Ribeiro, and William F. Schneider," DFT Comparison of Water Dissociation Steps on Cu, Au, Ni, Pd and Pt," *J. Phys. Chem. C*, accepted.
9. Cao, Jun, Ayush Goyal, Krista A. Novstrup, Samuel P. Midkiff, and James M. Caruthers, "An Optimizing Compiler for Parallel Chemistry Simulations," *IEEE Transactions on Parallel and Distributed Systems*. (2009) accepted.
10. Novstrup, Krista, Nicholas Travia, Grigori Medvedev, Cornel Stanciu, Jeffrey Switzer, W. Nicholas Delgass, Mahdi Abu-Omar, James Caruthers, "Punctuated Chain Transfer in [rac-(C<sub>2</sub>H<sub>4</sub>(1-Indenyl)<sub>2</sub>Zr(Me)<sub>2</sub>]-Catalyzed 1-Hexene Polymerization: New Mechanistic Insights from Kinetic Modeling of Rich Multi-Response Data", *to be submitted to JACS* (2009).

**Towards a Molecular Scale Understanding of Surface Chemistry and Photocatalysis on Metal Oxides: Surface Science Experiments and First Principles Theory**

Students and Postdocs: Peter Jacobson, Hongzhi Cheng, Yunbin He, Shao-Chun Li

Collaborators: C. Di Valentin (University of Milano-Bicocca), G. Pacchioni (University of Milano-Bicocca), Antonio Tilocca (University College London), Andreas Stierle (Max-Planck Institut Stuttgart, Germany)

Contacts: U. Diebold, Tulane University; phone: (504) 862-8279; Email:

[diebold@tulane.edu](mailto:diebold@tulane.edu); A. Selloni, Princeton University; phone (609) 258-3837; Email:

[aselloni@princeton.edu](mailto:aselloni@princeton.edu); web page: <http://www.surface.tulane.edu>

**Goal**

Our overall objective is to provide a complete picture of the relationship between atomic structure, electronic properties and (photo-)reactivity of TiO<sub>2</sub> surfaces. Macroscopic single crystalline surfaces are being studied, where these interrelated aspects can be identified. The project's major thrusts are : (i) characterization of intrinsic defects and impurities at TiO<sub>2</sub> anatase (101), the most relevant of all TiO<sub>2</sub> polymorphs, with atomically-resolved STM and accompanying DFT calculations; (ii) Adsorbates, especially water, oxygen, and aromatic molecules (model pollutants) on rutile (110), rutile (011) and anatase (101) surfaces, the resulting electronic structure, and their response to uv-light irradiation; (iii) the 'functionalization' of TiO<sub>2</sub> with noble metal nanoclusters, chromophores, and dopants.

**Recent Progress**

*Importance of subsurface defects at the anatase (101) surface [PRL '09].* Using DFT calculations we predicted that on anatase TiO<sub>2</sub>(101) oxygen vacancies are about 0.5 eV more stable at subsurface than at surface sites, see Fig. 1. Moreover, once formed, the activation energy for a vacancy to migrate from the surface into the bulk is smaller than the other way round. STM experiments have confirmed this unusual result: the (101) surfaces of anatase single crystals with different reduction states show no evidence of surface oxygen vacancies, which are instead quite numerous on the rutile TiO<sub>2</sub>(110) surface. The more reduced anatase sample showed clear evidence for ordered, subsurface defects, however. These are possibly of 'Frenkel'-type, which consist of oxygen vacancies and titanium atoms at interstitial positions. This result could be more than a mere curiosity. If surface oxygen vacancies are formed, they will not survive long in the ambient – almost immediately they will be covered by water or by other adsorbates. When such defects hide in a subsurface layer, they could provide a more subtle, but also more robust influence on surface reactivity.

*Rutile TiO<sub>2</sub>(011)-2x1: solution of the surface structure [Surf. Sci. Lett. '09].* An extensive search based on first principles DFT calculations allowed us to identify a number of structural models with much lower surface energies than previously-proposed models. These new structures were tested with surface x-ray diffraction (SXR) and voltage-dependent STM measurements. The model that is (by far) energetically most stable shows also the best agreement with SXR data. Calculated STM images agree with the experimental ones for appropriate tunneling conditions. The new surface

structure – which we call ‘brookite (001)-like’ because of its similarity to the brookite  $\text{TiO}_2(001)$  surface - exhibits two different types of undercoordinated oxygen and titanium atoms, and is, in its stoichiometric form, predicted to be rather inert towards the adsorption of probe molecules.

*Water on anatase (101) [Nat. Mater. accepted]* - By a combined experimental (STM) and theoretical (DFT-FPMD) study, we have obtained a detailed atomic-scale picture of the structural, dynamical, and electronic properties of water on anatase (101). Water adsorbs as an intact monomer with a computed binding energy of 730 meV. The charge rearrangement at the molecule-anatase interface affects the adsorption of further water molecules, resulting in short-range repulsive and attractive interactions along  $[010]$  and  $[\bar{1}11]/[\bar{1}\bar{1}\bar{1}]$  directions, respectively, and a locally-ordered  $(2 \times 2)$  superstructure of molecular water.

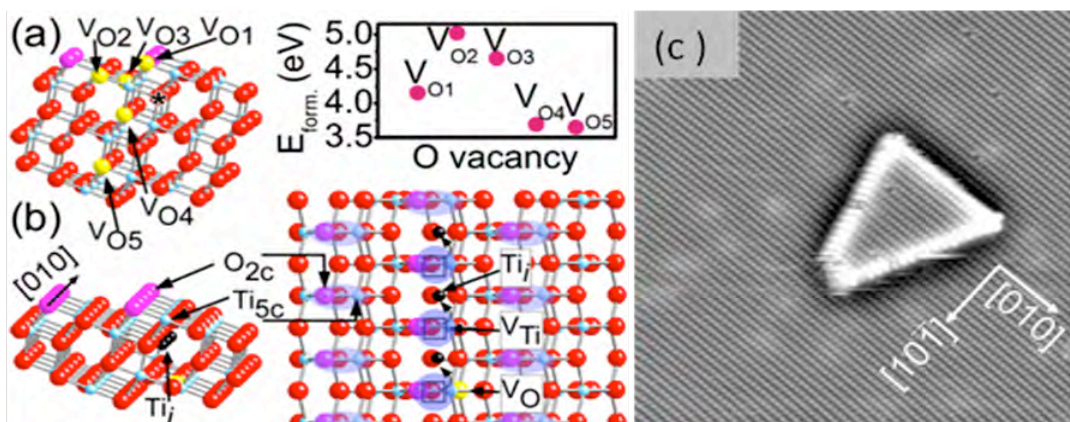


Fig. 1 (a) Various types of on- and sub-surface O vacancies (left) and their computed formation energies (right) at anatase  $\text{TiO}_2(101)$  (red balls: O; light blue balls: Ti). (b) Illustration of formation of ordered subsurface defects invoking Frenkel hops in side (left) and top (right) view. Formation of a subsurface O vacancy at the given site (yellow) initiates the migration of a neighboring Ti atom to an interstitial site ( $Ti_i$ , black), leaving behind a Ti vacancy ( $V_{Ti}$ , black square). Atomically-resolved STM images from the undisturbed surface show ovals that extend across undercoordinated surface  $O_{2c}$  and  $Ti_{5c}$  atoms (purple shading). (c) Large-scale STM image from a freshly-cleaved anatase (101) surface ( $300 \times 300 \text{ \AA}^2$ ;  $V_{\text{sample}} = +1.3 \text{ V}$ ,  $I_{\text{tunnel}} = 1.9 \text{ nA}$ ): no surface oxygen vacancy is present. Adapted from Ref. 2

**DOE Interest:** The project will provide an increased understanding of molecular processes and structure-activity relationships in photocatalytic systems. This can lead to guidelines on how to make  $\text{TiO}_2$ -based photocatalytic systems more efficient. This directly relates to the Program’s mission to develop a mechanistic understanding of chemical reactions that pertain to environmental remediation and pollution control; energy production (photoelectrochemical and production of hydrogen); and novel materials synthesis.

**Future Plans:** We will continue our work on the characterization of clean and doped  $\text{TiO}_2$  single crystalline surfaces and their interaction with selected adsorbates. In particular, we intend to investigate the influence of subsurface defects on the surface chemistry of anatase (101) and understand the origin of the “halos” observed on the STM images of this surface (see Fig. 1c). The chemistry of the reconstructed rutile  $\text{TiO}_2(011)$ - $2 \times 1$  surface will be investigated and compared to that of  $\text{TiO}_2(110)$ .

**Publications 2007 – 2009** (in reverse chronological order)

1. Y. He, A. Tilocca, O. Dulub, A. Selloni, U. Diebold, Submonolayer water on TiO<sub>2</sub> anatase (101): structural, dynamical, and electronic signatures, *Nature Materials*, accepted.
2. Y. He, O. Dulub, H. Cheng, A. Selloni, U. Diebold, Evidence for the Predominance of Subsurface Defects on Reduced Anatase TiO<sub>2</sub>(101), *Phys. Rev. Lett.* **2009**, *102*,106105.
3. H. Cheng and A. Selloni, Surface and subsurface oxygen vacancies in anatase TiO<sub>2</sub> and differences with rutile, *Phys Rev. B* **2009**, *79*, 092101.
4. S.-C. Li, J.-G. Wang, P. Jacobson, X.Q. Gong, U. Diebold, A. Selloni, Correlation between bonding geometry and band gap states at organic-inorganic interfaces: catechol on rutile, *J. Am. Chem. Soc.*, **2009**, *131*, 980-984.
5. X.-Q. Gong, N. Khorshidi, A. Stierle, H. Dosch, H. Z. Chen, A. Selloni, Y. He, O. Dulub, and U. Diebold, The 2×1 Reconstruction of the Rutile TiO<sub>2</sub>(011) Surface: a Combined Density Functional Theory, X-ray Diffraction, and Scanning Tunneling Microscopy Study, *Surf. Sci.*, **2009**, *603*, 138-144.
6. F. De Angelis, S. Fantacci, A. Selloni, Alignment of the dye's molecular levels with the TiO<sub>2</sub> band edges in dye-sensitized solar cells: a DFT-TDDFT study, *Nanotechnology*, **2008**, *19*,424002.
7. W.-K. Li, G. Z. Lu, X.-Q. Gong and A. Selloni, Different reactivities of TiO<sub>2</sub> polymorphs: Comparative DFT calculations of water and formic acid adsorption at anatase and brookite TiO<sub>2</sub> surfaces, *J. Phys. Chem C*, **2008**, *112*, 6594-6596.
8. X.-Q. Gong, A. Selloni, O. Dulub, P. Jacobson, U Diebold, Small Au and Pt clusters at the anatase TiO<sub>2</sub>(101) surface: behavior at terraces, steps and surface oxygen vacancies, *J. Am. Chem. Soc.* **2008**, *130*, 370-381.
9. P. Jacobson, S.-C. Li, C. Wang, U. Diebold, Decomposition of catechol and carbonaceous residues on TiO<sub>2</sub>(110): A model system for cleaning of EUVL optics, *J. Vacuum Sci. Technol.* **2008**, *26*, 2236-2240.
10. S.-C. Li, O. Dulub, U. Diebold, Scanning Tunneling Microscopy Study of a Vicinal TiO<sub>2</sub> Anatase Surface, *J. Phys. Chem. C* **2008**, *112*, 16166-16170.
11. X. Q. Gong, A. Selloni, First principles studied of the structures and energetics of stoichiometric brookite TiO<sub>2</sub> surfaces, *Phys. Rev. B* **2007**, *76*, 235307
12. C. Di Valentin, U. Diebold, and A. Selloni, Doping and functionalization of photoactive semiconducting metal oxides, *Chem. Phys.* **2007**, *339*, pages vii-viii
13. F. De Angelis, S. Fantacci, A. Selloni, M. Graetzel, M.K. Nazeeruddin, Influence of Sensitizer Adsorption Mode on the Open-Circuit Potential of Dye-Sensitized Solar Cells, *Nanoletters*, **2007**, *7*, 3189-3195.
14. C. Di Valentin, E. Finazzi, G. Pacchioni, A. Selloni, S. Livraghi, M.C. Paganini, E. Giamello, N-Doped TiO<sub>2</sub>: Theory and Experiment, *Chem. Phys.* **2007**, *339*, 44-56.
15. E. Finazzi, C. Di Valentin, A. Selloni, G. Pacchioni, First Principles Study of Nitrogen Doping at the Anatase TiO<sub>2</sub> (101) surface, *J. Phys. Chem. C*, **2007**, *111*, 9275-9282.
16. X.-Q. Gong, A. Selloni, Role of steps in the reactivity of the anatase TiO<sub>2</sub>(101) surface, *J. Catal.* **2007**, *249*, 134.
17. M. Batzill, E. H. Morales and U. Diebold, Surface studies of Nitrogen implanted TiO<sub>2</sub>, *Chem. Phys.* **2007**, *339*, 36-43.
18. O. Dulub, M. Batzill, S. Solovyev, E. Loginova, A. Alchagirov, T.E. Madey and U. Diebold, Electron-induced oxygen desorption from the TiO<sub>2</sub>(011)-2x1 surface leads to self-organized vacancies, *Science*, **2007**, *317*, 1052-1056.

**Early Transition Metal Oxides as Catalysts: Crossing Scales from Clusters to Single Crystals to Functioning Materials (C. Peden (PNNL) – PI)****Transition Metal Oxide Clusters – Electronic Structure, Chemical Bonding, and Reactivity Using Photoelectron Spectroscopy and Computational Chemistry**

Dr. David. A. Dixon, Co-Principal Investigator (Co-PI);<sup>1</sup> Dr. Lai-Sheng Wang, Co-PI;<sup>2</sup>  
Dr. Hua-Jin Zhai, Investigator.<sup>2</sup>

Postdoctoral Fellow: Shenggang Li<sup>1</sup>

Students: R. Craciun (graduate),<sup>1</sup> Rebecca Long (undergraduate),<sup>1</sup> Désirée Picone (undergraduate),<sup>1</sup> Natalie Gist (undergraduate)<sup>1</sup>

The University of Alabama,<sup>1</sup> Washington State University<sup>2</sup>

Contact: D.A. Dixon, Chemistry Department, Shelby Hall, Box 870336, The University of Alabama, Tuscaloosa, AL 35487-0336; Phone: 205-348-8441; Email: dadixon@bama.ua.edu

The focus of our subtask in the Catalysis Center led by PNNL is to obtain a molecular level understanding of the properties of supported TMOs, and catalytic reaction mechanisms based on cluster models. Our overall approach is a coordinated experimental (photoelectron spectroscopy (PES)) and computational (density functional (DFT) and molecular orbital (MO) theories) effort to understand and predict the properties of these clusters. Gas phase clusters provide molecular systems with controlled and well-defined structures and atomic connectivity. Their spectroscopic features provide a mechanism for validating electronic structure calculations which form a central part of our program. The chemical properties of free TMO clusters are useful in addressing issues about the nature of the reactive sites of supported clusters. The fact that chemical reactivity depends on cluster size and composition is established, but, there are few spectroscopic studies on early transition metal oxide clusters and little is known about their electronic and structural properties. This work has been done in close collaboration with the other parts of our program on surface catalytic studies.

We have made significant advances in our studies of such species. The work has focused on the structures and reactivity of TMO clusters involving the Group IVB and VIB metals. Important advances include the role of “d orbital aromaticity in transition metal oxide clusters; the high Lewis and Brønsted acidities of metal oxide clusters; the reliable prediction of the high electron affinities of MF<sub>6</sub> compounds; reliable heats of formation and bond energies for MF<sub>x</sub>, MH<sub>x</sub>, MO<sub>3</sub> and MO<sub>2</sub> based clusters, M(PH<sub>3</sub>)<sub>2</sub>, and MCl<sub>x</sub>(PH<sub>3</sub>)<sub>2</sub> (M-PH<sub>3</sub>, x = 0 and 2) at the CCSD(T)/complete basis set level; detailed benchmarking of DFT exchange-correlation functionals; the electronic structure and electron affinities of Group VIB transition metal oxides; CCSD(T)/CBS potential energy



surfaces for oxidative dehydrogenation; and water splitting on the ground and excited states of TiO<sub>2</sub> clusters.

### **Publications (2006 – 2008)**

“On the Structure and Chemical Bonding of Tri-Tungsten Oxide Clusters W<sub>3</sub>O<sub>n</sub><sup>-</sup> and W<sub>3</sub>O<sub>n</sub> (n = 7-10): W<sub>3</sub>O<sub>8</sub> As A Molecular Model for O-Deficient Defect Sites in Tungsten Oxides,” X. Huang, H. J. Zhai, J. Li, and L. S. Wang, *J. Phys. Chem. A* **2006**, *110*, 85.

“Experimental and Theoretical Characterization of Superoxide Complexes W<sub>2</sub>O<sub>6</sub>(O<sub>2</sub><sup>-</sup>) and W<sub>3</sub>O<sub>9</sub>(O<sub>2</sub><sup>-</sup>): Models for the Interaction of O<sub>2</sub> with Reduced W Sites on Tungsten Oxide Surfaces,” X. Huang, H. J. Zhai, T. Waters, J. Li, and L. S. Wang, *Angew. Chem. Int. Ed.* **2006**, *45*, 657.

“Formation of Monodisperse (WO<sub>3</sub>)<sub>3</sub> Clusters on TiO<sub>2</sub>(110),” O. Bondarchuk, X. Huang, J. Kim, B. D. Kay, L. S. Wang, J. M. White, and Z. Dohnálek, *Angew. Chem. Int. Ed.* **2006**, *45*, 4786.

“Photoelectron Spectroscopy of Free Multiply Charged Keggin Anions α-[PM<sub>12</sub>O<sub>40</sub>]<sup>3-</sup> (M = Mo, W) in the Gas Phase,” T. Waters, X. Huang, X. B. Wang, H. K. Woo, R. A. J. O’Hair, A. G. Wedd, and L. S. Wang, *J. Phys. Chem. A* **2006**, *110*, 10737.

“Probing the Electronic Properties of Dichromium Oxide Clusters Cr<sub>2</sub>O<sub>n</sub><sup>-</sup> (n = 1-7) Using Photoelectron Spectroscopy,” H. J. Zhai and L. S. Wang, *J. Chem. Phys.* **2006**, *125*, 164315.

“Molecular and Electronic Structures, Brønsted Basicities, and Lewis Acidities of Group VIB Transition Metal Oxide Clusters,” S. Li and D.A. Dixon, *J. Phys. Chem., A* **2006**, *110*, 6231.

“Bulky Alkylphosphines with Neopentyl Substituents as Ligands in the Amination of Aryl Bromides and Chlorides,” L. L. Hill, L. R. Moore, R. Huang, R. Craciun, A. Vincent, D. A. Dixon, J. Chou, C. J. Woltermann, and K. H. Shaughnessy, *J. Org. Chem.*, **2006**, *71*, 5117.

“Accurate Thermochemical Properties for Energetic Materials Applications. I. Heats of Formation of Nitrogen-containing Heterocycles and Energetic Precursor Molecules from Electronic Structure Theory,” K. E. Gutowski, R. D. Rogers, and D. A. Dixon, *J. Phys. Chem. A*, **2006**, *110*, 11890.

“Ab Initio Prediction of the Gas- and Solution-Phase Acidities of Strong Brønsted Acids: The Calculation of pK<sub>a</sub> Values Less Than -10” K. E. Gutowski and D. A. Dixon, *J. Phys. Chem. A*, **2006**, *110*, 12044.

“Density Functional Theory Study of the  $\beta$ -Carotene Radical Cation and Deprotonated Radicals,” Y. Gao, A. L. Focsan, L. D. Kispert, and D. A. Dixon, *J. Phys. Chem. B*, **2006**, *110*, 24750.

“Probing the Electronic Structure and Band Gap Evolution of Titanium Oxide Clusters  $(\text{TiO}_2)_n^-$  ( $n = 1-10$ ) Using Photoelectron Spectroscopy,” H. J. Zhai and L. S. Wang, *J. Am. Chem. Soc.* **2007**, *129*, 3022

“d-Aromaticity in  $\text{Ta}_3\text{O}_3^-$ ,” H. J. Zhai, B. B. Averkiev, D. Y. Zubarev, L. S. Wang, A. I. Boldyrev, *Angew. Chem. Int. Ed.* **2007**, *46*, 4277.

“Probing the Electronic Structure of Early Transition Metal Oxide Clusters: Polyhedral Cages of  $(\text{V}_2\text{O}_5)_n^-$  ( $n = 2-4$ ) and  $(\text{M}_2\text{O}_5)_2^-$  ( $\text{M} = \text{Nb}, \text{Ta}$ ),” H. J. Zhai, J. Döbler, J. Sauer, and L. S. Wang, *J. Am. Chem. Soc.* **2007**, *129*, 13270.

“Low-Lying Electronic States of  $\text{M}_3\text{O}_9^-$  and  $\text{M}_3\text{O}_9^{2-}$  ( $\text{M} = \text{Mo}, \text{W}$ ),” S. Li and D. A. Dixon, *J. Phys. Chem.*, **2007**, *111*, 11093.

“Benchmark Calculations on the Electron Detachment Energies of  $\text{MO}_3^-$  and  $\text{M}_2\text{O}_6^-$  ( $\text{M} = \text{Cr}, \text{Mo}, \text{W}$ ),” S. Li and D. A. Dixon, *J. Phys. Chem.*, **2007**, *111*, 11908.

“Accurate Thermochemical Properties for Energetic Materials Applications. II. Heats of Formation of Imidazolium-, 1,2,4-Triazolium-, and Tetrazolium-based Energetic Salts from Isodesmic and Lattice Energy Calculations,” Keith E. Gutowski, Robin D. Rogers and David A. Dixon, *J. Phys. Chem. B*, **2007**, *111*, 4708

“Coupled Cluster Study of the Energetic Properties of  $\text{S}_2^x$  ( $x = 0, +1, -1$ )”, D J. Grant, D. A. Dixon and J. S. Francisco, *J. Chem. Phys.* **2007**, *126*, 144308

“Coupled-Cluster Study of the Electronic Structure and Energetics of Tetrasulfur,  $\text{S}_4$ ,” M. H. Matus, D. A. Dixon, K. A. Peterson, J. A. W. Harkless, J. S. Francisco, *J. Chem. Phys.* **2007**, *127*, 174305

“Heats of Formation of Krypton Fluorides and Stability Predictions for  $\text{KrF}_4$  and  $\text{KrF}_6$  from High Level Electronic Structure Calculations,” by D. A. Dixon, T.-H. Wang, D. J. Grant, K. A. Peterson, K. O. Christe, and G. J. Schrobilgen, *Inorg. Chem.*, **2007**, *46*, 10016

“Theoretical Prediction of the Heats of Formation of  $\text{C}_2\text{H}_5\text{O}^\bullet$  Radicals Derived from Ethanol and of the Kinetics of  $\beta$ -C-C Scission in the Ethoxy Radical,” M. H. Matus, M. T. Nguyen, and D. A. Dixon, *J. Phys. Chem. A*, **2007**, *111*, 113

“Probing the Electronic and Structural Properties of Chromium Oxide Clusters  $(\text{CrO}_3)_n^-$  and  $(\text{CrO}_3)_n$  ( $n = 1-5$ ): Photoelectron Spectroscopy and Density Functional Calculations,” H. J. Zhai, S. G. Li, D. A. Dixon, and L. S. Wang, *J. Am. Chem. Soc.* **2008**, *130*, 5167.

“Probing the Electronic Structure and Chemical Bonding of Gold Oxides and Sulfides in  $\text{AuO}_n^-$  and  $\text{AuS}_n^-$  ( $n = 1, 2$ ),” H. J. Zhai, C. Bürgel, V. Bonacic-Koutecky, and L. S. Wang, *J. Am. Chem. Soc.* **2008**, *130*, 9156

“Molecular Structures and Energetic of the  $(\text{TiO}_2)_n$  ( $n = 1-4$ ) Clusters and Their Anions,” S. Li and D. A. Dixon, *J. Phys. Chem. A*, **2008**, *112*, 6646.

“Sterically Demanding, Sulfonated, Triarylphosphines: Application to Palladium-Catalyzed Cross-Coupling, Steric and Electronic Properties, and Coordination Chemistry,” L. R. Moore, E. C. Western, R. Craciun, J. M. Spruell, D. A. Dixon, K. P. O'Halloran, K. H. Shaughnessy, *Organometallics*, **2008**, *27*, 576.

“Benchmark Calculations on the Adiabatic Ionization Energies of the  $\text{M-NH}_3$  ( $\text{M} = \text{Na}, \text{Al}, \text{Ga}, \text{In}, \text{Cu}, \text{Ag}$ ) Complexes,” S. Li, K. A. Peterson and D. A. Dixon, *J. Chem. Phys.* **2008**, *128*, 154301.

“Neopentylphosphines as effective ligands in palladium-catalyzed cross-couplings of aryl bromides and chlorides,” L. L. Hill, J. M. Smith, W. S. Brown, L. R. Moore, P. Guevera, E. S. Pair, J. Porter, J. Chou, C. J. Wolterman, R. Craciun, D. A. Dixon, K. H. Shaughnessy, *Tetrahedron*, **2008**, *64*, 6920.

“Heats of formation of triplet ethylene, ethylidene, and acetylene,” by M. T. Nguyen, M. H. Matus, W. A. Lester, Jr., and D. A. Dixon, *J. Phys. Chem. A*, **2008**, *112*, 2082

“Pulsed EPR and DFT Characterization of Radicals Produced by Photo-Oxidation of Zeaxanthin and Violaxanthin on Silica-Alumina,” A. L. Focsan, T. A. Konovalova, M. K. Bowman, D. A. Dixon, L. D. Kispert, P. Molnár, and J. Deli, *J. Phys. Chem. B* **2008**, *112*, 1806.

“Energetics and Mechanism of Decomposition of Trifluoromethanol,” Minh Tho Nguyen, M. H. Matus, V. T. Ngan, R. Haiges, K. O. Christe, and D. A. Dixon, *J. Phys. Chem. A*, **2008**, *112*, 1298.

“Bond Dissociation Energies in Second Row Compounds,” D. J. Grant, M. H. Matus, J. Switzer, D. A. Dixon, J. S. Francisco, and K.O. Christe, *J. Phys. Chem. A*, **2008**, *112*, 3145.

“Thermochemical Properties of  $\text{CHFO}$ ,  $\text{CF}_2\text{O}$ , and  $\text{CFO}$ ” by M. H. Matus, M. T. Nguyen, D. A. Dixon, and K.O. Christe, *J. Phys. Chem. A*, **2008**, *112*, 4973

“Structure and Heats of Formation of Iodine Fluorides and the Respective Closed Shell Ions from CCSD(T) Electronic Structure Calculations and Reliable Prediction of the Steric Activity of the Free Valence Electron Pair in  $\text{ClF}_6^-$ ,  $\text{BrF}_6^-$  and  $\text{IF}_6^-$ ,” D. A. Dixon, D. J. Grant, K. O. Christe, and K. A. Peterson, *Inorg. Chem.* **2008**, *47*, 5485.

“A survey of factors contributing to accurate theoretical predictions of atomization energies and molecular structures,” D. Feller, K.A. Peterson, and D.A. Dixon, *J. Chem. Phys.*, **2008**, *129* 204015.

**Fundamental Studies of the Reforming of Oxygenated Compounds over Supported Metal Catalysts**

Students: Dante Simonetti, Juben Chheda, Edward Kunkes, Zhen Liu  
Collaborators: Manos Mavrikakis (University of Wisconsin); Jingguang Chen, Mark Barteau, Doug Buttrey (University of Delaware); Ricardo Soares (Universidade de Uberlândia); Robert J. Davis (University of Virginia); Abhaya Datye (University of New Mexico); Jeff Miller (Argonne)  
Contact: James A. Dumesic, Department of Chemical and Biological Engineering, University of Wisconsin, Madison, WI 53706; phone: (608) 262-1095; E-mail: dumesic@engr.wisc.edu  
Web page: [http://www.engr.wisc.edu/che/faculty/dumesic\\_james.html](http://www.engr.wisc.edu/che/faculty/dumesic_james.html)

**Goal**

The goal of this project is to elucidate the fundamental surface chemistry involved in the catalytic conversion of renewable biomass resources to produce energy. The primary focus of this work has been the catalytic production of mono-functional oxygenated hydrocarbons (i.e., C<sub>4</sub> – C<sub>6</sub> alcohols, ketones, carboxylic acids, and heterocyclic compounds) by aqueous-phase processing of biomass-derived sugars and polyols over supported metal catalysts. More recent work has involved the catalytic conversion of these mono-functional intermediates to targeted hydrocarbons for use in transportation fuels.

**Recent Progress**

We have developed a catalytic process whereby sugars and polyols are converted into mono-functional chemical intermediates in a single reactor over a carbon-supported PtRe catalyst. In this step, more than 80% of the initial oxygen content of the sugars and polyols is removed, yielding a spontaneously-separating organic phase. This step operates at moderate pressures (20-30 bar) and temperatures (483-523 K) and utilizes highly concentrated aqueous feeds (40-60%) of sorbitol or glucose. The overall oxygen removal process is accomplished via integration of endothermic reactions that produce hydrogen (involving C-C cleavage) with exothermic de-oxygenation reactions that consume hydrogen (involving C-O cleavage). The balance between reforming and de-oxygenation reactions determines the efficiency of the overall process.

At 503 K and 18 bar, PtRe/C showed excellent stability for longer than one month time-on-stream and yielded an organic stream (referred to as sorb\_503\_18) containing 52% of the carbon found in the 60 wt% sorbitol feed. Assuming a complete balance between the reforming and de-oxygenation reactions (no excess hydrogen produced), we have calculated that the maximum carbon conversion to a mixture of mono-functionalized products with a similar composition to sorb\_503\_18 is equal to 75%, with the remaining 25% of the carbon being converted to CO<sub>2</sub>. The actual conversion of the carbon in sorbitol to Sorb\_503\_18 corresponds to a yield of 70% of this maximum. The aforementioned yield corresponds to the production of 1 kg of Sorb\_503\_18 for every 4 kg of sorbitol. If Sorb\_503\_18 is converted entirely into alkane-based fuels, these fuels will retain 65% of the energy content of the sorbitol feed.

The carbon chain length of carbohydrate derived monofunctional species mentioned above is limited to six carbons by the chain length of parent carbohydrate. To produce higher molecular weight species required for gasoline, diesel and jet fuel applications, the mixture of monofunctional species is subsequently subjected to catalytic C-C coupling reactions. To that end, we have demonstrated the coupling of ketones and alcohols contained in sorb\_503\_18 via aldol condensation/hydrogenation. This reaction proceeds over metals (such as Cu and Pd) supported on mixed oxides with acidic and basic functionalities (such as MgAlO<sub>x</sub> and CeZrO<sub>x</sub>) between 573 and 623 K under low pressures of hydrogen (5 bar). This C-C coupling process yields C<sub>8</sub>-C<sub>12</sub> singly branched ketones that can be converted into diesel grade alkanes via deoxygenation over solid acid supported metal catalysts such as Pt/NbOPO<sub>4</sub>. We have also shown that the carboxylic acids are detrimental to aldol condensation catalysts, and can be rendered benign by ketonization: a reaction in which two carboxylic acid molecules react to form a linear ketone and CO<sub>2</sub>. By integrating aldol condensation over Pd/CeZrO<sub>x</sub> with ketonization over CeZrO<sub>x</sub>, we were able to convert 57% of the carbon in a glucose-derived mixture of monofunctional hydrocarbons into C<sub>7+</sub> ketones.

### **Future Plans**

In our future work, we plan to explore in greater detail the reactions of sugars and polyols over PtRe. For example, we plan to study the fundamental reaction kinetics and the effects of catalyst properties. We also plan to investigate the conversion of sugars/polyols over other bimetallic catalysts with the aim of identifying a less expensive alternative to PtRe/C. Preliminary results have shown that carbon-supported bimetallic catalysts consisting of platinum and oxophilic transition metals such as Cr, Mo and Mn yield similar distributions of mono-functional hydrocarbons as PtRe/C. Additionally, we have shown that palladium-based catalysts are capable of sorbitol reforming at elevated temperature (~543 K). In our previous work, we have shown that our PtRe/C catalyst contains Pt and Re in intimate contact, possibly forming an alloy. We have also concluded that the active sites for the reforming of sugars and polyols consist of platinum atoms with neighboring partially oxidized or hydroxylated Re atoms. The similar atomic numbers and electron backscattering properties of Pt and Re have complicated the characterization of this system by EXAFS and TEM analysis. By substituting rhenium with lighter, but chemically similar oxophilic metals, we not only intend to reduce catalyst cost but also improve contrast, thus allowing for more incisive characterization.

We plan to carry out EXAFS and XANES studies (in and ex-situ) on platinum and palladium bi-metallic catalysts to determine the oxidation state of the oxophilic additive and the nature of the interaction with Pt and Pd in the reduced catalyst and under reaction conditions. The reforming of a volatile model compound such as ethanol would serve as an in-situ probe reaction to measure the relative rates of C-C and C-O bond cleavage processes that also take place during sorbitol reforming. Lastly, transmission electron microscopy will be used to investigate the morphological characteristics of the bimetallic catalysts.

Another avenue of future research involves the study of the kinetics of C-C coupling processes (ketonization and aldol condensation/hydrogenation). Our ultimate objective is to combine these processes in a single reactor, where carbohydrate-derived mixtures of monofunctional hydrocarbons can be converted into C<sub>7+</sub> ketones in a single

step. Preliminary results indicate that water and CO<sub>2</sub> (products of ketonization) cause severe, but reversible inhibition of the PdCeZrO<sub>x</sub> aldol condensation/hydrogenation catalyst. We plan to identify the causes of this inhibition through various characterizations techniques, and use this knowledge to formulate more effective catalysts.

### **DOE Interest**

Environmental and political problems created by our dependence on fossil fuels, such as global warming and national security, combined with diminishing petroleum resources are causing our society to search for new renewable sources of energy and chemicals. In this respect, renewable biomass resources are promising options for the sustainable production of liquid transportation fuels in an age of diminishing fossil fuel reserves.

### **Publications from 2007 - 2009:**

1. J. N. Chheda, Y. Román-Leshkov, and J. A. Dumesic, Production of 5-hydroxymethylfurfural and furfural by dehydration of biomass-derived mono- and poly-saccharides, Green Chemistry **9**, 342 (2007).
2. J. Chheda and J. A. Dumesic, An overview of dehydration, aldol-condensation and hydrogenation processes for production of liquid alkanes from biomass-derived carbohydrates, Catalysis Today **123**, 59 (2007).
3. D. A. Simonetti, E. L. Kunkes, and J. A. Dumesic, Gas-phase conversion of glycerol to synthesis gas over carbon supported platinum and platinum-rhenium catalysts, Journal of Catalysis **247**, 298 (2007).
4. J. N. Chheda, G. W. Huber, and J. A. Dumesic, Liquid-phase catalytic processing of biomass-derived oxygenated hydrocarbons to fuels and chemicals, Angewandte Chemie International Edition **46**, 7164 (2007).
5. Y. Román-Leshkov, C. J. Barrett, Z. Y. Liu, and J. A. Dumesic, Production of 2,5-dimethylfuran from biomass-derived carbohydrates for liquid transportation fuels, Nature **447**, 982 (2007).
6. D. A. Simonetti, J. Rass-Hansen, E. L. Kunkes, R. R. Soares, and J. A. Dumesic, Coupling of glycerol processing with Fischer-Tropsch synthesis for production of liquid fuels, Green Chemistry **9**, 1073 (2007).
7. Ryan M. West, Zhen Y. Liu, Maximilian Peter, and J. A. Dumesic, Liquid alkanes with targeted molecular weights from biomass-derived carbohydrates, Chemistry and Sustainability **1**, 417 (2008).
8. E. L. Kunkes, D. A. Simonetti, R. M. West, J. C. Serrano-Ruiz, C. A. Gaertner, and J. A. Dumesic, Catalytic conversion of biomass to mono-functional hydrocarbons and targeted liquid fuel classes, Science **322**, 417 (2008).
9. D. A. Simonetti and J. A. Dumesic, Catalytic strategies for changing the energy content and achieving C-C coupling in biomass-derived oxygenated hydrocarbons, Chemistry and Sustainability **1**, 725 (2008).
10. D. A. Simonetti, E. L. Kunkes, W. D. Pyrz, L. Murillo, W. Lonergan, J. G. Chen, D. J. Buttrey, and J. A. Dumesic, The role of rhenium in the conversion of glycerol to synthesis gas over carbon supported platinum-rhenium catalysts, Journal of Catalysis **260**, 164 (2008).

## Engineering Catalytic Nanoporous Metals for Reactions Important to the Hydrogen Economy

Students: Joshua Snyder, Anant Mathur  
Contacts: Johns Hopkins University, 102 Maryland Hall, 3400 N. Charles St., Baltimore, MD 21218; [jonah.erlebacher@jhu.edu](mailto:jonah.erlebacher@jhu.edu)

### Goal

Fabricate new nanoporous electrocatalytic metals by electrochemical dealloying, develop methods to tailor their surface chemistry, test their activity for hydrogen oxidation and oxygen reduction, and integrate them into fuel cells as low precious metal loading catalysts.

### DOE Interest

The development of new catalysts for hydrogen fuel cell reactions is a critical step in the development of this technology. Factors for which there is room for improvement include improving catalyst activity, particularly toward oxygen reduction, and the development of carbon-free catalyst layers in the membrane electrode assembly that are not prone to corrosion. A materials system that may be a potential solution for both of these problems simultaneously are nanoporous metals made by selective electrochemical dissolution of one component of a multi-component alloy (dealloying). More specifically, alloys are chosen such that as the majority alloy component is dissolved, the secondary component diffuses along the alloy/electrolyte interface, reconstructing the material into a high surface area crystal with open porosity, high surface area/volume (ligament and pore sizes 5-10 nm), and intrinsic electrical contact to all surface area.

### Recent Progress

*Pt-plated nanoporous gold fuel cell electrodes:* We have made nanoporous gold foils, (15 nm pores, 100 nm thick-foils) by dealloying silver/gold, and then chemically coated them with 1-5 nm of Pt. These materials contain significantly less precious metals than common fuel cell electrodes ( $\sim 0.15$  mg/cm<sup>2</sup> of both Au and Pt combined, with Pt loading alone from 0.01 to 0.05 mg/cm<sup>2</sup>). In H<sub>2</sub>/O<sub>2</sub> fuel cells, this material provided specific power densities of approximately 5 kW/g Pt, and comparable polarization performance to nanoparticle-based catalysts. This demonstrates carbon-free nanoporous metal membranes are compatible with the architecture of proton exchange membrane fuel cells [2,6,7].

*Spontaneous formation of core-shell nanoporous metals:* The ligament size of the dealloyed porous metals (as well their surface area) is largely controlled by the surface diffusion rate of the component left behind. To slow this rate down in nanoporous gold, Pt was added as a minority ternary component to the base alloy. Upon dealloying, a porous metal with pore size  $\sim 4$  nm was formed. This material was found to be morphologically stable in highly acidic solutions and elevated



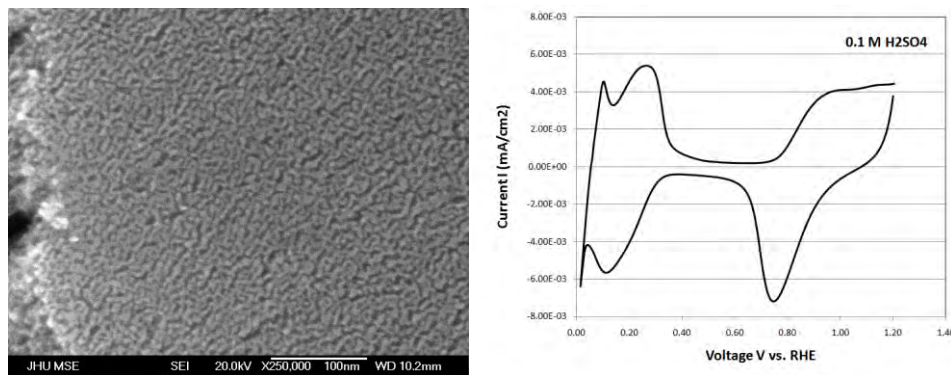


Figure 1. (left) Nanoporous dealloyed Ni<sub>80</sub>Pd<sub>15</sub>Pt<sub>5</sub>, showing ligaments ~5nm in diameter. (right) cyclic voltammetry of dealloyed Ni<sub>80</sub>Pd<sub>15</sub>Pt<sub>5</sub>, showing features associated with hydrogen adsorption/absorption into surface-enriched PdPt.

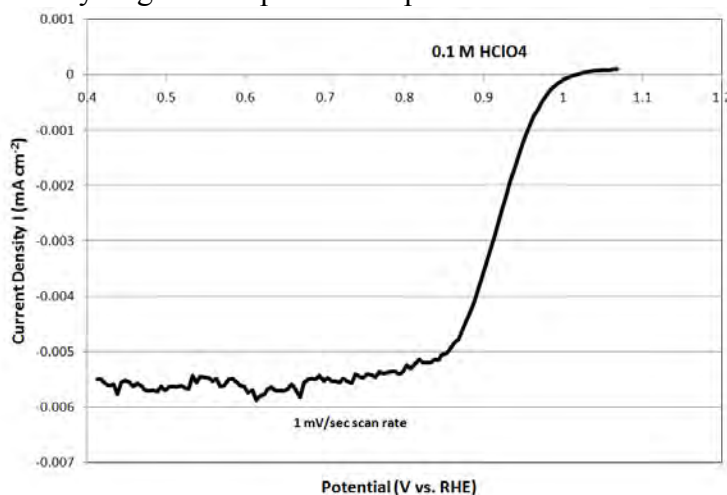


Figure 2. Oxygen reduction kinetics of dealloyed Ni<sub>80</sub>Pd<sub>15</sub>Pt<sub>5</sub> in 0.1 M perchloric acid, 1 mV/sec scan rate (rotating disk electrode, 1600 rpm).

temperatures up to 400 °C. Furthermore, the surface was found to be enriched in Pt and Au, leading to the conclusion that the material is essentially a porous alloy core, with an atomically thin skin comprised primarily of the more noble alloy components, allowing us to control the composition of the surface of porous metals without any post-dealloying processing [4,5].

*Nickel-based nanoporous metal catalysts for oxygen reduction:* In an effort to remove gold from the pre-dealloyed base alloy, nickel based alloys (Ni<sub>x</sub>(Pd, Pt)<sub>1-x</sub>) alloys with x=80 at.% alloys were examined for dealloying possibilities with an eye toward making Pt-skin over Ni-core nanoporous metals and assessing them for oxygen reduction. High quality, crack free films of nanoporous dealloyed Ni<sub>80</sub>Pd<sub>15</sub>Pt<sub>5</sub> and Ni<sub>80</sub>Pt<sub>20</sub> were made (pore size < 5nm), as shown in Figure 1. Voltammetry of the dealloyed materials show significant features associated with hydrogen adsorption on surface Pt, and hydrogen absorption into near-surface Pd.

Assessment of the dealloyed nickel-based alloys for oxygen reduction is highly promising, with half-wave potentials for oxygen reductions greater than 0.92 V (Figure 2), making these materials some of the most active for this reaction yet discovered.

### **Future Plans**

*Electron microscopy characterization of dealloyed Ni-based nanoporous metals.* How is the residual Ni, Pt and Pd distributed on and in the nanoporous metal? What is the density of surface defect sites such as step edges or other low-coordination sites? How good is the core-shell model for these materials?

*Integration of Ni-based nanoporous metals into fuel cell MEAs.* Examination of dealloyed Ni-based alloys in real fuel cell environments will be critical to assess their utility in this application.

*Characterization and measurement of reaction kinetics inside nanoporous metals.* Clues to the enhanced activity of the nanoporous catalysts toward various reactions will be found by measuring catalytic activity versus reactant concentration.

### **Publications (2006-2009)**

1. J. Erlebacher, "Materials Science of Proton Exchange Membrane Fuel Cell Catalysts," *Solid State Physics* **61** (2009), to appear.
2. Mathur, J. Erlebacher, "Effects of Substrate Shape, Curvature and Roughness on Thin Heteroepitaxial Films of Pt on Au(111)," *Surface Science* **602** (2008) 2863-2875.
3. T. Fujita, L. Qian, K. Inoke, J. Erlebacher, M. Chen, "Quantitative Transmission Electron Tomography of Nanoporous Gold," *Applied Physics Letters* **92** (2008) 251902.
4. J. Snyder, K. Livi, J. Erlebacher, "Dealloying Silver/Gold Alloys in Neutral Silver Nitrate Solution: Porosity Evolution, Surface Composition, and Surface Oxides", *Journal of the Electrochemical Society* **155** (2008) C464.
5. J. Snyder, P. Asanithi, A.B. Dalton, J. Erlebacher, "Stabilized nanoporous metals by dealloying ternary alloy precursors," *Advanced Materials* **20** (2008) 4883-4886.
6. R. Zeis, T. Lei, K. Sieradzki, J. Snyder, J. Erlebacher, "Catalytic reduction of oxygen and hydrogen peroxide by nanoporous gold," *J. Catalysis* **253** (2008) 132-138.
7. R. Zeis, A. Mathur, G. Fritz, J. Lee, J. Erlebacher, "Platinum-plated nanoporous gold: An efficient, low Pt loading electrocatalyst for PEM fuel cells", *J. Power Sources* **165** (2007) 65-72.
8. Mathur, J. Erlebacher, "Size Dependence of the Effective Young's Modulus of Nanoporous Gold ", *Appl. Phys. Lett.* **90** (2006) 061910.

**Nanostructured, metal-ion modified ceria and zirconia catalysts**

Co-PIs: Howard Saltsburg (Tufts U.); George Flynn (Columbia U.); Irving Herman (Columbia U.); Siu-Wai Chan (Columbia U.)

Post-docs: Rui Si (Tufts U.); Kwang Toer Rim (Columbia U.)

Graduate Students: Yanping Zhai (Tufts U.); Matthew Boucher (Tufts U.); Nan Yi (Tufts U.); Joan Raitano (Columbia U.); Wei Wang (Columbia U.)

Undergrad Students: Forrest Gittleson (Tufts U.); Glenn Ferreira (Tufts U.)

Collaborators: Anatoly Frenkel (Yeshiva U.); Jose Rodriguez (BNL); Jon Hanson (BNL), Syed Kalid (BNL); Steven Overbury (ORNL); Larry Allard (ORNL); Lihua Zhang (BNL)

Contact: M. Flytzani-Stephanopoulos, Department of Chemical and Biological Engineering, Tufts University, 4 Colby St., Medford, MA 02155; [maria.flytzani-stephanopoulos@tufts.edu](mailto:maria.flytzani-stephanopoulos@tufts.edu)  
Irving P. Herman, Department of Applied Physics and Applied Mathematics, Columbia University, New York, NY 10027; [iph1@columbia.edu](mailto:iph1@columbia.edu)

**Goal**

The overall goal of this project is to elucidate the role of metal ions anchored in oxide supports, and the role of oxide structures in stabilizing the metal ions in their active state for catalyzing reactions of interest to fuel reforming for hydrogen generation. The concentration and types of oxygen defects are strong functions of the size, shape, and composition of the oxide nanoparticles. Novel chemical synthesis techniques are employed to control the size and shape of oxide nanoparticles, and metal-doped oxides to elucidate these correlations. The nanocatalysts are characterized by a variety of analytical techniques, including in situ X-ray absorption spectroscopy, in situ Raman scattering, aberration-corrected electron microscopy, and by surface-probing methods, such as XPS and scanning tunneling microscopy and spectroscopy. Catalytic testing under steady-state and dynamic conditions, TPR, and TPSR provide important information about the activity, selectivity, and stability of catalysts in realistic reaction gas mixtures.

**DOE Interest**

The project is motivated by the original reports<sup>1,2</sup> by the PI's group at Tufts University that the activity of ceria-supported gold or platinum catalysts for the water-gas shift reaction is not due to the presence of the metal nanoparticles. Rather, a sub-structure of oxidized metal atoms embedded in ceria, i.e. Au-O-Ce and Pt-O-Ce, contains the active sites for this reaction. While the metal particle size distribution is not important, the particle size, shape, and oxygen defect density of the host oxide (ceria) are crucial for an active water-gas shift catalyst. These results have a major impact on catalyst design and development. The extension of these findings to other redox reactions in fuel processing is of interest. Also, under investigation are other nanoscale oxide hosts, such as zirconia, iron oxide, and zinc oxide. Lower-cost catalysts for hydrogen generation and purification are critical to the development and market penetration of fuel cells.

## Recent Progress

Recently, we have demonstrated that the catalytic properties of nanoscale Au-FeO<sub>x</sub> are identical to Au-CeO<sub>x</sub> in regards to their activity for the WGS and the CO oxidation reactions. Atomically dispersed gold in the iron oxide lattice, Au-O-Fe, catalyzes the WGS reaction<sup>3,4</sup>, while these species are inactive for the low-temperature CO oxidation reaction, as is true also for the gold-ceria system<sup>3,5</sup>. The oxygen potential of the reaction gas mixture determines the stability of the active Au-O-Ce,Fe sites at low temperatures. Deactivation is due to hydrogen-induced sintering of the gold particles. Full re-dispersion of the sintered gold particles is possible by heating in air at 400°C.<sup>3</sup> Extension of these findings to other gold-oxide systems is under investigation in the project. We have identified a strong shape effect of ceria on the activity of the gold/ceria nanocatalyst for the WGS reaction<sup>6</sup>. Shape effects are currently under investigation for some of the other oxides of interest to this project. Highlights from last year's findings of the project are presented below.

### Nano Au/FeO<sub>x</sub>

Direct imaging of catalyst evolution at the atomic scale was achieved by high-resolution aberration-corrected electron microscopy with an in-situ heating stage, in collaboration with researchers (Overbury, Allard) at Oak Ridge National Lab<sup>4</sup>.

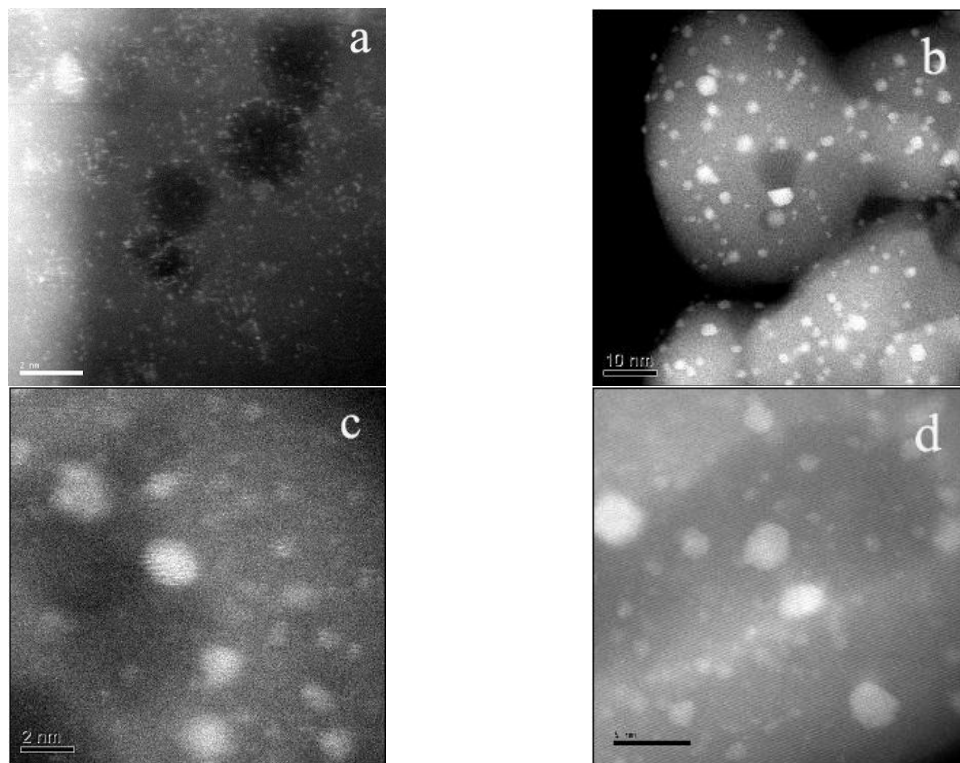


**Figure 1.** Aberration-corrected HREM images of the leached gold-iron oxide samples: (a) Fresh; (b) Fresh after 500 °C in vacuum for 7 min; (c) Used; (d) Reduced.

A series of samples derived from a parent material (2 at.% Au/Fe<sub>2</sub>O<sub>3</sub>, World Gold Council) by NaCN-leaching the surface gold and exposed to various treatments, including air at 400°C (fresh), water–gas shift (WGS) reaction gas (1%CO/3%H<sub>2</sub>O/He)

at 250°C (used), and hydrogen at 400 °C (reduced) were examined. The fresh sample was also subjected to in situ heating from RT to 700°C holding for several minutes at each temperature. Atomic gold throughout the iron oxide particles was identified in the fresh samples, along with a few embedded gold nanoparticles with contracted lattice constant (Figure 1a). Heating up to 500–700 °C in vacuum caused gold migration to the surface of the Fe<sub>2</sub>O<sub>3</sub> particles, collapse of the oxide nanopores, and growth and redistribution of Au nanoparticles (Figure 1b). The used (Figure 1c) and reduced (Figure 1d) samples show similar features; the distribution of gold is predominantly in 1-3 nm particles, together with a minority of atomically dispersed gold. These results demonstrate the value of in situ heating<sup>4</sup> for understanding structural changes in the catalyst with elevated temperature treatments<sup>4</sup>.

In on-going work, we are also evaluating new synthesis methods of nanoscale Au-FeO<sub>x</sub> catalysts with controlled crystal shapes. Hematite ( $\alpha$ -Fe<sub>2</sub>O<sub>3</sub>) nanotubes (200-300 nm in length; 100 nm in outer diameter) have been synthesized *via* a controlled hydrolysis method together with a hydrothermal treatment at 220°C. The as-prepared nanocrystals show good thermal stability up to 400°C in air. We are now introducing gold into iron oxide during this one-step preparation to evaluate the interaction between Au and FeO<sub>x</sub>.

#### In situ XANES/EXAFS

Combined in situ XANES and EXAFS studies were conducted using the X18B beamline at Brookhaven to follow gold structural changes of low-content (<1%Au) gold-ceria catalysts in WGS reaction tests; and after heating the used catalysts in oxygen gas<sup>7</sup>. Gold in the fresh (400°C-calcined) material was atomically dispersed in cerium oxide. The Au-Au coordination number is zero for the fresh material, but increases during reaction to 6.5±2.4 (after use at 100°C) and to 8.7±1.5 (after 200°C) in 5%CO/3%H<sub>2</sub>O/He. Loss of activity accompanies the gold particle formation. Attempts to reoxidize and redisperse the gold by heating in oxygen gas at 150 °C were not effective (Fig. 2). However, complete recovery of the surface oxygen amount and redispersion of gold in ceria was possible after a 400 °C- oxygen treatment, with concomitant recovery of the initial high activity<sup>7</sup>.

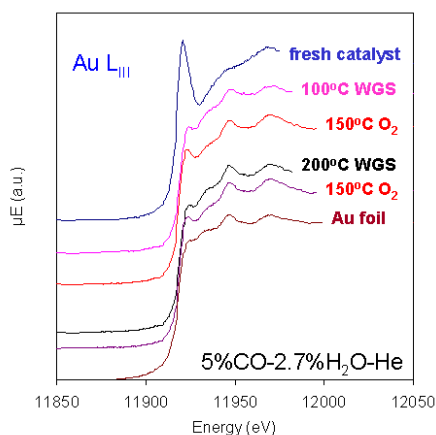


**Figure 2.** XANES of a 0.5 at.% Au-CeO<sub>2</sub> sample under different conditions.

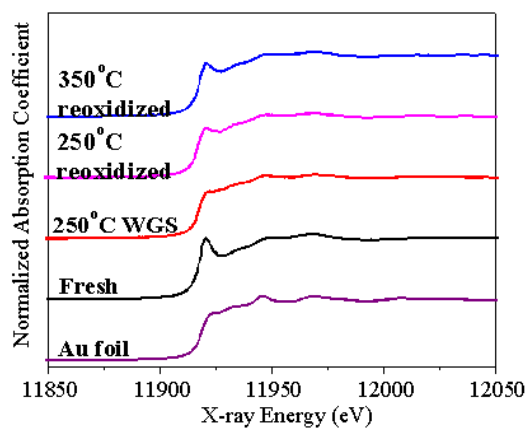


**Figure 3.** XANES of a 0.7 at.% Au-FeO<sub>x</sub> sample under different conditions.

Similar to the Au-CeO<sub>2</sub> system, gold can be partially re-dispersed in the iron oxide support by oxidation at low temperatures after use in the WGS reaction, and fully redispersed after a 400°C-oxygen treatment. This is depicted in Fig. 3 by a series of in situ XANES analyses of the 0.7 at.% Au-FeO<sub>x</sub> catalyst obtained by NaCN-leaching of World Gold Council 2at% Au/Fe<sub>2</sub>O<sub>3</sub> parent material. The leached sample contained only ionic gold, with a coordination number (CN) of Au-O in the fresh catalyst of 2.3±0.5 and without any Au-Au contribution. The CN of Au-Au was 7.2±1.3 after the 250°C WGS reaction, together with a drop of the CN of Au-O to 0.5±0.2. After the 350°C oxidation step (20%O<sub>2</sub>/He), the Au-Au shell disappeared and the CN of Au-O increased to 1.4±0.8.

#### Scanning Tunneling Microscopy Studies of Gold Nano-particles on an Iron Oxide

To elucidate the nature of the enhanced reactivity of gold in iron oxide, we have prepared a model catalyst system, consisting of vapor deposited gold on a single crystal iron oxide surface, in ultrahigh vacuum. This sample has been used to investigate the site-specific adsorption of Au nanoparticles and adatoms on the oxide and the relationship between the size of the formed Au nanoparticles and their oxidation state using Scanning Tunneling Microscopy (STM) and Spectroscopy (STS)<sup>8</sup>.

Gold forms two electrically distinct nanoparticles on an iron oxide surface upon annealing multilayer Au/Fe<sub>3</sub>O<sub>4</sub>(111) at 500°C for 15 minutes. I(V) curves taken via STS measurements show the presence of large gold nanoparticles (~8nm), which exhibit a metallic electronic structure and, thus, are likely neutral. Single gold adatoms are also observed and appear to be strongly bonded to the oxygen sites of the Fe<sub>3</sub>O<sub>4</sub>(111) surface. Electrons flow predominantly from these Au adatoms to oxygen sites of the surface. Site-specific adsorption at oxygen surface atoms and the size sensitive nature of the electronic structure suggest that the Au adatoms are likely positively charged. When this Au/Fe<sub>3</sub>O<sub>4</sub>(111) system is dosed with CO at 260K, adsorption of CO molecules normal to the surface takes place atop the gold adatom sites<sup>8</sup>. Experiments are under way to determine the behavior of water on this surface.

#### Synthesis of Nanoscale Zirconia and Doped Ceria and Zirconia Crystals

Nanoparticles of cubic, tetragonal and monoclinic ZrO<sub>2</sub> have been prepared by an aqueous method with subsequent annealing resulting in a single phase. Nanoparticles of either tetragonal or monoclinic ZrO<sub>2</sub> can be prepared in pure form while cubic ZrO<sub>2</sub> was stabilized by around 4% Y<sub>2</sub>O<sub>3</sub>. Furthermore, nanoparticles of Pd-CeO<sub>2</sub> and Pd-ZrO<sub>2</sub> have been prepared by aqueous co-precipitation resulting in single phase, cubic and tetragonal structures, respectively. Since palladium species are not visible in X-ray diffraction scans of either calcined oxide and a slight lattice contraction is observed in Pd-CeO<sub>2</sub> nanoparticles with respect to pure ceria, palladium is likely in at least partial solid solution with these oxides. Such solid solution formation in the Pd-CeO<sub>2</sub> nanoparticles is supported by Pd exhibiting a +2 oxidation state by XANES analysis and by the defective microstructure of the crystallites, unlike pure ceria. Testing of these catalysts in methanol reforming reactions is currently under investigation.

#### Methanol Decomposition and Steam Reforming Reactions

The shape effect of ceria on methanol reactions was recently investigated using Au- and Pt-ceria nanorods{110}+{100} and nanocubes{100}. The metal was added in a second

step on the pre-formed ceria nanoshapes. Methanol decomposition in a gas mixture containing (mol) 16% CH<sub>3</sub>OH balanced with He is shown in Figure 4a. A clear shape effect of ceria on the Pt-ceria nanorods and nanocubes was found. Steam reforming of methanol in a gas mixture containing (mol) 2% CH<sub>3</sub>OH, 2.6% H<sub>2</sub>O balanced with He is shown in Fig.4b; again a strong shape effect is observed for the Au-ceria catalyst.

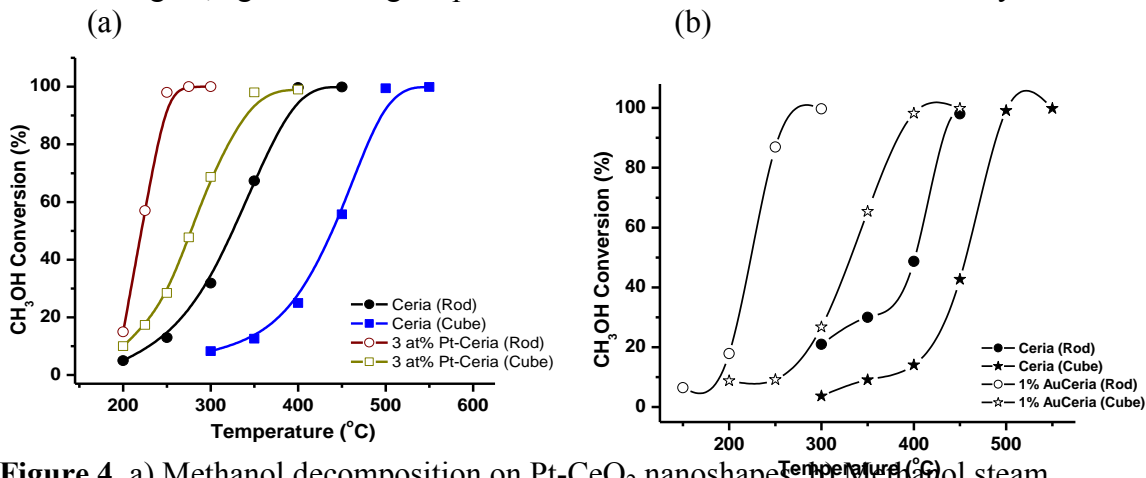


**Figure 4.** a) Methanol decomposition on Pt-CeO<sub>2</sub> nanoshapes; b) Methanol steam reforming on Au-CeO<sub>2</sub> nanoshapes.

#### In situ Raman Scattering of Au-doped CeO<sub>2</sub> nanoshapes in CO Gas Flow

We have investigated nanocrystalline ceria-supported Au with various morphologies in CO gas flow as a function of temperature. Bands at 340 cm<sup>-1</sup> and 831-872 cm<sup>-1</sup> have been observed in CO gas flow at temperatures from -150 °C to 150 °C; these peaks also exist in air, but with intensity much lower than that in CO. No shift is seen for either band with <sup>13</sup>CO gas flow, therefore the assignment of carbon-related species is excluded. The 340 cm<sup>-1</sup> and 831-872 cm<sup>-1</sup> bands are assigned to symmetric Ce-O vibration and O-O stretching vibration of the peroxide species coordinated at two-electron defect sites, respectively. Temperature-programmed measurements in CO flow allow peroxide species on isolated and aggregated two-electron defect sites to be distinguished. These peroxide bands are strong for 0.9% Au-doped CeO<sub>2</sub> nanorod catalysts (with high activity), and extremely weak for the pure CeO<sub>2</sub> nanorod or 0.9% Au-doped CeO<sub>2</sub> nanocube (both with very low activity) samples. The intensity of the peroxide bands could be increased at certain temperatures by introducing H<sub>2</sub>O into the gas flow for the 0.9% Au-doped CeO<sub>2</sub> nanorod catalyst. No changes are seen in the Raman spectrum when D<sub>2</sub>O is used instead. The ability to generate surface peroxide species in CO and CO/H<sub>2</sub>O gas flow tracks the catalytic activity of the Au-doped CeO<sub>2</sub> catalyst, indicating that peroxide species is likely a key intermediate in the CO oxidation and WGS reaction catalyzed by Au-doped CeO<sub>2</sub>.

#### **Future Directions**

All the activities highlighted above are continuing in the near future. A comprehensive and complementary approach is followed in the project to elucidate the metal-oxide interaction at the atomic scale. A new task in next year's plan is the synthesis, characterization and evaluation of surface alloys on nanoscale oxides for the reactions of methanol under study in the project. We will focus a major part of our effort on detailed examinations of the shape effect of the oxide host and propose general catalyst design

guidelines as appropriate. The desired outcome is a good mechanistic understanding of the chemistries under investigation, and the evolution of the key catalyst structures.

## **References and Publications (since 2006) acknowledging this DOE Grant**

Note: a reference in bold-face also belongs to the ‘publications’ list.

1. Q. Fu, H. Saltsburg, and M. Flytzani-Stephanopoulos, *Active nonmetallic Au and Pt species on ceria-based water-gas shift catalysts*, Science 30, 935-938 (2003).
2. Q. Fu, W. Deng, H. Saltsburg, M. Flytzani-Stephanopoulos, *Activity and stability of low-content gold-cerium oxide catalysts for the water-gas shift reaction*, Appl. Catal. B 56, 57–68 (2005).
3. W. Deng, D. Carpenter, N.Yi, and M.Flytzani-Stephanopoulos, *Comparison of the activity of Au/CeO<sub>2</sub> and Au/Fe<sub>2</sub>O<sub>3</sub> catalysts for the CO oxidation and the water-gas shift reactions*. Topics in Catalysis 44, 199-208 (2007)
4. L.F. Allard, A. Borisevich, W. Deng, R. Si, M. Flytzani-Stephanopoulos, S. H. Overbury, *Evolution of gold structure during thermal treatment of Au/FeOx catalysts revealed by aberration-corrected electron microscopy*, J. Electron Microscopy, published online (2009)
5. W. Deng, J. DeJesus, H. Saltsburg, M. Flytzani-Stephanopoulos, *Low-content gold-ceria catalysts for the water-gas shift and preferential CO oxidation reactions*, Appl. Catal. A 291, 126-135 (2005)
6. R. Si, M. Flytzani-Stephanopoulos, *Shape and crystal-plane effects of nanoscale ceria on the activity of Au-CeO<sub>2</sub> catalysts for the water-gas shift reaction*, Angew. Chem. Int. Ed. 47, 2884-2887 (2008)
7. W. Deng, A. Frenkel, R. Si, and M. Flytzani-Stephanopoulos, *Reaction-relevant gold structures in the low temperature water-gas shift reaction on Au-CeO<sub>2</sub>*. J. Phys. Chem. C 112, 12834-12840 (2008)
8. K.T. Rim, D. Eom, L. Liu, E. Stolyarova, J. M. Raitano, S.-W. Chan, M. Flytzani-Stephanopoulos, and G.W. Flynn, *Catalytic gold nanoparticles on an iron oxide surface: a scanning tunneling microscopy/spectroscopy study*, J. Phys. Chem.-C, in press (2009)
9. W. Deng and M. Flytzani-Stephanopoulos, Angew. Chem. Int. Ed. 45, 2285-2289 (2006)
10. F. Zhang, J. M. Raitano, Chih-Hao Chen, J. C. Hanson, W. Caliebe, S. Khalid, and S.-W. Chan, *Phase stability in ceria-zirconia binary oxide nanoparticles: The effect of the Ce<sup>3+</sup> concentration and the redox environment*, J. Appl. Phys. 99, 0843131-38 (2006)
11. D. Pierre, W. Deng and M. Flytzani-Stephanopoulos, Topics in Catalysis 46, 363-373 (2007)
12. F.C. Meunier, D. Reid, A. Goguet, S. Shekhtman, C. Hardacre, R. Burch, W. Deng and M. Flytzani-Stephanopoulos, J. Catal. 247, 269-79 (2007)
13. Po-Yi Wu, J. Pike, F. Zhang, and S.-W. Chan, *Low temperature synthesis of ZnO nanoparticles*, Int’l J. Appl. Cer.Techn. 3, 272-278 (2006)
14. M. Manzoli, F. Boccuzzi, A. Chiorino, F. Vindigni, W. Deng, M. Flytzani-Stephanopoulos, *Spectroscopic features and reactivity of CO adsorbed on different Au/CeO<sub>2</sub> catalysts*, J. Catal. 245, 308-315 (2007)
15. F. Zhang, P.J. Chupra, S. Lun, A. Lui, J.C. Hanson, W. Caliebe, P. L. Lee, and S.-W.Chan, Chem. Materials 19, 3118-3126 (2007)
16. W. Wang, R. Si, S. Banerjee, M. Flytzani-Stephanopoulos, I. P. Herman, *In situ Raman scattering study on water-gas-shift reaction catalysed by Au-CeO<sub>2</sub>*, JACS, to be submitted.



## Mechanistic Study of Ethylene Hydroformylation over Supported Rh Nanoparticles under Reaction Conditions by Time Resolved FTIR Spectroscopy

N. Sivasankar and H. Frei\*

Physical Biosciences Division, Lawrence Berkeley National Laboratory,  
Berkeley, CA 94720  
e-mail: HMFrei@lbl.gov

Hydroformylation or oxo-synthesis is an important industrial process in which an alkene reacts with CO in the presence of hydrogen to produce aldehydes. Development of viable heterogeneous catalytic paths for hydroformylation remains a critical challenge. The understanding of the mechanism of hydroformylation is of paramount interest to attain high product selectivity as well as to design efficient catalysts. Time resolved FTIR spectroscopic technique in the millisecond regime has been successfully used to detect kinetically relevant transient species in important heterogeneous catalytic reactions such as hydrogenation of CO, ethylene and propylene in our group. We report here millisecond FTIR spectroscopic investigation of ethylene hydroformylation over Rh/Al<sub>2</sub>O<sub>3</sub> catalyst at 443 K, resulting in the direct observation of growth and reaction of surface propionyl intermediate for the first time. Two consecutive reaction steps on the Rh nanoparticle surface were temporally resolved.

Monitoring of the reaction of C<sub>2</sub>H<sub>4</sub> and CO with H<sub>2</sub> under flow conditions (1 atm, H<sub>2</sub>/N<sub>2</sub> 0.07, 4.8 L min<sup>-1</sup>) at 443 K revealed complete selectivity towards hydroformylation at the expense of ethylene hydrogenation. Release of ethylene pulses into the H<sub>2</sub>/N<sub>2</sub> flow lead to efficient hydrogenation to gas phase ethane (monitored at 2893 cm<sup>-1</sup>) under direct observation of transient surface ethyl intermediate (CH<sub>3</sub>CH<sub>2</sub>Rh, 1196 cm<sup>-1</sup>). By contrast, pulsed release of ethylene and CO gas into the hydrogen flow results in hydroformylation with high selectivity; no ethane was formed. This implies that the competition between hydrogenation of surface ethyl species versus reaction with CO to yield surface propionyl is overwhelmingly in favor of reaction with CO. We have been able to directly monitor the reaction of surface ethyl intermediate with CO to form surface propionyl species (CH<sub>3</sub>CH<sub>2</sub>C(=O)Rh, 1675 cm<sup>-1</sup>), which reaches maximum intensity within 3,000 milliseconds. This step determines the product branching between hydrogenation and hydroformylation. The subsequent hydrogenation of surface propionyl to propionaldehyde (1735 cm<sup>-1</sup>) was resolved as well. This is the first example of a heterogeneous catalytic reaction in which two consecutive elementary steps are directly observed under reaction conditions. Spectral assignments were confirmed by experiments using isotopically labeled <sup>13</sup>CO.

**Mesoscopic behavior of supported metal clusters: Pt/ $\gamma$ -Al<sub>2</sub>O<sub>3</sub>**

Lead PI: Ralph G. Nuzzo

Potsdocs: Qi Wang (YU), L.L.Wang (UIUC), L. Li (Pitt)

Students: S. Sanchez, M. Small (UIUC), A. Bram (YU)

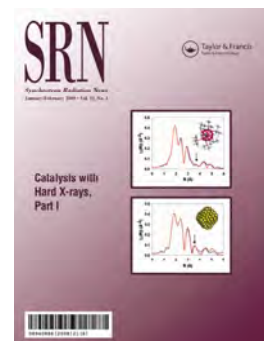
Collaborators: J. Rehr, F. Vila, J. Kas (U. Washington)

Contact: Physics Department, Yeshiva University, 245 Lexington Ave., New York, NY 10016; [anatoly.frenkel@yu.edu](mailto:anatoly.frenkel@yu.edu)

In 2006, we reported a number of structural anomalies (negative thermal expansion, enhanced bond length disorder, and non-bulk like electronic properties) in Pt nanoclusters supported on  $\gamma$ -Al<sub>2</sub>O<sub>3</sub>. Given its importance as a catalytic system, we undertook a combined, experimental and theoretical, effort to define scalings of such complexity with regards to cluster size, loading to adsorbates, support identity and alloying amongst other variables.<sup>1-3</sup> We now understand that the origins of the phenomena reside in the electronic consequences of the dynamic structure, elements of which are captured in the MD/DFT results obtained by us and our collaborators. Implicit in this rendering is the non-vibrational dynamics of the cluster diffusing over the substrate. Our more extended data obtained by a combination of EXAFS and electron microscopy (EM) studies have made it possible to separately analyze the competing influences of bonding to adsorbates and supports/ligands, cluster-size effects and heterogeneity, amongst others. Specific bonding interactions between a substrate and its support constitute an important influence for heterogeneous systems. First principles calculations by Johnson's group, for example, have convincingly demonstrated the role of oxygen vacancies in facilitating charge transfer between a  $\gamma$ -Al<sub>2</sub>O<sub>3</sub> substrate and a supported Pt cluster. Our recent experimental EM and EXAFS data, coupled with DFT modeling, allowed us to quantitatively measure, and understand the physical origin of, the size- and substrate- dependent crystallinity of Pt particles on different substrates. Our results demonstrate that these factors dominate the bonding developed within the cluster. It remains a challenge to bridge these new insights to the most fundamental question related to a chemical transformation mediated by such a prototypical heterogeneous catalyst—to demonstrate how the dynamical ensembles of the type revealed by the present work might act to promote specific forms of molecular transformations. This challenge motivates our future work in this field.

**References:**

1. A. I. Frenkel, J. C. Yang, D. D. Johnson, R. G. Nuzzo, "Complexity of nanoscale atomic clusters." In: Encyclopedia on Complexity and Systems Science, R. A. Meyers, Ed., Springer. 2009, in press.
2. M. Small, S. Sanchez, R. G. Nuzzo, A. I. Frenkel, "X-ray absorption spectroscopy studies of model catalysts." Synchrotron Radiation News, Special Issue "Catalysis with hard x-rays", J.-D. Grunwaldt and A. I. Frenkel, Editors., **22:1**, 6-11, 2009.
3. S. I. Sanchez, L. D. Menard, A. Bram, J. H. Kang, M. W. Small, R. G. Nuzzo, A. I. Frenkel, "The emergence of non-bulk properties in supported metal clusters: negative thermal expansion and atomic disorder in Pt nanoclusters supported on  $\gamma$ Al<sub>2</sub>O<sub>3</sub>". J. Am. Chem. Soc. 2009, in press.



**Exploiting Metastable Oxygen on Gold Surfaces for the Selective Functionalization of Olefins**

Students: Thomas A. Baker, Xingyi Deng, , Xiaoying Liu, Bingjun Xu

Postdoctoral Researchers: Dr. Jan Haubrich, Dr. Weiwei Gao, Dr. Byoung Koun Min

Collaborators: Prof. Marcus Bäumer (Bremen Univ.) Prof. Robert J. Madix (Harvard), Dr. Volkmar Zielasek (Bremen Univ.), Arne Wittstock (Bremen Univ.)

Contact: Cynthia M. Friend; Harvard University; 12 Oxford St., Cambridge, MA 02138

Phone: 617 495 4052; e-mail: [friend@chemistry.harvard.edu](mailto:friend@chemistry.harvard.edu)Web page: <http://www.chem.harvard.edu/groups/friend/index.html>**Goal:**

The proposed work aims to characterize the structures of nanoscale Au-based materials that are of potential importance in efficient catalytic synthesis of oxygenates and other key chemical building blocks. Most recently, we have focused on the oxidation of alcohols. Our objective is to develop a fundamental understanding of how *to control the activity and selectivity for important reactions* promoted by Au-based materials, with special emphasis on the use of transient, metastable states of oxygen.

**DOE Interest:**

DOE has interest in developing new materials, especially at the nanoscale for efficient chemical processes and for energy conversion. Our work provides fundamental insights into activating and improving the selectivity of nanoscale Au-based materials that are of potential importance in efficient catalytic synthesis of oxygenates and other key chemical building blocks. Our work has provided the fundamental underpinnings for controlling the activity and selectivity for oxidation of alcohols promoted by Au-based materials, with special emphasis on the use of transient, metastable states of oxygen. The mechanism of reaction developed in our work provides the basis for understanding alcohol oxidation on supported Au catalysts and on unsupported nanoporous Au.

**Recent Progress:****1.3.1. The state of active oxygen on Au.**

A combination of experiment and theory was used to demonstrate that gold nanoparticles are formed on top of Au(111) upon oxidation of the surface at low temperature. We find that the local bonding of atomic O on the Au nanoparticles and the overall morphology and structure of the surface is important in determining reactivity and selectivity of the surface. Importantly, *atomic oxygen bound to the Au nanoparticles is active for a wide range of oxidation reactions*, including CO, olefin, ammonia, and alcohols. We control the size and the local structures of the O/Au nanoparticles using surface temperature and the method of oxidation, which affects the rate. We establish that the islands formed at low temperature contain Au because

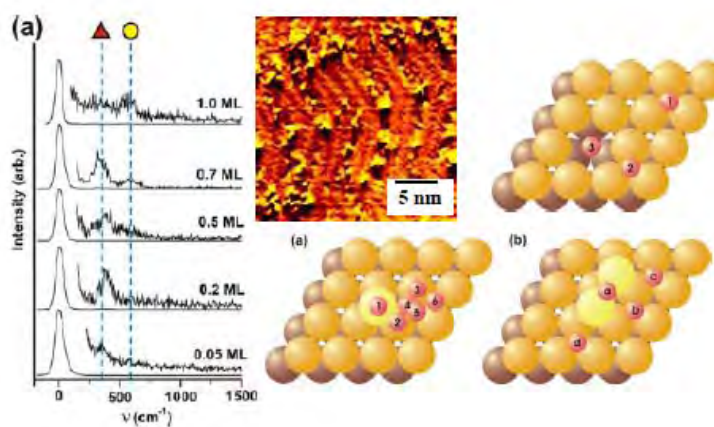


Figure 1: Oxygen bound to disordered, Au nanoparticles is predominantly bound in local 3-fold coordination sites at low O coverages, based on vibrational data (shown on the left) and density functional theory studies of defective Au at low O coverage. The preferred binding sites for O are at 3-fold sites near defects, e.g. sites 5 on the adatom surface on the left or 2 on the surface with a vacancy below. The simulated vibrational frequency is marked by the red triangle. Scanning tunneling microscope image shows the nanoparticles formation upon oxidation of the Au.

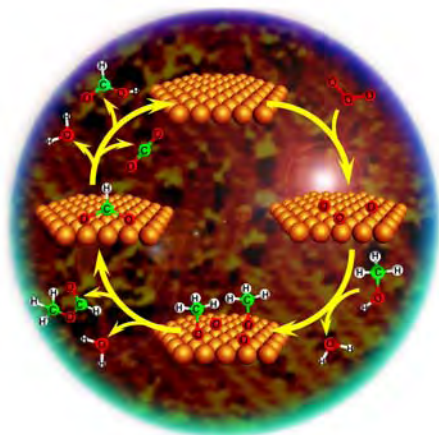


Figure 2: Schematic of methanol oxidation mechanism over oxidized Au nanoparticles. Key intermediates—methoxy and formate—have been identified using vibrational spectroscopy. An analogous mechanism has been established for other primary alcohols, e.g. ethanol.

results clearly establish that adsorbed *atomic* oxygen promotes olefin oxidation since there are no peroxy or other O<sub>2</sub>-species present under the conditions of our experiments. We also generalized our results to show that NH and N, formed from ammonia oxidation, added to the double bond of styrene, yielding the aziridine compound (the NH analog of styrene epoxide.) Thus, we demonstrate the predictive value of fundamental surface chemistry studies.

#### Selective Alcohol Oxidation:

We have established a general mechanistic framework for oxidation of alcohols, illustrated for methanol oxidation over oxidized Au nanoparticles (Figure 2). In our work, we demonstrate that coupling of primary alcohols leads to ester formation at low O coverage on metastable Au nanoparticles. After activation of the O-H bond to form methoxy, some formaldehyde is formed from subsequent  $\beta$ -C-H activation. The formaldehyde is rapidly attacked by methoxy remaining on the surface to afford methyl formate. The esterification pathway is favored at low O coverage. Secondary oxidation to CO<sub>2</sub> and organic acids is favored at higher coverage and proceeds via formate. These results provide a predictive framework for alcohol oxidation and have been generalized to ethanol and other alcohols.

#### Future Plans:

In our future work, we plan to extend our studies of oxidation over Au to higher pressure environments and to more complex materials—nanoporous Au and alloys of Au that can promote O<sub>2</sub> dissociation. We also plan to further investigate methods for improving the selectivity and activity for these important reactions by using promoters and adjustment of reaction conditions to favor more reactive phases.

#### Publications from DOE-supported work, 2006-2009:

1. V. Zielasek, B. Xu, X. Liu, M. Bäumer and C. M. Friend, "The Absence of Subsurface Oxygen Effects in the Oxidation of Olefins on Au: Styrene Oxidation over Sputtered Au(111)." *J. Phys. Chem. C*, **2009**, In Press.
2. X. Liu, B. Xu, J. Haubrich and C. M. Friend, "Surface-mediated self-coupling of ethanol on gold." *J. Am. Chem. Soc.*, **2009**, In press.
3. T. A. Baker, C. M. Friend, and E. Kaxiras, "Atomic Oxygen Adsorption on Au(111) with Defects." *J. Phys. Chem. C.*, **2009**, 113 (8), 3232-3238.

they remain essentially unchanged following the removal of the adsorbed oxygen by reaction with CO at 200K, indicating that they also include gold in their structure, since gold is not mobile at this temperature. We establish that O is present on the nanoclusters by the square symmetry of the clusters (pure Au would be hexagonal) and by using surface spectroscopy (XPS and HREELS). A combination of theory and experiment is used to determine the local bonding of the active oxygen. Importantly, we find that the *disordered, metastable Au-O phase created at low temperature, in which O is predominantly in sites of local 3-fold coordination, is most reactive and induces reactions with the highest selectivity.*

#### Olefin Oxidation:

We have extensively studied oxidation reactions on oxidized Au(111) and in all cases the disordered, metastable oxygen phase formed at low temperature is most reactive and most selective. We have investigated the oxidation of CO, styrene, propene, allyl alcohol, and acrolein, to date. Although clean Au adsorbs hydrocarbons reversibly, selective oxidation is promoted on oxygen-covered Au(111). Our

4. B. Xu, X. Liu, J. Haubrich, R. J. Madix, and C. M. Friend, "Selectivity Control in Gold-Mediated Esterification of Methanol." *Angewandte Chemie*, **2009**, *48*, 1-5.
5. T. A. Baker, C. M. Friend, and E. Kaxiras, "Effects of chlorine and oxygen coverage on the structure of the Au(111) Surface." *J. Chem. Phys.* **2009**, *130*, Art. No. 084701.
6. X. Liu, R. J. Madix, and C. M. Friend, "Unraveling molecular transformations on surfaces: a critical comparison of oxidation reactions on coinage metals." *Chemical Society Reviews* **2008**, *37*(10), 2243-2261.
7. R. J. Madix, C. M. Friend, and X. Liu, "Anticipating Catalytic Oxidation Reactions on Gold at High Pressure (Including Liquid Phase) From Ultrahigh Vacuum Studies." *J. Catalysis*. **2008**, *258* (2), 410-413.
8. X. Deng, S. Y. Quek, M. M. Biener, J. Biener, D.-H. Kang, R. Schalek, E. Kaxiras, and C. M. Friend, "Selective Thermal Reduction of Single-Layer MoO<sub>3</sub> Nanostructures on Au(111)." *Surf. Sci.* **2008**, *602*(6), 1166-1174.
9. X. Deng and C. M. Friend, "Selectivity Switch for Nitrogen Functionalization of Styrene on Au(111)." *Surf. Sci.* **2008**, *602*(5), 1066-1071.
10. W. Gao, T. A. Baker, L. Zhou, D. S. Pinnaduwege, E. Kaxiras, and C. M. Friend, "Chlorine Adsorption on Au(111): Chlorine Overlayer or Surface Chloride?" *J. Am. Chem. Soc.* **2008**, *130*(11), 3560-3565.
11. W. Gao, L. Zhou, D. S. Pinnaduwege, and C. M. Friend, "Interaction of Chlorine with Au-O Surface Complexes." *J. Phys. Chem. C*, **2007**, *111*(26), 9005-9007.
12. B. K. Min and C. M. Friend, "Heterogeneous Gold-Based Catalysis for Green Chemistry: Low-Temperature CO Oxidation and Propene Oxidation." *Chem. Rev.*, **2007**, *107*(6), 2709-2724.
13. X. Liu, A. Klust, R. J. Madix, and C. M. Friend, "Structure Sensitivity in the Partial Oxidation of Styrene, Styrene Oxide, and Phenylacetaldehyde on Silver Single Crystals." *J. Phys. Chem. C*, **2007**, *111*(9), 3675-3679.
14. D. S. Pinnaduwege, L. Zhou, W. Gao and C. M. Friend, "Chlorine Promotion of Styrene Epoxidation on Au(111)." *J. Am Chem. Soc.* **2007**, *129*(7), 1872-1873.
15. X. Deng, T. A. Baker, and C. M. Friend, "A Pathway for NH Addition to Styrene Promoted by Gold." *Angew. Chem. Int. Ed. Engl.* **2006**, *45*(42), 7075-7078.
16. X. Liu, R. J. Madix, and C. M. Friend, "Surface-Mediated NH and N Addition to Styrene on Ag(110)." *J. Am. Chem Soc.* **2006**, *128*(44), 14266-14267.
17. J. Biener, M. M. Biener, T. Nowitzki, A. V. Hamza, C. M. Friend, V. Zielasek, and M. Bäumer, "On the Role of Oxygen in Stabilizing Low-Coordinated Au Atoms." *ChemPhysChem.*, **2006**, *7*(9), 1906-1908.
18. X. Deng, B. K. Min, X. Liu, and C. M. Friend, "Partial Oxidation of Propene on Oxygen-Covered Au(111)." *J. Phys. Chem B* **2006**, *110*(32), 15982-15987.
19. B. K. Min, A. R. Alemozafar, D. Pinnaduwege, X. Deng, and C. M. Friend, "Efficient CO Oxidation at Low Temperature on Au(111)." *J. Phys Chem B* **2006**, *110*(40), 19833-19838.

**Dynamic Characterization of Structure and Bonding in Supported Molecular Catalysts**

Students: V. Aguilar-Guerrero, A. J. Liang, Y. Hao, I. Ogino

Collaborators: A. Corma (Valencia), H. Knözinger (Munich), K. Hadjiivanov (Sofia)

Contact: B. C. Gates, Dept. of Chemical Engineering & Materials Science, Univ. of California, Davis, CA 95616; email: [bcgates@ucdavis.edu](mailto:bcgates@ucdavis.edu); web site:

[www.chms.ucdavis.edu/research/web/catalysis/](http://www.chms.ucdavis.edu/research/web/catalysis/)

**Goals**

Extend molecular catalysis onto surfaces by precise synthesis of supported metal complexes and metal clusters and characterization by complementary spectroscopic and microscopic methods (especially of catalysts in the functioning state).

**DOE Interest**

Most catalysts for energy conversion are solids, many of them supported. Understanding supported metal catalysts at the most basic level requires characterization of the reacting species, including characterizing of the metal, the ligands on the metal, and the metal support interactions. Such understanding, with the aid of theory, provides a foundation for the design of new and improved supported catalysts.

**Recent Progress**

A supported CO oxidation catalyst was synthesized from  $\text{Au}(\text{CH}_3)_2(\text{acac})$  (acac = acetylacetonate) with partially dehydroxylated MgO powder and found by IR and EXAFS spectroscopies to incorporate dimethyl gold complexes bonded to the support. It lacked measurable catalytic activity for CO oxidation at room temperature, but as the temperature increased to  $>373$  K with the sample in flowing  $\text{CO} + \text{O}_2$  at 1 atm, removal of methyl ligands from the gold was observed by IR and EXAFS spectroscopies. Simultaneously, the sample became active for CO oxidation catalysis. EXAFS characterization of the sample right after the activation indicated aggregation of the gold into clusters of approximately 4–6 Au atoms each, on average. These are among the smallest supported gold clusters yet reported, and they are inferred to be the catalytically active species. The XANES data suggest that the gold in the activated catalyst had not been reduced to the metallic state.

Separately, the catalyst was activated for CO oxidation in flowing helium at 473 K. EXAFS and XANES spectra confirmed that the activation involved reduction of the gold and formation of clusters (with an average diameter  $<10$  Å) in which the gold was essentially zerovalent. During CO oxidation catalysis in a batch reactor, at least some of the gold was oxidized, as evidenced by the appearance of an IR  $\text{Au}^{\delta+}\text{-CO}$  band at  $2151\text{ cm}^{-1}$ . During operation in a flow reactor, the catalyst underwent deactivation, accumulating species such as carbonate and bicarbonate on its surface, as indicated by IR spectra. The accumulation of such species on the MgO support took place only during the initial period of operation, whereas the accumulation of such species on the gold continued throughout the operation, consistent with the inference that these species blocked catalytically active sites on the gold. The catalyst was reactivated by decomposition of these species by treatment in helium at 473 K. After three activation-deactivation cycles, the average diameter of the gold clusters increased to about 30 Å, and the catalytic activity increased. Thus, the results provide a resolution of the separate effects on the catalytic activity of gold aggregation and accumulation of species such as carbonates and bicarbonates.

Because the literature of CO oxidation catalyzed by supported gold is extensive, but reports of the kinetics of the reaction are incomplete and fragmented, we prepared a summary of such information presented in tables that state (1) how the catalysts were made, treated, and tested; (2) their physical properties, such as the average gold particle size; and (3) kinetics data, including

turnover frequencies, reaction orders, and apparent activation energies. This summary will appear in *Catalysis Letters*.

CeO<sub>2</sub>-supported gold synthesized from Au(CH<sub>3</sub>)<sub>2</sub>(acac) catalyzed CO oxidation at 353 K, with a TOF of  $6.3 \times 10^{-3}$  molecules of CO (Au atom s)<sup>-1</sup> at CO and O<sub>2</sub> partial pressures of 1.0 kPa; the apparent activation energy was  $138 \pm 2$  kJ mol<sup>-1</sup>. The activity increased as the catalyst functioned in a flow reactor, and after 48 h, the TOF at 298 K and the CO and O<sub>2</sub> partial pressures stated above was  $5.6 \pm 0.2 \times 10^{-2}$  molecules of CO (Au atom s)<sup>-1</sup>. X-ray absorption spectra show that the catalyst structure changed during operation, as the mononuclear cationic species present initially formed clusters consisting, on average, of roughly 15 Au atoms each. Reaction orders of CO oxidation catalyzed by the sample containing the clusters at 303 K were found to be 0.19, 0.18, and -0.4 in CO, O<sub>2</sub>, and CO<sub>2</sub>, respectively. The apparent activation energy characterizing the catalyst containing the clusters was found to be only about one-third of the value characterizing the catalyst incorporating the mononuclear cationic gold. An important result is that the gold clusters are more active for CO oxidation catalysis than the mononuclear gold species, and we present the first quantitative comparison of the activities of the respective species (Figure 1).

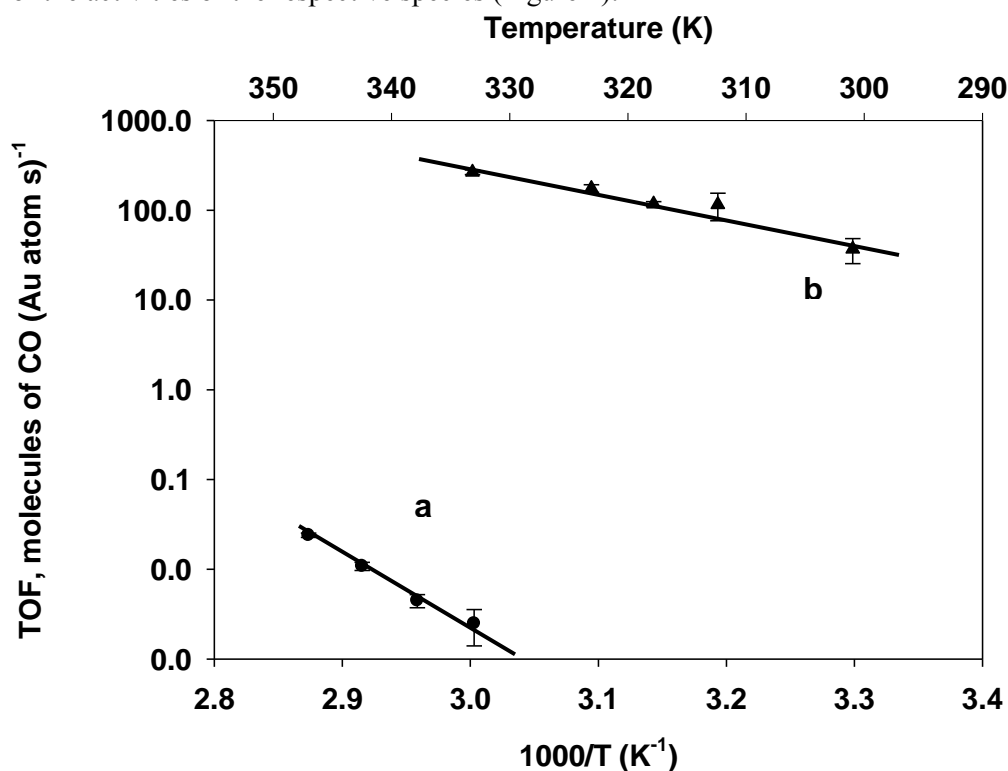


Figure 1. Arrhenius plot (a) characterizing CO oxidation by catalyst in which gold was present as mononuclear species, as indicated by EXAFS spectroscopy. Total feed flow rate: 100 mL(NPT) min<sup>-1</sup>;  $P_{CO}$  = 1.0 kPa,  $P_{O_2}$  = 0.5 kPa. For comparison (b), data are shown for the catalyst that had been activated by 48 h of operation in the flow reactor at 353 K followed by 48 h at 303 K, during which the gold aggregated to form clusters. Total feed flow rate in each experiment was 200 mL(NPT) min<sup>-1</sup>;  $P_{CO} = P_{O_2} = 1.0$  kPa. Conversions were <10% and differential;  $T$  is temperature.

Dealuminated Y zeolite was used as a support for a complex synthesized from *cis*-Ru(acac)<sub>2</sub>(C<sub>2</sub>H<sub>4</sub>)<sub>2</sub> (**I**). IR and EXAFS spectra indicate that the surface species were mononuclear ruthenium complexes, Ru(acac)(C<sub>2</sub>H<sub>4</sub>)<sub>2</sub><sup>2+</sup>, bonded tightly to the surface by two Ru–O bonds at Al<sup>3+</sup> sites of the zeolite when ruthenium loading was 1.0 wt%. A high degree of uniformity of the chemisorbed species was demonstrated by sharp bands in the IR spectrum characteristic of ruthenium

dicarbonyls, formed by reaction of the complex with CO. In the presence of ethene and H<sub>2</sub>, the surface-bound species entered into a catalytic cycle for ethene dimerization and operated stably. IR data show that at the start of the catalytic reaction an acac ligand of the Ru(acac)(C<sub>2</sub>H<sub>4</sub>)<sup>2+</sup> species was dissociated and captured by an Al<sup>3+</sup> site. Ethene dimerization proceeded approximately 600 times faster with a co-feed of ethene and H<sub>2</sub> than that without H<sub>2</sub>, providing evidence of the importance of the cooperation of Al<sup>3+</sup> sites in the zeolite and H<sub>2</sub> in the feed for the genesis of the catalytically active species.

The maximum loading of the anchored ruthenium complexes was one per two Al<sup>3+</sup> sites; at higher loadings, some of the *cis*-Ru(acac)<sub>2</sub>(C<sub>2</sub>H<sub>4</sub>)<sub>2</sub> was physisorbed. Investigation of supported samples with systematically varied ratios of chemisorbed to physisorbed species by ethene dimerization reaction experiment indicates that reaction proceeded much faster on the chemisorbed species than on the physisorbed species under our conditions. Consistent with these results, ethene ligands on the chemisorbed species reacted to form butenes when the temperature was raised to approximately 393 K; acac ligands remained bonded to Ru. In contrast, ethene ligands on the physisorbed complex simply desorbed under the same conditions. IR and EXAFS data characterizing the supported samples indicate that (1) the Ru center in the chemisorbed species became more electropositive than that in the physisorbed species and (2) Ru-ethene bonds in the chemisorbed species are less symmetric than those in the physisorbed species, suggesting that ethene ligands in the chemisorbed species are in a configuration appropriate for dimerization. In summary, the zeolite plays multiple roles: (1) a ligand to anchor the electropositive ruthenium complex with uniform in structure, (2) a ligand to activate ethene ligands in the chemisorbed species and (3) a support to aid the removal of acac ligands for genesis of catalytically active species.

### Publications (2007-2009)

1. "Increasing the Number of Oxygen Vacancies on TiO<sub>2</sub> by doping with Iron Activates Oxygen and Increases Catalytic Activity of Supported Gold, S. Carretin, Y. Hao, V. Aguilar-Guerrero, B. C. Gates, J. J. Calvino, and A. Corma, *Chem. Eur. J.*, **13**, 7771 (2007).
2. "Genesis of a highly active cerium oxide-supported gold catalyst for CO oxidation," V. Aguilar-Guerrero and B. C. Gates, *ChemComm*, **2007**, 3210.
3. "Oxidation by CO<sub>2</sub> of Au<sup>0</sup> and Au<sup>-</sup> Species on La<sub>2</sub>O<sub>3</sub>-Supported Gold Clusters," M. Mihaylov, E. Ivanova, Y. Hao, K. Hadjiivanov, B. C. Gates, and H. Knözinger, *ChemComm*, **2008**, 175.
4. "Catalysis by Gold Dispersed on Supports: The Importance of Cationic Gold," J. C. Fierro-Gonzalez and B. C. Gates, *Chem. Soc. Rev.*, **37**, 2127 (2008).
5. "Molecular Chemistry in a Zeolite: Genesis of a Zeolite Y-supported Ruthenium Complex Catalyst," I. Ogino and B. C. Gates, *J. Am. Chem. Soc.*, **130**, 13338 (2008).
6. "Gold Supported on La<sub>2</sub>O<sub>3</sub>: Structure and Reactivity with CO<sub>2</sub> and Implications for CO Oxidation Catalysis," M. Mihaylov, E. Ivanova, Y. Hao, K. Hadjiivanov, H. Knözinger, and B. C. Gates, *J. Phys. Chem. C*, **112**, 18,973 (2008).
7. "Kinetics of CO Oxidation Catalyzed by Highly Dispersed CeO<sub>2</sub>-Supported Gold," V. Aguilar-Guerrero and B. C. Gates, *J. Catal.*, **260**, 351 (2008).
8. "CO Oxidation Catalyzed by Gold Supported on MgO: Spectroscopic Identification of Carbonate-like Species Bonded to Gold during Catalyst Deactivation," Y. Hao, M. Mihaylov, E. Ivanova, K. Hadjiivanov, H. Knözinger, and B. C. Gates, *J. Catal.*, **261**, 137 (2009).
9. "Genesis of a Cerium Oxide-Supported Gold Catalyst for CO Oxidation: Transformation of Mononuclear Gold Complexes into Clusters as Characterized by X-Ray Absorption Spectroscopy," V. Aguilar-Guerrero, R. J. Lobo-Lapidus, and B. C. Gates, *J. Phys. Chem. C*, **113**, 3259 (2009).
10. "Activation of Dimethyl Gold Complexes on MgO for CO Oxidation: Removal of Methyl Ligands and Formation of Catalytically Active Gold Clusters," Y. Hao and B. C. Gates, *J. Catal.*, **263**, 83 (2009).
11. "Kinetics of CO Oxidation Catalyzed by Supported Gold: A Tabular Summary of the Literature," V. Aguilar-Guerrero and B. C. Gates, *Catal. Lett.*, in press.



**Enantioselective Explosions on Chiral Surfaces**

Lead PI: Andrew J. Gellman  
Postdoc: Feng Xu, Vladimir Pushkarev  
Contact: Department of Chemical Eng., Carnegie Mellon University, 5000 Forbes Ave., Pittsburgh, PA 15213, (412) 268-3848, [gellman@cmu.edu](mailto:gellman@cmu.edu)

There is a class of surface decomposition reactions that occurs by an explosive kinetic mechanism ( $A \rightarrow 2A$ ). These are typically adsorbate decomposition reactions that require multiple empty sites to initiate decomposition. Tartaric acid is known to exhibit such decomposition kinetics on the Cu(110) surface and this process has been studied using TPD measurements over a wide range of initial coverages and conditions. The reaction kinetics are highly non-linear:  $r = k \cdot \theta \cdot (1-\theta)^2$ . As a consequence, at coverages approaching saturation the entire decomposition process occurs over an extremely narrow temperature range in a typical TPD experiment. The same reaction has been studied on several naturally chiral, high Miller index surfaces of Cu. As a result of the chirality of the Cu(*hkl*)<sup>R&S</sup> surfaces, the decomposition of D- and L-tartaric acid is enantioselective. As a result of the highly non-linear reaction kinetics, the process leads to extremely high enantioselectivity. The work provides insight into mechanisms leading to high enantioselectivity. It also provides insight into the origins of enantioselectivity and the mechanism of surface explosions.

**The Physical and Chemical Properties of Nanostructured  
Metal and Mixed-Metal Catalysts**

Postdocs: Feng Gao, Sean McClure, Zhen Yan, Yilin Wang

Students: Matt Lundwall, Zihao Zhou, Zhoujun Wang, Stephanus  
Axnanda

Contact: Department of Chemistry, Texas A&M University, College  
Station, TX 77843; Email: goodman@mail.chem.tamu.edu

**Goal**

The synthesis of monodispersed nanoclusters of metals and mixed-metals on ultrathin oxide surfaces and the characterization of their detailed morphology using scanning probe techniques. The focus of the research is an understanding of the effects on catalytic activity of metal-substrate interactions and particle size for the single metal systems and the surface versus bulk composition and specific arrangement of the catalytically active site for the mixed-metal systems for key probe reactions.

**DOE Interest**

New strategies for the synthesis of well-defined nanostructured catalysts and an in-depth understanding of their electronic and chemical properties are necessary for the development of highly dispersed, size-limited catalysts for new catalytic applications. The development of in situ methods for characterizing the morphology of nanocatalysts and the surface species formed during reaction are keys to the ultimate development of practical commercial nanocatalysts. These are key issues central to the proposed work.

**Selected Significant Achievements**

*Catalysis by Gold-Palladium Alloys - The Role of Isolated Palladium Sites:*

A AuPd(100) single crystal model catalyst, suitable for studying surface segregation and structure-reactivity relationships, was used to study CO-O<sub>2</sub> and CO-NO reactions at CO pressures of ~0.01 atm. For the CO-O<sub>2</sub> reaction, exceedingly high CO<sub>2</sub> formation rates, e.g., 10<sup>3</sup> times higher than

Pd single crystals at 450 K under the same reaction conditions, was discovered. This reactivity is attributed to the significantly reduced CO binding energy ( $< 84$  kJ/mol compared with  $\sim 150$  kJ/mol on Pd single crystals) such that CO-inhibition of reaction is greatly reduced. In situ polarization-modulation infrared reflection absorption spectroscopy (PM-IRAS), coupled with reaction kinetic measurements, also reveal that  $O_2$  dissociation occurs exclusively on surface contiguous Pd sites, demonstrating that these sites are indispensable for CO oxidation. The CO-NO reaction was also found to proceed promptly below  $\sim 500$  K, temperatures at which (supported) Pt-group metals marginally catalyze this reaction. These results demonstrate the unusual ability of Au-Pd alloys to dissociate NO. Moreover, a AuPd(100) surface catalyzes the CO-NO reaction with exceedingly high  $N_2$  selectivity, presumably due to the low  $NO_{(ads)}$  coverage under reaction conditions, discovered using in situ PM-IRAS. These studies confirm that Au-Pd alloys are promising catalysts for emission control, especially during low-temperature operation.

*New insights into catalytic CO oxidation on Pt-group metals at elevated pressures:* Producing a definitive picture of the CO oxidation reaction ( $CO + O_2 \rightarrow CO_2$ ) on Pt group metals (Rh, Pd, Pt, and Ru) across the “pressure gap” has proved to be a challenging task. Recent work in our laboratory has examined CO oxidation kinetics on Pt-group single crystals using PM-IRAS, XPS, and mass spectrometry from low ( $10^{-8}$ - $10^{-3}$  Torr) to high ( $1$ - $10^2$  Torr) pressures. These studies have shown that at both low and high pressures (a) Langmuir-Hinshelwood kinetics adequately describe CO oxidation kinetics on Pt-group metals (Pt, Pd, Rh) (i.e. there is no pressure gap) and (b) the most active surface is one with minimal CO coverage. Additionally, investigations of high pressure CO oxidation kinetics on  $SiO_2$ -supported Rh nanoparticles prepared *in-situ* have shown the efficacy of using the CO oxidation reaction to count the surface sites and hence approximate particle sizes for known metal coverages.

### **Future Directions**

Current work is directed toward elucidating the basis for structure sensitivity of hydrogenolysis reactions over Rh and Pt catalysis with

well-defined particle sizes. Further studies are underway to explore the mechanisms by which mixed-metal catalysts enhance significantly the activity and selectivity for a wide range of reactions. This work utilizes the well-studied Au-Pd system from extended planar surfaces to nanostructured Au-Pd particles. We are presently investigating the use of nanostructured silica-supported Co particles for F-T synthesis as a prelude to studying alloy variations of this catalyst.

### **Publications (2007-2009)**

1. M. S. Chen, K. Luo, D. Kumar, W. T. Wallace, C. W. Yi, K. K. Gath and D. W. Goodman, "The structure of ordered Au films on TiO<sub>x</sub>", *Surf. Sci.*, 601(2007) 632-637.
2. D. Kumar, Y.-F. Han, and D. W. Goodman, "Ethylene Combustion on Unsupported and Supported Pd: A Comparative Study", *Topics in Catal.*, 46(2007), 169-174.
3. M. S. Chen, K. Luo, D. Kumar, W. T. Wallace, C.-W. Yi, K. K. Gath and D. W. Goodman, "The Structure of Ordered Au Films on TiO<sub>x</sub>", *Surf. Sci.*, 601(2007) 632-637.
4. D. Kumar, Y.-F. Han, and D. W. Goodman, "Ethylene Combustion on Unsupported and Supported Pd: A Comparative Study", *Top. Catal.*, 46(2007), 169-174.
5. M. S. Chen and D. W. Goodman, "Oxide-supported metal clusters", *Chapter in the The Chemical Physics of Solid Surfaces, Eds. D. P. Woodruff*, Vol. 12(2007) 201-269.
6. M. S. Chen and D. W. Goodman, "Synthesis of Vinyl Acetate on Pd-based Catalysts", D. Kumar, *Catal. Today*, 123(2007) 77-85.
7. T. Wei, J. Wang and D. W. Goodman, "Characterization and Chemical Properties of Pd-Au Alloy Surfaces", *J. Phys. Chem. C*, 111(2007) 8781-8788.
8. M. S. Chen and D. W. Goodman, "Interaction of Au with Titania: the Role of Reduced Ti", *Top. Catal.*, 44(2007) 41-47.

9. P. Han, S. Axnanda, I. Lyubinetsky and D. W. Goodman, "Atomic-Scale Assembly of a Heterogeneous Catalytic Site", *J. Am. Chem. Soc.*, 129(2007) 14355-14361.
10. D. W. Goodman, C. H. F Peden and M. S. Chen, "CO oxidation on ruthenium: The Nature of the Active Catalytic Surface", *Surf. Sci.*, 601(2007), L124-L126.
11. M. S. Chen, Y. Cai, Z. Yan, K. K. Gath, S. Axnanda and D. W. Goodman, "Highly Active Surfaces for CO Oxidation on Rh, Pd and Pt", *Surf. Sci.*, 601(2007) 5326-5331.
12. D. W. Goodman, C. H. F Peden and M. S. Chen, Reply to Comment on "CO oxidation on ruthenium: The Nature of the Active Catalytic Surface" by H. Over, M. Muhler and A. P. Seitsonen", *Surf. Sci.*, 601(2007) 5663-5665.
13. H.-J. Freund and D. W. Goodman, "Ultrathin Oxide Films", *Chapter in Handbook of Heterogeneous Catalysis*, Eds. G. ERTL, H. Knözinger, F. Schüth, Wiley-VCH Verlag GmbH & Co. KGaA, 8(2008) 1309-1338.
14. P. Han, and D. W. Goodman, "Controlling the Density and Size Distribution of Pd-Au Nanoparticles on TiO<sub>2</sub>(110)", *J. Phys. Chem. C*, 112(2008) 6390-6397.
15. B. Wang, G. F. Froment and D. W. Goodman, "CO-free Hydrogen Production via Dehydrogenation of a Jet A Hydrocarbon Mixture", *J. Catal.*, 253(2008), 239-243.
16. B. Wang, D. W. Goodman and G. F. Froment, "Kinetic Modeling of Pure Hydrogen Production from Decalin", *J. Catal.*, 253(2008) 229-238.
17. F. Gao, M. Lundwall and D. W. Goodman, "Infrared Reflection Absorption Spectroscopy Study of CO Adsorption and Reaction on Oxidized Pd(100)", *J. Phys. Chem. C*, 112(2008) 6057-6064.
18. M. S. Chen and D. W. Goodman, "Ultrathin, Ordered Oxide Films on Metal surfaces", *J. Phys.: Condensed Matter*, 20(2008), 264013.
19. T. Wei, D. Kumar, M. S. Chen, K. Luo, S. Axnanda, M. Lundwall and D. W. Goodman, "Vinyl Acetate Synthesis over Model Pd-Sn Bimetallic Catalysts", *J. Phys. Chem. C*, 112(2008) 8332-8337.

20. F. Yang, E. Trufan, R. D. Adams and D. W. Goodman, "The Structure of Molecular-Sized Ru<sub>3</sub>Sn<sub>3</sub> Clusters on a SiO<sub>2</sub> Film on Mo(112)", *J. Phys. Chem. C*, 112(2008), 14233-14235.
21. M. S. Chen and D. W. Goodman, "Catalytically Active Gold on Ordered Titania Supports", *Chem. Soc. Rev*, 37(2008)1860-1870.
22. D. Kumar, M. S. Chen and D. W. Goodman, "Ultra-thin Titanium Oxide Films on Mo(112), Measured by XPS", *Surf. Sci. Spectra*, 14(2008) 1-7.
23. F. Gao, S. M. McClure, Y. Cai, K. K. Gath, Y. Wang, M. S. Chen, Q. L. Guo and D. W. Goodman, "CO Oxidation Trends on Pt Group Metals from Ultrahigh Vacuum to Near Atmospheric Pressures: A Combined in situ PM-IRAS and Reaction Kinetics Study", *Surf. Sci.*, 603(2009) 65-70.
24. F. Gao, Y. Cai, K. K. Gath, Y. Wang, M. S. Chen, Q. L. Guo and D. W. Goodman, "CO Oxidation on Pt Group Metals from Ultrahigh Vacuum to Near Atmospheric Pressures I. Rhodium", *J. Phys. Chem. C*, 113(2008) 182-192.
25. M. S. Chen and D. W. Goodman, "Promotional effects of Au in Pd-Au Catalysts for Vinyl Acetate Synthesis", *Chinese J. Catal.*, 29(2008) 1178-1186.
26. F. Gao, Y. Cai, K. K. Gath, Y. Wang, M. S. Chen, Q. L. Guo and D. W. Goodman, "CO Oxidation on Pt Group Metals from Ultrahigh Vacuum to Near Atmospheric Pressures II. Palladium and Platinum", *J. Phys. Chem. C*, 113(2008) 174-181.
27. F. Yang, M. S. Chen and D. W. Goodman, "Sintering of Au Particles Supported on TiO<sub>2</sub>(110) during CO Oxidation", *J. Phys. Chem. C*, 113(2008) 254-260.

**Thermodynamic Properties of Supported Catalysts**

**Students:** Kevin Bakhmutsky, Parag Shah

**Collaborators:** J. M. Vohs (Penn), P. Fornasiero (Trieste), Jonathan Hanson (BNL)

**Contact:** Department of Chemical & Biomolecular Engineering,  
311 Towne Building, 220 S. 33rd Street, University of Pennsylvania  
Philadelphia, PA 19104 Ph: 215-898-4439; Fax: 215-573-2093  
gorte@seas.upenn.edu

**Goals:**

Understand how support and composition affect the thermodynamic properties for oxidation and reduction of various oxide and metal catalysts. Understand how redox properties at a surface differ from that of bulk materials.

**DOE Interest:**

The thermodynamic properties for oxidation and reduction of bulk materials are well known. However, typical catalytic materials are in the form of nano-particles, supported on high-surface-area oxides, and often in the form of a mixed oxide or solid solution. The redox properties of these types of materials are not usually known in detail. For selective oxidation reactions which proceed by a Mars-Van Krevelen mechanism, understanding the redox properties of the catalyst is critical to a fundamental understanding of the reaction and to the development of new and improved catalysts. For reactions involving steam or CO<sub>2</sub>, the thermodynamic properties of the catalyst affect the oxidation state of the catalyst under steady-state reaction conditions, thereby affecting the activity and selectivity of the reaction.

**Recent Progress:**

We have prepared a series of solid solutions of ceria with zirconia, titania, manganese oxide, hafnia, praseodymia, and terbium and measured their thermodynamic properties using coulometric titration. Mixed oxides of Ce-Hf, Ce-Zr and Ce-Ti showed greatly enhanced reducibility, with oxidation enthalpies between -500 and -550 kJ/mol O<sub>2</sub>, compared to an oxidation enthalpy of -760 kJ/mol O<sub>2</sub> for pure ceria. With Ce-Zr and Ce-Hf solutions, the oxidation enthalpies and entropies can be understood in terms of a local atomic picture, with the solid forming pyrochlore-like clusters (Zr<sub>2</sub>Ce<sub>2</sub>O<sub>7</sub>). Mixed oxides of Ce-Pr and Ce-Tb formed solid solutions; however, except for the fact that Pr and Tb could be completely oxidized to the +4 state, the solid solutions behaved similarly to the physical mixtures. Despite much effort to form ceria-manganese solid solutions, diffraction data was inconclusive that solid solutions were formed and the oxidation isotherms were similar to that expected for a physical mixture.

A series of V-containing oxides, including CeVO<sub>4</sub>, LaVO<sub>4</sub>, ZrV<sub>2</sub>O<sub>7</sub>, Mg<sub>3</sub>(VO<sub>4</sub>)<sub>2</sub>, CrVO<sub>4</sub>, AlVO<sub>4</sub>, and V<sub>2</sub>O<sub>5</sub>, were also prepared and the redox properties characterized. For each of the compounds, the oxygen uptakes corresponded to oxidation from V<sup>+3</sup> to V<sup>+5</sup> as oxygen fugacities increased from 10<sup>-25</sup> to 10<sup>-2</sup> atm at 973 K. With V<sub>2</sub>O<sub>5</sub> and ZrV<sub>2</sub>O<sub>7</sub>, the only materials in this

group that contain V-O-V linkages, there was evidence for two oxidation processes, corresponding to  $V^{+3}-V^{+4}$  and  $V^{+4}-V^{+5}$  equilibria, whereas oxidation occurred in a single step for the other materials.  $CrVO_4$  and  $AlVO_4$  were unstable to deep reduction, but isotherms measured from the oxidizing and reducing were similar. Oxidation enthalpies and entropies were determined for  $CeVO_4$ ,  $ZrV_2O_7$ ,  $Mg_3(VO_4)_2$ , and  $V_2O_5$ .  $-\Delta G$  of oxidation for the series  $CeVO_4$ ,  $LaVO_4$ ,  $Mg_3(VO_4)_2$ ,  $CrVO_4$ ,  $AlVO_4$ , was found to vary linearly with the electronegativity of the counter cation; but the catalytic activity for methanol oxidation and propane ODH was not affected.

Oxidation isotherms were measured for  $V_2O_5$ /zirconia catalysts at monolayer and submonolayer loadings. The monolayer catalyst showed evidence for  $V^{+3}-V^{+4}$  and  $V^{+4}-V^{+5}$  equilibria, whereas only a single oxidation step was observed for the submonolayer catalyst. The catalytic activities were not significantly different for these two catalysts.

### **Future Work:**

In a continuation of our past work, studies will be carried out to understand the redox properties of supported-vanadia catalysts as a function of loading on supports of different composition in order to determine how the support influences the redox properties of isolated  $VO_x$  species. Supported metals, particularly Co, Ni, and Fe, will be examined as a function of particle size to determine how redox properties are affected by particle size and surface properties. Finally, supported metals that appear to form alloys will be examined to determine whether alloy formation could provide a driving force for support reduction.

### **Publications Acknowledging DE-FG02-85ER13350, since 4/1/06**

1. "An Investigation of  $NO_x$  Storage on Pt-BaO- $Al_2O_3$ ", G. Zhou, T. Luo, and R. J. Gorte, *Applied Catalysis B*, 64 (2006) 88-95.
2. "A Thermodynamic Investigation of the Redox Properties of Ceria-Zirconia Solid Solutions", T. Kim, J. M. Vohs, and R. J. Gorte, *Industrial and Engineering Chemistry*, 45 (2006) 5561-65.
3. "Evidence for Entropy Effects in the Reduction of Ceria-Zirconia Solutions", Parag R. Shah, Taeyoon Kim, Gong Zhou, Paolo Fornasiero, and Raymond J. Gorte, *Chemistry of Materials*, 18 (2006) 5363-69.
4. "Oxidation Entropies and Enthalpies for Ceria-Zirconia Mixed Oxides", Gong Zhou, Parag R. Shah, Taeyoon Kim, Paolo Fornasiero, and Raymond J. Gorte, *Catalysis Today*, 123 (2007) 86-93.
5. "Probing the Effect of Local Structure on the Thermodynamic Redox Properties of  $V^{+5}$ : A Comparison of  $V_2O_5$  and  $Mg_3(VO_4)_2$ ", P. R. Shah, J. M. Vohs, and R. J. Gorte, *Journal of Physical Chemistry B*, 111 (2007) 5680-83.
6. "Oxidation Enthalpies for Reduction of Ceria Surfaces", Gong Zhou, P. R. Shah, T. Montini, P. Fornasiero, and R. J. Gorte, *Surface Science*, 601 (2007) 2512-19.
7. "A Study of Cerium-Manganese Mixed Oxides For Oxidation Catalysis", G. Zhou, P. R. Shah, and R. J. Gorte, *Catalysis Letters*, 120 (2008) 191-197.
8. "A Comparison of the Redox Properties of Vanadia-Based Mixed Oxides", P. R. Shah, M. M. Khader, J. M. Vohs, and R. J. Gorte, *Journal of Physical Chemistry C*, 112 (2008) 2613-2617.



9. "A Thermodynamic Investigation of the Redox Properties of Ceria-Titania Mixed Oxides", G. Zhou, R. J. Gorte, and J. Hanson, *Applied Catalysis A*, 335 (2008) 153-158.
10. "Redox Isotherms for Vanadia Supported on Zirconia", P. R. Shah, J. M. Vohs, and R. J. Gorte, *Catalysis Letters*, 125 (2008) 1.
11. "A Thermodynamic Investigation of the Redox Properties for Ceria-Hafnia, Ceria-Terbia, and Ceria-Praseodymia Solid Solutions", G. Zhou and R. J. Gorte, *Journal of Physical Chemistry B*, 112 (2008) 9869.
12. "The Water-Gas-Shift Reaction on Pd/Ceria-Praseodymia: The Effect of Redox Thermodynamics", K. Bakhmutsky, G. Zhou, S. Timothy, and R. J. Gorte, *Catalysis Letters*, accepted.

## Surface Termination of M1 Phase and Rational Design of Propane Ammoxidation Catalysts

**Students and Post-doc:** P. Korovchenko, J. Woo, N. R. Shiju, A. Govindasamy  
**Collaborators:** Drs. S. H. Overbury, D. R. Mullins, V. Schwartz, S. Dai, A. J. Rondinone, and Y. Xu (ORNL), D. J. Buttrey (University of Delaware), A. W. Weimer (University of Colorado)  
**Contact:** V. V. Guliants, Department of Chemical and Materials Engineering, University of Cincinnati, Cincinnati, OH 45221-0012; (513) 556-0203; [vguliant@alpha.che.uc.edu](mailto:vguliant@alpha.che.uc.edu); webpage: [alpha.che.uc.edu/matcat](http://alpha.che.uc.edu/matcat)

### Goal

Elucidate the roles of Nb and other catalytically significant metal ions in the bulk lattice of the M1 phase. Develop molecular models of surface termination of the M1 phase. Investigate propane ammoxidation over model M1 surface employing density functional theory.

### DOE Interest

Selective alkane (amm)oxidation over metal oxide catalysts is one of the most important areas of catalytic process improvement. The current fundamental understanding of catalytic mixed oxides is rather limited, because of the lack of model mixed oxide catalysts with well-defined ordered structures and compositions. This research is aimed at fundamental studies of the topmost surface chemistry and mechanism of propane ammoxidation over Mo-V-(Te-Nb)-O M1 catalysts in order to develop quantitative understanding of the surface molecular structure – reactivity relationships for this unique catalytic system. The Mo-V-(Te-Nb) oxides possess unique catalytic properties among mixed metal oxides, because they selectively catalyze three alkane transformation reactions, namely propane ammoxidation to ACN, propane oxidation to acrylic acid and ethane ODH, all of *considerable economic significance*. Therefore, the larger goal of this research is to expand this catalysis to other alkanes of commercial interest, and more broadly, demonstrate successful approaches to rational design of improved catalysts that can be applied to other selective (amm)oxidation processes.

### Recent Progress

*Roles of Nb and Other Significant Metal Ions in M1 Lattice:* The mixed metal Mo-V-M-O (M= Te, Nb) catalysts were synthesized employing microwave irradiation, which demonstrated that the synthesis of well-defined M1 phase catalysts may be accelerated 10-fold [1]. Nb was found to be important for the thermal stability of the M1 phase. In the absence of Nb, the Mo-V-Te-O M1 phase underwent phase transformation at elevated temperatures (>450°C) into the M2 phase, which is known to be inactive in propane (amm)oxidation, but can selectively transform the propylene intermediate into acrylonitrile [2]. This study confirmed the lack of synergy between the M1 and M2 phases at industrially relevant high conversion of propane. A subsequent study indicated that the substitution of W, Ga and particularly Fe for Te significantly improves thermal stability of the M1 phase while maintaining the reactivity of the Mo-V-Te-O phase in propane ammoxidation [3]. The structures of M1 phases with the Mo-V-O, Mo-V-Te-O and Mo-V-Te-Nb-O bulk compositions were solved by full profile refinement of the power XRD patterns,

which indicated significant differences in the occupancy of the 13 metal lattice sites depending on their bulk composition [4]. These structures are currently being employed in a theoretical study of Nb location in the M1 lattice [5]. In this study, several previously unknown forcefield types of metal ( $\text{Mo}^{5+}$ ,  $\text{V}^{4+}$ ,  $\text{Te}^{4+}$ ) and terminal  $\text{O}^{2+}$  ions were defined by reproducing experimental crystal structures of Nb-free M1 phases [4] employing GULP, a classical forcefield-based molecular modeling package.

*Surface Termination of M1 Phase:* The oxidation states and their changes in the surface region of the M1 phase catalysts were investigated by XANES at Brookhaven National Laboratory. This study indicated that only V ions undergo changes in their redox state under dynamic cycling conditions in  $\text{H}_2$  and  $\text{O}_2$ -containing atmospheres strongly suggesting that surface V sites are responsible for propane activation over the M1 phase [6]. The catalytic role of the surface *ab* planes of the M1 phase indicated as active and selective in propane ammoxidation to acrylonitrile in previous studies by the PI were investigated employing M1 phase catalysts in which all other crystal planes were covered by alumina ALD (Figure 1 and [7]). This study indicated that the *ab* planes possessed significantly enhanced reactivity in propane ammoxidation as compared to M1 catalysts with random exposure of surface crystal planes. Moreover, an isotope-labeling study employing  $^{13}\text{C}$ -labeled propane indicated that propane ammoxidation under typical reaction conditions occurs without any C3 backbone rearrangements or dimerization contrary to recent observations of propane oxidation over other V-containing mixed metal oxides [8]. The results of these recent studies have been discussed in a focused review [9].

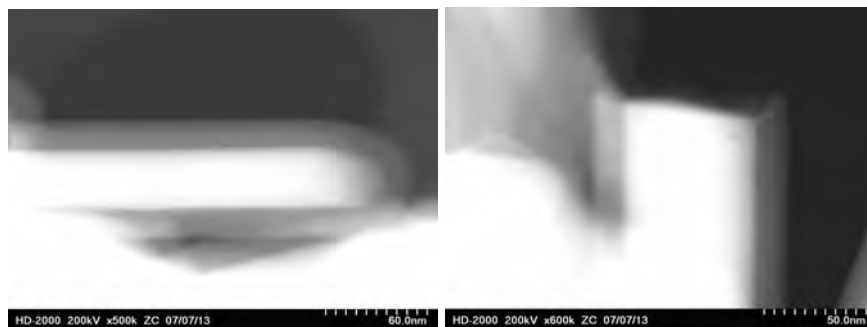


**Figure 1.** Z-contrast TEM images of Mo-V-Te-Nb-O M1 phase catalyst coated with alumina before crushing (left) and after crushing to expose *ab* planes (right). The former image shows the complete coverage of the particle by alumina [7].

*Mechanism of Propane Ammoxidation:* The results of the above experimental studies have been used to construct several realistic molecular models of the *ab* surface of the M1 phase [10]. These models explored the effects of V content (1 or 2), its location and the number of atomic layers on the electronic structure of small cluster models of the *ab* planes of the Mo-V-Te-Nb-O M1 phase employing VASP. These studies indicated that two-layer models containing 1 V atom in the “surface” are sufficiently accurate for initial investigations of a complete reaction pathway for propane ammoxidation to acrylonitrile [11].

## Future Plans

*Surface Termination of ab Planes of M1 Phase:* Develop fast silica ALD methodology for further LEIS studies of surface termination of the *ab* planes combined with the use of surface

chemical probes. Silica is expected to be a more inert catalytic component than alumina employed in a previous ALD study [7].

*Theoretical Models of O<sub>2</sub>, NH<sub>3</sub> and Propane Activation:* Complete this on-going study of the *ab* planes employing VASP.

*Mechanism of Propane Ammoxidation:* Conduct reaction a theoretical VASP study of the entire pathway of propane ammoxidation.

### **Publications (2007-2009)**

1. N. R. Shiju, V. V. Guliants, "Microwave-assisted hydrothermal synthesis of monophasic Mo-V-Te-Nb-O mixed metal oxide catalysts for the selective ammoxidation of propane", *ChemPhysChem* **8** (2007) 1615-1617.
2. P. Korovchenko, N. R. Shiju, A. K. Dozier, U. M. Graham, O. M. Guerrero-Perez, V. V. Guliants, "M1 to M2 Phase Transformation and Phase Cooperation in Bulk Mixed Metal Mo-V-M-O (M=Te, Nb) Catalysts for Selective Ammoxidation of Propane", *Topics in Catalysis* **50** (2008) 43-51.
3. N. R. Shiju, V. V. Guliants, "Mo-V-M-O (M=Te, W, Fe, Ga) catalysts for selective ammoxidation of propane", *Catal. Commun.* **9** (2008) 2253-2256.
4. N. R. Shiju, V. V. Guliants, S. H. Overbury, A. J. Rondinone, "Toward environmentally benign oxidations: bulk mixed Mo-V-(Te-Nb)-O M1 phase catalysts for the selective ammoxidation of propane", *ChemSusChem* **1** (2008) 519-523.
5. J. Woo, J. Yu, V. V. Guliants, "Nb Location in the Mo-V-Te-Nb-O M1 phase", *J. Phys. Chem. C*, submitted.
6. N. R. Shiju, A. J. Rondinone, D. R. Mullins, V. Schwartz, S. H. Overbury, V. V. Guliants, "XANES Study of Hydrothermal Mo-V-Based Mixed Oxide M1-Phase Catalysts for the (Amm)oxidation of Propane", *Chem. Mater.* **20** (2008) 6611-6616.
7. N. R. Shiju, X. Liang, A. W. Weimer, C. Liang, S. Dai, V. V. Guliants, "The Role of Surface Basal Planes of Layered Mixed Metal Oxides in Selective Transformation of Lower Alkanes: Propane Ammoxidation over Surface *ab* Planes of Mo-V-Te-Nb-O M1 Phase", *JACS* **130** (2008) 5850-5851.
8. N. R. Shiju, R. R. Kale, S. S. Iyer, V. V. Guliants, "Isotope Labeling Study of Propane Ammoxidation over M1 Phase Mo-V-Te-Nb-O Mixed Oxide catalyst", *J. Phys. Chem. C* **111** (2007) 18001-18003.
9. N. R. Shiju, V. V. Guliants, "Recent developments in catalysis using nanostructured materials", *Appl. Catal. A* **356** (2009) 1-17.
10. A. Govindasamy, Y. Kapustin, V. V. Guliants, [585f] Theoretical Study of Propane, Dioxygen and Ammonia Activation Over Cluster Models of the Surface *ab* Planes of Mo-V-Te-Nb-O M1 Phase Catalyst, 2008 Annual AIChE Meeting, Philadelphia, PA, 11/20/2008.
11. A. Govindasamy, Y. Xu and V. V. Guliants, "Electronic structure of the cluster models of the Mo-V-Te-Nb-O M1 phase catalyst for propane ammoxidation", *Molecular Simulations*, submitted.

### Nanoporous Structured Silica (MCM-41 and SBA-15) Catalysts and Catalyst Supports

Posdoc: Sungchul Lee  
Students: Chuan Wang and Xiaoming Wang  
Collaborators: Lisa Pfefferle and Tarek Fahmy (both at Yale University)  
Contacts: Yale University, Department of Chemical Engineering, P. O. Box  
208286, New Haven, CT 06520-8286; [gary.haller@yale.edu](mailto:gary.haller@yale.edu)

#### Goal

Develop the concepts of pore radius of curvature effect and cation and occlusion stabilization of metal particles for high temperature catalyzed reactions.

#### DOE Interest

Structured silicas (MCM-41 and SBA-15) provide uniform pore structures in the range of 2-10 nm that can be varied in a systematic way. Most transition metals can be partially substituted for silicon to provide a tailored cation-metal particle anchor and/or simple pore size constraint on metal particle size. Anchored metal particles of uniform size can be used to template other nano-structures such as single walled carbon nanotubes (SWNT) and both the structured silica and the SWNT can be excellent catalysts supports with surface areas that are  $> 1000 \text{ m}^2/\text{g}$ . These catalysts have novel properties for energy related reactions such as aqueous reforming and fuel solubilized catalyst for aviation propulsion.

#### Recent Progress

*The Na Effect on SWNT Synthesis:* SWNT have been synthesized using two different catalysts with 3 wt % of Co incorporated in the MCM-41 mesoporous silica. The mesoporous silica has been prepared by using the same experimental conditions, but different silica sources. One MCM-41 was prepared using sodium silicate and the other one using Cab-O-Sil colloidal silica and tetramethylammonium silicate (TMASi) as silica sources. The physical and chemical properties of the catalysts were determined by nitrogen physisorption, XRD, TPR, EXAFS and used in the synthesis of SWNT by CO disproportionation. The carbon nanotubes were characterized by TGA, TEM, and RAMAN. The results showed that even though the structural regularity of both catalysts was similar, their chemical properties are quite different. The sodium ions hamper the adequate cobalt isomorphic substitution in the mesoporous structure, giving way to several metal ion species on silica, which are reduced at lower temperatures in comparison to the incorporated species in the catalyst without sodium, as shown by TPR. These different species of cobalt on

MCM-41 produce carbon nanotubes with heterogeneous distribution of diameters and generate amorphous carbon, reducing considerably the reaction yield. The metal particles, formed after reduction, are more homogeneous and showed lower average diameter in the catalyst without sodium.

*Co-SBA-15 SWNT Synthesis Catalyst:* Highly dispersed cobalt on SBA-15 was successfully prepared by a post synthesis grafting of cobalt. Of the cobalt precursors tested, Co(II) acetylacetonate was found to be the best source for high dispersion of cobalt. The Co-SBA-15 catalysts were characterized with several techniques: N<sub>2</sub> physisorption, XRD, TPR, TEM and X-ray adsorption analysis. The mesoporous structure of SBA-15 was retained after cobalt grafting with up to 10 wt.% Co loading. There were no large cobalt oxide particles formed, which indicates all the cobalt ions are highly dispersed in the surface and the direct bonding to the silica surfaces results in a high reduction temperature (1123K) relative to Co oxides. X-Ray absorption analysis demonstrates a local structure of Co ions with all Co ions isolated and bonded with oxygen. XANES analysis requires that the local environment for Co ions be that of either a distorted tetrahedral or an octahedral structure and the fitting of EXAFS data further shows a Co-O bond coordination number of 3.58 +/- 0.48, confirming that the Co is in a distorted tetrahedral environment. The catalytic activity of Co-SBA-15 catalyst was studied for the synthesis of SWNT. The high reduction stability of Co-SBA-15 makes a favorable catalyst for this high temperature reaction. Raman spectroscopy and TEM photographs show that good quality carbon SWNT was synthesized by Co-SBA-15. Moreover, Co-SBA-15 has a higher yield of carbon SWNT compared with Co-MCM-41 (C16 alkyl template) under the same reaction conditions.

*Co-Silicalite-1 SWNT Synthesis Catalyst:* Crystalline cobalt silicalites with the MFI structure (Co-Silicalite-1) catalysts have been prepared. The reducibility of Co-silicate-1 catalyst was characterized by temperature programmed reduction analysis (TPR). It shows a wide distribution of reduction peaks in TPR due to the multiple substitutable sites for Co ions in the silicate-1 structure. The catalytic performance of such crystalline Co catalysts was compared with amorphous silica supported mesoporous Co catalysts, incorporated Co-MCM-41 and grafted Co-SBA-15g catalysts for the synthesis of SWNT. Unlike Co-MCM-41 and Co-SBA-15g catalysts, which have the high selectivity of smaller diameter tubes (1nm), Co-silicalite-1 catalyst can grow large diameter SWNT (5nm) when reacted at 1023K.

### **Future Plans**

*Co Bi-metallic Catalysts for SWNT Synthesis:* There is significant evidence that the activity and selectivity of Co can be modified by a second metal this is not active for SWNT synthesis, e.g., Mo. We plan to investigate the Co-Mo interaction for SWNT

synthesis as a function of matrix (MCM-41 and SBA-15) and method of deposition/incorporation.

*Large Diameter (1-5 nm) SWNT Synthesis:* Co-silicalite-1 has been shown to catalyze SWNT of diameter as large as 5 nm, mostly unbundled. This synthesis will be optimized for a narrow diameter distribution and for yield of SWNT.

*SWNT as Catalyst Supports:* Functionalization of SWNT to produce high dispersions of supported metals, e.g., Pt, Co, etc., will be investigated.

### **Publications (2006-2008)**

1. Du, Guoan; Lim, Sangyun; Pinault, Mathieu; Wang, Chuan; Fang, Fang; Pfefferle, Lisa; Haller, Gary L. **Synthesis, characterization, and catalytic performance of highly dispersed vanadium grafted SBA-15 catalyst.** *Journal of Catalysis* (2008), 253(1), 74-90.
2. Lim, Sangyun; Li, Nan; Fang, Fang; Pinault, Mathieu; Zoican, Codruta; Wang, Chuan; Fadel, Tarek; Pfefferle, Lisa D.; Haller, Gary L. **High-Yield Single-Walled Carbon Nanotubes Synthesized on the Small-Pore (C10) Co-MCM-41 Catalyst.** *Journal of Physical Chemistry C* (2008), 112(32), 12442-12454.
3. Lim, Sangyun; Yang, Yanhui; Pfefferle, Lisa D.; Haller, Gary L. **Formation of size controllable sub-nanometer metallic clusters by pore radius of curvature effect and the stability explained by anchoring/occlusion effect.** *Studies in Surface Science and Catalysis* (2007), 321-324.
4. Lim, Sangyun; Wang, Chuan; Yang, Yanhui; Ciuparu, Dragos; Pfefferle, Lisa; Haller, Gary L. **Evidence for anchoring and partial occlusion of metallic clusters on the pore walls of MCM-41 and effect on the stability of the metallic clusters.** *Catalysis Today* (2007), 123(1-4), 122-132.
5. Chen, Yuan; Wei, Li; Wang, Bo; Lim, Sangyun; Ciuparu, Dragos; Zheng, Ming; Chen, Jia; Zoican, Codruta; Yang, Yanhui; Haller, Gary L.; Pfefferle, Lisa D. **Low-Defect, Purified, Narrowly (n,m)-Dispersed Single-Walled Carbon Nanotubes Grown from Cobalt-Incorporated MCM-41.** *ACS Nano* (2007), 1(4), 327-336.
6. Chen, Yuan; Wang, Bo; Li, Lain-Jong; Yang, Yanhui; Ciuparu, Dragos; Lim, Sangyun; Haller, Gary L.; Pfefferle, Lisa D. **Effect of different carbon sources on the growth of single-walled carbon nanotube from MCM-41 containing nickel.** *Carbon* (2007), 45(11), 2217-2228.
7. Du, Guoan; Lim, Sangyun; Yang, Yanhui; Wang, Chuan; Pfefferle, Lisa; Haller, Gary L. **Methanation of carbon dioxide on Ni-incorporated MCM-41 catalysts: The influence of catalyst pretreatment and study of steady-state reaction.** *Journal of Catalysis* (2007), 249(2), 370-379.

In situ measurement of metal oxide and metal rearrangement of  $\text{CuFe}_2\text{O}_4$  spinel during catalyst activation for Water Gas Shift (WGS) reaction catalysis.

Lead PI: Jonathan Hanson

Postdoc: L Barrio, W. Wen, X-Q Wang, G. Zhou

Student: M. Estrella

Contact: Department of Chemistry, Brookhaven National Laboratory, Upton, NY 11973  
[rodriguez@bnl.gov](mailto:rodriguez@bnl.gov), [hrbek@bnl.gov](mailto:hrbek@bnl.gov)

It has been shown by using in situ X-ray diffraction and X-ray absorption spectroscopy that the metal to metal oxide interaction plays an important role in the catalysis of the WGS reaction[1]. In many cases the precursor has been a mixed metal oxide[2]. In the current study we have used commercially prepared  $\text{CuFe}_2\text{O}_4$  spinel (with 6% CuO) as a precursor to a WGS catalyst. We studied the structural changes of the catalyst during preparation and under WGS reaction conditions. The active catalyst was shown to be Cu supported on  $\text{Fe}_3\text{O}_4$ . In the starting  $\text{CuFe}_2\text{O}_4$  spinel, the Cu cations are predominately at the octahedral site and the Fe cations are distributed between the octahedral and tetrahedral sites.

The diffraction data were collected to a  $q$  of  $18\text{\AA}^{-1}$  ( $q=4\pi\sin\theta/\lambda$ ). With powder profile refinement of this data we were able to observe the changes to the cation distribution at the octahedral site during catalyst activation. This included a decrease in electron density at the Cu site as the spinel transformed from  $\text{CuFe}_2\text{O}_4$  to  $\text{Fe}_3\text{O}_4$ .

We also analyzed this data with the pair distribution function method (PDF). The PDF method uses the Fourier transform of appropriately corrected high  $q$  diffraction data to calculate a function like the radial distribution. For measurements under WGS conditions, the time resolved PDF maps showed changes in the cation distribution of the spinel and the appearance of the metallic copper.

This study is a new example of the use of in situ X-ray diffraction, PDF and X-ray absorption spectroscopy for the determination of catalyst structure under operating conditions[3, 4].

- 1 J. A. Rodriguez, P. Liu, X. Wang, W. Wen, J. Hanson, J. Hrbek, M. Pérez and J. Evans, Water-gas shift activity of Cu surfaces and Cu nanoparticles supported on metal oxides Catalysis Today, ((web)).
- 2 W. Wen, J. Liu, M. G. White, M. Marinkovic and J. A. Rodriguez, In situ Time-resolved Characterization of Novel Cu-MoO<sub>2</sub> Catalysts during the Water-Gas Shift Reaction, Catal. Letters, **113**, 1 (2007).
- 3 J. A. Rodriguez, and J. Hanson, In situ Characterization of Heterogeneous Catalysts Using Time-resolved X-ray Diffraction., Ciencia, **14**, 177 (2006).
- 4 P. Norby, and J. Hanson, Hydrothermal Synthesis of the Microporous Aluminosphate CoAPO-5; *In-Situ* Time Resolved Synchrotron X-Ray Powder Diffraction Studies, Catalysis Today, **39**, 301 (1998).



**Supported Molecular Catalysts: Synthesis, in-situ Characterization and Performance**

Dr. J. F. Haw (PI),<sup>1</sup> Dr. Bruce C. Gates, (Co-PI),<sup>2</sup> Dr. David A. Dixon (Co-PI)<sup>3</sup>

Students: M. McAfee (graduate),<sup>1</sup> A. Joyce(graduate),<sup>1</sup> A. J. Liang (graduate),<sup>2</sup> R. J. Lobo-Lapidus,<sup>2</sup> A. Uzun,<sup>2</sup> M. Chen (graduate),<sup>3</sup> T.-H. Wang (graduate),<sup>3</sup> T. Glenn Kelly, (undergraduate),<sup>3</sup> Désirée Picone (undergraduate)<sup>3</sup>

University of Southern California,<sup>1</sup> Univeristy of California-Davis,<sup>2</sup> The University of Alabama<sup>3</sup>

Contact: J.F. Haw, Chemistry Department, The University of Southern California, 840 Downey Way, Los Angeles, CA 90089-0744; Phone: 213-740-1022; Email: jhaw@usc.edu

Oxide-supported metal complexes are a widely investigated and industrially important class of catalyst. Understanding of their chemistry is hindered by the complexity of their structures, which is linked to the intrinsic non-uniformity of the support surfaces. A precise synthesis of zeolite-supported metal complex can be accomplished via a one-step reaction of an organometallic precursor  $[\text{Rh}(\text{C}_2\text{H}_4)_2(\text{acac})]$  ( $\text{acac} = \text{CH}_3\text{COCHCOCH}_3$ ) or  $\text{cis-Ru}(\text{acac})_2(\eta^2\text{-C}_2\text{H}_4)_2$  with the zeolite. (Liang et al. *J. Phys. Chem. B* **2005**, *109*, 24236; Ogino and Gates, *J. Am. Chem. Soc.* **2008**, *130*,13338) Rhodium diethylene complexes on dealuminated Y zeolite were shown by temperature-dependent  $^{13}\text{C}$  NMR spectroscopy to have a degree of dynamic uniformity unprecedented for supported species (Ehresmann et al. *Angew. Chem. Int. Ed.* **2006**, *45*, 574). Because the ethylene ligands undergo facile conversions and the complexes are site-isolated, such supported complexes open the way to precise characterization of a family of related complexes in the absence of complications that characterize the solution chemistry such as solvent effects and metal-metal bond formation. Precisely synthesized structures on zeolites, in contrast to those on oxides (the reactive sites of which are often defects or edge and corner sites), can be determined with a precision unattainable for the non-uniform oxide-supported metal complexes. A distinct advantage of the uniform zeolitic species is that electronic structure calculations at the density functional theory (DFT) level can be used to verify spectroscopic assignments and resolve structures characterized by subtly different spectra. Thus, zeolite-supported metal complexes offer the prospects of (a) surface chemistry determined with a rigor rivaling that attainable with molecular metal complexes in solution, but in the absence of the complications characteristic of solution chemistry, and (b) ultimately, blurring of the distinctions between homogeneous and surface reactions. We have begun to realize these prospects in an investigation of reactions of zeolite-supported rhodium complexes. We have found that is advantageous to use isotopically labeled gas-phase reactants that can displace the olefin ligands on the site-isolated rhodium atoms. The newly formed complexes can then be characterized by spectroscopic techniques including IR,  $^{13}\text{C}$  NMR, and extended X-ray absorption fine structure (EXAFS) spectroscopies, guided by electronic structure calculations at the DFT level. This combination of techniques enabled the identification of heretofore unknown species, including an activated rhodium hydride complex.

Structures of zeolite-anchored organorhodium complexes undergoing conversions with gas-phase reactants were characterized by infrared spectra bolstered by calculations with density functional theory and analysis of the gas-phase products. Structurally well-defined zeolite-supported rhodium diethylene complexes were synthesized by chemisorption of  $\text{Rh}(\text{C}_2\text{H}_4)_2(\text{acac})$  ( $\text{acac} = \text{CH}_3\text{COCHCOCH}_3$ ) on dealuminated Y zeolite, being anchored by two Rh-O bonds, as shown by EXAFS spectroscopy. The predicted structures of a  $\text{Rh}^+$  which has displaced the proton in a model zeolite acid site are consistent with the EXAFS structural assignments. In contrast to the nonuniformity of metal complexes anchored to metal oxides, the near uniformity of the zeolite-supported species allowed precise determination of their

chemistry, including the role of the support as a ligand. The anchored rhodium diethylene complex underwent facile, reversible ligand exchange with deuterated ethylene at 298 K, and ethylene ligands were hydrogenated by reverse spillover of hydrogen from support hydroxyl groups to form the C<sub>2</sub>H<sub>5</sub> ligand and ethane. The supported complexes reacted with CO to form rhodium *gem*-dicarbonyls, which, in the presence of ethylene, gave rhodium monocarbonyls. The facile removal of ethylene ligands from the complex in H<sub>2</sub>-N<sub>2</sub> mixtures created coordinatively unsaturated rhodium complexes; the coordinative unsaturation was stabilized by the site isolation of the complexes, allowing reaction with N<sub>2</sub> to form rhodium complexes with one and with two N<sub>2</sub> ligands. The results also provide evidence of a new rhodium monohydride species incorporating a CO ligand, although we cannot rule out the possibility that some C<sub>2</sub>H<sub>4</sub> might have been present in place of the CO. The use of isotope labeling in combination with DFT calculations of the frequencies was critical to analyzing the experimental spectra and the observation of new intermediates. A summary of some of the reactions is shown in Figure 1.

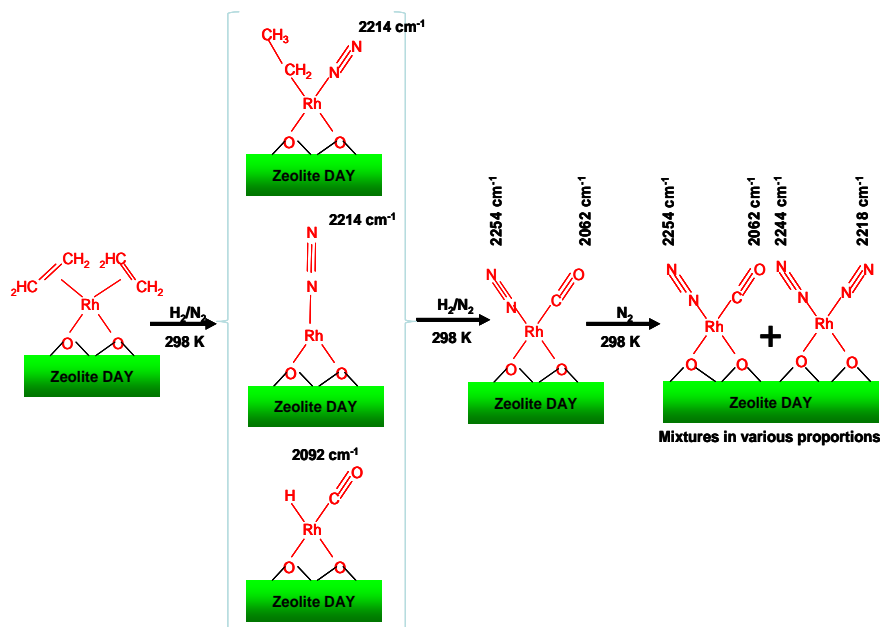


**Figure 1.** Reaction scheme showing intermediates assigned on the basis of isotope labeling and DFT calculations.

Ligand dissociation energies (LDEs) were calculated for the supported rhodium complexes with an accuracy of  $\pm 5$  kcal/mol. For a complex zeolite-RhLL' (2 ligands bonded to Rh), the average Rh–L dissociation energies (in kcal/mol) are:  $\Delta E(\text{H}) = 64 > \Delta E(\text{CO}) = 53 > \Delta E(\text{C}_2\text{H}_5) = 45 > \Delta E(\text{C}_2\text{H}_4) = 40 > \Delta E(\text{N}_2) = 28 \sim \Delta E(\text{H}_2) = 27$ . These values are slightly higher than the ligand dissociation energies for the complex zeolite–Rh–L with a single ligand bonded to the Rh. Thus we would expect CO to displace C<sub>2</sub>H<sub>4</sub>, for example, in an equilibrium situation. However, the results must be used carefully in any analysis of the exchange reactions in the flow experiments—which are far from equilibrium—so that the treatments in the flow system can lead to endothermic exchange processes.

We have studied the catalytic cyclotrimerization of acetylene using our site-isolated metal complexes in zeolites as catalysts. The C<sub>2</sub>H<sub>4</sub> on the Rh was displaced by C<sub>2</sub>H<sub>2</sub> to form the initial reactant. NMR, IR, and EXAFS measurements coupled with DFT calculations were used to map out the catalytic pathway in detail. The DFT calculations were used to assign the <sup>13</sup>C nmr spectra to within about 5 to 10 ppm, consistent with an error of 6 ppm in C<sub>6</sub>H<sub>6</sub>. Figure 2 is a schematic representation of the catalytic cycle determined on the basis of our computations and experimental results for the conversion of acetylene on the supported catalyst, with the structures of the intermediates and a summary of the characterization methods used to identify each species, including PRE. Of the significant intermediates along the reaction pathway, two (SI<sub>1</sub> and SI<sub>3</sub>) have been observed by solid-state NMR spectroscopy with their assignments as the *bis*-acetylene and benzene complexes, in agreement with <sup>13</sup>C shift for analogous solution complexes. The third intermediate (SI<sub>2</sub>) has been inferred on the basis of our DFT calculations to be in equilibrium with a structurally related spectator cyclobutadiene complex (SPEC) that we also observe by <sup>13</sup>C solid-state NMR spectroscopy. The benzene complex SI<sub>3</sub> was characterized by NMR spectroscopy after entering the cycle in either the forward direction, by exchange of PRE with acetylene-

$^{13}\text{C}_2$ , or the reverse direction, by exchange with benzene- $^{13}\text{C}_6$ . The key to the rigorous elucidation of the catalytic intermediates is the near uniformity of the supported rhodium complexes, as demonstrated by the dynamic uniformity evidenced by  $^{13}\text{C}$  NMR spectroscopy of the ethylene ligands in the supported as-synthesized complex **PRE**. In a more typical supported catalyst, exemplified by platinum particles supported on alumina, adsorption of acetylene led to a  $^{13}\text{C}$  MAS

NMR spectrum consisting only of a broad signal attributed to benzene at a shift close to the solution value. Even when putative intermediates in surface catalysis are observed spectroscopically, they often prove to be spectators—species present in low-energy states that are equilibrated with reactive species in the catalytic cycle.

The overall catalytic cycle is qualitatively in agreement with previous models of the cyclotrimerization reaction in solution catalyzed by  $\text{CpCo}^+$  and various  $\text{Co}^+$ ,  $\text{Rh}^+$ , and  $\text{Ir}^+$  complexes. Our results are also consistent with the gas phase ion-cyclotron resonance spectroscopy studies of benzene formation in reactions of cyclobutadiene and acetylene with complexes of  $\text{Rh}^+$  and of  $\text{Ru}^+$ . These authors determined the reactivities of the  $\text{C}_4\text{H}_4$  complex of  $\text{Rh}^+$  with acetylene, finding that the catalytic cycle turned over six times as  $\text{MC}_4\text{H}_4^+$  reacted with acetylene to form free benzene and bare  $\text{Rh}^+$ . Ion-molecule collision experiments established that  $\text{RhC}_4\text{H}_4^+$  was a key intermediate, most likely present as a cyclobutadiene complex rather than a metallacycle, although the latter cannot be ruled out on the basis of the experimental results. Results characterizing the products of the gas phase ion-molecule reaction indicate that it most likely takes place on the triplet surface, corresponding to the most stable metal ion spin state.

Our calculations show that the bonding of the hydrocarbon ligands is not significantly affected by the presence of the zeolite support, as the benzene complexes with the bare atomic ion and with the rhodium complex incorporating the zeolite as a ligand are characterized by similar bonding of the benzene, which is predicted to bind  $\eta^2$  to  $\eta^4$  in each. Thus, there are similarities between the gas-phase cyclotrimerization reaction in the presence of  $\text{Rh}^+$  and in the presence of our isolated zeolite-bound surface site, although we note that there may be differences in the spin states that may control the reactivity.

Other results are summarized in the publications listed below.

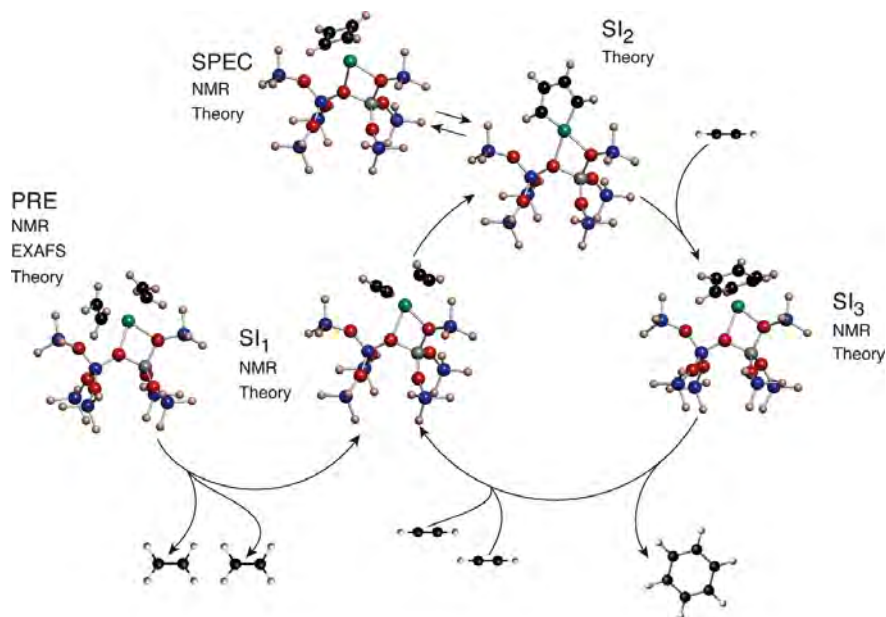


**Figure 2.** Catalytic cycle for cyclotrimerization of acetylene catalyzed by a single-site  $\text{Rh}^+$  center bonded to a zeolite support by two  $\text{Rh-O}$  bonds. The reactive organic groups bonded to  $\text{Rh}$  in the as-synthesized catalyst (at left, **PRE**), two ethylenes, allow facile entry into a catalytic cycle. (Characterization methods for all the species are shown on the figure.) When the sample is brought in contact with gas-phase acetylene, the ethylene is replaced by acetylene, to form the stable intermediate **SI<sub>1</sub>**, initiating the catalytic cycle. This intermediate undergoes ring closure via transition state **TS<sub>1→2</sub>**, forming the metallacycle **SI<sub>2</sub>**, which equilibrates with the more stable cyclobutadiene complex (**SPEC**, a spectator species). The pool consisting of **SI<sub>2</sub>** and **SPEC** crosses via transition state **TS<sub>2→3</sub>** into the stable benzene complex **SI<sub>3</sub>**. Dissociation of product benzene into the gas phase, compensated by adsorption of reactant acetylene, closes the cycle.

## Publications: 2007 -2009

1. "Synthesis and Crystal Structure of  $\text{Ir}(\text{C}_2\text{H}_4)_2(\text{C}_5\text{H}_7\text{O}_2)$ ," V. A. Bhirud, A. Uzun, P. W. Kletnieks, R. Craciun, J. F. Haw, D. A. Dixon, M. M. Olmstead, and B. C. Gates, *J. Organometallic Chem*, **2007**, 692, 2107.
2. "Molecular Heterogeneous Catalysis: A single-site Zeolite-Supported Rhodium Complex for Acetylene Cyclotrimerization," P. W. Kletnieks, A. J. Liang, R. Craciun, J. O. Ehresmann, D. M. Marcus, V. A. Bhirud, M. M. Klaric, M. J. Hayman, D. R. Guenther, O. P. Bagatchenko, D. A. Dixon, B. C. Gates, and J. F. Haw, *Chem. Eur. J.*, **2007**, 13, 7294.
3. "Probing Defect Sites on  $\text{TiO}_2$  with  $\text{H}_3\text{Re}_3(\text{CO})_{12}$ : Spectroscopic Characterization of the Surface Species," K. Suriye, R. J. Lobo-Lapidus, G. J. Yeagle, P. Praserthdam, R. D. Britt, and B. C. Gates, *Chem. Eur. J.*, **2008**, 14, 1402.
4. "Alumina-Supported Trirhenium Clusters: Stable High-Temperature Catalysts for Methylcyclohexane Conversion," R. J. Lobo-Lapidus, M. J. McCall, M. Lanuza, S. Tonnesen, S. R. Bare, and B. C. Gates, *J. Phys. Chem. C*, **2008**, 112, 3383.
5. "Real-Time Characterization of Formation and Breakup of Iridium Clusters in Highly Dealuminated Zeolite Y," A. Uzun and B. C. Gates, *Angew. Chem., Int. Ed.*, **2008**, 47, 9245.
6. "Time-Resolved Structural Characterization of Formation and Break-up of Rhodium Clusters supported in Highly Dealuminated Y Zeolite," A. J. Liang and B. C. Gates, *J. Phys. Chem. C*, **2008**, 112, 18,039
7. "Site-Isolated Iridium Complexes on MgO Powder: Individual Ir Atoms Imaged by Scanning Transmission Electron Microscopy," A. Uzun, V. Ortalan, N. D. Browning, and B. C. Gates, *ChemComm*, in press.
8. "Zeolite-Supported Organorhodium Fragments: Essentially Molecular Surface Chemistry Elucidated with Spectroscopy and Theory," A. J. Liang, R. Craciun, M. Chen, T. G. Kelly, P.W. Kletnieks, J. F. Haw, D. A. Dixon, and B. C. Gates, *J. Am. Chem. Soc.* submitted, 2009.

DE-FG02-03ER15463  
DE-FG02-03ER15464  
DE-FG02-07ER15842

Tony F. Heinz/Stephen P. O'Brien (Columbia U.)  
Ludwig Bartels (UC Riverside)  
Talat S. Rahman (U. Central Florida)

### **Controlling Structural, Electronic, and Energy Flow Dynamics of Catalytic Processes through Tailored Nanostructures**

Post-docs: Zhihai Cheng (UCR), Daejin Eom (Columbia), Limin Huang (Columbia), Christophe Huchon (UCR), Sampyo Hong (UCF), Marisol Alcantara Ortigoza (UCF), K. L. Wong (UCR).

Students: Zhang Jia (Columbia), D. H. Kim (UCR), Duy Tran Le (UCF), M. M. Luo (UCR), Greg Pawin (UCR), Ghazal Shafai (UCF) Dezheng Sun (UCR), Jon Wyrick (UCR), Hui Zhou (Columbia).

Collaborators: Radoslav R. Adzic (Brookhaven), Gerhard Ertl and Karl Jakobi (Fritz-Haber Inst., Berlin), Christopher Murray (U. Penn), Mark Hybertsen (Brookhaven), Matthew Sfeir (Brookhaven), Feng Wang (UC Berkeley) Yumei Zhu (Brookhaven), and Columbia U. collaborators: Louis E. Brus, George W. Flynn, Irving Herman, Jim Hone, Gertrude Neumark, Colin Nuckolls, Nicholas Turro.

Contact: Tony. F. Heinz, Dept. of Physics, Columbia University, New York, NY, 10027; tel: 212-854-6564; email: [tony.heinz@columbia.edu](mailto:tony.heinz@columbia.edu); web page: <http://heinz.phys.columbia.edu>  
Ludwig Bartels, Dept. of Chemistry, U. of California, Riverside, CA 92506; tel: 951-827-2041; email: [ludwig.bartels@ucr.edu](mailto:ludwig.bartels@ucr.edu); web page: <http://research.chem.ucr.edu/groups/bartels/>  
Talat S. Rahman, Dept. of Physics, University of Central Florida, Orlando, FL 32816; tel: 407-823-1480; email: [trahman@mail.ucf.edu](mailto:trahman@mail.ucf.edu); web page: <http://www.physics.ucf.edu/~talat>

#### **Goal**

The overall goal of this project, which is being carried out jointly with PIs Ludwig Bartels (UC Riverside), Tony Heinz and Stephen O'Brien (Columbia University) and Talat Rahman (University of Central Florida), is to pursue the development of new catalysts that control the flow of reactants to and products from optimized reaction sites and, to the extent possible, control the flow of energy released in the surface reactions through the use of tailored nanostructured materials. The research program involves three principal thrust areas: (1) The synthesis of nanostructured materials suitable for novel catalysts; (2) experimental investigations of non-equilibrium surface processes, particularly on nanostructured materials; (3) and theoretical investigations to understand the electronic properties and reactivity of the corresponding systems. Within the experimental surface-science component, research involves the traditional tools of surface science, but also places special emphasis on scanning tunneling microscopy to understand the nature of behavior on heterogeneous surfaces and laser sources to induce and probe non-equilibrium processes. Elementary surface processes and model reactions with nanoscale materials will be examined to pursue these ambitious goals.

#### **DOE Interest**

The development of new highly selective catalysts is critical to the future of cleaner, more efficient management of energy consumption and distribution, with major potential impacts across the

energy value chain, including fuels process and new (e.g. bio-) fuels, large scale energy generation, feedstocks and pollution control. To seek new methods that can inform or enhance parallel current catalyst technology is therefore of high importance to the DOE. Furthermore, much of our collaborative research attempts to address two of the five proposed grand challenges in basic energy science materials science research: control over materials process at the level of electrons, and control over matter (including control over matter away from equilibrium). It is the aim of this project to explore new approaches that rely on recent developments in nanostructured materials and on advances in our fundamental understanding of molecule/surface interactions to produce catalysts with higher efficiency and greater selectivity, with the potential for impact on a diverse and significant set of chemical processes. Our approach is to start with the concept of a model catalyst, that would feature atomically-defined active sites at high density and predetermined relative position, which would lead to the ability to perform catalytic reactions through a series of planned and concerted reactions. Key to this design is not only facilitation of the actual catalytic reaction step(s), but also management of the surface transport of reactants/products between the catalyst components and their exchange with the surrounding phase.

## Recent Progress

### *Controlling Site Selectivity in Binary Nanoparticles*

Proton exchange fuel cells are promising tools for the efficient use of hydrogen in many applications. However, trace amounts of CO, inevitably present in hydrogen, block active Pt sites of anode and, hence, poison its reactivity. The Adzic group at Brookhaven National Laboratory has recently shown that nanoclusters of Ru with sub-monolayer of Pt (PtRu<sub>20</sub>) are much more tolerant to CO poisoning than commercial PtRu catalysts. It is important to note that the content of Pt in these novel materials is much lower than that in PtRu alloys. From estimates of the average diameter of Ru nanoparticles and Pt/Ru ratio, Adzic concludes that the deposited Pt forms small islands on the facets of the Ru nanoparticles. Rahman's group has examined this model problem in catalytic selectivity theoretically. Her calculations using density-functional theory (DFT) have established that while Pt wets Ru surfaces, Pt islets are stable on facets of Ru nanoparticles as a result of the high diffusion barrier for the Pt dimer and larger clusters to cross the nanoparticles edges.

These calculations also establish that CO has the lowest adsorption energy at the center of the islet, and its bonding increases as it moves to the edge of the island and further onto the substrate. Activation energy barriers for CO diffusion from the islet to the Ru surface are found to be lower than 0.3 eV (Figure 1), making the process feasible and leading to the conclusion that this hydrogen oxidation catalyst is CO tolerant because of the spillover of CO from active Pt sites to the Ru substrate. The rate of CO oxidation by OH is found to be substantially enhanced when the former is adsorbed on the edge of Pt islands and the latter on nearby. We will further explore how by changing of the support dimensions and corresponding electronic confinement effect, binary metallic mixtures can be manipulated to adopt geometries that are particularly favorable for the activation of desired catalytic reactions.

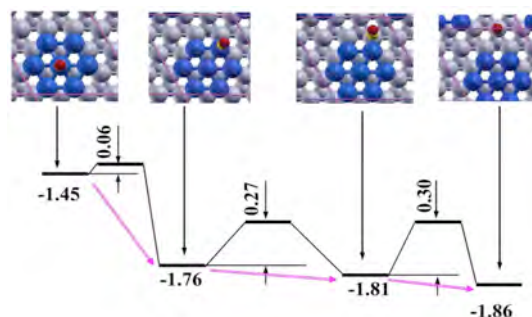


**Figure 1:** Density functional theory calculations of the diffusion barriers and binding energies for CO adsorbed molecules (red) adsorbed on an islet of Pt (blue) atoms on a Ru (grey) surface.

### Complete CO Oxidation by Copper Oxide Nanoparticles

A joint experimental (O'Brien's group) and theoretical (Rahman's group) effort has examined the reactivity of nearly monodisperse copper oxide nanoparticles. These nanoparticles prepared via the thermal decomposition of a Cu(I) precursor, were found to exhibit exceptional activity toward CO oxidation in CO/O<sub>2</sub>/N<sub>2</sub> mixtures. Greater than 99.5% conversion of CO to CO<sub>2</sub> could be achieved at temperatures less than 250 °C for over 12 h for a preparation of nanoparticles on a silica gel (Fig. 2).

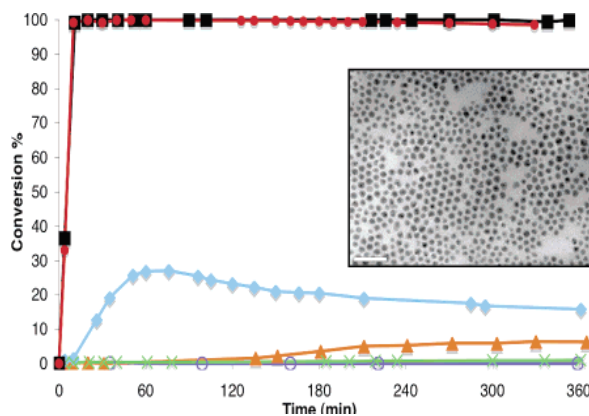


**Figure 2:** Experimental results on the oxidation of CO by different forms of copper oxide. The red curve corresponds to the highly monodisperse copper oxide nanoparticles shown in the micrograph.

The (*P,T*) phase diagram of the Cu<sub>2</sub>O(100) surface in equilibrium with gas-phase O<sub>2</sub> obtained from an *ab-initio* thermodynamics approach finds the O-terminated surface to have lower free energy than the Cu-terminated one within the entire range of pressure and temperature for which the compound exists. The quasi-stable Cu-terminated Cu<sub>2</sub>O(100) is found to undergo a surface reconstruction in agreement with experiments. CO is found to be oxidized spontaneously on Cu<sub>2</sub>O(100) by consuming surface O atoms. These calculations also show that the surface O vacancies left in the course of the CO oxidation can be easily filled with dissociative adsorption of the gas phase O<sub>2</sub> (activation barrier of 0.3 eV) and that one O atom fills the vacancy while the other occupies the hollow site next to the vacancy, thereby restoring the surface.

### Selectivity in Ammonia oxidation on an oxide surface

To address the high selectivity for NO formation in ammonia oxidation on RuO<sub>2</sub>(110) observed by collaborator Ertl and colleagues, Rahman has performed DFT calculations of the activation energy barriers for the associated reaction processes and applied them in kinetic Monte Carlo (KMC) simulations of the reaction rates. These simulations reproduce the selectivity towards formation of NO for a substrate saturated with oxygen. When several intermediates and their reactions (18 processes) were included, the KMC simulations show about 70% selectivity toward NO within the experimental O<sub>2</sub> pressure range (fig. 3.) Beyond this particular system, this study is evidence that activation energy barriers obtained from DFT calculations together with KMC simulations serve as powerful tools for assisting in the design of catalytic materials. In another Rahman/Ertl collaboration involving a comparison of the reactivity of RuO<sub>2</sub>(110) to CO and NO oxidation, we traced the experimentally observed lack of reactivity for NO oxidation to the NO-Ru bond at coordinatively unsaturated substrate sites. This bond was found to be

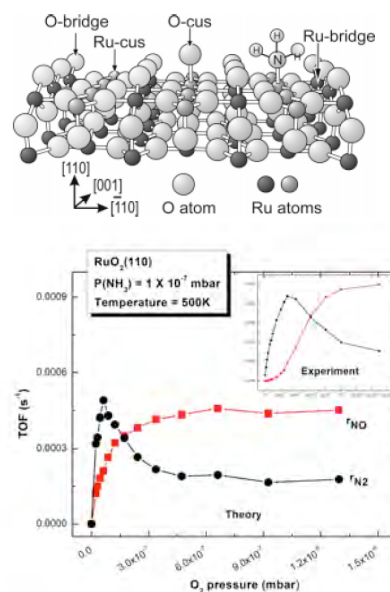


**Figure 3:** Experimental (inset) and theoretical results by KMC simulations for ammonia oxidation on the RuO<sub>2</sub>(110) surface. The surface structure is shown above.

much stronger than the CO-Ru bond at such sites, with the difference arising from the contribution of the unpaired  $2\pi^*$  electrons of NO.

### ***Catalytic Growth and Properties of Carbon Nanotubes and Graphene***

The major impediment to the widespread use of carbon nanotubes in various important technologies is the lack of sufficient control of the precise crystallographic structure or chiral indices ( $n,m$ ) of the material. This issue is in fact a problem in catalytic growth and selectivity, since the dominant method of nanotube production is through catalytic decomposition of various carbon-bearing species on metal nanoparticles. Recent dramatic results show that graphene (a monolayer of  $sp^2$  hybridized carbon) may also be a revolutionary new material for electronics and nanomechanics applications. Its use, however, is currently limited by poorly developed growth techniques, which are also expected to be catalytic in nature.

O'Brien and Heinz working jointly have grown and characterized ultralong (mm-length) nanotubes produced by a chemical vapor deposition process using ethanol as the feedstock and Co nanoparticles as the catalyst. This method has been shown to yield ultrahigh quality nanotubes, which can, moreover, be grown from a given location (by catalyst placement) in a given direction (by reactor gas flow conditions). Although rough diameter control has been achieved by the growth conditions, full specification of chiral index remains a challenge.

Using a similar approach to that employed for carbon nanotube growth, Heinz and collaborators have recently examined the growth of graphene using catalytic dehydrogenation of a hydrocarbon precursor on the Co(0001) surface. Well-ordered islands of graphene were produced with uniform single monolayer thickness and perfect substrate alignment. The favorable growth characteristics are attributed to the nearly perfect lattice match between the graphene lattice and the Co(0001) lattice. Also, the role of the specific structure of the hydrocarbon precursor, particularly, the presence or absence of fused benzene rings, is currently being investigated.

### ***Guiding Surface Motion***

Hexagonal surfaces exhibit the highest symmetry of all crystalline surfaces. They are also among the least reactive, which renders transport across them towards sites of greater activity (e.g., step-edges, defects, and regions of different composition) particularly important.

Adsorbates generally diffuse in an isotropic fashion on metal surfaces, i.e., in all possible surface directions with equal probability. Surfaces of lower symmetry are known to guide the diffusion of adsorbates along their structural features (e.g., atomic rows on (110) surfaces, step-edges on regularly stepped surfaces, etc.). STM investigations have been tremendously useful in both elucidating and quantifying the details of such processes. Experimental investigations by the Bartel's group have shown that 1-dimensional guidance can also be achieved on the hexagonal fcc(111) surface despite the *absence of structural differences along the three equivalent in-plane directions*. The origin of this guidance effect is completely different from the familiar influence of the inherent surface anisotropy. It arises from the detailed molecule/substrate interaction. We

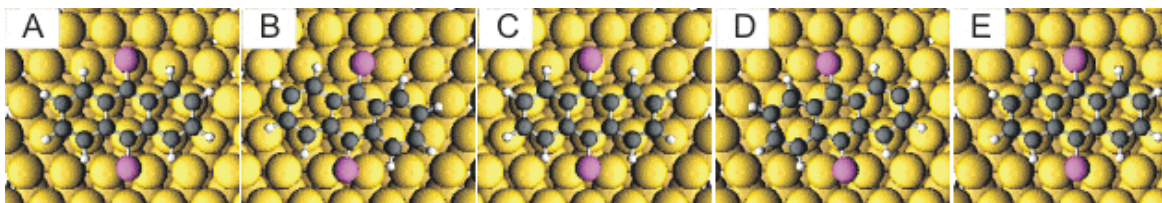


**Figure 4:** Molecular configurations during the linear diffusive motion of DTA on a Cu(111) surface. At any instant either one of the sulfur (purple) substrate linkers is outside a favorable hollow site or the ring system as a whole is misaligned with the substrate.



initially demonstrated this effect using a molecule, 9,10-diacetylthioanthracene (DTA) that we designed for this purpose. We found that when deposited on a Cu(111) substrate, DTA diffuses exclusively along the direction in which it is initially aligned. This converts a 2D random walk into a 1D phenomenon. A combination of theoretical modeling and density functional theory calculations by Rahman allowed us to elucidate the fundamental steps underlying this process. We find that the molecule's motion resembles bipedal stepping across the surface (Fig. 4).

Bartels has recently extended this counter-intuitive concept of uniaxial surface motion to the transport of "cargo" molecules along a given direction. This was achieved using a combination of anthraquinone, the oxygen counterpart of dithioanthracene, as a carrier and CO<sub>2</sub> as cargo. STM measurements show, that anthraquinone can carry up to two CO<sub>2</sub> molecules, each of which is reversibly attached to one of the carbonyl substrate linkers by means of relatively weak substrate mediated interactions.

Once the barriers for linear motion were established, Bartels used these systems to study the strength of hydrogen bonds at surfaces. Formation and cleavage of hydrogen bonds is a common intermediate step in many catalyzed reactions both at surfaces and in the solution phase. While it can be studied quite precisely in the gas phase, prior to this study little experimental information on the strength of hydrogen bonds at surfaces was available.

### Future Plans

In the coming period, the research team intends to make use of the combined advances in experimental and theoretical understanding to examine a more restricted class of catalytic reactions in which nanostructured materials play an essential role. To this end, the Cu/ZnO catalyst, with its widespread application in methanol synthesis, will be a subject of particular attention. In addition, photoexcitation, already investigated in this project for adsorbates on flat Cu surfaces, will be examined as a route to achieving efficient methanol synthesis through the reduction of CO<sub>2</sub>. The focus of the research will continue to be on understanding and controlling the fundamental steps in catalytic conversion process using detailed experimental and theoretical studies at the molecular level, as illustrated in the work presented above.

### Publications for 2007-2009:

1. K. L. Wong, G. Pawin, K-Y. Kwon, X. Lin, T. Jiao, U. Solanki, R. H. J. Fawcett, L. Bartels, S. Stolbov, and T. S. Rahman, "A Molecule Carrier," *Science* **315**, 1391 (2007).
2. T. S. Rahman, S. Stolbov, and F. Mehmood, "Alkali Induced Effects on Metal Substrates and Coadsorbed Molecules," *App. Phys. A* **87**, 367 (2007).
3. L. Zhang, J. Zhang, L. Huang, S. O'Brien, and Z. Yu, "Imaging and Raman Spectroscopy of Individual Single-Wall Carbon Nanotubes on a Large Substrate," *J. Phys. Chem. C* **111**, 11240 (2007).
4. L. Huang, Z. Jia, and S. O'Brien, "Oriented Assembly of Single-Walled Carbon Nanotubes and Applications," *J. Mater. Chem.* **17**, 3863 (2007).
5. E. Stolyarova, K. T. Rim, S. Ryu, J. Maultzsch, P. Kim, L. E. Brus, T. F. Heinz, M. H. Hybertsen, and G. W. Flynn, "High-Resolution Scanning Tunneling Microscopy Imaging of Graphene Sheets on an Insulating Surface," *Proc. Nat. Acad. Sci.* **104**, 9209 (2007).
6. M. Yin, Z. Chen, B. Deegan, and S. O'Brien, "Wustite Nanocrystals: Synthesis, Structure and Superlattice Formation," *J. Mater. Res.* **22**, 1987 (2007).
7. T. Andelman, Y. Gong, G. Neumark, and S. O'Brien, "Diameter Control and Photoluminescence of ZnO Nanorods from Trialkylamines," *J. Nanomater.* 2007, 73824 (2007).
8. F. Wang, W. Liu, Y. Wu, M. Y. Sfeir, L. Huang, J. Hone, S. O'Brien, L. E. Brus, T. F. Heinz, and Y. R. Shen, "Multiphonon Raman Scattering from Individual Single-Walled Carbon

- Nanotubes,” *Phys. Rev. Lett.* **98**, 047402 (2007).
9. Y. Wu, J. Maultzsch, E. Knoesel, B. Chandra, M. Huang, M. Y. Sfeir, L. E. Brus, J. Hone, and T. F. Heinz, “Variable Electron-Phonon Coupling in Isolated Metallic Carbon Nanotubes Observed by Raman Scattering,” *Phys. Rev. Lett.* **99**, 027402 (2007).
  10. F. Wang, D. Cho, B. Kessler, J. Deslippe, P. J. Schuck, S. G. Louie, A. Zettl, T. F. Heinz, and Y. R. Shen, Y.R., “Observation of Excitons in One-Dimensional Metals,” *Phys. Rev. Lett.* **99**, 227401 (2007).
  11. T. F. Heinz, “Rayleigh Scattering Spectroscopy in Carbon Nanotubes, in *Advanced Topics in the Synthesis, Structure, Properties and Applications*, A. Jorio, G. Dresselhaus, and M. S. Dresselhaus, Eds; (Springer, Berlin, 2007), Ch. 11.
  12. S. Hong, T. S. Rahman, K. Jacobi, G. Ertl, “The Interaction of NO with a RuO<sub>2</sub>(110) Surface: a First Principles Study,” *J. Phys. Chem. C* **111**, 12361 (2007).
  13. G. Pawin, U. Solanki, K. Y. Kwon, K. L. Wong, X. Lin, T. Jiao, and L. Bartels, “A Quantitative Approach to Hydrogen Bonding at a Metal Surface,” *JACS* **129**, 12056 (2007).
  14. G. Pawin, K. L. Wong, D. Kim, D. Sun, L. Bartels, S. Hong, T. S. Rahman, R. Carp, and M. Marsella, “A Surface Coordination Network Based on Substrate-Derived Metal Adatoms with Local Charge Excess,” *Angew. Chem. Int. Ed.* **47**, 8442 (2008).
  15. G. Pawin, K. L. Wong, K-Y. Kwon, R. J. Frisbee, T. S. Rahman, L. Bartels, “Surface Diffusive Motion in a Periodic and Asymmetric Potential,” *J. Amer. Chem. Soc.* **130**, 15244 (2008).
  16. M. Alcántara-Ortigoza, S. Stolbov, and T. S. Rahman, “Formation of Pt Islets on Facets of Ru Nanoparticles: First-Principles Study,” *Phys. Rev. B* **78**, 195417 (2008).
  17. K. F. Mak, M. Y. Sfeir, Y. Wu, C. H. Lui, J. Misewich, and T. F. Heinz, “Measurement of the Optical Conductivity of Graphene,” *Phys. Rev. Lett.* **101**, 196405 (2008).
  18. D. Song, F. Wang, G. Dukovic, M. Zheng, E. D. Semke, L. E. Brus, and T. F. Heinz, “Direct Measurement of the Lifetime of Optical Phonons in Single-Walled Carbon Nanotubes,” *Phys. Rev. Lett.* **100**, 225503 (2008).
  19. C. Lu, Z. Chen, and S. O’Brien, “Optimized Conditions for the Self-Organization of CdSe-Au and CdSe-CdSe Binary Nanoparticle Superlattices,” *Chem. Mater.* **20**, 3594 (2008).
  20. L. Liu, K. T. Rim, D. Eom, T. F. Heinz, and G. W. Flynn, “Direct Observation of Atomic Scale Graphitic Layer Growth,” *Nano Lett.* **8**, 1872 (2008).
  21. S. Ryu, M. Y. Han, J. Maultzsch, T. F. Heinz, P. Kim, M. L. Steigerwald, and L. E. Brus, “Reversible Basal Plane Hydrogenation of Graphene,” *Nano Lett.* **8**, 4597 (2008).
  22. Z. Chen, and S. O’Brien, “Structure Direction of II-VI Semiconductor Quantum Dot Binary Nanoparticle Superlattices by Tuning Radius Ratio, *ACS Nano* **2**, 1219 (2008).
  23. S. Berciaud, S. Ryu, L. E. Brus, and T. F. Heinz, “Probing the Intrinsic Properties of Exfoliated Graphene: Raman Spectroscopy of Free-Standing Monolayers,” *Nano Lett.* **9**, 346 (2009).
  24. M. Alcántara-Ortigoza, T. S. Rahman, R. Heid, and K. P. Bohnen, “Effect of c(2x2)-CO Overlayer on the Phonons of Cu(001): A First-Principles Study,” *Phys. Rev. B* **79**, 125432 (2009).
  25. S. Stolbov, M. Alcántara Ortigoza, T. S. Rahman, and R. Adzic, “High CO Tolerance of Pt /Ru Nanocatalyst: Insights from First Principles Calculations,” *J. Chem. Phys.* **130**, 124714 (2009).
  26. Ki-Y. Kwon, G. Pawin, K. Wong, E. Peters, D-H. Kim, S. Hong, T. S. Rahman, M. Marsella, and L. Bartels, “H-atom Position as Pattern-Determining Factor in Arenethiol Films,” *J. Amer. Chem. Soc.* (in press)
  27. D. T. Le, S. Stolbov, and T. S. Rahman, “Reactivity of the Cu<sub>2</sub>O(100) Surface: Insight from First Principles Calculations,” *Surface Sci.* (in press) (Special Issue for Nobel Laureate Ertl)
  28. D. Eom, D. Prezzi, K. T. Rim, H. Zhou, M. Lefenfeld, C. Nuckolls, M. S. Hybertsen, T. F. Heinz, and G. W. Flynn, “Structure and Electronic Properties of Epitaxial Graphene on Co(0001),” submitted to *Nano Lett.*
  29. S. Stolbov, M. Alcántara Ortigoza and T. S. Rahman, “Application of Density Functional Theory to the Fuel Cell Problem,” submitted to *J. Phys. Condens. Mat*

**Fundamental Studies of Heterogeneous Photocatalysis on Model TiO<sub>2</sub> Surfaces**

Additional PIs: Scott A. Chambers, Michel Dupuis, Igor Lyubinetsky  
Post-docs: N. Aaron Deskins, Robert T. Zehr, Dong J. Kim  
Graduate Students: none  
Undergrad Students: none  
Collaborators: D.A. Dixon (U. Alabama), H. Idriss (Auckland, NZ), M.A. Langell, (U. Nebr.), H. Onishi (Kobe, Jpn), K.M. Rosso (PNNL), J.M. White (U.Texas, Austin, deceased)  
Contact: M.A. Henderson, Pacific Northwest National Laboratory, PO Box 999, MS K8-80, Richland, WA 99352; phone: (509) 376-2192; Email: [ma.henderson@pnl.gov](mailto:ma.henderson@pnl.gov);

**Goal**

The goal of this project is to provide the field of heterogeneous photocatalysis with unique insights into the molecular-level properties of photocatalytic transformations through joint experimental and theoretical studies of organic photooxidation reactions on model TiO<sub>2</sub> materials. In this project, molecular-level expertise at PNNL in material synthesis, surface chemistry, theory, photodynamics and scanning probe microscopy will be used to study three areas of fundamental importance to heterogeneous photocatalysis on TiO<sub>2</sub>. These are: (1) detailed reaction mechanisms, (2) mechanisms of charge transfer, charge trapping and energy redistribution, and (3) surface structure and material dependences, each as they relate to organic photooxidation reactions. These issues will be explored using a variety of model TiO<sub>2</sub> systems including single crystal surfaces and epitaxially grown films of rutile and anatase, mixed phase films of the two, and surfaces prepared with controlled structural and electronic defects and varying degrees of porosity.

**DOE Interest**

Heterogeneous photocatalysis on TiO<sub>2</sub> has received considerable attention of late due to increased interest in using light to promote chemical transformations in remediation and energy technologies. Fundamental questions remain unaddressed, e.g., reaction and charge transfer mechanisms, specific surface reaction sites, selectivity, and interplay between thermal and non-thermal processes. The vast majority of research effort in the literature has been phenomenological, resulting in conflicting explanations for such crucial issues as the performance differences between the polymorphs of TiO<sub>2</sub> (rutile, anatase or mixtures thereof). Work in this project is of direct relevance to DOE's mission of increasing fundamental scientific understanding of heterogeneous catalysis and of light-to-chemical energy conversions.

**Recent Progress (FY06 to FY09)**

*Photodesorption of Organic Fragments* We have discovered that acetone photodecomposition on TiO<sub>2</sub>(110) occurs via a two-step process involving thermal conversion of acetone into a C<sub>3</sub> 'acetone diolate' followed by photodecomposition of this diolate to a C<sub>2</sub> acetate, with

concomitant ejection of a methyl radical from the surface. This combined thermal chemistry and photochemistry is not restricted to acetone, but is observed for a variety of other ketones and aldehydes on  $\text{TiO}_2(110)$ . For example, acetaldehyde and butanone both photodecompose through this two-step mechanism (generalized in Figure 1). The diolates photodecompose by ejection of an organic radical from the surface leaving behind a carboxylate species. In the acetaldehyde case, only methyl radical photodesorption was detected, with formate left on the surface.

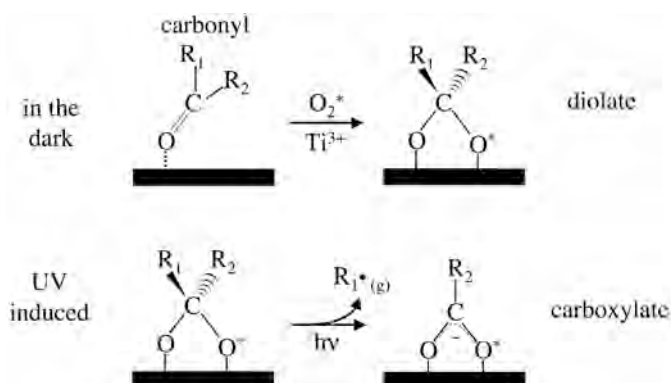


Figure 1: Two-step reaction scheme for photodecomposition of organic carbonyls on  $\text{TiO}_2$  surfaces.

In the butanone case there was a possibility of either methyl or ethyl radical ejection, with propionate or acetate left behind, respectively. However, only ethyl ejection was observed. The preference of which radical is ejected is based on the relative stabilities of the C-R bonds. We have explored a large list of ketones with varying  $\text{R}_1$  and  $\text{R}_2$  groups (e.g., benzophenone, chloroacetones and 3,3-dimethylbutanone) and find that the photochemistry observed for acetone, butanone and acetaldehyde represents a general mechanistic description for how C=O containing organics photodecompose on  $\text{TiO}_2(110)$ .

First Principles Modeling of  $e^-/h^+$  Polaron Transport in  $\text{TiO}_2$  We have examined the intrinsic  $e^-/h^+$  transport in stoichiometric  $\text{TiO}_2$  and the characterization of mixed phase interfaces using a combination of quantum mechanical (QM) and molecular dynamics (MD) theories, with QM-derived energetics for polarons being used to parameterize classical shell-model potentials for MD simulations. Electron hopping was described by a polaron model whereby a negative polaron is localized at a  $\text{Ti}^{3+}$  site and hops to an adjacent  $\text{Ti}^{4+}$  site. The theory is Marcus and/or Holstein formulated for polaronic systems in the solid state. Lattice distortions associated with both  $e^-$  and  $h^+$  polarons in rutile and anatase were calculated, as well as the transfer rates to adjacent sites along varied unique directions. For both types of polarons the Ti-O bonds around the polaron sites were found to be longer than Ti-O bonds in stoichiometric solids. Transport is more facile along directions that enable adiabatic thermal hopping. Activation barriers for  $e^-$  hopping were calculated to be  $\sim 0.07$  eV, in good accord with the experimental value of 0.09 eV, while activation energies for  $h^+$  transport were found to be  $\sim 0.16$  eV, slightly larger than for experimental observation.

Structure of Rutile/Anatase  $\text{TiO}_2$  Interfaces and  $e^-/h^+$  transport Little detailed characterization of interfaces between rutile and anatase forms of  $\text{TiO}_2$  is available. These interfaces are important for understanding mixed-phase catalysts, such as the Degussa P25 catalyst. Experimentally, we have explored the systematics of  $\text{TiO}_2$  polymorph nucleation during film growth by MBE on perovskite substrates. The lattice match between anatase (001) and  $\text{LaAlO}_3(001)$  or  $\text{SrTiO}_3(001)$  typically results in anatase nucleation at the interface, but varying growth conditions can promote rutile nucleation within the resulting anatase film. Candidate anatase-rutile interface have been identified from these films using HRTEM. Computational models of these candidate interfaces were constructed using MD with the shell-model potentials. Construction of these interfaces was

based on the near-coincidence-site lattice (NCSL) theory. The results showed adhesion energies for the most stable interfaces typically near  $-2 \text{ J/m}^2$ . The interfaces were characterized as disordered, with the disorder limited to very thin interfaces, in agreement with our HRTEM data. Formation of rutile octahedral structures occurred at the anatase side of the interface that appeared to be the beginning of an anatase-to-rutile phase transition. For one such interface, we calculated the energy associated with an  $e^-$  polaron assigned to every Ti site in the model system (see Figure 2). Away from the interface all the  $e^-$  binding energies are essentially constant. Near the interface some Ti sites show strong binding energies on the anatase side of the interface with non-favorable binding energies on the rutile side. The calculations indicated a large ( $\sim 1 \text{ eV}$ ) potential step across the interface, the magnitude of which being at odds with electrostatic potentials calculated with DFT. The discrepancy was traced to the classical shell-model not describing well the dielectric constant of rutile or anatase. This finding points to the need for increased accuracy of the shell-model potential when describing the bulk dielectric constants of the phases.

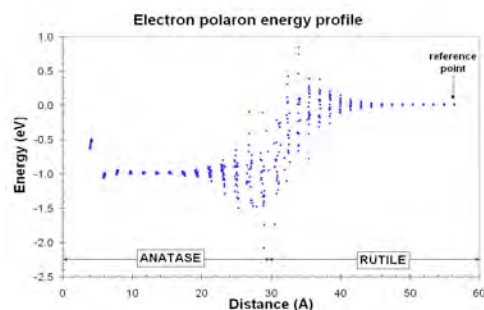


Figure 2: Simulation of electron trapping across a candidate anatase-rutile interface.

Surface Photochemistry on Anatase  $\text{TiO}_2$  Surfaces of  $\text{TiO}_2$  in both rutile and anatase polymorphs have attracted significant attention in catalysis and photochemistry. The (110) orientation of rutile, and to a lesser extent other rutile orientations, have been studied on an atomic scale, yielding information on surface structure and chemical reactivity. In contrast, the thermal and photochemistry of well-defined, single-crystal anatase surfaces has not received near the intensity of investigation, largely because of the metastable nature of anatase and unavailability of high-quality surfaces. We have extended our studies of trimethyl acetate (TMA) photoreactivity on rutile (110) to the (001) surface of anatase  $\text{TiO}_2$ . Structurally excellent anatase (001) epitaxial thin films were grown by molecular beam epitaxy on lattice-matched  $\text{SrTiO}_3(001)$ . An STM image of TMA adsorbed on the  $(4 \times 1)/(1 \times 4)$  reconstructed surface of anatase (001) is presented in Figure 3. The large bright spots are individual TMA groups. Only TMA groups residing on the ridges of this reconstructed surface are observable by STM even though XPS analysis (through comparison with TMA on rutile (110)) indicates TMA groups must also reside in the troughs. UV photodecomposition of TMA on anatase (001) in UHV is clearly seen in the image by the disappearance of TMA groups. These data and those from photodesorption studies indicate that UV light promotes hole-mediated photodecomposition of TMA on this anatase surface in a similar manner seen on rutile (110), resulting in decarboxylation to yield a *t*-butyl radical (which subsequently decomposes and desorbs as isobutane and/or isobutene) and  $\text{CO}_2$ . The photochemical rate constant for TMA photodecomposition on anatase (001) was obtained using photodesorption and compared to that for TMA from a rutile (110) surface under identical conditions. The rate of

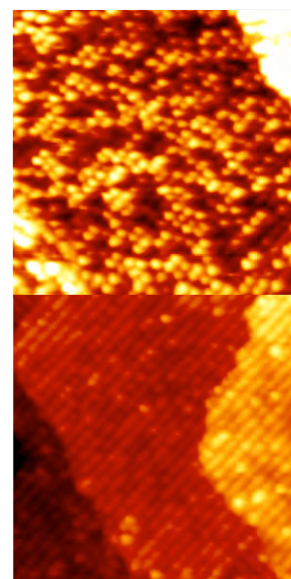


Figure 3: STM of  $\sim 0.3$  ML TMA on anatase (001) (top) and after 5 min. of UV exposure (bottom).

TMA photodecomposition in UHV on rutile (110) was similar to, if not slightly greater than, that on anatase (001). This result provides one setting (hole-mediated organic photodecomposition) that dispels the prevailing presumption in the literature that the anatase form is necessarily the most active polymorph of TiO<sub>2</sub>.

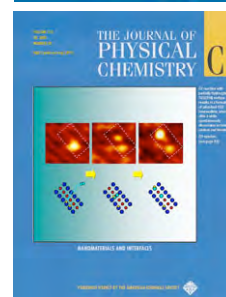
### Future Plans

- Studies of site specificity, influence of co-adsorbates (e.g., water/OH, oxygen, alkali and simple organics), and material/structural sensitivities in the photodecomposition of TMA on rutile (110), (100) and (111), and anatase (001) and (101) surface.
- Examinations of the photocatalytic properties of highly dispersed Ti<sup>4+</sup> centers in microporous structures (e.g., mesoporous silica or zeolites) with development of similar model photocatalysts supported on photocatalytically inert single crystal oxide surfaces (e.g.,  $\alpha$ -Al<sub>2</sub>O<sub>3</sub>(0001)).
- Exploration of the nucleation, growth and photoactivity of epitaxial TiO<sub>2</sub> anatase nanostructures on lattice-matched and mis-matched oxide surfaces.
- Modeling of charge trapping in the bulk and surfaces of anatase and rutile TiO<sub>2</sub> surfaces including the influence of adsorbates on surface trapping.
- Simulating dissociative hole attachment to adsorbed carboxylates on TiO<sub>2</sub>(110) with emphasis on exploring the relationship between the thermodynamic stabilities of the starting carboxylate, the resulting photodecomposition products, and the charge transfer mechanism and rate for hole attachment.
- Modeling charge transport across and trapping at the interfaces of mixed phase TiO<sub>2</sub> materials.

### Publications (FY06-FY09)

- O. Bondarchuk and I. Lyubinetsky, "Preparation of TiO<sub>2</sub>(110)-(1x1) surface via UHV cleavage: An scanning tunneling microscopy study," *Review of Scientific Instruments* 78 (2007) 113907.
- M.D. Cai, S.C. Langford, M.J. Wu, W.M. Huang, G. Xiong, T.C. Droubay, A.G. Joly, K.M. Beck, W.P. Hess and J.T. Dickinson, "Study of martensitic phase transformation in a NiTiCu thin-film shape-memory alloy using photoelectron emission microscopy," *Advanced Functional Materials* 17 (2007) 161.
- S.A. Chambers, T. Ohsawa, C.M. Wang, I. Lyubinetsky and J. Jaffe, "Band Offsets at the Epitaxial Anatase TiO<sub>2</sub>/n-SrTiO<sub>3</sub>(001) Interface," *Surface Science* 603 (2009) 771.
- N.A. Deskins and M. Dupuis, "Electron transport via polaron hopping in bulk TiO<sub>2</sub>: A density functional theory characterization," *Physical Review B* 75 (2007) 195212.
- N.A. Deskins and M. Dupuis, "Intrinsic Hole Migration Rates in TiO<sub>2</sub> from Density Functional Theory," *Journal of Physical Chemistry A* 113 (2009) 346.

- N.A. Deskins, S. Kerisit, K.M. Rosso and M. Dupuis, "Molecular dynamics characterization of rutile-anatase interfaces," *Journal of Physical Chemistry C* 111 (2007) 9290. (Featured on the Journal cover.)
- Y. Du, N.A. Deskins, Z. Zhang, Z. Dohnálek, M. Dupuis and I. Lyubinetsky, "Imaging Consecutive Steps of O<sub>2</sub> Reaction with Hydroxylated TiO<sub>2</sub>(110): Identification of HO<sub>2</sub> and Terminal OH Intermediates," *Journal of Physical Chemistry C* 113 (2009) 666. (Featured on the Journal cover.)
- Y. Du, N.A. Deskins, Z. Zhang, Z. Dohnálek, M. Dupuis and I. Lyubinetsky, "Two Pathways for Water Interaction with Oxygen Adatoms on TiO<sub>2</sub>(110)," *Physical Review Letters* 102 (09) 096102.
- Y. Du, J.F. Groves, I. Lyubinetsky and D.R. Baer, "Formation of Cu<sub>2</sub>O quantum dots on SrTiO<sub>3</sub>(100): Self-assembly and directed self-assembly," *Journal of Applied Physics* 100 (2006) 094315.
- J.F. Groves, Y. Du, I. Lyubinetsky and D.R. Baer, "Focused Ion Beam Directed Self-Assembly (Cu<sub>2</sub>O on SrTiO<sub>3</sub>): FIB Pit and Cu<sub>2</sub>O Quantum Dot Evolution," *Superlattices and Microstructures* 44 (2008) 677.
- M.A. Henderson, "Relationship of O<sub>2</sub> photodesorption in photooxidation of acetone on TiO<sub>2</sub>," *Journal of Physical Chemistry C* 112 (2008) 11433.
- M.A. Henderson, "Effect of coadsorbed water on the photodecomposition of acetone on TiO<sub>2</sub>(110)," *Journal of Catalysis* 256 (2008) 287.
- M.A. Henderson, "Ethyl radical ejection during photodecomposition of butanone on TiO<sub>2</sub>(110)," *Surface Science* 602 (2008) 3188.
- M.A. Henderson, J.M. White, H. Uetsuka and H. Onishi, "Selectivity changes during organic photooxidation on TiO<sub>2</sub>: Role of O<sub>2</sub> pressure and organic coverage," *Journal of Catalysis* 238 (2006) 153.
- J.E. Jaffe, R.A. Bachorz and M. Gutowski, "Band offset and magnetic property engineering for epitaxial interfaces: A monolayer of M<sub>2</sub>O<sub>3</sub> (M=Al,Ga,Sc,Ti,Ni) at the α-Fe<sub>2</sub>O<sub>3</sub>/α-Cr<sub>2</sub>O<sub>3</sub>(0001) interface," *Physical Review B* 75 (2007) 205323.
- S. Kerisit, N.A. Deskins, K.M. Rosso and M. Dupuis, "A shell model for atomistic simulation of charge transfer in titania," *Journal of Physical Chemistry C* 112 (2008) 7678.
- I. Lyubinetsky, Z.Q. Yu and M.A. Henderson, "Direct observation of adsorption evolution and bonding configuration of TMAA on TiO<sub>2</sub>(110)," *Journal of Physical Chemistry C* 111 (2007) 4342.
- T. Ohsawa, I. Lyubinetsky, Y. Du, M.A. Henderson, V. Shutthanandan and S.A. Chambers, "Crystallographic Dependence of Visible-Light Photoactivity in Epitaxial TiO<sub>2-x</sub>N<sub>x</sub> Anatase and Rutile," *Physical Review B* 79 (2009) 085401.
- R. Shao, C.M. Wang, D.E. McCready, T.C. Droubay and S.A. Chambers, "Growth and structure of MBE grown TiO<sub>2</sub> anatase films with rutile nano-crystallites," *Surface Science* 601 (2007) 1582.
- W. Wei, S.L. Parker, Y.M. Sun, J.M. White, G. Xiong, A.G. Joly, K.M. Beck and W.P. Hess, "Study of copper diffusion through a ruthenium thin film by photoemission electron microscopy," *Applied Physics Letters* 90 (2007) 111906.
- G. Xiong, A.G. Joly, K.M. Beck, W.P. Hess, M.D. Cai, S.C. Langford and J.T. Dickinson, "In situ photoelectron emission microscopy of a thermally induced martensitic transformation in a CuZnAl shape memory alloy," *Applied Physics Letters* 88 (2006) 091910.



- G. Xiong, A.G. Joly, G.P. Holtom, C.M. Wang, D.E. McCready, K.M. Beck and W.P. Hess, "Excited carrier dynamics of  $\alpha$ -Cr<sub>2</sub>O<sub>3</sub>/ $\alpha$ -Fe<sub>2</sub>O<sub>3</sub> core-shell nanostructures," *Journal of Physical Chemistry B* 110 (2006) 16937.
- G. Xiong, R. Shao, T.C. Droubay, A.G. Joly, K.M. Beck, S.A. Chambers and W.P. Hess, "Photoemission electron microscopy of TiO<sub>2</sub> anatase films embedded with rutile nanocrystals," *Advanced Functional Materials* 17 (2007) 2133.
- Z.Q. Yu, C.M. Wang, Y. Du, S. Thevuthasan and I. Lyubinetsky, "Reproducible Tip Fabrication and Cleaning for UHV STM," *Ultramicroscopy* 108 (2008) 873.
- Z.Q. Yu, C.M. Wang, M.H. Engelhard, P. Nachimuthu, D.E. McCready, I.V. Lyubinetsky and S. Thevuthasan, "Epitaxial growth and microstructure of Cu<sub>2</sub>O nanoparticle/thin films on SrTiO<sub>3</sub>(100)," *Nanotechnology* 18 (2007) 115601.
- R.T. Zehr and M.A. Henderson, "Acetaldehyde photochemistry on TiO<sub>2</sub>(110)," *Surface Science* 602 (2008) 2238.
- R.T. Zehr and M.A. Henderson, "Influence of O<sub>2</sub>-induced surface roughening on the chemistry of water on TiO<sub>2</sub>(110)," *Surface Science* 602 (2008) 1507.



KC0302010

J. Hrbek hrbek@bnl.gov

**Catalysis: Reactivity and Structure (FWP CO-009)**

Co-PIs: J.A. Rodriguez rodriguez@bnl.gov; J.C. Hanson hanson1@bnl.gov; P. Liu pingliu3@bnl.gov

Research associates: W. Wen; A. Nambu; D. Stacchiola

Brookhaven National Laboratory, Chemistry Department 555, Upton, NY 11973

**Goals**

The goal of this program is to provide an improved understanding of chemical catalysis by elucidating details of the fundamental properties of molecules, surfaces, and their reactions that are critical to catalysis and energy conversion. Reactivity-structure correlations explored and unraveled by utilization of synchrotron radiation are a key aspect of these studies. Complexities stemming from the inherent multi-component aspects of heterogeneous catalysis are explored using both ultra-high-vacuum Surf. Sci. investigations of well-defined model systems, and powder diffraction and x-ray absorption studies of "real-world" systems. In the former, emphasis is placed on understanding of basic principles of surface reactivity and its control by surface modification, on identification of active sites and full characterization of their electronic and structural properties. X-ray photoemission and absorption spectroscopies at the U7A beamline at the National Synchrotron Light Source (NSLS) are essential to this work. In the latter systems, in-situ time-resolved studies of the formation and transformations of supported metal clusters and metal oxides and carbides under catalytic reaction conditions are carried out using our X-ray diffraction facility at beamline X7B. Quantum-chemical calculations based on density-functional theory are performed to help in interpretation of experimental results and to study basic aspects of catalytic reactions.

**DOE Interest**

The objective of this program is to provide new insights into the nature of matter and energy and (i) to provide improved understanding of catalysis for energy conversion and (ii) to increase fundamental understanding of surface chemical reactivity and its modification and (iii) to operate NSLS beam lines U7A and X7B as a state-of-the-art resources in support of the "Fuel of the Future", "Protect our Living Planet" and "Provide Extraordinary Tools for Extraordinary Science" themes of the OS as outlined in the Science and Technology Statement of the DOE Strategic Planning document.

**Recent Progress**

During this time period, the Catalysis Group has been examining the links between surface modification and reactivity in several important areas of catalysis: production of hydrogen through water-gas shift reaction and photocatalysis of water, desulfurization reactions on metal compounds, and synthesis/reforming of alcohols as novel fuels. In addition, surface science experiments were carried out on gold, ruthenium and ruthenium oxide single crystals, and on pure or oxidized metal carbide substrates. The group remains very active in the development of in situ techniques for the characterization of catalysts at NSLS I and NSLS II. The following paragraphs summarize the major results and research activities.

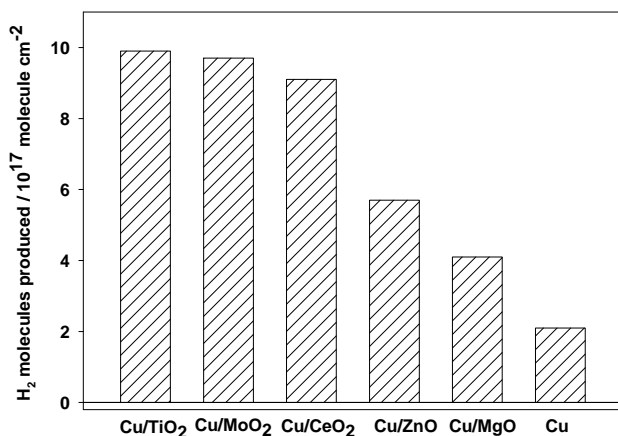
*Dissociation of thiophene on Au/TiC(001): Effects of Au-C interactions and charge polarization.* High resolution photoemission and DFT calculations were used to study the interaction of thiophene with Au/TiC(001) surfaces. Thiophene is adsorbed weakly on TiC(001), desorbing at temperatures below 180 K. However, the special electronic properties that Au nanoparticles have on a metal carbide substrate give Au/TiC(001) an extremely high desulfurization activity. In our DFT calculations spontaneous dissociation was observed when thiophene was set in the interface of carbide and very small Au nanoparticles. Au and C sites work in a cooperative way during the cleavage of the S-C bonds, where Au grabs the dissociated S and the hydrocarbon fragment sits at the carbide

site. The polarization of charge induced by the Au-C interactions maximizes the flow of electrons from Au into the LUMO of the thiophene molecule, which helps the S-C bond breaking. With the increasing of coverage, Au wets the TiC(001) surface in one-layer, and the charge polarization due to the Au-C interactions still exist; however, the polarization is not strong enough to dissociate thiophene, but strongly chemisorbing. When 3D Au particles are formed, the polarization decreases significantly and only physisorbed thiophene is observed. Experimental tests showed that a TiC(001) surface with 0.2 ML of Au was more active for the hydrodesulfurization of thiophene than conventional Ni/MoS<sub>x</sub> catalysts. The Au clusters increase the hydrodesulfurization activity of TiC(001) by enhancing the bonding energy of thiophene and by helping in the dissociation of H<sub>2</sub> to produce the hydrogen necessary for the hydrogenolysis of C-S bonds and the removal of S.

XRD and XAFS Studies of the Water-Gas Shift Reaction on CuFe<sub>2</sub>O<sub>4</sub>. Cu-Fe oxides are used as WGS catalysts in some industrial processes. The structure of CuFe<sub>2</sub>O<sub>4</sub>, known as an “inverse spinel”, contains both octahedral and tetrahedral cation sites. Copper ions sit predominantly on octahedral sites and iron atoms split between the two. CuFe<sub>2</sub>O<sub>4</sub> is cubic at elevated temperatures (> 400 °C) and tetragonal with the axial ratio  $c/a > 1$  at room temperature. XRD data collected while performing the WGS on CuFe<sub>2</sub>O<sub>4</sub> showed that up to ~ 200 °C, there were no changes in the tetragonal structure of CuFe<sub>2</sub>O<sub>4</sub> and no WGS activity was detected. From 200 to 300 °C, the CO attacks the oxide and partial reduction leads to the segregation of metallic Cu with the onset of WGS activity. At 350 °C, one has an active WGS catalyst which contains a mixture of Cu, CuFe<sub>5</sub>O<sub>8</sub> and/or Fe<sub>3</sub>O<sub>4</sub>. The intensity of the Cu(200) diffraction line becomes constant and a Scherrer’s analysis of its width gave a Cu particle size of ~ 23 nm. A Rietveld refinement gave a mole ratio of ~ 1 for the diffraction lines of Cu and the CuFe<sub>5</sub>O<sub>8</sub>/Fe<sub>3</sub>O<sub>4</sub> spinel. In situ experiments of x-ray absorption spectroscopy at the Cu K-edge indicated that essentially all the Cu<sup>2+</sup> initially present in CuFe<sub>2</sub>O<sub>4</sub> was reduced to metallic Cu<sup>0</sup>. Our XRD and XAFS results point to metallic copper as an active species for the WGS.

Water-Gas Shift Activity of Au and Cu Nanoparticles supported on Metal Oxides.

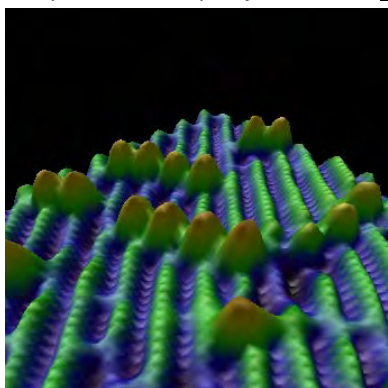
Catalytic tests performed over CuFe<sub>2</sub>O<sub>4</sub>, Ce<sub>1-x</sub>Cu<sub>x</sub>O<sub>2</sub> or CuMoO<sub>4</sub> show significant water-gas shift activity only when the Cu cations in the mixed-metal oxide are reduced to metallic copper. Thus, Cu nanoparticles were deposited on different oxide surfaces and their WGS activity was measured in a batch reactor. The WGS activity of the Cu nanoparticles supported on MgO(100) was 2-3 times larger than that of Cu(100). Even better WGS catalysts were obtained when Cu was deposited on CeO<sub>2</sub>(111) or TiO<sub>2</sub>(110). An apparent activation energy of 13.8 kcal/mol was found for the WGS on Cu/MgO(100). This is smaller than the value of 15.2



kcal/mol observed on Cu(100), and substantially larger than the values of 7-9 kcal/mol seen for the apparent activation energies of the Cu/CeO<sub>2</sub>(111) and Cu/TiO<sub>2</sub>(110) catalysts. Post-reaction surface characterization pointed to the lack of O vacancies in the Cu/MgO(100) catalysts. This is in contrast to results found for Cu/CeO<sub>2</sub>(111) and Cu/TiO<sub>2</sub>(110), where the oxide support exhibits a significant concentration of O vacancies as a consequence of the WGS reaction. The oxygen vacancies present in Cu/CeO<sub>2</sub>(111) and Cu/TiO<sub>2</sub>(110) help in the dissociation of the water molecule and reduce the apparent activation energy for the WGS process. Such a phenomenon cannot

occur on the Cu/MgO(001) catalysts, and the main steps of the WGS probably take place on the Cu nanoparticles.

Controlling the Nature of Mixed-Metal Oxide Catalysts at the Nanometer Level: High Catalytic Activity of Au/CeO<sub>x</sub>/TiO<sub>2</sub>(110) Surfaces.

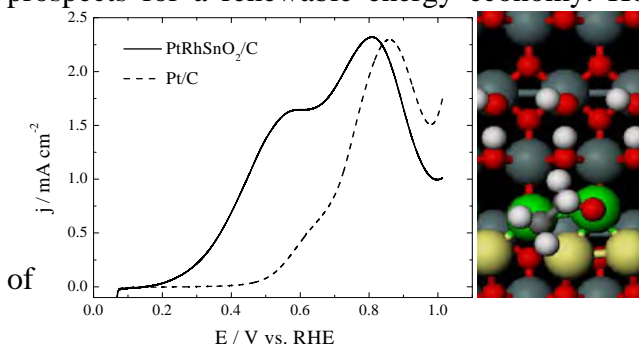


Mixed-metal oxides play a very important role in many areas of chemistry, physics, materials science and geochemistry. Recently, there has been a strong interest in understanding phenomena associated with the deposition of oxide nanoparticles on the surface of a second (host) oxide. At BNL, scanning tunneling microscopy, photoemission, and density-functional calculations were used to study the behavior of ceria nanoparticles deposited on a TiO<sub>2</sub>(110) surface. The titania substrate imposed non-typical coordination modes on the ceria nanoparticles. In the CeO<sub>x</sub>/TiO<sub>2</sub>(110) system, the Ce cations adopt an structural geometry and an oxidation state (+3) which are quite different from those seen in bulk ceria or for

ceria nanoparticles deposited on metal substrates. The results of scanning tunneling microscopy show the formation of Ce<sub>2</sub>O<sub>3</sub> dimers which form small linear arrays on top of the TiO<sub>2</sub>(110) substrate. An increase in the stability of the Ce<sup>3+</sup> oxidation state leads to an enhancement in the chemical and catalytic activity of the ceria nanoparticles. The co-deposition of ceria and gold nanoparticles on a TiO<sub>2</sub>(110) substrate generates catalysts with an extremely high activity for the production of hydrogen through the water-gas shift reaction for the oxidation of carbon monoxide. The enhanced stability of the Ce<sup>3+</sup> state is an example of structural promotion in catalysis found here for the first time on the atomic level. Thus, the exploration of mixed-metal oxides at the nanometer level may open new avenues for optimizing catalysts through stabilization of unconventional surface structures with special chemical activity.

Theoretical and experimental study of Ternary Pt/Rh/SnO<sub>2</sub> Electrocatalysts for Oxidizing Ethanol to CO<sub>2</sub>.

The direct ethanol-oxidation fuel cell (DEFC) could afford an excellent alternative solution to energy-generation problems, and entail major improvements in the prospects for a renewable energy economy. However, the development of DEFC has



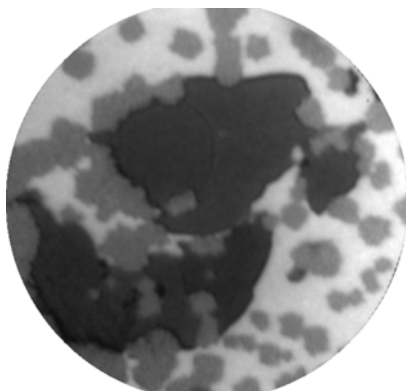
Left panel: polarization curves for the oxidation of ethanol on PtRhSnO<sub>2</sub>/C- and Pt/C- (20% Pt on C E-TEK Co. Right panel: optimized geometry of CH<sub>2</sub>CH<sub>2</sub>O adsorption on a Rh,Pt/SnO<sub>2</sub>(110) surface using DFT. (Sn: large grey; Pt: large yellow; Rh: large green; C: small grey; O: small red; H: small white)

been impeded by its slow and incomplete oxidation kinetics even on the best electrocatalysts. Thus far, the best binary catalysts for ethanol oxidation in acid environments are Pt–Sn alloys. In situ spectroscopic studies have shown that acetaldehyde and acetic acid are the main products the oxidation of ethanol in acid solution, with carbon dioxide appearing at very high positive potentials. Although it is inconsequential for DEFC, adding Sn to Pt inhibits the splitting of C–C bonds. Indications are that adding Rh to Pt may aid this reaction above 0.6 V, but the overall activity of these

electrocatalysts is lower than that of Pt–Sn. We synthesized the ternary PtRhSnO<sub>2</sub>/C electrocatalyst, effective in splitting the C–C bond of ethanol at room temperature, whose predominant oxidation pathway leads to carbon dioxide at low potentials. The generation of carbon dioxide was verified using in situ infrared spectroscopy. Our analysis using both experimental and theoretical techniques reveal that its catalytic activity rests on the

synergy between the three constituents of the electrocatalyst. Thus, SnO<sub>2</sub> provides a strong interaction to the Pt and Rh deposited on its surface and, by strongly adsorbing water at the interface, precludes the Rh and Pt sites from reacting with H<sub>2</sub>O to form M-OH, so making them available for ethanol oxidation. The high activity of SnO<sub>2</sub> with H<sub>2</sub>O provides OH species to oxidize the dissociated CO at Rh sites, while Pt contributes to ethanol dehydrogenation. It also modifies the electronic structure of Rh to afford moderate bondings to ethanol, intermediates, and products, which facilitates C-C bond breaking and, therefore, ethanol oxidation. Our PtRhSnO<sub>2</sub> electrocatalyst effectively splits the C-C bond in ethanol at room temperature in acid solutions. These findings open new possibilities for studies of C-C bond splitting in variety of important reactions, while this electrocatalyst holds great promise for resolving the major impediment to developing direct ethanol fuel cells.

Structural Imaging of surface oxidation and oxidation catalysis on Ru(0001). Using simultaneous LEEM imaging and structural fingerprinting under reaction conditions, we



probed the initial oxidation pathway and CO oxidation catalysis on Ru(0001). Oxidation beyond an initial (1x1)-O adlayer phase produces a heterogeneous surface, comprising a disordered trilayer-like surface oxide and an ordered RuO<sub>2</sub>(110) thin-film oxide, which form independently and exhibit similar stability. The surface oxide and RuO<sub>2</sub> phases both show high intrinsic catalytic activity. The oxygen adlayer is inactive in isolation but becomes active due to cooperative effects in close proximity to the surface oxide. (LEEM image diameter 10 μm; three visible phases: chemisorbed oxygen (white), surface tri-layer oxide (grey) and RuO<sub>2</sub>(110) surface(black))

NLS Beam Lines X7B and U7A – 26 papers. Our group operates, maintains and upgrades two endstations at the NLS beam lines: X7B and U7A. In addition to our own basic science program (projects 1 - 3 below) conducted at NLS beam lines, we also provide support to many outside users (projects 4 - 7 below). Examples of projects studied at X7B in the last period with in situ time-resolved XRD include: (1) activation of metal/oxide catalysts (Cu-CeO<sub>2</sub>, Pd-CeO<sub>2</sub>, Pt-CeO<sub>2</sub>, Pt-TiO<sub>2</sub>, Cu-Fe<sub>2</sub>O<sub>3</sub>, Cu/Cr<sub>2</sub>O<sub>3</sub>-Fe<sub>2</sub>O<sub>3</sub>, Ni-MoO<sub>2</sub>) during the water-gas shift reaction; (2) behavior of metal/oxide catalysts (Pd-CeO<sub>2</sub>, Rh-CeO<sub>2</sub>, Pd-Rh-CeO<sub>2</sub>) during the reforming of ethanol, (3) synthesis of nanosized molybdenum carbide, titanium oxide and titanium nitride (4) substrate binding in zeolites and other framework compounds; (5) reduction /oxidation of oxide catalysts;; (6) operando studies of NO<sub>x</sub> removal on supported BaO; and (7) operando studies of desulfurization of Pt-BaO/Al<sub>2</sub>O<sub>3</sub> catalysts.

### **Future Plans**

Manipulating the Active Site in Catalytic Reactions for the Efficient Use of Energy.

Despite considerable scientific effort over many years, our knowledge of what exactly the active sites are and how they really work is in most cases very primitive. The complexity of catalytic processes is the main impediment to their thorough understanding. Foremost, it is necessary to identify the active site and fully characterize its electronic and structural properties. Subsequently, one must understand how these properties affect the different steps of a catalytic reaction and how an active site interacts within a given chemical environment. In the scientific design of catalysts, a key issue is how the behavior of an active site changes when modifying the size of the system (molecular to nano to bulk), the media (homogeneous to heterogeneous) or the type of chemical reaction (oxidation vs. reduction chemistry). What we propose here is a unique effort that closely couples sophisticated experimental techniques and state-of-the-art theory to investigate the behavior of active sites in several important catalytic systems.

Ethanol as a fuel: partial oxidation and steam reforming. Partial oxidation and steam reforming of ethanol can yield the molecular hydrogen necessary for operating conventional fuel cells or other industrial applications. This is an exothermic process, but the catalyst must not transform the hydrogen into water. This problem does not exist in the steam reforming process, however, one must supply energy to the system. For either of these two processes, a good catalyst must be efficient at C-C bond dissociation, CO oxidation and H-H association. Thus, catalysts that are good for the water-gas shift reaction and are able to induce C-C bond cleavage should also be good catalysts for the partial oxidation or steam reforming of ethanol. Alloys of Pd-Rh and Pt-Rh supported on ceria satisfy this requirement and are able to catalyze the partial oxidation or reforming of ethanol through gas/solid interactions. Rh/CeO<sub>2</sub> is an excellent catalyst for C-C bond breaking, but the supported Rh has a limited ability to hydrogenate CH<sub>x</sub> fragments and with time is deactivated by a carbonaceous layer. In contrast Pd/CeO<sub>2</sub> and Pt/CeO<sub>2</sub> are very good hydrogenation catalysts, however, they are not very good at cleaving C-C bonds. At an atomic or fundamental level, it is not known how exactly the catalysts for the processing of ethanol work. We have started a research program aimed at understanding the active sites and mechanisms for the partial oxidation and steam reforming of ethanol.

Fundamental studies of the reaction mechanism of alcohol synthesis from CO, CO<sub>2</sub> and H<sub>2</sub> on metal, alloy and metal/oxide catalysts. Our research aims to understand and develop efficient catalytic processes for the synthesis of C1-C4 alcohols through the hydrogenation of CO<sub>2</sub> or CO. The main limitation in the industrial synthesis of higher alcohols from CO<sub>2</sub> or CO has been the lack of a selective and durable catalyst that leads to the efficient production of the alcohols. The optimization of these catalytic systems is hindered by controversy about basic questions regarding the nature of their active sites and the reaction mechanism for the synthesis of alcohols. Currently, supported Rh catalysts are the most selective for ethanol synthesis from syngas, but even Rh produces primarily methane without promoters, which are typically alkali or transition metal cations. A major challenge is the evaluation of new catalytic materials. Theoretical and experimental studies will be carried out to understand the key issues involved in the synthesis of alcohols from CO or CO<sub>2</sub>.

Catalysis at NSLS Beam Lines. We will continue the in situ XRD characterization of catalyst under process conditions to obtain a better understanding of the relationship between structure and function of metal oxides, carbide, nitrides and sulfides. New X7B beamline capabilities will allow for identification of structural features from amorphous catalyst. We will also use EXAFS techniques and combined EXAFS and XRD as members of the SCC. We will continue to develop the improved in situ measurement capability and rapid data acquisition techniques which will be transferred to beam lines at NSLS II.

### **Publications (2009-2007) – 25 papers**

J.I. Flege, J. Hrbek, P. Sutter, Structural Imaging of surface oxidation and oxidation catalysis on Ru(0001), Phys. Rev. B 78, 165407 (2008).

Graciani, J.; Fdez. Sanz, J.; Asaki, T.; Nakamura, K.; Rodriguez, J., Interaction of Oxygen with TiN(001): N↔O Exchange and Oxidation Process, J. Chem. Phys., 126, 244713(2007).

J. Hrbek, F. M. Hoffmann, J. B. Park, P. Liu, D. Stacchiola, Y. Soo Hoo, S. Ma, A. Nambu, J.A. Rodriguez, and M. G. White, Adsorbate driven morphological changes of a gold surface at low temperatures, J. Am. Chem. Soc. 130, 17272-17273 (2008).

Hrbek, J.; Chang, Z.; Hoffmann, F. M., The Adsorption of 1,3-butadiene on Ag(111): A TPD/IRAS Study and Importance of Lateral Interactions. Surf. Sci., 601, 1409-1418 (2007).

A. Kowal, M. Li, M. Shao, K. Sasaki, M. B. Vukmirovic, J. Zhang, N. S. Marinkovic, P. Liu, A. Frenkel, and R. R. Adzic, "Ternary Pt/Rh/SnO<sub>2</sub> Electrocatalysts for Oxidizing Ethanol to CO<sub>2</sub>", Nature Mater, 2009 doi:10.1038/nmat2359

P. Liu, J.A. Rodriguez, Y. Takahashi, and K. Nakamura, Water-gas-shift reaction on a Ni<sub>2</sub>P(001) catalyst: Formation of oxy-phosphides and highly active reaction sites", J. Catal., 262, 294-303 (2009).

- Ma, S., Zhao, X., Rodriguez, J.A. and Hrbek, J., STM and XPS study of growth of Ce on Au(111). *J. Phys. Chem. C*, 111, 3685-3691 (2007).
- K. Manandhar, K.T. Park, S. Ma and J. Hrbek, Heteroepitaxial Thin Film of Iron Phthalocyanine on Ag(111), *Surf. Sci.* 603, 636-640 (2009).
- O. Ozturk, J.B. Park, T.J. Black, J.A. Rodriguez, J. Hrbek and D.A. Chen, Methanethiol Chemistry on TiO<sub>2</sub>-supported Ni Clusters”, *Surf. Sci.* 602, 3077-3088 (2008).
- J. B. Park, J. Graciani, J. Evans, D. Stacchiola, S. Ma, P. Liu, A. Nambu, J. Fernandez-Sanz, J. Hrbek and J. A. Rodriguez, High catalytic activity of Au/CeO<sub>x</sub>/TiO<sub>2</sub>(110) controlled by the nature of the mixed-metal oxide at the nanometer level, *PNAS* 2009 doi:10.1073/pnas.0812604106
- Parks, G. L., M. L. Pease, A. Burns, M. E. Bussell, X. Wang, J. Hanson and J. A. Rodriguez, Characterization, and hydrodesulfurization properties of catalysts derived from amorphous metal-boron materials. *J. Catal.*, 246, 277-292 (2007).
- J.A. Rodriguez, P. Liu, F. Viñes, F. Illas, Y. Takahashi, and K. Nakamura, Dissociation of SO<sub>2</sub> on Au/TiC(001): Effects of Au-C Interactions and Charge Polarization”, *Angew. Chem. Intl. Ed.* 47, 6685-6689 (2008).
- J.A. Rodriguez and P. Liu, Theoretical Studies in Heterogeneous Catalysis: Towards a Rational Design of Novel Catalysts for Hydrodesulfurization and Hydrogen Production”, in *New Developments in Quantum Chemistry*, Transworld Research Network (2008), invited book chapter.
- Rodriguez, J.A.; Ma, S.; Liu, P.; Hrbek, J.; Evans, J.; Perez, M., Water-Gas Shift Reaction on Inverse CeO<sub>x</sub>/Au(111) and TiO<sub>x</sub>/Au(111) Catalysts: Active Role of Oxide Nanoparticles, *Science*, 318, 1757-1760 (2007).
- Rodriguez J.A.; Liu P.; Hrbek J.; Evans, J.; Perez, M., Water gas shift reaction on Cu and Au nanoparticles supported on CeO<sub>2</sub>(111) and ZnO(0001): Intrinsic activity and importance of support interactions, *Angew. Chem. Intl. Ed.*, 46, 1329-1332 (2007).
- Szanyi, J.; Kwak, J.H.; Kim, D.H.; Wang, X.; Chimentao, R.; Hanson, J.; Epling, W.S.; Peden, C.H.F., Water-Induced Morphology Changes in BaO/ $\gamma$ -Al<sub>2</sub>O<sub>3</sub> NO<sub>x</sub> Storage Materials: an FTIR, TPD, and Time-Resolved Synchrotron XRD Study, *J. Phys. Chem. C*, 111, 4678-4687 (2007).
- Szanyi, J.; Kwak, J.H.; Kim, D.H.; Wang, X.; Hanson, J.; Chimentao, R.J.; Peden, C.H.F., Water-Induced Morphology Changes in BaO/ $\gamma$ -Al<sub>2</sub>O<sub>3</sub> NO<sub>x</sub> Storage Materials, *Chem. Comm.*, 9, 881-988 (2007).
- X. Teng, Q. Wang, P. Liu, W.-Q. Han, A. Frenkel, W. Wen, N. Marinkovic, J.C. Hanson and J.A. Rodriguez, Formation of Pd/Au Nanostructures from Pd Nanowires via Galvanic Replacement Reaction”, *J. Am. Chem. Soc.*, 130, 1093-1101 (2008).
- Ventrice, Jr., C.A.; Borst, D.R.; Geisler, H.; van Ek, J.; Losovj, Y.B.; Robbert, P.S.; Diebold, U.; Rodriguez, J.A.; Miao, G.X.; Gupta, A., Are the Surfaces of CrO<sub>2</sub> Metallic? *J. Phys. Cond. Matter*, 19, 315207 (2007).
- Vines, F.; Sousa, C.; Illas, F.; Liu, P.; Rodriguez, J. A., Density Functional Study of the Adsorption of Atomic Oxygen on the (001) Surface of Early Transition-Metal Carbides. *J. Phys. Chem. C*, 111, 1307 -1314 (2007).
- Vines, F.; Sousa, C.; Illas, F.; Liu, P.; Rodriguez, J.A., A Systematic Density Functional Study of Molecular Oxygen Adsorption and Dissociation on the (001) Surface of Group IV, V and VI Transition Metal Carbides, *J. Phys. Chem. C*, 111, 16982-16989 (2007).
- W. Wen, J.E. Calderon, J.L. Brito, N. Marinkovic, J.C. Hanson, and J.A. Rodriguez, “In situ Time-resolved Characterization of Ni-MoO<sub>2</sub> Catalysts for the Water-Gas Shift Reaction”, *J. Phys. Chem. C*, 112, 2121-2128 (2008).
- Wen, W., J. Liu, M. G. White, M. Marinkovic and J. A. Rodriguez, In situ Time-resolved Characterization of Novel Cu-MoO<sub>2</sub> Catalysts during the Water-Gas Shift Reaction. *Catal. Lett.*, 113, 1-6 (2007).
- Zhao, X.; Ma, S.; Hrbek, J.; Rodriguez, J.A., Reaction of Water with Ce-Au(111) and CeO<sub>x</sub>/Au(111) Surfaces: Photoemission and STM Studies, *Surf. Sci.*, 601, 2445-2452 (2007).
- Zhou, G., R. Gorte, and J. Hanson, A Thermodynamic Investigation of the Redox Properties of Ceria-Titania Mixed Oxides. *Appl. Catal. A.*, 335, 153-158 (2008).

## Designing new electrocatalysts: A case study of the hydrogen evolution reaction (HER)

Thomas F. Jaramillo

Dept. of Chemical Engineering, Stanford University  
Stanford, CA 94305 USA

Email: Jaramillo@stanford.edu

phone +1-650-498-6879, fax +1-650-723-9780, cheme.stanford.edu

Combining theory and experiment is a strong approach to designing and developing improved electrocatalytic materials [1,2]. The goal of this work is to gain insight into the hydrogen evolution reaction (HER) using theoretical methods, use that insight to predict new electrocatalytically active catalysts, and then use experimental methods to synthesize and characterize those specific surface structures. Our search strategy began with metal alloy surfaces, where computational screening on 736 different surfaces identified a Pt-Bi surface alloy to be more active than Pt [1]. Moving away from Pt-based systems, we examined different forms of molybdenum sulfide [2-5]. In order to identify relationships between structure and catalytic activity within MoS<sub>2</sub> nanoparticles, well-defined MoS<sub>2</sub> nanoparticles were synthesized in ultra-high vacuum (UHV), imaged by scanning tunnelling microscopy (STM), and transferred to an electrochemical cell where catalytic activity for the HER could be measured [3]. This approach has been extended to the investigation of other metal sulfide systems, including supported [Mo<sub>3</sub>S<sub>4</sub>]<sup>4+</sup> molecular complexes [4] and cobalt-promoted MoS<sub>2</sub> and WS<sub>2</sub> [5].

- [1] J. Greeley, T. F. Jaramillo, J. Bonde, I. Chorkendorff, and J. K. Nørskov, *Nature Mater.*, **11** (2006) 909.
- [2] B. Hinnemann, P.G. Moses, J. Bonde, K.P. Jørgensen, J.H. Nielsen, S. Horch, I. Chorkendorff, J.K. Nørskov, *J. Am. Chem. Soc.*, **127** (2005) 5308.
- [3] T.F. Jaramillo, K.P. Jørgensen, J. Bonde, J.H. Nielsen, S. Horch, I. Chorkendorff, *Science*, **317** (2007) 100.
- [4] T.F. Jaramillo, J. Bonde, J. Zhang, B.L. Ooi, K. Andersson, J. Ulstrup, I. Chorkendorff, *J. Phys. Chem. C* **112** (2008) 17492.
- [5] J. Bonde, P.G. Moses, T.F. Jaramillo, J.K. Nørskov, I. Chorkendorff, *Faraday Discussions*, **140** (2008) 219.

*“Developing the Science of Immobilized Molecular Catalysts”*

Co-PI's: Weck, M.; Davis, R.; Ludovice, P.; Sherrill, D.;

Postdocs: Zheng, X.; Madhavan N.; Norman, A.; Venkatasubbaiah, K.; Zhu, X.

Students: Sears, J.; Swann, A.; Jain, S.; Gill, C.; Goyal, P.; Pinon, V.; Shiels, R.; Takatani, T.;  
Richardson, J. Key, R.

**Goal**

Immobilized organometallic catalysts, in principle, can give high rates and selectivities like homogeneous catalysts with the ease of separation enjoyed by heterogeneous catalysts. However, the science of immobilized organometallics has not been developed because the field lies at the interface between the homogeneous and heterogeneous catalysis communities. Researchers at Georgia Tech, NYU and the University of Virginia are developing design principles for supported metallated salen catalysts that follow a monometallic (Ru- and Mn-Salen) or a bimetallic (Co- and Al-Salen) pathway. Using these model systems, the fundamental principles to be used to understand and design future classes of immobilized organometallic catalysts are being elucidated.

**DOE Interest**

The work performed in this program elucidates fundamental principles important in the design of immobilized catalysts. These catalysts have the potential of being very active and selective while being easy to separate for the reaction medium. All of these aspects provide a substantial energy advantage in chemical processing.

**Recent Progress (2007-present)**

A major focus of research the past two years centered on reactions that require the cooperative interaction of two metal centers in the transition state of the slow step in the reaction. We rationalized that an optimized support structure can significantly increase the activity of catalytic transformations that follow a bimetallic pathway by bringing the two catalytic moieties within close proximity of each other. Initially, we have focused our efforts on the Co(III)-Salen catalyzed hydrolytic kinetic resolution (HKR) of epoxides. The HKR reaction has been shown to follow a bimetallic mechanism as evident from a second-order dependency of activity upon the concentration of Co(III) sites. The first cobalt center is proposed to activate the hydroxide, which then performs a nucleophilic attack on the  $\alpha$  carbon of the epoxide coordinated to the second cobalt center. Hydrolysis of the intermediate species then purportedly regenerates the two active sites as the catalytic cycle repeats. Accordingly, activities of the original homogeneous Co(III)-Salen catalyst suffered, owing to unfavorable statistical interactions between the catalytic active sites in solution, resulting in very slow rates at low catalyst concentrations.

Based on our reports from 2006 describing a straight forward one-pot synthesis of unsymmetrically functionalized salen complexes, we synthesized a series of Co-Salen functionalized polymers and investigated the resulting supported catalysts in the HKR of terminal epoxides. The structural parameters that were varied and the resulting supported catalysts evaluated for the HKR were: (i) polymer backbone structure, (ii) salen-support linker structure, (iii) support solubility, and (iv) type of salen pairing (Figure 1).



In 2006, we reported the synthesis of poly(norbornene) and poly(styrene) supported C-Salen catalysts. We found a direct correlation between catalyst activity and polymer support flexibility. Therefore, we sought to support Co-Salen on an alternative, even more flexible backbone.

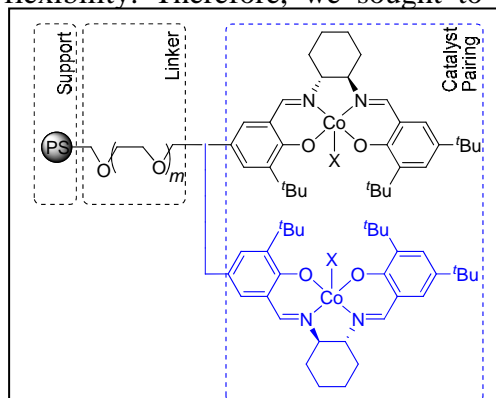


**Figure 1.** Structural components of supported M-Salen catalysts, including support type, linker structure, metal-ligand complex structure, and Salen pairing (one per side chain in black, multiple per side chain in blue). In this work, the metal-ligand complex is fixed as shown.

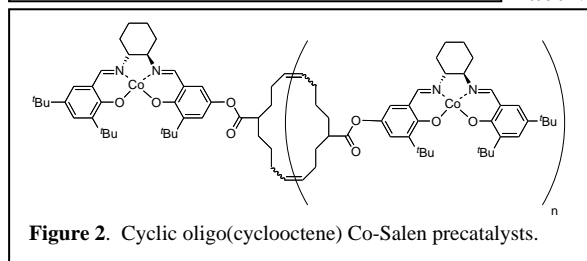


**Figure 2.** Cyclic oligo(cyclooctene) Co-Salen precatalysts.

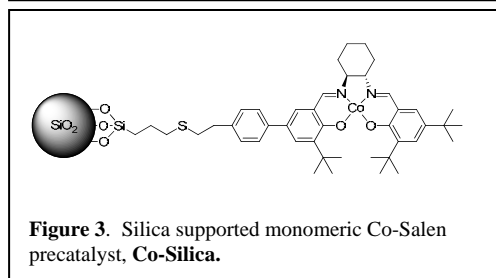


**Figure 3.** Silica supported monomeric Co-Salen precatalyst, Co-Silica.

We hypothesized that poly(cyclooctene)s derived from ROMP would provide a highly flexible catalyst support. Interestingly, the ruthenium-based olefin metathesis resulted in the formation of ring cycles rather than linear polymers (Figure 2). The oligo(cyclooctene)-supported Co-Salen complexes were examined for their catalytic efficiency in the HKR of terminal epoxides. For most epoxides, an exceptionally low catalyst loading of 0.01 mol% was employed. In all cases, enantiomeric excesses above 99% were observed within several hours and isolated yields of 43-48% were obtained (crude conversions measured by GC or HPLC were usually ~5% higher). At the same catalyst loading, the original unsupported Co-Salen catalyst showed effectively no catalytic activity, demonstrating the high activity the cyclic catalysts against a benchmark system.

Compared to the poly(styrene) system under identical conditions, our cyclic oligomeric system derived from cyclooctene metathesis is ~25x more active and equally selective.

Based on the cooperative mechanism of the HKR reaction, we hypothesized that the traditional way of supporting molecular

complexes on porous oxide supports would result in relatively inactive catalysts and perhaps catalysts that were completely inactive if complete site isolation were achieved. Mesoporous SBA-15 silica supported monomeric Co-Salen (Figure 3) proved to be active, but less active than the homogeneous catalyst at similar loadings. Given the low loading of cobalt on this catalyst (~0.35 mmol/g), one might assume that

cooperative interactions will be severely limited. This might be interpreted to be consistent with the presence of an alternative slower monomeric pathway in the HKR reaction.

One component that was hypothesized to affect activity and selectivity of supported Co-Salen catalysts was the salen-support linker structure. Using poly(styrene) as the support, we systematically varied the linker structure to probe its influence on the catalytic properties (Figure 4). We found that copolymer supports were slower than their homopolymeric analogs. Furthermore, the catalyst with the rigid phenylene linker was by far the slowest, followed by the catalyst with the shortest flexible linker. The catalysts with the longer, flexible poly(ethylene glycol) linkers were similarly active, although there appeared to be an optimum with the catalyst that contained 6 atoms in the linker. These data suggest that the linker structure affects the catalytic activity, although the cause of the changes needs to be further examined. The data also support the notion that linker flexibility is important.

We hypothesized that polymer-oxide hybrid catalysts would allow for easy catalyst recovery through the oxide-induced insolubility in liquid media, while the polymer chain would induce partial solubility, allowing for cooperative complex-complex interactions. We thus designed solid-supported polymer brush catalysts (Figure 5). The first generation catalyst used nonporous nanoparticulate silica as a support, off of which poly(styrene) chains containing salen units were grown. Use of atom-transfer radical polymerization (ATRP) allowed for surface initiation of the polymerization, and linear copolymers of salen-functionalized styryl monomers and styrene were prepared. Building on the work described above using soluble, purely polymeric styrene systems, we chose the rigid phenylene linker and a flexible, PEG-based linker for use in the silica-supported polymer brush catalysts. The most active catalyst was based on the flexible PEG linker, with the catalyst that utilized the rigid phenylene linker being markedly less efficient. This is the same trend as observed with the soluble polymeric systems, indicating that the observations with the purely polymeric systems transfer to these hybrid systems. It should be noted that at much lower loadings of 0.01 mol% catalyst, the polymeric catalysts with enhanced salen-salen cooperativity are still very active (first order kinetics), whereas the monomeric small molecule catalysts are essentially inactive (second order kinetics). These catalysts were easily recovered and reused multiple times with consistent selectivity. The activity decayed with each recycle and the catalyst deactivation was carefully studied.

The cooperativity associated with the supported Co-Salen catalysts described above is controlled by preparing side-chain functionalized polymers with manipulations of (i) salen density along the side-chains, (ii) backbone structure and flexibility, and (iii) linker structure,

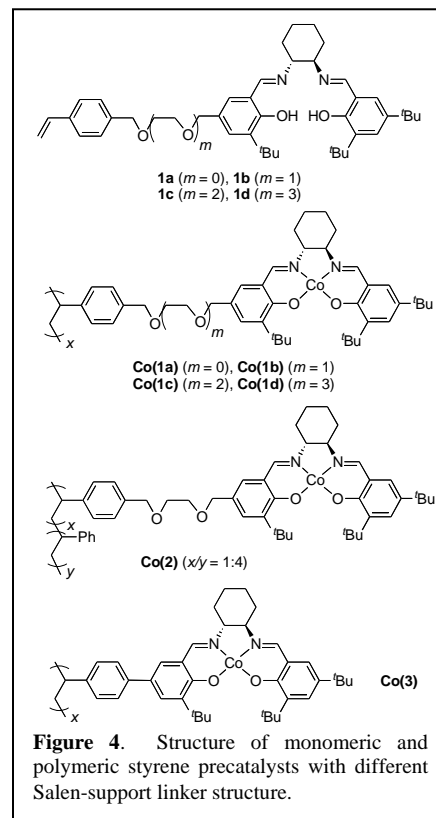


**Figure 4.** Structure of monomeric and polymeric styrene pre-catalysts with different Salen-support linker structure.

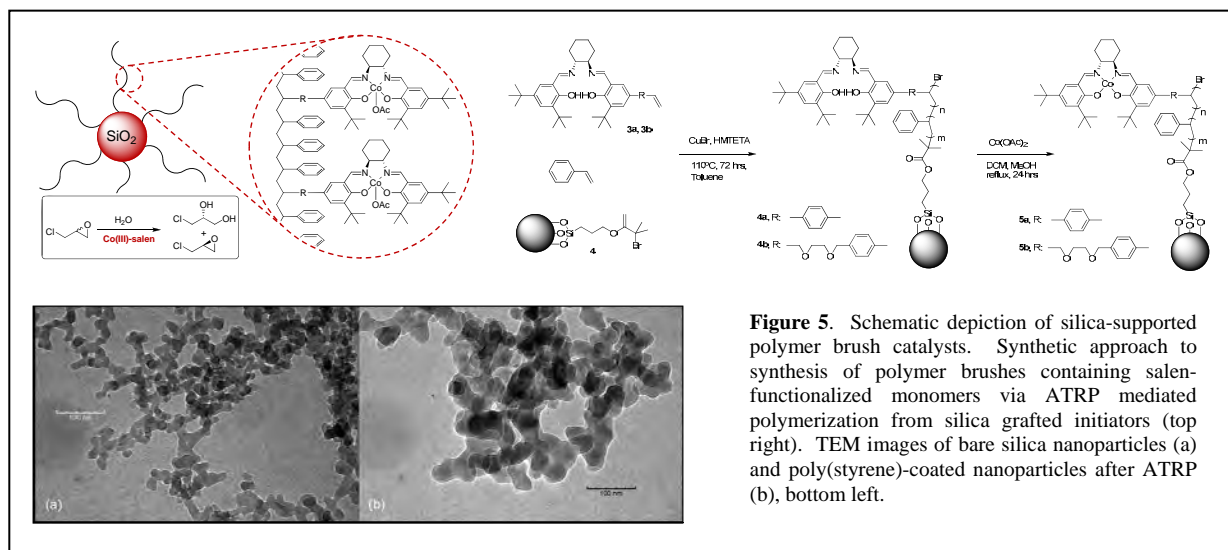
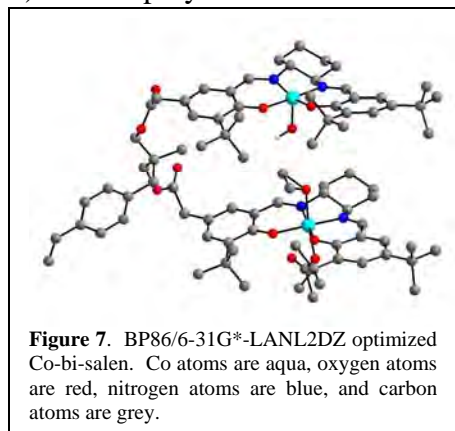


**Figure 5.** Schematic depiction of silica-supported polymer brush catalysts. Synthetic approach to synthesis of polymer brushes containing salen-functionalized monomers via ATRP mediated polymerization from silica grafted initiators (top right). TEM images of bare silica nanoparticles (a) and poly(styrene)-coated nanoparticles after ATRP (b), bottom left.

length and flexibility. An alternate approach to enhance cooperativity further is to develop building blocks or fragments with multiple salen units per reactive group. We sought to create reactive, multimeric salen fragments that could be used to give heterogeneous catalysts that are easy to recover via simple techniques such as filtration. The first strategy we pursued was the synthesis of a dendron that contained multiple Co-Salen units on one fragment and could be immobilized on insoluble polymer resins in one step. The three components of our system were: a cross-linked poly(styrene) resin, a dendron based linker and the target Co-Salen catalysts. The resulting catalytic system upon activation showed high activities and enantioselectivities in the HKR of a variety of terminal epoxides with activities similar to the soluble poly(styrene) and poly-(norbornene) supported systems. The catalyst was easily separated from the product mixture by simple filtration.

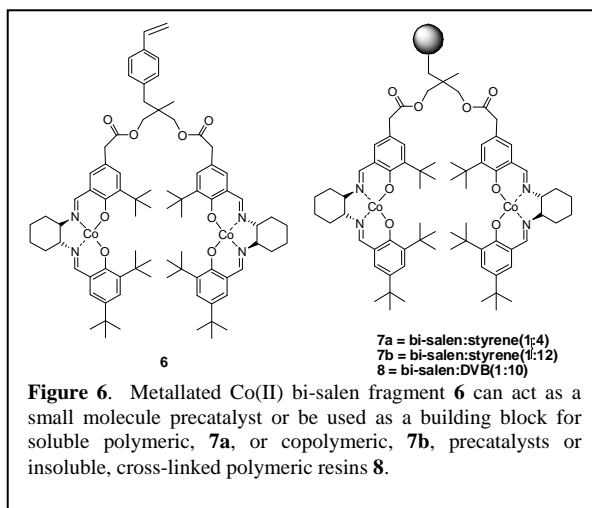
In addition to the dendron-functionalized polymer resin catalyst, we developed another multimeric salen catalyst based on a dimeric Salen fragment that can be used to create a wide-variety of different cooperative salen catalysts.

Referred to as a bi-salen unit (Figure 6), it is composed of a styrene molecule that has been functionalized with two salens linked in a manner such that effective cooperative catalytic interactions are possible. Density functional theory (DFT) computations were performed using the Jaguar suite of programs to model the binding of hydroxide to one metal center and the epoxide to the other center (Figure 7). We employed the BP86 functional in conjunction with the LANL2DZ effective core potential



for Co and the 6-31G\* basis for other atoms. The resulting DFT structure allowed us to predict that our design can accommodate structures where two salens are in very close proximity and can cooperate in the bimetallic transition state. With this confirmation in hand, we synthesized the bi-salen fragment and used it to construct an array of different Co-Salen catalysts. The versatile Co-bi-salen motif can (6) can act as (i) a soluble small molecule catalyst or it can be employed as a building block in the synthesis of (ii) soluble homogeneous copolymer complexes (7a & 7b), (iii) insoluble cross-linked polymeric resin complex (8), or (iv) insoluble silica-supported complex (9), all of which contain the cooperative bi-salen motif. All these catalysts were highly active. Interestingly, the polymeric and copolymeric bi-salen catalysts 7a and 7b were measurably more active than the small molecule, cooperative bi-salen catalyst 6. This suggested that cooperation occurs not only between the two salen units on a single bi-salen monomer, but also with salen units on the neighboring bi-salen unit in the polymer chain. This system and related systems may allow an unprecedented ability to study catalyst cooperativity along a single polymeric backbone.

The second class of cooperative catalysts that was investigated is based on supported Al-Salen complexes. Al-Salen complexes catalyze a variety of reactions such as conjugate additions,

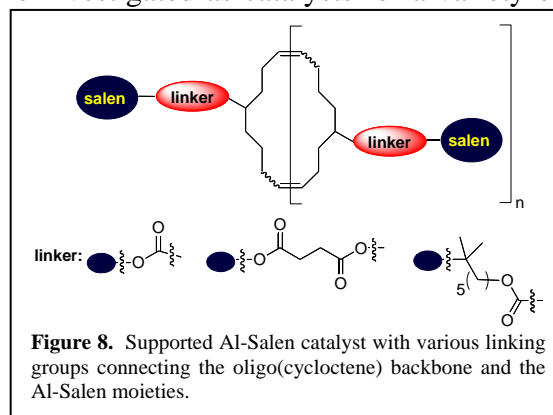
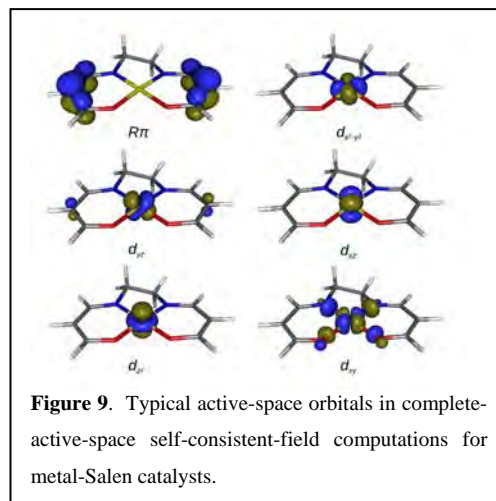


CO<sub>2</sub> addition to epoxides and lactide polymerization. The conjugate addition of cyanides to  $\alpha,\beta$ -unsaturated imides catalyzed by Al-Salen affords highly enantiopure cyano adducts that are important precursors for the pharmaceutical and fine chemical industries. The reaction is hypothesized to follow a bimetallic pathway, wherein one Al-Salen complex binds to the imide as a Lewis acid, while the other complex activates the cyanide nucleophile. In contrast to the Co-Salen systems, the Al-Salen catalysts are typically required in high catalyst loadings (10-15 mol%). Therefore, it is an ideal system for application of polymeric supports with high catalyst loadings, as such an approach can simultaneously promote cooperativity and lead to more efficient catalyst separation from the products.

Motivated by the excellent performance of cyclic cyclooctene-supported Co-Salen catalysts (*vide supra*), we investigated the effect of linker length and support structure on the transformations catalyzed by Al-Salen catalysts using cyclooctene-derived macrocyclic Al-Salen catalysts (Figure 8). These supported complexes were investigated as catalysts for a variety of reactions such as the bimetallic cyanide addition and the monometallic indole addition to  $\alpha,\beta$ -unsaturated ketones. While the flexible, cyclic oligomeric support significantly enhanced the rate of the cyanide addition reaction, most likely by promoting salen-salen interactions as in the Co-Salen case, it decreased the reaction rate for the monometallic indole reaction. For both reactions, a significant increase in catalytic activity was observed for catalysts with the longest backbone-salen linkers.

We have also synthesized poly(norbornene)-supported Al-Salen catalysts that were highly active in the enantioselective addition of cyanide to  $\alpha,\beta$ -unsaturated imides and efficiently performed the catalytic transformation within 6 hrs in high yields and enantioselectivities, with a low catalyst loading of 5 mol%, which represents 66% lower catalyst loading than is typically used by the homogeneous analogues. In addition, the poly(norbornene)-supported catalysts could also be recycled up to 5 times with undiminished selectivities. The poly(norbornene) Al-Salen catalyst is an excellent example successful implementation of what we learned from the bimetallic Co-Salen reactions to the Al-Salen system through translation of design principles.

In parallel with the catalyst design studies described above, we have carried out experimental and theoretical evaluations of the Co-Salen and Al-Salen systems to gain insight into the reaction mechanisms. Our theoretical electronic structure work has focused on exploration and then systematic testing of the reliability of DFT for metal-salen catalysts. Leveraging experience gained in very challenging theoretical benchmark studies of oxo-Mn-Salen carried out in 2005-2006, we massively expanded the effort to systematically investigate a variety of metal-salen catalysts as a function of the metal and the formal charge on the metal. We



carried out extensive comparisons of DFT vs CASSCF and CASPT2 for geometries and spin-state splittings for low-lying electronic states of a variety of  $3d^0$ ,  $3d^2$ , and  $4d^2$  metals. As in the oxo-Mn-Salen case, these systems often feature nearly-degenerate singlet and triplet states, followed by a relatively low-lying quintet state. Fortunately, our studies indicate that relatively few active orbitals are required in the CASSCF wavefunction, and they are qualitatively similar for all species studied to date (see Figure 9). Unfortunately, standard DFT approximations disagree on the energetic ordering of the states and tend to overstabilize the higher-lying quintet state. Geometries are generally well-predicted by DFT methods, but not in all cases. These investigations will prove indispensable to future computational studies by us and other researchers because they set guidelines for choosing appropriate computational models for these molecules.

Armed with the knowledge about when DFT is reliable for M-Salen catalysts, we focused our attention on experiments of direct relevance to the experimental and molecular modeling efforts. In a joint study utilizing both computational experiments and synthetic efforts, the effect of the linker on the activity of Al-Salen catalysts was investigated. Al-Salen catalysts were specifically targeted in this phase of the project because they are much more accessible to accurate theoretical studies by modest computational methods (e.g., DFT). In this work, the linker was found to influence the catalytic activity of the Al-Salen catalysts. However, our computations indicate that the electronic structure around the metal center changes very little as a function of different linkers. This indicates that the differences in catalytic activity are therefore due to differences in sterics or dynamics of the linkers, an important conclusion that can guide further catalyst design.

We have also carefully followed our catalyst deactivation profiles and our ability to recycle. We have done this by monitoring the kinetics of our recycle reactions, as well as via application of spectroscopic and physical characterization of the catalysts after reactions. For Co-Salen catalysts during HKR, the general mode of catalyst deactivation has been suggested to be the change of the active Co(III)-Salen complex to an inactive Co(II)-Salen complex. Unfortunately, no detailed spectroscopic studies have been carried out to confirm this suggestion. We investigated the deactivation of both homogeneous and supported Co-Salen catalysts in the HKR of terminal epoxides. Possible modes of deactivation of Co-Salen catalysts during the HKR of epichlorohydrin were explored by UV-Vis, IR and X-ray absorption spectroscopies and electrospray ionization mass spectrometry combined with recycling studies. In addition, the role of the Co-Salen counterion on the HKR reaction mechanism, catalytic activity, enantioselectivity and stability was explored. In addition to the bimetallic reaction path for HKR, Jacobsen has suggested there is a less selective and slower monometallic reaction path. Different counterions with varying nucleophilicities were used to elucidate when a bimetallic or monometallic transition state was formed during the HKR of a terminal epoxide and how the nature of the reaction path (mono vs bimetallic) affects the observed catalyst lifetime.

Spectroscopy results showed that the cobalt in Co-Salen catalysts maintained its +3 oxidation state throughout the reaction, although an active homogeneous, molecular Co(III) Salen catalyst deactivated substantially after multiple cycles without regeneration. Thus, deactivation of Co-Salen during HKR was not the result of Co reduction. The mass spectrum of a deactivated material showed that catalyst dimerization does not account for the loss of activity. However, the extent of counterion addition to epoxide was influenced by the exposure time and the nucleophilicity of the counterion. The rate of counterion addition to epichlorohydrin, which ultimately is suggested to form a less active Co(III)OH-Salen complex. In particular, on

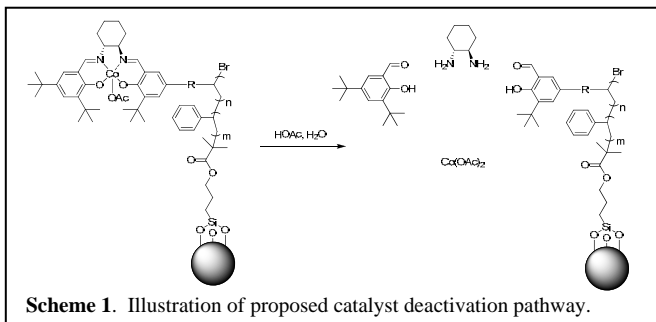
recycling Co(III)X-Salen catalysts, the loss in catalyst activity during HKR of epichlorohydrin occurred in the following order with X: iodide > chloride > acetate > tosylate. However, the measured activity of the fresh catalysts in the first run showed the same trend with counterion.

Given the knowledge developed on the homogeneous Co-Salen system, we sought to understand how our polymer brush supported catalysts deactivated during recycle. In addition to the role of counterion exchange, we sought to investigate the stability of the supported Co-Salen complexes. In recycle studies on the most active catalyst **7b**, high enantioselectivities of the remaining epoxide ( $\geq 99\%$ ) were retained after each of five runs. The time required to achieve  $\geq 99\%$  *ee* increased by roughly a factor of ten (45 to 420 min) and maximum initial turnover frequencies (TOFs) dropped from 30.2 to 4.1  $\text{min}^{-1}$  after five cycles. These results echo our results of the supported dendron-resin system.

Several possibilities existed to explain the catalyst deactivation: cobalt leaching, ligand decomposition, polymer loss (non-surface-bound or cleavage of surface-bound polymer), and/or counter-ion exchange. Elemental analysis (EA) and FT-IR of fresh and spent catalysts were compared to elucidate possible deactivation mechanisms. These data suggested ligand decomposition as the underlying cause of catalyst deactivation (Scheme 1). Results suggest that ligand decomposition is associated with regeneration of the Co(OAc) complexes. It may also be possible that counter-ion exchange was occurring at long reaction times, compounding the problem of salen decomposition.

Molecular modeling was used to investigate the behavior of the poly(norbornene) catalyst supports. The initial hypothesis was that this polymer would form a helix or at least be partially helical, thereby increasing the number of accessible catalytic side-chains. This hypothesis was based on the similarity of poly(norbornene) synthesized via ROMP to poly(norbornene) fabricated using addition-polymerization. It is the presence of alternating non-rotatable backbone bonds and bulky side-groups that is known to stabilize helical conformations in polymers. We found that the cyclopentyl group of the poly(norbornene) backbone was quite flexible and that this fact may thwart the formation of stable helices. We investigated the conformation and effect of this flexible bond, side-groups and tether structure on the conformation of poly(norbornene) as well as the accessibility of side-groups. It was asserted that this accessibility should scale with the effectiveness of the catalyst supported on these polymers.

Following MD simulations of poly(norbornene) using various initial conformations, the accessibility of a spherical LennardJones pseudo-atom grafted to the cyclopentyl ring via an undecanoic ester group was determined using the alpha-shape method of Edelsbrunner. The results showed that the side-chain accessibility is not significantly different for a variety of configurations. Similarly, there was a decrease in accessibility with polymer molecular weights using probes of different radii. While accessibility showed the expected decrease with effective tethered catalyst size and increase with alkyl linker length, all the configurations exhibited conformations and scaling of radius of gyration and accessibility indicative of a random coil polymer. This suggests that poly(norbornene) is not helical. This is of particular importance because it is difficult to determine the backbone structure experimentally. We hypothesize that this failure to form stable helices is due to the inability of the flexible cyclopentyl group to



Scheme 1. Illustration of proposed catalyst deactivation pathway.

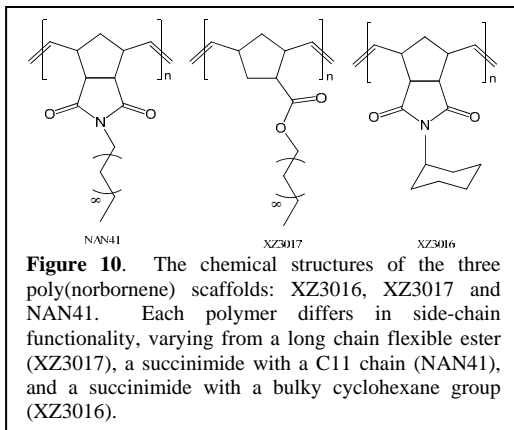
approximate a non-rotatable bond and the lack of bulky side-groups on the double bond. To investigate this hypothesis, we have restricted the pseudo-rotation of the cyclopentyl group by fusing it with a succinimide group. We found that the steric hindrance does play a role in creating local helices in the backbone.

To evaluate whether helical conformations can be induced by reducing the pseudo-rotation of the cyclopentyl group, it was fused with a succinimide ring to make the cyclopentyl group behave like a non-rotatable bond. Three polymers were both simulated and prepared in the laboratory for parallel experimental and computational study. The three poly(norbornene)s shown in Figure 10 were evaluated using SAXS and WAXS at Brookhaven National Laboratory. The MD and WAXS/SAXS results showed that poly(norbornene) is not helical by nature. However, helix formation can be induced by locking the cyclopentyl rings.

Computer simulations of oligo(cyclooctene) macrocycles with pendant Co-Salen complexes were carried out to determine the origin of the improved reactivity in the cyclic oligomeric supports. Using quantum calculations, a classical force field was first developed to model the Co-Salen catalyst site. This force field was then used to simulate the frequency with which the salen complexes could interact to form the required dimeric species that is required for cooperative catalysis. This frequency, normalized for constant cobalt loading was called a “reaction score”. We computed that the cis oligomer appears to be more reactive than the trans oligomer and the results are consistent with experimental observation that the cyclic oligomers are significantly more reactive than the linear oligomer. This increased reactivity occurs because of the increased ability of adjacent salen groups to favorably interact with each other. The modeling indicates that the optimal cis oligomer has 3 units and the optimal trans oligomer contains 4 units. The optimal cis trimer alternates between complexes formed from two adjacent pairs. It is not known if the experimentally synthesized sample is predominantly cis, trans, or a mixture of the two, but it is known that it is mainly a mixture of oligomers varying between approximately 3 and 6 repeat units. Thus, the simulations predict that the synthesized sample may be nearly optimal from a site-pairing probability perspective.

## Summary

During the past two years, we have developed design principles for supported metallated salen catalysts that follow a monometallic (Ru- and Mn-Salen) or a bimetallic (Co- and Al-Salen) pathway. For monometallic transformations, catalysts should be site-isolated along the support to enhance access while eliminating bimetallic decomposition pathways. In contrast, catalysts that follow a bimetallic pathway should be presented close to each other in a highly flexible manner. Furthermore, an optimal linker length and flexibility exist to enhance the bimetallic catalysis. Oligomeric poly(cyclooctene)-based catalysts fulfill all these requirements and are the most active and selective catalysts studied. Clearly, through variation of four variables: (i) the nature of the support, (ii) the linker length and rigidity, (iii) catalyst density along the polymer support, and (iv) the nature of the connectivity of the catalyst to the support, one can design optimized supports for supported salen catalysts that follow either a monometallic or a bimetallic reaction pathway.



We have also carried out extensive studies into the decomposition pathways of metallated salen catalysts under reaction conditions and investigated whether DFT level computation adequately predict the electronic states of  $3d^0$ ,  $3d^2$ , and  $4d^2$  metals, a prerequisite for the computing of transition states which is proposed for the next funding period. Finally, we have established that typical ROMP poly(norbornene)s do not exist in a helical conformation. These research accomplishments have resulted in a total of 24 manuscripts that have been published or are under review from 2007 to the present.

### **Publications From This Project (2007-present)**

1. Madhavan, N.; Takatani, T.; Sherrill, C. D.; Weck, M., Macrocyclic Cyclooctene-supported Salen(AlCl) Catalysts for Conjugated Addition Reactions: Effect of Linker and Support-structure on Catalysis. *Chem. Eur. J.* **2009**, *15*, 1186-1194.
2. Sears, J. S.; Sherrill, C. D., Assessing the Performance of Density Functional Theory for the Electronic Structure of Metal-Salens: The  $3d^0$ -Metals. *J. Phys. Chem. A* **2008**, *112*, 3466-3477.
3. Sears, J. S.; Sherrill, C. D., Assessing the Performance of Density Functional Theory for the Electronic Structure of Metal-Salens: The  $d^2$ -Metals. *J. Phys. Chem. A* **2008**, *112*, 6741-6752.
4. Takatani, T.; Sherrill, C. D., Performance of Spin-Component-Scaled Second-Order Møller-Plesset Perturbation Theory (SCS-MP2) for Potential Energy Curves of Noncovalent Interactions. *PhysChemChemPhys* **2007**, *9*, 6106-6114.
5. Venkatasubbaiah, K.; Gill, C. S.; Takatani, T.; Sherrill, C. D.; Jones, C. W., A Versatile Co(bisalen) Unit for Homogeneous and Heterogeneous Cooperative Catalysis in the Hydrolytic Kinetic Resolution of Epoxides. *Chem. Eur. J.* **2009**, in press.
6. Jain, S.; Zheng, X.; Jones, C. W.; Weck, M.; Davis, R. J., Importance of Counterion Replacement on the Deactivation of Co-Salen Catalysts in the Hydrolytic Kinetic Resolution of Epichlorohydrin. *Inorg. Chem.* **2007**, *46*, 8887-8896.
7. Jain, S.; Zheng, X.; Venkatasubbaiah, K.; Jones, C. W.; Weck, M.; Davis, R. J., Investigation of Deactivation of Co-Salen Catalysts in the Hydrolytic Kinetic Resolution of Epichlorohydrin. *Proc. Org. Reac. Catal. Soc.* **2009**, 389-398.
8. Gill, C. S.; Price, B. A.; Jones, C. W., Sulfonic Acid Functionalized Silica Coated Magnetic Nanoparticle Catalysts. *J. Catal.* **2007**, *251*, 145-152.
9. Gill, C. S.; Venkatasubbaiah, K.; Jones, C. W., Recyclable Polymer and Silica Supported Ruthenium(II)-Salen Bis-Pyridine Catalysts for the Asymmetric Cyclopropanation of Olefins. **2009**, submitted.
10. Gill, C. S.; Venkatasubbaiah, K.; Phan, N. T. S.; Weck, M.; Jones, C. W., Enhanced Cooperativity via Design: Pendant Co(III)-Salen Polymer Brush Catalysts for the Hydrolytic Kinetic Resolution of Epichlorohydrin. *Chem. Eur. J.* **2008**, *14*, 7306-7313.
11. Richardson, J. M.; Jones, C. W., Strong Evidence of Solution Phase Catalysis Associated with Palladium Leaching from Immobilized Thiols during Heck and Suzuki Coupling of Aryl Halides. *J. Catal.* **2007**, *251*, 80-93.
12. Richardson, J. M.; Jones, C. W., Leached Nickel Promotes Catalysis Using Supported Ni(II) Complex Precatalysts in Kumada-Corriu Reactions. *J. Mol. Catal. A* **2009**, *297*, 127-134.
13. Shiels, R. A.; Jones, C. W., Homogeneous and Heterogeneous 4-(N,N-Dialkylamino)pyridines as Effective Single Component Catalysts in the Synthesis of Propylene Carbonate. *J. Mol. Catal. A* **2007**, *261*, 160-171.
14. Shiels, R. A.; Venkatasubbaiah, K.; Jones, C. W., Polymer and Silica Supported Tridentate Schiff Base Vanadium Catalysts for the Asymmetric Oxidation of Ethyl Mandelate: Activity, Stability and Recyclability. *Adv. Synth. Catal.* **2008**, *350*, 2823-2834.



15. Weck, M.; Jones, C. W., Mizoroki-Heck Coupling Using Immobilized Molecular Precatalysts – Pd Pincers, Entrapped Pd Salts and Pd NHC Complexes. *Inorg. Chem.* **2007**, *46*, 1865-1875.
16. Goyal, P.; Zheng, X.; Weck, M., Enhanced Cooperativity in Hydrolytic Kinetic Resolution of Epoxides using Poly(styrene) Resin-Supported Dendronized Co-(Salen) Catalysts. *Adv. Synth. Catal.* **2008**, *350*, 1816-1822.
17. Madhavan, N.; Jones, C. W.; Weck, M., Rational Approach to Polymer-Supported Catalysts: Synergy between Catalytic Reaction Mechanism and Polymer Design. *Acc. Chem. Res.* **2008**, *41*, 1153-1165.
18. Madhavan, N.; Weck, M., Highly Active Polymer-Supported (salen)Al Catalysts for the Enantioselective Addition of Cyanide to  $\alpha,\beta$ -Unsaturated Imides. *Adv. Synth. Catal.* **2008**, *350*, 419-425.
19. Sommer, W.; Weck, M., Supported N-Heterocyclic Carbene Complexes in Catalysis. *Coord. Chem. Rev.* **2007**, *251*, 860-873.
20. Sommer, W.; Weck, M., Facile Functionalization of Gold Nanoparticles via Microwave Assisted 1,3 Dipolar Cycloaddition. *Langmuir* **2007**, *23*, 11991-11995.
21. Zheng, X.; Jones, C. W.; Weck, M., Unsymmetrical Macrocyclic Oligomeric Co-Salen Complexes Generated via Ring-Expanding Olefin Metathesis: Highly Reactive and Enantioselective Catalysts for the Hydrolytic Kinetic Resolution of Terminal Epoxides. *J. Am. Chem. Soc.* **2007**, *129*, 1105-1112.
22. Zheng, X.; Jones, C. W.; Weck, M., Engineering Polymer-Enhanced Bimetallic Cooperative Interactions in the Hydrolytic Kinetic Resolution of Epoxides. *Adv. Synth. Catal.* **2008**, *350*, 255-261.
23. Swann, A.; Ludovice, P. J., Helical Conformations in ROMP Poly(norbornene). *Macromol. Theory Simul.* **2009**, accepted.
24. Richardson, J. M.; Jones, C. W.; Assessing Catalyst Homogeneity/Heterogeneity via Application of Insoluble Metal Scavengers: Application to Heck and Suzuki Reactions. *Proc. Org. React. Catal. Soc.* **2009**, 193-202.
25. Swann, A.; Ludovice, P. "Cyclopentane Dynamics: Force Field and Simulation Algorithm Effects," **2009**, submitted.
26. Swann, A.; Takatani, T.; Sherrill, D.; Ludovice, P. "Molecular Modeling of Co-salen Complex Supported by Poly(cyclooctene) for Optimization as Catalyst," **2009**, submitted.

**Controlling Heterogeneous Ti-Epoxidation Activity via Support Effects**

Students: Jarred M. Ghilarducci, Andrew Solovyov, Niladri Maity  
Collaborators: Enrique Iglesia (UC Berkeley)  
Contact: A. Katz, Dept of Chem Eng MC 1462, Berkeley, CA 94720-1462;  
Phone: (510) 643-3248; Email: katz@cchem.berkeley.edu  
web page: <http://www.cchem.berkeley.edu/katzgrp/>

**Goal**

Inspired by observed solvent effects in TS-1 catalysis, in which a decade increase in epoxidation catalyst activity is observed upon changing pKa of solvent from tert-butanol (pKa 18) to methanol (pKa 15) (cannot be explained with reactant partitioning effects), as well as observed activation of peroxide for olefin epoxidation via hydrogen bonding in related homogeneous systems, we have set out to explore the role of defect sites, and, in general, environment as defined by the heterogeneous support, in epoxidation catalysis when using Ti(IV)-calixarene active sites anchored on silica as catalyst. This approach benefits from the rigorous isolation aspects of calixarene active sites, which enforce a non-coordinatively saturated geometry around the metal center, and builds on previously observed rate enhancements when comparing heterogeneous Ti(IV)-calixarene sites on silica and the corresponding homogeneous triphenylsilyl complex **1**, which was shown to be at least an order of magnitude less active.

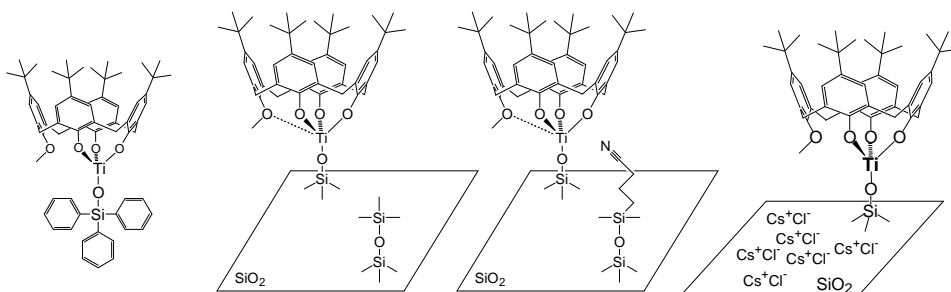
**Recent Progress*****Replacement of Silanols with Organosilane***

The current investigation includes rigorous capping of silanol groups on silica with organosilanes to synthesize new materials **2** and **3**, in which silanols are replaced with aprotic groups consisting of either cyano or alkane (methyl) functionality, respectively. These approaches replace silanols in the vicinity surrounding the Ti metal center using either chlorosilane or silazane-based capping agents and a highly dehydroxylated silica support. The hypothesis is that if silanol groups external to the Ti(IV)-calixarene active site are critical for catalysis, then activity should be decreased significantly (corresponding to behavior observed with the homogeneous triphenylsilyl adduct **1** as catalyst). Capped material **2** has been characterized via FTIR spectroscopy, and consists of a greatly silanol-depleted silica surface when compared with corresponding, previously published, uncapped materials (FTIR of the capped material demonstrates only inaccessible internal silanols). Yet no decrease in epoxidation activity (per Ti site) was observed (in all cases used cyclohexene epoxidation in octane solvent with TBHP as oxidant at 60 °C as probe reaction). Other materials consisting of fluorinated alkane capping agents (not shown), which were hypothesized to interact with peroxide, produced similar epoxidation catalytic activity. Only a slight decrease was observed with the cyano groups in material **3** presumably as a result of weak coordination to the Ti metal center during catalysis (when the Ti(IV)-calixarene active site comes off of the surface), resulting in a higher degree of coordination and a less Lewis acidic active site. This data

demonstrates that relatively few silanols are required for promoting epoxidation catalysis, and, minimally, catalysis may only require the single silanol that is synthesized upon cleaving the Ti-O-Si bond upon hydroperoxide binding to the metal center. Also, complete exclusion of silanols is difficult to guarantee in any of the organosilane-capped materials because the unexpected mode of attachment of Ti(IV)-calixarene to the surface appears to be ring opening of silica network Si-O-Si bonds as opposed to/in conjunction with consumption of capping-group-inaccessible silanols.

### ***Poisoning of Silanols on Silica Using Cesium Chloride:***

Based on our previous demonstration of titrating silanols on silica with excess CsCl, we set out to remove all silanols in the system, even those that would be generated during catalysis via cleavage of Ti-O-Si bonds. This was performed by impregnating the silica support with 6 CsCl/nm<sup>2</sup> prior to dehydration and Ti(IV)-calixarene anchoring. Some residual silanols remained accessible after this impregnation procedure presumably as a result of uneven CsCl deposition. The hypothesis was that these remaining silanols as well as any other ones generated during catalysis would be titrated by the excess CsCl present (calixarene coverage less than 150-fold less than CsCl coverage). Catalysis results demonstrate a dramatic decrease in initial catalytic activity of four-fold in the CsCl-capped material relative to an unmodified Ti(IV)-calixarene catalyst. Interestingly, much like the previously reported for homogeneous **1**, deactivation of catalysis is observed after ~10 turnovers, presumably as a result of active site dimerization on the surface due to lack of available silanols for covalent anchoring.



Rate	<b>1</b>	<b>2</b>	<b>3</b>	<b>4</b>
Constant	0.5 M <sup>-2</sup> s <sup>-1</sup>	17 M <sup>-2</sup> s <sup>-1</sup>	4.3 M <sup>-2</sup> s <sup>-1</sup>	2.9 M <sup>-2</sup> s <sup>-1</sup>
	<b>deactivates rapidly</b>	no deactivation	no deactivation	<b>deactivates rapidly</b>

### **Future Plans**

Given the critical observed role of tuning support defect sites in Ti-catalyzed epoxidation of olefins using organic hydroperoxide, mixed oxide supports consisting of a mixture of silica and other inorganic oxides will be investigated. An additional hypothesis is that given the confinement of the metal center in the resting state of catalyst **3**, the Ti should be uncoordinated to the cyano groups and becomes coordinated only during catalysis. This hypothesis will be investigated using Ti K-edge XANES on both the catalyst resting state as well as during an in-situ measurement. The hypothesis is that if the confinement is occurring as expected, only during in-situ measurement should a higher coordination mode Ti be observed. Finally, other Lewis acid-catalyzed systems consisting of metallocalixarene catalysts with V(V) and Sn(IV) active sites will be investigated.

## Publications 2007-2009

“Structural Assessment and Catalytic Consequences of the Oxygen Coordination Environment in Grafted Ti-Calixarenes” by J. M. Notestein, L. R. Andrini, V. I. Kalchenko, F. G. Requejo\*, A. Katz\*, and E. Iglesia\*, *J. Am. Chem. Soc.* **2007**, *129*, 1122-1131.

“The Role of Outer-Sphere Surface Acidity in Alkene Epoxidation Catalyzed by Calixarene-Ti(IV) Complexes” J. M. Notestein, A. Solovyov, L. R. Andrini, F. G. Requejo, A. Katz\*, and E. Iglesia\*, *J. Am. Chem. Soc.* **2007**, *129*, 1122-1131.

“Fluorescence and Charge Transfer Complexes in Calixarenes Grafted on Anatase Nanoparticles” by J. M. Notestein, E. Iglesia\*, and A. Katz\*, *Chem. Mater.* **2007**, *19*, 3998 - 5005 .

“Graftable Chiral Ligands for Surface Organometallic Materials: Calixarenes Bearing Asymmetric Centers Directly Attached to the Lower Rim” by A. Solovyov, J. M. Notestein, K. A. Durkin, A. Katz\*, *New Journal of Chemistry* **2008**, *32*, 1314 - 1325.

“Primary Amine Confinement at the Interface of Grafted Calixarenes and Silica” by A. Solovyov, T. J. Amundsen, J. D. Daniels, Y.G. Kim, A. Katz\*, *Chem. Mater.* **2008**, *20*, 6316 - 6318.

“Vanadocalixarenes on Silica: Requirements for Permanent Anchoring and Electronic Communication” by N. de Silva, S.-J. Hwang, K. A. Durkin, A. Katz\*, *Chem. Mater.*, in press.

## Modeling Coverage Dependence in Surface Reaction Networks

Students: Spencer Miller, Nilay Inoglu

Contacts: Carnegie Mellon University, 5000 Forbes Ave, Doherty Hall A207F, Pittsburgh, PA 15213; [jkitchin@andrew.cmu.edu](mailto:jkitchin@andrew.cmu.edu)

### Goal

To develop simple, fast and accurate methods for simulating coverage effects on transition metal catalyst surfaces that also explain in physical terms how adsorbates modify catalyst reactivity.

### DOE Interest

Heterogeneous catalysis involves the adsorption, reaction and desorption of molecular species at metal surfaces. The reaction rates depend on the details of how the species interact with each other and the surface. The difficulties associated with experimentally measuring all of these details make modeling and simulation a complementary approach to studying these systems. Quantum chemical calculations are computationally too expensive to consider every possible detail, and new methods and algorithms are needed to facilitate the simulations of surface reactions, as well as to explain the results obtained from quantum chemical calculations.

### Recent Progress

*Corresponding adsorption states:*

The adsorption energies of atomic C, N, O and S on the late transition metal (111) surfaces are highly correlated with each other at all coverages [1, 2]. We have discovered that the coverage dependence can be reduced to a single master curve (Figure 1) by scaling the adsorption energies. The correlations work provided the geometry and bonding mechanisms of the adsorbates on each surface are similar. These correlations suggest a simple and efficient way to estimate the adsorption behavior of simple adsorbates on other metal surfaces from the detailed adsorption behavior of the adsorbate on a reference surface that is determined by quantum chemical calculations.

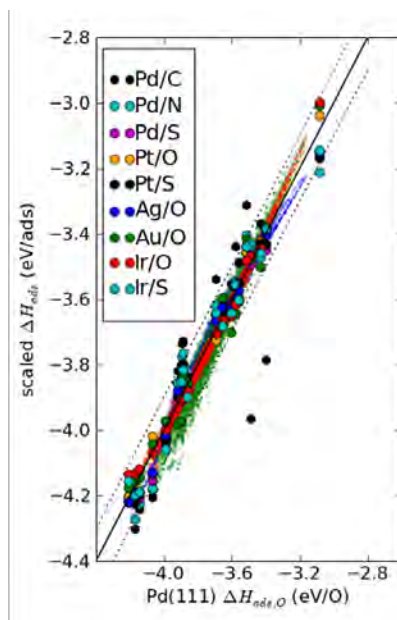


**Figure 1. Master curve illustrating the correlations between scaled coverage dependent atomic adsorption energies on late transition metal (111) surfaces. The two outliers are geometrically dissimilar due to reconstructions compared to the same configurations on the other metal surfaces, and thus do not follow the correlations.**

*Common mechanism for coverage dependent adsorption behavior:* The reason that the correlations observed above exist has been found to be a result of a common mechanism of adsorbate-induced changes to the surface electronic structure.

As the coverage increases, the increased overlap between the adsorbate orbitals and the surface metal *d*-orbitals results in a broadening of the surface *d*-band. The number of *d*-electrons in the band is conserved, however, resulting in a decrease in the average energy of the *d*-band and a weakening of subsequent adsorption energies.

*Similarity in thermodynamically relevant adsorbate structures:* Many of the possible adsorbate structures that can form are thermodynamically irrelevant as they are very high in energy. Near the ground state convex hull, however, there are many thermodynamically accessible configurations. Many of these configurations are configurationally similar (Figure 2) and are related defect structures.

### Future Plans

*Extensions of configurational correlations:* Determine if configurational correlations can be extended to alloy and thin film systems such as oxides and sulfides.

*Generalization of surface electronic structure modification:* Catalyst surface electronic structures can be modified by alloying, ligand effects, strain and coverage effects. Develop a generalized model that describes the electronic structure in terms of adsorbate and surface metal orbital overlaps.

*Incorporation of cluster expansion models into molecular simulations:* The cluster expansion models enable us to rapidly and accurately calculate adsorption properties of configurations. The computational speed will enable us to simulate the phase behavior and reactivity of larger systems than density functional theory can handle. We will be incorporating the cluster expansion models into kinetic Monte Carlo algorithms to simulate coverage dependent temperature programmed desorption spectra and to predict surface alloy phase behavior.

### Publications

1. Miller, S. and J.R. Kitchin, *Uncertainty and Figure Selection for DFT based Cluster Expansions for Oxygen Adsorption on Au and Pt (111) Surfaces*. Molecular Simulation 2009. **Accepted 2009**.
2. Miller, S.D. and J.R. Kitchin, *Relating the coverage dependence of oxygen adsorption on Au and Pt fcc(1 1 1) surfaces through adsorbate-induced surface electronic structure effects*. Surface Science, 2009. **603**(5): p. 794-801.

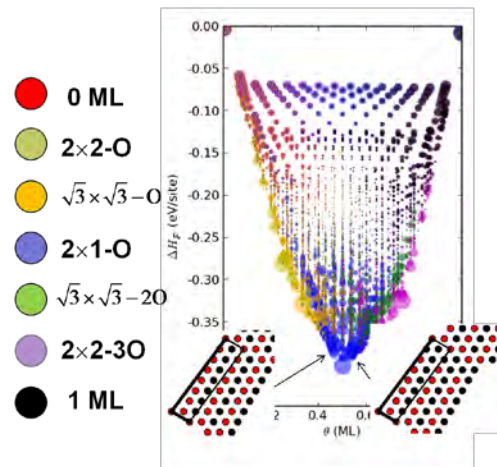


**Figure 2. Structural similarity phase diagram. Each dot corresponds to the stability of a particular adsorbate configuration and its similarity to a reference structure found on the ground state convex hull. The size of the colored dot is a function of the similarity; larger colored dots indicate more similarity to the reference structure.**

**Nanostructure Catalytic Materials: An Investigation of Effect of Active Site Environment**

Postdoc: Jeong Kyu Lee  
Students: Michael Missaghi, John Galloway  
Collaborators: Mayfair Kung (Northwestern), Chris Downing (Northwestern)  
Contacts: Chemical and Biological Engineering Department, Northwestern University, 2145 Sheridan Road, E136, Evanston, IL 60208-3120. hkung@northwestern.edu

**Goal**

Develop an understanding and methodology to incorporate chemical/catalytic functionalities into artificial structures so as to capture the desirable catalytic properties found in enzymes with materials that are more stable and tolerant to process conditions, such as temperature and pH.

**DOE interest**

Achieving high reaction selectivity is an ultimate goal in catalysis research, since elimination of undesirable byproducts reduces environmental impact of the process and the energy demand for separation and purification, which often accounts for the majority of the process energy requirement. Whereas enzymes, the nature's catalyst, are highly selective and active, they are not used widely in industry because of their fragility to processing conditions. Heterogeneous catalysts are much more robust, but have not been able to capitalize on the properties found in enzymes to enhance selectivities in catalytic reactions. There is a need to develop the capability to achieve this.

**Recent Progress**

We have been focusing on structures built from silicon-based material. In our earlier work, we used a micelle-templating method to synthesize a 2 nm-diameter nanocage, defined by a thin, 2 to 3 atom-layer thick siloxane shell with interior amine groups [1]. These amine groups are chemically active; they can catalyze the decarboxylation of acetylacetone and react positively in the ninhydrin test. Extending from this work, we synthesized a ~5 nm diameter nanocage using a dendrimer-templating method [2]. An immolative dendrimer (Figure 1) was constructed using carbamate linkages between generations, such that upon cleavage, the dendrimer would degrade into small fragments that can be removed by diffusion through the cage wall [3]. By using dendrimers of different generations, nanocages of different sizes can be synthesized with this method. We demonstrated the synthesis of a carbosilane nanocage possessing interior hydroxyl groups, which, upon activation with p-nitrophenyl chloroformate, were shown to react with smaller amines but not larger amines, demonstrating size-selectivity (Figure 2).

In support of the nanostructure synthesis program, we have developed a convenient method to prepare the class of organosilicon hydride halide compounds that are very useful for synthesis of designed siloxane oligomers. The syntheses of silicon chlorohydride containing various ligands including those containing C=C, chlorophenyl, and pyridyl groups are demonstrated. These compounds are being used to synthesize target siloxane oligomers for catalyst preparation [4].

This synthesis methodology enables our study of the effect of binding of bis(3-pyridyl)siloxane compounds of different separation distances between pyridyl groups to Pd(OAc)<sub>2</sub> in the aerobic oxidation of primary and secondary alcohols to aldehydes and ketones. The pyridine ligand is essential in stabilizing this catalytic system from formation of Pd black, but excess ligand suppresses the activity. Bispyridyl ligands may be able to stabilize the complex at a low concentration without suppressing the activity. Indeed, the activity was found to be independent of the bispyridylsiloxane concentration while free pyridine suppresses the activity.

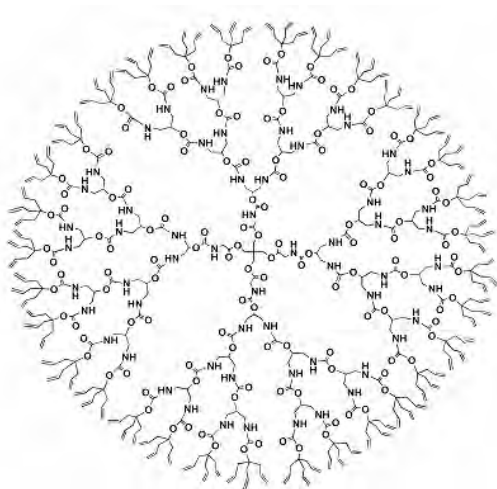


Figure 1. Generation 4 dendrimer with immolative carbamate bonds used to synthesize nanocages.

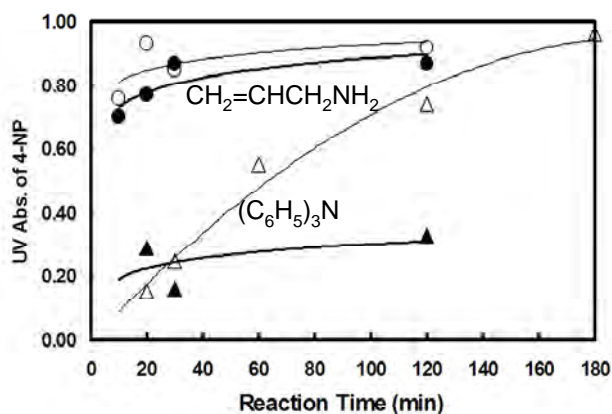


Figure 2. Formation of 4-nitrophenol from the reaction of allylamine (circles) or tritylamine (triangles) with PNP-activated interior OH groups in nanocages (filled points) and with a control PNP carbonate in solution (empty points), showing size-selectivity for the nanocage shell.

### Future Plans

Future plan is to continue to synthesize novel, designed structures suitable for anchoring chemically active groups to explore cooperative effects of functional groups in catalysis. Two multifunctional structures to be examined are bipyridyl carboxylate and bis-carboxylate structures.

### Publications (2006-2009)

1. "Size-Selective Shell Cross-Linked Interior Functionalized Siloxane Nanocages," Young-Woong Suh, Mayfair C. Kung, Yingmin Wang, Harold H. Kung, *J. Amer. Chem. Soc.* 128 (2006) 2776-2777.
2. "Nanotechnology: Opportunities for Chemical Engineering," Harold H. Kung, *J. Chin. Inst. Chem. Engrs.* 37 (2006) 1.
3. "Catalytic Nanomotors – Promising leads for new catalytic applications," Harold H. Kung, Mayfair



- C. Kung, *Appl. Catal. A: General*, 309 (2006) 159-161.
4. "Efficient Synthesis of Immolative Carbamate Dendrimer with Olefinic Periphery," Jeong-Kyu Lee, Young-Woong Suh, Mayfair C. Kung, Christopher M. Downing, and Harold H. Kung, *Tetrahedron Lett.* 48 (2007) 4919-4923
  5. "Understanding Au-catalyzed low temperature CO oxidation," Mayfair C. Kung, Robert J. Davis, Harold H. Kung, *J. Phys. Chem. C*, 111(32), (2007) 11767-11775. Featured article.
  6. "Engineered nanostructures for catalysis." Kung, Mayfair C.; Kung, Harold H.. Chemical and Biological Engineering Department, Preprints - American Chemical Society, Division of Petroleum Chemistry (2007), 52(2), 54.
  7. "Cooperative Catalysis: a New Development in Heterogeneous Catalysis," Jeong-Kyu Lee, Mayfair C. Kung, Harold H. Kung, *Topics in Catalysis*, 49 (2008) 136-144.
  8. "Discrete Molecular-size Nanocages Derived from Disintegratable Dendrimer Templates," Jeong-Kyu Lee, Mayfair C. Kung, Harold H. Kung, *Chem. Mater.* 2008; 20(2); 373-375.
  9. "Use of Dendrimers in Catalyst Design," Bert D. Chandler, Jeong-Kyu Lee, Harold H. Kung and Mayfair C. Kung, in *Design of Heterogeneous Catalysts, New Approaches based on Synthesis, Characterization and Modeling*, U. Ozkan ed., Wiley-VCH publ., 2009, p.59-81.
  10. "Synthesis of Organofunctional Silicon Hydride Halides from Methylchlorosilane," Michael N. Missaghi, Christopher M. Downing, Mayfair C. Kung, and Harold H. Kung, *Organometallics*, 2008, 27 (23), pp 6364-6366.
  11. "Engineered structures as catalysts for environmentally friendly reactions." Kung, Harold H, Preprints of Symposia - American Chemical Society, Division of Fuel Chemistry (2008), 53(1), 1.

## References

- [1] Y.-W. Suh, M.C. Kung, Y. Wang, and H.H. Kung, Size-selective shell cross-linked interior functionalized siloxane nanocages. *Journal of the American Chemical Society* 128 (2006) 2776-2777.
- [2] J.-K. Lee, M.C. Kung, Y.-W. Suh, and H.H. Kung, Discrete Molecular-Sized Nanocages Derived from Disintegratable Dendrimer Templates. *Chemistry of Materials* 20 (2008) 373-375.
- [3] J.-K. Lee, Y.-W. Suh, M.C. Kung, C.M. Downing, and H.H. Kung, Efficient synthesis of immolative carbamate dendrimer with olefinic periphery. *Tetrahedron Letters* 48 (2007) 4919-4923.
- [4] M.N. Missaghi, C.M. Downing, M.C. Kung, and H.H. Kung, Synthesis of Organofunctional Silicon Hydride Halides from Methylchlorosilane. *Organometallics* 27 (2008) 6364-6366.

## Selective and Efficient Catalysis in 3-D Controlled Environments

**Graduate Students and Postdocs:** H.-T. Chen, T.-W. Kim, Y. Cai, C.-W. Wu, J.L. Rapp, P.-W. Chung, and Y. Huang.

**Collaborators:** A. Bakac, M.S. Gordon, J.W. Evans, A.D. Sadow, and J.W. Wiench

Ames Laboratory and Department of Chemistry, Iowa State University, Ames, IA 50011-3111  
[vsylin@iastate.edu](mailto:vsylin@iastate.edu), [mpruski@iastate.edu](mailto:mpruski@iastate.edu)

### Goal

Develop and characterize multifunctionalized mesoporous materials that integrate the selectivity of homogeneous catalysts with thermal/chemical stability and separability of heterogeneous catalysts. Investigation of the selectivity, reactivity, and kinetics of these 3-D heterogeneous catalysts to gain fundamental mechanistic understanding at the molecular level.

### DOE Interest

Developing catalytic systems that can coherently unite the best features of the homogeneous and heterogeneous areas of catalysis has been the key interest of the DOE. By controlling the structure, reactivity and morphology of the mesoporous solid support and its interaction with the active sites, these studies provide truly unique opportunities for the design of a new generation of highly efficient and selective catalysts. This research also provides fundamental knowledge about catalysis by deconvoluting the key factors that affect selectivity, reactivity and kinetics.

### Recent Progress

#### (1) *Synthesis of Multifunctional Mesoporous Silica Materials with Controllable Mesochannel Orientation*

We have developed a one-pot synthesis of *organically multi-functionalized* mesoporous silica nanoparticles (MSNs) with the precise control of both incorporated amount of functional group and the orientation of two-dimensional hexagonal mesoporous channels.<sup>1</sup> We used ureidopropyltrimethoxysilanes (UDP-TMS) with strong hydrogen-bonding ability that cooperatively interacts with the cationic CTAB surfactant micelles in a NaOH-catalyzed condensation reaction of tetraethoxysilane (TEOS). As depicted in **Figure 1**, the mesochannels

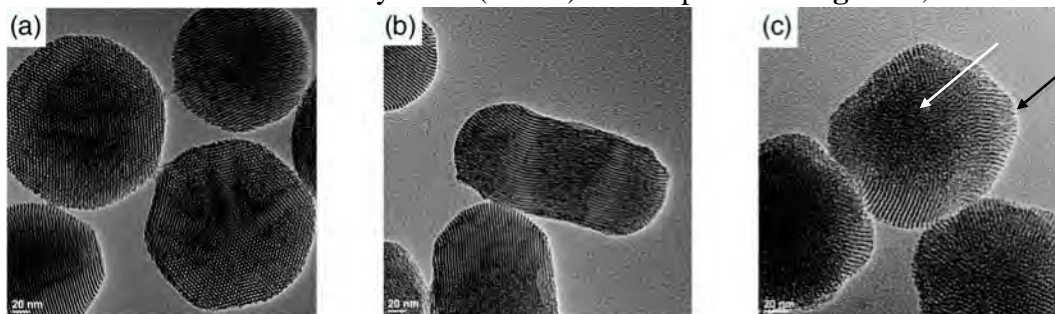


**Figure 1.** TEM micrographs of ureidopropyl-functionalized mesoporous silica nanoparticles (UDP-MSNs) with straight mesochannels (a), helical mesochannels (b), and with radical mesochannels (black arrow) and worm-like mesostructured core (white arrow) (c) depending on the loading of UDP.<sup>1</sup> All scale bars = 20 nm.

in ureidopropyl-functionalized MSNs (UDP-TMS) can be controlled and fine-tuned from typically straight hexagonal mesopores to the twisted helical mesochannels, and then to the radical aligned channels from the central core with worm-like mesostructure depending on the extent of organic functionalization. Moreover, we are able to synthesize multifunctional MSNs with the same ratio of organic groups while altering the 3-D mesostructures by varying the sequence of introduction of the different organosilane precursors. This newly gained ability of manipulating the 3-D mesoporous structure while controlling the particle morphology and organic functionalization of these mesoporous solid supports would foreseeably play a crucial role for the design of highly efficient and selective single-sited catalytic systems.

## (2) Synthesis of Thermo-responsive Polymer Immobilized Mesoporous Silica Nanoparticle Materials for Selective Catalysis

Recently, the selectivity of several organic/inorganic hybrid mesoporous catalytic systems was shown to be regulated by immobilizing stimuli-responsive “gate-keepers” that can control the diffusion of reactants and products to the catalytic sites inside the mesopores (*J. Am. Chem. Soc.*, **2004**, *126*, 1010-1011). To further advance this burgeoning area, we have successfully synthesized a temperature-responsive poly(*N*-isopropylacrylamide) immobilized MSN material (PNiNAm-MSN) via a surface-initiated living radical polymerization with a reversible addition-fragmentation chain transfer (RAFT) reaction.<sup>15</sup> The PNiNAm polymer is selectively attached

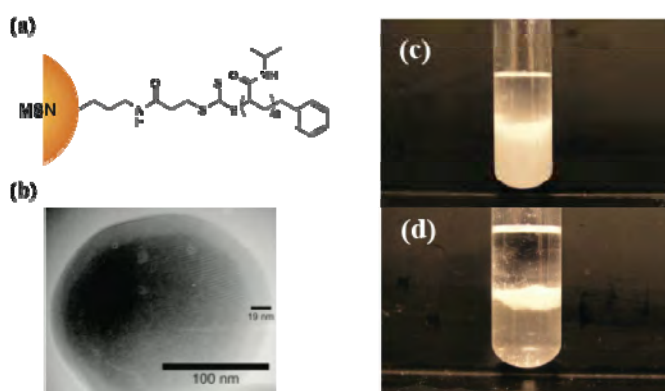


**Figure 2.** (a) Schematic representation of PNiNAm functionalized MSN (PNiNAm-MSN). (b) TEM image of PNiNAm-MSN. The opaque thick layer represents the PNiNAm polymer coating. The partition of PNiNAm-MSNs in the biphasic solution system (toluene/water) at temperature at 25 °C (c) and > 40 °C (d).<sup>15</sup>

on the exterior surface of MSNs. As shown in **Figure 2(a)**, the degree of polymerization could be controlled. We have demonstrated that the properties of PNiPAM-MSN could indeed be tuned reversibly. As depicted in the **Figure 2(c, d)**, the partition property of PNiPAM-MSN in hydrophilic and hydrophobic solution could be switched repeatedly simply by changing the solution temperature.

## (3) One-Pot Reaction Cascade Catalyzed by Acid- and Base-Functionalized Mesoporous Silica Nanoparticles

In many biological reaction cascades involving reversible equilibria, enzymes with different reactions kinetics are often synergistically work together in a sequential fashion to prevent the undesired reverse reactions. Incorporating this catalytic principle to artificial catalysts (both homogeneous and heterogeneous systems) has been difficult. We have recently demonstrated that a reaction cascade involving reversible equilibria could be successfully catalyzed by two MCM-41 type MSN materials that are functionalized with a 4-ethylphenylsulfonic acid (SAMSN) and an aminopropyl functionality (APMSN).<sup>14</sup> Our results showed that SAMSN and APMSN could serve as acid and base catalysts, respectively, for the wolf-and-lamb type of one-pot reaction cascades. As a proof of principle, we examined the catalytic conversion of 4-nitrobenzaldehyde dimethyl acetal to (*E*)-1-nitro-4-(2-nitrovinyl)benzene, which involved two separate reactions, i.e., an acid-catalyzed deprotection to yield the 4-nitrobenzaldehyde, followed

by a base-catalyzed Henry reaction in nitromethane to generate the final product (*E*)-1-nitro-4-(2-nitrovinyl)benzene as summarized in **Table 1**. We have demonstrated that by confining organic acid and base inside of mesoporous silica nanoparticles with different particle sizes and pore diameters, these opposing reagents can serve as effective catalysts for a one-pot reaction cascades.<sup>14</sup> We envision that this approach can be further developed into a general design principle for biomimetic catalytic cascades.

**Table 1.** One-pot reaction cascade catalyzed by SAMSNS and APMSNS.<sup>14</sup>

Entry	SAMSNS (mol %)*	APMSNS (mol %)*	Conversion of A (%)	Yield of B (%)	Yield of C (%)
1	1.0	1.0	99.9	56.4	43.5
2	1.0	2.0	100	22.0	78.0
3	1.0	4.0	100	5.0	95.0
4	1.0	6.0	100	2.3	97.7
5	1.0	0	98.1	98.1	0
6	0	1.0	0	0	0
7	Pure MSN	Pure MSN	0	0	0

\* No reaction occurred when the MSN catalysts replaced by corresponded homogeneous analog.

#### (4) Control of Spatial Distribution and Coordination of Metal Oxide

We developed a mesoporous aluminum silicate (Al-MS) catalyst via our modified interfacial condensation reaction (**Figure 3**).<sup>22</sup> Solid-state NMR studies showed that the aluminum atoms are tetrahedrally coordinated and are stable up to at least 400 °C. The double resonance <sup>27</sup>Al-<sup>29</sup>Si NMR experiment provided the first direct evidence that all Al atoms are surrounded by Si atoms

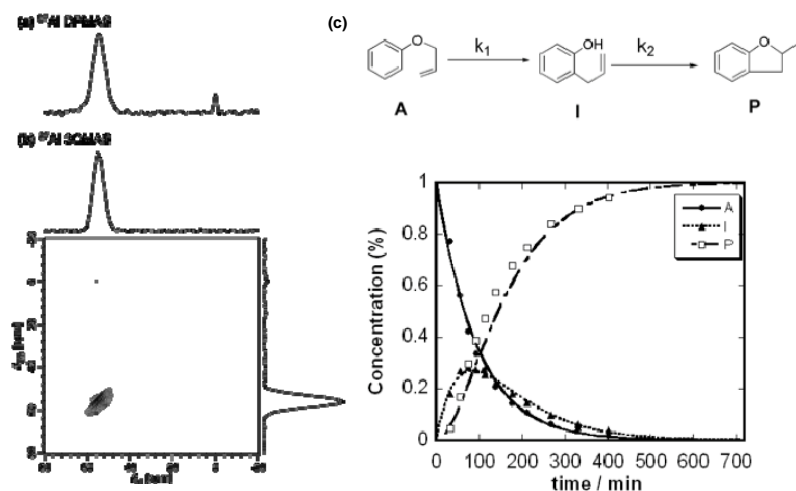


**Figure 3.** (a) <sup>27</sup>Al DPMAS and (b) <sup>27</sup>Al MQMAS spectra of hydrated Al-MS acquired with  $\nu_R = 10$  kHz. The MQMAS experiment was performed using  $\nu_{RF}^{Al} = 83$  kHz during hard pulses,  $\nu_{RF}^{Al} = 8$  kHz during the soft pulse, 48  $t_1$  increments of 40  $\mu$ s, and 7200 scans per  $t_1$  increment in the hypercomplex acquisition mode. The spectrum is displayed after shearing, using the isotropic scale  $\delta_{ISO}$  in the MQ (vertical) dimension. (c) Reaction scheme and kinetic study of Claisen rearrangement of allyl phenyl ether.<sup>22</sup>

forming Al-O-Si bonds in the framework. The silicon to aluminum atomic ratio at the surface (Si/Al)<sub>s</sub> is estimated at around 100, which exceeds the overall Si/Al ratio of 60. Reactivity study of the mesoporous aluminosilicate shows an excellent catalytic reactivity for the Claisen rearrangement of allyl phenyl ether, despite the low surface concentration of Al.

### (5) Solid-state NMR characterization of nanostructured heterogeneous catalysts

We have used solid-state NMR spectroscopy as a primary tool for characterization of new catalysts invented in this Program<sup>2,9,12,13,15,16,18,20-22</sup> and developed new NMR methods for such studies.<sup>3,5,8,12,17,23</sup>

#### (a) Sensitivity enhancement by indirect detection.

We demonstrated remarkable new capabilities of solid-state NMR spectroscopy by combining fast magic angle spinning (MAS) at 2-3 million rpm with new multiple RF pulse sequences.<sup>3,8,17</sup> The latest exploit was to seek sensitivity gain in *through-space* and *through-bond* heteronuclear correlation (HETCOR) spectroscopy through the detection of high- $\gamma$  (<sup>1</sup>H) rather than low- $\gamma$  (e.g., <sup>13</sup>C, <sup>15</sup>N) nuclei.<sup>3,17</sup> This so-called indirect detection method has been hitherto impossible due to the lack of adequate <sup>1</sup>H homonuclear decoupling schemes. In addition, *through-bond* HETCOR NMR was prohibitively inefficient due to decoherence of magnetization during the polarization transfer. These difficulties were overcome to the extent that two-dimensional (2D) <sup>1</sup>H{<sup>13</sup>C} HETCOR spectra of surface bound molecules can now be acquired under natural abundance within minutes or hours, a result that earlier would have been considered unrealistic. The new methods were used to detail the conformational changes in molecules on solid-liquid interfaces and in structural studies of new catalysts (see below).<sup>3,9</sup> We are currently testing the applicability of these experiments to the studies of solid biomolecules (**Figure 4**).

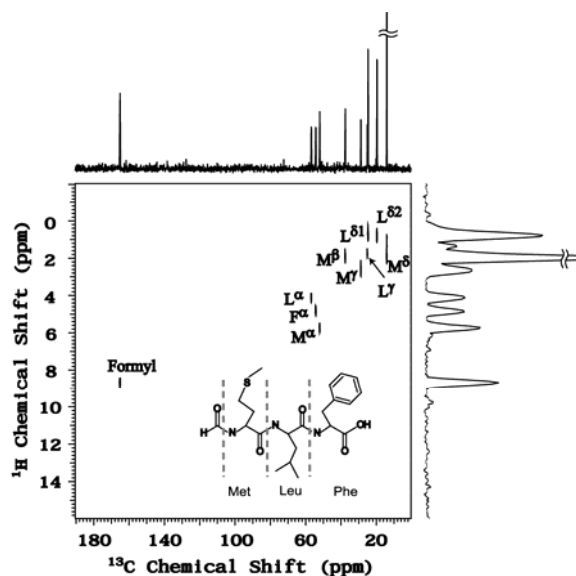


**Figure 4.** 2D <sup>13</sup>C{<sup>1</sup>H} HETCOR spectrum of naturally abundant tripeptide (f-MLF-OH) acquired using INEPT mixing. The experiment was performed using  $\nu_R = 42$  kHz, homonuclear PMLG5 decoupling during  $t_1$  (<sup>1</sup>H) evolution and during INEPT, and low power SPINAL-64 heteronuclear decoupling during <sup>13</sup>C detection.

(b) *MSN-supported rhodium catalysts.* An in-depth solid-state NMR study of MSNs functionalized with rhodium-phosphine ligands showed that covalent attachment of the ligand to the MSN surfaces was successful, and provided structural assignments of the ligand and the MSNs themselves.<sup>9</sup> The assignments were unambiguously determined by employing the indirectly detected <sup>13</sup>C{<sup>1</sup>H} and <sup>31</sup>P{<sup>1</sup>H} experiments, which indicated that oxidation of the attached phosphinosilyl groups and detachment of Rh was enhanced upon syngas conversion. Such structural details of oxidized and non-oxidized phosphine species were indiscernible in conventional 1D NMR experiments.

(c) *Studies of mesoporous frameworks composed of mixed oxides.* We have introduced the RAPT-CPMAS-CPMG NMR experiment, which provided high quality 2D <sup>27</sup>Al-<sup>29</sup>Si HETCOR spectra of aluminosilicates, including a new type of industrial zeolite ZSM-4.<sup>12,13</sup> By separating the resonances in two dimensions, the spectra provided clear indication of random distribution of

aluminum and silicon within the ZSM-4 network. Additionally, unexpected correlations were observed between different components of inhomogeneously broadened  $^{29}\text{Si}$  and  $^{27}\text{Al}$  lines, which are most likely due to differences in the second coordination sphere environments. Similar 1D and 2D techniques will be further developed and exploited to characterize other mesoporous scaffolds composed e.g. of CaO, MgO, MnO, and SrO.

### Future Plans

- *Influence of the mesopore environment on catalyst selectivity and activity.* Our ability to anchor two types of groups on mesopore walls allows us to tether not only the catalyst but also other functional moieties. The influence of these auxiliary groups will be directed toward achieving various catalyst functions, such as enantioselectivity. These studies will use the concept of gatekeepers, which will be tested in the development of catalysts for the stereochemically controlled polymerization, selective hydrolysis, etc.
- *Control of the orientation and activity of tethered transition metal complex catalysts.* In order to understand the activity and selectivity of metal complex catalysts tethered on the walls of mesopores, we will characterize and control the location and the exact structure of the tethered catalysts on the surface.
- *Catalyst characterization.* Solid state NMR techniques will be further developed to better characterize the catalytic surfaces, especially to probe the spatial organization of the surface species and to provide key dynamic information about catalysts that will be prepared and tested during the next stages of this research. We will focus on further exploitation of J-spectroscopy,  $^1\text{H}$ - $^1\text{H}$  decoupling, and the CPMG-based schemes for enhancing the sensitivity.

### Publications (2007-present)

1. S.-G. Wang, C.-W. Wu, K. Chen and V.S.-Y. Lin, "Fine-tuning Mesochannel Orientation of Organically Functionalized Mesoporous Silica Nanoparticles," *Chem. Asian. J.*, DOI: 10.1002/asia.200900015 (2009).
2. E. Szajna-Fuller, Y. Huang, J. L. Rapp, G. Chaka, V. S.-Y. Lin, M. Pruski and A. Bakac, "Kinetics of Oxidation of an Organic Amine With a Cr(V) Salen Complex in Homogeneous Aqueous Solution and on the Surface of Mesoporous Silica," *Dalton Trans.*, DOI: 10.1039/B900043G (2009).
3. K. Mao, J. W. Wiench, V. S.-Y. Lin and M. Pruski, "Indirectly Detected Through-Bond Chemical Shift Correlation NMR Spectroscopy in Solids under Fast MAS: Studies of Organic-Inorganic Hybrid Materials," *J. Magn. Reson.*, 196, 92-95 (2009).
4. V. S.-Y. Lin, "Veni, vidi, vici and then... vanished," *Nat. Mater.*, 8, 252-253 (2009).
5. J. P. Amoureux and M. Pruski, "MQMAS NMR: *Experimental Strategies and Applications*". in Encyclopedia of Magnetic Resonance, eds R. K. Harris and R. Wasylishen, John Wiley: Chichester, DOI: 10.1002/9780470034590.emrstm0211, 2009.
6. D. Zorn, V. S.-Y. Lin, M. Pruski and M. S. Gordon, "An Interface between the Universal Force Field and the Effective Fragment Potential Method," *J. Phys. Chem. B*, 112, 12753-12760 (2008).
7. D. Zorn, V. S.-Y. Lin, M. Pruski and M. S. Gordon, "Comparison of Nitroaldol Reaction Mechanisms Using Accurate Ab Initio Calculations," *J. Phys. Chem. A*, 112, 10635-10649 (2008).
8. J. W. Wiench, V. S.-Y. Lin and M. Pruski, " $^{29}\text{Si}$  NMR in Solid State with CPMG Acquisition under MAS," *J. Magn. Reson.*, 193, 233-242 (2008).

9. J. L. Rapp, Y. Huang, M. Natella, Y. Cai, V. S.-Y. Lin and M. Pruski, "A Solid-State NMR Investigation of the Structure of Mesoporous Silica Nanoparticle Supported Rhodium Catalysts," *Solid State NMR.*, <http://dx.doi.org/10.1016/j.ssnmr.2008.1012.1004> (2008).
10. V. S.-Y. Lin, Y. Huang and Y. Cai, "Mesoporous Silica Nanoparticle-Supported Metal Catalyst for Bioenergy Applications," *Prepr. Symp. - Am. Chem. Soc., Div. Fuel Chem.*, 53, 192-193 (2008).
11. T.-W. Kim, P.-W. Chung, I. I. Slowing, M. Tsunoda, E. S. Yeung and V. S.-Y. Lin, "Structurally Ordered Mesoporous Carbon Nanoparticles as Transmembrane Delivery Vehicle in Human Cancer Cells," *Nano Lett.*, 8, 3724-3727 (2008).
12. G. J. Kennedy, J. W. Wiench and M. Pruski, "Determination of  $^{27}\text{Al}$ - $^{29}\text{Si}$  Connectivities in Zeolites with 2D  $^{27}\text{Al}$ → $^{29}\text{Si}$  RAPT-CPMG-HETCOR NMR," *Solid State NMR.*, 33, 76-81 (2008).
13. G. J. Kennedy, J. W. Wiench and M. Pruski, "Determination of Si-Al Connectivities in Zeolites with 2D Al-Si RAPT CPMAS CPMG HETCOR NMR Techniques," *Stud. Surf. Sci. Catal.*, 174B, 769-774 (2008).
14. Y. Huang, B. G. Trewyn, H.-T. Chen and V. S.-Y. Lin, "One-pot Reaction Cascades Catalyzed by Base- and Acid-Functionalized Mesoporous Silica Nanoparticles," *New J. Chem.*, 32, 1311-1313 (2008).
15. P.-W. Chung, R. Kumar, M. Pruski and V. S.-Y. Lin, "Temperature Responsive Solution Partition of Organic-Inorganic Hybrid Poly(N-isopropylacrylamide)-Coated Mesoporous Silica Nanospheres," *Adv. Funct. Mater.*, 18, 1390-1398 (2008).
16. B. Baird, A. V. Pawlikowski, J. Su, J. W. Wiench, M. Pruski and A. D. Sadow, "Easily Prepared Chiral Scorpionates: Tris(2-oxazolonyl)boratoiridium(I) Compounds and Their Interactions with MeOTf," *Inorg. Chem. (Washington, DC, U. S.)*, 47, 10208-10210 (2008).
17. J. W. Wiench, C. E. Bronnimann, V. S.-Y. Lin and M. Pruski, "Chemical Shift Correlation NMR Spectroscopy with Indirect Detection in Fast Rotating Solids: Studies of Organically Functionalized Mesoporous Silicas," *J. Am. Chem. Soc.*, 129, 12076-12077 (2007).
18. J. W. Wiench, Y. S. Avadhut, N. Maity, S. Bhaduri, G. K. Lahiri, M. Pruski and S. Ganapathy, "Characterization of Covalent Linkages in Organically Functionalized MCM-41 Mesoporous Materials by Solid-State NMR and Theoretical Calculations," *J. Phys. Chem. B*, 111, 3877-3885 (2007).
19. B. G. Trewyn, I. I. Slowing, S. Giri, H.-T. Chen and V. S.-Y. Lin, "Synthesis and Functionalization of a Mesoporous Silica Nanoparticle Based on the Sol-Gel Process and Applications in Controlled Release," *Acc. Chem. Res.*, 40, 846-853 (2007).
20. J. A. Nieweg, C. Kern, B. G. Trewyn, J. W. Wiench, M. Pruski and V. S.-Y. Lin, "Environmentally Friendly Cooperative Acid-Base Mixed Oxide Catalytic Systems for the Synthesis of Biodiesel," *Prepr. - Am. Chem. Soc., Div. Pet. Chem.*, 52, 89-90 (2007).
21. H.-T. Chen, S. Huh and V. S. Y. Lin, "Fine-Tuning the Functionalization of Mesoporous Silica," *Catal. Prep.*, 45-73 (2007).
22. Y. Cai, R. Kumar, W. Huang, B. G. Trewyn, J. W. Wiench, M. Pruski and V. S.-Y. Lin, "Mesoporous Aluminum Silicate Catalyst with Single-Type Active Sites: Characterization by Solid-State NMR and Studies of Reactivity for Claisen Rearrangement Reactions," *J. Phys. Chem. C*, 111, 1480-1486 (2007).
23. J. P. Amoureux, J. Trebosc, J. Wiench and M. Pruski, "HMQC and Refocused-INEPT Experiments Involving Half-integer Quadrupolar Nuclei in Solids," *J. Magn. Reson.*, 184, 1-14 (2007).

## Understanding the Interfacial Structures-Chemistry Relationships in Solid Oxide Fuel Cells (SOFCs)

Postdoc: YongMan Choi  
Students: Harry Abernathy, Kevin Blinn, Matt Lynch, and Lei Yang  
Collaborator: M. C. Lin (Emory University); J. L. Bredas (Chemistry and Biochemistry)  
Contact: Georgia Institute of Technology, 771 Ferst Drive, Atlanta, GA 30332-0245  
Phone: (404) 894-6114; E-mail: [meilin.liu@mse.gatech.edu](mailto:meilin.liu@mse.gatech.edu)

### Goal

Develop a better understanding of the reaction processes at electrode surfaces/interfaces that limit the performance of SOFCs, especially those involving contamination sources: poisoning of the cathode by chromium from metallic interconnect layers, poisoning of the anode from H<sub>2</sub>S contaminants in the fuel gas, and coking on anodes from the use of carbon-containing fuels. Develop *in situ* Raman spectroscopic techniques for probing and mapping new phases and species on electrode surfaces under fuel cell operating conditions, alongside electrochemical measurements to correlate directly with cell performance, as well as mass spectrometry to monitor the immediate chemical environment of an operating cell.

### DOE Interest

Characterizing new phases and surface species involved in electrode processes under fuel cell operating conditions is important to gaining detailed knowledge of interfacial structures and electrode reaction mechanisms, which is vital to achieving rational design of new electrode materials and microstructures for electrochemical devices that are exceptionally efficient in energy storage and conversion. The acquired knowledge may help to develop new materials<sup>[1-3]</sup> for SOFCs that can directly utilize hydrocarbon fuels, coal gas, and other renewable fuels.

### Recent Progress

Work performed in our lab has demonstrated the utility of Raman spectroscopy for studying various SOFC electrode materials and surface/interfacial processes, especially those involving oxygen, sulfur, and carbon.<sup>[4-8]</sup>

**Coking:** Carbon deposition on the anode lends itself readily to *in situ* measurements. All major carbon allotropes (diamond, graphite, graphene, carbon nanotubes, carbon black, diamondlike carbon) are Raman-active. Based on the presence and relative intensity of different first and second order peaks, these phases can be distinguished from one another using Raman spectroscopy. In particular, our sample chamber is mounted on an X-Y-Z motorized stage that can move in 20 nm increments. We have studied the formation of amorphous carbon on various types of anodes: dense and porous Ni/YSZ, patterned Ni and Cu anodes on YSZ substrates. Carbon deposition was detected under methane and propane fuel gases at various temperatures. Figure 1 shows typical spectra collected from a patterned Ni electrode on a YSZ substrate exposed to methane at 625°C for 24 hrs. The SEM micrograph in Figure 1a reveals the presence of carbon spheroids on the Ni surface (the lighter region). We have also demonstrated the capability to monitor the deposition of carbon as a function of time, as shown in Figure 1b. The



Raman map in Figure 1c shows the intensity of the ‘G’ band for carbon at  $1580\text{ cm}^{-1}$  (associated with  $\text{sp}^2$ -bonded carbon). The carbon deposits cover the nickel surface almost entirely.

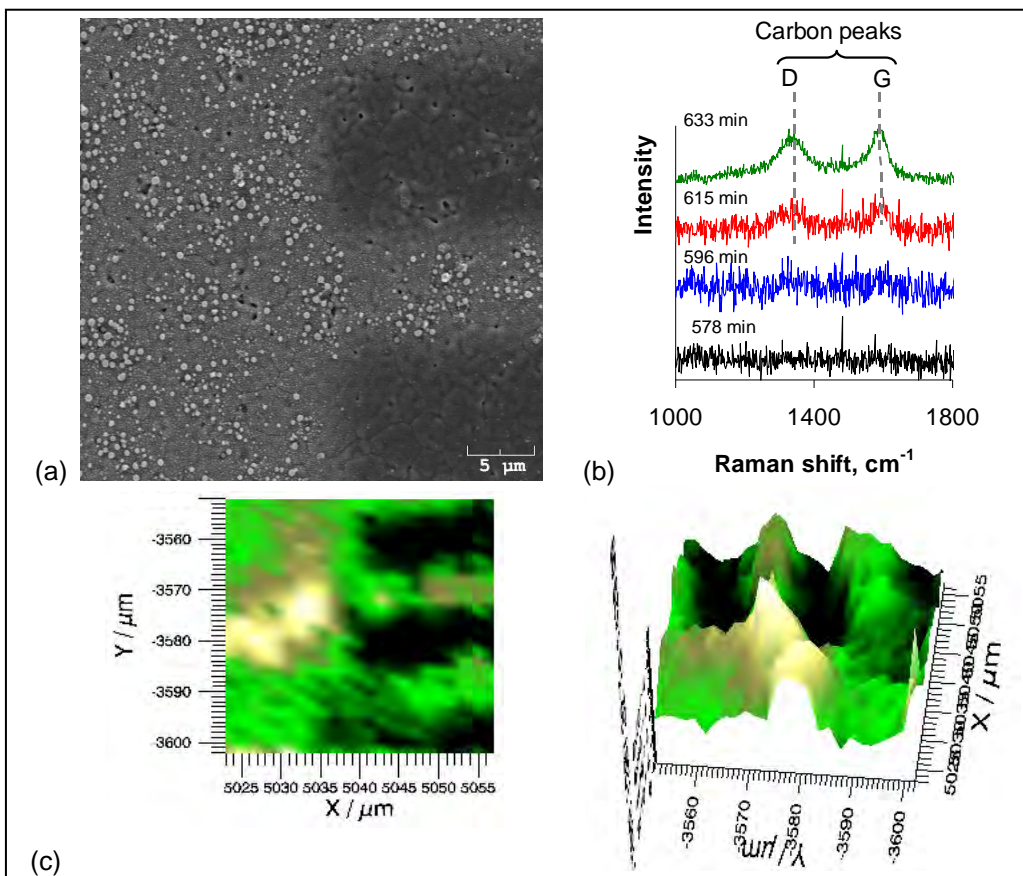


**Figure 1.** A study of carbon deposition on a patterned Ni anode on a YSZ substrate exposed to  $\text{CH}_4$  at  $625^\circ\text{C}$ . (a) SEM micrograph showing carbon particles on the Ni surface (the lighter phase) after 24 hrs exposure to  $\text{CH}_4$ . (b) Raman spectra collected from the Ni surface as a function of time. (c) Raman map of the  $1580\text{ cm}^{-1}$  carbon peak. A lighter shade indicates higher peak intensity.

***A new material with remarkable tolerance to sulfur poisoning and coking:***<sup>[1-3]</sup> We have developed a new material for SOFCs that shows astonishing tolerance to coking and  $\text{H}_2\text{S}$  poisoning. First, it displays the highest ionic conductivity below  $750^\circ\text{C}$  among all SOFC electrolyte materials ever reported, thus allowing fabrication of anode-supported thin-electrolyte SOFCs of high power output at lower temperatures. Second, it exhibits exceptional tolerance to sulfur poisoning – there is no observable change in power output when the fuel is switched to one contaminated with  $\text{H}_2\text{S}$ , which is attributed to its excellent catalytic activity for conversion of  $\text{H}_2\text{S}$  to  $\text{SO}_2$ . Third, it displays significant activity for *in situ* reforming of hydrocarbon fuels, which minimizes the tendency of coking. Finally, it demonstrates adequate chemical and electrochemical stability over a wide range of conditions relevant to SOFC operation, implying long-term stability and long operational life. We have systematically investigated this material as the anode in  $\text{H}_2\text{S}$ -contaminated  $\text{H}_2$  and hydrocarbon fuels. The test cells displayed not only impressive power output in clean hydrogen but also superior tolerance to coking and sulfur poisoning. The new material has great potential to dramatically improve the economical competitiveness and commercial viability of SOFCs that are driven by cost-effective and renewable fuels.

## Future Plans

While a new class of materials have been developed that demonstrate remarkable tolerance to sulfur poisoning and coking, the detailed reaction mechanism is yet to be determined and many scientific questions still remain. We will apply the *in situ* Raman spectroscopic techniques developed in our laboratory under this DOE support to probe and map the active surface sites for the reactions involved in anode operation, to elucidate how and where H<sub>2</sub>S was removed from electrode surfaces, and to clarify how and where hydrocarbons are effectively reformed. Specific tasks to be performed include (1) to probe and map new phases and species adsorbed on electrode surfaces using *in situ* Raman spectroscopy and to monitor the chemical environment of the functional surface using mass spectrometry; (2) to determine electrochemical performance of electrode surfaces using various electrochemical measurements performed on cells with electrodes of well-controlled geometries, alongside *in situ* Raman measurements and *on-line* mass spectrometry; (3) to correlate phenomenological behavior to surface structure/chemistry and to the chemical environment of the functional surface in order to gain a profound understanding of the detailed electrode reaction mechanism and rate-limiting steps of SOFC electrode processes; and (4) to develop and validate predictive models<sup>[10-14]</sup> for electrode processes in order to achieve rational design of better electrode materials and microstructures.

## Publications (2006-2008)

1. L. Yang, C. Zuo, S. Wang, Z. Cheng, and M. Liu, "A Novel Composite Cathode for Low-Temperature SOFCs Based on Oxide Proton Conductors," *Advanced Materials*, **20**(17), 3280-3283, 2008.
2. L. Yang, S. Wang, K. Blinn, M. F. Liu, Z. Liu, Z. Cheng, M. Liu "Remarkable Tolerance to Sulfur Poisoning and Coking of a Mixed Ion Conductor for Solid Oxide Fuel Cells", *Nature*, submitted.
3. Z. Cheng, J. H. Wang, and M. Liu, "Anodes", Chapter 2, in "Solid Oxide Fuel Cells: Materials Properties and Performance", Editors: J. W. Fergus, R. Hui, X. G. Li, D. P. Wilkinson, and J. J. Zhang, CRC Press, p.73-130, 2008.
4. H. Abernathy, E. Koep, C. Compson, Z. Cheng, and M. Liu, "Monitoring Ag-Cr Interactions in SOFC Cathodes Using Raman Spectroscopy," *J. Physical Chemistry C* **112**(34), 13299-13303, 2008.
5. Z. Cheng, H. Abernathy, and M. Liu, "Raman Spectroscopy of Nickel Sulfide Ni<sub>3</sub>S<sub>2</sub>," *Journal of Physical Chemistry C*, **111**, 17997-18000, 2007.
6. K. Blinn, H. Abernathy, and M. Liu, "Surface Enhanced Raman Spectroscopy for Investigation of SOFC Cathodes", *Ceramic Engineering and Science Proceedings*, in press.
7. J. H. Wang, Z. Cheng, J.L. Bredas, and M. Liu, "Electronic and vibrational properties of nickel sulfides from first principles," *Journal of Chemical Physics*, **127**, 214705, 2007.
8. J. H. Wang and M. Liu, "Surface Regeneration of Sulfur-Poisoned Ni surfaces under SOFC Operation Conditions Predicted by First-Principles Based Thermodynamic Calculations," *Journal of Power Sources*, **176**(1), 23-30, 2008
9. S. Choi, J. H. Wang, Z. Cheng, and M. Liu, "Surface modification of Ni-YSZ using niobium oxide for sulfur tolerant anodes in solid oxide fuel cells," *J. Electrochem. Soc.*, **155**(5), B449-B454, 2008.
10. Y. M. Choi, M. C. Lin, M. Liu, "Computational Study on the Catalytic Mechanism toward Oxygen Reduction on La<sub>0.5</sub>Sr<sub>0.5</sub>MnO<sub>3</sub>(110) in SOFCs," *Angewandte Chemie, Int. Ed.*, **46**, 7214, 2007.
11. Y. M. Choi, D. S. Mebane, J. H. Wang, M. Liu, "Continuum and Quantum-Chemical Modeling of Oxygen Reduction on the Cathode in a Solid Oxide Fuel Cell," *Catalysis Today*, **46**, 386-401, 2007.
12. M. E. Lynch, D. S. Mebane, Y. Liu and M. Liu, "Triple Phase Boundary and Surface Transport in Mixed Conducting Patterned Electrodes," *J. Electrochem. Soc.*, **155**(6), B635-B643, 2008.
13. D. S. Mebane, Y. J. Liu, and M. Liu, "Refinement of the Bulk Defect Model for La<sub>x</sub>Sr<sub>1-x</sub>MnO<sub>3±δ</sub>," *Solid State Ionics*, **178**(39-40), 1950-1957, 2008.
14. D. S. Mebane, Y. Liu, M. Liu, "A Two-Dimensional Model and Numerical Treatment for Mixed-Conducting Thin Films: The Effect of Sheet Resistance," *J. Electrochem. Soc.*, **154**, A421, (2007).

**Water-gas-shift Reaction on Metal-oxide Catalysts: a Density Functional Study**

Lead PI: Jose A. Rodriguez

Postdoc: Jesus Graciani

Contact: Department of Chemistry, Brookhaven National Laboratory, Upton, NY11973;  
[pingliu3@bnl.gov](mailto:pingliu3@bnl.gov)

The water-gas-shift reaction (WGS) reaction ( $\text{CO} + \text{H}_2\text{O} \rightarrow \text{H}_2 + \text{CO}_2$ ) is a critical process in providing pure hydrogen for fuel cells and other applications. However, current industrial catalysts (Fe-Cr or Zn-Al-Cu oxides) are pyrophoric and require complex activation steps before usage. A fascinating puzzle has recently emerged: Au(Cu)/CeO<sub>2</sub>(TiO<sub>2</sub>) nanomaterials show very efficient for WGS catalysis. However, the nature of the active phase(s) in these metal-oxide nanocatalysts is unclear at the present time, which impedes the design and optimization of WGS catalysts. To address it, we have made coordinated effects from both experiment and theory. The experiment show that the model catalysts, Au(Cu)/CeO<sub>2</sub>(111) or Au(Cu)/TiO<sub>2</sub>(110) and inverse TiO<sub>2</sub>(CeO<sub>2</sub>)/Au(111), display activities comparable to good WGS catalysts (e.g. Cu(100), Cu(111)) [1-3]. Theoretical calculations based on density functional theory (DFT) are also carried out to understand the active sites in the oxide-metal catalysts, by probing reaction scenarios on Au, Cu, titania, and Au-TiO<sub>2</sub> (Au(Cu)/TiO<sub>2</sub> and TiO<sub>2</sub>/Au(111)) catalyst model structure [1-4]. In accordance with experiment, our calculations show a very high barrier for the dissociation of water on Au and the formation of very stable formate species on titania that prevents the production of H<sub>2</sub> and CO<sub>2</sub>. The model metal-oxide catalyst overcomes these bottlenecks: the moderate chemical activity of metal is coupled to the more reactive oxide. The dissociation of water takes place on the oxide easily, a reaction that are highly activated on extended surfaces and nanoparticles of metal. CO adsorbs on metal sites located nearby (bifunctional catalyst). Then all the subsequent steps occur at the oxide-metal interface at a reasonable speed. Our results imply that the high performances of metal-oxide nanocatalysts in the WGS rely heavily on the direct participation of metal-oxide interface.

**References**

1. J. A. Rodriguez, S. Ma, P. Liu, J. Hrbek, J. Evans, and M. Pérez, "Water-gas shift Reaction on inverse CeO<sub>x</sub>/Au(111) and TiO<sub>x</sub>/Au(111) catalysts: Active role of oxide nanoparticles", *Science*, **318**, 1757 (2007).
2. J. A. Rodriguez, P. Liu, J. Hrbek, J. Evans and M. Pérez, "Water-gas shift reaction on Cu and Au nanoparticles supported on CeO<sub>2</sub>(111) and ZnO(000̄1): intrinsic activity and importance of support interactions", *Angewandte Chemie International Edition*, **46**, 1329 (2007).
3. J. A. Rodríguez, J. Evans, J. Graciani, J. Park, P. Liu, J. Hrbek and J. F. Sanz, "High Water-Gas Shift Activity in TiO<sub>2</sub>(110) supported Cu and Au Nanoparticles: Role of the Oxide and Metal Particle Size", *Journal of Physical Chemistry C*, in press.
4. P. Liu, J. A. Rodriguez, "Water-gas-shift reaction on metal nanoparticles and surfaces" *Journal of Chemical Physics*, **126**, 164705 (2007).

## Novel Photocatalysts with One-Dimensional and Two-Dimensional Nanostructures

**Additional co-PIs:** Douglas Doren

**Students:** Bharat Bhopana, Heather Schmidt, Liu Yang and Tim Lucas

**Contacts:** Center for Catalytic Science and Technology, Department of Chemical Engineering and Department of Chemistry and Biochemistry, University of Delaware, Newark, DE 19716. 302-831-1261, [lobo@udel.edu](mailto:lobo@udel.edu)

**Collaborators:** Prof. Tatyana Polenova, Department of Chemistry and Biochemistry, University of Delaware

### Goal

To develop novel photocatalytic materials capable of using a portion of the visible light spectrum to facilitate the partial and total oxidation of organic compounds in the gas and liquid phase.

### DOE Interest

Semiconductor photocatalysis is one of the most promising approaches for the destruction or transformation of hazardous chemicals. A major emphasis has been centered on TiO<sub>2</sub> photocatalysis as TiO<sub>2</sub> is abundant, inexpensive, and useful in the destruction of many types of substances. Despite its many advantages, TiO<sub>2</sub> has the serious disadvantage that its bandgap (~3.2 eV) is relatively high and only a small fraction of the photons from sunlight are used efficiently (<10%). We are developing novel photocatalyst compositions that have bandgaps below 3.0 eV following evidence by the Domen's group that bimetallic oxy nitrides (and related compounds) have lower bandgaps than their oxide counterparts while maintaining most of their photocatalytic activity.

### Recent Progress

*Synthesis of Zn-Ga ox-y-nitrides from oxide precursors:* Zinc Gallium Oxy Nitrides (ZGONs) have been prepared traditionally by high temperature nitridation of ZnO and Ga<sub>2</sub>O<sub>3</sub> in ammonia. The disadvantage of the current process is the limited control over the zinc content in the final product ZGONs, relatively higher band gaps obtained (2.63 to 3.22 eV) attributable to higher volatilization of zinc (loss of Zn 3d orbitals) from the precursor mixture and low surface areas. The samples we have prepared are similar in composition and properties to others reported in the literature.

*Synthesis of Zn-Ga oxy-nitrides from sol-gel precursors:* Sol-gel methods have been used to synthesize high surface area photocatalysts with controllable band gaps. The advantage of this process is the avoidance of high temperature sample changes like sintering, volatilization etc. In our synthesis zinc-gallium precursors were precipitated from a solution of zinc and gallium nitrate hydrates (the Zn/Ga ratio was varied from 0.5 to 2) in the presence of ammonium hydroxide at pH 7 to 8. The resulting samples were subsequently nitrided in ammonia (250 SCCM) for 15 hours (between 550°C and 850°C).

The precursors obtained from the sol-gel synthesis were a combination of ZnGa<sub>2</sub>O<sub>4</sub> (spinel) and GaOOH phases, the fraction of GaOOH decreasing with increasing Zn/Ga ratios.

The XRD patterns and UV-Vis spectra for the ZGONs obtained by nitridation of Zn/Ga of  $\frac{1}{2}$  are shown in Figure 1. The sample prepared at 850°C was found to be a wurzite with unit cell dimensions of  $a = 0.3215$  nm and  $b = 0.5219$  nm consistent with a solid solution of ZnO and GaN. The ZGON prepared at 550°C is of particular interest: it has a spinel structure (JC PDS # 86-0415) similar to zinc gallate ( $\text{ZnGa}_2\text{O}_4$ ) but with smaller unit cell dimensions (see inset in Figure 1) and has a 40% reduction in band gap compared to zinc gallate. The reduction in band gap for wurzitic ZGONs is attributed to the presence of N orbitals and volatilization of zinc but EDAX for the spinel indicates the final Zn/Ga content to be  $\frac{1}{2}$  and is equal to the maximum value that is possible according to the stoichiometry of  $\text{ZnGa}_2\text{O}_4$ . Furthermore, the sample's BET surface area of  $36 \text{ m}^2/\text{g}$  is comparable to commercial  $\text{TiO}_2$  Degussa P-25 ( $50 \text{ m}^2/\text{g}$ ). To the best of our knowledge, this is the first reported sample of a spinel ZGON with a band gap within the visible light energy range wherein Zn is tetrahedrally and Ga octahedrally coordinated. Further analysis of the sample is presently underway to quantify the presence of N in the sample. The nitrided samples red shift, as expected, with respect to zinc gallate and an increase in temperature leads to a decrease in surface areas from  $114 \text{ m}^2/\text{g}$  (zinc gallate) to  $4 \text{ m}^2/\text{g}$  (850°C sample) due to sintering. The effects of calcination of zinc gallate and post-treatment (2 stage nitridation with excess ZnO) are also being studied.

*Synthesis of Zn-Ga oxynitrides supported on mesoporous silicas:* To increase the surface area of the ZGONs, we are also investigating the effect of supporting the material on mesoporous silica (SBA-15). At this time, we have shown that it is possible to form ZGONs supported on SBA-15 using wet impregnation of zinc nitrate and gallium nitrate hydrate dissolved in ethanol (3% w/w (Zn+Ga)/ $\text{SiO}_2$ ). The support withstands the reaction temperatures (850°C) with a moderate reduction in surface area of  $\sim 25\%$  and maintaining the mesoporosity. Studies are underway to determine the fraction of the ZGONs that is occluded in the pores of the support and to analyze its electronic and photocatalytic properties.

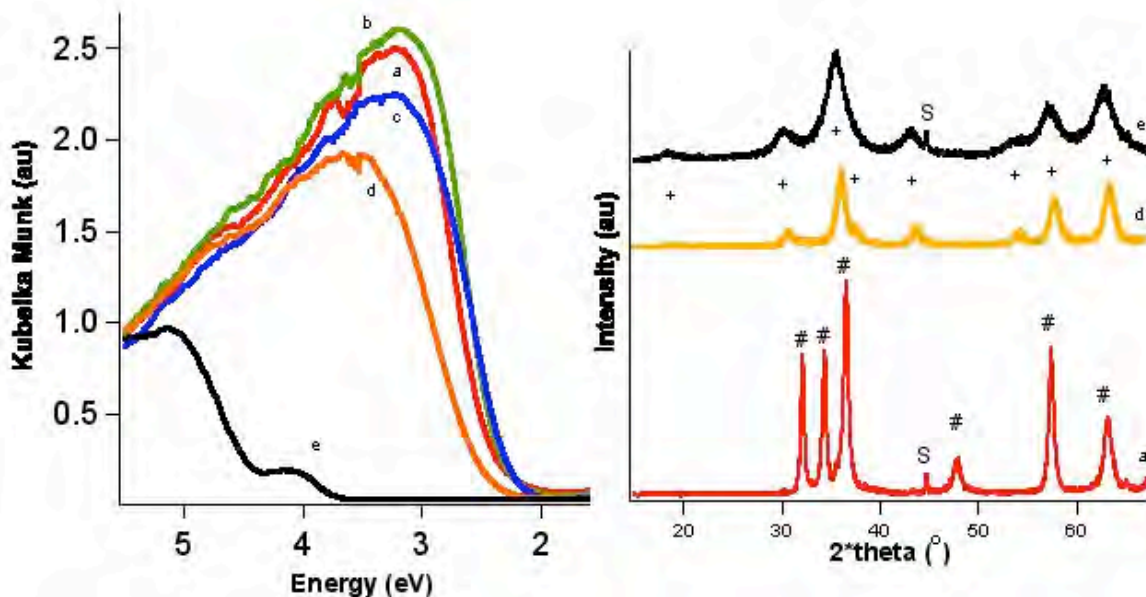


Figure 1: Left panel: UV – Vis spectra of Sol-Gel samples nitrided at 850°C (a), 750°C (b), 650°C (c), 550°C (d). Zinc gallate (e) is given as a reference. Right panel: XRD patterns of selected samples; + and # symbols identify spinel and wurzite reflections respectively. S denotes a peak from the Al sample holder.

## Future Plans

*Synthesis and Testing of Oxynitrides:* We will investigate in more detail the structure of the new spinel oxy nitrides. We will determine if Ga is present in both octahedral and tetrahedral coordination environments using X-ray spectroscopy and we will use NEXAFS to investigate the coordination environment of nitrogen in the sample. The photocatalytic activity of the samples will be measured using the acetaldehyde oxidation reaction on a photoreactor that will be soon completed.

*Electronic Structure Calculations of Mixed-Metal Oxynitrides:* We will investigate the electronic structure of the novel ZGON spinel materials using cluster and periodic models to understand what is the impact of the nitrogen and gallium coordination on the bandgap and potential for photocatalytic activity.

## Publications (2007-2009)

Sole Funding by DOE-BES (this grant)

- (1) Nash, M.; Lobo, R.F.; Rikov, S.; Doren, D.J.; "Photocatalytic Activity of Vanadium-substituted ETS-10", *J. Phys. Chem. C.* **2007** *111*, 7029.
- (2) Shough, A.M., Lobo, R. F., Doren, D. J., "A visible light photocatalyst: effects of vanadium substitution on ETS-10", *Phys. Chem. Chem. Phys.*, **2007** *9*, 5096-5104.
- (3) Shough, A.M.; Doren, D.J.; Nash, M.; Lobo, R.F.; "Effects of vanadium substitution on the structure and photocatalytic behavior of ETS-10", *J. Phys. Chem. C.*; **2007**, *111*, 1776-1782.
- (4) Nash, M.J., Lobo, R. F., Doren, D.J.; "Photocatalytic oxidation of Ethylene by Ammonium Exchanged ETS-10 and AM-5", *Appl. Catal. B, Env. Catal.*, **2009**, 889, 209.

Join Funding by DOE (this grant) and other federal agencies.

- (1) Nash, M. J., Shough, A. M., Fickel, D. W., Doren, D.J., Lobo, R. F., "High Temperature Dehydrogenation of Bronsted Acid Sites in Zeolites", *J. Am. Chem. Soc.*, **2008** *130*, 2460-2462.
- (2) Lobo, R.F., "Chemical Diversity of Zeolite Catalytic Sites", *AIChE J.*, **2008**, *54*, 1402-1409.
- (3) W. Liu, R.H. Wood, D.J. Doren, "Sodium Chloride in Supercritical Water as a Function of Density: Potentials of Mean Force and an Equation for the Dissociation Constant from 723 to 1073 K and from 0 to 0.9 g/cm<sup>3</sup>", *J. Phys. Chem. B.*, **2008**, *112*, 2289.
- (4) Shough, A.M., Doren, D.J., Di Toro, D.M., "Polyfunctional Methodology for Improved DFT Thermodynamical Predictions", *J. Phys. Chem. A.*, **2008**, *112*, 10624.
- (5) Ooms, K, Polenova, T., Shough, A.M., Doren, D.J., Nash, M.J., Lobo R. F., "Identification of mixed valence vanadium in ETS-10 using EPR, 51-V solid-state NMR and DFT studies", *J. Phys. Chem. C.*, submitted (2009).

**Supported Organometallic Complexes: Surface Chemistry, Spectroscopy, Catalysis and Homogeneous Models**

Postdoc: Maximilliano DelFerro  
Graduate students: Brandon Rodriguez, Linda Williams, Staci Wegener, Michael Weberski  
Collaborators: Tim Wenzel, Peter Nickias (Dow Chemical Co.), Ignazio Fragala (U. Catania), Alceo Macchioni (U. Perugia), Scott Collins (U. Akron), Jeremy Kropf, Jeffery Miller, Chris Marshall (Argonne National Laboratory).  
Contact: Department of Chemistry and the Center for Catalysis and Surface Science, Northwestern University, Evanston IL 60208-3113  
[t-marks@northwestern.edu](mailto:t-marks@northwestern.edu) <http://chemgroups.northwestern.edu/marks/>

**Goal**

Elucidate, model, elaborate, tune, and exploit pathways by which mononuclear and polynuclear organometallic molecules undergo chemisorptive activation and catalytic reactivity modifications on solid surfaces. Such processes are closely connected to the function of real-world, large-scale industrial processes and manufacturing cleaner, greener, more environmentally acceptable products, including those from renewal resources. Research combines organometallic synthesis, surface chemistry, homogeneous analogue exploration, catalysis, and computational modeling. This effort involves collaboration with national laboratory and industrial scientists. Specific objectives in the past year were: 1) Understand binuclear organometallic molecule chemisorption on “super Brønsted acid” oxides, 2) Synthesize and characterize mononuclear and polynuclear catalyst precursors for chemisorption and homogeneous catalysis, 3) Characterize the structures, molecular dynamics, and catalytic mechanisms of these species, 4) Computationally model catalytic properties.

**DOE Interest**

The catalyst syntheses, mechanistic studies, and product characterization activities that are the central part of this project relate directly to the efficiency, selectivity, and “greenness” of real-world industrial catalytic processes that are practiced on a huge scale and to the ability of these processes to produce cleaner, more environmentally acceptable products. This includes catalytic processes that use renewable, bio-feedstocks such as Dow’s production of polyethylene from sugar cane in Brazil on a world scale. These multifaceted, highly interdisciplinary projects provide ideal training for young scientists needed as part of a highly skilled U.S. technical workforce.

**Recent Progress**

*Metal Hydrocarbyl Chemisorption on Sulfated Metal Oxide Surfaces:* Electrophilic zirconium surface alkyls are created in very high coverages by chemisorptive protonolysis of group 4-alkyl bonds and these species exhibit very high activity for arene and olefin hydrogenation as well as olefin polymerization. Benzene hydrogenation rates exceed that of any catalyst yet discovered. The kinetics and mechanism were characterized in detail, revealing that ~ 97% of the surface Zr species are catalytically significant--unusual for any heterogeneous catalyst. We expanded this investigation to other sulfated metal oxides and to other mononuclear and binuclear organometallic precursors. Thus, mono- and binuclear “constrained-geometry catalyst” (CGC)

group 4 hydrocarbyls  $\text{Me}_2\text{Si}(\text{Me}_5\text{C}_5)(^t\text{BuN})\text{ZrMe}_2$  [CGCZrMe<sub>2</sub>, **1**], 1-Me<sub>2</sub>Si(3-ethylindenyl)(<sup>t</sup>BuN)ZrMe<sub>2</sub> [EICGCZrMe<sub>2</sub>; **Zr<sub>1</sub>**, **2**],  $(\mu\text{-CH}_2\text{CH}_2\text{-3,3}')\{(\eta^5\text{-indenyl})[1\text{-Me}_2\text{Si}(^t\text{BuN})](\text{ZrMe}_2)_2\}$  [EBICGC(ZrMe<sub>2</sub>)<sub>2</sub>, **Zr<sub>2</sub>**, **3**], and  $(\mu\text{-CH}_2\text{CH}_2\text{-3,3}')\{(\eta^5\text{-indenyl})[1\text{-Me}_2\text{Si}(^t\text{BuN})](\text{TiMe}_2)_2\}$  [EBICGC(TiMe<sub>2</sub>)<sub>2</sub>, **Ti<sub>2</sub>**, **4**] undergo rapid chemisorption on highly Brønsted acidic sulfated alumina (AIS) surfaces. <sup>13</sup>C CPMAS NMR spectroscopy of the chemisorbed <sup>13</sup>C<sub>α</sub>H<sub>3</sub>-enriched complexes EICGCZr<sup>13</sup>Me<sub>2</sub>/AIS (**2\*/AIS**) and EBICGC(Zr<sup>13</sup>Me<sub>2</sub>)<sub>2</sub>/AIS (**3\*/AIS**) reveals that chemisorption involves two processes, M-C σ-bond protonolysis at the strong surface Brønsted acid sites, as well as heterolytic M-C scission with methide transfer to strong surface Lewis acid sites, forming similar “cation-like” electrophilic organo-group 4 complexes such as EICGCM<sup>13</sup>Me<sup>+</sup>. Relative rates of ethylene homopolymerization mediated by the catalysts prepared via chemisorption on AIS are **4/AIS** > **2/AIS** > **3/AIS** > **1/AIS**, for ethylene polymerization at 75 psi ethylene and 25°C. Ethylene/1-hexene copolymerizations mediated by the same set of catalysts display relative polymerization rates of **4/AIS** > **3/AIS** > **2/AIS** > **1/AIS**, for copolymerizations at 75 psi ethylene, 0.8 M 1-hexene, and 25°C. EXAFS studies are underway in collaboration with Drs. Neng Guo, Jeff Miller, Jeremy Kropf, and Chris Marshall at Argonne National Laboratory. For Cp\*ZrMe<sub>3</sub>/AIS, in which ~ 95% of the Zr sites are catalytically active, the Cp\*ZrMe<sub>2</sub><sup>+</sup> cation essentially “floats” above the AIS<sup>-</sup> anion with *very weak* ion pairing.

*Theoretical Studies:* To better understand the above chemisorption and catalytic chemistry, we focused on the catalytic properties of the organozirconium precatalyst Cp<sub>2</sub>Zr(CH<sub>3</sub>)<sub>2</sub> chemisorbed on dehydroxylated γ-alumina (Al<sub>2</sub>O<sub>3</sub>), as analyzed via density functional theory. The interactions of the catalytically active cationic Cp<sub>2</sub>ZrCH<sub>3</sub><sup>+</sup> adsorbate species are scrutinized at two possible model Al<sub>2</sub>O<sub>3</sub> (110) surface sites, namely μ<sub>2</sub>-O and μ<sub>3</sub>-O, representing the principal reactive species on the alumina surface. It is found that zirconocenium coordination occurs via two different geometries (dioxo-bridged and oxo-bridged) at both the μ<sub>3</sub>-O and μ<sub>2</sub>-O surface sites. This process is compared to that for forming the related homogeneous phase Cp<sub>2</sub>ZrCH<sub>3</sub><sup>+</sup>H<sub>3</sub>CB(C<sub>6</sub>F<sub>5</sub>)<sub>3</sub><sup>-</sup> ion pair structure. It is found that the interaction of the Cp<sub>2</sub>ZrCH<sub>3</sub><sup>+</sup> adsorbate species with the μ<sub>2</sub>-O sites is far stronger than with the μ<sub>3</sub>-O sites due to the greater unsaturation of the former. Furthermore, the interaction with the μ<sub>3</sub>-O sites is weaker than in the parent homogeneous ion pair. The catalytic activity of the chemisorbed Cp<sub>2</sub>ZrCH<sub>3</sub><sup>+</sup> systems for ethylene polymerization is investigated at both μ<sub>2</sub>-O and μ<sub>3</sub>-O sites and compared with the analogous Cp<sub>2</sub>ZrCH<sub>3</sub><sup>+</sup>H<sub>3</sub>CB(C<sub>6</sub>F<sub>5</sub>)<sub>3</sub><sup>-</sup> - mediated process in solution. A Cossee enchainment mechanism proceeds via ethylene π-complex formation and an α-agostic assisted transition state to yield γ- and β- agostic insertion products. The overall kinetics of enchainment are closely correlated with the energetics of π-complex formation, and it is suggested that the differing kinetic behaviors of the surface-bound Cp<sub>2</sub>ZrR<sup>+</sup> species on the various Al<sub>2</sub>O<sub>3</sub> coordination sites and the analogous homogeneous species reflect differences in the olefin π-complex stabilization energies. These computational results agree well with the experimental data which indicate that only fractions of the surface bound species are catalytically significant, but that these are far more catalytically active than the homogeneous analogues.

In theoretical work complementary to the nuclearity studies reported below, we focused on the distinctive center-to-center cooperative catalytic properties exhibited by bimetallic “constrained geometry catalysts” (CGCs), and analyzes metal-metal proximity effects on ethylene polymerization processes mediated by  $(\mu\text{-CH}_2\text{-3,3}')\{(\eta^5\text{-indenyl})[1\text{-H}_2\text{Si}(^t\text{BuN})](\text{ZrMe}_2)_2\}$  (**Zr<sub>2</sub>**)



-derived catalysts using density functional theory. Precatalyst geometries were first analyzed, and then ion pair formation/heterolytic dissociation processes involving the binuclear bisborane cocatalyst 1,4-(C<sub>6</sub>F<sub>5</sub>)<sub>2</sub>BC<sub>6</sub>F<sub>4</sub>B(C<sub>6</sub>F<sub>5</sub>)<sub>2</sub> (**BN**<sub>2</sub>), were analyzed and compared with those in the parent mononuclear analogue. It is found that on proceeding from the mononuclear to binuclear catalyst system, ion-pair dissociation energies increase due to the stronger catalyst center-counteranion interactions. Moreover, in the binuclear case, the interaction energies are markedly sensitive to geometrical matching between the binuclear bisborane and the precatalyst Zr-methyl positions. Binuclear catalytic effects between the metal centers are then explored, with the specific contribution from the proximity of the second metal center. Possible agostic interactions of  $\alpha$ -alkenes  $\pi$ -coordinated to one Zr center with the second Zr center of the binuclear catalyst are scrutinized for the case of 1-octene. It is argued that these agostic interactions are at least partly responsible for the unusual enchainment properties of the bimetallic catalysts. In particular, the greater polyethylene product branch densities found experimentally for the bimetallic catalysts can be correlated with an intramolecular reinsertion process, assisted by agostic interactions. Moreover, these same agostic interactions involving a chain growing at one metal site with the second metal site of the binuclear catalyst, modify the environment to increase propagation/termination rate ratios, in turn favoring increased product molecular weight ( $M_n$ ). These effects are observed experimentally at closer Zr...Zr proximities in olefin polymerizations mediated by binuclear CGC catalysts.

*Nuclearity Effects on Single-Site Polymerization Catalyst Structure, Activity, and Selectivity:* For electrophilic cation-anion ion-paired catalyst systems, nuclearity effects on enchainment rates, chain transfer processes, and catalyst stability/longevity can be significant, reflecting subtle non-covalent, cation-anion interaction/-molecular recognition effects. As part of our continuing effort to elucidate and enhance interactions between proximate single-site polymerization catalyst centers, we studied the homopolymerization of styrene and the copolymerization of ethylene and styrenic comonomers mediated by the single-site bimetallic “constrained geometry catalysts” (CGCs), ( $\mu$ -CH<sub>2</sub>CH<sub>2</sub>-3,3') $\{(\eta^5$ -indenyl)[1-Me<sub>2</sub>Si(<sup>t</sup>BuN)](TiMe<sub>2</sub>)<sub>2</sub> [EBICGC(TiMe<sub>2</sub>)<sub>2</sub>; **Ti**<sub>2</sub>], ( $\mu$ -CH<sub>2</sub>CH<sub>2</sub>-3,3') $\{(\eta^5$ -indenyl)[1-Me<sub>2</sub>Si(<sup>t</sup>BuN)](ZrMe<sub>2</sub>)<sub>2</sub> [EBICGC(ZrMe<sub>2</sub>)<sub>2</sub>; **Zr**<sub>2</sub>], ( $\mu$ -CH<sub>2</sub>-3,3') $\{(\eta^5$ -indenyl)[1-Me<sub>2</sub>Si(<sup>t</sup>BuN)](TiMe<sub>2</sub>)<sub>2</sub> [MBICGC(TiMe<sub>2</sub>)<sub>2</sub>; **C1-Ti**<sub>2</sub>], and ( $\mu$ -CH<sub>2</sub>-3,3') $\{(\eta^5$ -indenyl)[1-Me<sub>2</sub>Si(<sup>t</sup>BuN)](ZrMe<sub>2</sub>)<sub>2</sub> [MBICGC(ZrMe<sub>2</sub>)<sub>2</sub>; **C1-Zr**<sub>2</sub>], in combination with the borate activator/cocatalyst Ph<sub>3</sub>C<sup>+</sup>B(C<sub>6</sub>F<sub>5</sub>)<sub>4</sub><sup>-</sup> (**B**<sub>1</sub>). Under identical styrene homopolymerization conditions, **C1-Ti**<sub>2</sub> + **B**<sub>1</sub> and **Ti**<sub>2</sub> + **B**<sub>1</sub> exhibit ~ 65 and ~ 35 times greater polymerization activities, respectively, than does monometallic [1-Me<sub>2</sub>Si(3-ethylindenyl)(<sup>t</sup>BuN)]TiMe<sub>2</sub> (**Ti**<sub>1</sub>) + **B**<sub>1</sub>. **C1-Zr**<sub>2</sub> + **B**<sub>1</sub> and **Zr**<sub>2</sub> + **B**<sub>1</sub> exhibit ~ 8 and ~ 4 times greater polymerization activities, respectively, than does the monometallic control [1-Me<sub>2</sub>Si(3-ethylindenyl)(<sup>t</sup>BuN)]ZrMe<sub>2</sub> (**Zr**<sub>1</sub>) + **B**<sub>1</sub>. NMR analyses show that the bimetallic catalysts suppress the regiochemical insertion selectivity exhibited by the monometallic analogues. In ethylene copolymerization, **Ti**<sub>2</sub> + **B**<sub>1</sub> enchains 15.4% more styrene (**A**), 28.9% more 4-methylstyrene (**B**), 45.4% more 4-fluorostyrene (**C**), 41.2% more 4-chlorostyrene (**D**), and 31.0% more 4-bromostyrene (**E**) than does **Ti**<sub>1</sub> + **B**<sub>1</sub>. This observed bimetallic chemoselectivity effect follows the same general trend as the electron density on the styrenic *ipso* carbon (**C** > **D** > **E** > **B** > **A**). Kinetic studies reveal that both **Ti**<sub>2</sub> + **B**<sub>1</sub> and **Ti**<sub>1</sub> + **B**<sub>1</sub>-mediated ethylene + styrene copolymerizations follow second-order Markovian statistics and tend to be alternating. Moreover, calculated reactivity ratios indicate that **Ti**<sub>2</sub> + **B**<sub>1</sub> favors styrene insertion more than does **Ti**<sub>1</sub> + **B**<sub>1</sub>. All the organozirconium complexes (**C1-Zr**<sub>2</sub>,

**Zr<sub>2</sub>**, and **Zr<sub>1</sub>**) are found to be incompetent for ethylene + styrene copolymerization, yielding only mixtures of polyethylene and polystyrene. Model compound ( $\mu$ -CH<sub>2</sub>CH<sub>2</sub>-3,3') $\{(\eta^5$ -indenyl)[1-Me<sub>2</sub>Si(<sup>t</sup>BuN)][Ti(CH<sub>2</sub>Ph)<sub>2</sub>]<sub>2</sub> {EBICGC[Ti(CH<sub>2</sub>Ph)<sub>2</sub>]<sub>2</sub>} was designed, synthesized, and characterized. In situ activation studies with cocatalyst B(C<sub>6</sub>F<sub>5</sub>)<sub>3</sub> suggest an  $\eta^1$ -coordination mode for the benzyl groups, thus supporting the proposed mechanism. For ethylene + styrene copolymerization, polar solvents are found to increase copolymerization activities and coproduce atactic polystyrene impurities in addition to ethylene-co-styrene, without diminishing the comonomer incorporation selectivity. Both homopolymerization and copolymerization results argue that substantial cooperative effects between catalytic sites are operative.

The synthesis and characterization of the bimetallic 2,7-di-[(2,6-diisopropylphenyl)imino]-1,8-naphthalenediolato group 10 metal polymerization catalysts {[Ni(CH<sub>3</sub>)<sub>2</sub>][1,8-(O)<sub>2</sub>C<sub>10</sub>H<sub>4</sub>-2,7-[CH=N(2,6-<sup>i</sup>Pr<sub>2</sub>C<sub>6</sub>H<sub>3</sub>)](PMe<sub>3</sub>)<sub>2</sub>]} and {[Ni(1-naphthyl)]<sub>2</sub>[1,8-(O)<sub>2</sub>C<sub>10</sub>H<sub>4</sub>-2,7-[CH=N(2,6-<sup>i</sup>Pr<sub>2</sub>C<sub>6</sub>H<sub>3</sub>)](PPh<sub>3</sub>)<sub>2</sub>]} [**FI<sup>2</sup>-Ni<sub>2</sub>(PR<sub>3</sub>)<sub>2</sub>**] were realized, along with the synthesis and characterization of the mononuclear analogues {Ni(CH<sub>3</sub>)[3-<sup>t</sup>Bu-2-(O)C<sub>6</sub>H<sub>3</sub>CH=N(2,6-<sup>i</sup>Pr<sub>2</sub>C<sub>6</sub>H<sub>3</sub>)](PMe<sub>3</sub>)<sub>3</sub>} and {Ni(1-naphthyl)[3-<sup>t</sup>Bu-2-(O)C<sub>6</sub>H<sub>3</sub>CH=N(2,6-<sup>i</sup>Pr<sub>2</sub>C<sub>6</sub>H<sub>3</sub>)](PPh<sub>3</sub>)<sub>3</sub>} [**FI-Ni (PR<sub>3</sub>)**]. Monometallic Ni catalysts were also prepared by functionalizing one ligation center of the bimetallic ligand with a trimethylsilyl group (TMS), yielding {Ni(CH<sub>3</sub>)[1,8-(O)(TMSO)C<sub>10</sub>H<sub>4</sub>-2,7-[CH=N(2,6-<sup>i</sup>Pr<sub>2</sub>C<sub>6</sub>H<sub>3</sub>)](PMe<sub>3</sub>)<sub>2</sub>]} [**TMS-FI<sup>2</sup>-Ni(PMe<sub>3</sub>)**]. The **FI<sup>2</sup>-Ni<sub>2</sub>** catalysts exhibit significant increases in ethylene homopolymerization activity versus the monometallic analogues, as well as increased branching and methyl branch selectivity, even in the absence of a Ni(cod)<sub>2</sub> cocatalyst. Increasing ethylene concentrations significantly suppresses branching and branch morphology. **FI<sup>2</sup>-Ni<sub>2</sub>**-mediated copolymerizations with ethylene + polar-functionalized norbornenes exhibit a four-fold increase in comonomer incorporation versus **FI-Ni**, yielding copolymers with up to 10% norbornene copolymer incorporation. **FI<sup>2</sup>-Ni<sub>2</sub>**-catalyzed copolymerizations with ethylene + methylacrylate or methyl methacrylate incorporate up to 11% acrylate comonomer, while the corresponding mononuclear **FI-Ni** catalysts incorporate negligible amounts. Furthermore, the **FI<sup>2</sup>-Ni<sub>2</sub>**-mediated polymerizations exhibit appreciable polar solvent tolerance, turning over in the presence of ethyl ether, acetone, and even water. The mechanism by which the present cooperative effects take place was investigated, as was the nature of the copolymer microstructures produced.

## Future Plans

In the area of novel supports for group 4 mononuclear and binuclear molecule-based catalysts, we will investigate supports claimed to be even more Brønsted acidic sulfated metal oxides, seeking catalytic effects only possible via the agency of an adjacent catalytic center. Thus, a variety of binuclear catalyst precursors will be chemisorbed and studied. Structural characterization will include <sup>13</sup>C CPMAS NMR and EXAFS/XANES studies at ANL, with attempts at operando studies of catalysts turning over and/or being inhibited. In this regard, systems with virtually 100% active sites present a unique opportunity. We also plan to continue our investigations of cooperative effects in homogeneous binuclear group 10 catalysts, focusing on transformations that are normally exceeding difficult by virtue of steric congestion and/or unfavorable substrate basicity. Catalysts will include Ni<sub>2</sub>, Pd<sub>2</sub>, and heterobinuclear NiPd and group 4- group 10 systems.

### Publications (2007-2009)

1. Roberts, J.A.S.; Chen, M.-C.; Seyam, A.M.; Li, L.; Zuccaccia, C.; Stahl, N.G.; Marks, T.J. Diverse Stereocontrol Effects Induced by Weakly Coordinating Anions. Mono- and Polynuclear Halo-Perfluoroarylmethylates as Cocatalysts for Stereospecific Olefin Polymerization at Archetypal  $C_3$ - and  $C_7$ -Symmetrical Catalysts, *J. Am. Chem. Soc.* **2007**, *129*, 12713-12733.
2. Motta, A.; Fragala, I.L.; Marks, T.J. Stereochemical Control Mechanisms in Propylene Polymerization Mediated by  $C_7$ -Symmetric CGC Titanium Catalyst Centers, *J. Amer. Chem. Soc.* **2007**, *129*, 7327-7338.
3. Guo, N.; Stern, C.L.; Marks, T.J. Bimetallic Effects in the Homopolymerization of Styrene and Copolymerization of Ethylene and Styrenic Comonomers. Scope, Kinetics, and Mechanism, *J. Am. Chem. Soc.* **2008**, *130*, 2246-2261.
4. Amin, S.B.; Marks, T.J. Versatile Routes to In Situ Polyolefin Functionalization with Heteroatoms. Catalytic Chain Transfer, *Angew. Chem. Int. Ed.*, **2008**, *47*, 2006-2025.
5. Amin, S.B.; Marks, T.J. Organo- $f^n, d^0$ -Mediated Synthesis of Amine-Capped Polyethylenes. Scope and Mechanism, *Organometallics*, **2008**, *27*, 2411-2420.
6. Motta, A.; Fragala, I.L.; Marks, T.J. Pathways for Chemisorptive Organozirconium Catalyst Activation and Reactivity on Oxide Surfaces. A DFT Study for Dehydroxylated  $\gamma$ -Alumina, *J. Am. Chem. Soc.*, **2008**, *130*, 16533-16546.
7. Rodriguez, B.A.; Delferro, M.; Marks, T.J. Neutral Bimetallic Ni(II) Phenoxyiminato Catalysts for Highly Branched Polyethylenes and Ethylene-Norbornene Copolymerizations, *Organometallics*, **2008**, *27*, 2166-2168.
8. Motta, A.; Fragala, I.L.; Marks, T.J. Proximity and Cooperativity Effects in Binuclear  $d^0$  Olefin Polymerization Catalysts. Theoretical Analysis of Structure and Mechanism, *J. Amer. Chem. Soc.*, **2009**, *131*, 3974-3984.
9. Rodriguez, B.A.; Delferro, M.; Marks, T.J. Neutral Binuclear Nickel Catalysts for Ethylene Polymerization in Polar Media and Ethylene Copolymerization with Functionalized Polar Comonomers, *J. Amer. Chem. Soc.*, **2009**, *131*, ASAP.
10. Williams, L.A.; Marks, T.J. Chemisorption Pathways and Catalytic Olefin Polymerization Properties of Group 4 Mono- and Binuclear Constrained Geometry Complexes on Highly Acidic Sulfated Alumina, *Organometallics*, **2009**, *28*, ASAP.
11. Rodriguez, B.A.; Weberski, M.P.; Marks, T.J. Neutral Heterobimetallic Ni/Pd Catalysts for Ethylene-co-Methyl Methacrylate Polymerization and Block Copolymer Synthesis, submitted.

## Structure/Composition/Function Relationships in Supported Nanoscale Catalysts for Oxidative Hydrolysis Cellulose to Monosaccharide Sugars and their Derivatives

Additional PIs: Stefan Vajda; Jeffrey Elam  
 Postdoc: Weiling Deng; Sungsik Lee  
 Contacts: Argonne National Laboratory  
 9700 S. Cass Avenue, Argonne, IL 60439  
[marshall@anl.gov](mailto:marshall@anl.gov)

### Goal

Investigate the fundamentals of selective oxidation of glycosidic-like bonds. Model compounds with appropriate C-O-C linkages are used to understand the reaction pathways and changes in catalyst morphology that lead to the oxidative breakdown of this key bond.

### DOE interest

Renewable biofuel and chemical production from the degradation of biomass (such as cellulose) is one of the grand challenges. However, the chemical steps involved in the oxidative hydrolysis of cellulose to monosaccharide sugars and their derivatives are not understood. Improving our fundamental understanding of composition/structure/function relationships in supported, heterogeneous catalysts for reactions that oxidatively convert cellulose to monosaccharide sugars will help overcome the current technology difficulty.

### Recent Progress

#### *Nanometer Metal Catalyst Preparation by Atomic Layer Deposition (ALD)*

Catalytic nanolith samples beginning with nanostructured templates consisting of anodic aluminum oxide (AAO) membranes are fabricated with 60nm uniform pore size. These AAO membranes are then coated using ALD to have a series of functional layers. Figure 1 is an example of Pd ALD synthesis. During this nucleation period, the Pd ALD initiates on a small number of discrete sites, and proceeds via growth and coalescence of the Pd islands. The Pd loading increases much more rapidly on the ZnO substrate than on the Al<sub>2</sub>O<sub>3</sub> substrate. Pd ALD has been shown to have a very long nucleation period on Al<sub>2</sub>O<sub>3</sub> surfaces.

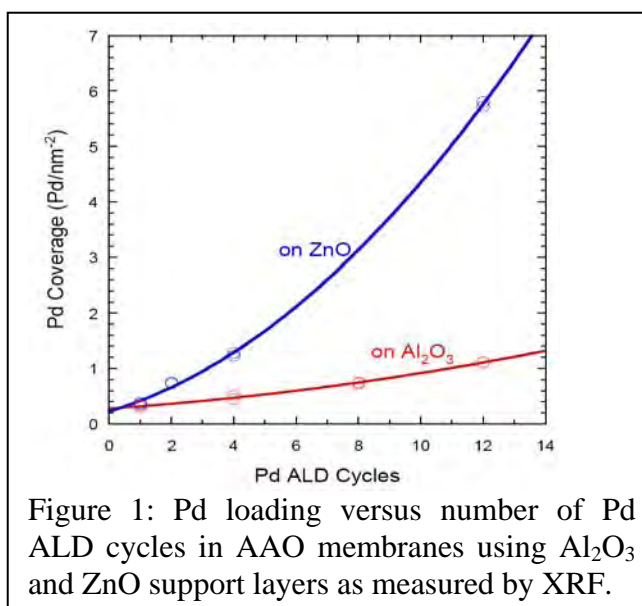


Figure 1: Pd loading versus number of Pd ALD cycles in AAO membranes using Al<sub>2</sub>O<sub>3</sub> and ZnO support layers as measured by XRF.

### Sub-nanometer Co Clusters Preparation by Cluster Deposition (CD)

In addition to well defined size of the nanoclusters, the CD technique can precisely control the location of the clusters at either the entrance or exit of the AAO nanochannels. This enables straightforward studies of the effect of the contact times on catalytic activity and tuning selectivity. Figure 2 shows how the  $\text{Co}_{17-33}$  clusters were prepared by this technique.

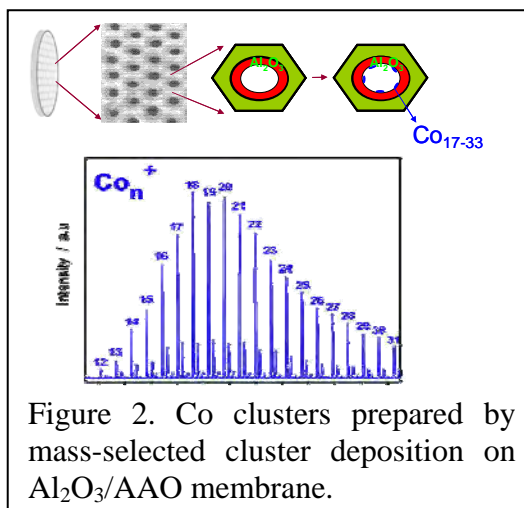
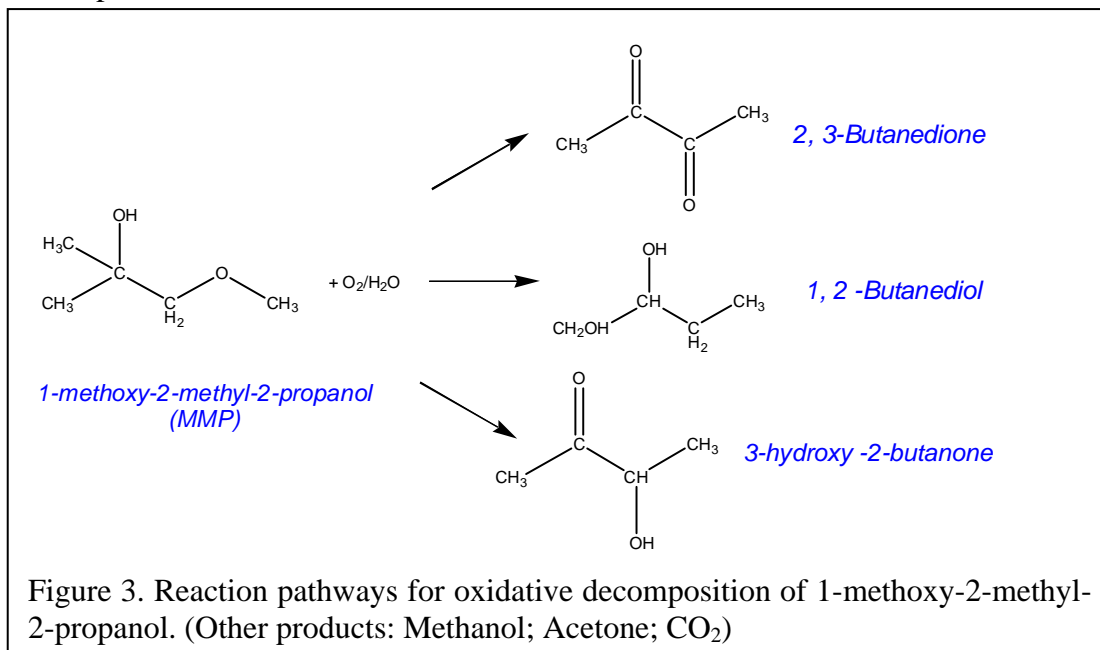


Figure 2. Co clusters prepared by mass-selected cluster deposition on  $\text{Al}_2\text{O}_3/\text{AAO}$  membrane.

### C-O-C Bond Cleavage

The probe molecule in our work is 1-methoxy-2-methyl-2-propanol (MMP). Products from the C-O-C bond cleavage have been identified by GC-MS, as shown in Figure 3. Catalytic studies of support effect ( $\text{Al}_2\text{O}_3$ , ZnO), metal effect (Pd, Pt,  $\text{VO}_x$ , Co) and preparation effect (ALD and CD) in the oxidative MMP hydrolysis reaction have been completed.



### Contact vs. Selectivity

As shown in Figure 4, Co clusters placed at the gas entrance yield more secondary products while those placed at the exit create more primary products, indicating the effects of re-adsorption versus single contact on product selectivity.

## Future Plans

### *Nucleation of Metals on Metal Oxides*

The nucleation of ALD metals on metal oxides is not well understood, but is extremely relevant to catalyst synthesis because it will control both the size and the loading of the metal clusters on the surface. We will prepare additional samples of ALD Pt and Pd on different oxide surfaces and examine the coating process using XAS, XRF, SEM, AFM, and

other techniques. More detailed studies of CD coverage and support effects in the breakdown of cellulose precursors with the goal to determine optimal catalyst size and composition and support chemistry.

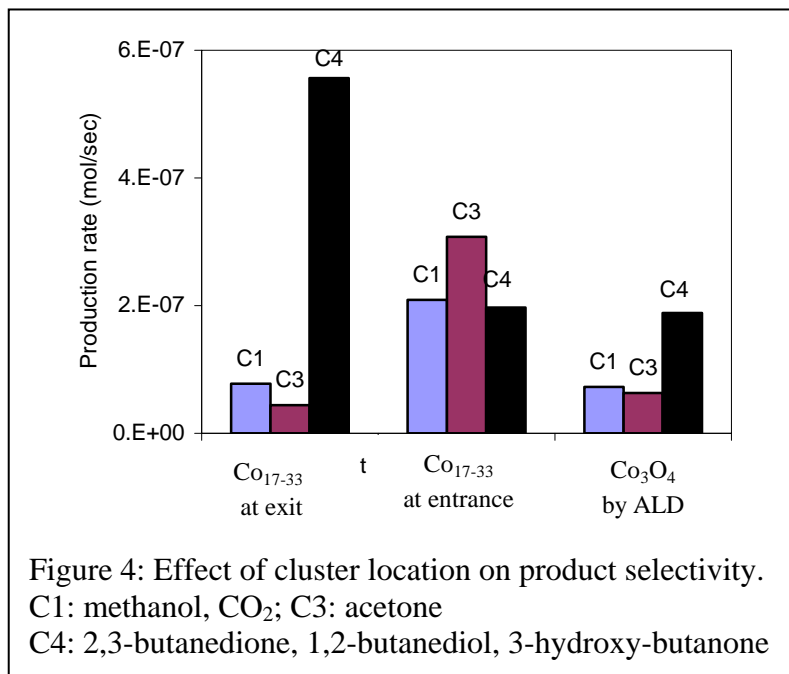


Figure 4: Effect of cluster location on product selectivity. C1: methanol, CO<sub>2</sub>; C3: acetone C4: 2,3-butanedione, 1,2-butanediol, 3-hydroxy-butanone

### *Other Model Compounds C-O-C Bond Cleavage*

The catalytic systems identified in previous work in the C-O-C bond breakage will be further studied to determine how to improve the selectivity. Detailed studies using other model compounds will help identify key reaction pathways.

### *Oxidative Hydrolysis vs. Direct Hydrolysis*

Reaction pathway analysis will be accomplished to compare two reaction systems: using oxygen and water in the feed gas vs. water only.

## Publications (2007-2009)

1. W. Deng, S. Vajda, S. Lee, J. A. Libera, J. W. Elam, C. L. Marshall, "Cobalt clusters reactivity in C-O bond breakage", in preparation, March 2009.
2. W. Deng, S. Lee, S. Vajda, J. A. Libera, J. W. Elam, C. L. Marshall, 21<sup>st</sup> North American Catalysis Society, "Oxidative Decomposition of Cellulosic Materials", June 9, 2009.
3. W. Deng, S. Lee, S. Vajda, J. A. Libera, J. W. Elam, C. L. Marshall, 2009 Spring Symposium, Catalysis Club of Chicago, "C-O-C bond cleavage in oxidative hydrolysis of cellulosic materials", May 18, 2009.
4. W. Deng, S. Lee, S. Vajda, J. A. Libera, J. W. Elam, C. L. Marshall, 2008 Argonne Postdoctoral Symposium, "Oxidative Decomposition of Cellulosic Materials", September 11, 2008.

## Investigations of Electronic Promotion of C-x Bond Transformations

**Undergraduate Students:** Roy Kerney, Christie Rei

**Graduate Students:** Wei Tang

**Post Docs:** Jung-Nam Park, Zhenpeng Hu

**Collaborator:** Raj Pala (IIT, Kanpur, India)

**Contacts:** Professor Eric McFarland (805-8934343, mcfar@engineering.ucsb.edu), Dept. of Chemical Engineering, Professor Horia Metiu (805-8932256, metiu@chem.ucsb.edu), Dept. of Chemistry and Biochemistry, University of California, Santa Barbara, CA 93106

### Overall Goals:

To create and characterize experimentally the activity of new catalysts, predicted by density functional theory, capable of activating C-x bonds. This joint experimental-theory project is aimed at the controlled activation of the C-H bond for the partial oxidation and oxidative dehydrogenation of methane, propane, and propene.

### DOE Interest:

Understanding and controlling hydrocarbon reactivity is essential for developing technical strategies to improve and optimize existing processes and develop new routes for the production of fuels and chemicals. Doped oxides, in which a few cations in a host oxide are replaced with heteroatoms, are interesting new catalysts for alkane activation. Very few have been studied and it is very likely that among so many possible dopant/oxide combinations there are some dopant-host pairs that can break efficiently the C-H bond in methane, propane or propene, to initiate useful partial oxidation or oxidative dehydrogenation chemistry.

### Recent Progress:

#### 1. DFT based calculations to determine the ability of various doped oxides to break the C-X bond:

Oxidation with oxygen on metal oxides traditionally proceeds through a Mars-van Krevelen (MVK) pathway whereby the metal oxide surface supplies oxygen atoms to the reductant through formation of a surface oxygen vacancy and gas phase oxygen refills the vacancies. Using a combination of theory and experiments, we showed that ZnO (in itself inactive) substitutionally doped with Ti or Al promotes the adsorption and activation of dioxygen on the Ti sites for reaction with CO. The proposed mechanisms were supported by density functional theory calculations and by experiments involving isotopically labeled dioxygen. (manuscript submitted to J. Cat. Jan 2009).

Electrophilic Pt atoms were used as atomic dopants in ceria hosts to improve the oxidative power of the oxygen atoms of the host oxide. Whereas complete combustion of methane in oxygen occurs on supported Pt catalysts, high selectivity for the partial oxidation of methane to CO and H<sub>2</sub> was achieved on Pt-doped CeO<sub>2</sub>. The critical step in facilitating synthesis gas formation is the decrease in oxygen vacancy formation energy caused by the Pt doping of CeO<sub>2</sub>. (manuscript to be submitted May 2009).

(i) Doped ZnO for CO oxidation

We have performed state-of-the-art density functional calculations building on our prior work [10] where we found that doping ZnO with Ti, V, Zr, Nb, Hf, Ta or W increased substantially the energy required for making an oxygen vacancy at the surface of the oxide. These dopants, whose preferred valence is higher than that of Zn, are not satisfied with the number of oxygen atoms surrounding them and compensate by binding the neighboring oxygen more strongly. Our recent calculations (submitted to J. Cat.) show that such dopants adsorb O<sub>2</sub> from the gas-phase. If their valence is satisfied by binding to one additional O atom then the system will be inclined, after adsorbing an O<sub>2</sub> molecule, to provide the other oxygen atom for an oxidation reaction. This mechanism is different from the usual Mars-van

Krevelen (MVK) mechanism[11], which is invoked for explaining the majority of oxidation reactions catalyzed by oxides[12]. We found three mechanisms which all start with O<sub>2</sub> adsorption on the dopant (see structure Fig. 1b). The next step in all three mechanisms is the reaction of CO with the adsorbed oxygen to form a “carbonate” (see structure Fig. 1.1c), which takes place without an energy barrier. After these common steps several different mechanisms are possible. *Mechanism 1*: the adsorbed O<sub>2</sub> reacts with CO to form a carbonated, which decomposes producing a O atom on the dopant and CO<sub>2</sub> in the gas-phase. The O atom reacts with CO and forms a CO<sub>2</sub> molecule which desorbs.

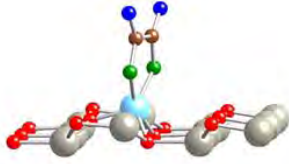


Figure 1: The structure of the oxalate intermediate formed in mechanism 3.

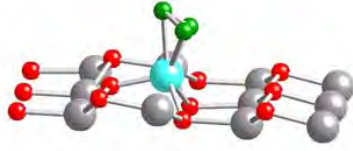


Figure 2. The structure of the tri-oxygen intermediate (green oxygen and cyan the

*Mechanism 2*: Proceeds like mechanism 1 up to the point when an O atom is left on the dopant. This reacts with a gas-phase O<sub>2</sub> molecule to form a tri-oxygen species bound to the Ti dopant (see Fig. 1). The tri-oxygen reacts with CO forming CO<sub>2</sub>, which desorbs leaving behind an O<sub>2</sub> molecule adsorbed on the Ti atom.

*Mechanism 3*: Proceeds like mechanism 1 up to carbonate formation. The carbonate reacts with stable in the absence of atomic hydrogen. CO to form an oxalate, whose structure is shown in Fig. 2. This decomposes to produce two CO<sub>2</sub> molecules which desorb and leave behind an O<sub>2</sub> molecule adsorbed on the Ti atom. The activation energy was calculated only for one critical step: the reaction of the adsorbed O<sub>2</sub> with CO. We thought that it would be better to do experiments to find whether the activation energies are small enough to produce CO<sub>2</sub>.

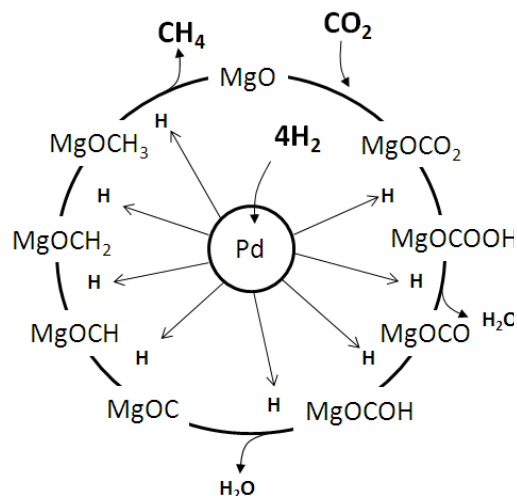
**2. Experimental synthesis and characterization of doped oxides:** Synthesis and characterization methods have been developed to establish true atomic doping (SEM, Rietveld refinement of XRD, BET, FTIR, TPR). *i) CO oxidation by Ti doped ZnO.* Our main objective was to prove that the oxidation of CO by this catalyst is due to the oxygen adsorbed on the dopant and not to the oxygen atoms in the oxide’s surface layer. We did this by using <sup>18</sup>O<sub>2</sub> and showing that C<sup>16</sup>O<sup>18</sup>O is produced. In parallel the reaction produces some C<sup>16</sup>O<sub>2</sub> and C<sup>18</sup>O<sub>2</sub>, and theory was used to provide an explanation for the mechanism through which these compounds are produced. *(ii) Methane partial oxidation by Pt<sub>x</sub>C<sub>1-x</sub>O<sub>2</sub> catalyst.* Pt doped CeO<sub>2</sub> was synthesized by three methods, XRD shows that all materials are single phase with the CeO<sub>2</sub> fluorite structure. One (DP) yields neutral Pt atom clusters supported on CeO<sub>2</sub> (this is the structure we intended for comparison with the doped oxides). The other two samples contain Pt<sup>0</sup>, Pt<sup>II</sup> and Pt<sup>IV</sup> in different proportions. A sol-gel sample was also exposed to a cyanide solution to remove Pt<sup>0</sup> from the surface. TPR of methane oxidation with the four samples was performed with steady-state at selected temperatures. The samples show remarkable differences. The Pt<sup>0</sup> rich sample showed complete methane combustion, when ionic Pt was present we observed combustion accompanied by methane reforming with CO<sub>2</sub> and H<sub>2</sub>O produced. Thus samples containing ionic Pt have different and more interesting chemistry than the ones containing exclusively Pt<sup>0</sup>. This study was then augmented by measurements of the dependence of CH<sub>4</sub> oxidation on the O<sub>2</sub>/CH<sub>4</sub> ratio. Separately we have studied CO<sub>2</sub> reforming of methane by Pt doped CeO<sub>2</sub>. To differentiate the catalysts prepared by different methods we have also performed temperature programmed desorption with CO.

*Theoretical study of Pt/CeO<sub>2</sub> Catalyst.* To complement these experiments we have started DFT calculations on this system. Because there are doubts that the ordinary GGA-DFT deals correctly with CeO<sub>2</sub> we use a variety of methods: rPBE-GGA, GGA+U, B3LYP and PB0. The last two methods are assumed to be more reliable (though more demanding in computer power) because they remove the electron self-interactions that may plague GGA. We are examining the structure and the stability of Pt<sub>x</sub>Ce<sub>1-x</sub>O<sub>2</sub> for different dopant positions, the role of the dopant in activating the neighboring oxygen atoms on the oxide’s surface and the ability of the surface to break the C-H bond in alkanes.

**3. Activation of carbon dioxide on Pd-Mg/SiO<sub>2</sub>.** A unique synthesis approach allows intimate mixing of Pd in MgO without sintering or phase separation. Whereas supported Pd catalysts are active for WGS and form CO and water from carbon dioxide and hydrogen, the bi-functional Pd-Mg/SiO<sub>2</sub> catalysts make only methane at high carbon dioxide conversion. Replacing the Mg with Fe or Ni maintained the high activity for carbon dioxide



activation and the divalent Ni maintained a high methane selectivity; however, the redox active Fe has little selectivity for methane. The bi-functional Pt-MgO/SiO<sub>2</sub> catalyst for CO<sub>2</sub> methanation was investigated and its catalytic activity and selectivity were compared with other known methanation catalysts. The performance for CO<sub>2</sub> methanation compared with Pt-MgO/SiO<sub>2</sub> catalysts prepared by conventional impregnation was significantly better and major functional differences were observed. A bi-functional mechanism whereby the Pd component of the catalyst dissociates H<sub>2</sub> and makes available hydrogen atoms for transfer and reaction with carbonate intermediates formed by the reaction of CO<sub>2</sub> on MgO has been proposed to explain the results observed for CO<sub>2</sub> methanation.



### Future Plans:

1. Continue DFT based calculations of various doped oxides with emphasis on C-H bond activation and CO<sub>2</sub> as a source of surface active oxygen.
2. Continue the development of consistent methods to synthesize and demonstrate that true “doped oxides” are achieved and not mixed phases.
3. Extend exciting results from the Pd-Mg system to other hydrogen transfer metals and basic oxides (Pd,Pt,Au)-(Mg,La,Zr) for the hydrogenation of carbon dioxide and more general reactions of CO<sub>2</sub> and C<sub>n</sub>H<sub>m</sub>O<sub>x</sub> as hydrogen donors.
4. Continue the development of effective characterization methods (physical, structural, and optoelectronic) to investigate doped oxide catalysts.
5. Analysis of the reactivity results to provide iterative feedback to theoretical work for additional modeling.

### References:

- [1] G. Kresse, J. Furthmüller, Phys. Rev. B. 54 (1996) 11169-11186.
- [2] G. Kresse, J. Furthmüller, Comput. Mater. Sci. 6 (1996) 15-50.
- [3] G. Kresse, D. Joubert, Phys. Rev. B. 59 (1999) 1758-1775.
- [4] J.P. Perdew, Y. Wang, Phys. Rev. B. 45 (1992) 13244.
- [5] J.A. Dean, Lange’s Handbook of Chemistry, 14 ed., McGraw-Hill, Inc., 1992.
- [6] G.V. Samsonov, The oxide handbook, 1982.
- [7] C.H. Bates, W.B. White, R. Roy, Science. 137 (1962) 993.
- [8] B. Meyer, D. Marx, Phys. Rev. B. 67 (2003) 035403.
- [9] G. Kresse, O. Dulub, U. Diebold, Phys. Rev. B. 68 (2003) 245409.
- [10] R.G.S. Pala, H. Metiu, J. Phys. Chem. C. 111 (2007) 8617.
- [11] P. Mars, D.W. van Krevelen, Chem. Eng. Sci. Spec. Suppl. 3 (1954) 41-59.
- [12] C. Doornkamp, V. Ponc, Journal of Molecular Catalysis a-Chemical. 162 (2000) 19-32.
- [13] R. Bader, Atoms in Molecules: A Quantum Theory, Clarendon, Oxford, 1994.
- [14] G. Henkelman, A. Arnaldsson, H. Jonsson, Computational Materials Science. 36 (2006) 354-360.
- [15] L.F. Liao, C.F. Lien, D.L. Shieh, M.T. Chen, J.L. Lin, The Journal of Physical Chemistry B. 106 (2002) 11240-11245.
- [16] V. Shapovalov, H. Metiu, J. Catal. 245 (2007) 205.
- [17] S. Chrétien, H. Metiu, Catalysis Lett. 107 (2006) 143-147.
- [18] R.G.S. Pala, H. Metiu, J. Phys. Chem. C. 111 (2007) 8617-8622.
- [19] H.Y. Kim, R.G.S. Pala, V. Shapovalov, H.M. Lee, H. Metiu, J. Phys. Chem. C. 112 (2008) 12398-12408.
- [20] S. Wendt, R. Schaub, J. Matthiesen, E.K. Vestergaard, E. Wahlstrom, M.D. Rasmussen, P. Thostrup, L.M. Molina, E. Laegsgaard, I. Stensgaard, B. Hammer, F. Besenbacher, Surface Science. 598 (2005) 226-245.
- [21] M.A. Henderson, W.S. Epling, C.L. Perkins, C.H.F. Peden, U. Diebold, J. Phys. Chem. B. 103 (1999) 5328-5337.
- [22] W.S. Epling, C.H.F. Peden, M.A. Henderson, U. Diebold, Surface Science. 412-413 (1998) 333-343.
- [23] S. Chrétien, H. Metiu, J. Chem. Phys. 129 (2008) 0747705-0747701-0747716.
- [24] F.J. Maldonado-Hódar, C. Moreno-Castilla, A.F. Pérez-Cadenas, Applied Catalysis B: Environmental. 54 (2004) 217-224.
- [25] G.C. Torres, E.L. Jablonski, G.T. Baronetti, A.A. Castro, S.R. de Miguel, O.A. Scelza, M.D. Blanco, M.A. Pena Jiménez, J.L.G. Fierro, Applied Catalysis A: General. 161 (1997) 213-226.
- [26] F. Coloma, A. Sepulveda-Escribano, J.L.G. Fierro, F. Rodriguez-Reinoso, Langmuir. 10 (1994) 750-755.
- [27] L. Pino, V. Recupero, S. Beninati, A.K. Shukla, M.S. Hegde, P. Bera, Applied Catalysis a-General. 225 (2002) 63-75.
- [28] J.M. Wei, E. Iglesia, Journal of Physical Chemistry B. 108 (2004) 4094-4103.
- [29] J.D.A. Bellido, E.M. Assaf, Applied Catalysis A: General. 352 (2009) 179-187.
- [30] F.B. Noronha, A. Shamsi, C. Taylor, E.C. Fendley, S. Stagg-Williams, D.E. Resasco, Catalysis Letters. 90 (2003) 13-21.
- [31] S.M. Stagg-Williams, F.B. Noronha, G. Fendley, D.E. Resasco, J. Catal. 194 (2000) 240-249.
- [32] X. Liu, K. Zhou, L. Wang, B. Wang, Y. Li, Journal of the American Chemical Society. 131 (2009) 3140-3141.
- [33] M. Boutonnet, S. Logdberg, E.E. Svensson, Current Opinion in Colloid & Interface Science. 13 (2008) 270-286.
- [34] S. Eriksson, U. Nýlen, S. Rojas, M. Boutonnet, Applied Catalysis a-General. 265 (2004) 207-219.
- [35] S.J. Choe, H.J. Kang, S.J. Kim, S.B. Park, D.H. Park, D.S. Huh, Bulletin of the Korean Chemical Society. 26 (2005) 1682-1688.
- [36] L.F. Liotta, G.A. Martin, G. Deganello, J. Catal. 164 (1996) 322-333.
- [37] N. Yoshida, T. Hattori, E. Komai, T. Wada, Catalysis Letters. 58 (1999) 119-122.

## **Exploring Visible-light Photocatalysts via the Dye-sensitization of Titanium Dioxide Materials**

M. W. McKittrick

University at Buffalo, Chemical & Biological Engineering, Buffalo, NY 14051

e-mail: [mm355@buffalo.edu](mailto:mm355@buffalo.edu)

The development of visible light active photocatalysts can enable and improve energy efficient chemical transformations of small organic molecules. Progress in this important area will enhance capabilities in a number of areas, including the treatment of hazardous chemicals. While  $\text{TiO}_2$  is an important material in photocatalysis, the material's bandgap limits its visible spectrum absorption. A number of researchers have explored expanding  $\text{TiO}_2$ 's usefulness as a visible light catalyst by a number of approaches, including doping and variations in architecture. Of interest to this work are approaches to create hybrid materials via functionalizing the  $\text{TiO}_2$  surface with visible light active dye molecules. However, the outstanding potential of visible light photocatalysis has not been fully achieved due to difficulty in understanding the host of interactions that occur between the dyes and supports. Not only must the dye and surface interact to increase enhanced activity, but aggregation, surface accessibility, and material architecture all play a role in the photoactivity of the resulting materials.

We are working to develop a number of well-defined dye-sensitized  $\text{TiO}_2$  materials and begin to clarify the parameters which play a role in the overall photoactivity of the system, specifically for the photodegradation of small organic pollutants. By better understanding how these important interactions work together to govern the photoactivity of the system, we can rationally optimize the system to develop highly active materials.

## Surface Chemistry of Gold Model Catalysts

Additional PIs: N/A  
 Postdocs: N/A  
 Students: Jinlong Gong, Ting Yan  
 Collaborators: Graeme Henkelman (UT-Austin), J. M. White (UT-Austin), B. D. Kay (PNNL), Z. Dohnalek (PNNL)  
 Contacts: Department of Chemical Engineering, University of Texas at Austin, 1 University Station C0400, Austin, TX 78712-0231; (512) 471-5817; [mullins@che.utexas.edu](mailto:mullins@che.utexas.edu)

### Goal

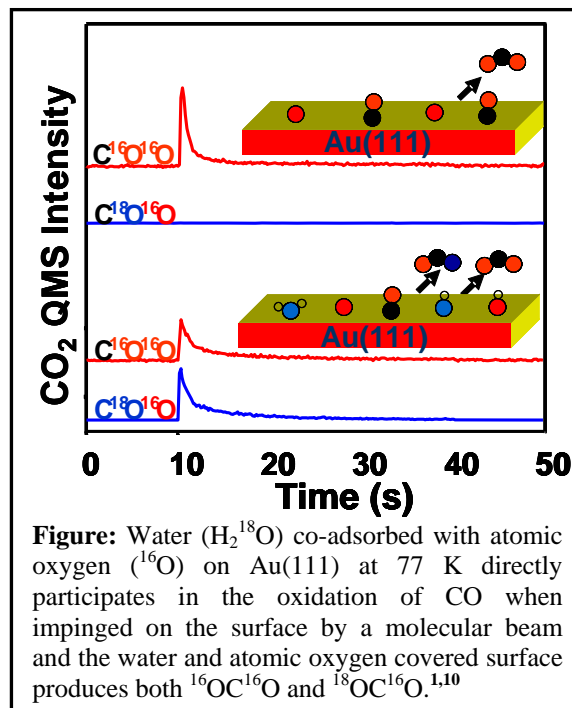
Our goals involve contributing to the understanding of issues related to gold catalysis through the study of specific surface chemical reactions on gold model catalysts in vacuum, including: What is the origin of the gold particle size effect? What is the nature and structure of the active site? What mechanisms drive the reaction [e.g., what is the role of moisture, which seems to be required for so many gold-catalyzed reactions]? What is the role of a metal oxide support?

### DOE Interest

Catalysis by metal-oxide supported gold is of interest to the Department of Energy since this catalytic system holds some promise for low-temperature one-step chemical conversions (e.g., epoxidation of propylene). Additionally, fundamental catalysis science is of interest to the DOE.

### Recent Progress

Gold-based heterogeneous catalysis has been explored via a considerably increased number of experimental and theoretical investigations including both nano-sized gold clusters and gold single crystals. However, mechanistic aspects regarding the activity of supported gold nanoclusters are still debated, especially, the active site structure, particle size dependence, and the molecular oxygen activation process. In our recent investigations we have demonstrated that bulk gold pre-covered by atomic oxygen is very active for low temperature oxidation of CO, oxidation of ammonia, NO, amines, and alcohols. The presence of oxygen atoms is crucial as they act as a Brønsted base or a nucleophilic base. Our investigations have demonstrated the intrinsic



activity of gold with an activated oxygen species (i.e., atomic oxygen) in the absence of a support, which show the same general patterns of reactivity and selectivity as observed on high surface area Au-based catalysts.

### Future Plans

We propose to study surface chemical reactions on model gold catalysts using ultrahigh vacuum surface science techniques including temperature programmed desorption and molecular beam methods. In particular, the primary model catalyst surfaces we will study include (i) planar wafers of a metal oxide [ $\text{TiO}_2(110)$  and  $\text{CeO}_2(111)$ ] decorated with gold clusters and (ii) “inverse” model catalysts composed of metal oxide nanoparticles (ceria and titania) dispersed on a  $\text{Au}(111)$  surface. Several valuable studies investigating the physical characterization of such “inverse” surfaces have been conducted recently along with a few studies of their chemistry and we plan to build upon this previous work as well as recent research of our own. We propose three major themes regarding the surface chemistry of these model gold surfaces: (i) the influence and role of adsorbed water in CO oxidation and the water gas shift reaction, (ii) the selective catalytic oxidation of ammonia to dinitrogen and hydrogen, and (iii) the partial oxidation of alcohols.

### Publications (2006-2009)

1. T. S. Kim, J. Gong, R. Ojifinni, J. M. White, and C. B. Mullins, “Water Activated by Atomic Oxygen on  $\text{Au}(111)$  to Oxidize CO at Low Temperatures” *J. Am. Chem. Soc.* **128**, 6282-6283 (2006).
2. S. M. McClure, D. J. Safarik, T. M. Truskett, and C. B. Mullins, “Evidence that amorphous solid water below 160 K is not a fragile liquid,” *J. Phys. Chem. B* **110**, 11033-11036 (2006).
3. Jinlong Gong, Rotimi A. Ojifinni, Tae S. Kim, J. M. White, and C. B. Mullins, “Selective catalytic oxidation of ammonia to nitrogen on atomic oxygen precovered  $\text{Au}(111)$ ,” *J. Am. Chem. Soc.* **128**, 9012-9013 (2006).
4. J. D. Stiehl, J. Gong, R. A. Ojifinni, T. S. Kim, S. M. McClure, and C. B. Mullins, “Reactivity of Molecularly Chemisorbed Oxygen on a  $\text{Au}/\text{TiO}_2$  Model Catalyst,” *J. Phys. Chem. B* **110**, 20337-20343 (2006).
5. S. M. McClure, E. Barlow, M. Akin, D. J. Safarik, T. M. Truskett, and C. B. Mullins, “Transport in amorphous solid water films: Implications for self-diffusivity,” *J. Phys. Chem. B* **110**, 17987-17997 (2006).
6. D. W. Flaherty, Z. Dohnalek, A. Dohnalkova, B. W. Arey, D. E. McCready, N. Pnnusamy, C. B. Mullins, and B. D. Kay, “Reactive ballistic deposition of porous  $\text{TiO}_2$  films: growth and characterization,” *J. Phys. Chem. C* **111**, 4765-4773 (2007).
7. J. Gong, R. A. Ojifinni, T. S. Kim, J. D. Stiehl, S. M. McClure, J. M. White, and C. B. Mullins, “Low temperature CO oxidation on  $\text{Au}(111)$  and the role of adsorbed water,” *Top. Catal.* **44**, 57-63 (2007).
8. S. M. McClure, E. Barlow, M. Akin, D. J. Safarik, T. M. Truskett, and C. B. Mullins, “Effect of dilute nitric acid on crystallization and fracture of amorphous solid water films,” *J. Phys. Chem. C* **111**, 10438-10447 (2007).
9. C. B. Mullins and G. O. Sitz, “Taking a selective bite out of methane,” *Science* **319**, 736-737 (2008).

10. R. A. Ojifinni, N. S. Froemming, J. Gong, T. S. Kim, M. Pan, J. M. White, G. Henkelman, and C. B. Mullins, "Water-enhanced low-temperature CO oxidation and isotope effects on atomic oxygen covered Au(111)," *J. Am. Chem. Soc.* **130**, 6801-6812 (2008).
11. J. Gong, D. W. Flaherty, R. A. Ojifinni, J. M. White, and C. B. Mullins, "Surface chemistry of methanol on clean and atomic oxygen pre-covered Au(111)" *J. Phys. Chem. C* **112**, 5501-5509 (2008).
12. R. A. Ojifinni, J. Gong, Nathan S. Froemming, D. W. Flaherty, M. Pan, G. Henkelman, and C. B. Mullins, "Carbonate formation and decomposition on atomic oxygen pre-covered Au(111)," *J. Am. Chem. Soc.* **130**, 11250-11251 (2008).
13. J. Gong and C. B. Mullins, "Enhanced carbonate formation on gold," *J. Phys. Chem. C* **112**, 17631-17634 (2008).
14. J. Gong, D. W. Flaherty, T. Yan, and C. B. Mullins, "Selective oxidation of propanol on Au(111): Mechanistic insights into aerobic oxidation of alcohols," *ChemPhysChem* **9**, 2461-2466 (2008).
15. J. Gong and C. B. Mullins, "Selective oxidation of ethanol to acetaldehyde on gold," *J. Am. Chem. Soc.* **130**, 16458-16459 (2008).
16. J. Gong, T. Yan, and C. B. Mullins, "Selective oxidation of propylamine to propionitrile and propaldehyde on oxygen-covered gold," *Chem. Comm.* 761-763 (2009).

DE-FG02-03ER15461

Djamaladdin G. Musaev  
Craig L. Hill  
Keiji Morokuma

**Principles of Selective O<sub>2</sub>-Based Oxidation by Optimal (Multinuclear) Catalytic Sites**

**Postdocs:** Yurii Geletti, Alexsey Kuznetsov,

**Students:** Zhen Luo, Daniel A. Hillesheim, Jie Song, Rui Cao,  
Yu Hou, Kevin O'Halloran

**Collaborators:** Alex Kaledin (Emerson Center),  
David Quiñonero (Visiting scientist, Universitat de les Illes  
Balears, Spain)

**Affiliations:** Emory University, Department of Chemistry  
[dmusaev@emory.edu](mailto:dmusaev@emory.edu), [chill@emory.edu](mailto:chill@emory.edu), [morokuma@emory.edu](mailto:morokuma@emory.edu)  
phone: 404-727-2382, 404-727-6611, 404-727-2180

**Goals.** Develop a combined experimental and theoretical approach to elucidate the mechanisms of selective (non-radical), reductant-free, O<sub>2</sub>-based oxidation of organic substrates catalyzed by metal oxide cluster systems (polyoxometalates or "POMs") with two or more proximal and synergistically interacting metal centers. The objectives entail clarification of the structural, solution and catalytic properties of two classes of complexes: those with two adjacent d-electron transition metals (formula:  $\gamma$ -XM<sup>I</sup>M<sup>II</sup>(OH)<sub>2</sub>(M<sub>FW</sub>)<sub>10</sub>O<sub>38</sub><sup>n-</sup>) and the new Late Transition Metal Oxo (LTMO) complexes.

**DOE Interest.** The proposed research addresses the catalytic selective oxidation of organic substrates by O<sub>2</sub>. Realization of synthetic catalysts capable of such transformations remains a monumental challenge. The most promising such catalysts in chemistry and biology remain those with multiple proximal d-electron-containing metal centers. The POM complexes targeted herein, those with two adjacent d-electron-containing metals and the LTMO complexes, address core issues of intellectual and potential practical importance and provide a foundation for addressing principles central to realizing optimal synthetic catalysts and understanding related catalytic biological processes. One reaction (of several) the goals of this effort address that impacts energy transportation and utilization significantly is the catalytic O<sub>2</sub>-based oxidation of methane (96% of natural gas) selectively at high conversion to methanol, a process that has yet to be achieved satisfactorily by a non-biological catalyst.

**Recent Progress:**

Our ongoing program focuses in part on oxidatively robust POM complexes in which a catalytic active site interacts with proximal metal centers in a synergistic manner. Two classes of such POM complexes are of particular interest: (I) those with two

adjacent d-electron transition metals ( $\gamma$ -M<sub>2</sub>-Keggin complexes) and **(II)** the newly developed Late Transition Metal Oxo (LTMO) complexes.

**I.** Complexes with two adjacent d-electron transition metals ( $\gamma$ -M<sub>2</sub>-Keggin complexes).

**I.1.** Now, we have fully characterized (using X-ray crystallography, IR spectrometry, computational, electrochemical, potentiometrical, UV-vis titration, and other techniques) the previously prepared first homogeneous (molecular) catalyst for H<sub>2</sub>O oxidation to O<sub>2</sub>, Rb<sub>8</sub>K<sub>2</sub>[{Ru<sub>4</sub>O<sub>4</sub>(OH)<sub>2</sub>(H<sub>2</sub>O)<sub>4</sub>}( $\gamma$ -SiW<sub>10</sub>O<sub>36</sub>)<sub>2</sub>] $\cdot$ 25H<sub>2</sub>O (**1**) (Figure 1). We have elucidated stability, electronic and geometry structures of various oxidation states of this polyanion involved in H<sub>2</sub>O oxidation. We have shown that all Ru-centers of **1** are in their +4 oxidation states [this species will be denoted as **1(0)**, where the number **n** given in parenthesis indicates the n-electron oxidation (+) or/and reduction (-) states of **1**]. Kinetic studies show that the four electron oxidized state of **1**, **1(+4)**, is the most likely reactive intermediate oxidizing water to O<sub>2</sub>. We have suggested the following reaction mechanism,

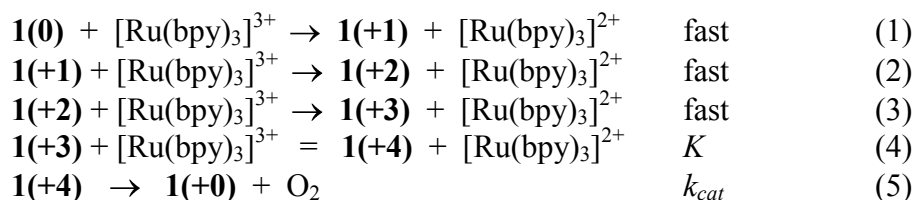
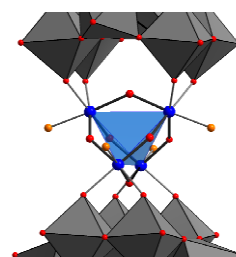


**Figure 1.** Structure of the polyanion in **1(0)**, highlighting the central [Ru<sub>4</sub>( $\mu$ -O)<sub>4</sub>( $\mu$ -OH)<sub>2</sub>(H<sub>2</sub>O)<sub>4</sub>]<sup>6+</sup> core (ball-and-stick representation, Ru: blue,  $\mu$ -O: red, O(H<sub>2</sub>): orange, H omitted for clarity) and the slightly distorted Ru<sub>4</sub> tetrahedron (transparent blue). The polytungstate fragments are shown as gray polyhedra; Si as yellow spheres.



The reactions in eqs 1-3 are thermodynamically very favorable and therefore are considered to proceed very quickly. Consequently, the steady state concentrations of **1(0)**, **1(+1)**, and **1(+2)** are negligible compared with the concentrations of **1(+3)** and **1(+4)**. The latter two complexes are in fast equilibrium because the electron transfer reaction in eq 4 is estimated to be thermodynamically neutral.

**I.2.** The complex analogous to **1(0)**, TBA<sub>(10-x)</sub>H<sub>x</sub>[{Ru<sub>4</sub>O<sub>4</sub>(OH)<sub>2</sub>(H<sub>2</sub>O)<sub>4</sub>}( $\gamma$ -SiW<sub>10</sub>O<sub>36</sub>)<sub>2</sub>], where TBA is tetrabutylammonium cation, soluble in organic solvents has been synthesized and characterized. The catalytic activity of this compound was tested in oxidation of 3,5,3',5'-tetra-*t*-butyl-biphenyl-4,4'-diol (BPH<sub>2</sub>) by dioxygen to 3,5,3',5'-tetra-*t*-butyl-diphenoquinone (DPQ). Several turnover numbers, TON = DPQ/**1(0)** ~4, have been achieved in the presence of small amounts of bases, e.g. 2,6-di-*t*-butylpyridine. The catalytic cycle includes the reduction of **1(-1)** by BPH<sub>2</sub> to **1(-2)** with a slow regeneration of **1(-2)** to **1(-1)** by O<sub>2</sub>. No catalytic activity was found in oxidation of tetrahydrothiophene, 2-chloroethyl ethyl sulfide, and cyclohexene by O<sub>2</sub>.

**I.3.** We have demonstrated that lacunary polyoxometalates can function as ligands for isolable polymetal-nitrido compounds. The dinuclear polytungstates,  $\gamma$ -[XW<sub>10</sub>O<sub>38</sub>{RuN<sub>2</sub>}<sub>2</sub>]<sup>6-</sup>, X = Si (**2**) and Ge (**3**) were synthesized and thoroughly characterized (X-ray structure, computation, several spectroscopic and other techniques). We have elucidated the geometry, electronic structure and reactivity of these complexes. It was shown that the small ionic radius of the high oxidation state precursor [Ru<sup>VI</sup>NCl<sub>4</sub>]<sup>-</sup> facilitates formation of “in-pocket”  $\gamma$ -[XW<sub>10</sub>O<sub>36</sub>]<sup>8-</sup> (X=Si, Ge) complexes, with the two ruthenium atoms firmly set in the lacuna, when in water (either prepared in or residing in aqueous media). Interestingly, reduction of **2** triggers the controlled removal of the nitrogen atoms from the complex. The different protonation and reduction processes for NH<sub>3</sub> production are summarized in Figure 2.

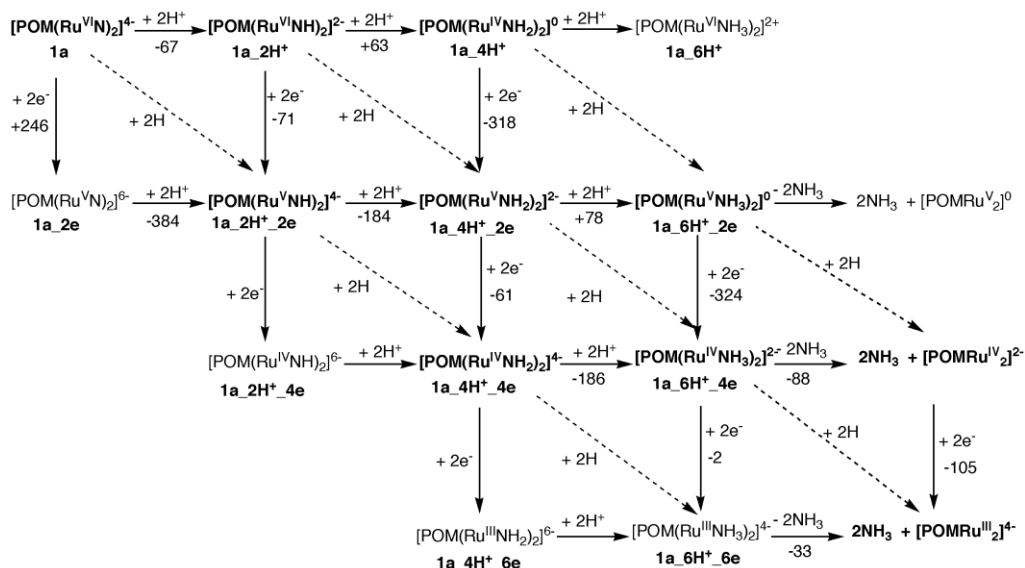


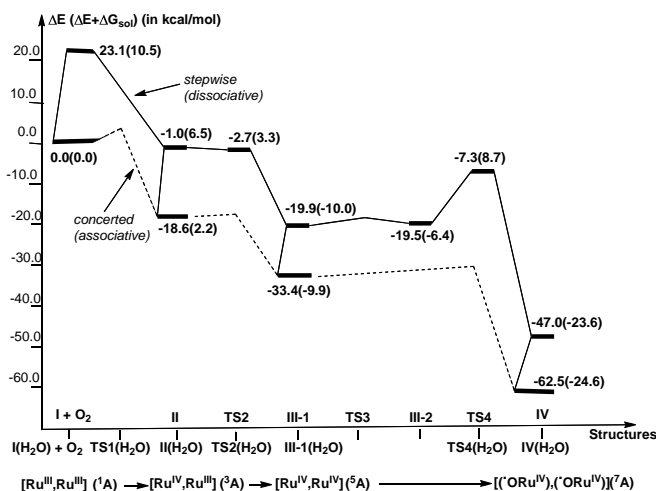
**Figure 2.** The protonation and redox processes involved in reduction of [SiW<sub>10</sub>O<sub>38</sub>{RuN<sub>2</sub>}<sub>2</sub>]<sup>6-</sup>, **2** (**1a** in this scheme) and release of NH<sub>3</sub>. The values are the B3LYP calculated energies in kcal mol<sup>-1</sup>.

**I.4.** Now, we have completed studies on stability and reactivity of  $[\gamma$ -(1,2)-H<sub>2</sub>SiRu<sub>2</sub>W<sub>10</sub>O<sub>40</sub>(H<sub>2</sub>O)<sub>2</sub>]<sup>4-</sup> complex. DFT calculations show that reaction of the Ru<sub>2</sub>-substituted  $\gamma$ -Keggin polyoxotungstate  $\{\gamma$ -[(H<sub>2</sub>O)Ru<sup>III</sup>-( $\mu$ -OH)<sub>2</sub>-Ru<sup>III</sup>(H<sub>2</sub>O)][SiW<sub>10</sub>O<sub>36</sub>]<sup>4-</sup>, **I(H<sub>2</sub>O)**, with O<sub>2</sub> is a 4-electron highly exothermic process [ $\Delta E_{\text{gas}} = 62.5$  ( $\Delta E_{\text{gas}} + \Delta G_{\text{solv(water)}} = 24.6$ ) kcal/mol] and leads to formation of (H<sub>2</sub>O){ $\gamma$ -[(O)Ru-( $\mu$ -OH)<sub>2</sub>-Ru(O)](H<sub>2</sub>O)[SiW<sub>10</sub>O<sub>36</sub>]<sup>4-</sup>, **IV(H<sub>2</sub>O)** (see Figure 3). The first 1e-oxidation is achieved by the H<sub>2</sub>O-to-O<sub>2</sub> substitution which is calculated to occur with a maximum of 23.1 (10.5) kcal/mol barrier and leads to formation of  $\{\gamma$ -[(OO)Ru-( $\mu$ -OH)<sub>2</sub>-Ru(H<sub>2</sub>O)](H<sub>2</sub>O)[SiW<sub>10</sub>O<sub>36</sub>]<sup>4-</sup>, **II(H<sub>2</sub>O)**. The second 1e-oxidation is initiated by the proton transfer from the coordinated water molecule to the superoxide (OO<sup>-</sup>) ligand in **II(H<sub>2</sub>O)** and is completed upon formation of hydroperoxo-hydroxo intermediate,  $\{\gamma$ -[(OOH)Ru-( $\mu$ -OH)<sub>2</sub>Ru(OH)](H<sub>2</sub>O)[SiW<sub>10</sub>O<sub>36</sub>]<sup>4-</sup>, **III-1(H<sub>2</sub>O)**. The final 2e-oxidation occurs upon the proton transfer from the terminal OH-ligand to the Ru-coordinated OOH fragment and is completed at the formation of (H<sub>2</sub>O)<sup>·-</sup>{ $\gamma$ -[(O)Ru-( $\mu$ -OH)<sub>2</sub>-



$\text{Ru}(\text{O})[(\text{H}_2\text{O})[\text{SiW}_{10}\text{O}_{36}]]^{4-}$ , **IV**( $\text{H}_2\text{O}$ ), with two multiply bonded  $\text{Ru}=\text{O}$  (terminal ruthenium-oxo) units. The resulting **IV**( $\text{H}_2\text{O}$ ) with a  $\{\text{Ru}(\text{O})-(\mu\text{-OH})_2\text{-Ru}(\text{O})\}$  core should be formulated to have  $\text{Ru}^{\text{IV}}=\text{O}\cdot$  units, rather than the  $\text{Ru}^{\text{V}}=\text{O}$  groups. The reverse reaction, water oxidation by **IV**( $\text{H}_2\text{O}$ ), is found to be highly endothermic and cannot occur; this finding is different from that reported for the “blue-dimer” intermediate,  $\{(\text{bpy})_2[(\text{O}^\bullet)\text{Ru}-(\mu\text{-O})\text{-Ru}(\text{O}^\bullet)](\text{bpy})_2\}^{4+}$ , which readily oxidizes an incoming water molecule to produce  $\text{O}_2$ . The main reason for this difference in reactivity of  $\text{Ru}_2$ -POM and the “blue-dimer” intermediates towards the water molecule is found to be a high stability of the former compared with the analogous “blue-dimer” intermediate relative to  $\text{O}_2$  formation.

**Figure 3.** Schematic presentation of the potential energy surface of the stepwise and concerted pathways of the reaction of  $\{\gamma\text{-}[(\text{H}_2\text{O})\text{Ru}^{\text{III}}-(\mu\text{-OH})_2\text{Ru}^{\text{III}}(\text{H}_2\text{O})]\text{-}[\text{SiW}_{10}\text{O}_{36}]]^{4-}$ , I( $\text{H}_2\text{O}$ ) with  $\text{O}_2$ . The relative energies  $\Delta E$  (and  $\Delta E + \Delta G_{\text{solv}(\text{water})}$  in parentheses) are given in kcal/mol.



This, in turn, derives from the electron-rich nature of  $[\text{SiW}_{10}\text{O}_{36}]^{4-}$  compared to bpy ligands. It was concluded that the lack of reactivity of the intermediate  $\{\gamma\text{-}[(\text{O}^\bullet)\text{Ru}-(\mu\text{-OH})_2\text{Ru}(\text{O}^\bullet)][\text{SiW}_{10}\text{O}_{36}]]^{4-}$  towards the water molecule facilitates its complexation with another  $\{\gamma\text{-}[\text{Ru}^{\text{III}}-(\mu\text{-OH})_2\text{Ru}^{\text{III}}][\text{SiW}_{10}\text{O}_{36}]]^{4-}$  molecule forming the experimentally isolated and thoroughly characterized water oxidation catalyst  $[\{\text{Ru}_4\text{O}_4(\text{OH})_2(\text{H}_2\text{O})_4\}(\gamma\text{-}\text{SiW}_{10}\text{O}_{36})_2]^{10-}$  described in section 1.

**I.5.** Water oxidation by  $\{\gamma\text{-}[(\text{O})\text{Ru}-(\mu\text{-OH})_2\text{Ru}(\text{O})][\text{XW}_{10}\text{O}_{36}]]^{4-}$ , **IV<sub>x</sub>**, complex, where X = Si, P and S. Previously, in course of this project (in 2006-2007), we predicted that the heteroatom, X, in the di-Ru substituted  $\gamma$ -Keggin POMs,  $[(\text{X}^{\text{n}+}\text{O}_4)\text{Ru}_2(\text{OH})_2(\text{M}_{\text{FW}})_{10}\text{O}_{32}]^{(8-n)-}$ , for X =  $\text{Al}^{\text{III}}$ ,  $\text{Si}^{\text{IV}}$ ,  $\text{P}^{\text{V}}$  and  $\text{S}^{\text{VI}}$ , where  $\text{M}_{\text{FW}}$  (framework metals) = Mo and W, can function as an “internal switch” for defining the ground electronic states and, consequently, the reactivity of the  $\gamma$ -M<sub>2</sub>-Keggin POM complexes. In order to test this prediction we have studied reaction mechanism and energetics of the reaction of  $\{\gamma\text{-}[(\text{O})\text{Ru}-(\mu\text{-OH})_2\text{Ru}(\text{O})][\text{XW}_{10}\text{O}_{36}]]^{4-}$ , **IV<sub>x</sub>**, complex with water molecule for X = Si, P and S. DFT calculations show that complexes **IV<sub>P</sub>** and **IV<sub>S</sub>** are *not* more reactive with water molecules than complex **IV<sub>Si</sub>**: Reaction **IV<sub>x</sub>** +  $\text{H}_2\text{O} \rightarrow \{\gamma\text{-}[(\text{O}_2)\text{Ru}-(\mu\text{-OH})_2\text{Ru}(\text{H}_2\text{O})][\text{XW}_{10}\text{O}_{36}]]^{n-}$  is calculated to be endothermic by 25.5, 21.3 and 23.2 kcal/mol for X = Si, P and S, respectively.

## II. Late-Transition-Metal-oxo (LTMO) complexes.

**II.1. Au-oxo:** We have now completed an unusually thorough characterization of the previously prepared first terminal oxo complexes of the coinage metals, namely two Au-oxo complexes. These complexes relate to O<sub>2</sub>/air-based oxidations catalyzed by Au(0) systems which include supported Au(0) films, Au nanoclusters, and other species. We have now completed the first set of experiments on the terminal Au-oxo complexes: (1) established the structures of these compounds by both very low temperature X-ray diffraction and neutron diffraction (the latter in collaboration with our DOE Argonne National Laboratory colleagues, T. Koetzle, A. Schultz and P. Piccoli); (2) formulated the oxidation states of the Au-oxo complexes using 5 complementary approaches: chemical titration, controlled potential coulometry, ultra-low-temperature optical spectroscopy (in collaboration with the group of M. Kirk at U. New Mexico), X-ray absorption spectroscopy (XAS) (in collaboration with the group at Stanford University and the Stanford Synchrotron Radiation Laboratory, SSRL), and from detailed analysis of bond distances and more subtle structural effects.

**II.2. (Pd-oxo)<sub>2</sub>:** The first complex with two terminal Pd-oxo units proximal in the same molecule has been prepared and characterized. The complex has been characterized by multiple single crystal X-ray structure determinations and <sup>17</sup>O NMR has confirmed that presence of the terminal oxo oxygen on the noble metal. (All the LMTO oxo oxygens have a chemical shift that is in a unique window, based on hundreds of published POM <sup>17</sup>O NMR spectra, and this chemical shift is consistent experimentally and theoretically with some  $\pi$  bonding between the noble metal (Pd in this case) and its terminal oxygen.

#### **Future Plans:**

Our team in ongoing efforts will continue to (1) prepare and study physicochemical and catalytic properties of  $\gamma$ -Ru<sup>III</sup><sub>2</sub>-Keggin complexes with different central heteroatom(s) X (P and S) and counterions in each POM; (2) investigate the factors controlling stability of LMTO complexes in aqueous solution (these include the POM ligand(s) themselves, counter cations, ionic strength and temperature); (3) develop the chemistry (physicochemical and catalytic properties) of LTMO complexes in organic solvents (the complexes are far more stable in organic media than in H<sub>2</sub>O); (4) probe more quantitatively the electronic structure of the metal-oxo unit and its impact on oxo transfer to organic molecules and other key processes; (5) develop the ONIOM approach to study LTMO structure, stability and reactivity.

#### **Publications (2007-2009):**

##### **a. Sole funding by DOE-BES:**

1. Quiñonero, D.; Morokuma, K.; Geletii, Y. V.; Hill, C. L.; Musaev, D. G. "A Density Functional Study of Geometry and Electronic Structure of [(SiO<sub>4</sub>)(M<sup>III</sup>)<sub>2</sub>(OH)<sub>2</sub>W<sub>10</sub>O<sub>32</sub>]<sup>4-</sup> for M = Mo, Ru and Rh." *J. Mol. Catal. A, Chem.* **2007**, 262, 227-235.
2. Fang, X.; Hill, C. L. "Multiple Reversible Protonation of Polyoxoanion Surfaces: Direct Observation of Dynamic Structural Effects from Proton Transfer", *Angew. Chem. Int. Ed.* **2007**, 46, 3877-3888

3. Botar, B.; Kögerler, P.; Hill, C. L. "Tetrairon and Hexairon Hydroxo/Acetato Clusters Stabilized by Multiple Polyoxometalate Scaffolds. Structures, Magnetic Properties and Chemistry of a Dimer and a Trimer", *Inorg. Chem.* **2007**, 46, 5398-5403.
4. Prabhakar, R.; Morokuma, K.; Geletii, Y. V.; Hill, C. L.; Musaev, D. G. "Insights into the Mechanism of H<sub>2</sub>O<sub>2</sub>-based Olefin Epoxidation Catalyzed by the Lacunary  $[\gamma-(\text{SiO}_4)\text{W}_{10}\text{O}_{32}\text{H}_4]^{4-}$  and di-V-substituted- $\gamma$ -Keggin  $[\gamma-1,2-\text{H}_2\text{SiV}_2\text{W}_{10}\text{O}_{40}]^{4-}$  Polyoxometalates. A Computational Study." In "Computational Modeling for Homogenous and Enzymatic Catalysis", Morokuma, K.; Musaev, D. G. Eds. Wiley: New York, **2008**, 215-230.
5. Kuznetsov, A. E.; Geletii, Y. V.; Hill, C. L.; Morokuma, K.; Musaev, D. G. "On the Mechanism of the Divanadium-substituted Polyoxotungstate  $[\gamma-1,2-\text{H}_2\text{SiV}_2\text{W}_{10}\text{O}_{40}]^{4-}$  Catalyzed Olefin Epoxidation by H<sub>2</sub>O<sub>2</sub>: A Computational Study." *Inorg. Chem.*, **2009**, 48, 1871-1878
6. Kuznetsov, A. E.; Geletii, Y. V.; Hill, C. L.; Morokuma, K.; Musaev, D. G. "Dioxygen and Water Activation Processes on Multi-Ru-substituted Polyoxometalates: Comparison with the "Blue Dimer" Water Oxidation Catalyst" *J. Am. Chem. Soc.* **2009**, 131, in revision.

**b. Joint funding by DOE:**

7. Yurii V. Geletii, Bogdan Botar, Paul Kogerler, Daniel A. Hillesheim, Djamaladdin G. Musaev, Craig L. Hill, „An All-Inorganic, Stable, and Highly Active Tetra Ruthenium Homogenous Catalyst for Water Oxidation“, *Angew. Chem. Intern. Ed.* **2008**, 47, 3896-3899. *Selected as the VIP ("Very Important Article") by the reviewers and editor.*

**c. Joint funding by DOE and other Sources:**

8. Zheng, G.; Witek, H.; Bobadova-Parvanova, P.; Irle, S.; Musaev, D. G.; Prabhakar, R.; Morokuma, K.; Lundberg, M.; Elstner, M.; Kohler, C.; Frauenheim, T. "Parameterization of Transition Metal Elements for the Spin-Polarized Self-Consistent-Charge Density-Functional Tight-Binding Method: 1. Parameterization of Ti, Fe, Co, and Ni." *J. Chem. Theory and Comp.*, **2007**, 3(4); 1349-1367.
9. Cao, R.; Anderson, T. M.; Piccoli, P. M. B.; Schultz, A. J.; Koetzle, T. F. Geletii, Y. V.; Slonkina, E.; Hedman, B.; Hodgson, K. O.; Hardcastle, K. I.; Fang, X.; Kirk, M. L.; Knottenbelt, S.; Kögerler, P.; Musaev, D. G.; Morokuma, K.; Hill, C. L. "Reactive terminal gold-oxo units" *J. Am. Chem. Soc.* **2007**, 129(36); 11118-11133.
10. Hill, C. L.; Delannoy, L.; Duncan, D. C.; Weinstock, I. A.; Renneke, R. F.; Reiner, R. S.; Atalla, R. H.; Han, J. W.; Hillesheim, D. A.; Cao, R.; Anderson, T.; Okun, N. M.; Musaev, D. G.; Geletii, Y. "Complex catalysts from self repairing ensembles to highly reactive air-based oxidation systems" *Comptes Rendus Chimie*, **2007**, 10, 305-312.
11. Hill, C. L. "Progress and challenges in polyoxometalate-based catalysis and catalytic materials chemistry", *J. Mol. Catal. A., Chem.* **2007**, 262, 2-6.
12. Rui Cao, Jong Woo Han, Traves M. Anderson, Daniel A. Hillesheim, Martin L. Kirk, Djamaladdin G. Musaev, Keiji Morokuma, Yurii V. Geletii, Craig L. Hill, „Late Transition Metal Oxo Compounds and Open Framework Materials that Catalyze Aerobic Oxidations“, *Prog. Inorg. Chem.*, **2008**, pp.245-272.

**Theory Aided Design of Active and Durable Nanoscale Cathode Catalysts**

**Postdoc:** Michael Paul  
**Students:** Anirban Chatterjee  
**Collaborators:** Dr. Paul Kent, University of Tennessee and Oak Ridge National Laboratory, Dr. David Thompsett, Johnson Matthey.  
**Contact:** Departments of Chemical Engineering and Chemistry, University of Virginia, Charlottesville, VA 22904-4741, Phone: (434) 924-6248. Fax (434) 982-2658. e-mail: [mn4n@virginia.edu](mailto:mn4n@virginia.edu)

**Overall Goals and Objectives and Achievements**

A number of critical challenges currently prevent the commercialization of the proton exchange membrane (PEM) fuel cell for light-duty transportation and portable power. One of the greatest technological hurdles relates to the sluggish activity, low durability and the high cost of the catalysts that are currently employed. It has been estimated that for automotive PEM fuel cells to become commercially viable, the Pt-specific power density would need to be reduced to less than 0.2gPt/kW (at cell voltages >0.65 V). This would require the Pt loadings to be less than 0.15 mg<sub>Pt</sub>/cm<sup>2</sup><sub>MEA</sub> within the membrane electrode assembly. This could be achieved by enhancing the catalytic activity at the cathode, thus lowering its overpotential. Various different Pt-alloys have shown 2-4 times enhanced activities over Pt alone but still suffer some of the same durability issues as that of the pure Pt. There is a general loss of active Pt due to dissolution and sintering. While there have been a number of elegant fundamental experimental and theoretical studies on ideal single crystal Pt and Pt alloy surfaces which have helped to elucidate the factors that control the activity, there have been very few fundamental studies focused on the stability, reactivity and durability of well-defined Pt nanoparticles. We ab initio density functional theory together with a novel double reference method that we have developed to simulate constant potential electrochemical systems in order to model the electrocatalytic reduction of oxygen over model Pt alloy nanoparticles and test their stability to dissolution. The ab initio simulations will be used to determine the reaction energies and activation barriers for a comprehensive array of different elementary adsorption, desorption, surface reaction and diffusion steps over Pt and Pt alloys involved in the electroreduction of oxygen as a function of potential and temperature. The calculations will examine potential dependent adsorption and surface reaction energies along with activation barriers in order to determine the kinetics for different surface structures and structural features (step edge and corner sites) to provide the necessary input for kinetic studies. More coarse-grained simulated annealing methods will be used together with electronic structure calculations to establish the lowest energy structures and morphologies for different Pt and Pt-alloy nanoparticles that form. The results from these structural studies will be used together with the ab initio-derived kinetic database to provide the necessary input to a 3D kinetic Monte Carlo code that will be used to simulate the electrocatalytic performance over different particle sizes, shapes and compositions. The ab initio calculations together with the kinetic Monte Carlo simulations will be used to complete the following objectives: 1) *Determine the controlling elementary reaction pathways and intrinsic kinetics involved in ORR and their potential dependent behavior;* 2) *Establish the influence of the extrinsic reaction environment including*

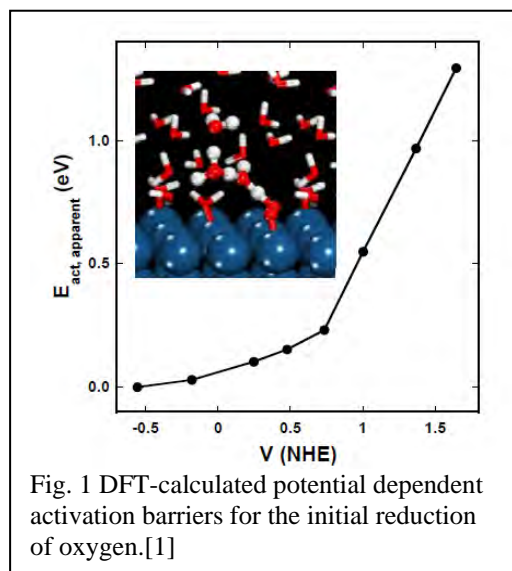
surface structure, alloy composition and spatial arrangement and the humidity on ORR kinetics; 3) Elucidate the effects of particle size and morphology as well as the atomic structure and composition of nanoparticles of Pt, Pt<sub>3</sub>Co, Pt<sub>3</sub>Ni, Pt<sub>3</sub>Fe and other Pt-alloys on the electrocatalytic activity and reaction selectivity; 5) Construct surface Pourbaix phase diagrams for different Pt and Pt-alloys in order to map out the most stable surface phases for different material compositions and reaction conditions; 6) Elucidate the mechanisms that control dissolution and re-deposition of Pt.

### Potential Impact on DOE

The goals of the proposed research are to elucidate and control electrocatalysis at the aqueous/metal interface for PEM fuel cell systems. This matches the longer term DOE Basic Energy Science program measure of *understanding, modeling, and controlling of chemical reactions on surfaces for energy-related applications, employing lessons from inorganic, organic and self-assembling systems*. The methods developed along with the knowledge gained should crosscut various areas in electrocatalysis, catalysis and electrochemistry important to BES. The proposed effort will utilize the tools developed herein to aid in the design novel alloy catalysts for the cathode that are active and resilient to dissolution and degradation. This is directly related to the long term BES program measure of *“designing, modeling, fabricating, characterizing, analyzing, assembling and using new materials and structures, including metals and alloys, particularly at the nanoscale, for energy-related applications.”*

### Recent Progress

The ab initio double reference method that we developed previously to simulate electrochemical

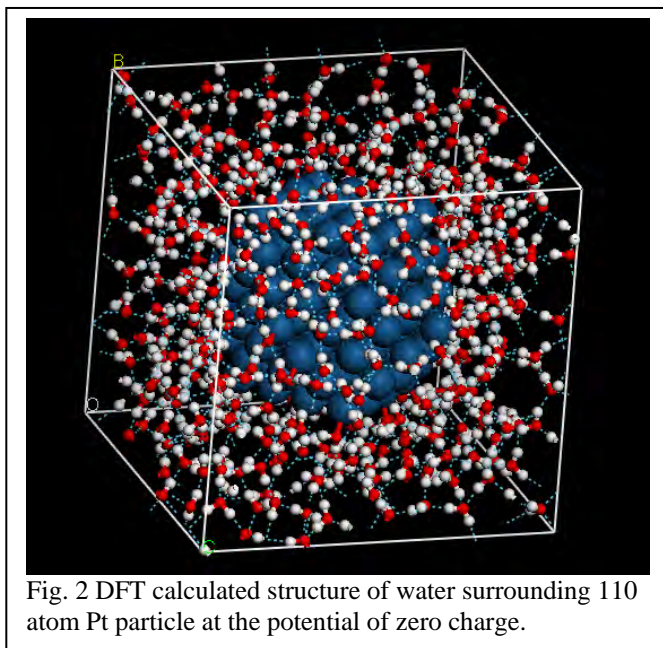


systems was adopted here to examine the potential dependent behavior for the electrocatalytic reduction of oxygen over model Pt surfaces. The results indicate that the initial reduction of O<sub>2</sub> to form the hydroperoxo intermediate and the reductive removal of OH from the surface limit the rate at operating cell potentials of interest[1]. The initial reduction of the adsorbed O<sub>2</sub> tends to limit the rate at higher potentials. The free energy for the reduction of O<sub>2</sub>\* to form OOH\* was calculated to be endothermic at potentials above 0.7 V NHE, in line with the expectation that transport of the proton nearer to the positively charged surface is successively more endothermic with increasing proximity. The first step of moving the proton near to the adsorbed O<sub>2</sub> has a reaction free energy increases with increasing potential and has a slope of 1. This indicates that electron transfer occurs prior to

formation of the OO-H bond. A detailed analysis of charge corroborates that reduction occurs prior to hydrogen addition and the electron which transfers resides in the oxygen adsorbate layer near to the surface. The hydrogen subsequent transfers to the adsorbed O<sub>2</sub> to form the OOH\* intermediate. The activation barrier for this step increases exponentially with an increase in potential as is shown in Fig. 1. The calculated barrier at 0.8 V-NHE of 0.34 eV agrees well with that measured by Damjanovic and Sepa (0.26 eV).[2] Similar calculations were carried out for

all the steps in O<sub>2</sub> reduction over Pt(111). As is well established PtCo, PtNi alloys and Pt/Pd pseudomorphic overlayers lead to an optimal balance for the initial O<sub>2</sub> reduction and OH reduction reactions. We have recently extended the calculations to treat the influence of surface coverages.

In addition to these studies on the mechanism of ORR, we also adopted the ab initio double reference approach to examine the oxidative and reductive activation of water and the dissolution of Pt (and Co) over model Pt and PtCo alloys. The results were used to construct surface Pourbaix diagrams for the activation of water to form surface hydride, hydroxide and oxide as a function of potential. The work agrees well with experimental work on the surface phase transitions. Dissolution requires significantly higher potentials which indicates that it occurs at coordinatively unsaturated sites such as step edges or corners. In addition, we have been carrying out the ab initio double reference approach to simulate the oxidative and reductive activation of water over more open surfaces and over very large Pt<sub>110</sub> atom nanoparticles in the presence of 450 water molecules to represent the solution phase. The Pt<sub>110</sub>/water structure at the potential of zero charge is shown in Fig. 2.



### Future Efforts

We are currently extending the work to examine ORR chemistry as well as the dissolution of Pt from the large Pt<sub>110</sub> atom nanoparticle structure shown in Fig. 2. The simulations will be used to examine in detail the influence of coverage as well as the influence of alloying Co, Ni and Fe.

### Publications (2008-2009)

Janik, M.J., C.D. Taylor, and M. Neurock, Oxygen reduction reaction mechanism over Pt(111) from periodic density functional theory: Potential dependence of the activation barrier for the first reduction step, *J. Electrochem. Soc.*, 156, 1, B126-B135, 2008.

Neurock, M., "Theory Aided Catalyst Design", Design of Heterogeneous Catalysts: New Approaches based on Synthesis, Characterization and Modelling, VCH-Wiley, 2008.

Janik, M.J., S.A. Wasileski, C.D. Taylor, and M. Neurock, "First Principles Simulation of the Active Sites and Reaction Environment in Electrocatalysis", Fuel Cell Catalysis: A Surface Science Approach, J.Wiley & Sons, ed. M. Koper, 2009, in Press.

M. Neurock, First-Principles Modeling for the Electrooxidation of Small Molecules, Handbook of Fuel Cells, ed. H. Gasteiger, H. Yokokawa and W. Vielstich, Wiley and Sons, 2009.

## **Novel Structures of Supported Metal Oxide Catalysts Using Calixarene and Macrocyclic Amine Complexes on Hybrid Organic-Inorganic Surfaces**

Justin M. Notestein,\* Andrew W. Korinda, Nick J. Schoenfeldt, Lisa E. Felberg, Dario Prieto-Centurion, Pria D. Young, and Natalia Morlanes-Sanchez

Northwestern University, Department of Chemical and Biological Engineering, Evanston IL 60208

e-mail: [j-notestein@northwestern.edu](mailto:j-notestein@northwestern.edu)

Novel hybrid organic-inorganic catalysts are described that employ multidentate organic ligands and grafted exchange sites to control the degree of site isolation, coordination number, and synergistic arrangement of functional groups around supported metal oxide sites. Selected results are chosen from emerging work on routes to creating isolated sites via ligand-protected grafting of single Ti, Mn, Ta, and Fe cations for applications in epoxidation, hydroxylation, photocatalysis, and model hydrotreating reactions such as deoxygenation or denitrogenation. A novel synthetic technique for supporting oxides of defined nuclearity is also presented. Oxide supports (e.g.  $\text{SiO}_2$  or  $\text{Al}_2\text{O}_3$ ) are functionalized with organic exchange sites and active and selective catalysts are created when the resulting surfaces are loaded with pre-formed metal oxide dimers and related structures synthesized in solution with atomic precision. The solid materials have substantial catalytic oxidation reactivity as synthesized, or subsequent calcination of the material can be performed to result in uniform and highly dispersed oxide active sites whose structure and reactivity are nonetheless dependent on the nuclearity of the precursor. Finally, techniques are described for creating supramolecular arrangements combining molecular catalytic groups and reactant binding sites on hybrid organic/inorganic surfaces. All catalyst materials are probed by TGA, diffuse reflectance UV/Vis, X-ray diffraction, solid state NMR, and temperature programmed techniques to gain insight into the surface structure and domain size of the active sites. Creating uniform populations of atomically-precise surface structures is critical for developing an enhanced fundamental understanding of heterogeneous catalysis and for the rational development of transformative new materials.

**The Reactivity and Structural Dynamics of Supported Metal Nanoclusters Using Electron Microscopy, in situ X-Ray Spectroscopy, Electronic Structure Theories, and Molecular Dynamics Simulations.**

Additional PIs: Judith Yang (U. Pittsburgh), Duane Johnson (Illinois), Anatoly Frenkel (Yeshiva U.)  
Post-docs: Long Li (U. Pittsburgh), Qi Wang (Yeshiva U.), Lin-lin Wang (Illinois)  
Graduate Students: Sergio Sanchez (Illinois), Matthew Small (Illinois), Zhongfan Zhang (U. Pittsburgh)  
Undergrad Students: M. Bromberg (YU)  
Collaborators: J. Rehr (U. Washington), V. Petkov (Central Mich. Univ.), X. Teng (U. New Hampshire), K. Guy, C. Werth, J. Shapley (Illinois)

Contact:

R. Nuzzo, Chemistry Dept., Univ. of Illinois, 600 S Mathews Avenue, Urbana, IL, 61801; [r-nuzzo@illinois.edu](mailto:r-nuzzo@illinois.edu)  
J. Yang, Dept. of Mech. Eng. Mat. Sci., Univ. of Pittsburgh, 3700 O'Hara St, Pittsburgh, PA 15261; [judyang@pitt.edu](mailto:judyang@pitt.edu)  
A. Frenkel, Dept. of Physics, Yeshiva Univ., 245 Lexington Avenue, New York, NY 10016; [Anatoly.Frenkel@yu.edu](mailto:Anatoly.Frenkel@yu.edu)  
D. Johnson, Dept. of Mat. Sci. Eng., Univ. of Illinois, 1304 W. Green, Urbana, IL 61801; [duanej@illinois.edu](mailto:duanej@illinois.edu)

**Goal**

This project involves the characterization of metal nanoparticles (NPs) with the goal of achieving a fundamental understanding of their dynamical and structural properties and the correlations these have with behavior seen in catalytic chemistry. Nanomaterials prepared via controlled chemical syntheses are characterized using a variety of analytical techniques, highlighted by the complementary use of X-ray absorption spectroscopy (XAS) and advanced transmission electron microscopy (TEM). Theoretical calculations further augment an understanding of structures that are characteristic of the nanometer dimensions of catalyst materials or of the local environment of the catalyst.

**DOE Interest**

Our program of collaborative research develops atomistically rationalized understandings of the structural dynamics of nanoscale heterogeneous catalysts. We highlight coordinated efforts to characterize heretofore poorly understood physico-chemical behaviors seen in such systems and the critical role that bonding interactions with adsorbates and supports play in mediating them. This work emphasizes the development, integration, and exploitation of state of the art experimental and theoretical methods to elucidate the fundamental science of complex phenomena whose understanding is of central importance to the development of new types of catalysts and advanced energy conversion systems based on them. The systems explored in this work include exceptionally well-defined metal and metal-alloy catalysts supported in diverse forms—materials that are synthesized by the collaborating team and chosen for the insights they empower into fundamental electronic, structural, and dynamical behaviors.



## Recent Progress

**A. Interactions in supported mono- and heterometallic nanoparticles:** Our studies of the prototypical heterogeneous reforming catalyst Pt supported on  $\gamma$ -Al<sub>2</sub>O<sub>3</sub> are now quite advanced. The most remarkable of the behaviors we uncovered in this work, and one subjected to extensive validation efforts because of the significant questions it raises, involved the inherently non-bulk-like occurrence of “negative thermal expansion” (NTE) in Pt<sub>n</sub>/ $\gamma$ -Al<sub>2</sub>O<sub>3</sub>. We uncovered multiple correlations between the dynamic and structural characteristics of different sized NP, supported on different substrates and subjected to different gas environments. For NP sizes of 0.9 to 3 nm, the changes in the NP properties revealed by XAFS are most significant. For example, the 1 nm size Pt NPs demonstrate strong sensitivities to: 1) the substrate, where C-supported clusters evidence bulk-like dynamics and electronic properties while those Pt<sub>n</sub>/ $\gamma$ -Al<sub>2</sub>O<sub>3</sub> of the same size reveal strong perturbations in terms of atomic and electronic structure, and dynamical features such as NTE; 2) adsorbates, where the bond lengths found in Pt<sub>n</sub>/ $\gamma$ -Al<sub>2</sub>O<sub>3</sub> in inert atmospheres are much shorter than under H<sub>2</sub> but longer than those in a weakly oxidizing atmosphere. The most striking aspect of these data is the dynamical perturbations that are evidenced in the context of marked (and adsorbate dependent) M-M bond-length disorder and anomalous structural and electronic thermal behaviors. Supported Pt-Ir clusters of 1 nm size exhibited competing interactions between the metal atoms and adsorbates, metals and substrate, as well as the charge transfer between the alloying elements (figure 1).

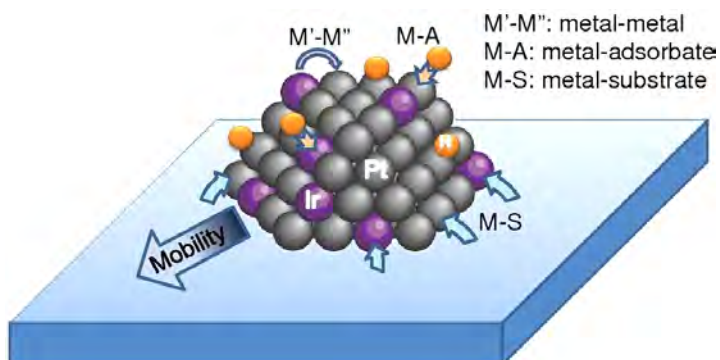


**Figure 1.** Schematic of the complex interactions in supported bimetallic clusters in [IrPt]/ $\gamma$ -Al<sub>2</sub>O<sub>3</sub>.

**B. Size dependent Pt NPs supported on  $\gamma$ -Al<sub>2</sub>O<sub>3</sub>:** We observed size-dependent crystallinity of Pt<sub>n</sub>/ $\gamma$ -Al<sub>2</sub>O<sub>3</sub>. The supported NPs were synthesized with different wt% Pt via a Pt<sup>2+</sup> precursor, Pt(NH<sub>3</sub>)<sub>4</sub>(OH)<sub>2</sub>·H<sub>2</sub>O, to produce a size range from sub- to several nm in diameter. The focal series reconstruction (FSR) of the HRTEM data revealed size-dependent crystallinity of clusters: Pt NPs <1 nm in diameter had a disordered structure while those >2.5 nm had FCC structure. A transition range exists from 1.1 to 2.4 nm, in which more than 85% of NPs appeared disordered and less than 15% ordered, see figure 2 (a)-(d). Figure 2(e) shows the static disorder parameters measured by temperature-resolved EXAFS, where a general trend of increased static disorder is noted as the NP sizes or coordination number decreases. Simulations via *ab initio* Molecular Dynamics (AIMD) demonstrated that the ground state structure of Pt<sub>37</sub>/ $\gamma$ -Al<sub>2</sub>O<sub>3</sub> (100) (size of ~1.1 nm) has a disordered structure (figure 2g), which is more favorable than the FCC structure (figure 2f) by 1.53 eV (or 0.04 eV per Pt atom). The calculated average first nearest-neighbor bond length and coordination number is 2.67 Å and 6.4, respectively, for the ordered particle (figure 2f), and 2.65 Å and 6.3 for the disordered particle (figure 2g). The disordered structures of Pt NPs between 1.1 and 2.4 nm were more frequently observed by HRTEM (>85%) than the ordered ones as a consequence of the small energy preference (0.04 eV per Pt atom) for the disordered structure.

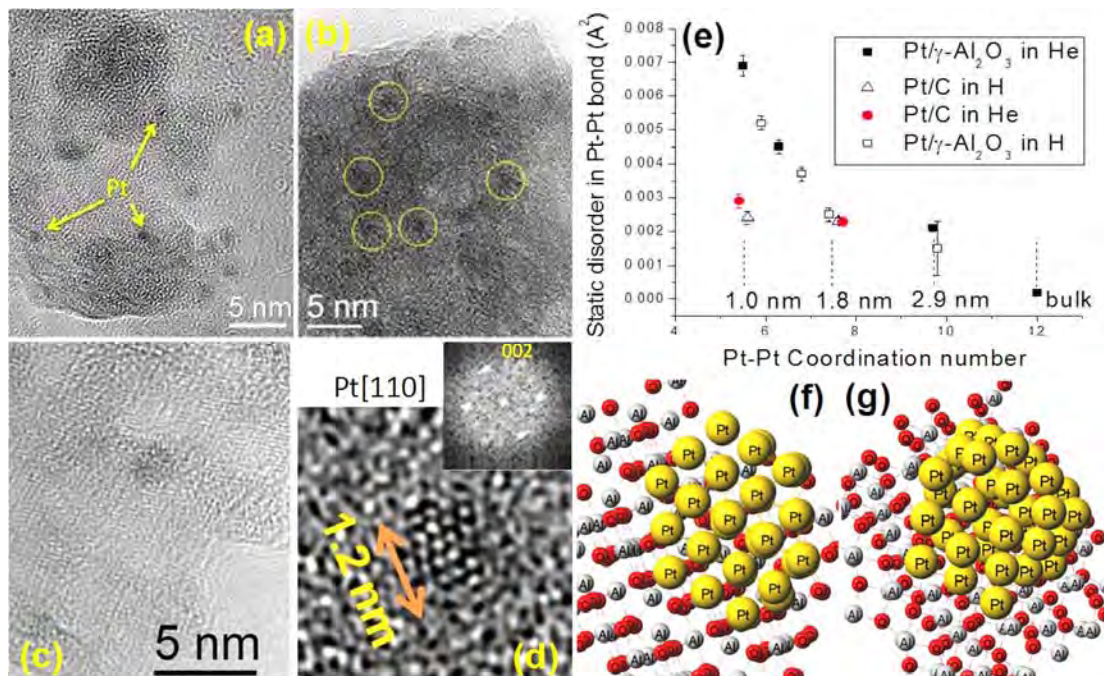
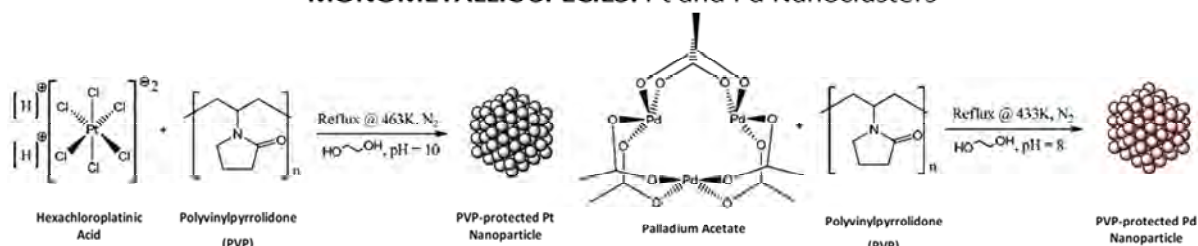


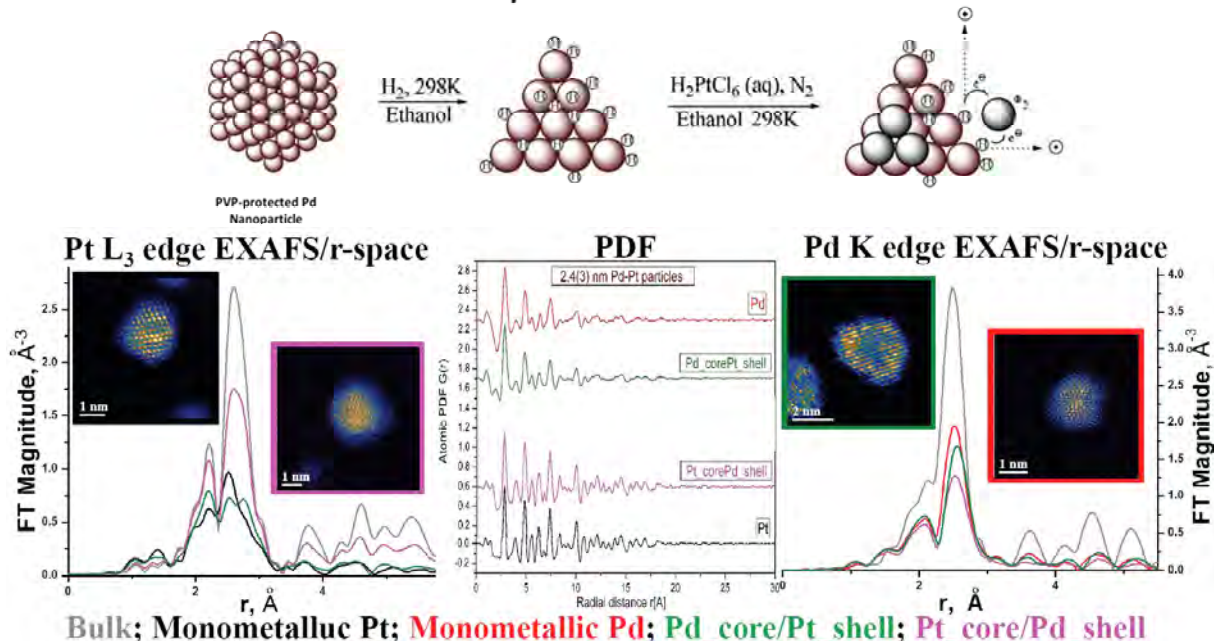
**Figure 2.** HRTEM observations: representative images showing the disordered habits of supported Pt nanoparticles with sizes of (a) sub-nm , (b) 1.1-1.5 nm, (c)~2 nm, and (d) an ordered Pt particle of 1.2 nm; more than 85% of the supported Pt particles (1.1 to 2.4 nm) were disordered; (e) EXAFS data illustrating strong sensitivity of the presence of static bond-length disorder and its dependence on the cluster size and substrate; MD simulation of a  $\text{Pt}_{37}/\gamma\text{-Al}_2\text{O}_3$  (001): (f) ordered truncated cuboctahedron with FCC-stacking and (g) disordered structure, both configurations with sizes of ~1.1 nm. The energy preference of (g) over (f) is 0.04 eV per Pt atom. The average first nearest neighbor bond length and coordination number is 2.67 Å and 6.4 for (f), and 2.65 Å and 6.3 for (g), respectively.

**C. Latest results on aberration-corrected Scanning TEM (STEM):** An important addition to our experimental effort is a state of the art aberration-corrected ( $C_s$ ) STEM, where single atoms can be resolved. The aberration-corrected JEM-2200FS microscope is equipped with a 200 kV field emission gun (FEG), a CEOS probe  $C_s$ -corrector, and an in-column energy filter (Omega filter) that allows elemental analysis and chemical analysis of specimens. It is also equipped with an energy dispersive X-ray spectrometer (EDS) and a CCD-camera. Most importantly, with an available small probe size of ~0.1 nm, atomic level high-resolution high-angle annular dark-field (Z-contrast) images and high-resolution EELS spectrum imaging can be obtained. As we illustrate with preliminary data coming from an exemplary current study, this new addition to our instrumental resources will provide an unprecedented capability to structurally characterize and speciate with atomic precision the clusters present in a heterogeneously supported catalyst sample—the model materials developed in the program component described immediately above. We highlight here the specific example of the polymer encapsulated Pt-Pd and Pd-Pt core shell particles prepared according to a variant of the protocol schematically depicted in figure 3.

### MONOMETALLIC SPECIES: Pt and Pd Nanoclusters



### CONTROLLED BIMETALLIC CORE/SHELL STRUCTURE: Core shell motif with Pd at the core



**Bulk; Monometallic Pt; Monometallic Pd; Pd\_core/Pt\_shell; Pt\_core/Pd\_shell**

**Figure 3.** Above is a schematic showing the synthesis of monometallic Pt and Pd nanoclusters and the template syntheses of a core-shell structure directed by a sacrificial hydrogen layer. Below are Fourier transform magnitudes of the EXAFS data for the Pt L<sub>3</sub> and Pd K edge. The EXAFS data shown are for the monometallic Pt, Pd, bimetallic Pt(core)-Pd(shell), Pd(core)-Pt(shell), bulk Pt and bulk Pd. The insets show atomic resolution HAADF-STEM micrographs. These images revealed the highly crystalline nature of the Pt cluster and the apparent structural strain characterizing the structure of similarly sized Pd clusters. The core-shell structures can be qualitatively characterized by intensity maps dependence on atomic number where higher intensity implies a stronger scattering element (Pt) compared to a lower scattering element (Pd). The PDF data contrasts the coherency and long range order in the crystal structures for the different monometallic and bimetallic samples.

**D. DFT/MD study on Pt<sub>10</sub> supported on  $\gamma$ -Al<sub>2</sub>O<sub>3</sub> [110]: role of dynamic structure and vacancies:** We have developed needed theoretical approaches to understanding the physics unique to matter at this scale. First-principles calculations by Johnson's group have demonstrated the role of *oxygen vacancies* in stabilizing supported Pt<sub>n</sub>/ $\gamma$ -Al<sub>2</sub>O<sub>3</sub>. The results (figure 4) suggest that the clusters can adopt strongly varying structures and in ways that are responsive to the specific bonding arrangements present on different sites on the surface. Due to the shallow nature of the energy barriers as compared to the clusters' thermal energy, metastable structures are directly accessible, and with an increasing facility at higher temperatures. The larger time scales (and, hence, slower) dynamics emerging from this new picture are directly relevant to structural explorations made in an EXAFS experiment. The

focus of Johnson's work on longer time scales that are not feasible for treatment within *ab initio* molecular dynamics, required an assessment of thermally averaged Pt-Pt bond lengths by Boltzmann statistics analysis (using a database of fully relaxed local NP configurations) as opposed to a direct measurement of the pair distribution function in an MD run (figure 5, done by Rehr). These results complementing and extending those coming from our collaborations with J. Rehr's group, reveal a broader impact of cluster librational motion (figure 5) on anomalous structural and electronic properties found in experiment. It remains a challenge, though, to bridge these new insights to the most fundamental question related to a chemical transformation mediated by such a prototypical heterogeneous catalyst—to demonstrate how the dynamical ensembles revealed by the present work might act to promote specific forms of molecular transformations. This challenge is one we have already begun to address and which will motivate work significant aspects that we propose to carry out in the next grant period.

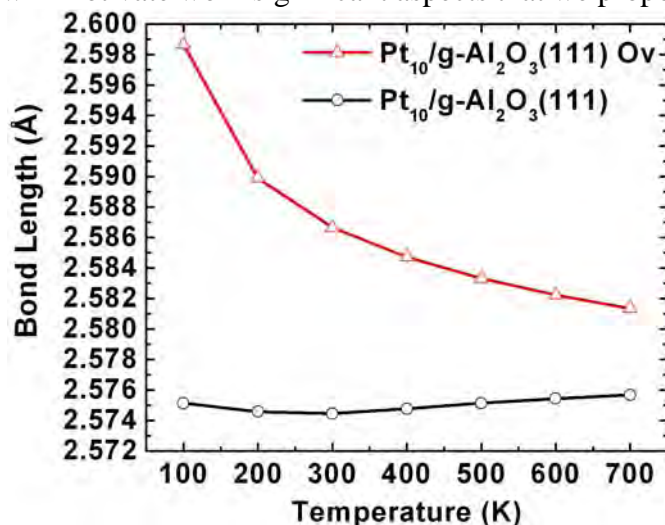


**Figure 4.** Thermally-averaged Pt-Pt bond length according to Boltzmann distribution for Pt<sub>10</sub> supported on  $\gamma$ -Al<sub>2</sub>O<sub>3</sub> surface with(out) oxygen vacancy.

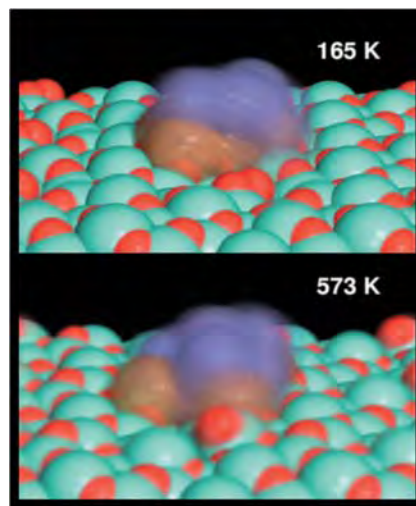


**Figure 5.** Time-elapsing rendering of the structure of a Pt<sub>10</sub> cluster on  $\gamma$ -Al<sub>2</sub>O<sub>3</sub> [110].

### Future Plans

- We will develop new forms of model materials to establish with atomic precision the nature of the bonding that mediates metal support interactions in heterogeneous catalysis, including compositionally complex systems that mediate important electrocatalysis and environmental remediation. We will characterize important classes of promoters and active supports.
- We will undertake development efforts to extend broadly the capacities and reach of the correlated use of advanced forms of electron microscopy and synchrotron X-ray based characterization methods. Furthermore, spatially separating catalytically active species by DAFS coupled to time domain measurements from XAFS will advance understandings of catalytic reaction pathways.
- We will utilize theory and DFT/MD simulations to address the much more challenging goal of correct prediction of catalytic rates and selectivity—to establish a critical linkage between atomic and electronic structure to the specific forms of chemistry promoted by a catalyst.

**Selected Publications (2007-2009) (56 in total: 9 in preparation, 5 submitted, 42 published)**

1. A. I. Frenkel, J. C. Yang, D. D. Johnson, R. G. Nuzzo, *Complexity of nanoscale atomic clusters*, Springer Encyclopedia of Complexity and Systems Science, 5589-5912 (2009).
2. A. Kowal, M. Li, M. Shao, K. Sasaki, M. B. Vukmirovic, J. Zhang, N. S. Marinkovic, P. Liu, A. I. Frenkel, R. R. Adzic, *Ternary Pt/Rh/SnO<sub>2</sub> electrocatalysts for oxidizing ethanol to CO<sub>2</sub>*, Nature Materials **8**, 325-330 (2009).
3. L. Li, J. H. Kang, S. I. Sanchez, Q. Wang, L.-l. Wang, Z. Zhang, D. D. Johnson, A. I. Frenkel, R. G. Nuzzo, J. C. Yang, *Size-dependent crystallinity and relative orientations of nano-Pt/ $\gamma$ -Al<sub>2</sub>O<sub>3</sub>*, Microscopy and Microanalysis **14**, 184-185 (2008).
4. W. J. Huang, R. Sun, J. Tao, L. D. Menard, R. G. Nuzzo, J. M. Zuo, *Coordination-dependent surface atomic contraction in nanocrystals revealed by coherent diffraction*, Nature Materials **7**, 308-313 (2008).
5. X. W. Teng, W. Q. Han, Q. Wang, L. Li, A. I. Frenkel, J. C. Yang, *Hybrid Pt/Au nanowires: Synthesis and electronic structure*, Journal of Physical Chemistry C **112**, 14696-14701 (2008). (Letters)
6. X. W. Teng, Q. Wang, P. Liu, W. Han, A. Frenkel, W. Wen, N. Marinkovic, J. C. Hanson, J. A. Rodriguez, *Formation of Pd/Au nanostructures from Pd nanowires via galvanic replacement reaction*, Journal of the American Chemical Society **130**, 1093-1101 (2008).
7. F. Vila, J. J. Rehr, J. Kas, R. G. Nuzzo, A. I. Frenkel, *Dynamic structure in supported Pt nanoclusters: Real-time density functional theory and X-ray spectroscopy simulations*, Physical Review B **78**, 121404/1-4 (2008).
8. L. L. Wang, D. D. Johnson, *Electrocatalytic properties of PtBi and PtPb intermetallic line compounds via DFT: CO and H adsorption*, Journal of Physical Chemistry C **112**, 8266-8275 (2008).
9. Z. Liu, K. A. Guy, J. R. Shapley, C. J. Werth, Q. Wang, A. I. Frenkel, J. C. Yang, *Microstructural characterization of colloid-derived bimetallic Pd-Cu nanocatalysts supported on  $\gamma$ -Al<sub>2</sub>O<sub>3</sub> for Nitrate Reduction*, Microscopy and Microanalysis **14**, 186-187 (2008).
10. N. A. Zarkevich, T. L. Tan, D. D. Johnson, *First-principles prediction of phase-segregating alloy phase diagrams and a rapid design estimate of their transition temperatures*, Physical Review B **75**, 104203/1-12 (2007).
11. A. I. Frenkel, *Solving the 3D structure of metal nanoparticles*, Zeitschrift für Kristallographie **222**, 605-611 (2007). (Invited article for the special issue "Structure Studies of Nanocrystals")
12. O. Guliamov, A. I. Frenkel, L. D. Menard, R. G. Nuzzo, L. Kronik, *Tangential ligand-induced strain in icosahedral Au<sub>13</sub>*, Journal of the American Chemical Society **129**, 10978-10979 (2007). (Communications)
13. L. Li, L. D. Menard, F. Xu, J. Kang, R. G. Nuzzo, J. C. Yang, *Quantitative studies on Au nano-catalysts by STEM and HRTEM*, Microscopy and Microanalysis **13**, 566-567 (2007).
14. A. I. Frenkel, L. D. Menard, P. Northrup, J. A. Rodriguez, F. Zypman, D. Glasner, S.-P. Gao, H. Xu, J. C. Yang, R. G. Nuzzo, *Geometry and Charge State of Mixed-Ligand Au<sub>13</sub> Nanoclusters*, AIP Conf. Proc. **882**, 749-751 (2007).
15. L. L. Wang, D. D. Johnson, *Shear instabilities in metallic nanoparticles: Hydrogen-stabilized structure of Pt<sub>37</sub> on carbon*, Journal of the American Chemical Society **129**, 3658-3664 (2007).

**Fundamentals of Heterogeneous Catalysis on Surfaces and Nanostructures**

Co-PI: Sheng Dai, David R. Mullins, Zili Wu

Collaborators: Ye Xu, Viviane Schwartz, De'en Jiang, Albina Borisevich, Edward W. Hagaman, Larry Allard, Stephen J. Pennycook, R.J. Harrison, Sergey Rashkeev (INL), Takeshi Egami (U. Tennessee), W. Dmowski (U. Tennessee)

Postdocs: Zhen Ma, Meijun Li, Tsung-Liang Chen, Ariana Beste, Wesley Gordon (VPI), Jason Clark (SudChemie), Sanjaya Senanayake (BNL), Jing Zhou (U. Wyoming)

Contact: Chemical Sciences Division, Oak Ridge National Laboratory, Oak Ridge, TN 37831-6201, [overburysh@ornl.gov](mailto:overburysh@ornl.gov)

**Goals**

The overarching goal of this project is to understand the interactions between metals and their supports and the crucial role these play in promoting or altering catalytic pathways and controlling surface chemistry. Work described in this abstract focuses upon two major aspects 1) understanding how surface chemistry and redox reactions occurs on reducible oxide surfaces, 2) understanding the role of *support type and surface structure* on the catalytic activity of Au catalysts in catalytic reactions.

**DOE interest**

New catalysts are needed to achieve incremental or revolutionary improvements in technologies related to emission control, fuel cells and hydrogen utilization. This work provides a research basis for preparing, testing and understanding catalysts with potential application in these technologies.

**Recent Progress**

A portion of our project focuses on probing the adsorption of a variety of molecules on well ordered films of CeO<sub>2</sub>(111) by TPD, soft x-ray photoemission spectroscopy (sXPS) and reflection absorption spectroscopy. DFT calculations are used to determine the stability and pathways of decomposition for molecules on this model surface and how they are affected by reduction of the CeO<sub>2</sub>(111) surface. We have studied the adsorption of C<sub>1</sub> – C<sub>3</sub> alcohols to determine how alcohol chain length, branching (i.e. primary vs. secondary alcohols) and cerium oxidation state affects the surface chemistry of the ceria surface. sXPS indicates that alcohols universally adsorb on oxidized and reduced surfaces as deprotonated alkoxy species. On oxidized ceria, the secondary alcohol 2-propanol exhibits primarily dehydration to propylene whereas the primary alcohols show significant dehydrogenation to aldehydes. On the reduced surface the alkene fraction increases, driven by the tendency to leave the ceria surface more oxidized. Alkoxy adsorption appears to occur at O vacancy site. The reduced ceria surface clearly demonstrates stronger redox properties than the oxidized surface.

DFT calculations were performed of methanol adsorption on both oxidized and reduced surfaces.<sup>8</sup> DFT finds that methanol adsorption is exothermic on the fully oxidized as well as on the partially reduced surface. The dissociation of methanol on the surface is enhanced by the presence of an oxygen vacancy. An on-top methoxy species, where the methoxy oxygen binds to a single, second layer cerium atom, appears to be the stable dissociation product on the fully oxidized surface. On the partially reduced surface the dissociation product is a triply

bridged methoxy species, where the methoxy oxygen partly fills an oxygen vacancy in the surface. Although adsorption energies are influenced by the introduction of the Hubbard U term, the relative energy differences between surface species such as dissociation energies on the surface are less sensitive.

Acetone was studied as a model ketone.<sup>5</sup> On the reduced surface three unique types of C are detected by high resolution C 1s sXPS. These are attributed to Ce- $\underline{\text{C}}\text{H}_2$ , C- $\underline{\text{C}}\text{H}_3$  and  $\underline{\text{C}}\text{-O}$  species. C 1s NEXAFS indicates the presence of C=C and C=O bonds (**Fig. 1**). It is postulated that the intermediate is a carbanion bonded through both O and C atoms to Ce cations. On an oxidized surface, the chemisorbed molecule binds to the surface as the  $\eta_1$ -acetone rather than through a bridge-bonded dioxy-configuration as seen in formaldehyde.

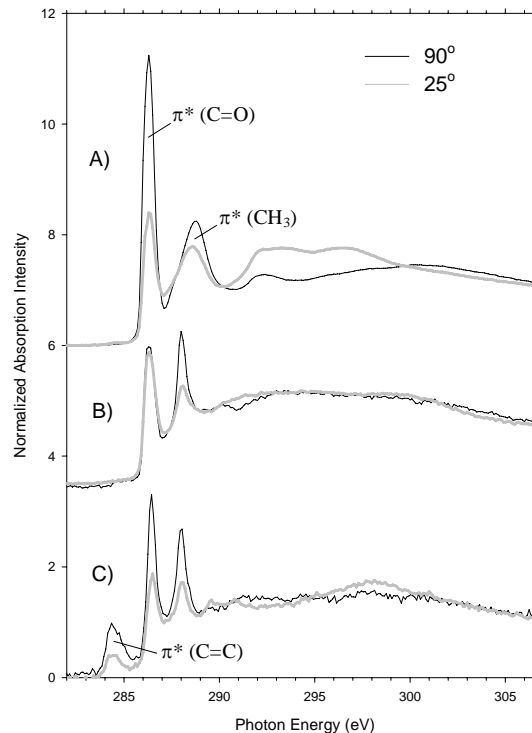


**Fig 1:** C1s NEXAFS from acetone multilayer (A) adsorption on  $\text{CeO}_2(111)$  (B) and reduced ceria (C).

Adsorption of formate on oxide surfaces is of interest because it may play a role as an intermediate in the water-gas shift (WGS) reaction and other reactions related to  $\text{H}_2$  production and  $\text{CO}_2$  utilization. We have applied sXPS, TPD and reflection absorption infra-red spectroscopy (RAIRS) to study the adsorption and thermal evolution of formic acid and formate on highly ordered films of fully oxidized  $\text{CeO}_2(111)$  and highly reduced  $\text{CeO}_x(111)$  surfaces under ultra-high vacuum (UHV) conditions, and the experimental results are combined with density functional theory (DFT) calculations to probe the identity, symmetry, and bonding of the surface intermediates.<sup>2,12</sup>

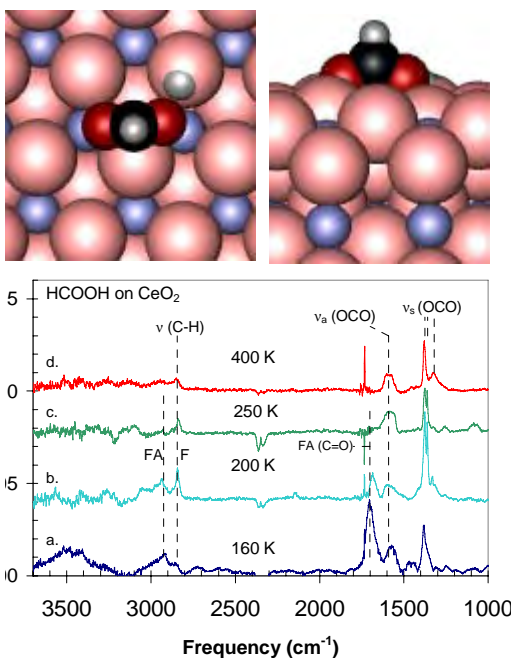


**Fig. 2.** DFT structure of deprotonated formate interacting with H atom on  $\text{CeO}_2$ . RAIRS shows thermal deprotonation of formic acid.

Disordered ice, ordered  $\alpha$ -polymorph and molecular formic acid bonded through the carbonyl are observed at low temperatures. By 250 K, desorption and deprotonation lead to formate co-existing with hydroxyl. DFT results suggest that bridging bidentate formate, coordinated to surface Ce cations in nearly  $\text{C}_{2v}$  symmetry and interacting strongly with neighboring H, is the dominant surface species at this temperature (**Fig. 2**). Changes in the spectra at higher temperatures are consistent with additional tilting of the formate.

This change in bonding symmetry is caused primarily by interaction with oxygen vacancies introduced by water desorption. On reduced ceria, multiple formate states of low symmetry exist due to interactions with clustered oxygen vacancies and neighboring H. Isotopic studies demonstrate that the formyl hydrogen does not contribute to H incorporated in hydroxyl on the surface, and that both formate oxygen atoms may exchange with lattice oxygen at 400 K.

Another portion of our program focuses on the role of support structure and metal support interactions upon catalytic activity in Au catalysts. Our work established that Au supported on non-reducible SiO<sub>2</sub> can be highly active. For this support, the use of a positively charged Au precursor (Au(en)<sub>2</sub>Cl<sub>3</sub>) leads to highly active Au catalysts.<sup>31</sup> The essential synthetic concept is adapting the charge of the Au precursor to the negatively charged SiO<sub>2</sub> that exists under basic conditions of deposition-precipitation.

Extensive studies of the reaction pathways for CO oxidation on the SiO<sub>2</sub> supported Au have been carried out using a transient reactor with FTIR for monitoring the surface species.<sup>7,13</sup> Activating this catalyst requires first calcination at high temperature, but then slow activation is observed under reaction conditions. FTIR indicates that the slow activation is related to the reduction of Au that occurs slowly under reactions conditions. CO oxidation activity is found in good correlation with the reduction degree of Au species, a clear indication of the essential role of metallic Au species played in CO oxidation. (Fig. 3) The

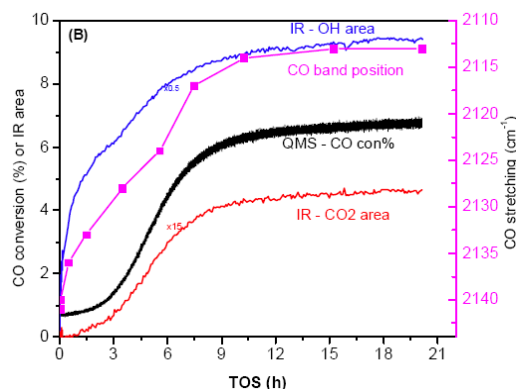


**Fig. 3** Correlation between activity and CO frequency for Au/SiO<sub>2</sub> catalyst.

accompanying slight deactivation with the oxidation of metallic Au species on reductively treated Au/SiO<sub>2</sub> in CO oxidation suggests that cationic Au species may play a negative role in CO oxidation. The effect of water in CO oxidation on Au/SiO<sub>2</sub> was also investigated. Two positive roles played by water in CO oxidation have been identified: activation of O<sub>2</sub> and assistance in the reduction of cationic Au species.

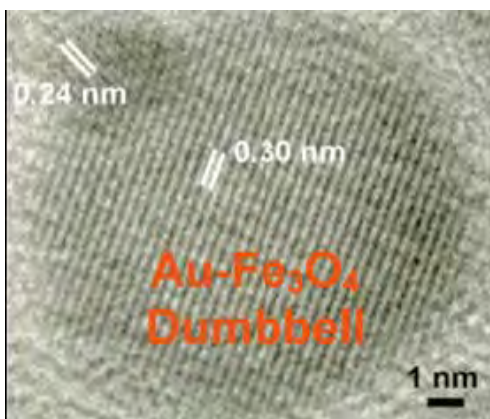


**Fig. 4** Au/Fe<sub>3</sub>O<sub>4</sub> heterostructure

We have also investigated preparation of Au particles supported on nanoparticle supports. A new colloidal deposition methodology was used to introduce Au catalysts on supports via dumbbell-structured Au-Fe<sub>3</sub>O<sub>4</sub> nanoparticles.<sup>16</sup> These heterostructures (Fig. 4) could be deposited onto a many supports (SiO<sub>2</sub>, TiO<sub>2</sub> or C). Au-Fe<sub>2</sub>O<sub>3</sub> heterostructures supported on SiO<sub>2</sub> were very active and stable with respect to sintering. This high stability is attributed to the extra activation energy against the sintering of metal nanoparticles induced by the difference in the metal-support interactions of gold with Fe<sub>3</sub>O<sub>4</sub> and SiO<sub>2</sub>. In other

work we have found that a variety of oxide promoters also had the effect of stabilizing Au particles. Au/TiO<sub>2</sub> modified by several different alkaline earth, rare earth or transition metal



oxides could retain significant activity at ambient temperature even after aging in O<sub>2</sub>-He at 500 °C, whereas unmodified Au/TiO<sub>2</sub> lost its activity.<sup>24</sup> The metal oxide promoter suggest a general methodology of using textural promoters to stabilize Au catalysts, although they may also alter the electronic properties of the active metal or be the source of reactive oxygen caused by certain additives. Modification of supports by phosphates was also explored.<sup>22</sup>

Besides oxide supports, we have also explored the use of non-oxide supports for Au catalysts, especially phosphates. We have investigated different phosphates as supports for Au catalysts and find a fairly wide range of activity and stability, depending upon the support. Au/M-P-O (M = Mg, Al, Zn, Zr) catalysts are not particularly active, regardless of the pretreatment temperature. On the other hand Au/M-P-O (M = Fe, Co) catalysts are active after 200 °C pretreatment, but significantly deactivate after 500 °C-pretreatment. Many active Au/M-P-O catalysts can withstand high-temperature treatment without dramatic loss of activity.<sup>10</sup> We have chosen Au/FePO<sub>4</sub> as a system for detailed kinetic studies.<sup>4</sup> Oxidative pretreatment (in O<sub>2</sub>) leads to cationic Au species that can be reduced by CO, as indicated by changes in CO stretching frequency (**Fig 5**). *In situ* reduction of the cationic Au during CO oxidation generates metallic Au that is active for CO oxidation. Reductive pretreatment (in H<sub>2</sub>) leads to metallic Au species that are more active for CO oxidation than those on an oxidatively pretreated catalyst. FTIR and Raman results indicate that there is active structural oxygen on the Au/FePO<sub>4</sub> catalysts that can be consumed by CO and then replenished by gaseous O<sub>2</sub> at rt. It is found that this active oxygen is not due to any chemisorbed O<sub>2</sub>-like species (superoxide, peroxide) but is due to structural oxide within the phosphate lattice. Au activates both CO and O<sub>2</sub> so that the FePO<sub>4</sub> support can undergo reduction by CO and reoxidation by O<sub>2</sub>. CO oxidation with labeled <sup>18</sup>O<sub>2</sub> demonstrates two parallel reaction pathways at 300 K, 1) a redox pathway in which FePO<sub>4</sub> supplies active oxygen and 2) a direct pathway on metallic Au, via either Langmuir-Hinshelwood or Eley-Rideal mechanisms, in which gas phase O<sub>2</sub> provides the active oxygen.

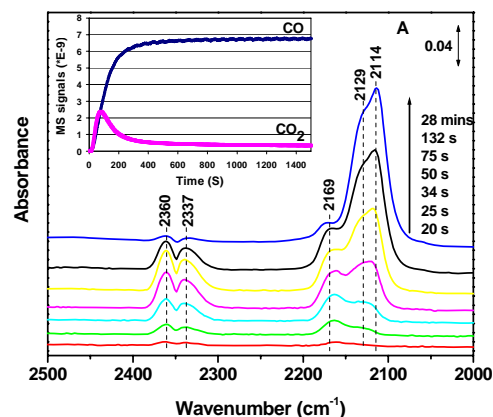


**Fig. 5** FTIR spectra under transient adsorption of CO shows multiple Au sites

### Future Plans

The surface chemistry of oxides is dependent upon the structural termination of the oxide. We will probe this effect in the chemistry on oxidized and reduced CeO<sub>2</sub> surfaces, with and without supported metal particles. We will study molecular adsorption in UHV on CeO<sub>2</sub> films that terminate on different crystallographic planes. In another approach, we have learned how to synthesize CeO<sub>2</sub> nanoparticles which uniformly terminate on only the (100) face (cubes) or only on the (111) faces (octahedra). We plan to use these as supports for metal particles and use this methodology as a means to probe the effect of support structure on catalytic properties in systems with high surface area. These two approaches will be used and compared to probe the chemistry of small molecules (C<sub>1</sub>-C<sub>3</sub> alcohols, aldehydes and acids). We will also investigate the role of support structure in catalytic reactions, especially CO oxidation, WGS and dehydration / dehydrogenation reactions.

We plan to examine how the functionalization of supports affects catalytic activity for supported metals (Au and Rh) on oxide and functionalized oxide supports. In general we find that the stability of the Au particle size and its catalytic behavior may be altered by functionalizing layers on the support particles. For example, functionalizing SiO<sub>2</sub> with a sub-monolayer of TiO<sub>2</sub> can alter both the interaction of the Au precursor with the SiO<sub>2</sub> support during synthesis and also the stability of the resulting Au particles during exposure to subsequent heat treatments and reaction conditions. We will explore how the surface chemistry and reaction pathways are affected by the modifying layer. We will employ two approaches, one based upon highly dispersed nanomaterials using synthesis methods such as layer-by-layer surface sol-gel or atomic layer deposition. Characterization techniques and *operando* methodology appropriate for high surface area samples will be utilized. The second approach will be based upon UHV techniques for preparation of thin layers on single crystal or highly ordered surfaces and characterization of structure and reactivity in UHV.

### Publications (2007-2009)

1. L. F. Allard; A. Borisevich; W. Deng; R. Si; M. Flytzani-Stephanopoulos; S. H. Overbury (2009) Evolution of Gold Structure During Thermal Treatment of Au/FeO<sub>x</sub> Catalysts Revealed by Aberration-Corrected Electron Microscopy, *Journal of Electron Microscopy*, **in press**.
2. W. O. Gordon; Y. Xu; D. R. Mullins; S. H. Overbury (2009) Structure and Bonding of Formic Acid and Formates on fully oxidized and reduced CeO<sub>2</sub>(111), *Journal of Physical Chemistry C*, **submitted**.
3. D.-E. Jiang; S. Dai (2009) Diffusion of the Linear CH<sub>3</sub>S-Au-SCH<sub>3</sub> Complex on Au(111) from First Principles, *Journal of Physical Chemistry C*, **113**, 3763.
4. M. Li; Z. Wu; Z. Ma; V. Schwartz; D. Mullins; S. Dai; S. H. Overbury (2009) CO oxidation on Au/FePO<sub>4</sub> catalyst: Reaction pathways and nature of Au sites, *Journal Catalysis*, **submitted**.
5. S. D. Senanayake; W. O. Gordon; S. H. Overbury; D. R. Mullins (2009) Adsorption and Reaction of Acetone over CeO<sub>x</sub>(111) Thin Films, *Surface Science*, **in press**.
6. G. M. Veith; A. R. Lupini; S. Rashkeev; S. J. Pennycook; D. R. Mullins; V. Schwartz; C. A. Bridges; N. J. Dudney (2009) Thermal stability and catalytic activity of gold nanoparticles supported on silica *Journal of Catalysis*, **262**, 92.
7. Z. Wu; S. Zhou; H. Zhu; S. Dai; S. H. Overbury (2009) DRIFTS-QMS study of room temperature CO oxidation on Au/SiO<sub>2</sub> catalyst: nature and role of different Au species, *Journal of Physical Chemistry C*, **113**, 3726.
8. A. Beste; D. R. Mullins; S. H. Overbury; R. J. Harrison (2008) Adsorption and dissociation of methanol on the fully oxidized and partially reduced (111) cerium oxide surface: Dependence on the configuration of the cerium 4f electrons, *Surface Science*, **602**, 162.
9. Z. Ma; S. Brown; J. Y. Howe; S. H. Overbury; S. Dai (2008) Surface modification of Au/TiO<sub>2</sub> catalysts by SiO<sub>2</sub> via atomic layer deposition, *Journal of Physical Chemistry C*, **112**, 9448.
10. Z. Ma; H. Yin; S. H. Overbury; S. Dai (2008) Metal Phosphates as a New Class of Supports for Gold Nanocatalysts, *Catalysis Letters*, **126**, 20.
11. D. R. Mullins; T. S. McDonald (2008) Adsorption and reaction of methanethiol on thin-film cerium oxide, *Surface Science*, **602**, 1280.
12. S. D. Senanayake; D. R. Mullins (2008) Redox pathways for HCOOH decomposition over CeO<sub>2</sub> surfaces, *Journal of Physical Chemistry C*, **112**, 9744.
13. Z. Wu; S. Zhou; H. Zhu; S. Dai; S. H. Overbury (2008) Oxygen-assisted reduction of Au species on Au/SiO<sub>2</sub> catalyst in room temperature CO oxidation, *Chemical Communications*, **2008**, 3308.
14. W. F. Yan; Z. Ma; S. M. Mahurin; J. Jiao; E. W. Hagaman; S. H. Overbury; S. Dai (2008) Novel Au/TiO<sub>2</sub>/Al<sub>2</sub>O<sub>3</sub> · xH<sub>2</sub>O catalysts for CO oxidation, *Catalysis Letters*, **121**, 209.

15. H. F. Yin; Z. Ma; S. H. Overbury; S. Dai (2008) Promotion of Au(en)<sub>2</sub>Cl<sub>3</sub>-derived Au/fumed SiO<sub>2</sub> by treatment with KMnO<sub>4</sub>, *Journal of Physical Chemistry C*, **112**, 8349.
16. H. F. Yin; C. Wang; H. G. Zhu; S. H. Overbury; S. H. Sun; S. Dai (2008) Colloidal deposition synthesis of supported gold nanocatalysts based on Au-Fe<sub>3</sub>O<sub>4</sub> dumbbell nanoparticles, *Chemical Communications*, **2008**, 4357.
17. J. Zhou; A. P. Baddorf; D. R. Mullins; S. H. Overbury (2008) Growth and characterization of Rh and Pd nanoparticles on oxidized and reduced CeO<sub>x</sub>(111) thin films by scanning tunneling microscopy, *Journal of Physical Chemistry C*, **112**, 9336.
18. Z. Ma; S. H. Overbury; S. Dai. Gold Nanoparticles as Chemical Catalysts. In *Nanomaterials: Inorganic and Bioinorganic Perspectives*; Lukehart, C. M., Scott, R. A., Eds.; John Wiley & Sons.: Chichester, 2007 Vol. in press.
19. Z. Ma; H. Zhu; W. Yan; S. H. Overbury; S. Dai. Functionalized Mesoporous Materials for Gold Catalysis. In *Nanoporous Materials-V* Sayari, A., Jaroniec, M., Eds.; World Scientific Publishing, : Singapore, 2007 Vol. in press.
20. J. C. Clark; S. Dai; S. H. Overbury (2007) Operando studies of desorption, reaction and carbonate formation during CO oxidation by Au/TiO<sub>2</sub> Catalysts, *Catalysis Today*, **126**, 135.
21. W. Dmowski; T. Egami; K. Swider-Lyons; W. Yan; S. Dai; S. H. Overbury (2007) Local atomic structure in disordered and nanocrystalline catalytic materials., *Zeitschrift für Kristallographie*, **222** 617.
22. Z. Ma; S. Brown; S. H. Overbury; S. Dai (2007) Au/PO<sub>4</sub><sup>3-</sup>/TiO<sub>2</sub> and PO<sub>4</sub><sup>3-</sup>/Au/TiO<sub>2</sub> catalysts for CO oxidation: Effect of synthesis details on catalytic performance, *Applied Catalysis A - General*, **327**, 226.
23. Z. Ma; C. Liang; S. H. Overbury; S. Dai (2007) Gold nanoparticles on electroless-deposition-derived MnO<sub>x</sub>/C: synthesis, characterization, and catalytic CO oxidation, *Journal of Catalysis*, **252** 119.
24. Z. Ma; S. H. Overbury; S. Dai (2007) Au / M<sub>x</sub>O<sub>y</sub> / TiO<sub>2</sub> catalysts for CO oxidation: Promotional effect of main-group, transition, and rare-earth metal oxide additives, *Journal of Molecular Catalysis a-Chemical*, **273**, 186.
25. D. R. Mullins; T. S. McDonald (2007) Adsorption and Reaction of Hydrogen Sulfide on Thin-film Cerium Oxide, *Surface Science*, **601**, 4931.
26. O. Ozturk; J. B. Park; S. Ma; J. S. Ratliff; J. Zhou; D. R. Mullins; D. A. Chen (2007) Probing the interactions of Pt, Rh and bimetallic Pt–Rh clusters with the TiO<sub>2</sub>(110) support, *Surface Science*, **601**, 3099.
27. S. N. Rashkeev; A. R. Lupini; S. H. Overbury; S. J. Pennycook; S. T. Pantelides (2007) The role of the nanoscale in catalytic CO oxidation by supported Au and Pt nanostructures *Physical Review B*, **76**, 035438.
28. V. Schwartz; D. R. Mullins; W. Yan; H. Zhu; S. Dai; S. H. Overbury (2007) Structural investigation of Au catalysts on TiO<sub>2</sub>-SiO<sub>2</sub> supports – on the nature of the local structure of Ti and Au atoms by EXAFS and XANES, *Journal of Physical Chemistry C*, **111**, 17322.
29. S. D. Senanayake; J. Zhou; A. P. Baddorf; D. R. Mullins (2007) The reaction of carbon monoxide with palladium supported on cerium oxide thin films, *Surface Science*, **601**, 3215.
30. W. Yan; B. Chen; S. M. Mahurin; S. H. Overbury; S. Dai (2007) Gold supported on microporous aluminophosphate AlPO<sub>4</sub>-H1 for selective oxidation of CO in a H<sub>2</sub>-rich stream, *Studies in Surface Science and Catalysis*, **170**, 1065.
31. H. G. Zhu; Z. Ma; J. C. Clark; Z. W. Pan; S. H. Overbury; S. Dai (2007) Low-temperature CO oxidation on Au/fumed SiO<sub>2</sub>-based catalysts prepared from Au(en)<sub>2</sub>Cl<sub>3</sub> precursor, *Applied Catalysis a-General*, **326**, 89.
32. H. G. Zhu; Z. Ma; S. H. Overbury; S. Dai (2007) Rational design of gold catalysts with enhanced thermal stability: post modification of Au/TiO<sub>2</sub> by amorphous SiO<sub>2</sub> decoration, *Catalysis Letters*, **116**, 128.

**Early Transition Metal Oxides as Catalysts:  
Crossing Scales from Clusters to Single Crystals to Functioning Materials**

Dr. David. A. Dixon<sup>1</sup>, Co-Principal Investigator (Co-PI); Dr. Zdenek Dohnalek<sup>2</sup>, Co-PI; Dr. Dr. Jianzhi Hu<sup>2</sup>, Investigator; Dr. Enrique Iglesia<sup>3</sup>, Co-PI; Dr. Bruce D. Kay<sup>2</sup>, Co-PI; Ja Hun Kwak<sup>2</sup>, Investigator; Dr. Jun Liu<sup>2</sup>, Co-PI; Dr. Charles H. F. Peden<sup>2</sup>, Co-PI and Project Director; Dr. Roger Rousseau<sup>2</sup>, Co-PI; Dr. Lai-Sheng Wang<sup>4</sup>, Co-PI; Dr. Yong Wang<sup>2</sup>, Co-PI; Dr. John M. White<sup>5,\*</sup>, Co-PI; Dr. Hua-Jin Zhai<sup>4</sup>, Investigator.

Postdocs: <sup>2</sup>H.-Y. Fan, <sup>5</sup>Y.K. Kim, <sup>1</sup>S. Li, <sup>2</sup>X. She, <sup>3</sup>T. Stuchinskaya, <sup>2</sup>D. Wang, <sup>3</sup>X. Yin, <sup>2</sup>Z. Zhang, <sup>2</sup>K. Zhu.

Students: <sup>3</sup>R. Carr, <sup>1</sup>R. Craciun, <sup>1</sup>N. Gist (undergrad), <sup>1</sup>D Picone (undergrad), <sup>1</sup>R.T. Long (undergrad), <sup>3</sup>J. Macht

<sup>1</sup>University of Alabama, <sup>2</sup>Pacific Northwest National Laboratory, <sup>3</sup>University of California, Berkeley, <sup>4</sup>Washington State University, <sup>5</sup>University of Texas at Austin

\*Deceased, August 31, 2007

Contact information: C.H.F. Peden, P.O. Box 999, MS K2-12, Pacific Northwest National Laboratory, Richland, WA 99352 chuck.peden@pnl.gov

**Goal**

We are employing an integrated experimental/theoretical approach to advance our current ability to understand, design, and control the catalytic and surface chemistry of transition metal oxides, specifically for redox and acid-base chemistries. The approach combines novel solid-state inorganic synthesis, surface science, experimental and theoretical/computational chemical physics, and mechanistic organic chemistry to address this complex and important challenge.

**DOE Interest**

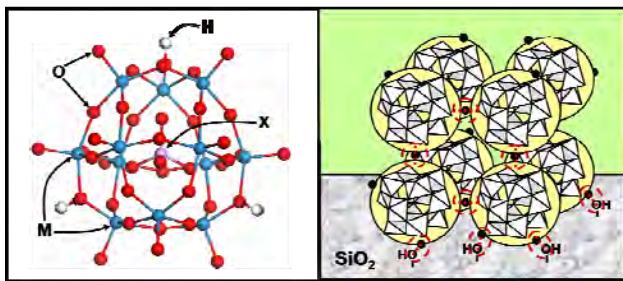
The proportion of chemical industry processes using catalysts exceeds 80%. Current commercial heterogeneous catalysts are structurally and chemically complex and data gathered from them can seldom be interpreted with atomic-level precision. We seek to reduce the complexity of TMO catalysts to levels addressable and controllable at the atomic level, while maintaining intimate linkages with practical catalysis and catalytic materials. The focus of the proposed work is to gain a fundamental understanding of chemical transformations in order to design and construct new catalysts with more precise control of specific chemical reactions. This will enable us to help DOE reach its goals of doing fundamental science to address the energy needs of the country by (1) improving energy conservation by new means of energy conversion and storage; (2) enable direct chemical conversions previously economically unfeasible and produce new routes to novel materials while at the same time minimizing by-products and environmental impact; and (3) protecting the environment

**Recent Progress**

Selected highlights from the results obtained in the last year are presented in this section.

### Catalyst synthesis, characterization, and kinetics studies

**Oxidation and Acid Catalysis on Polyoxometalate Clusters:** Polyoxometalate (POM)-based clusters exhibit uniform and well-defined cluster size and atomic connectivity, diverse chemical compositions, and relatively high stability. These properties make them ideally suited to elucidate the effects of chemical composition, atomic connectivity, and cluster size on acid and redox properties, as well as the consequences of these properties for catalysis by transition metal oxides. Their known and stable structures provide also a unique opportunity for rigorous comparisons with theoretical estimates of their thermodynamic properties and catalytic reactivity. In this program, we have systematically varied the identity of exchanged cations (Me), central atoms (X), and addenda atoms (M) in Keggin POM clusters ( $\text{Me}_x\text{H}_y\text{X}^{n+}\text{M}_{12}\text{O}_{40}$ ; Me =  $\text{Cs}^+$ ,  $\text{Na}^+$ ,  $\text{Cu}^{2+}$ ; X = P, Si, B, Al or Co; M = W, Mo, V or Nb) to examine their effects on the intrinsic reactivity of these clusters in acid and oxidation reactions. These materials crystallize into secondary structures consisting of cubic packings of primary clusters (Scheme 1); as a result, the accessibility and reactivity of intracrystalline acid or redox sites depends on the reaction media and the reactivity and adsorptive properties of active sites may differ between external and internal environments. We have addressed these challenges by developing grafting synthetic methods that enforce significant isolation and reproducible accessibility, by exploiting site titration and spectroscopic protocols that allow measurements of the number of acid sites, and by ensuring the integrity of the grafted clusters *during* catalysis and their minimal fragmentation into lacunary structures.<sup>1</sup> These enabling tools, developed during the previous reporting period, have allowed us to advance our understanding of these systems to an unprecedented level of detail and to provide concepts and knowledge broadly applicable to acid and oxidation catalysis. As part of this program, we have developed rigorous relations between the acid<sup>2</sup> and redox properties of these materials to their reactivity for general reactions of these two types. Theoretical aspects of this program have been carried out in collaboration and consultation with Professor Matthew Neurock of the University of Virginia.



**Scheme 1:** (a) Primary Keggin structure of  $\text{H}_{(8-n)}\text{X}^{n+}\text{M}_{12}\text{O}_{40}$  (colors indicate atomic identity; red = oxygen; blue = addenda (W, Mo); white = hydrogen; purple = central atom (P, Si, Al, Co)). (b) Cubic secondary structure of Keggin POM with hydrogen bonding interactions between clusters and support.

**Mechanistic Consequences of Composition in Acid Catalysis by Polyoxometalate Keggin Clusters:** We have provided evidence for the kinetics and mechanism of ether cleavage and alkanol elimination on Brønsted acids based on dispersed polyoxometalates in terms of elementary steps and of the stability of the transition states involved.<sup>1-6</sup> Measured rates, kinetic isotope effects, and theoretical calculations showed that the energy of cationic transition states and intermediates depends on properties of reactants (proton affinity), POM clusters (deprotonation energy), and ion-pairs in transition states or intermediates (stabilization energy).<sup>2</sup> These represent the critical features for the design of acid catalysts for specific and general reactions proceeding via cationic transition states. The rate equations and elementary steps were identical for all elimination reactions examined (2-propanol, 1- and 2-butanol, *tert*-butanol, *sec*-butyl-methyl ether elimination) on POM clusters with different central atoms (P, Si, Al, Co) and on acidic zeolites. Dehydration rates are determined by the rate constant for elimination from adsorbed alkanols or ethers and on the equilibrium constant for the formation of unreactive reactant dimers.

Elimination involves E1 pathways and late carbenium-ion transition states, consistent with small kinetic isotope effects for all deuterated alkanols, with strong effects of substituents on elimination rates, and with similar alkene stereoselectivities in alkanol dehydration and alkene isomerization.<sup>2</sup> *n*-Donor species, such as alkanols, ethers, or water, inhibit elimination rates by forming stable dimers. These data resolve issues about the nature of elimination transition states; they also rule out E2 elimination pathways

and provide a rigorous and predictive basis to describe the effects of solvation on transition states. Elimination rate constants increased with increasing valence of the central POM atom,<sup>1</sup> because deprotonation energies (DPE) concurrently decrease and form more stable anionic clusters at transition states (Fig. 1).<sup>2</sup> DPE influences rates more weakly than the proton affinity of reactants. These trends reflect the higher charge density at the conjugate base of weaker acids, which stabilize transition state cationic fragments more effectively than less charged conjugate bases of stronger acids. These compensation effects are ubiquitous in acid chemistry and play a critical role in catalytic inhibition by n-donors and in the selectivity of acid catalysis.

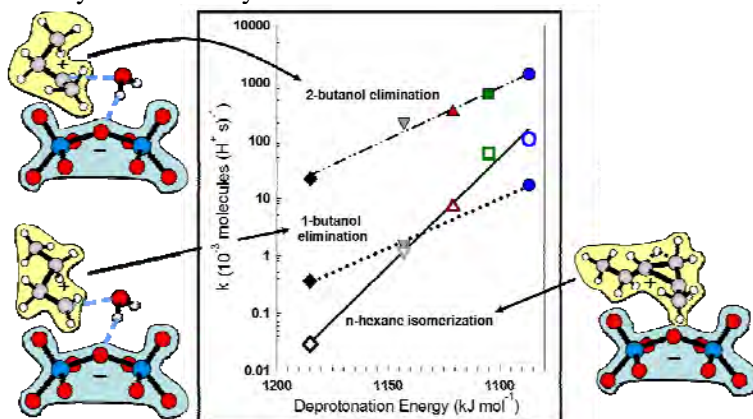


**Fig. 1:** 1-Butanol and 2-butanol elimination (full symbols) and n-hexane isomerization (open symbols) rate constants as a function of deprotonation energy on 0.04H<sub>3</sub>PW/Si (●), 0.04H<sub>4</sub>SiW/Si (■), 0.04H<sub>5</sub>AlW/Si (▲) and 0.04H<sub>6</sub>CoW/Si (▼) and H-BEA (◆) for alkanol elimination and as physical mixtures with Pt/Al<sub>2</sub>O<sub>3</sub> for n-hexane isomerization. Late ion-pair transition state structures for each of the reactions are also shown.

***In-situ High Field, High Resolution NMR Spectroscopy:*** We showed<sup>7</sup> for the first time that the spin-lattice relaxation time,  $T_1$ , corresponding to zeolite-exchanged molybdenum species in Mo/HZSM-5 catalysts is about two orders of magnitude shorter than the corresponding  $T_1$  for small MoO<sub>3</sub> crystallites. Such a difference can be utilized to differentiate the exchanged Mo species from MoO<sub>3</sub> agglomerates in Mo/HZSM-5 catalysts, and to readily estimate their relative fractions present in catalysts with varying Mo loading. A good linear correlation between the amount of zeolite-exchanged species and the aromatics formation rate during catalytic methane dehydroaromatization is obtained. This result together with our recently published data<sup>8</sup> from NMR lineshape simulation unambiguously indicates that the exchanged Mo species are the precursors of the active centers for this reaction on Mo/HZSM-5 catalysts. Of more general interest for Mo-exchanged zeolites, the results may provide useful data for analyzing the binding of exchanged Mo species in zeolite cages. In particular, the NMR data suggest a possible saturation loading for the exchanged Mo species at a Mo/Al ratio of approximately 0.5 for the ZSM-5 zeolite used in this study (Si/Al=25). Furthermore, for polycrystalline MoO<sub>3</sub> powder samples, the parameters related to the electric-field-gradient (EFG) tensor, the chemical shift anisotropy (CSA), and the three Euler angles required to align the CSA principal axis system with the quadrupolar principal axis system are determined by analyzing both the MAS and static <sup>95</sup>Mo spectra. The new results obtained from this study on MoO<sub>3</sub> powders should help to clarify some of the contradictions in prior literature reports of studies of Mo-containing solids by <sup>95</sup>Mo NMR.

We have investigated surface acid sites in dispersed tungsten oxide catalysts supported on SBA-15 mesoporous silica using a combination of pyridine titration, both fast-, and slow-MAS <sup>15</sup>N NMR spectroscopies, and quantum chemical calculations.<sup>9</sup> We find that the <sup>15</sup>N NMR peak corresponding to pyridine reaction with the Brønsted acid site (W-OH) is well separated from the rest of the peaks, while the peaks corresponding to pyridine adsorbed on both the Lewis acid (W=O) and silanol (Si-OH) sites are severely overlapped in the fast-MAS spectra. However, in the slow-MAS spectrum, the spinning sideband families corresponding to all of these sites are uniquely defined, from which the principal values of the

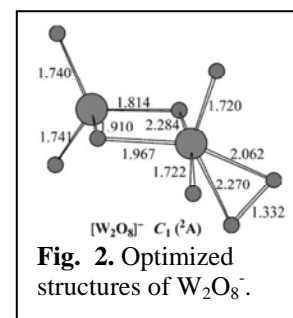
<sup>15</sup>N chemical shift tensors can be determined. Our results indicate that pyridine is capable of acquiring the proton from the Brønsted acid site, suggesting that the acidity of the W-OH group is quite strong. Furthermore, the molecular interactions between pyridine molecules and the Brønsted or the Lewis acid sites for the dispersed tungsten oxide species is strong, making the interacting pyridine molecules rigid even at room temperature. This property also makes it possible to quantitatively determine the relative ratio of the Brønsted to Lewis acid sites in the catalyst using the slow-MAS method. The results suggest that the stable surface acid structure most likely has the form of  $\equiv WO - OH$ ; i.e., each surface bound W site is associated with one Brønsted and one Lewis acid site.

A novel in-situ NMR probe based on both magic angle turning (MAT)<sup>10</sup> and magic angle hopping (MAH)<sup>11</sup> strategies has been developed. Proof-of-concept experiments have been successfully carried out<sup>12</sup> using solid powder samples of adamantane and 1,2,3-trimethoxybenzene and adamantane, where a line narrowing factor of as much as 72 was achieved. Using a method called "discrete magic angle turning" or DMAT, the sample is rotated back and forth as in an MAH experiment, albeit by less than 360°. Since a less than 360° sample rotation is involved, the design potentially allows for in-situ control over physical parameters such as pressure, flow conditions, feed compositions, and temperature so that true in-situ NMR investigations can be carried out.

### Geometric and electronic structure of oxide clusters

#### *Experimental and Theoretical Characterization of Superoxide Complexes $W_2O_6(O_2^-)$ and $W_3O_9(O_2^-)$ : Models for the Interaction of $O_2$ with Reduced W Sites on Tungsten Oxide Surfaces:*<sup>13</sup>

Tungsten oxides are a major focus of this catalysis group project and tungsten oxide clusters have also been a natural focus of this program component. Among the many related studies on  $W_xO_y^-$  type clusters in this funding period, we investigated two O-rich tungsten oxide clusters,  $W_2O_8^-$  and  $W_3O_{11}^-$ , using PES and density functional theory (DFT) calculations. We found that the two anions are best considered as  $O_2^-$  bonded to  $W_2O_6$  and  $W_3O_9$  (Fig. 2), each containing a side-on bound superoxide ligand. In contrast, the neutral clusters  $W_2O_8$  and  $W_3O_{11}$  are predicted to contain a physisorbed  $O_2$  to the  $W_2O_6$  or  $W_3O_9$  stoichiometric cluster. This study shows that the extra electron in the  $W_2O_6^-$  or  $W_3O_9^-$  anionic cluster is capable of activating dioxygen by non-dissociative electron transfer ( $W\ 5d \rightarrow O_2\ \pi^*$ ), and the two anionic clusters can be viewed as models for reduced defect sites on tungsten oxide surfaces for the chemisorption of  $O_2$ .



**Probing the Electronic and Structural Properties of Stoichiometric 3d Transition Metal Oxide Clusters,  $(TiO_2)_n^-$  ( $n = 1-10$ ),<sup>14</sup>  $(V_2O_5)_n^-$  ( $n = 2-4$ ),<sup>15</sup> and  $(CrO_3)_n^-$  ( $n = 1-5$ ):<sup>16</sup>** Bulk oxides of the three early 3d transition metal oxides ( $M = Ti, V, Cr$ ) are insulators with large band gaps. PES provides an ideal means to examine how the band gaps evolve as a function of cluster size. We found that the band gap of  $(TiO_2)_n$  clusters strongly depends on the size and approaches the bulk value at  $n = 7$ . The band gap of  $(CrO_3)_n$  clusters increases monotonically with size and reaches the bulk value for  $n = 4$ , whereas the band gaps of  $(V_2O_5)_n$  clusters for  $n = 2-4$  are all higher than the bulk oxide. The band gap evolution is consistent with the cluster structures. The  $(CrO_3)_n$  clusters possess cyclic structures, in which each Cr is tetracoordinated. The structural parameters for  $(CrO_3)_n$  clusters rapidly converge to those of the bulk oxide just as found for the band gap. The unusually large band gaps in the  $(V_2O_5)_n$  clusters are a consequence of their unique cage structures. We also found that the extra electron in the  $(TiO_2)_n^-$  cluster anions is mainly localized on a Ti site, whereas it is quite delocalized in the  $(CrO_3)_n^-$  clusters.

**Low Lying Electronic States in  $M_3O_9^-$  ( $M = Mo, W$ ):** Multiple low-lying electronic states of  $M_3O_9^-$  and  $M_3O_9^{2-}$  ( $M = Mo, W$ ) arise from the occupation of the near degenerate low-lying virtual orbitals in the neutral clusters. The ADEs and VDEs of the neutral clusters were calculated at the CCSD(T) and DFT levels, the latter with 27 exchange-correlation functionals.<sup>17</sup> Our CCSD(T) calculations including core-valence correlation corrections predict the Jahn-Teller distorted  $^2A_1$  state to be the ground state of  $Mo_3O_9^-$  and that the  $^2A_1$  and  $^2A_1'$  states are of essentially the same energy for  $W_3O_9^-$ . We found that different DFT exchange-correlation functionals yield qualitatively different results for

$W_3O_9^-$ . With core-valence correlation corrections and estimates for the basis set extrapolation corrections included, the CCSD(T) method give good agreement with the experimental electron detachment energies.  $M_3O_9^{2-}$  was predicted to be a delocalized singlet in its ground electronic state, and it was calculated to be less stable than  $M_3O_9^-$  for  $M = Mo$ , but more stable for  $M = W$ . The existence of many low-lying states for these species may have significant implication on the cluster reactivity, which can contribute to the catalytic activity of these transition metal oxide clusters.

#### **Electronic Properties of $TiO_2$ Clusters.**

$TiO_2$  with band gaps of 3.0 eV for rutile and 3.2 eV for anatase is an active photocatalyst as well as an important catalyst support. We predicted the properties of the neutral nanoclusters  $(TiO_2)_n$  and their anions for  $n = 1-4$  at the CCSD(T) and DFT levels.<sup>18</sup> For  $n > 1$ , numerous conformations are possible. The calculated ADEs and VDEs of the anionic clusters to the ground and first excited states of the neutral clusters were calculated to be in good agreement with the experimental results and provide definitive assignment of the ground state structures of the anionic clusters. We developed an approach to reliably predict the heats of formation of metal oxide clusters on the basis of normalized clustering energies. Our CCSD(T) and DFT calculations show that the first excitation energy gaps exhibit a strong dependence on the cluster structures.

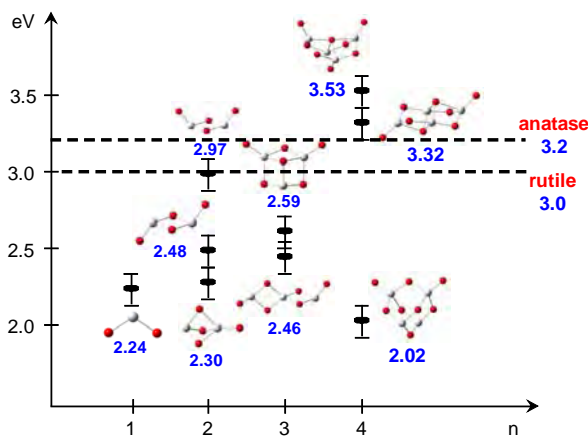


**Fig. 4.** Adiabatic energy gaps for the low-lying structures of the  $(TiO_2)_n$  ( $n = 1-4$ ) clusters calculated at the CCSD(T)/aug-cc-

Fig. 4 displays the adiabatic energy gaps (the energy differences between the first triplet excited states and the ground states of the neutral clusters) at the CCSD(T) level. These gaps, except for the tetramer are below the band gap of the bulk material and show that controlling the particle size and structure will be important in controlling the photocatalytic activity of  $TiO_2$  nanoparticles. The energies of the ground state of the low-lying conformations lie within  $\sim 15$  kcal/mol at the CCSD(T) level to the ground states of these clusters. Thus, they may be present on the surface of  $TiO_2$  catalysts, depending on the manufacturing process, the support, and other environmental effects. As there are a number of low-lying structures with distinct energy gaps, one should be able to tune the photocatalytic properties of the titanium dioxide particles by varying the size and structural distribution with different preparation methods and/or different supports. The anions contain electron-rich titanium center(s) with strong electron donating capability. These anions are expected to be very reactive, which may contribute to the photocatalytic activity of  $TiO_2$ .

### **Surface structure and chemistry of Model, Planar Supported Oxides**

**Interactions of Alcohols with  $(WO_3)_3$  Clusters:** To probe the catalytic activity of the  $(WO_3)_3$  trimers we have carried out reactivity studies with 2-Propanol using TPD studies combined with DFT calculations of possible reaction channels.<sup>19</sup> Our results show that the clusters provide an extremely efficient dehydration reaction channel, which utilizes both strong Lewis acid W(VI) sites and doubly-bonded oxygen tungstyl (W=O) groups. For this specific reaction, the activation energy for dehydration is practically unaffected by the cluster proximity and/or binding to  $TiO_2(110)$ .

To more clearly elucidate general structure-activity trends we studied the reactions of all C1 – C4 aliphatic alcohols (methanol, ethanol, 1- and 2-propanol, and 1-, 2-, and t-butanol) with  $(WO_3)_3$  clusters. In these experiments  $(WO_3)_3$  clusters were deposited into multilayers of alcohols to provide conditions that represent the reactivity of isolated  $(WO_3)_3$  clusters. TPD measurements were used to determine reaction products and infrared reflection absorption spectroscopy (IRAS) was used to probe the bonding between the alcohols and the  $(WO_3)_3$  clusters by examining the W=O bond stretching mode. Concurrently we employed DFT calculations, and the climbing image nudged elastic band method<sup>20</sup> for determining the minimum-energy reaction paths in order to provide a mechanistic framework for interpretation of our



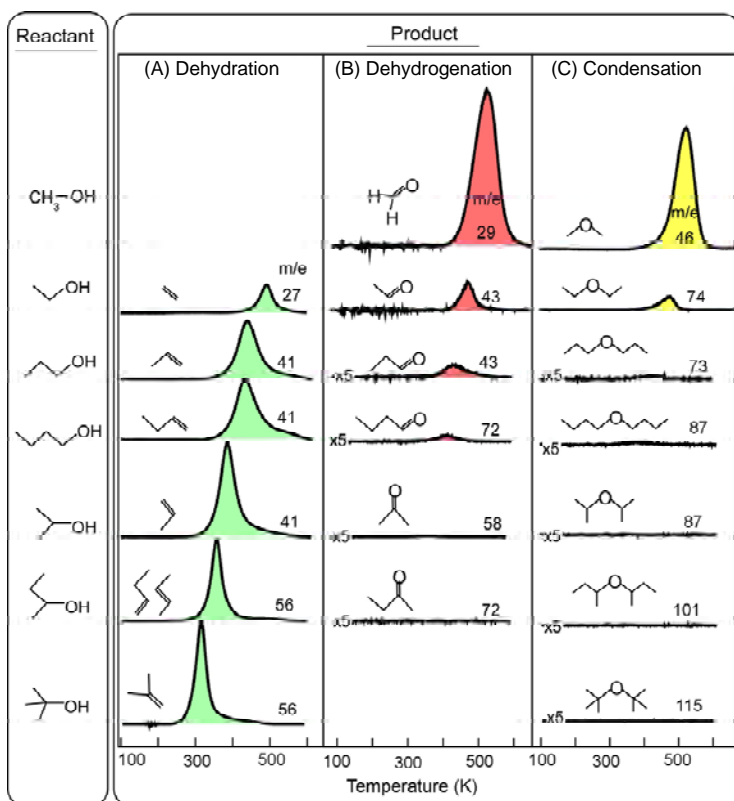


**Fig. 4.** TPD spectra of all three reaction products (alkene, aldehyde, and dialkyl ether), corresponding to dehydration, dehydrogenation, and alcohol condensation, respectively obtained from  $(\text{WO}_3)_3$  clusters ( $1.1 \text{ nm}^{-2}$ ) dropped into a multilayer ( $24 \text{ molecules nm}^{-2}$ ) of C1 to C4 aliphatic alcohols at 100 K.

experimental results. This study was designed to elucidate individual reaction channels under well-controlled stoichiometric conditions thereby yielding quantitative mechanistic information. Our results experimental results. This study was designed to elucidate individual reaction channels under well-controlled stoichiometric conditions thereby yielding quantitative mechanistic information. Our results indicate that the length and number of alkyl chains has a pronounced effect and determines the product branching ratios among the potential dehydration, dehydrogenation, and alcohol condensation reactions. Dehydration was observed for all C2 – C4 alcohols, while dehydrogenation was found to be active only for primary alcohols. Ether formation via condensation was observed only for methanol and ethanol. A summary figure displaying all reaction products is shown in Fig. 4.

Our theoretical calculations reveal possible low-energy barrier mechanisms for all three reactions with dehydration being energetically

favored over the other channels in agreement with experiment. The barrier for dehydration is found to be lowered proportionally with the electron donating ability of the alkyl groups due to stabilization of the transition state.<sup>21</sup> This is similar to the trend observed in our prior studies of alcohol dehydration on bridge-bonded oxygen vacancies of  $\text{TiO}_2(110)$ .<sup>21,22</sup> Interestingly, the dehydration barrier on  $(\text{WO}_3)_3$  clusters is found to be  $\sim 11 \text{ kcal/mol}$  lower than that on  $\text{TiO}_2(110)$  thereby reducing the reaction temperature by over 150K.<sup>21</sup>

## Cited References

- [1] Macht, J; MJ Janik, M Neurock, and E Iglesia, *Angew. Chem. Int. Ed.*, **2007**, *46*, 7864.
- [2] Macht J, M Janik, M Neurock and E Iglesia, *J. Am. Chem. Soc.* **2008**, *130*, 10369.
- [3] Macht J, and E Iglesia, *Phys. Chem. Chem. Phys.* **2008**, *10*, 5331.
- [4] Janik M, J Macht, E Iglesia and M Neurock, *J. Phys. Chem. C* **2009**, in press.
- [5] Macht J, RT Carr and E Iglesia, *J. Catal.* **2009**, submitted.
- [6] Macht J, RT Carr and E Iglesia, *J. Am. Chem. Soc.* **2009**, submitted.
- [7] Hu JZ, JH Kwak, Y Wang, CHF Peden, H Zheng, D Ma and X Bao, *J. Phys. Chem. C* **2009**, *113*, 2936.
- [8] Zheng H, D Ma, X Bao, JZ Hu, JH Kwak, Y Wang and CHF Peden, *J. Am. Chem. Soc.* **2008**, *130*, 3722.
- [9] Hu JZ, JH Kwak, Y Wang and CHF Peden, *Catal. Communications* **2009**, submitted.
- [10] Hu JZ, W Wang, F Liu, MS Solum, DW Alderman, RJ Pugmire and DM Grant, *J. Mag. Res. A* **1995**, *113*, 210.
- [11] Hu JZ, AM Orendt, DW Alderman, C Ye and RJ Pugmire, *Solid State NMR* **1993**, *2*, 235.

- [12] Hu JZ, JA Sears, JH Kwak, DW Hoyt, Y Wang and CHF Peden, *J. Mag. Res.* **2009**, in press.
- [13] X. Huang, H. J. Zhai, T. Waters, J. Li, and L. S. Wang, *Angew. Chem. Int. Ed.* **45**, 657 (2006).
- [14] H. J. Zhai and L. S. Wang, *J. Am. Chem. Soc.* **129**, 3022 (2007).
- [15] H. J. Zhai, Jens Döbler, Joachim Sauer, and L. S. Wang, *J. Am. Chem. Soc.* **2007**, *129*, 13270.
- [16] H. J. Zhai, S. G. Li, D. A. Dixon, and L. S. Wang, *J. Am. Chem. Soc.* **2008**, *130*, 5167.
- [17] S. Li and D. A. Dixon, *J. Phys. Chem. A* **2007**, *111*, 11093.
- [18] S. Li and D. A. Dixon, *J. Phys. Chem. A* **2008**, *112*, 6646.
- [19] Y.K. Kim, R. Rousseau, B.D. Kay, J.M. White, and Z. Dohnálek, *J. Am. Chem. Soc.* **2008**, *130*, 5059.
- [20] X. Huang, H.J. Zhai, B. Kiran, and L.S. Wang, *Angew. Chem., Int. Ed. Engl.* **2005**, *44*, 7251.
- [21] Y.K. Kim, B.D. Kay, J.M. White, and Z. Dohnálek, *Catal. Lett.* **2007**, *119*, 1.
- [22] Y.K. Kim, B.D. Kay, J.M. White, and Z. Dohnálek, *J. Phys. Chem. C* **2007**, *111*, 18236.

## Publications 2007-2009

- Zhang, Z; OA Bondarchuk, BD Kay, JM White, and Z Dohnálek. "Direct Visualization of 2-butanol Adsorption and Dissociation on TiO<sub>2</sub>(110)." *J. Phys. Chem. C* 111 (2007) 3021-3027.
- Zhang, Z; Q Ge, S-C Li, JM White, BD Kay, and Z Dohnálek. "Imaging Intrinsic Diffusion of Bridge-bonded Oxygen Vacancies on TiO<sub>2</sub>(110)." *Phys. Rev. Lett.* 99 (2007) 126105 (4 pages).
- Kim, J; O Bondarchuk, BD Kay, JM White, and Z Dohnálek. "Preparation and Characterization of Monodispersed WO<sub>3</sub> Nanoclusters on TiO<sub>2</sub>(110)." *Catalysis Today* 120 (2007) 186-195.
- Matus, MH; MT Nguyen, and DA Dixon. "Theoretical Prediction of the Heats of Formation of C<sub>2</sub>H<sub>5</sub>O\* Radicals Derived from Ethanol and of the Kinetics of β-C-C Scission in the Ethoxy Radical." *J. Phys. Chem. A* 111 (2007) 113-126.
- Wang, Y; KY Lee, S Choi, J Liu, L-Q Wang, and CHF Peden. "Grafting Sulfated Zirconia on Mesoporous Silica." *Green Chemistry* 9 (2007) 540-544.
- Chimentao, RJ; JE Herrera, JH Kwak, F Medina, Y Wang, and CHF Peden. "Oxidation of Ethanol to Acetaldehyde over Na-promoted Vanadium Oxide Catalysts." *Appl. Catal. A* 332 (2007) 263-272.
- Bondarchuk, OA; YK Kim, JM White, J Kim, BD Kay, and Z Dohnálek. "Surface Chemistry of 2-Propanol on TiO<sub>2</sub>(110): Low and High Temperature Dehydration, Isotope Effects, and Influence of Local Surface Structure." *J. Phys. Chem. C* 111 (2007) 11059-11067.
- Kim, YK; BD Kay, JM White, and Z Dohnálek. "Alcohol Chemistry on Rutile TiO<sub>2</sub>(110): The Influence of Alkyl Substituents on Reactivity and Selectivity." *J. Phys. Chem. C* 111 (2007) 18236-18242.
- Zhai, HJ and LS Wang. "Probing the Electronic Structure and Band Gap Evolution of Titanium Oxide Clusters (TiO<sub>2</sub>)<sub>n</sub> (n = 1-10) Using Photoelectron Spectroscopy." *J. Am. Chem. Soc.* 129 (2007) 3022-3026.
- Kim, YK; BD Kay, JM White, and Z Dohnálek. "Inductive Effect of Alkyl Chains on Alcohol Dehydration at Bridge-bonded Oxygen Vacancies of TiO<sub>2</sub>(110)." *Catal. Lett.* 119 (2007) 1-4.
- Zhai, HJ; BB Averkiev, DY Zubarev, LS Wang, and AI Boldrev. "δ-Aromaticity in Ta<sub>3</sub>O<sub>3</sub><sup>3-</sup>" *Angew. Chem. Int. Ed.* 46 (2007) 4277-4280.
- Zhai, HJ; J Döbler, J Sauer, and LS Wang. "Probing the Electronic Structure of Early Transition Metal Oxide Clusters: Polyhedral Cages of (V<sub>2</sub>O<sub>5</sub>)<sub>n</sub> (n = 2-4) and (M<sub>2</sub>O<sub>5</sub>)<sub>2</sub> (M = Nb, Ta)" *J. Am. Chem. Soc.* 129 (2007) 13270-13276.
- Goodman, DW; MS Chen, and CHF Peden. "CO Oxidation on Ruthenium: The Nature of the Active Catalytic Surface." *Surf. Sci.* 601 (2007) L124-L126.
- Goodman, DW; CHF Peden, and MS Chen. "Reply to Comment on "CO Oxidation on Ruthenium: The Nature of the Active Catalytic Surface" by H. Over, M. Muhler and A.P. Seitsonen" *Surf. Sci.* 601 (2007) 5663-5665.
- Gutowski, KE; RD Rogers, and DA Dixon. "Accurate Thermochemical Properties for Energetic Materials Applications. II. Heats of Formation of Imidazolium-, 1,2,4-Triazolium-, and Tetrazolium-based Energetic Salts from Isodesmic and Lattice Energy Calculations." *J. Phys. Chem. B* 111 (2007) 4708-4800.
- Bhirud, VA; A Uzun, PW Kletnieks, R Craciun, JF Haw, DA Dixon, MM Olmstead, and BC Gates. "Synthesis and Crystal Structure of Ir(C<sub>2</sub>H<sub>4</sub>)<sub>2</sub>(C<sub>5</sub>H<sub>7</sub>O<sub>2</sub>)." *J. Organometallic Chem.* 692 (2007) 2107-2113.
- Grant, DJ; DA Dixon, and JS Francisco. "Coupled Cluster Study of the Energetic Properties of S<sub>2</sub><sup>x</sup> (x = 0, +1, -1)." *J. Chem. Phys.* 126 (2007) 144308 (6 pages).
- Kletnieks, PW; AJ Liang, R Craciun, JO Ehresmann, DM Marcus, VA Bhirund, MM Klaric, MJ Hayman, DR Guenther, OP Bagatchenko, DA Dixon, BC Gates, and JF Haw. "Molecular Heterogeneous Catalysis: A Single-site Zeolite-supported Rhodium Complex for Acetylene Cyclotrimerization." *Chemistry--A European Journal* 13 (2007) 7294-7304.

- Matus, MH; DA Dixon, KA Peterson, JAW Harkless, and JS Francisco. "Coupled-Cluster Study of the Electronic Structure and Energetics of Tetrasulfur, S<sub>4</sub>." *J. Chem. Phys.* 127 (2007) 174305 (7 pages).
- Li, S and DA Dixon. "Low-Lying Electronic States of M<sub>3</sub>O<sub>9</sub><sup>-</sup> and M<sub>3</sub>O<sub>9</sub><sup>2-</sup> (M = Mo, W)." *J. Phys. Chem.* 111 (2007) 11093-11099.
- Dixon, DA; T-H Wang, DJ Grant, KA Peterson, KO Christe, and GJ Schrobilgen. "Heats of Formation of Krypton Fluorides and Stability Predictions for KrF<sub>4</sub> and KrF<sub>6</sub> from High Level Electronic Structure Calculations." *Inorg. Chem.* 46 (2007) 10016-10021.
- Li, S and DA Dixon. "Benchmark Calculations on the Electron Detachment Energies of MO<sub>3</sub><sup>-</sup> and M<sub>2</sub>O<sub>6</sub><sup>-</sup> (M = Cr, Mo, W)." *J. Phys. Chem.* 111 (2007) 11908-11921.
- Peng Z; F Xu, A Navrotsky, J Lee, S Kim, and J Liu. "Surface Enthalpies of Nanophase ZnO with Different Morphologies." *Chem. Matls.* 19 (2007) 5687-5693.
- Macht, J; MJ Janik, M Neurock, and E Iglesia. "Catalytic Consequences of Composition in Polyoxometalate Clusters with Keggin Structure." *Angew. Chem. Int. Ed.* 46 (2007) 7864-7868.
- Sounart TL; J Liu, JA Voigt, M Huo, ED Spoerke, and B Mckenzie. "Secondary Nucleation and Growth of ZnO." *J. Am. Chem. Soc.* 129 (2007) 15786-15793.
- Nguyen, MT; MH Matus, WA Lester, Jr., and DA Dixon. "Heats of Formation of Triplet Ethylene, Ethylidene, and Acetylene." *J. Phys. Chem. A* 112 (2008) 2082-2087.
- Zheng, H; D Ma, X Bao, JZ Hu, JH Kwak, Y Wang, and CHF Peden. "Direct Observation of the Active Center for Methane Dehydroaromatization using an Ultra-High Field 95Mo NMR Spectroscopy." *J. Am. Chem. Soc.* 130 (2008) 3722-3723.
- Zbavre, DY; BB Averkiev, HJ Zhai, LS Wang, and AI Boldyrev. "Aromaticity and Antiaromaticity in Transition-metal Systems." *Phys. Chem. Chem. Phys.* 10 (2008) 257-267.
- Macht, J and E Iglesia. "Structure and Function of Oxide Nanostructures: Catalytic Consequences of Size and Composition." *Phys. Chem. Chem. Phys.* 10 (2008) 5331-5343.
- Zhai, HJ; SG Li, DA Dixon, and LS Wang. "Probing the Electronic and Structural Properties of Chromium Oxide Clusters (CrO<sub>3</sub>)<sub>n</sub> and (CrO<sub>3</sub>)<sub>n</sub> (n = 1-5): Photoelectron Spectroscopy and Density Functional Calculations." *J. Am. Chem. Soc.* 130 (2008) 5167-5177.
- Herrera, JE; JH Kwak, JZ Hu, Y Wang, and CHF Peden. "Effects of Novel Supports on the Physical and Chemical Properties of Tungstophosphoric Acid for Alcohol Dehydration Reactions." *Topics in Catalysis* 49 (2008) 259-267.
- Wang, D.; Z Ma, S Dai, J Liu, Z Nie, MH Engelhard, Q Huo, C Wang, and R Kuo. "Low-Temperature Synthesis of Tunable Mesoporous Crystalline Transition Metal Oxides and Applications as Au Catalyst Supports." *J. Phys. Chem. C* 112 (2008) 13499-13509.
- Macht, J.; M Janik, M Neurock, and E Iglesia. "Mechanistic Consequences of Composition in Acid Catalysis by Polyoxometalate Keggin Clusters." *J. Am. Chem. Soc.* 130 (2008) 10369-10379.
- Zhai, HJ; C Bürgel, V Bonacic-Koutecky, and LS Wang. "Probing the Electronic Structure and Chemical Bonding of Gold Oxides and Sulfides in AuO<sub>n</sub><sup>-</sup> and AuS<sub>n</sub><sup>-</sup> (n = 1, 2)." *J. Am. Chem. Soc.* 130 (2008) 9156-9167.
- Li, S and DA Dixon. "Molecular Structures and Energetic of the (TiO<sub>2</sub>)<sub>n</sub> (n = 1-4) Clusters and Their Anions," *J. Phys. Chem. A*, 2008, 112, 6646.
- Kim, YK; BD Kay, JM White, and Z Dohnálek. "2-Propanol Dehydration on TiO<sub>2</sub>(110): The Effect of Bridge-bonded Oxygen Vacancy Blocking." *Surf. Sci.* 602 (2008) 511-516.
- Moore, LR; EC Western, R Craciun, JM Spruell, DA Dixon, KP O'Halloran, and KH Shaughnessy. "Sterically Demanding, Sulfonated, Triarylphosphines: Application to Palladium-Catalyzed Cross-Coupling, Steric and Electronic Properties, and Coordination Chemistry." *Organometallics* 27 (2008) 576-593.
- Focsan, AL; TA Konolvalova, MK Bowman, DA Dixon, LD Kispert, P Molnár, and J Deli. "Pulsed EPR and DFT Characterization of Radicals Produced by Photo-Oxidation of Zeaxanthin and Violaxanthin on Silica-Alumina." *J. Phys. Chem. B* 112 (2008) 1806-1819.
- Nguyen, MT; MH Matus, VT Ngan, R Haiges, KO Christe, and DA Dixon. "Energetics and Mechanism of Decomposition of Trifluoromethanol." *J. Phys. Chem. A* 112 (2008) 1298-1312.
- Du, Y; Z Dohnálek, and I Lyubinsky. "Transient Mobility of Oxygen Adatoms upon O<sub>2</sub> Dissociation on Reduced TiO<sub>2</sub>(110)." *J. Phys. Chem. C* 112 (2008) 2649-2653.
- Grant, DJ; MH Matus, J Switzer, DA Dixon, JS Francisco, and KO Christe. "Bond Dissociation Energies in Second Row Compounds." *J. Phys. Chem. A* 112 (2008) 3145-3156.
- Li, S; KA Peterson, and DA Dixon. "Benchmark Calculations on the Adiabatic Ionization Energies of the M-NH<sub>3</sub> (M = Na, Al, Ga, In, Cu, Ag) Complexes." *J. Chem. Phys.* 128 (2008) 154301 (12 pages).
- Li, SC; Z Zhang, D Sheppard, BD Kay, JM White, Y Du, I Lyubinsky, G Henkelman, and Z Dohnálek. "Intrinsic Diffusion of Hydrogen on Rutile TiO<sub>2</sub>(110)." *J. Amer. Chem. Soc.* 130 (2008) 9080-9088.

- Hill, LL; JM Smith, WS Brown, LR Moore, P Guevera, ES Pair, J Porter, J Chou, CJ Wolterman, R Craciun, DA Dixon, KH Shaughnessy. "Neopentylphosphines as Effective Ligands in Palladium-catalyzed Cross-couplings of Aryl Bromides and Chlorides." *Tetrahedron* 64 (2008) 6920-6934.
- Feller, D; KA Peterson, and DA Dixon. "A Survey of Factors Contributing to Accurate Theoretical Predictions of Atomization Energies and Molecular Structures." *J. Chem. Phys.* 129 (2008) 204015 (32 pages).
- Matus, MH; MT Nguyen, DA Dixon, and KO Christe. "Thermochemical Properties of CHFO, CF<sub>2</sub>O, and CFO." *J. Phys. Chem. A* 112 (2008) 4973-4981.
- Dixon, DA; DJ Grant, KO Christe, and KA Peterson. "Structure and Heats of Formation of Iodine Fluorides and the Respective Closed Shell Ions from CCSD(T) Electronic Structure Calculations and Reliable Prediction of the Steric Activity of the Free Valence Electron Pair in ClF<sub>6</sub><sup>-</sup>, BrF<sub>6</sub><sup>-</sup> and IF<sub>6</sub><sup>-</sup>." *Inorg. Chem.* 47 (2008) 5485-5494.
- Kim, YK; R Rousseau, BD Kay, JM White, and Z Dohnálek. "Catalytic Dehydration of 2-Propanol on (WO<sub>3</sub>)<sub>3</sub> Clusters on TiO<sub>2</sub>(100)." *J. Am. Chem. Soc.* 130 (2008) 5059-5061.
- Zhang, Z; R Rousseau, J Gong, S-C Li, BD Kay, Q Ge, JM White, and Z Dohnálek. "Vacancy Assisted Diffusion of Alkoxy Species on Rutile TiO<sub>2</sub>(110)." *Phys. Rev. Lett.* 101 (2008) 156103 (4 pages).
- Hu, JZ; JA Sears, JH Kwak, DW Hoyt, Y Wang, and CHF Peden. "An Isotropic Chemical Shift-Chemical Shift Anisotropic Correlation Experiment Using Discrete Magic Angle Turning." *J. Mag. Reson.* (2009) in press.
- Janik, M; J Macht, E Iglesia, and M Neurock. "Correlating Acid Properties and Catalytic Function: A First-Principles Analysis of Alcohol Dehydration Pathways on Polyoxometalates." *J. Phys. Chem. C* (2009) in press.
- Zhang, Z; Y Du, NG Petrik, GA Kimmel, I Lyubinetsky, and Z Dohnálek. "Water as a Catalyst: Imaging Reactions of O<sub>2</sub> with Partially and Fully Hydroxylated TiO<sub>2</sub>(110) Surfaces." *J. Phys. Chem. C* (2009) in press.
- Hu, JZ; JH Kwak, Y Wang, CHF Peden, H Zheng, D Ma, and X Bao. "Studies of the Active Sites for Methane Dehydroaromatization Using Ultra-High Field Solid State <sup>95</sup>Mo NMR Spectroscopy." *J. Phys. Chem. C* (2009) in press.
- Du, Y; NA Deskins, Z Zhang, Z Dohnálek, M Dupuis, and I Lyubinetsky. "Imaging "Elusive" HO<sub>2</sub> and Terminal OH Species during O<sub>2</sub> Reaction with Hydroxylated TiO<sub>2</sub>(110)." *J. Phys. Chem. C* (2009) in press.

## Methylrheniumtrioxide activation on amorphous silica-alumina: benchmark test of DFT model, an aluminum site model, and preliminary results on initiation pathways

S. M. Stewart, S. L. Scott, Baron Peters  
Department of Chemical Engineering, UCSB, Santa Barbara, CA 93106  
email: baronp@engineering.ucsb.edu

Methylrheniumtrioxide (MTO) is highly active for olefin metathesis when supported on amorphous silica-alumina, but many questions surround the activation and deactivation mechanisms. Details of the local support structure are important, but not understood. For example, zeolites are inactive supports despite having the same composition as amorphous silica-alumina. Even on amorphous silica-alumina, most MTO precursors do not become active catalytic centers.[1] Propagation is likely by the Chauvin mechanism, but the pathway from MTO to the active metal carbene ( $\text{Re}=\text{CH}_2$ ) is unknown. Finally, the active sites are easily deactivated by contaminants. *Ab initio* modeling can contribute much to our atomistic level knowledge of these mechanisms, but basis sets and effective core potentials for Rhenium are relatively new and untested compared to those for other elements and the amorphous support also presents significant modeling challenges.[2] We compare calculated and measured kinetics and thermodynamics for reactions between hydrogen peroxide and MTO in solution.[3] These calculations use combinations of two effective core potentials for rhenium with three basis sets for description of the rhenium valence electrons. We find agreement with experiment using the Stuttgart small core effective core potential when combined with the rhenium basis set developed by A. K. Rappe and coworkers.[4] We also present a model of the aluminum environment in amorphous silica-alumina that, in accordance with the hypothesis by Omegna et al.[5], enables aluminum to retain a coordination number of at least four both before and after MTO adsorption. The aluminum site model and the benchmarked model for rhenium chemistry are then combined to investigate the tautomerization and pseudo-Wittig pathways for MTO activation on amorphous silica-alumina.

### References

1. A. W. Moses, C. Raab, R. C. Nelson, H. D. Leifeste, N. A. Ramsahye, S. Chattopadhyay, J. Eckert, B. F. Chmelka, S. L. Scott, *J. Am. Chem. Soc.* **129** 8912 (2007)
2. S. M. Stewart, S. L. Scott, B. Peters, in preparation (2009)
3. W. D. Wang, J. H. Espenson, *Inorganic Chemistry* **36** 5069 (1997)
4. M. A. Pietsch, T. V. Russo, R. B. Murphy, R. L. Martin, A. K. Rappe, *Organometallics* **17** 2716 (1998).
5. A. Omegna, J. A. von Bokhoven, R. Prins, *J. Phys. Chem. B.* **107** 8854 (2003).

**Enhanced Reactivity and Selectivity of Oxide Nanostructures**

Lead PI: T. F. Heinz (Columbia University)

Postdoc: Sampyo Hong (UCF)

Students: Duy Tran Le (UCF), B. White (CU), M. Yin (CU), A. Hall (CU), N. Turro (CU)

Collaborators: G. Ertl and K. Jacobi

Contact: Dept. of Physics, Univ. of Central Florida, Orlando, FL 32816 ([talat@physics.ucf.edu](mailto:talat@physics.ucf.edu))

Dept. Applied Physics, Columbia Univ., New York, NY 10027 ([so188@columbia.edu](mailto:so188@columbia.edu))

Towards the goal of developing of an understanding of factors that control the reactivity and selectivity of nanocatalysts, such as oxide nanoparticles and nanostructured surfaces, through joint experimental and theoretical investigations, we present here some recent results.

In one such effort between O'Brien and Rahman groups we note that nearly monodisperse copper oxide nanoparticles prepared via the thermal decomposition of a Cu(I) precursor exhibit exceptional activity toward CO oxidation in CO/O<sub>2</sub>/N<sub>2</sub> mixtures. Greater than 99.5% conversion of CO to CO<sub>2</sub> could be achieved at temperatures less than 250 °C for over 12 h. The (*P, T*) phase diagram of the Cu<sub>2</sub>O(100) surface, mimicking a nanoparticle facet, in equilibrium of with gas phase O<sub>2</sub> built using the *ab-initio* thermodynamics approach finds the O-terminated surface to have lower free energy than the Cu-terminated one within the entire range of pressure and temperature for which the compound exists. The quasi-stable Cu-terminated Cu<sub>2</sub>O(100) is found to undergo a surface reconstruction in agreement with experiments. A major finding is that CO is oxidized spontaneously on Cu<sub>2</sub>O(100) by consuming surface O atoms. These calculations also show that the surface O vacancies left in the course of the CO oxidation can be easily filled with dissociative adsorption of the gas phase O<sub>2</sub> (activation barrier of 0.3 eV) and that one O atom fills the vacancy while the other occupies the hollow site next to the vacancy, thereby restoring the surface. We present results of microkinetic modeling to justify our claims.

To accompany the above findings, we also present results from Rahman's group, in collaboration with Ertl and Jacobi, on the high selectivity for NO formation in ammonia oxidation on RuO<sub>2</sub>(110). Activation energy barriers and reaction paths for possible competing processes are calculated using density functional theory and the results applied in kinetic Monte Carlo (KMC) simulations of the reaction rates. These simulations reproduce the selectivity towards formation of NO for a substrate saturated with oxygen. The inclusion of several intermediates and their reactions (18 processes) in the KMC simulations shows about 70% selectivity toward NO within the experimental O<sub>2</sub> pressure range. The remarkable agreement between experimental data and theoretical predictions of the relative rates of NO and N<sub>2</sub>, under steady state conditions, provides insights into the reaction paths and mechanisms most suitable for the oxidation process.

References:

1. B. White, M. Yin, A. Hall, D. Le, S. Stolbov, T. S. Rahman, N. Turro, and S. O'Brien, "Complete CO oxidation over Cu<sub>2</sub>O nanoparticles supported on silica gel," *Nano Letters* **6**, 2095 (2006).
2. D. T. Le, S. Stolbov, and T. S. Rahman, "Reactivity of the Cu<sub>2</sub>O(100) surface: Insight from first principles calculations," *Surf. Sci.*, in press <http://dx.doi.org/10.1016/j.susc.2008.12.039>
3. S. Hong, T. S. Rahman, K. Jacobi, G. Ertl, "The Interaction of NO with a RuO<sub>2</sub>(110) Surface: a first principles Study," *Jour. Phys. Chem, C* **111**, 12361 (2007).

### Fundamental Studies on the Kinetics of Oxidation Reactions

Students: Andrew D. Smeltz, Bradley R. Fingland

Collaborators: W. F. Schneider (Notre Dame), Jeffrey T. Miller (BP), Eric Stach (Purdue), D. Zemlyanov (Purdue University), A. Jeremy Kropf (Argonne National Laboratory), Stefan Vajda (Argonne National Laboratory), B.S. Mun (Lawrence Berkeley National Laboratory)

Contact: Fabio H. Ribeiro, Purdue University, 480 Stadium Mall Drive, West Lafayette, IN 47907-2100, phone: (765) 494-7799, E-mail: fabio@purdue.edu

#### Goal

The goal is to develop model catalysts and *operando* tools to study the mechanism of heterogeneous catalytic reactions. We studied Pt single crystal surfaces, Pt clusters deposited on single crystal titania and Pt clusters on various supports for the reaction of NO oxidation.

#### DOE Interest

Development of techniques based on model catalysts and *operando* measurements will help to understand the mechanism of heterogeneous catalytic reactions. Model catalysts, due to the control afforded by the precise variation of surface morphology, allow the testing of mechanisms with an unprecedented level of detail. *Operando* techniques developed for supported catalysts allow the study of structure-property relationships in a direct way.

#### Recent Progress

##### Structure sensitivity of the NO Oxidation Reaction Studied on Single Crystals of Platinum:

NO oxidation was studied on the Pt(321) surface, a surface which represents the surface structure of small 1-3nm particles due to the high degree of coordinative surface unsaturation. Turnover rates (TOR) were measured under a wide range of conditions which allowed us to determine the apparent activation energies and reaction orders for NO, NO<sub>2</sub> and O<sub>2</sub> as a function of the ratio of NO to NO<sub>2</sub>. Further, the previous kinetic study on Pt(111) [1], a surface which represents large 5-10nm particles, was expanded to study the effect of NO:NO<sub>2</sub> on these kinetic parameters. In our previous studies using *in situ* XPS on Pt(111) [1], the ratio of NO to NO<sub>2</sub> was found to be the most important variable in controlling the atomic oxygen, O\*, the most abundant surface intermediate on the surface. This study will investigate how that ratio affects the intrinsic kinetics of NO oxidation.

Figures 1 and 2 show the temperature dependence ( $E_a$ ) and the apparent O<sub>2</sub> order on the kinetics of NO oxidation as a function of NO:NO<sub>2</sub> respectively. The Pt(321) surface had a higher  $E_a$  over the range studied which also increased more rapidly as NO:NO<sub>2</sub> decreased as compared to Pt(111). Further the TOR dependence on O<sub>2</sub> pressure was more pronounced on Pt(321) vs Pt(111), approaching 1<sup>st</sup> order at higher NO:NO<sub>2</sub>. Figures 3 and 4 show the apparent order in NO and NO<sub>2</sub> as a function of the midpoint NO:NO<sub>2</sub> respectively. The NO order is identical for both surfaces over the range, showing a non-linear dependence. The NO<sub>2</sub> orders for both surfaces show a similar non linear dependence. The data suggests that the NO<sub>2</sub> order is more negative at a given NO:NO<sub>2</sub> indicating NO oxidation on Pt(321) is inhibited more by NO<sub>2</sub> than on Pt(111).

Turnover rates, in general, were within a factor of two of each other over a wide range of conditions.

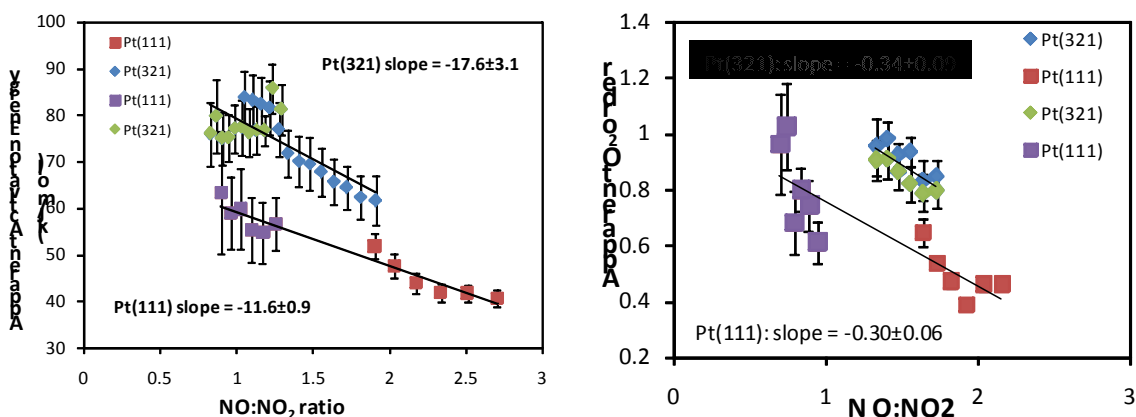


Fig 1 (left): Temperature dependence ( $E_a$ ) and apparent O<sub>2</sub> order, Fig 2: (right), for the NO oxidation reaction as function of NO:NO<sub>2</sub> for Pt(321) and Pt(111). Temperature range for each  $E_a$  was generally 40°C in the range of 200-280°C depending on conditions with 10% O<sub>2</sub>. For the O<sub>2</sub> order, 5-17% O<sub>2</sub> was used at 300°C. Error bars represent standard deviation from the regressions and different colors for each face represent results obtained using different sets of batch data.

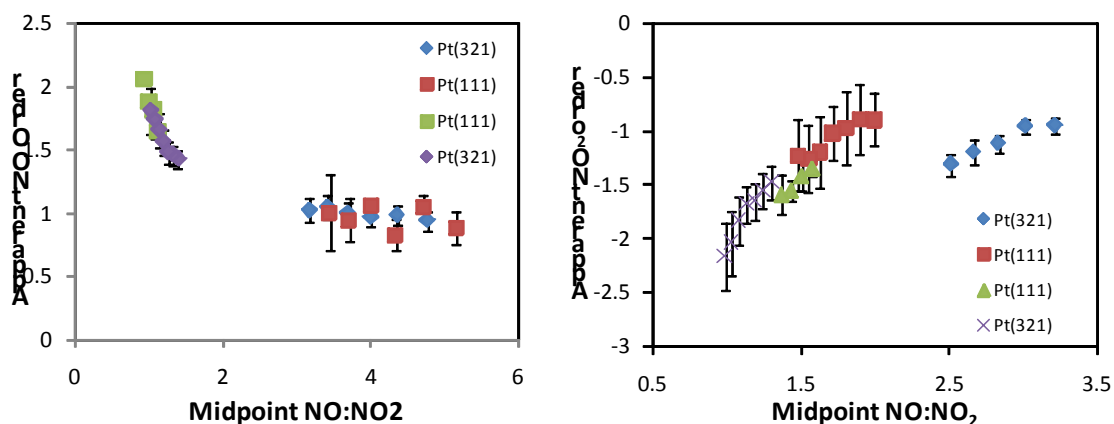


Fig 3 (left): Apparent NO order and NO<sub>2</sub> order, Fig 4: (right), for the NO oxidation reaction as function of NO:NO<sub>2</sub> for Pt(321) and Pt(111) at 300°C. Error bars represent standard deviation from the regressions and different colors for each face represent results obtained using different sets of batch data.

Oxygen coverage measurements *ex situ* after reaction using AES indicated that the Pt(321) had a higher surface coverage of chemisorbed oxygen, O\*, than Pt(111) and that some of the oxygen on Pt(321) may have been in the form of PtO<sub>x</sub>. For example, from the  $E_a$  data set, at a NO:NO<sub>2</sub> equal to 0.89, O\* was 0.85 ± 0.14 ML on Pt(321) and 0.52 ± 0.08 ML on Pt(111). No significant dependence of O\* was found on O<sub>2</sub> pressure or on temperature. On Pt(321), O\* increased significantly with decreasing NO:NO<sub>2</sub>, however, the data on Pt(111) is inconclusive. However on Pt(111), using *in situ* XPS [2], we were able to show that O\* did increase with decreasing NO:NO<sub>2</sub>. XPS of the O1s region on Pt(321) after reaction showed two types of oxygen at 530.0eV and 531.5eV which may indicate surface PtO<sub>x</sub> formation. Our *in situ* XPS results on Pt(111) [2] never showed this 2<sup>nd</sup> oxygen peak under NO oxidation conditions.



The kinetic and AES/XPS results suggest that the kinetic parameters are functions of  $O^*$  which is determined mainly by  $NO:NO_2$ . The experimental results combined with DFT results from our collaborators can be used to postulate a new microkinetic model for NO oxidation based on an Eley-Rideal type mechanism, which is the subject of our paper [3], currently in preparation.

**Water Gas Shift Reaction (WGS):** Preliminary WGS kinetic experiments have been completed on Pt(111). Previous reported results were found to be invalid due to the presence of ppm levels of  $O_2$ . After eliminating sources of  $O_2$ , current results show a very low TOR, equal to or less than the least active supported Pt catalyst, Pt/ $Al_2O_3$ . This is in agreement with previous studies which suggest that WGS on supported Pt or Pd is bi-functional with the noble metal providing a supply of chemisorbed CO to the support/metal interface where the water dissociation takes place.

**Operando X-ray Absorption Spectroscopy (XAS):** An inexpensive fixed-bed, plug-flow *operando* reactor has been developed in which X-ray absorbance and kinetic data can be measured simultaneously [4]. Pt  $L_3$  (11.56 keV) XANES and EXAFS data were obtained on a 1.5% Pt/silica catalyst in borosilicate glass reactors of different diameter and thickness, some of which are capable of operation at pressures up to about 40 atm. Additionally, polyimide, tubular reactors with low absorbance can be used for lower energy edges of the 3d transition metals, or fluorescence detection for low concentration or highly absorbing supports. With the polyimide reactor, however, the pressure is limited to  $\sim 3.5$  atm and the reaction temperature to about 300 °C. To validate the reactor, the rate and activation energies for the water-gas shift reaction on 2% Pd, 13.7% Zn on  $Al_2O_3$  catalyst were within 15% of those obtained in a standard laboratory reactor, which is within laboratory reproducibility. In addition, the Pd K edge (24.35 keV) XANES and EXAFS data on pre-reduced catalyst were identical to that previously determined on a regular cell. The EXAFS data show that the degree of Pd-Zn alloy formation changes with reaction temperature demonstrating the importance of characterizing the catalyst under reaction conditions.

### Future Plans

NO oxidation experiments similar to those completed on Pt(111) and Pt(321) will be completed on the Pt(100) surface, the other dominant surface on large, 5-10nm, Pt particles. We will continue the experiments on WGS on the various Pt crystal planes.

### Publications

1. A.D. Smeltz, R.B. Getman, W.F. Schneider, F.H. Ribeiro, Catalysis Today 136 (2008) 84, "Coupled theoretical and experimental analysis of surface coverage effects in Pt-catalyzed NO and  $O_2$  reaction to  $NO_2$  on Pt(111)"
2. R. B. Getman, W. F. Schneider, A. D. Smeltz, W. N. Delgass, and F. H. Ribeiro, Physical Review Letters, 102 (2009) 076101, "Oxygen Coverage Effects on Molecular Dissociations at a Pt Metal Surface"
3. A.D. Smeltz, W.N. Delgass, F.H. Ribeiro, R.B. Getman and W.F. Schneider, To be submitted, "The reaction of NO oxidation on Pt is not sensitive to the structure of the catalyst"
4. B. R. Fingland, F. H. Ribeiro, J. T. Miller, Catalysis Letters, Submitted "Simultaneous measurement of x-ray absorption spectra and kinetics: a fixed-bed, plug-flow *operando* reactor"

# Thermal, X-Ray and Electrical Probes of the Liquid-Solid Interface during the Synthesis of Heterogeneous Catalysts

Robert M. Rioux\*, Jason Binz, Joon Hyun Baik

Department of Chemical Engineering, Pennsylvania State University, University Park, PA  
16802-4400

Email: rioux@enr.psu.edu

The synthesis of heterogeneous catalysts is still considered art more than science. While there have been considerable advances in the field of catalyst synthesis by Brunelle [1], Schwarz [2], and more recently, by Regalbuto [3] and Che [4], the molecular mechanisms of catalyst precursor association with the metal oxide and carbon surfaces are unknown. In this work, we demonstrate that titration methods combined with calorimetry enable the determination of adsorption energies – both inner sphere and outer sphere – of metal complexes on specific surface sites on  $\gamma$ -Al<sub>2</sub>O<sub>3</sub> surfaces, as well as the influence of hydroxyl density on the adsorption of metal precursors on mesoporous silica surfaces [5]. We are able to build adsorption isotherms for metal precursor adsorption on these surfaces, which are then correlated with the final metallic dispersion after the proceeding unit operations (i.e. drying, calcination and reduction) essential to catalyst synthesis are completed. Using recent solid-state NMR results in which the absolute concentration of coordination sites on  $\gamma$ -Al<sub>2</sub>O<sub>3</sub> was determined [6], we have demonstrated that the coverage dependent heat of adsorption is due to association with sites of specific coordination. In parallel, we have examined the dynamic changes of the electrostatic environment using streaming potential measurements [7] of the surface of Al<sub>2</sub>O<sub>3</sub> during the adsorption of metal precursors throughout the adsorption isotherm. These are some of the first studies aimed at understanding how dynamic changes in zeta potential (surface charge) during precursor adsorption influence the thermochemistry at this complex liquid-solid interface. In the future, this work will be complemented with *in-situ* x-ray absorption fine structure and x-ray tomography in order to understand the initial coordination chemistry as well as the distribution of metal precursors within the porous host matrix. The objective of this work is develop a more quantitative understanding of ion-exchange and electrostatic strong adsorption catalyst synthesis routes by quantitative studies of the relevant interfacial solid-liquid chemistry.

## References

1. J. P. Brunelle, Pure Appl. Chem. 50 (1978) 1211-1229.
2. J. A. Schwarz, C. Contescu, A. Contescu, Chem. Rev. 95 (1995) 477-510.
3. X. Hao, W.A. Spieker, J.R. Regalbuto, J. Coll. Inter. Sci 267 (2003) 259–264.
4. S. Boujday, J. F. Lambert, M. Che, Top. Catal. 24 (2003) 37-42.
5. J. S. Binz, R. M. Rioux, In preparation, (2009); R. M. Rioux, In preparation (2009).
6. P. J. Sides, J. D. Hoggard, Langmuir 20 (2004) 11493-11498.
7. J. H. Kwak, J. Z. Hu, A. Lukaski, D. H. Kim, J. Szanyi, C. H. F. Peden, J. Phys. Chem. C 112 (2008) 9486-9492.; J. H. Kwak, J. Z. Hu, D. H. Kim, J. Szanyi, C. H. F. Peden, J. Catal. 251 (2007) 189-194.

## Active Sites and Mechanisms for the Water-Gas Shift Reaction on Metal and Metal/Oxide Catalysts (BNL FWP CO-027)

Co-PIs: J. Hrbek hrbek@bnl.gov; J.C. Hanson hanson1@bnl.gov; P. Liu pingliu3@bnl.gov, J.T. Muckerman muckerm1@bnl.gov, M. White mgwhite@bnl.gov  
Research associates: L. Barrio, J. Graciani; F. Yang; S. Senanayake  
Brookhaven National Laboratory, Chemistry Department 555, Upton, NY 11973

### Goals

Our goal is to obtain the knowledge necessary to predict the behavior, and ultimately design, improved cost-effective water-gas shift low temperature catalysts. Most hydrogen is currently derived from steam reforming of hydrocarbons (reacting steam with natural gas):  $C_nH_m + nH_2O \rightarrow nCO + (n-m/2)H_2$ . The reformed fuel contains 1-10% of CO, which degrades the performance of the platinum catalysts used in polymer electrolyte membrane (PEM) fuel cell systems. The water-gas shift reaction (WGS:  $CO + H_2O \rightarrow H_2 + CO_2$ ) is a critical process in providing pure hydrogen for fuel cells and other applications. Current industrial catalysts for the water-gas shift reaction are commonly mixtures of Fe-Cr and Zn-Al-Cu oxides, used at temperatures between 350-500C and 180-250C, respectively. These oxide catalysts are pyrophoric and normally require lengthy and complex activation steps before usage. Improved catalysts are being sought, particularly for lower temperature (e.g., at  $T < 150C$ , equilibrium lowers the product CO concentration into ranges for direct fuel cell use without further purification.). Ceria (Au, Cu or Pt on  $CeO_2$ ), titania (Au, Pd or Pt on  $TiO_2$ ) and molybdena (Ni, Cu and Au on  $MoO_2$ ) based nanostructured catalysts are very promising new candidates for high activity, lower temperature operation in WGS systems. However, the design and optimization of these and other metal/oxide WGS nanocatalysts are hindered by controversy about basic questions regarding the nature of the active sites and the reaction mechanism. Here, we follow a coordinated experimental and theoretical effort to better understand these promising metal/oxide catalysts, and to develop concepts for their improvement.

### DOE Interest

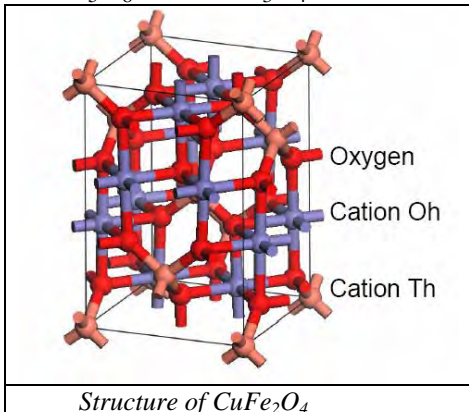
The project contributes to the DOE long term goal of understanding and controlling chemical processes for energy-related applications. This work effort may support at a minimum level or concurrently, projects within the “Fuel of the Future” and “Protect our Living Planet” themes of the OS as outlined in the Science and Technology Statement of the DOE Strategic Planning document.

### Recent Progress

This is the first year of the project. This research program has benefited from background studies performed in previous years at BNL (Catalysis: Structure and Reactivity, CO-009 FWP) and work is currently being performed combining three main thrusts: (i) *in situ* studies to determine catalyst structure, oxidation state and chemistry under reaction conditions; (ii) studies of relevant model systems, primarily based on nanoparticles supported on single crystal substrates; and (iii) computational modeling. As a result of these efforts, eight articles have been published or submitted for publication in the last fiscal year. The following paragraphs highlight the main efforts.

*In-situ XRD and XAFS Studies of the Water-Gas Shift Reaction on  $CuFe_2O_4$ .* Cu-Fe oxides are used as WGS catalysts in several industrial processes. The structure of  $CuFe_2O_4$ , known as an “inverse spinel”, contains both octahedral and tetrahedral cation sites. Copper ions sit predominantly on octahedral sites and iron atoms split between the two.  $CuFe_2O_4$  is cubic at elevated temperatures ( $> 400$  °C) and tetragonal with the axial

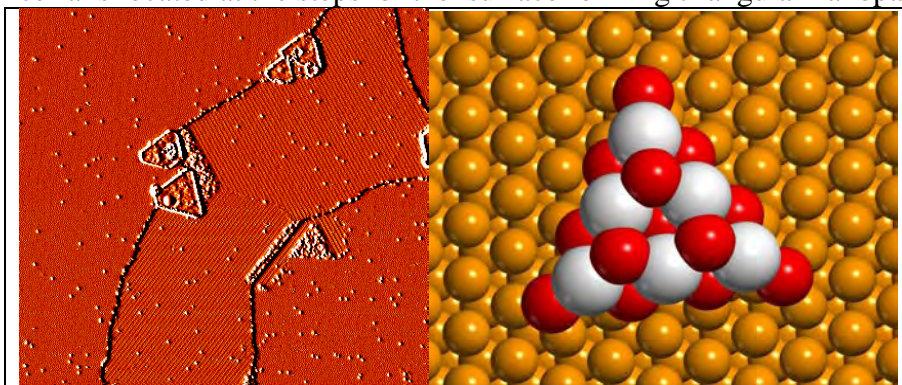
ratio  $c/a > 1$  at room temperature. XRD data collected while performing the WGS on  $\text{CuFe}_2\text{O}_4$  showed that up to  $\sim 200^\circ\text{C}$ , there were no changes in the tetragonal structure of  $\text{CuFe}_2\text{O}_4$  and no WGS activity was detected. From 200 to  $300^\circ\text{C}$ , the CO attacks the oxide and partial reduction leads to the segregation of metallic Cu with the onset of WGS activity. At  $350^\circ\text{C}$ , one has an active WGS catalyst which contains a mixture of Cu,  $\text{CuFe}_5\text{O}_8$  and/or  $\text{Fe}_3\text{O}_4$ . The intensity of the Cu(200) diffraction line becomes constant



and a Scherrer's analysis of its width gave a Cu particle size of  $\sim 23$  nm. A Rietveld refinement gave a mole ratio of  $\sim 1$  for the diffraction lines of Cu and the  $\text{CuFe}_5\text{O}_8/\text{Fe}_3\text{O}_4$  spinel. *In-situ* experiments of x-ray absorption spectroscopy at the Cu K-edge indicated that essentially all the  $\text{Cu}^{2+}$  initially present in  $\text{CuFe}_2\text{O}_4$  was reduced to metallic  $\text{Cu}^0$ . Our XRD and XAFS results point to metallic copper as an active species for the WGS. This is consistent with studies performed in our group for the water-gas shift on  $\text{CuMoO}_4$ ,  $\text{Ce}_{1-x}\text{Cu}_x\text{O}_{2-x}$ , and  $\text{CuO-ZnO}$  powder catalysts. In all of these systems, catalytic activity was seen only after a  $\text{Cu}^{2+} \rightarrow \text{Cu}^0$

transformation. The active phase consists of metallic Cu dispersed on a partially reduced oxide support ( $\text{MoO}_2$ ,  $\text{CeO}_{2-x}$ ,  $\text{Fe}_3\text{O}_{4-x}$ ).

Water-gas shift reaction on inverse  $\text{CeO}_x/\text{Cu}(111)$  catalysts: Active role of oxide nanoparticles? Our work with high-surface area powders and well-defined single crystal surfaces indicates that  $\text{Cu-CeO}_2$  is a very efficient catalyst for the water-gas shift reaction. The exact role of the oxide in the catalytic process and the WGS reaction mechanism are unclear at the present time. The ceria support may not be a simple spectator in these systems. Several studies dealing with metal/oxide powder catalysts and the WGS indicate that the oxide plays a direct role in the reaction, but due to the complex nature of these systems there is no agreement on what exactly this role is. With this in mind, we have planned a series of experiments aimed at testing the chemical and catalytic properties of  $\text{CeO}_2$  nanoparticles dispersed on a  $\text{Cu}(111)$  template, as inverse model catalysts. This year we have investigated different methods for the generation of  $\text{CeO}_x/\text{Cu}(111)$  inverse catalysts. After depositing Ce atoms on  $\text{Cu}(111)$  under an atmosphere of  $\text{O}_2$ , one obtains  $\text{CeO}_x/\text{Cu}_2\text{O}/\text{Cu}(111)$  systems. STM images indicate that ceria is located at the steps of the surface forming triangular nanoparticles, and terraces



Left side: STM image of  $\text{CeO}_x/\text{Cu}_2\text{O}/\text{Cu}(111)$ ,  $200\text{ nm} \times 200\text{ nm}$ . Right side: Structure calculated with DFT for a supported ceria particle, red spheres denote O, white are Ce

exhibit different faces of  $\text{Cu}_2\text{O}$ . Upon interaction with CO, the  $\text{Cu}_2\text{O}$  is easily reduced yielding a  $\text{CeO}_x/\text{Cu}(111)$  inverse catalysts. The oxidation state of Ce in these systems is a mixture of  $\text{Ce}^{3+}$  and  $\text{Ce}^{4+}$ . DFT calculations have

been used to study these ceria nanosystems showing that they are easier to reduce than extended surfaces of bulk ceria. Among the surfaces of bulk copper,  $\text{Cu}(111)$  probably has the lowest catalytic activity for the water-gas shift. The future experiments with these

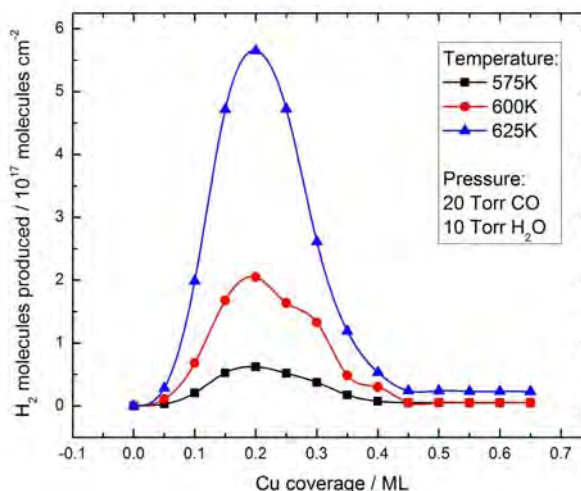
inverse model catalysts hopefully will show the role of the oxide in Au-CeO<sub>2</sub> WGS catalysts.

Controlling the Nature of Mixed-Metal Oxide Catalysts at the Nanometer Level: High Catalytic Activity of Au/CeO<sub>x</sub>/TiO<sub>2</sub>(110) Surfaces for the Water-Gas Shift reaction.

Mixed-metal oxides play a very important role in many areas of chemistry, physics, materials science and geochemistry. Recently, there has been a strong interest in understanding phenomena associated with the deposition of oxide nanoparticles on the surface of a second (host) oxide. At BNL, scanning tunneling microscopy, photoemission, and density-functional calculations were used to study the behavior of ceria nanoparticles deposited on a TiO<sub>2</sub>(110) surface. The titania substrate imposed non-typical coordination modes on the ceria nanoparticles. In the CeO<sub>x</sub>/TiO<sub>2</sub>(110) system, the Ce cations adopt an geometry and an oxidation state (+3) which are quite different from those seen in bulk ceria or for ceria nanoparticles on metal substrates. The results of scanning tunneling microscopy show the formation of Ce<sub>2</sub>O<sub>3</sub> dimers which form small linear arrays on top of the TiO<sub>2</sub>(110) substrate. An increase in the stability of the Ce<sup>3+</sup> oxidation state leads to an enhancement in the chemical and catalytic activity of the ceria nanoparticles. The co-deposition of ceria and gold nanoparticles on a TiO<sub>2</sub>(110) substrate generates catalysts with an extremely high activity for the production of hydrogen through the water-gas shift reaction. Au/CeO<sub>x</sub>/TiO<sub>2</sub>(110) was found to be much more active than Au/TiO<sub>2</sub>(110) or Au/CeO<sub>2</sub>(111). The enhanced stability of the Ce<sup>3+</sup> state in CeO<sub>x</sub>/TiO<sub>2</sub>(110) is an example of structural promotion in catalysis found here for the first time on the atomic level. Thus, the exploration of mixed-metal oxides at the nanometer level may open new avenues for optimizing catalysts through stabilization of unconventional surface structures with special chemical activity. In the future, we plan to extend this type of studies to high-surface area powders and the Cu/CeO<sub>x</sub>/TiO<sub>2</sub> and Pt/CeO<sub>x</sub>/TiO<sub>2</sub> systems.

Multiscale Modeling of Catalysis and its Application to the Water Gas Shift Reaction on Copper Nanoparticles.

We have adopted a multiscale modeling paradigm in which density functional theory can be used to determine the behavior of systems at much larger length and time scales by coupling it with kinetic Monte Carlo methods. In this work we developed a multiscale modeling framework based on density functional theory and the kinetic Monte Carlo approach. It has enabled us to study the steady-state conditions of the WGS reaction on Cu surfaces and on Cu nanoparticles supported on ZnO(0001) surfaces. In other words, to bridge the gap between theoretical and experimental time/length scales, we adopted a computational paradigm in which information from the atomic and microscopic level can be used to determine the behavior of the system at much longer (i.e., experimental) length and time



Kinetic Monte Carlo results showing the number of hydrogen molecules produced during the WGS reaction on Cu nano islands supported by a ZnO(0001) surface as a function of Cu adatom coverage.

scales. We focused on basic studies regarding the nature of the active sites, structural/size effects of nanoparticles on their catalytic activities, thermochemistry, and detailed energetic aspects of the kinetics for the elementary steps involved in different mechanisms of the WGS reaction. The outcome of this work has an impact not only in the specific problem but on the way we approach complex, multi-scale problems of immense scientific and technological import using powerful hybrid computational techniques. Our KMC simulations show that, in agreement with experiments, the hydrogen production rate strongly depends on size and structure of the nanoparticles. As shown in the figure above, the hydrogen production rate increases with Cu coverage on the ZnO(0001) support. The production rate is at a maximum around 0.25 ML and it decreases at higher coverage. This trend suggests that the edges of the nano islands play a significant role in the WGS reaction. The edge length of a nano island increases with its size and area.

Development of instrumentation for in-situ time-resolved characterization of water-gas shift powder catalysts. The development of techniques for characterizing the structural properties of catalysts under the high-pressure conditions of industrial processes is widely recognized as a top priority in the area of heterogeneous catalysis. To optimize the performance of WGS catalyst, it is desirable to know what its active phase is. In collaboration with the National Synchrotron Light Source (NSLS) and the Synchrotron Catalysis Consortium (SCC) we are setting up a facility for rapid collection of combined EXAFS and X-ray diffraction from *in situ* cells at beamline X18A of the NSLS. This facility will allow for the combined structure determination of the catalyst and the oxidation state determination of the catalytic metal atoms under operating conditions. The measurements will be alternate between EXAFS and diffraction while maintaining nearly identical operating conditions. The EXAFS data will be collected by the QEXAFS technique which we have developed at the NSLS in previous years. It provides full EXAFS spectra in 0.3sec. In addition, the X-rays at X18A are focused to less than 1mm and consequently provide stronger signal from the small opening on the active area in the *in situ* cells. We are currently using a linear detector for collecting X-ray data, but we are trying to obtain a silicon strip detector. This detector can read out a partial powder pattern in 15 msec. In many cases partial patterns will be adequate to monitor structure changes. If necessary, the detector can rapidly be repositioned to obtain full powder patterns. When completed this facility will give our project a unique tool for the *in-situ* characterization of WGS catalysts.

### **Future Plans**

We will be using a combination of experiment and theory to continue our studies on the behavior of WGS nanocatalysts that contain three different types of oxides: Ceria- (Cu/CeO<sub>2</sub>, Au/CeO<sub>2</sub>, Pd/CeO<sub>2</sub>, Pt/CeO<sub>2</sub>), titania- (Au/TiO<sub>2</sub>, Pd/TiO<sub>2</sub>, Pt/TiO<sub>2</sub>) and molybdena-based (Au/MoO<sub>2</sub>, Cu/MoO<sub>2</sub>, Ni/MoO<sub>2</sub>) systems. The future research can be divided in three major thrusts:

*i) In-situ Characterization of High-Surface Area Powder Catalysts.* There is not generally accepted picture for the oxidation state, structure or morphology of WGS catalysts under working conditions. For example, is the reaction happening on the metal, the oxide or the metal/oxide interface? Since powder catalysts are extremely complex, their characterization *in-situ* as they evolve in time with a changing chemical environment is a real challenge and one needs a combination of several techniques. In the next years we will perform systematic experiments that will focus on examining the chemical state and structural/morphological properties of metal/oxide WGS catalysts using a unique suite of techniques (XAFS, XRD, TEM) for *in-situ* characterization. A new capability for environmental transmission electron microscopy (ETEM) is being established at the Center for Functional Nanomaterials (CFN) in BNL. The new ETEM is a custom-designed instrument for advanced *in-situ* electron microscopy, including experiments for

chemical reaction and crystal growth in various gas environments. It is the first of its kind and will be applied for three dimensional (3D) tomography and near-edge x-ray absorption spectroscopy with powder catalysts. After the structural and morphological characterization of the catalysts, experiments that use IR spectroscopy to probe the WGS reaction mechanism will be carried out. We will be able to validate or discard controversial claims. The combination of *in-situ* XANES, XRD, TEM and IR spectroscopy will allow us to establish meaningful correlations between structure and reactivity that can be directly used to improve the performance of WGS industrial catalysts. The studies described in this part of the proposal will give basic information that will be used in the other two parts of the project for modeling the catalytic process at an atomic level and for testing fundamental concepts.

*ii) Experimental Studies with Model Well-defined Catalysts.* The powder nanocatalysts under study in the previous part are complex by nature. Investigators have a limited control over the structural and electronic properties that can affect the chemical reactivity of the system. This makes difficult to study in detail basic phenomena associated with the water-gas shift reaction: How does the reaction changes with particle size? ; What is the nature of the electronic interactions between the admetal and oxide support?; Are electronic effects more important than structural or ensemble effects?; Is the oxide a simple spectator?; How the reaction rate changes depending on the oxide surface structure? These fundamental questions need to be answered as a pre-requisite for a rational design of WGS catalysts. Previous works have proved that well-defined single crystal surfaces are very good models for examining individual adsorption steps, the kinetics, and mechanism of the WGS reaction on Cu(111) and Cu(110), on Cu/ZnO(000 $\bar{1}$ ), and on Cu or Au nanoparticles deposited over CeO<sub>2</sub>(111).

In this part of the project, we plan to do WGS studies on several well-defined model catalysts. These model systems will be used to examine fundamental issues that have raised from *in-situ* studies of high-surface area powder catalysts and will provide results that are essential for the theoretical work described in next section. Specifically, we are planning to use four complementary models. Metal nanoparticles will be deposited by physical vapor deposition on single crystal oxide surfaces. The same oxide supports will be used for mass- or size-selected metal cluster deposition. These experiments will be performed on a newly developed instrument at BNL which uses mass spectrometry to size-select metal cluster cations produced in a gas-phase source and deposit them at low energy (“soft-landing”) onto surfaces under UHV conditions. Metal monolayers on ultra thin oxide films will serve as models to explore metal $\leftrightarrow$ oxide interactions. Finally, the fourth model will be an “inverse” catalyst consisting of oxide nanoparticles supported on Au(111) or Cu(111) single crystals. We have been successful preparing nanoarrays of MoO<sub>x</sub>, TiO<sub>x</sub> and CeO<sub>x</sub> on Au(111). We also know how to prepare CeO<sub>x</sub>/Cu(111) “inverse” model catalysts. The model systems are flexible in such a way that they can be modified to test new concepts or hypothesis that will come from the future theoretical studies. Since we will be dealing with new materials or catalyst configurations, these studies also can give novel ideas on what should be considered when designing new industrial catalysts.

*In-situ* data collected with IR spectroscopy and moderate-pressure XPS on the well-defined metal/oxide and oxide/metal systems will point to key intermediates in the WGS reaction mechanism and will be extremely useful as a check-point in the theoretical studies described in the next section.

*iii) Theoretical Studies of Reaction Mechanism and the Behavior of Active Sites.* Despite extensive efforts, there are some issues involved in the WGS reaction that cannot be addressed directly by experiment. What is the detailed reaction pathway including the geometries and energetics of reactants, possible intermediates and transition states? On which sites does the reaction take place? How are the WGS activities of metal and metal

oxide nanoparticles affected by differences in their electronic structure and geometry associated with particle size and shape, the metal oxidation state, the support, and particle↔support interactions? Here, our project incorporates a strong theoretical component that is based on systematic density functional theory (DFT) calculations to facilitate the interpretation of experimental results and provide information that is very difficult to obtain by means of experimental methods.

We will be performing calculations on systems similar to those under study in the previous sections (i) and (ii). When going from extended surfaces to isolated nanoparticles and oxide supported nanoparticles, the effects of size, shape, and metal↔oxide interactions on the catalysis will be determined. Our calculations on these materials will be coordinated with extensive experiments, especially for the model catalysts discussed in section (ii), so that meaningful comparisons can be made. Our DFT study of a system will start with the calculation of the reaction pathway, where the computationally identified possible intermediates can be compared with the results from our experimental *in-situ* studies. With the calculated information on the energetics of intermediates and transition states, a micro-kinetic model will be developed to estimate the catalytic activity. In addition, features of the reaction pathway obtained from static DFT studies will be explored by molecular dynamics (MD) simulations. With this close interaction between theory and experiment, we should be able to provide definitive information about the behavior of WGS catalysts. The DFT calculations will be carried out using the DMol<sup>3</sup>, CASTEP and VASP codes. For a few of these systems, we will perform MD simulations using the algorithms available in CASTEP, VASP or CPMD. We will also augment the micro-kinetic model calculations with kinetic Monte Carlo (KMC) simulations.

**Publications (2008-2009)** – 8 papers published or in press.

J. A. Rodriguez, P. Liu, J. Hrbek, M. Pérez and J. Evans, “Water-Gas Shift Activity of Au and Cu Nanoparticles supported on Molybdenum Oxides”, *J. Molecular Catal. A*, **281** (2008) 59-65.

W. Wen, J.E. Calderon, J.L. Brito, N. Marinkovic, J.C. Hanson, and J.A. Rodriguez, “*In-situ* Time-resolved Characterization of Ni-MoO<sub>2</sub> Catalysts for the Water-Gas Shift Reaction”, *J. Phys. Chem. C*, **112** (2008) 2121-2128.

J. Graciani, A. Nambu, J. Evans, J.A. Rodriguez and J. Fernandez-Sanz, “Au↔N Synergy and N-Doping of Metal Oxide-Based Photocatalysts”, *J. Am. Chem. Soc.* **130** (2008) 12056-12063.

X. Wang, J.A. Rodriguez, J.C. Hanson, D. Gamarra, A. Martinez-Arias, and M. Fernandez-García, “Ceria-based Catalysts for the Production of H<sub>2</sub> through the Water-Gas Shift Reaction: Time-resolved XRD and XAFS Studies”, *Top. Catal.* **49** (2008) 81-88.

J.A. Rodriguez, J. Evans, J. Graciani, J.B. Park, P. Liu, J. Hrbek, J. Sanz, J., “High Water-Gas Shift Activity in TiO<sub>2</sub>(110) supported Cu and Au Nanoparticles: Role of the Oxide and Metal Particle Size”, *J. Phys. Chem. C*, in press (2009).

J.A. Rodriguez, P. Liu, X. Wang, W. Wen, J.C. Hanson, J. Hrbek, M. Pérez and J. Evans, “Water-Gas Shift Activity of Cu Surfaces and Cu Nanoparticles Supported on Metal Oxides”, *Catal. Today*, in press (2009), doi:10.1016/j.cattod.2008.08.022.

J.A. Rodriguez, J.C. Hanson, W. Wen, and X. Wang, “*In-situ* Characterization of Water-Gas Shift Catalysts using Time-resolved X-ray Diffraction”, *Catal. Today*, in press (2009). doi:10.1016/j.cattod.2008.11.018.

J. B. Park, J. Graciani, J. Evans, D. Stacchiola, S. Ma, P. Liu, A. Nambu, J. Fernandez-Sanz, J. Hrbek and J. A. Rodriguez, High Activity of Au/CeO<sub>x</sub>/TiO<sub>2</sub>(110) in the Water-Gas Shift Reaction: Unique Properties of ceria Nanoparticles in Mixed-Metal Oxide, *Proceedings of the National Academy of Sciences*, in press (2009), doi:10.1073/pnas.0812604106.



## Ligand-based approaches for preparation and characterization of surface supported transition metal centers for catalytic applications

Lead PI: Victor S. -Y. Lin

Student: KaKing Yan

Student: Kuntal Manna

Contact: Department of Chemistry and Ames Laboratory, Iowa State University, 1605 Gilman Hall, Ames, IA 50011; sadow@iastate.edu

As part of the Ames Laboratory Catalysis Program, we have been developing new transition-metal complexes that maintain similar coordination geometries under homogeneous and surface-supported conditions for the preparation of well-defined catalytic sites.

For part of this project, we have prepared tris(4,4-dimethyl-2-oxazoliny)borane [ $\text{B}(\text{Ox}^{\text{Me}2})_3$ ] as an ancillary ligand that control surface...transition-metal complex interactions and provides versatile spectroscopic handles for surface and solution characterization. In particular, the oxazoline's  $\nu_{\text{N}=\text{C}}$  is a intense band in the infrared region, and  $^{11}\text{B}$ ,  $^{13}\text{C}$ , and  $^{15}\text{N}$  NMR spectroscopy allow for the comparison of solution and surface organometallic species.[1] For example, we have prepared the soluble complex  $\text{PhB}(\text{Ox}^{\text{Me}2})_3\text{Re}(\text{CO})_3$  and the silica-supported complex  $\equiv\text{SiO-B}(\text{Ox}^{\text{Me}2})_3\text{Re}(\text{CO})_3$ . These species were synthesized by salt metathesis reactions of  $\text{ReBr}(\text{CO})_5$  with  $[\text{PhB}(\text{Ox}^{\text{Me}2})_3]\text{Li}$  or  $\equiv\text{Si-O-B}(\text{Ox}^{\text{Me}2})_3\text{K}$ , respectively. Infrared spectroscopy reveals similar  $\nu_{\text{N}=\text{C}}$  bands for soluble and supported compounds at 1581 and 1606  $\text{cm}^{-1}$ , respectively. Additionally, bands for the carbonyl ligands in soluble (2011 and 1888  $\text{cm}^{-1}$ ) and supported (2017 and 1892  $\text{cm}^{-1}$ ) compounds indicate that the coordination environment and electronic structure of the rhenium center (6-coordinate,  $C_{3v}$ -symmetric) is similar in both systems. These results indicate that the surface-supported  $\text{B}(\text{Ox}^{\text{Me}2})_3$  ligand is capable of reacting with metal halides via salt metathesis, and this will provide a general route to  $\equiv\text{Si-O-B}(\text{Ox}^{\text{Me}2})_3\text{ML}_n$  compounds for catalytic applications.

A second aspect of our approach focuses on alkyl ligands containing  $\beta$ -SiH groups. The silicon-hydride moiety is easily detected with IR and NMR spectroscopy, and as a group located beta to a metal center,  $\beta$ -agostic interactions and  $\beta$ -hydride abstraction and elimination provide strategies for developing further reactivity. Thus, we have prepared and characterized  $[\text{Y}(\text{C}(\text{SiHMe}_2)_3)_3]$  as a precursor for surface supported organometallic compounds.[2] IR spectroscopy and low temperature  $^1\text{H}$  and  $^{13}\text{C}\{^1\text{H}\}$  NMR spectroscopy reveal that  $[\text{Y}(\text{C}(\text{SiHMe}_2)_3)_3]$  contains six  $\beta$ -agostic and three non-agostic SiH groups. In particular,  $\nu_{\text{SiH}}$  1845  $\text{cm}^{-1}$  are indicative of agostic interactions. This compound reacts with isolated SiOH groups on the surface of silica to give a grafted material that contains a broad band assigned to  $\nu_{\text{SiH}}$ ; this band indicates that the surface-supported yttrium alkyl compound contains  $\beta$ -agostic interactions in its structure. Furthermore, the soluble  $[\text{Y}(\text{C}(\text{SiHMe}_2)_3)_3]$  and its silica-supported derivative are catalysts for amino olefins cyclization.

[1] B. Baird, A. V. Pawlikowski, J. Su, J. W. Wiench, M. Pruski, A. D. Sadow, "Easily Prepared Chiral Scorpionates: Tris(2-oxazoliny)boratoiridium(I) Compounds and Their Interactions with MeOTf," *Inorganic Chemistry*, **22**, 10208 (2008).

[2] K. Yan, A. V. Pawlikowski, C. Ebert, and A. D. Sadow, "A Tris(alkyl)yttrium Compound Containing Six  $\beta$ -Agostic Si-H Interactions," *Chemical Communications*, 656 (2009).

**Biofuels from Biomass by Catalytic Autothermal Reforming**

Students: Brian Michael, David Nare, Christine Balonek, Joshua Colby  
Contacts: Department of Chemical Engineering and Materials Science, University of Minnesota Minneapolis MN 55455, [schmidt@cems.umn.edu](mailto:schmidt@cems.umn.edu), 612 625 9391

**Goal**

Systematically examine the catalytic partial oxidation in millisecond autothermal reactors of solid biomass and the liquid products formed by pyrolysis of solid biomass. Alcohols, polyols, esters, solid carbohydrates, and lignocellulose will be studied to try to maximize formation of either hydrogen and syngas or olefins and oxygenated chemicals.

**DOE Interest**

Renewable fuels will play an increasing role in US energy demands. This research explores the fundamental catalysis of conversion of solid and liquid and liquid biomass into useful fuels by catalytic autothermal reforming at millisecond contact times.

**Recent Progress**

Spatial Profiles in Millisecond Reactors. We have within the past two years developed a technique to measure spatial profiles within the working catalyst with minimal disruption of flow and temperature profiles. In the technique we developed, we drill a 650  $\mu\text{m}$  hole in the ceramic monolith and fill the hole with a 600  $\mu\text{m}$  quartz capillary (a GC capillary). The capillary protrudes above the catalyst to completely block gas bypass. One end of the capillary is sealed off and the other end leads to a computer driven motor drive assembly through which thermocouple (gas temperature) and a quartz optical fiber (surface temperature) can be inserted. A 200  $\mu\text{m}$  hole is ground in the side of the capillary for gas sampling, and the capillary fiber also leads to a differentially pumped quadrupole mass spectrometer for gas composition measurements.

Autothermal Reforming of Bio Liquids. We have also examined many catalysts and supports for these reactions. Generally we find that Rh is the most robust catalyst and that Ce addition can improve syngas yields by several percent. Pt makes more olefins, and other metals such as Ni exhibit narrower windows of operation, generally because of formation of carbon and metal oxides. We have examined several supports including foam monoliths of alumina, zirconia, aluminosilicate, and fecralloy. We have also done extensive characterization of catalysts by microscopy, XPS, XRD, and surface area measurements. While optimizing catalysts and morphologies help define and optimize the catalyst, our major emphasis in this research program is to explore the **reaction engineering** and the **reaction chemistry** that enables extension of autothermal catalytic processes to more interesting and valuable applications involving biomass.

Autothermal reforming of Solid Biomass. Within the past two years we have successfully reformed solid biomass particles using related techniques. We have used Avacil cellulose (a food grade of 500  $\mu\text{m}$  cellulose particles), as well as sugar, starch, lignocellulose (aspen wood), and polyethylene particles (not biomass but interesting as a prototype for plastics recycling). The process also involves reactive flash volatilization as with bio liquids, but the delivery and mixing methods are entirely different. Solids are fed from a hopper through a screw drive and mixed with air or  $\text{O}_2$  to form a uniform distribution of particles in air or  $\text{O}_2$  that then impact the hot front face of the catalyst where they almost instantly decompose and volatilize. As with liquids, we have successfully reformed these solids into nearly equilibrium syngas for  $\text{C/O} < 1$  with no higher products formed and no carbon accumulation on the catalyst for periods of at least 24 hours.

### **Future Plans**

We plan to continue research on each of these topics. Spatial profiles will be examined for more complex biomass systems to identify the intermediate species produced and the reaction networks involved. For bio oils we will examine more complex liquids to determine the products formed and their mechanisms for different reactant functional groups to determine the reactivity of mixtures. For solids we will examine components of lignocellulose to determine strategies for biomass gasification to particular products.

### **Publications (2007-2009)**

R. Horn, K.A. Williams, N.J. Degenstein, L.D. Schmidt, "Mechanism of  $\text{H}_2$  and  $\text{CO}$  formation in the catalytic partial oxidation of  $\text{CH}_4$  on Rh probed by steady-state spatial profiles and spatially resolved transients," *Chemical Engineering Science* **62** (2007) 1298-1307.

L.D. Schmidt, P.J. Dauenhauer, "Hybrid Routes to Biofuels," *Nature* **447** (2007) 914-915.

R. Horn, K.A. Williams, N.J. Degenstein, A. Bitsch-Larsen, D. Dalle Nogare, S.A. Tupy, L.D. Schmidt, "Methane catalytic partial oxidation on autothermal Rh and Pt foam catalysts: Oxidation and reforming zones, transport effects, and approach to thermodynamic equilibrium," *Journal of Catalysis* **249** (2007) 378-391.

K.A. Williams, R. Horn, L.D. Schmidt, "Performance of mechanisms and reactor models for methane oxidation on Rh," *AIChE Journal* **53**(8), (2007) 2097-2113.

A. Bitsch-Larsen, N.J. Degenstein, L.D. Schmidt, "Effect of sulfur in catalytic partial oxidation of methane over Rh-Ce coated foam monoliths," *Applied Catalysis B: Environmental* **78**(3-4), (2008) 364-370.

D.C. Rennard, P.J. Dauenhauer, S.A. Tupy, L.D. Schmidt, "Autothermal catalytic partial oxidation of bio-oil functional groups: esters and acids," *Energy & Fuels*. **22** (2008) 1318-1327.

G.J. Panuccio and L.D. Schmidt, "Species and temperature profiles in a differential sphere bed reactor for the catalytic partial oxidation of n-octane," *Applied Catalysis A: General* 332, 171-182 (2007).

J.L. Colby, P.J. Dauenhauer, L.D. Schmidt, "Millisecond Autothermal Steam Reforming of Cellulose for Synthetic Biofuels by Reactive Flash Volatilization," *Green Chemistry* 10 (2008) 773-783.

Anders Bitsch-Larsen, "Catalytic Partial Oxidation of Methane on Rhodium & Platinum: Spatial Profiles at Elevated Pressure," *Applied Catalysis A: General* 348 (2008) 165–172.

David C. Rennard, Paul J. Dauenhauer, Sarah A. Tupy, and Lanny D. Schmidt. "Autothermal Catalytic Partial Oxidation of Bio-Oil Functional Groups: Esters and Acids." *Energy and Fuels* 2008, **22**,1318–1327

David C. Rennard, Jacob S. Kruger, and Lanny D. Schmidt. "Autothermal Catalytic Partial Oxidation of Glycerol to Syngas and to Non-Equilibrium Products." *ChemSusChem* **2**, 2009, 89-98

Brian C. Michael, Alessandro Donazzi and Lanny D. Schmidt "Effects of H<sub>2</sub>O and CO<sub>2</sub> addition in catalytic partial oxidation of methane on Rh", *J. Catal.*, to be published

Alessandro Donazzi, Brian C. Michael, Lanny D. Schmidt. "Chemical and geometric effects of Ce and washcoat addition on catalytic partial oxidation of CH<sub>4</sub> on Rh probed by spatially resolved measurements." *Journal of Catalysis* **260** (2008) 270–275.

Nogare DD, Degenstein NJ, Horn R, L. D. Schmidt, "Modeling spatially resolved profiles of methane partial oxidation on a Rh foam catalyst with detailed chemistry", *J. Catalysis* 258, 131-142, 2008

## Towards Realistic Models of Heterogeneous Catalysis: Simulations of Redox Catalysis from First Principles

Students: Rachel Getman, Hangyao Wang, Jason Bray  
 Post-doc: Dr. Chao Wu  
 Collaborators: Fabio Ribeiro (Purdue), Nick Delgass (Purdue), Ye Xu (ORNL)  
 Contact: W. F. Schneider, 182 Fitzpatrick Hall, Notre Dame, IN 46556;  
 Phone: (574) 631-8754; Email: [wschneider@nd.edu](mailto:wschneider@nd.edu)  
 Web page: [www.nd.edu/~wschnei](http://www.nd.edu/~wschnei)

### Goal

Develop first-principles-based approaches to describing and quantifying the kinetics of catalytic oxidations under realistic reaction conditions.

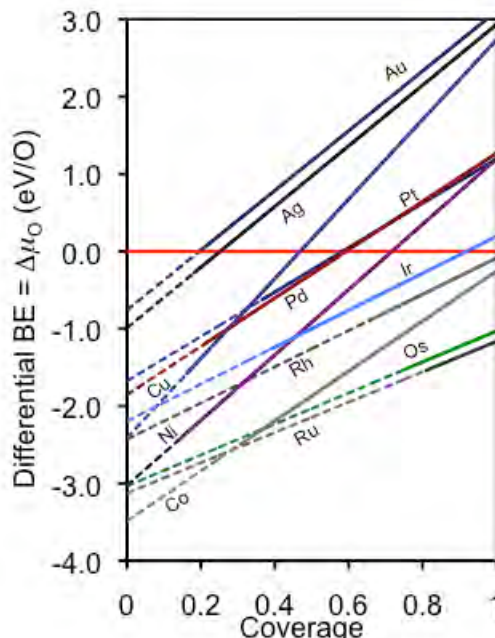
### DOE Interest

Catalytic O<sub>2</sub> activation is practically important for applications ranging from the effective use of fuels (e.g. in fuel cells) to chemical manufacture to emissions control. There is growing recognition that the rates and mechanisms of these reactions are sensitive to reaction conditions, both because these conditions modify catalyst surface chemistry and because microscopic reaction rates are sensitive to this surface composition. This research program uses DFT simulations to contribute qualitative understanding and quantitative modeling of oxidation kinetics at realistic conditions. Such models are valuable for interpreting experiment, for optimizing existing catalysts, and for discovering new materials.

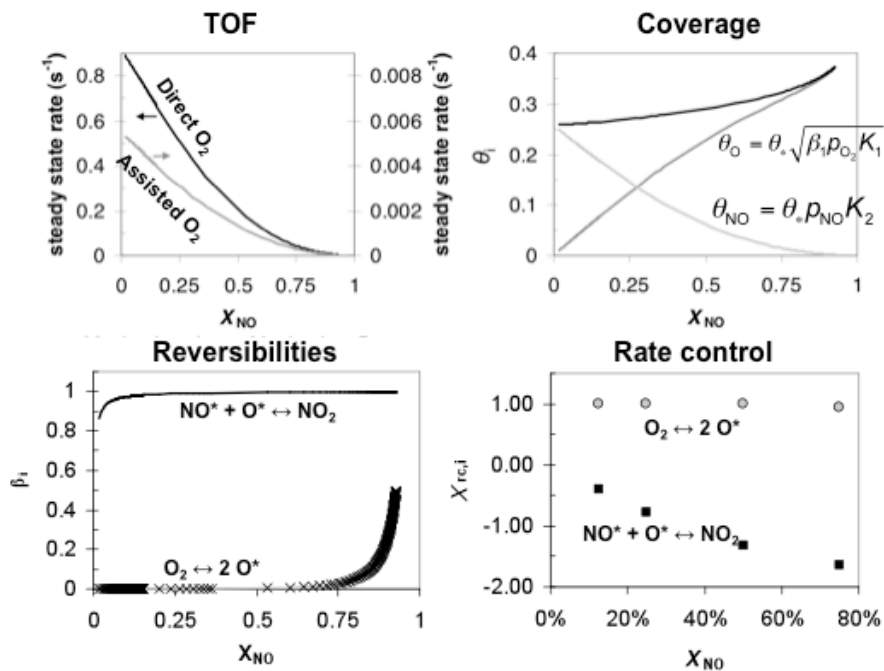
### Recent Progress

*Energetics of Oxygen Adsorption at Metal Surfaces:* DFT calculations have been performed to quantify oxygen adsorption energy vs. oxygen coverage on a range of metals (see figure). Adsorbate-adsorbate repulsions cause binding energies to uniformly decrease with increasing coverage, a property that affects both the overall energetics and rates of surface reactions.

*Coverage-Dependent Rates of Surface Reactions:* To quantify the influence of coverage effects on reaction rates, we determined O<sub>2</sub> and NO<sub>2</sub> dissociation barriers at various oxygen coverages on Pt(111). O<sub>2</sub> dissociation barriers follow a BEP trend, increasing with decreasing O adsorption energy. NO<sub>2</sub> dissociation is predicted to be much less



$T = 300^\circ\text{C}$ ,  $P = 1$  bar,  $p_{\text{O}_2} = 0.1$  bar,  $p_{\text{NO},0} = 0.0001$  bar



coverage sensitive. High-pressure XPS experiments by collaborators at Purdue confirm these differences in reaction rates and thus the non-linear dependence of surface kinetics on surface coverage.

*Kinetics of Catalytic NO Oxidation:* These results have been used to create a mean-field microkinetic model of NO oxidation over Pt that incorporates explicit coverage-dependence into individual reaction rates (see figure above). This is the first microscopic model that captures the main experimentally observed features, including TOF and NO<sub>2</sub> inhibition.

*Configurational Effects on O<sub>2</sub> Dissociation Rates:* To contrast catalytically active metals and oxides, we have studied coverage-dependent O<sub>2</sub> dissociation at an RuO<sub>2</sub>(110) surface. Coverage has a modest effect on adsorption energies, but a large effect on the statistics of sites available for dissociative adsorption. By quantifying these configurational effects, we can reproduce the observed TPD of O<sub>2</sub> from RuO<sub>2</sub>(110).

## Future Plans

*Beyond the Mean-Field:* Mean field kinetic models are difficult to develop for reactions happening at finite surface coverages. We are developing a lattice-based, hybrid approach that will (a) provide proper, coverage-dependent reaction rates, (b) allow more reliable mean-field models to be created, and (c) provide better connections between experimentally observed kinetic data and microkinetic models.

*Beyond Chemisorbed Oxygen:* Research to date has focused on the effects of chemisorbed oxygen on metal surface reactivity. Surface oxidation is potentially important to surface activity and deactivation. Recent literature reports describe the structure of a surface-oxidized Pt(111) surface. We want to understand the implications

of this oxidation on surface energies and kinetics and incorporate these into kinetic models.

*Beyond Surfaces:* Coverage is undoubtedly also important in reactions on very small catalyst particles. We will use simulation to develop coverage-dependent kinetic models that can be contrasted with surface models.

This work will all be done in close collaboration with experimental colleagues at Purdue.

**Publications (2007-2009):**

R. B. Getman and W. F. Schneider, "DFT-Based Characterization of the Multiple Adsorption Modes of Nitrogen Oxides on Pt(111)," *J. Phys. Chem. C*, **2007**, *111*, 389-397.

H. Wang and W. F. Schneider, "The Effects of Coverage on the Structures, Energetics, and Electronics of Oxygen Adsorption on RuO<sub>2</sub>(110)," *J. Chem. Phys.*, **2007**, *127*, 064706.

A. D. Smeltz, R. B. Getman, W. F. Schneider, and F. H. Ribeiro, "Coupled Theoretical and Experimental Analysis of Surface Coverage Effects in Pt-Catalyzed NO and O<sub>2</sub> Reaction to NO<sub>2</sub> on Pt(111)," *Catal. Today*, **2008**, *136*, 84-92.

R. B. Getman, Y. Xu, and W. F. Schneider, "Thermodynamics of Environment Dependent Oxygen Adsorption on Pt(111)," *J. Phys. Chem. C* (Centennial Feature Article), **2008**, *112*, 9559-9572.

Y. Xu, R. B. Getman, W. A. Shelton, and W. F. Schneider, "A First-Principles Investigation of the Effect of Pt Cluster Size on CO and NO Oxidation Intermediates and Energetics," *Phys. Chem. Chem. Phys.*, **2008**, *10*, 6009-6018.

L. Xiao and W. F. Schneider, "Surface Environmental Effects on Metal Atom Adsorption on  $\alpha$ -Alumina," *Surf. Sci.*, **2008**, *602*, 3445-3453.

R. B. Getman, W. F. Schneider, A. D. Smeltz, W. N. Delgass, and F. H. Ribeiro, "Oxygen-coverage effects on molecular dissociations at a Pt metal surface," *Phys. Rev. Lett.*, **2009**, *102*, 076101.

H. Wang, D. Schmidt, and W. F. Schneider, "Intermediates and Spectators in O<sub>2</sub> Dissociation at the RuO<sub>2</sub>(110) Surface," *J. Phys. Chem. C*, **2009**, submitted for publication.

**Atomic Resolution Imaging and Quantification of Chemical Functionality of Surfaces**

Additional PIs: Eric I. Altman  
Postdocs: Dr. Todd Schwendemann  
Students: Boris Albers, Mehmet Baykara  
Collaborators: Adam Foster (Helsinki), Carlos Vaz (Yale), Charles Ahn (Yale), Victor Henrich (Yale).  
Contact: Prof. Udo D. Schwarz, Department of Mechanical Engineering, Yale University, PO Box 208284, New Haven, CT 06520-8284; Phone (203) 432-7527; E-mail udo.schwarz@yale.edu

**Goal**

Develop noncontact atomic force microscopy (NC-AFM) into a tool for experimentally mapping out chemical forces acting between functional groups attached to a tip and individual atoms on surfaces with picometer resolution in  $x$ ,  $y$  and  $z$  and piconewton force sensitivity. Use this new technique to map out the functional chemical properties of individual surface atoms on catalytically relevant surfaces.

**DOE Interest**

Surface phenomena ranging from thin film growth, to friction and wear, to heterogeneous catalysis all inherently depend on the local, short-range interactions of the surface atoms with adsorbed atoms and molecules, and atoms on opposing surfaces in the case of tribology. All of these phenomena are central to DOE's mission of increasing energy efficiency and creating new chemical routes for efficient use of scarce resources with minimal environmental impact. Despite the broad technological importance of these local chemical interactions, they have only been theoretically accessible, and thus inherently subject to limitations in theory and computational constraints. Therefore, adding this chemical dimension to scanning probe microscopy offers great promise in advancing scientific areas that are at the core of DOE's mission.

**Recent Progress**

Since the advent of atomic force microscopy (AFM) it has been recognized that collecting force versus distance curves can provide insight into the local force field acting between the probe tip and sample. In principle, by collecting tens of thousands of such curves, a three dimensional map of the surface force field could be obtained. In conventional AFM, however, the tip makes contact with the surface and so the resolution is on the order of nanometers. Further, collecting tens of thousands of force curves requires so much time, that thermal drift renders any maps generated by such a method largely meaningless. During this reporting period we overcame these difficulties and established an AFM-based imaging method for quantitatively mapping out the entire force field acting between a tip and surface with *atomic resolution* and piconewton sensitivity. We term this new technique 3D-AFM and have applied it to highly oriented pyrolytic graphite (HOPG) as a test case.

The issues outlined above were overcome by operating in the non-contact mode where the tip oscillates above, but does not touch the surface, by using a highly-stable microscope specifically designed for this purpose with extremely low drift rates, and by a judicious data



collection strategy. In the non-contact mode, the tip-surface interaction shifts the resonant frequency of the cantilever; converting this frequency shift to a quantifiable force, requires collecting data back to a distance far from the surface where the cantilever oscillation is unaffected by the surface. By realizing that past a certain distance from the surface the force field does not vary laterally, the data collection time was greatly reduced by collecting this tail of the curve only once. Further, collecting series of NC-AFM images at progressively greater distances from the surface, rather than sequentially collecting force curves point-by-point, allowed post-data collection correction of residual drift. This resulted in dense, virtually drift-free arrays of  $(x, y, z, F_z)$  data. In addition, the potential energy,  $E$ , the energy dissipated during an individual oscillatory cycle,  $E_{\text{diss}}$ , and the tunneling current  $I$  have been recorded simultaneously. As a result, cuts along any plane deliver high-resolution maps of  $F_z$ ,  $E$ ,  $E_{\text{diss}}$ .

The power of this new method was demonstrated with results for HOPG. The full 3D data sets for the interaction force (a), potential energy (b), and energy dissipated during an individual oscillation cycle (c) are displayed in Fig. 1, representing  $256 \times 119$  pixel laterally, which is equivalent to the acquisition of 30464  $\Delta f(z)$  curves. To increase the contrast for the eye, the average force/energy in each plane of constant  $z$  was subtracted for all diagrams, rendering the atomic-scale contrast clearly visible. Note that the force corrugation caused by the atoms, e.g., is only about 3 % of the total force acting on the tip (the maximum averaged attractive force measured between tip and sample was  $-2.35$  nN at the distance of closest approach).

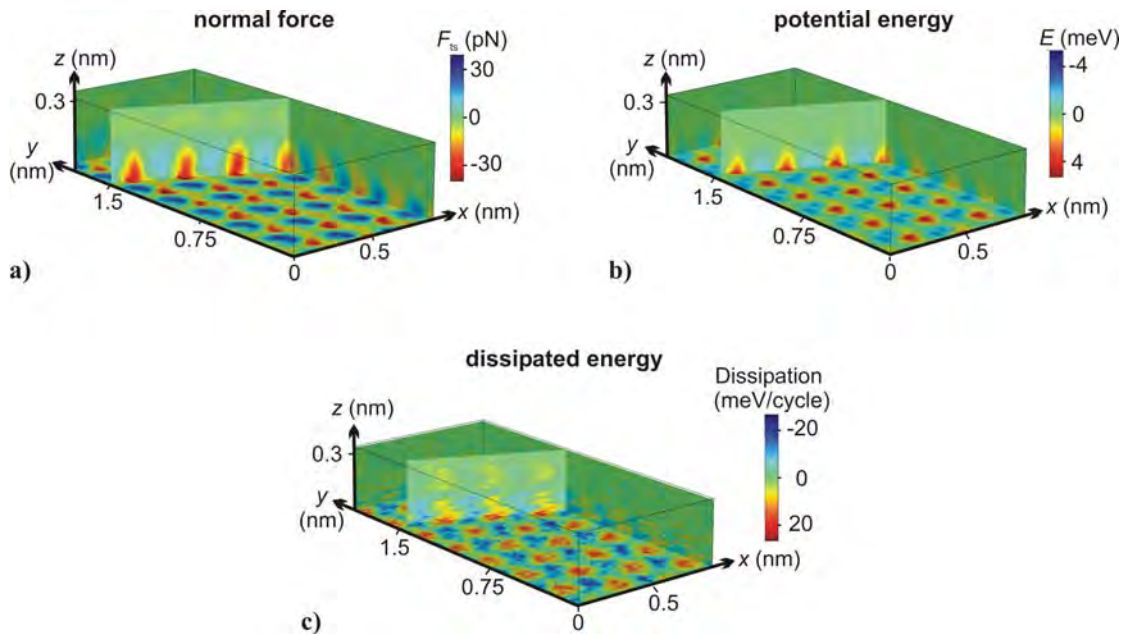


**Figure 1.** Three-dimensional data sets for the normal interaction force  $F_z$  (a), the tip-sample potential energy  $E$  (b), and the energy dissipated per cycle  $E_{\text{diss}}$  (c) recorded on HOPG. The average force/energy was removed in each plane of constant  $z$  to make the respective atomic-scale contrasts visible.

Much important information can be deduced from these plots. For example, we can observe how spatial changes in the short-range forces cause the contrast changes with distance. Especially interesting is the distance dependence of the dissipated energy. For most heights, dissipation images show three-fold symmetry (Fig. 2a) similar to other scanning probe images of this surface, but dissipation images recorded further above the surface reveal a honeycomb structure. Symmetry arguments allow identifying these spots with the locations of the atoms in

the graphite lattice. Therefore, we can clearly pinpoint the exact positions of all atoms in the lattice for the dissipation images, as indicated by the hexagons in Fig 2. This result proves the method's usefulness to *gain additional chemical information about the imaged surfaces*, allowing the *identification of the chemical nature of specific sites*.

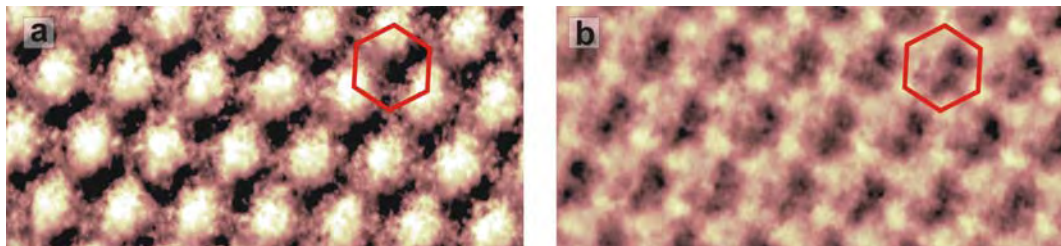


**Figure 2.** Dissipation images acquired at different heights above the surface. (a) 12 pm above closest approach and (b) 97 pm above closest approach. The hexagons and arrows identify the same spots in the two images.

In addition to the graphite work, we have shown that by recording the tunneling current during NC-AFM imaging of oxide layers on Cu(100) the atoms in the images can be uniquely identified while this is not possible using NC-AFM or STM measurements alone. We have also uncovered interesting surface phenomena during epitaxial growth of spinel (110) surfaces, and demonstrated imaging with Au tips ready for functionalization, and atomic-resolution imaging of the TiO<sub>2</sub>(110) surface.

### Future Plans

We are now working on 3D-AFM imaging of oxide surfaces with the rutile (110) surface as a prototype. We are also moving towards imaging with functionalized Au tips and establishing interactions with functional groups tethered to the surface as a means to provide a standard for identification of the tip termination. Longer term, we will be working on increasing the speed and robustness of the technique to allow it to be more widely adopted, and on quantifying specific chemical interactions on surfaces important to heterogeneous catalysis.

### Recent Publications

1. B. J. Albers, M. Liebmann, T. C. Schwendemann, M. Z. Baykara, M. Heyde, M. Salmeron, E. I. Altman, and U. D. Schwarz. *Combined low-temperature scanning tunneling/atomic force microscope for atomic resolution imaging and site-specific force spectroscopy*. Review of Scientific Instruments **79**, 033704-1 to 033704-9 (2008).
2. C. A. F. Vaz, H.-Q. Wang, C. H. Ahn, V. E. Henrich, M. Z. Baykara, T. C. Schwendemann, N. Pilet, B. J. Albers, U. D. Schwarz, L. H. Zhang, Y. Hzu, J. Wang, and E. I. Altman. *Interface and electronic characterization of thin epitaxial Co<sub>3</sub>O<sub>4</sub> films*. Surface Science **603**, 291-297 (2009).
3. B. J. Albers, T. C. Schwendemann, M. Z. Baykara, N. Pilet, M. Liebmann, E. I. Altman, and U. D. Schwarz. *Three-dimensional probing of short-ranged chemical forces with picometer resolution*. Nature Nanotechnology, DOI # 10.1038/NNANO.2009.57 (published online April 6, 2009).
4. C. A. F. Vaz, C. H. Ahn, V. E. Henrich and E. I. Altman. *Growth and Characterization of Thin Epitaxial Co<sub>3</sub>O<sub>4</sub>(111) Thin Films*. Journal of Crystal Growth, DOI # 10.1016/j.jcrysgro.2009.03.006.
5. B. J. Albers, T. C. Schwendemann, M. Z. Baykara, N. Pilet, M. Liebmann, E. I. Altman, and U. D. Schwarz. *Data acquisition and analysis procedures for high-resolution atomic force microscopy in three dimensions*. Nanotechnology, in press.
6. A. Schirmeisen, H. Hölscher, and U. D. Schwarz. *Force field spectroscopy in three dimensions*. In: Non-contact Atomic Force Microscopy, 2<sup>nd</sup> edition, Eds. S. Morita, R. Wiesendanger, F. Giessibl, Springer-Verlag, Heidelberg, Germany, in press.

**CATALYSIS SCIENCE INITIATIVE:  
Hierarchical Design of Heterogeneous Catalysts for Hydrocarbon Transformations**

Additional PIs: Bradley F. Chmelka, Baron Peters  
 Postdoctoral fellows: Ryan Nelson, Ming-Yung Lee, Ziyad Taha, H  l  ne Dozol, Swarup Chattopadhyay, Naseem Ramsahye  
 Graduate students: Miyako Hisamoto, Ramzy Shayib, S. Michael Stewart, Anthony Moses, Christina Raab, Eric Deguns  
 Collaborators: Stacey Zones (Chevron), Rick Wormsbecher (Grace-Davison)  
 Contact: Department of Chemical Engineering, University of California, Santa Barbara CA 93106-5080; sscott@engineering.ucsb.edu

### Goal

Dispersed metal oxides of the mid-transition metals (Cr, Mo, W, Re) show the remarkable ability to self-activate in the presence of olefinic substrates, generating metal alkyl and/or alkylidene active sites that catalyze the olefin metathesis, oligomerization and polymerization. We aim to understand the molecular mechanism(s) of spontaneous activation as well as deactivation, in order to design more active and more robust metal oxide catalysts.

### DOE Interest

The nature of the interaction between the active site and the catalyst support leading to activation of dispersed metal oxides is a perplexing problem in heterogeneous catalysis, because of the difficulty in probing amorphous materials. Support acidity, which varies widely even among similar oxides such as silica, alumina, silica-alumina and aluminosilicates, is likely key to the activation process. A better understanding of the origin and role(s) of Lewis and Br  nsted acidity can lead to more effective catalyst supports, and more efficient activation processes.

### Recent Progress

*High-field NMR studies of Al environments in amorphous silica-aluminas.* The use of very high magnetic fields significantly improves both the resolution and sensitivity of the solid-state  $^{27}\text{Al}$  MAS measurements of amorphous silica-alumina. Quantitative analyses of solid-state single-pulse  $^{27}\text{Al}$  MAS spectra acquired at 19.6 T for three amorphous silica-aluminas with varying aluminum contents (6.2, 11.0, and 27.3 wt% Al, corresponding to Si/Al molar ratios of 9, 4, and

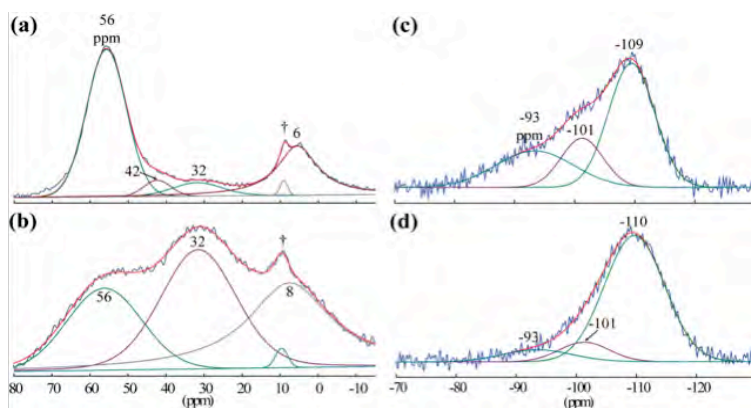


**Figure 1.** Quantitative (a,b)  $^{27}\text{Al}$  MAS and (c,d)  $^{29}\text{Si}$  MAS NMR spectra of MS-13 silica-alumina (a,c) as-synthesized/hydrated and (b,d) steamed/hydrated.  $^{27}\text{Al}$  MAS spectra were acquired at room temperature at 19.6 T under MAS conditions ( $\sim 30$  kHz) and  $^{29}\text{Si}$  MAS spectra at room temperature at 11.7 T and  $\sim 10$  kHz MAS. The signal at approximately 9 ppm in the  $^{27}\text{Al}$  MAS NMR spectra (a,b), denoted by the symbol ‘†’, corresponds to an  $\text{Al}_2\text{O}_3$  impurity in the AlN standard (whose  $^{27}\text{Al}$  signal at 113 ppm is present, but outside the range shown.)

0.5, respectively) were conducted to determine the population distributions of possible grafting sites, **Figure 1**. Correlations between aluminum content and the types and relative population distributions of Al species were determined before and after hydrothermal steam treatment. An increase in the relative populations of distorted four- and five-coordinate Al is observed upon hydrothermal steaming. From  $^{29}\text{Si}$  MAS spectra acquired at 11.7 T (500 MHz for  $^1\text{H}$ ) on the same as-synthesized and steamed materials, quantitative compositional and structural differences in the spectra reflect a greater fraction of fully siliceous  $^{29}\text{Si}$  (-110 ppm) after steaming, consistent with partial dealumination of the silica-alumina framework.

*Systematic computational investigation of Lewis acidity in amorphous silica-alumina.* Our model for isolated aluminum atoms in amorphous silica-alumina incorporates the ability of a surface aluminum atom to accept an electron pair from an underlying framework oxygen. This passivation results in a four-coordinate site even when no external Lewis base is adsorbed. **Figure 2** shows an example of an internally-bonded surface aluminum site. When an external Lewis base such as acetonitrile is present, the internally-bonded aluminum can become five-coordinate by binding with acetonitrile while continuing to interact with the framework oxygen. However, this five-coordinate structure is too high in energy to overcome the expected loss in translational free energy. The optimum structure appears to retain a weak, largely electrostatic, interaction with the fifth (oxygen) ligand. The binding energy for acetonitrile in this structure is sufficient to overcome the loss of translational free energy loss and to give high coverage at 300 K.

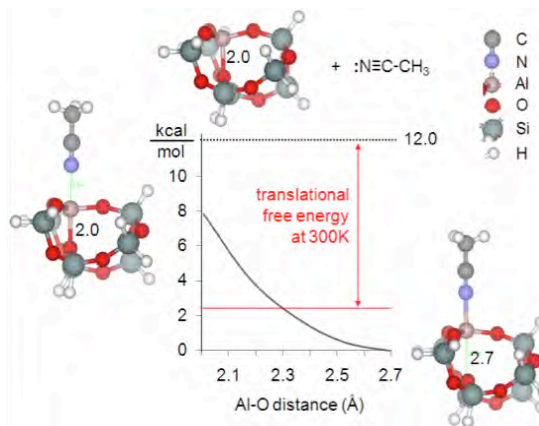


**Figure 2.** A model for Lewis acidity in silica-alumina. When an external Lewis base is present, Al prefers to bind to it instead of an underlying framework oxygen.

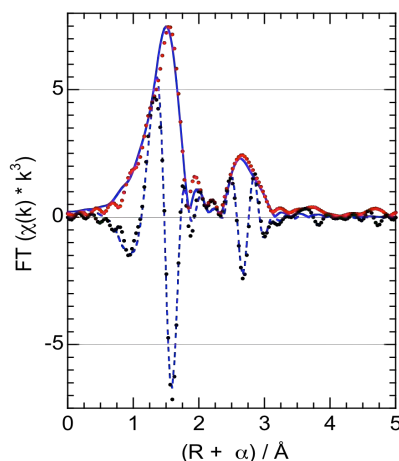


**Figure 3.** Ga K-edge EXAFS of silica pretreated at 800 °C then modified with  $\text{GaMe}_3$ , showing fit to a dimer model  $[\text{Me}_2\text{Ga}(\mu\text{-OSi=})_2]$  with Ga-Ga path at 2.98 Å.

*Trimethylgallium as a probe of the spatial relationship between Brønsted acid sites.* We probed the relationship between hydroxyl groups on silica dehydroxylated at 800 °C, for which all of the residual hydroxyl groups ( $0.4/\text{nm}^2$ ) are supposedly ‘isolated’ due to the very large average interhydroxyl distance. On this silica, the EXAFS shows some of the grafted  $\text{GaMe}_2$  sites are still paired, **Figure 3**. The correlation break analysis of the coordination number for the Ga-Ga path returns a value of 1.0, indicating that most, if not all, of the hydroxyl groups are paired. This can be explained by the very high barrier for forming the highly strained  $\text{Si}_2\text{O}_2$  rings by dehydroxylation of vicinal silanol pairs, which makes their mutual condensation prohibitive at temperatures below ca. 800 °C. A similar hydroxyl distribution appears to be present on low-Al silica-aluminas.

## Future Plans

We are undertaking a combined experimental-computational approach to the structure and strength of Lewis and Brønsted sites on a variety of alumino-silica and related materials used widely as supports for dispersed metal oxides. We are also studying initiation mechanisms for the active sites, involving reaction with the olefinic substrate.

## Publications acknowledging this grant (2007-2009)

1. M. Hisamoto, R.C. Nelson, M.-Y. Lee, J. Eckert, S.L. Scott, "Mode of Adsorption of  $(\text{CH}_3)_2\text{Au}(\text{acac})$  onto Partially Dehydroxylated Silica", *J. Phys. Chem. C*, **2009**, in press.
2. M. Hisamoto, S. Chattopadhyay, J. Eckert, G. Wu, S.L. Scott, "Solid-state Spectroscopic and Structural Investigation of *cis*- $(\text{CH}_3)_2\text{Au}(\text{O},\text{O}'\text{-acac})$ " *J. Chem. Crystallogr.* **2009**, *39*, 173-177.
3. D. Serrano, J. Aguado, G. Morales, J. M. Rodríguez, A. Peral, M. Thommes, J.D. Epping, B.F. Chmelka, "Molecular, meso- and macroscopic properties of hierarchical nanocrystalline ZSM-5 zeolite prepared by seed silanization," *Chem. Mater.*, **2009**, *21*, 641-654.
4. S. Cadars, D.H. Brouwer, B.F. Chmelka, "Probing the Local Structures of Siliceous Zeolite Frameworks Using Solid-State NMR and DFT Calculations of  $^{29}\text{Si}-\text{O}-^{29}\text{Si}$  Scalar Couplings," *Phys. Chem. Chem. Phys.*, **2009**, *11*, 1825-1837.
5. S. Bracco, A. Comotti, B.F. Chmelka, P. Sozzani, "Molecular rotors in hierarchically-ordered mesoporous organosilica frameworks," *Chem. Commun.*, **2008**, 4798-4800.
6. S. Cadars, N. Mifsud, A. Lesage, J.D. Epping, N. Hedin, B.F. Chmelka, L. Emsley, "Dynamics and Disorder in Surfactant-Templated Silicate Layers Studied by Solid-State NMR Dephasing Times and Correlated Lineshapes," *J. Phys. Chem. C*, **2008**, *112*, 9145-9154.
7. Y.I. Kim, S. Cadars, R. Shayib, T. Proffen, C.S. Feigerle, B.F. Chmelka, R. Seshadri, "Local structure of polar wurtzites  $\text{Zn}_{1-x}\text{Mg}_x\text{O}$  by Raman and  $^{25}\text{Mg}/^{67}\text{Zn}$  NMR spectroscopy and by total neutron scattering," *Phys. Rev. B*, **2008**, *78*, 195205.
8. G. Morales, G.L. Athens, B.F. Chmelka, R. van Grieken, J.A. Melero, "Aqueous-sensitive reaction sites in sulfonic acid-functionalized mesoporous silicas," *J. Catal.*, **2008**, *254*, 205-217.
9. M. Hisamoto, S.L. Scott, "IR Spectroscopic Investigation of *cis*- $(\text{CH}_3)_2\text{Au}(\text{O},\text{O}'\text{-acac})$  and *cis*- $(\text{CD}_3)_2\text{Au}(\text{O},\text{O}'\text{-acac})$ ", *Spectrochim. Acta A*, **2008**, *71*, 969-974.
10. A.W. Moses, C. Raab, R.C. Nelson, H.D. Leifeste, N.A. Ramsahye, S.K. Chattopadhyay, J. Eckert, B.F. Chmelka, S.L. Scott, "Spectroscopically Distinct Sites Present in Methyltrioxorhenium Grafted onto Silica-Alumina, and Their Abilities to Initiate Olefin Metathesis," *J. Am. Chem. Soc.*, **2007**, *129*, 8912-8920.
11. A.W. Moses, H.D. Leifeste, N. Ramsahye, J. Eckert, S.L. Scott, "Supported Re Catalysts for the Metathesis of Functionalized Olefins", Chemical Industries (CRC Press), *Catal. Org. React.* **2007**, *115*, pp. 13-22.
12. S.L. Scott, "Catalytic Transformation of Seed Oil Derivatives via Olefin Metathesis", *Helia*, **2007**, *30*, 133-142.

**Analysis of Events in Oxygen Reduction using GENIP**

Lead PI: Perla B. Balbuena  
Postdoc: Juan M. Sotelo-Campos  
Student: Pablo Salazar and Shiv Meka  
Contact: Department of Chemical Engineering, Texas A&M University  
3122 TAMU, College Station, TX 77843; [seminario@tamu.edu](mailto:seminario@tamu.edu)

We report here our exploratory work on the events at oxygen reduction sites from the basis of our ab initio procedure for materials participating in electron transfer reactions, the Generalized Electron-Nano-Interface Program (GENIP) [1-6], to consider bi-atomic backgrounds (e.g., substrates, catalysts, electrodes). Our aim is twofold: first, elucidate some of the basic mechanisms governing the interaction between a molecule and a catalyst. Second, analyze new class of catalysts, which may hold great promise for catalytic oxidation and reduction processes in modern fuel cells, as well as for hydrogenation reactions in liquid and gaseous phases. Therefore, we also introduce and analyze a family of supported metal clusters based on the typical transition metal components. Supported metal clusters have been studied intensively in recent years because of their technological application in heterogeneous catalysis, magnetic storage devices, mesoscopic, and nanoscopic electronics. The size-dependence of many physical and chemical properties at the nanoscale has been exploited to change, design, and tailor these properties aimed at modifying or creating new systems with desired specifications, unusual or absent in their bulk counterparts.

**References**

- [1] J. C. Sotelo, L. Yan, M. Wang, and J. M. Seminario, "Field Induced Conformational Changes in Bimetallic Oligoaniline Junctions," *Phys. Rev. A*, vol. 75, p. 022511 (13 pages), 2007.
- [2] P. B. Balbuena, D. Altomare, L. A. Agapito, and J. M. Seminario, "Theoretical analysis of Oxygen adsorption on Pt-based clusters alloyed with Co, Ni, or Cr embedded in a Pt matrix," *J. Phys. Chem. B*, vol. 107, pp. 13671-13680, 2003.
- [3] P. B. Balbuena, D. Altomare, N. Vadlamani, S. Bingi, L. A. Agapito, and J. M. Seminario, "Adsorption of O, OH, and H<sub>2</sub>O on Pt-based bimetallic clusters alloyed with Co, Cr, and Ni," *J. Phys. Chem. A*, vol. 108, pp. 6378-6384, 2004.
- [4] J. M. Seminario, L. A. Agapito, L. Yan, and P. B. Balbuena, "Density functional theory study of adsorption of OOH on Pt-based bimetallic clusters alloyed with Cr, Co, and Ni," *Chem. Phys. Lett.*, vol. 410, pp. 275-281, 2005.
- [5] J. C. Sotelo and J. M. Seminario, "Biatomic substrates for bulk-molecule interfaces: The PtCo-oxygen interface," *J. Chem. Phys.*, vol. 127, p. 244706 (13 pp), 2007.
- [6] J. C. Sotelo and J. M. Seminario, "Local reactivity of O<sub>2</sub> to Pt<sub>3</sub> on Co<sub>3</sub>Pt and related backgrounds," *J. Chem. Phys.*, vol. 128, pp. 204701 (1-11), 2008.

**Nanoscience and Nanoparticles for 100% Selective Catalytic Reactions****Personnel:**

The project has Principal Investigators (PIs) and Associate Members (AMs) who are experts in the three emphasis areas of the program.

- 1) nanoparticle synthesis: G. A. Somorjai (PI), F. D. Toste (PI), P. Yang (AM), and P. Alivisatos (AM)
- 2) characterization: H. Frei (PI), M. Salmeron (PI), and G. Somorjai (PI)
- 3) reaction studies: H. Frei (PI), Toste (PI), and G. Somorjai (PI)

**Goal**

In this project we are using nanotechnology approaches to understand and control catalyst selectivity and to design and synthesize new catalyst systems based on this knowledge. To achieve 100% selectivity, catalyst materials science will have to undergo major developments in order to achieve atomic-level control of parameters such as type of surface active sites, promoters, geometry, and distance between active sites. Our approach is to fabricate metal nanoparticles of platinum, rhodium, cobalt, and copper of equal size in the 1-10 nm range and controlled shape, and disperse them on high-surface-area mesoporous oxide supports or deposit them as monolayer films on metal or oxide wafers. Both the metal nanoparticles and the oxide supports are synthesized in our laboratories. The catalysts are characterized by a combination of techniques at each phase of preparation. These include X-ray diffraction, electron microscopy, light scattering, static and time-resolved Raman and FTIR spectroscopies, scanning probe techniques, high-pressure photoelectron spectroscopy, physical adsorption, and chemisorption. We then carry out catalytic reactions to evaluate selectivity and activity using flow or batch reactors. We use ethylene hydrogenation, a surface structure insensitive reaction, to independently determine the surface area of the exposed metal. Cyclohexene hydrogenation and dehydrogenation are employed to explore selectivity for a relatively simple reaction as a function of metal particle size, particle shape, and the type of the oxide support. Selectivities in multipath reactions are explored for hydrogenation of benzene or crotonaldehyde, pyrrole, and furane on platinum and for carbon monoxide hydrogenation for rhodium and cobalt as a function of metal particle size, shape, surface structure, and oxide support.

**DOE Interest**

Heterogeneous catalysts are nanoparticles. They are utilized in most industrial chemical processes in the form of metal clusters dispersed on high-surface-area oxide supports. Recent breakthroughs in nanotechnology have created the ability to control material structures on scales that are relevant for catalyst design (1–10 nm). The research conducted in this program is designed to develop new and useful catalysts with 100% selectivity, which can be used in the development of “clean manufacturing” processes that do not produce byproducts (green chemistry). If successful, there will be major gains in energy efficiency as undesirable byproducts that become waste are eliminated. This is one of the important missions of the DOE Basic Energy Sciences. Since we focus on the

hydrocarbon conversion reactions over platinum and other transition metals and bimetallic systems to high-octane branched isomers and aromatic molecules, higher concentration of naphtha is converted to fuels. Similarly, our studies of carbon monoxide hydrogenation address the science of synthetic gas conversion to chemicals and fuels through the formation of oxygenates such as methanol and ethanol, etc. This is also part of the energy mission of Basic Energy Sciences of the Department of Energy.

## Recent Progress

### 1. Nanoparticle Synthesis

#### *Thermally stable Pt/mesoporous silica core-shell nanocatalysts for high-temperature reactions*

We have reported the design of a high-temperature-stable model catalytic system that consists of a Pt metal core coated with a mesoporous silica shell (Pt@mSiO<sub>2</sub>). Inorganic silica shells encaged the Pt cores up to 750 °C in air and the mesopores providing direct access to the Pt core made the Pt@mSiO<sub>2</sub> nanoparticles as catalytically active as bare Pt metal for ethylene hydrogenation and CO oxidation. The high thermal stability of Pt@mSiO<sub>2</sub> nanoparticles enabled high-temperature CO oxidation studies, including ignition behaviour, which was not possible for bare Pt nanoparticles because of their deformation or aggregation. The results suggest that the Pt@mSiO<sub>2</sub> nanoparticles are excellent nanocatalytic systems for high-temperature catalytic reactions or surface chemical processes, and the design concept used in the Pt@mSiO<sub>2</sub> core-shell catalyst can be extended to other metal/metal oxide compositions.

#### *Tuning of Catalytic CO Oxidation by Changing Composition of Rh-Pt Bimetallic Nanoparticles*

Here, we have shown that the catalytic activity of CO oxidation by Rh/Pt bimetallic nanoparticles can be changed by varying the composition at a constant size (9 ± 1 nm). Two-dimensional Rh/Pt bimetallic nanoparticle arrays were formed on a silicon surface via the Langmuir-Blodgett technique. Composition analysis with X-ray photoelectron spectroscopy agrees with the reaction stoichiometry of Rh/(Pt + Rh). CO oxidation rates that exhibit a 20-fold increase from pure Pt to pure Rh show a nonlinear increase with surface composition of the bimetallic nanoparticles that is consistent with the surface segregation of Pt. The results demonstrate the possibility of controlling catalytic activity in metal nanoparticle-oxide systems via tuning the composition of nanoparticles with potential applications for nanoscale design of industrial catalysts.

#### *Near-Monodisperse Ni-Cu Bimetallic Nanocrystals of Variable Composition: Controlled Synthesis and Catalytic Activity for H<sub>2</sub> Generation*

Near-monodisperse Ni<sub>1-x</sub>Cu<sub>x</sub> (x = 0.2-0.8) bimetallic nanocrystals were synthesized by a one-pot thermolysis approach in oleylamine/1-octadecene, using metal acetylacetonates as precursors. The nanocrystals form large area 2D superlattices, and display a catalytic synergistic effect in the hydrolysis of NaBH<sub>4</sub> to generate H<sub>2</sub> at x = 0.5 in a strongly basic



medium. The Ni<sub>0.5</sub>Cu<sub>0.5</sub> nanocrystals show the lowest activation energy, and also exhibit the highest H<sub>2</sub> generation rate at 298 K.

*Dendrimer Templated Synthesis of One Nanometer Rh and Pt Particles Supported on Mesoporous Silica: Catalytic Activity for Ethylene and Pyrrole Hydrogenation*

Monodisperse rhodium (Rh) and platinum (Pt) nanoparticles as small as 1 nm were synthesized within a fourth generation polyaminoamide (PAMAM) dendrimer, a hyperbranched polymer, in aqueous solution and immobilized by depositing onto a high-surface-area SBA-15 mesoporous support. X-ray photoelectron spectroscopy indicated that the as-synthesized Rh and Pt nanoparticles were mostly oxidized. Catalytic activity of the SBA-15 supported Rh and Pt nanoparticles was studied with ethylene hydrogenation at 273 and 293 K in 10 torr of ethylene and 100 torr of H<sub>2</sub> after reduction (76 torr of H<sub>2</sub> mixed with 690 torr of He) at different temperatures. Catalysts were active without removing the dendrimer capping but reached their highest activity after hydrogen reduction at a moderate temperature (423 K). When treated at a higher temperature (473, 573, and 673 K) in hydrogen, catalytic activity decreased. By using the same treatment that led to maximum ethylene hydrogenation activity, catalytic activity was also evaluated for pyrrole hydrogenation.

## 2. Nanoparticle Characterization

*Reaction-Driven Restructuring of Rh-Pd and Pt-Pd Core-Shell Nanoparticles*

The nanoscale changes that catalysts undergo during a chemical reaction were observed directly for the first time. By understanding more completely how a catalyst functions, smarter catalysts can be developed to, for example, fight pollution, feed hydrogen fuel cells, and produce fuel more efficiently. Catalysts speed up the rates of chemical reactions and are essential to the production of many industrially important chemicals. They also play an important role in environmental chemistry, most famously exemplified by automobile catalytic converters.

Heterogeneous catalysts that contain bimetallic nanoparticles may undergo segregation of the metals, driven by oxidizing and reducing environments. The structure and composition of core-shell Rh<sub>0.5</sub>Pd<sub>0.5</sub> and Pt<sub>0.5</sub>Pd<sub>0.5</sub> nanoparticle catalysts were studied in situ, during oxidizing, reducing, and catalytic reactions involving NO, O<sub>2</sub>, CO, and H<sub>2</sub> by x-ray photoelectron spectroscopy at near ambient pressure. The Rh<sub>0.5</sub>Pd<sub>0.5</sub> nanoparticles underwent dramatic and reversible changes in composition and chemical state in response to oxidizing or reducing conditions. In contrast, no substantial segregation of Pd or Pt atoms was found in Pt<sub>0.5</sub>Pd<sub>0.5</sub> nanoparticles. The different behaviors in restructuring and chemical response of Rh<sub>0.5</sub>Pd<sub>0.5</sub> and Pt<sub>0.5</sub>Pd<sub>0.5</sub> nanoparticle catalysts under the same reaction conditions illustrates the flexibility and tunability of the structure of bimetallic nanoparticle catalysts during catalytic reactions.

*Charge-Transfer Interaction of Poly(vinylpyrrolidone) with Platinum and Rhodium Nanoparticles*

The vibrational spectra of platinum and rhodium nanoparticles (2.4-7 nm) capped with poly(vinylpyrrolidone) (PVP) were investigated by deep UV-Raman and Fourier transform infrared (FTIR) spectroscopy. Raman spectra of PVP/Pt and PVP/Rh showed

selective enhancement of CdO, C-N, and CH<sub>2</sub> vibrational modes of the pyrrolidone ring as a result of donor-acceptor interactions between polymer functional groups and surface metal atoms. This was observed in the UV-Raman spectra of PVP-capped metal nanoparticles by in-situ measurements in both reduced and oxidized states. Charge-transfer interactions between the polymer donor groups and surface Pt atoms in the first layer of the PVP/Pt system changed reversibly as a function of metal oxidation state (Pt(II) and Pt(0)), induced by heating under a flow of H<sub>2</sub> or O<sub>2</sub>.

### 3. Reaction Selectivity Studies

#### *Influence of Particle Size on Reaction Selectivity in Cyclohexene Hydrogenation and Dehydrogenation over Silica-Supported Monodisperse Pt Particles*

The role of particle size during the hydrogenation/dehydrogenation of cyclohexene (10 Torr C<sub>6</sub>H<sub>10</sub>, 200–600 Torr H<sub>2</sub>, and 273–650 K) was studied over a series of monodisperse Pt/SBA-15 catalysts. The conversion of cyclohexene in the presence of excess H<sub>2</sub> (H<sub>2</sub>: C<sub>6</sub>H<sub>10</sub> ratio = 20:60) is characterized by three regimes: hydrogenation of cyclohexene to cyclohexane at low temperature (423 K), an intermediate temperature range in which both hydrogenation and dehydrogenation occur; and a high temperature regime in which the dehydrogenation of cyclohexene dominates (573 K). The rate of both reactions demonstrated maxima with temperature, regardless of Pt particle size. For the hydrogenation of cyclohexene, a non-Arrhenius temperature dependence (apparent negative activation energy) was observed.

#### *Platinum Nanoparticle Shape Effects on Benzene Hydrogenation Selectivity*

Benzene hydrogenation was investigated in the presence of a surface monolayer consisting of Pt nanoparticles of different shapes (cubic and cuboctahedral) and tetradecyltrimethylammonium bromide (TTAB). Infrared spectroscopy indicated that TTAB binds to the Pt surface through a weak C-H-Pt bond of the alkyl chain. The catalytic selectivity was found to be strongly affected by the nanoparticle shape. Both cyclohexane and cyclohexene product molecules were formed on cuboctahedral nanoparticles, whereas only cyclohexane was produced on cubic nanoparticles. These results are the same as the product selectivities obtained on Pt(111) and Pt(100) single crystals in earlier studies. The apparent activation energy for cyclohexane production on cubic nanoparticles is  $10.9 \pm 0.4$  kcal/mol, while for cuboctahedral nanoparticles, the apparent activation energies for cyclohexane and cyclohexene production are  $8.3 \pm 0.2$  and  $12.2 \pm 0.4$  kcal/mol, respectively. These activation energies are lower, and corresponding turnover rates are three times higher than those obtained with single-crystal Pt surfaces.

#### *Sub-10 nm Platinum Nanocrystals with Size and Shape Control: Catalytic Study for Ethylene and Pyrrole Hydrogenation*

Platinum nanocubes and nanopolyhedra with tunable size from 5 to 9 nm were synthesized by controlling the reducing rate of metal precursor ions in a one-pot polyol synthesis. A two-stage process is proposed for the simultaneous control of size and shape. In the first stage, the oxidation state of the metal ion precursors determined the nucleation rate and consequently the number of nuclei. The reaction temperature controlled the

shape in the second stage by regulation of the growth kinetics. These well-defined nanocrystals were loaded into MCF-17 mesoporous silica for examination of catalytic properties. Pt loadings and dispersions of the supported catalysts were determined by elemental analysis (ICP-MS) and H<sub>2</sub> chemisorption isotherms, respectively. Ethylene hydrogenation rates over the Pt nanocrystals were independent of both size and shape and comparable to Pt single crystals. For pyrrole hydrogenation, the nanocubes enhanced ring-opening ability and thus showed a higher selectivity to n-butylamine as compared to nanopolyhedra.

#### *Oxidized Pt Nanoparticles for Electrophilic Catalysis*

Here, we investigate the synthesis of heterogeneous catalysts that mimic known homogeneous species for selective, solution phase carbon-carbon and carbon-heteroatom bond forming reactions typical of Pt catalysts. We report a method of treating Pt nanoparticles with oxidizing PhICl<sub>2</sub>. With these electrophilic NPs, we are able to catalyze a range of carbon-carbon and carbon-heteroatom forming cyclization reactions. These reactions, previously known to be catalyzed by homogeneous Pt(II) species, can now be accomplished heterogeneously. PAMAM dendrimer capped NPs supported on SBA-15 proved to be the most stable and robust catalyst system tested, and displayed excellent recyclability.

#### **Future Plans**

We shall synthesize another type of nanoparticles called core-shell structures, based on the Kirkendall effect, under which when two substances diffuse to form a compound, one diffuses much faster than the other. We can use this phenomenon to provide a shell of cobalt oxide around a platinum seed. Iron oxide shells around gold, or iron oxide shells around iron have all been synthesized. The core-shell nanoparticles combining oxide and transition metal will be synthesized. New catalysts composed of metal oxides (ZnO, MnO<sub>2</sub>, TiO<sub>2</sub>, Fe<sub>3</sub>O<sub>4</sub>) and transition metals (Pt, Pd, Ru, Ni, Co, Fe, Au, Cu) can be used to investigate the catalytic activity and selectivity. The bimetallic and core-shell nanoparticle structure allows maximization of the density of interface sites and permits tailoring the composition of multicomponent catalytic systems, which gives new opportunity to control the activity

Many of the organic reactions that we are studying employ metal catalysts in higher oxidation states than those typical for reduced metal nanoparticles. In order to allow for a more direct comparison of nanoparticle and homogeneous catalysts, we will explore methods for modification/oxidation of the nanoparticle catalysts. For example, preliminary experiments suggest that treatment of Pt/C with iodosobenzene dichloride produces a recyclable catalyst that is capable of catalyzing reactions previously catalyzed by homogeneous platinum(II) complexes. We will characterize these modified catalysts by ICP (Inductively Coupled Plasma) optical emission spectroscopy. In addition, we will also study the application of these methods and the development of novel methods for nanoparticle activation. In this context, X-ray photoelectron spectroscopy will be used to probe the oxidation state of the modified nanoparticles.

In the immediate future we will continue the study of the Fischer-Tropsch hydrocarbon synthesis on Co NP to clarify and complete many of the promising results obtained in recent years. In particular we will explore the NP size effects on selectivity of the reaction

to produce higher hydrocarbons (C<sub>2</sub>, C<sub>3</sub>, etc). A particularly interesting way to enhance the formation of higher hydrocarbons is by the use of initiators such as H<sub>2</sub>=CH-CH<sub>3</sub> seeded in the reactant flow. For these reactions, where selectivity is the most important aspect, acquisition or access to a gas chromatograph is crucial. We will also explore the synthesis of CH<sub>4</sub> and higher hydrocarbons from CO<sub>2</sub> and H<sub>2</sub>.

### Selected Publication (2007-2009)

1. Borodko, Y., Humphrey, S.M., Tilley, T.D., Frei, H. & Somorjai, G.A. Charge-transfer interaction of poly(vinylpyrrolidone) with platinum and rhodium nanoparticles. *J. Phys. Chem. C* **111**, 6288-6295 (2007).
2. Bratlie, K.M., Lee, H., Komvopoulos, K., Yang, P.D. & Somorjai, G.A. Platinum nanoparticle shape effects on benzene hydrogenation selectivity. *Nano Lett.* **7**, 3097-3101 (2007).
3. Grass, M.E. et al. A Reactive Oxide Overlayer on Rhodium Nanoparticles during CO Oxidation and Its Size Dependence Studied by In Situ Ambient-Pressure X-ray Photoelectron Spectroscopy. *Angewandte Chemie-International Edition* **47**, 8893-8896 (2008).
4. Habas, S.E., Lee, H., Radmilovic, V., Somorjai, G.A. & Yang, P. Shaping binary metal nanocrystals through epitaxial seeded growth. *Nature Materials* **6**, 692-697 (2007).
5. Huang, W. et al. Dendrimer templated synthesis of one nanometer Rh and Pt particles supported on mesoporous silica: Catalytic activity for ethylene and pyrrole hydrogenation. *Nano Lett.* **8**, 2027-2034 (2008).
6. Humphrey, S.M. et al. Rhodium nanoparticles from cluster seeds: Control of size and shape by precursor addition rate. *Nano Lett.* **7**, 785-790 (2007).
7. Joo, S.H. et al. Thermally stable Pt/mesoporous silica core-shell nanocatalysts for high-temperature reactions. *Nature Materials* **8**, 126-131 (2009).
8. Kuhn, J.N., Huang, W.Y., Tsung, C.K., Zhang, Y.W. & Somorjai, G.A. Structure Sensitivity of Carbon-Nitrogen Ring Opening: Impact of Platinum Particle Size from below 1 to 5 nm upon Pyrrole Hydrogenation Product Selectivity over Monodisperse Platinum Nanoparticles Loaded onto Mesoporous Silica. *Journal of the American Chemical Society* **130**, 14026-+ (2008).
9. Park, J.Y., Zhang, Y., Grass, M., Zhang, T. & Somorjai, G.A. Tuning of catalytic CO oxidation by changing composition of Rh-Pt bimetallic nanoparticles. *Nano Lett.* **8**, 673-677 (2008).
10. Rioux, R.M., Hsu, B.B., Grass, M.E., Song, H. & Somorjai, G.A. Influence of Particle Size on Reaction Selectivity in Cyclohexene Hydrogenation and Dehydrogenation over Silica-Supported Monodisperse Pt Particles. *Catalysis Letters* **126**, 10-19 (2008).
11. Tao, F. et al. Reaction-Driven Restructuring of Rh-Pd and Pt-Pd Core-Shell Nanoparticles. *Science* **322**, 932-934 (2008).
12. Zhang, Y.W. et al. One-step polyol synthesis and langmuir-blodgett monolayer formation of size-tunable monodisperse rhodium nanocrystals with catalytically active (111) surface structures. *J. Phys. Chem. C* **111**, 12243-12253 (2007).
13. Zhang, Y.W. et al. Highly selective synthesis of catalytically active monodisperse rhodium nanocubes. *Journal of the American Chemical Society* **130**, 5868-+ (2008).
14. Zhang, Y.W. et al. Near-monodisperse Ni-Cu bimetallic nanocrystals of variable composition: Controlled synthesis and catalytic activity for H<sub>2</sub> generation. *J. Phys. Chem. C* **112**, 12092-12095 (2008).

## The Influence of Electron Flow at Oxide-Metal Interfaces on the Selectivity and Turnover Rates of Catalytic Reactions

Gabor A. Somorjai (Principal Investigator)

### Goal

Our aim is to determine how electron flow influences catalytic reaction mechanisms. The exothermic reactions to be studied include carbon monoxide hydrogenation and oxidation, the oxidation of hydrogen, and NO/CO. We are studying how electron transport across the oxide-metal interface correlates with and influences catalytic activity and selectivity by using reactors that permit simultaneous monitoring of current flow and the reaction rates and product distributions. We shall use oxides such as  $\text{TiO}_x$ ,  $\text{NbO}_x$ ,  $\text{TaO}_x$  and  $\text{CeO}_x$  which have been shown to enhance catalytic turnover rates of reactions on transition metals and correlate these with their electron transport properties. We use metals such as Pt, Pd, Au, Ni and Rh in thin film nanowire and nanoparticle forms deposited on the various oxides to explore the oxide-metal interface and particle size dependence of hot electron flow. We shall attempt to modify turnover rates and reaction selectivities by applying an external potential across the catalytic nanodiode. With Professor Martin Head-Gordon, Chemistry Department, UCB, we shall investigate the theoretical model that is responsible for the generation of hot electrons under exothermic catalytic reactions.

### Recent Progress

#### 1. Fabrication and characterization of catalytic nanodiodes

##### *Interfacial and Chemical Properties of Pt/TiO<sub>2</sub>, Pd/TiO<sub>2</sub>, and Pt/GaN Catalytic Nanodiodes Influencing Hot Electron Flow*

The influence of physical and chemical properties of Pt/TiO<sub>2</sub>, Pd/TiO<sub>2</sub>, and Pt/GaN metal-semiconductor Schottky diodes on the yield of collected hot electron flow (number of hot electrons per product molecule) was investigated. We measured both the chemicurrent (electron flow) and chemical turnover rate during oxidation of carbon monoxide (at pressures of 100 Torr of O<sub>2</sub> and 40 Torr of CO in the 373-513 K range) using reaction systems equipped for simultaneous reaction rate and current measurements. The chemicurrent was found to be correlated with the turnover rate and can be used to detect the turnover rate for the three diodes. Thermoelectric current was observed in the presence of O<sub>2</sub> or CO gas in the absence of catalytic reaction. The chemicurrent was observed only under catalytic reaction conditions. The chemicurrent yield of Pt/GaN ((3.5 (0.8 x 10<sup>-3</sup>)) was higher than that of Pt/TiO<sub>2</sub> or Pd/TiO<sub>2</sub> ((2-3) x 10<sup>-4</sup>) by one order of magnitude. We found that the metal-semiconductor interface structure (roughness, grain size, and step terrace) is important in controlling the magnitude of chemicurrent yield.

## 2. Instruments for combined studies of hot electron flow and reaction turnover

### *The genesis and importance of oxide–metal interface controlled heterogeneous catalysis; the catalytic nanodiode*

We have shown that electronic excitations at the metal surface induced by exothermic catalytic reactions lead to the generation of energetic (hot) electron flows. We detected the flow of hot electrons during oxidation of carbon monoxide using Pt/ TiO<sub>2</sub> Schottky diodes. The thickness of the Pt film used as catalyst was 5 nm, less than the electron mean free path, resulting in the ballistic transport of hot electrons through the metal. The electron flow was detected as a chemicurrent if the excess electron kinetic energy generated by the exothermic reaction was larger than the effective Schottky barrier formed at the metal semiconductor interface. We found that heat generated by the reaction caused a negligible increase of temperature in our experimental range, suggesting that this thermal effect is not responsible for the generation of hot electron flow. We tested the stability and reversibility of chemicurrent generated during CO oxidation at 413 ~ 573 K. The activation energy calculated from the measurement of chemicurrent is quite close to that of the turnover rate of chemical reaction, which indicates that the generation mechanism of hot electrons is closely correlated with the chemical reaction. This correlation suggests that hot electron flow could be a new tool to probe the role of oxide–metal interfaces in heterogeneous catalysis.

## 3. Detection of hot electron flow on Pt colloid nanoparticles

### *Probing Hot Electron Flow Generated on Pt Nanoparticles with Au/TiO<sub>2</sub> Schottky Diodes during Catalytic CO Oxidation*

Hot electron flow generated on colloid platinum nanoparticles during exothermic catalytic carbon monoxide oxidation was directly detected with Au/TiO<sub>2</sub> diodes. Although Au/TiO<sub>2</sub> diodes are not catalytically active, platinum nanoparticles on Au/TiO<sub>2</sub> exhibit both chemicurrent and catalytic turnover rate. Hot electrons are generated on the surface of the metal nanoparticles and go over the Schottky energy barrier between Au and TiO<sub>2</sub>. The continuous Au layer ensures that the metal nanoparticles are electrically connected to the device. The overall thickness of the metal assembly (nanoparticles and Au thin film) is comparable to the mean free path of hot electrons, resulting in ballistic transport through the metal. The chemicurrent and chemical reactivity of nanoparticles with citrate, hexadecylamine, hexadecylthiol, and TTAB (tetradecyltrimethylammonium bromide) capping agents were measured during catalytic CO oxidation at pressures of 100 Torr O<sub>2</sub> and 40 Torr CO at 373-513 K. We found that chemicurrent yield varies with each capping agent but always decreases with increasing temperature. We suggest that this inverse temperature dependence is associated with the influence of charging effects due to the organic capping layer during hot electron transport through the metal-oxide interface.

#### 4. Theoretical studies of hot electron generation for CO oxidation (CO/O<sub>2</sub>) and hydrogen oxidation (H<sub>2</sub>/O<sub>2</sub>)

##### *Hydrogen Oxidation-Driven Hot Electron Flow in Catalytic Nanodiodes: Detection and Mechanism*

Hydrogen oxidation on platinum is shown to be a surface catalytic chemical reaction that generates a steady state flux of hot (> 1 eV) conduction electrons. These hot electrons are detected as a steady-state chemiurrent across Pt / TiO<sub>2</sub> Schottky diodes whose Pt surface is exposed to hydrogen and oxygen. Kinetic studies establish that the chemiurrent is proportional to turnover frequency for temperatures ranging from 298 K to 373 K, for P<sub>H<sub>2</sub></sub> between 1 and 8 Torr and P<sub>O<sub>2</sub></sub> of 760 Torr. Both chemiurrent and turnover frequency exhibit first order dependence on P<sub>H<sub>2</sub></sub>. These results can be understood within a phenomenological model: hot electrons are produced by an oxidation-reduction electron pump that draws metal electrons to the surface during the chemisorption of reactant gases, and then releases them back in the form of hot electrons during activated steps such as reactive desorption of water.

##### **Future plans**

- Measurement of hot electron flows and catalytic activity under exothermic catalytic reactions including hydrogen oxidation and NO/CO reaction.
- Studies of the isotope effect of hot electron generation under hydrogen oxidation/deuterium oxidation
- Measurement of chemiurrent on Rh nanoparticles on Au/TiO<sub>2</sub> Schottky diode.
- Fabrication of catalytic nanodiodes with different oxide materials such as CeO<sub>2</sub>, ZrO<sub>2</sub>, and ZnO.

##### **Selected Publication (2007-2009)**

1. Park, J.Y., Lee, H., Renzas, J.R., Zhang, Y.W. & Somorjai, G.A. Probing hot electron flow generated on Pt nanoparticles with Au/TiO<sub>2</sub> Schottky diodes during catalytic CO oxidation. *Nano Lett.* 8, 2388-2392 (2008).
2. Park, J.Y., Renzas, J.R., Contreras, A.M. & Somorjai, G.A. The genesis and importance of oxide-metal interface controlled heterogeneous catalysis; the catalytic nanodiode. *Topics in Catalysis* 46, 217-222 (2007).
3. Park, J.Y., Renzas, J.R., Hsu, B.B. & Somorjai, G.A. Interfacial and chemical properties of Pt/TiO<sub>2</sub>, Pd/TiO<sub>2</sub>, and Pt/GaN catalytic nanodiodes influencing hot electron flow. *J. Phys. Chem. C* 111, 15331-15336 (2007).
4. Hervier, A. et al. Hydrogen Oxidation-Driven Hot Electron Flows in Catalytic Nanodiodes: Detection and Mechanisms. *Nature Chemistry*, submitted.
5. Somorjai, G.A. & Park, J.Y. Molecular Ingredients of Catalytic Selectivity. *Angewandte Chemie Intl. Ed.* 47, 9212-9228 (2008).
6. Somorjai, G.A., Tao, F. & Park, J.Y. The nanoscience revolution: Merging of colloid science, catalysis and nanoelectronics. *Topics in Catalysis* 47, 1-14 (2008).

## Synthesis and Understanding of Novel Catalysts

Postdocs: Junling Lu  
Students: Paula Allotta, Dana Sauter  
Contact: Peter C. Stair, Department of Chemistry, Northwestern University, Evanston, IL 60208; phone: (847) 491-5266; Email: [pstair@northwestern.edu](mailto:pstair@northwestern.edu)

### Goal

The objectives are to synthesize highly uniform metal oxide materials in order to investigate and understand the relationships between the composition, atomic structure, and electronic properties of a catalytically active oxide and, where appropriate, a support and the corresponding chemical and catalytic properties.

### DOE Interest

Since bulk, thin film and supported oxides are among the most significant classes of catalytic materials, advances in their synthesis and the fundamental understanding of their catalytic properties can make an important contribution to the production of fuels and chemicals relevant to the DOE mission. This project addresses both the methods for synthesis of highly uniform cluster and thin film catalytic materials (a prerequisite to achieving a highly selective catalytic process) and their characterization.

### Recent Progress

*Synthesis and Characterization of Zeolite-Supported Iron Oxide Clusters:* Iron loaded zeolites are of particular interest as an alternative to expensive and rare transition metals for hydrocarbon oxidation reactions. Zeolites are an optimal support due to their uniform and rigid structure with few lattice imperfections and the ability to contain a variety of silicon-aluminum ratios (SAR). In previous research it was assumed that a specific loading method would yield uniform iron oxide clusters once excess iron had been removed from the system. We have compared several methods for loading iron oxide and used multiple characterization techniques to examine the reproducibility of the resulting materials. Over 150 samples have been synthesized using zeolites Mordenite (MOR), Beta and ZSM-5 (MFI; SAR= 33, 90, 120) prepared from  $\text{FeCp}_2$ ,  $\text{Fe}(\text{acac})_2$  or  $\text{FeCl}_3$  as the iron precursor. Loading methods included incipient wetness impregnation, chemical vapor deposition (CVD) and atomic layer deposition (ALD). Of these three methods only ALD, in our hands, provides iron cluster sizes at the limit of TEM resolution (**Fig. 1**) as well as consistently

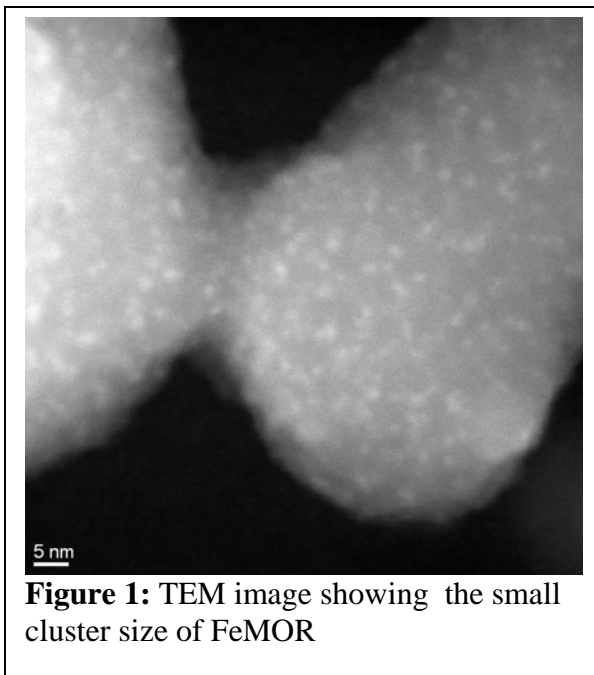


**Figure 1:** TEM image showing the small cluster size of FeMOR



reproducible iron/aluminum ratios (ICP) and identical structures by EXAFS. With the CVD method iron/aluminum ratios can vary by as much as twofold and the EXAFS data is indicative of irreproducible structures (Fig. 2).

*Surface Acidity of TiO<sub>2</sub> Films Supported on SiO<sub>2</sub>:* TiO<sub>2</sub>/SiO<sub>2</sub> supported oxides have been considered as substitutes for pure TiO<sub>2</sub> due to their improved mechanical strength, thermal stability, and high dispersion for TiO<sub>2</sub>. While these materials exhibit the catalytic properties of

solid acids the mechanism of their acidity is still debated. Recent work provides strong evidence that high purity TiO<sub>2</sub>-SiO<sub>2</sub> mixed oxides do not have Brønsted acid sites, in conflict with previous studies in the 1990's. We have prepared highly uniform, submonolayer to multilayer, thin films of titanium dioxide supported on high surface area silica gel by ALD using TiCl<sub>4</sub> and titanium isopropoxide (TTIP). UV-Vis DRS shows that the coordination geometry of Ti cations depends on the number of ALD cycles and the precursor but is essentially independent of deposition temperature. DRIFTS and visible-excitation Raman spectroscopy of pyridine as a probe molecule were used to study the surface acidity. As-prepared titania films synthesized using TiCl<sub>4</sub> exhibited both Lewis and Brønsted acidity. Films prepared using TTIP exhibited only Lewis acidity after removal of carbonyl groups by calcination. Similarly, when chlorine impurities, detected by ICP, were removed from TiCl<sub>4</sub>-prepared films by prolonged heating in flowing, humid air, only Lewis acidity was observed. Thus, we conclude that only films containing either chloride or carbonyl impurities possessed Brønsted acid sites.

### Future Plans

*Characterization of ALD-Synthesized Supported Iron Oxide Clusters:* The structure and uniformity of the ALD-synthesized iron oxide clusters will be probed by in-situ EXAFS and UV Raman spectroscopy.

*Chemistry and Catalysis:* The redox activity and catalytic performance in oxidation reactions of iron oxide clusters supported in zeolites and on silica will be investigated and compared with the objective of determining the relationships between size and catalytic performance.

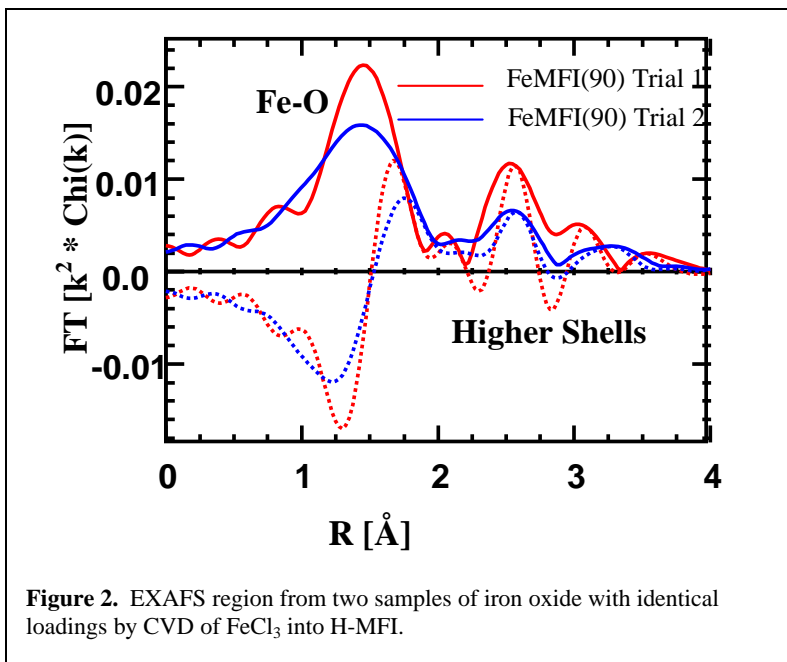


**Figure 2.** EXAFS region from two samples of iron oxide with identical loadings by CVD of FeCl<sub>3</sub> into H-MFI.

### Publications (2007-2009)

1. UV-Raman and Fluorescence Spectroscopy of Benzene Adsorbed Inside Zeolite Pores, C. Zhang, P.M. Allotta, G. Xiong, and P.C. Stair, *Journal of Physical Chemistry C* **112**, 14501-14507 (2008).
2. Z. Wu, H.-S. Kim, and P.C. Stair, *Resonance Raman Spectroscopy –  $\theta$ -Al<sub>2</sub>O<sub>3</sub> - Supported Vanadium Oxide Catalysts as an Illustrative Example*, in *Metal Oxide Catalysis*, J.S.J. Hargraves and S.D. Jackson, Editors. 2008, Wiley-VCH: Weinheim. p. 177-194.
3. Advanced synthesis for advancing heterogeneous catalysis, P.C. Stair, *Journal of Chemical Physics* **128**, 182507/1-182507/4 (2008).
4. Raman Spectroscopic Study of V/ $\theta$ -Al<sub>2</sub>O<sub>3</sub> Catalysts: Quantification of Surface Vanadia Species and Their Structure Reduced by Hydrogen, Z. Wu, P.C. Stair, S. Rugmini, and S.D. Jackson, *Journal of Physical Chemistry C* **111**, 16460-16469 (2007).
5. The Application of UV Raman Spectroscopy for the Characterization of Catalysts and Catalytic Reactions, P.C. Stair, *Advances in Catalysis* **51**, 75-98 (2007).
6. Surface Acidity and Properties of TiO<sub>2</sub>/SiO<sub>2</sub> Catalysts Prepared by Atomic Layer Deposition: UV-Visible Diffuse Reflectance, DRIFTS, and Visible Raman Spectroscopies Studies, J. Lu, C. Stair Peter, K.M. Kosuda, and R.P. Van Duyne, *Journal of Physical Chemistry C* Submitted, (2009).
7. UV Raman Studies of Coke Formation During Catalytic Methanol-to-Hydrocarbons, C. Zhang and P.C. Stair, In Preparation, (2009).
8. Quantitative Raman Analysis of Alky-substituted Naphthalenes Solution, C. Zhang and P.C. Stair, *Journal of Physical Chemistry A* In Preparation, (2009).

**Institute for Catalysis in Energy Processes (ICEP)**

Additonal PIs: Argonne: Larry Curtiss, Jeff Elam, Nada Dimitrijevic, Jeff Miller, Mike Pellin, Peter Zapol  
Northwestern University: Mike Bedzyk, Linda Broadbelt, Don Ellis, Franz Geiger, Kim Gray, Mark Hersam, Joe Hupp, Harold Kung, Mayfair Kung, Laurence Marks, Tobin Marks, SonBinh Nguyen, Justin Notestein, Ken Poeppele, Randy Snurr, Rick Van Duyne, Eric Weitz

Research Staff: Hack-Sung Kim (NU/ANL)

Postdocs: Chang-Yong Kim (NU), Gonghu Li (NU), Xufeng Lin (NU), Gordana Ostojic (NU), Sai Setthapun (ANL), Shuxia Yin (NU)

Graduate Students: Avi Buchbinder, Le Chen, Steve Christensen, Alon Danon, Chris Downing, Jim Enterkin, Hao Feng, Zhenxing Feng, Tendai Gadzikwa, Kathryn Kosuda, Tony Liang, Ryan Malecky, Neema Mashayekhi, Mike Missaghi, Brian Quezada, Federico Rabuffetti, Patrick Ryan, Ashi Savara, Avi Shultz, Chun-Yi Sung, Staci Wegener

Collaborators: Chris Marshall (ANL), Tijana Rajh (ANL), Wolfgang Sachtler (NU), Stan Zygmunt (Valpariso U.)

Contacts:

P. Stair, [pstair@northwestern.edu](mailto:pstair@northwestern.edu)  
L. Curtiss, [curtiss@anl.gov](mailto:curtiss@anl.gov)  
N. Dimitrijevic, [dimitrijevic@anl.gov](mailto:dimitrijevic@anl.gov)  
J. Elam, [jelam@anl.gov](mailto:jelam@anl.gov)  
J. Miller, [millerjt@anl.gov](mailto:millerjt@anl.gov)  
M. Pellin, [pellin@anl.gov](mailto:pellin@anl.gov)  
P. Zapol, [zapol@anl.gov](mailto:zapol@anl.gov)  
M. Bedzyk, [bedzyk@northwestern.edu](mailto:bedzyk@northwestern.edu)  
L. Broadbelt, [broadbelt@northwestern.edu](mailto:broadbelt@northwestern.edu)  
D. Ellis, [don-ellis@northwestern.edu](mailto:don-ellis@northwestern.edu)  
F. Geiger, [f-geiger@northwestern.edu](mailto:f-geiger@northwestern.edu)  
K. Gray, [k-gray@northwestern.edu](mailto:k-gray@northwestern.edu)  
M. Hersam, [m-hersam@northwestern.edu](mailto:m-hersam@northwestern.edu)  
J. Hupp, [j-hupp@northwestern.edu](mailto:j-hupp@northwestern.edu)  
H. Kung, [hkung@northwestern.edu](mailto:hkung@northwestern.edu)  
M. Kung, [m-kung@northwestern.edu](mailto:m-kung@northwestern.edu)  
L. Marks, [l-marks@northwestern.edu](mailto:l-marks@northwestern.edu)  
T. Marks, [t-marks@northwestern.edu](mailto:t-marks@northwestern.edu)  
S. Nguyen, [stn@northwestern.edu](mailto:stn@northwestern.edu)  
J. Notestein, [j-notestein@northwestern.edu](mailto:j-notestein@northwestern.edu)  
K. Poeppele, [krp@northwestern.edu](mailto:krp@northwestern.edu)  
R. Snurr, [snurr@northwestern.edu](mailto:snurr@northwestern.edu)  
R. Van Duyne, [vanduyne@northwestern.edu](mailto:vanduyne@northwestern.edu)  
E. Weitz, [weitz@northwestern.edu](mailto:weitz@northwestern.edu)

## Goal

ICEP seeks to understand at the molecular level catalytic and photocatalytic transformations relevant to energy harvesting, storage, and utilization and to further the discovery and development of highly efficient catalytic and photocatalytic processes. ICEP has been organized into three (3) subtasks: 1) Model Catalytic and Photocatalytic Processes has the goal to develop fundamental, atomic level understanding of the relationship between catalytic chemistry and the surface atomic structure and electronic properties of the catalyst. 2) Nanostructured Membrane Catalysis develops fundamental understanding of the relationship between catalyst structure at the nanoscale and the resulting catalytic chemistry. 3) Catalytic and Photocatalytic Chemical Transformations has the goals to achieve a fundamental understanding of factors that influence elementary catalytic and photocatalytic reaction steps and to advance the development of highly effective catalytic and photocatalytic systems

## DOE Interest

The understanding and control of reactions catalyzed on solid surfaces *at the molecular-level* is a “grand challenge” for 21<sup>st</sup> Century catalysis science. The development of fundamental understanding of structure-function relationships between catalytically active sites and the chemical reactions they catalyze are at the heart of this challenge.

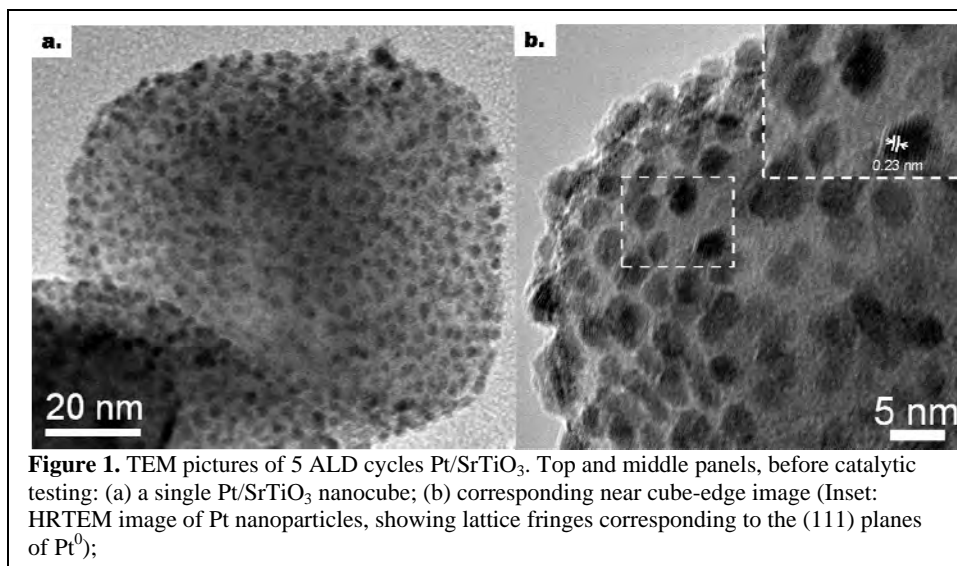
## Recent Progress

- *Synthesis*

Highly uniform supported nanoparticles of Pt and Pd have been prepared by atomic layer deposition (ALD). **Fig. 1** shows a TEM image of Pt nanoparticles supported on single crystal SrTiO<sub>3</sub> supports.

Synthesis of exceptionally uniform, small particles at high density is an important advantage for ALD over other preparation methods.

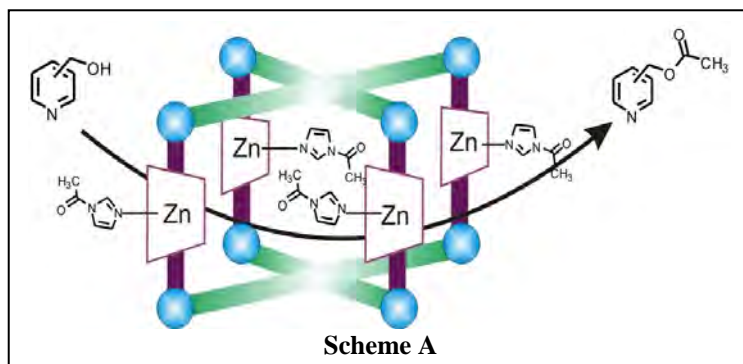
Permanently microporous metal organic frameworks (MOFs) that contain catalytically



competent metalloporphyrins have been synthesized. While many porphyrinic MOFs are known, none are ineffective as porous catalysts. The problems have been: a) insufficient stability, b) blockage of metal active sites due to strut ligation, and/or c) insufficient pore sizes. The ICEP group developed a mixed-strut, open-framework synthesis strategy that circumvent these problems. As illustrated in **Scheme A**, the new material behaves in a fashion reminiscent of enzymatic transferases; specifically the material catalyzes acyl-transfer reactions.

- **Characterization**

Raman spectra measured at several excitation wavelengths combined with density functional theory calculations have revealed the presence of several, previously unknown,  $\theta$ -alumina-supported vanadia monomer species with different catalytic properties (**Fig. 2**).



- **Photocatalysis**

The methane production by photocatalytic reduction of  $\text{CO}_2$  using different  $\text{TiO}_2$  materials was normalized to surface area and is compared in **Fig. 3**. Insignificant methane formation was observed in the presence of Degussa P25, whereas the sputtered mixed phase films displayed visible light activity using  $\text{H}_2\text{O}$  as the reductant. After being sintered at high temperature (823 K), a sputtered powder sample also showed visible light photoactivity in  $\text{CO}_2$  reduction.

**Future Plans**

- **Chemical Catalysis: Selective Oxidation of Light Alkanes to Fuels:** Specific questions to be addressed are: how do the nature of the metal, the oxygen, and the metal–oxygen bond at the catalytic site determine the reaction pathway of alkanes, leading to selective formation of oxygenates, and how can we modify them systematically to achieve high product yields. ICEP will focus on elucidating and understanding the chemistry and catalytic properties of monoatomic oxygen present in oxometal clusters or as adsorbed O on metal particles, and dioxygen present as a bound peroxy or related species. The ability of the ICEP team to synthesize and characterize well-defined metal oxo centers consisting of combinations of redox-active metals and/or non-redox active metals anchored on/in designed supports or supports of known surface atomic structures constitute the unique feature of the proposed program. Three types of supports will be used: metal organic framework structures, siloxane oligomers, and titanates of known surface atomic structures. The catalytic centers will be formed by atomic layer deposition and by using custom-synthesized metal oxo clusters of different nuclearity. The materials will be characterized by a combination of UV laser Raman and FTIR spectroscopies, X-ray absorption spectroscopy, and controlled atmosphere EPR spectroscopy. Reaction kinetics and product selectivities will be determined,

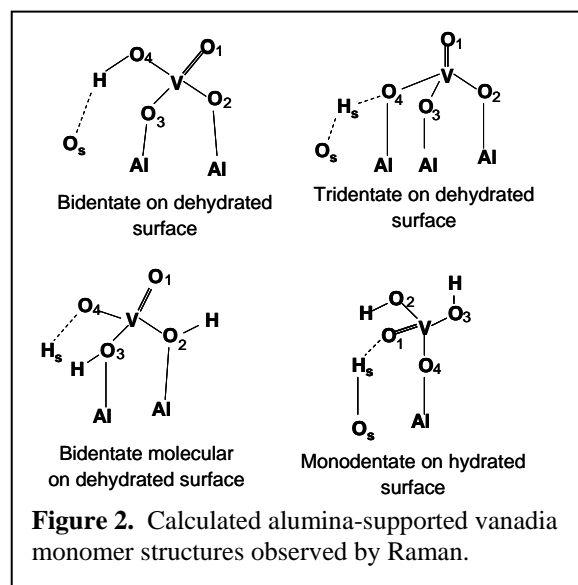


**Figure 2.** Calculated alumina-supported vanadia monomer structures observed by Raman.

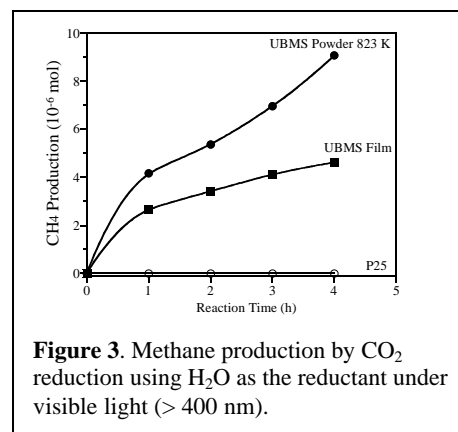


**Figure 3.** Methane production by  $\text{CO}_2$  reduction using  $\text{H}_2\text{O}$  as the reductant under visible light ( $> 400 \text{ nm}$ ).

assisted by isotope labeling, to gain mechanistic information. Quantum chemical computational investigation coupled to microkinetic modeling will be employed for detailed interpretation of the data. Modeling methods will include DFT, G4 theory, molecular dynamics simulations, and hybrid quantum chemical/molecular mechanics methods.

- *Photocatalysis: Reduction of Carbon Oxides*: Specific issues to be addressed are: 1) What is the initially adsorbed species, both in the presence and absence of water, and what is the structure of the photoactive defect site?; 2) What is the fate of the photogenerated electron hole pair, and how does charge transfer take place?; 3) What are the subsequent reactive steps after activation of the initially adsorbed species?

### Publications (2008-2009)

1. Albo, S.E., R.Q. Snurr, and L.J. Broadbelt, *Designing nanostructured membranes for oxidative dehydrogenation of alkanes: A multiscale modeling approach*. Ind. Eng. Chem. Res., submitted.
2. S. T. Christensen, J. W. Elam, B. Lee, Z. Feng, M. J. Bedzyk, and M. C. Hersam, “*Nanoscale structure and morphology of atomic layer deposition platinum on SrTiO<sub>3</sub> (001)*”, Chemistry of Materials, (in press) 2009.
3. Christensen, S.T., J.W. Elam, F. Rabuffetti, Q. Ma, S. Weigand, B. Lee, S. Seifert, C. Stair Peter, K.R. Poepelmeier, M.C. Hersam, and M.J. Bedzyk, *Controlled Growth of Platinum Nanoparticles on Strontium Titanate Nanocubes by Atomic Layer Deposition*. Small, 5, 750-757 (2009).
4. L. Chen, M.E. Graham, G. Li, D. Gentner, K.A. Gray (2009) “Photoreduction of CO<sub>2</sub> by TiO<sub>2</sub> Nanocomposites Synthesized through Reactive DC Magnetron Sputter Deposition,” *Thin Solid Films*, accepted.
5. Chiamonti, A.N., C.H. Lanier, L.D. Marks, and P.C. Stair, *Time, temperature, and oxygen partial pressure-dependent surface reconstructions on SrTiO<sub>3</sub> (1 1 1): A systematic study of oxygen-rich conditions*. Surface Science, 2008. **602**: p. 3018-3025.
6. Curet-Arana, M.C., Emberger, G.A., Broadbelt, L.J. and Snurr, R.Q., “*Quantum Chemical Determination of Stable Intermediates for Alkene Epoxidation with Mn-Porphyrin Catalysts*”, *J. Molec. Catal. A*, **2008**, 285, 120-127.
7. Curet-Arana, M.C., Snurr, R.Q.; and Broadbelt, L.J., “*Quantum Chemical Analysis of the Reaction Pathway for Styrene Epoxidation Catalyzed by Mn-Porphyrins*”, in *Mechanisms in Homogeneous and Heterogeneous Epoxidation Catalysis*, edited by T. Oyama, Elsevier, Amsterdam (2008); pp. 471-486.
8. Emberger, G.A.; Curet-Arana, M.C., Majumder, D.; Gurney, R.W.; Merlau, M.L.; Nguyen, S.T.; Snurr, R.Q.; Broadbelt, L.J., “*Microkinetic Analysis of the Epoxidation of Styrene Catalyzed by (Porphyrin)Mn Encapsulated in Molecular Squares*”, in preparation.
9. Chang-Yong Kim, Jeffrey Klug, Peter C. Stair, and Michael J. Bedzyk, “*Hydration and reduction of MBE grown VO<sub>x</sub>/a-Fe<sub>2</sub>O<sub>3</sub> (0001): Ambient pressure study*”, *J. Phys. Chem.* (in press) 2009.
10. Chiamonti, A.N., et al., *A Model for the Pseudo-Incommensurate 9x9 Reconstruction on SrTiO<sub>3</sub> (111)*. In Preparation, 2009.
11. Chiamonti, A.N., C.H. Lanier, L.D. Marks, and P.C. Stair, *Time, temperature, and oxygen partial pressure-dependent surface reconstructions on SrTiO<sub>3</sub>(111): A systematic study of oxygen-rich conditions*. Surface Science, 2008. **602**(18): p. 3018-3025.
12. Chiamonti, A.N., et al., *A Solution to the Valence Charge Problem for a Polar Oxide Surface: SrTiO<sub>3</sub>(111) 3x3*. In Preparation, 2009.
13. Chiamonti, A.N., et al., *SrTiO<sub>3</sub>(111) Surface Reconstructions in Oxidizing Environments*. In Preparation, 2009.
14. Curet-Arana, M.C., Emberger, G.A., Broadbelt, L.J., and Snurr, R.Q., *Quantum Chemical Determination of Stable Intermediates for Alkene Epoxidation with Mn-Porphyrin Catalysts*. *J. Molecular Catalysis A* 285, 120-127 (2008).

15. Curet-Arana, M.C., Snurr, R.Q., and Broadbelt, L.J., *Quantum Chemical Analysis of the Reaction Pathway for Styrene Epoxidation Catalyzed by Mn-Porphyrins*, in Mechanisms in Homogeneous and Heterogeneous Catalysis, Elsevier, S.T. Oyama, Editor. Elsevier, Amsterdam (2008) 471-486.
16. Dash, A.K.F., H.; Elam, J.W.; Pellin, M.J.; Stair, P.C.; Marks, T.J.; , *Product Selectivity in Oxidative Dehydrogenation of Cyclohexane by Single-Site Molecular Precursors of Vanadium Anchored in Nano-structured AAO-membranes*. In Preparation.
17. Feng, H., J.W. Elam, J.A. Libera, M.J. Pellin, and P.C. Stair, *Oxidative Dehydrogenation of Cyclohexane over Vanadium Oxide Catalysts Supported on the Nanoporous Alumina Structure*. Journal of Catalysis, 2009. **Submitted**.
18. Feng, H., J.W. Elam, J.A. Libera, M.J. Pellin, and P.C. Stair, *Catalytic Nanoliths*. Chemical Engineering Science, 2009. **64**: p. 560-7.
19. Gadzikwa, T.; Zeng, B.-S.; Hupp, J. T.; Nguyen, S. T., Ligand-elaboration as a strategy for engendering structural diversity in porous metal-organic framework compounds. *Chem. Commun.* **2008**, (31), 3672-3674.
20. Gadzikwa, T.; Farha, O. K.; Mulfort, K. L.; Hupp, J. T.; Nguyen, S. T., A Zn-based, pillared paddlewheel MOF containing free carboxylic acids via covalent post-synthesis elaboration. *Chem. Commun.* **2009**, submitted.
21. Hiu-Ying Law, M.C.K., Harold H. Kung, *Low Temperature NO<sub>x</sub> Removal from Diesel Exhaust by Coupling Ethylene Glycol Reforming with SCR*. Catalysis Today, 136, 40-45, (2008).
22. Kim, C.-Y., J.A. Klug, P.C. Stair, and M.J. Bedzyk, *Hydration and Reduction of Molecular Beam Epitaxy Grown VO<sub>x</sub>/alpha -Fe<sub>2</sub>O<sub>3</sub>(0001): Ambient Pressure Study*. J. Phys. Chem. C, 2009. **113**(4): p. 1406-1410.
23. Kim, H.-S. and P.C. Stair, *Resonance Raman spectroscopic study of alumina supported vanadium oxide catalysts with 220 nm and 287 nm excitation*. Journal of Physical Chemistry C, 2009. **113**: p. Accepted.
24. Lanier, C.H., et al., *The Fe<sub>3</sub>O<sub>4</sub>-based origin of the so-called Biphase termination of alpha-Fe<sub>2</sub>O<sub>3</sub>*. In Preparation, 2008.
25. J.K. Lee, M. C. Kung, and H. H. Kung, Discrete Molecular-size Nanocages Derived from Disintegratable Dendrimer Templates, *Chemistry of Materials* **20**(2) 373-375 (2008).
26. Jeong-Kyu Lee, Mayfair C. Kung, Harold H. Kung, Cooperative Catalysis: a New Development in Heterogeneous Catalysis, *Topics in Catalysis*, **49** 136-144 (2008).
27. Jeong-Kyu Lee, Mayfair C. Kung, Lynn Trahey, Michael N. Missaghi, and Harold H. Kung, Nanocomposites Derived from Phenol-Functionalized Si Nanoparticles for High Performance Lithium Ion Battery Anodes, *Chemistry of Materials*. **21** 6-8 (2009).
28. Lee, J.; Farha, O. K.; Roberts, J.; Scheidt, K. A.; Nguyen, S. T.; Hupp, J. T., Metal Organic Framework Materials as Catalysts. *Chem. Soc. Rev.* **2009**, 38, in press.
29. G. Li, N.M. Dimigtrijevic, L. Chen, T. Rajh, K.A. Gray (2008). "Photoactive CuO-TiO<sub>2</sub> Nanocomposites Prepared by a Chemical Method," *Jour. Phys. Chem. C*, **112**, 19040-19044.
30. G. Li, N.M. Dimitrijevic, L. Chen, J.M. Nichols, T. Rajh, K.A. Gray (2008) "The Important Role of Tetrahedral Ti<sup>4+</sup> Sites in the Phase Transformation and Photocatalytic Activity of TiO<sub>2</sub> Nanocomposites," *JACS*, **130**:5402-5403.
31. G. Li, S.M. Ciston, N. Dimitrijevic, T. Rajh, K.A. Gray (2008). "Photooxidation and Photoreduction using Mixed-phase Titanium Dioxide," *Journal of Catalysis*, **253**:105-110.
32. Michael N. Missaghi, Christopher M. Downing, Mayfair C. Kung, and Harold H. Kung, Synthesis of Organofunctional Silicon Hydride Halides from Methylchlorosilane, *Organometallics*, **27** (23) 6364-6366 (2008).
33. G. N. Ostojic, J. R. Ireland, and M. C. Hersam, "Noncovalent functionalization of DNA-wrapped single-walled carbon nanotubes with platinum-based DNA cross-linkers," *Langmuir*, **24**, 9784 (2008).

34. Petkov, V., Y. Ren, I. Saratovsky, P. Pasten, S.J. Gurr, M.A. Hayward, K.R. Poeppelmeier, and J.F. Gaillard, *Atomic-Scale Structure of Biogenic Materials by Total X-ray Diffraction: A Study of Bacterial and Fungal MnOx*. ACS Nano, 2009: p. ACS ASAP.
35. Rabuffetti, F.A., H.S. Kim, J.A. Enterkin, Y.M. Wang, C.H. Lanier, L.D. Marks, K.R. Poeppelmeier, and P.C. Stair, *Synthesis-dependent first-order Raman scattering in SrTiO<sub>3</sub> nanocubes at room temperature*. Chemistry of Materials, 2008. **20**(17): p. 5628-5635.
36. Ramachandran, C.E., Du, H., Kim, Y.J., Kung, M.C., Snurr, R.Q., and Broadbelt, L.J., *Solvent Effects in the Epoxidation Reaction of 1-Hexene with Titanium Silicalite-1 Catalyst*. J. Catal., 2008. **253**: p. 148-158.
37. Savara, A., C.M. Schmidt, F.M. Geiger, and E. Weitz, *Adsorption Entropies and Their Implications for Surface Science*. in press J. Phys. Chem. A, 2008.
38. Schmerberg, C. M.; Cho, S.-H.; Gadzikwa, T.; Hupp, J. T.; Nguyen, S. T., [Fe<sup>III</sup>(salen)]<sub>2</sub>O Complexes as Catalysts for Asymmetric Sulfoxidation. *Eur. J. Inorg. Chem.* **2009**, In preparation..
39. Shultz, A. K.; Farha, O. K.; Hupp, J. T.; Nguyen, S. T., A Catalytically Active, Permanently Microporous MOF with Metallaporphyrin Struts. *J. Am. Chem. Soc.* **2009**, 131, submitted.
40. Smit, J.P., T.M. McDonald, and K.R. Poeppelmeier, *Li<sub>3</sub>Ti<sub>0.75</sub>(MoO<sub>4</sub>)<sub>3</sub>: A Lyonsite Type Oxide*. Solid State Sciences, 10, 396-400 (2008).
41. Stair, P.C., *Advanced synthesis for advancing heterogeneous catalysis*. Journal of Chemical Physics, 2008. **128**(18): p. 182507/1-182507/4.
42. Stokes, G.Y., A.M. Buchbinder, J.M. Gibbs-Davis, K.A. Scheidt, and F.M. Geiger, *Heterogeneous Ozone Oxidation Reactions of 1-Pentene, 2-Hexene, Cyclopentene, Cyclohexene, and a Menthenol Derivative Studied by Sum Frequency Generation*. (in press) J. Phys. Chem., 2008.
43. Sung, C.-Y., Broadbelt, L.J. and Snurr, R.Q., "A DFT Study of Adsorption of Intermediates in the NO<sub>x</sub> Reduction Pathway over BaNaY Zeolites", *Catalysis Today*, **2008**, 136, 64-75.
44. Sung, C.-Y., Snurr, R.Q.; and Broadbelt, L.J., "Insights into the Reaction Mechanism of NO<sub>x</sub> Reduction over BaNaY Zeolites from DFT Calculations in the Gas Phase", *J. Phys. Chem. A*, submitted.
45. J. Sung, K. Kosuda, J. W. Elam, K. G. Spears, and R. P. Van Duyne, "Stability of Silver Nanoparticles Fabricated by Nanosphere Lithography and Atomic Layer Deposition to Femtosecond Laser Excitation," *J. Phys. Chem. C*, **112**, 5707-5714 (2008)
46. Warschkow, O., Y.M. Wang, A. Subramanian, M. Asta, and L.D. Marks, *Structure and Thermodynamics of the c(2x2) reconstruction of TiO<sub>2</sub> (100)*. Physical Review Letters, 2008. **100**: p. 86102.
47. Y. Yao, G. Li, K.A. Gray, R.M. Lueptow (2008) "Single-walled Carbon Nanotube Facilitated Dispersion of Particulate TiO<sub>2</sub> on ZrO<sub>2</sub> Ceramic Membranes," *Langmuir*, 24:7072-7075.
48. S-X Yin and D.E. Ellis, *H<sub>2</sub>O adsorption and dissociation on defective hematite (0001) surfaces: a DFT study*, Surf. Sci. **602**, 2047 (2008).
49. S. Yin and D.E. Ellis, "DFT studies of Cr (VI) complex adsorption on hydroxylated hematite (1  $\bar{1}$  02) surfaces", Surf. Sci. **603**, 736-746 (2009).



## Structure/Composition/Function Relationship in Supported Nanoscale Catalysts for Hydrogen

Additonal PIs: Larry Curtiss, Jeff Elam, Chris Marshall, Stefan Vajda  
Postdocs: Hao Feng, Sungsik Lee, Faisal Mehmood, Sai Setthapun,  
Collaborators: Peter Chupas, Jeffrey Greeley, Hack-Sung Kim, Randy Winans  
Contacts: P. Stair, Dept. Of Chemistry, Northwestern University, Evanston, IL 60208; [pstair@northwestern.edu](mailto:pstair@northwestern.edu)  
L. Curtiss, CSE Division, Argonne National Laboratory, 9700 S. Cass Ave., Argonne, IL 60439; [curtiss@anl.gov](mailto:curtiss@anl.gov)  
J. Elam, ES Division, Argonne National Laboratory, 9700 S. Cass Ave., Argonne, IL 60439; [jelam@anl.gov](mailto:jelam@anl.gov)  
C. Marshall, CSE Division, Argonne National Laboratory, 9700 S. Cass Ave., Argonne, IL 60439; [marshall@anl.gov](mailto:marshall@anl.gov)  
S. Vajda, CSE Division, Argonne National Laboratory, 9700 S. Cass Ave., Argonne, IL 60439; [vajda@anl.gov](mailto:vajda@anl.gov)

### Goal

The objective of the research is to improve our fundamental understanding of composition/structure/function relationships in supported, heterogeneous catalysts for reactions that produce hydrogen from hydrogen-rich molecules. The particular focus of this project is supported metal clusters with sub-nanometer dimensions. The influence of size and structure on the catalytic properties of clusters having dimensions <1 nm (<50 atoms) has been studied to a much lesser degree than particles >1 nm because the small clusters are difficult to prepare, stabilize, and characterize. The project will accomplish its objectives through highly integrated efforts in: 1) Novel catalyst synthesis, using advanced techniques, of highly uniform supported sub-nanometer catalytic metal and alloy clusters (<1 nm), 2) Measurements of catalyst atomic and nanoscopic structure and composition under synthesis, pretreatment and operating catalytic reaction conditions, 3) Experimental elucidation of kinetics and mechanisms for selected, model catalytic reactions and surface chemical reactions involving catalytic intermediates, and 4) Computational studies designed to facilitate interpretation of experimental measurements and understanding of the relationships between catalyst properties and catalytic chemistry.

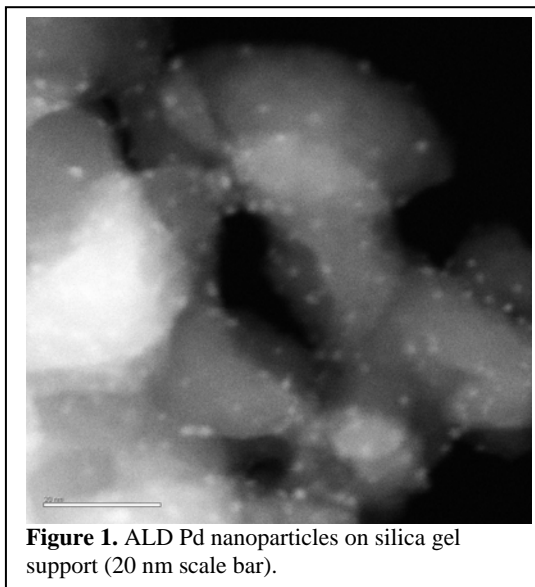
### DOE Interest

The understanding and control of reactions catalyzed on solid surfaces *at the molecular-level* is a “grand challenge” for 21<sup>st</sup> Century catalysis science. The development of fundamental understanding of structure-function relationships between catalytically active sites and the chemical reactions they catalyze that are at the heart of this challenge. This project brings together a team of national laboratory researchers who develop methods for the controlled design and synthesis of active catalytic metal sites and tailored supporting oxides at the atomic scale, diverse spectroscopy, and x-ray scattering techniques for detailed characterization (both ex-situ and in-situ) of catalyst structure and dynamics, elucidation of catalytic reaction mechanisms, and theory applied to catalytic processes.

## Recent Progress

• **Development of Metal Nanocluster Synthesis by Atomic Layer Deposition:** We have explored the use of atomic layer deposition (ALD) to prepare size-selected metal nanoclusters to improve our fundamental understanding of structure-property relationships in supported, heterogeneous catalysts capable of producing hydrogen from hydrogen-rich molecules. Our initial studies have focused on Pd nanoparticles and nanoclusters. We began by examining the nucleation and growth of these Pd nanoparticles on planar surfaces to facilitate analysis using thin film characterization methods. Using in situ quartz crystal microbalance and quadrupole mass spectrometry measurements, we investigated the influence of the catalyst support layer ( $\text{Al}_2\text{O}_3$ , ZnO, MgO, SrO, and  $\text{Al}_2\text{O}_3$ -ZnO mixtures) on the nucleation and growth of Pd by ALD. These measurements revealed that the Pd growth begins promptly on the ZnO surfaces, but the nucleation is delayed on the other oxide surfaces. Next, we prepared Pd ALD samples on ALD support layers on planar silicon and quartz substrates and analyzed these samples using scanning electron microscopy, ellipsometry, x-ray fluorescence, and optical absorption. These measurements confirmed the in-situ studies that the Pd ALD is efficient on the ZnO surface but inhibited on the other oxide surfaces, and also showed that the Pd nucleation proceeds by the growth and coalescence of Pd nanoparticles.

• **Preparation of High-Surface-Area Supported Pd Nanoparticles:** A series of Pd ALD catalyst samples were prepared on high surface area silica gel substrates by first depositing ALD catalyst support layers of ZnO and  $\text{Al}_2\text{O}_3$ . X-ray fluorescence and inductively coupled plasma atomic emission spectroscopy were used to quantify the Pd loading. These measurements showed that the Pd loading could be controlled precisely by the number of Pd ALD cycles as well as the precursor exposure times. The influence of the substrate chemistry on the Pd nucleation was less dramatic on the silica gel than on the planar substrates, and this difference is attributed to the much larger exposures used to coat the silica gel as compared to the planar substrates. These larger exposures will drive the Pd ALD surface reactions to completion even on less reactive surfaces such as the  $\text{Al}_2\text{O}_3$ . Cross-sectional scanning electron microscopy and energy dispersive X-ray analysis were used to evaluate the degree of infiltration of the ALD Pd into the porous silica gel particles. Transmission electron microscopy (TEM) was performed on ALD Pd samples prepared on alumina nanoparticles, and these measurements showed that the Pd deposits as ~2 nm particles. Further analysis using high angle annular dark field (HAADF) scanning transmission electron microscopy (STEM) revealed Pd particles as small as 0.8 nm (see **Fig. 1**).



• **Catalytic Evaluation:** A new catalytic testing station was designed and constructed for use on this project. The ALD Pd samples were tested using this system for methanol decomposition in the temperature range of 40-250°C with methanol feed concentration of 3.6% in Argon. Palladium surface densities were in the range of 0.3-6 Pd/nm<sup>2</sup>. We determined that the Pd

catalysts prepared on ZnO surfaces are active for methanol decomposition showing 30% conversion and almost 100% H<sub>2</sub> selectivity at 240°C, but these samples deactivate over time probably due to coking. In contrast, similar Pd catalysts prepared on Al<sub>2</sub>O<sub>3</sub> surfaces exhibit 100% conversion with 99% H<sub>2</sub> selectivity at 270°C with no evidence of deactivation. Preliminary studies indicate that at 250°C, methanol TOF increases with decrease in Pd loading. This may be due to the decrease in Pd cluster size and over-coating the Pd catalysts prepared on ZnO surfaces with one cycle of ALD Al<sub>2</sub>O<sub>3</sub> inhibits the deactivation.

• **Support Preparation:** From these ALD Pd studies as well as our related work exploring ALD Pt nanoparticles, we have learned that while the surface chemistry for noble metal ALD is self-limiting and the nanoparticle size can be controlled by the number of ALD cycles, particle sintering and agglomeration also strongly influence the ALD nanoparticle size. This agglomeration is driven by surface diffusion during the reduction step of the ALD reaction sequence. We hypothesize that by lowering the temperature of the reduction step we should reduce the diffusion rate and therefore the particle size. To test this hypothesis, we have designed and constructed a custom fixture for our ALD systems that will allow powder substrates as well as planar samples to be rapidly heated and cooled inside of the ALD reactor. This fixture will enable individual reactant exposures (such as Pd(hfac)<sub>2</sub> and HCOH for Pd ALD) to be performed at different temperatures. This capability will also enable a broader range of chemical precursors to be used for ALD catalyst synthesis, and ultimately should allow better control over nanoparticle size, dispersion, and morphology.

• **Combined TPRx/GISAXS experiments on size-selected Pd clusters:** The production of hydrogen from methanol by steam reforming and partial oxidation was studied over a series of Pd<sub>17-20</sub> clusters supported on ALD-synthesized Al<sub>2</sub>O<sub>3</sub>-based catalysts, using a mixture of methanol, oxygen and water vapor seeded in helium carrier gas. The nanocatalysts were prepared by size selected cluster deposition method and tested with temperature programmed reaction (Fig. 2). In situ GISAXS was applied to monitor possible change in cluster size via sintering during the reaction.

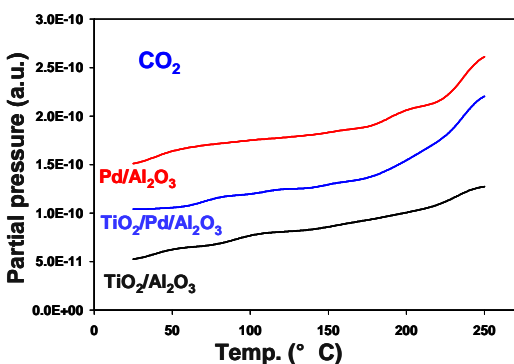


**Figure 2a.** Evolution of CO<sub>2</sub> on alumina supported Pd<sub>17-20</sub> catalyst and by ALD titania overcoated Pd/alumina catalyst. The signal obtained with the blank titania overcoated alumina support is also shown.

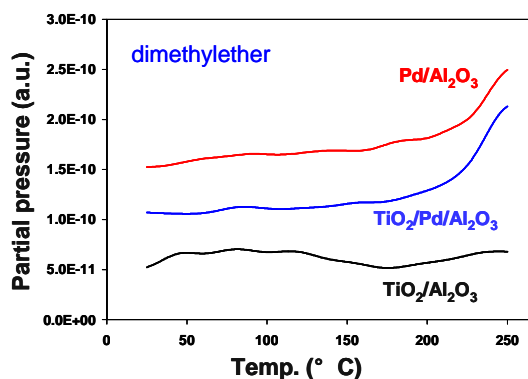


**Figure 2b.** Evolution of dimethyl ether on alumina supported Pd<sub>17-20</sub> catalyst and by ALD titania overcoated Pd/alumina catalyst. The signal obtained with the blank titania overcoated alumina support is also shown.

Special attention was paid to the effect of cluster size and catalyst supports (Al<sub>2</sub>O<sub>3</sub>, TiO<sub>2</sub>) and overcoating the Pd with ALD-TiO<sub>2</sub> on reactivity and selectivity. Some clear differences were observed with respect to catalyst functionality. The alumina supported Pd nanocatalyst system

shows a low light-off temperature and a low level of CO by-product. As second dominant product, dimethylether was identified based from the analysis of the mass spectral pattern. A very strong promotional effect of hydrogen to the reaction was observed – after a short injection of hydrogen, the partial pressure of the products increased by over an order of magnitude.

• **Synthesis of Pd- and Co-cluster based samples for further tests:** A set of size selected Pd samples on ALD-coated AAO nanoliths was fabricated, with cluster sizes in the range of Pd<sub>4</sub>, Pd<sub>8</sub> and Pd<sub>16</sub> on ZnO and Al<sub>2</sub>O<sub>3</sub> surfaces with the goal to study size and support effects. Accompanying calculations by Larry Curtiss focus on four and eight atom clusters. Samples of size-selected Co clusters on AAO nanoliths were also produced and are awaiting catalytic tests. Pd and Co clusters samples were also prepared on flat supports with various ALD-oxide coatings for combined GISAX/TPRx studies.

• **Development of operando grazing incidence X-ray techniques:** The technique of GISAXS/TPRx has been extended by grazing incidence X-ray absorption (GIXAS) to allow monitoring the nature of the nanocatalysts under reaction conditions.

• **Design of a new cluster deposition apparatus:** A new cluster beam apparatus has been designed which makes possible higher throughput and more flexibility for the synthesis of size-selected metal and alloy clusters. The apparatus is currently under construction.

• **Density functional studies of methanol decomposition on small Pd clusters:** Palladium based catalysts have been found to be very effective for the decomposition of methanol, a reaction of great interest because methanol is an attractive, clean, and reliable energy source. While Pd surfaces and nanoparticles have been extensively studied for this reaction, no study of methanol decomposition has been carried out on small (subnanometer) Pd clusters. The catalytic properties of these clusters have not traditionally been studied experimentally because of difficulties in stabilizing them under realistic conditions, but recent breakthroughs in this area have shown that supported subnanometer clusters do, indeed, exhibit novel catalytic properties. For example, small Pt clusters have been found to exhibit a surprisingly high activity and selectivity for oxidative dehydrogenation of propane to propylene compared to Pt surfaces.

We have carried out a density functional study of the reaction pathways for methanol dissociation on Pd<sub>4</sub> and Pd<sub>8</sub> clusters.

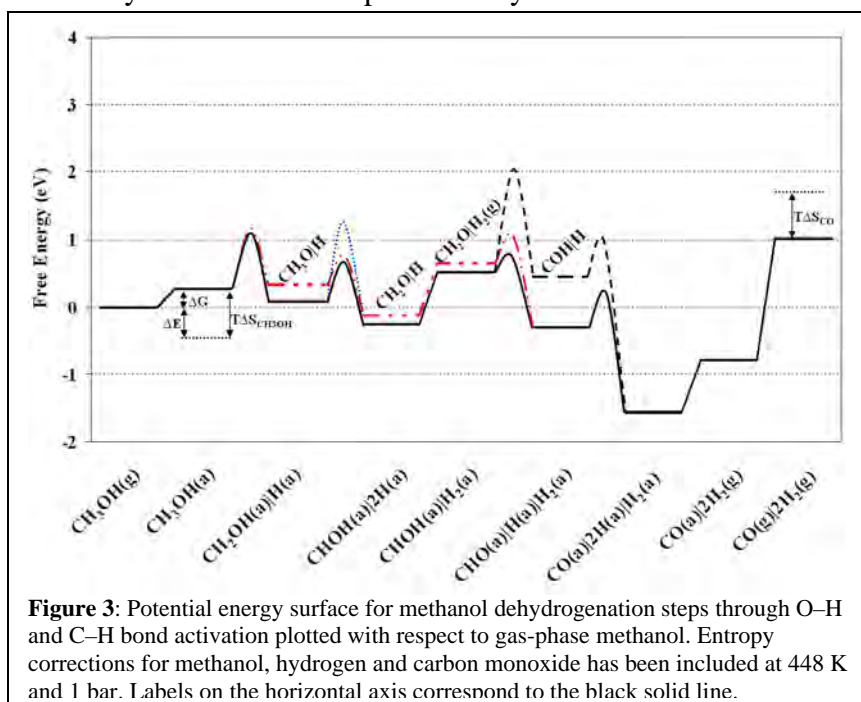


**Figure 3:** Potential energy surface for methanol dehydrogenation steps through O–H and C–H bond activation plotted with respect to gas-phase methanol. Entropy corrections for methanol, hydrogen and carbon monoxide has been included at 448 K and 1 bar. Labels on the horizontal axis correspond to the black solid line.

Calculated reaction pathways are shown in **Fig. 3**. This study represents the first study of reaction pathways for methanol decomposition on a Pd cluster and is more comprehensive than any comparable investigations that have been reported for Pd surfaces. We have used periodic density functional theory to calculate adsorption energies, geometries, reaction pathways and activation energy barriers. The results were used to estimate free

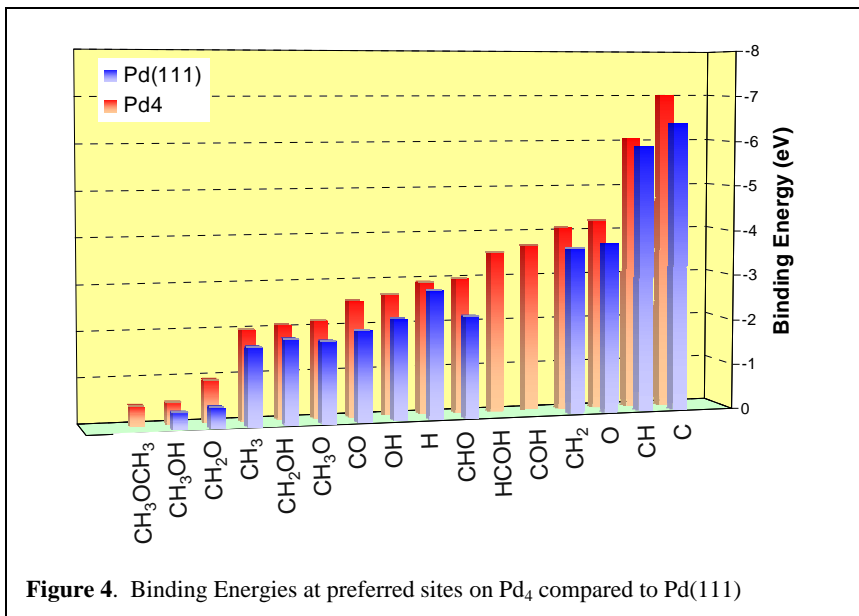


**Figure 4.** Binding Energies at preferred sites on Pd<sub>4</sub> compared to Pd(111)

energies for the different methanol decomposition pathways and were used to help understand the experimental studies being carried out in this project. We used the results to help identify the differences in reaction pathways on sub-nanometer clusters and those on nanoparticles or single crystal surfaces.

The main conclusions from this study are as follows. First, the most favorable reaction pathways for decomposition of methanol lead to formation of CO and H<sub>2</sub>. The pathways involving CO bond breaking on Pd clusters are unfavorable. These results are consistent with observations from experiment in this project. Secondly, the Pd clusters have slightly stronger binding for the decomposition fragments than do single-crystal Pd surfaces or larger nanoparticles, as shown in **Fig. 4**.

Thirdly, we investigated dimethyl ether formation on Pd clusters and have not found any favorable reaction pathways. Finally, we have constructed Brønsted-Evans-Polanyi (BEP) plots that show a qualitative relationship between the activation barriers for elementary reaction steps and the corresponding overall reaction energies, as shown in **Fig. 5**. This is the first time that such a

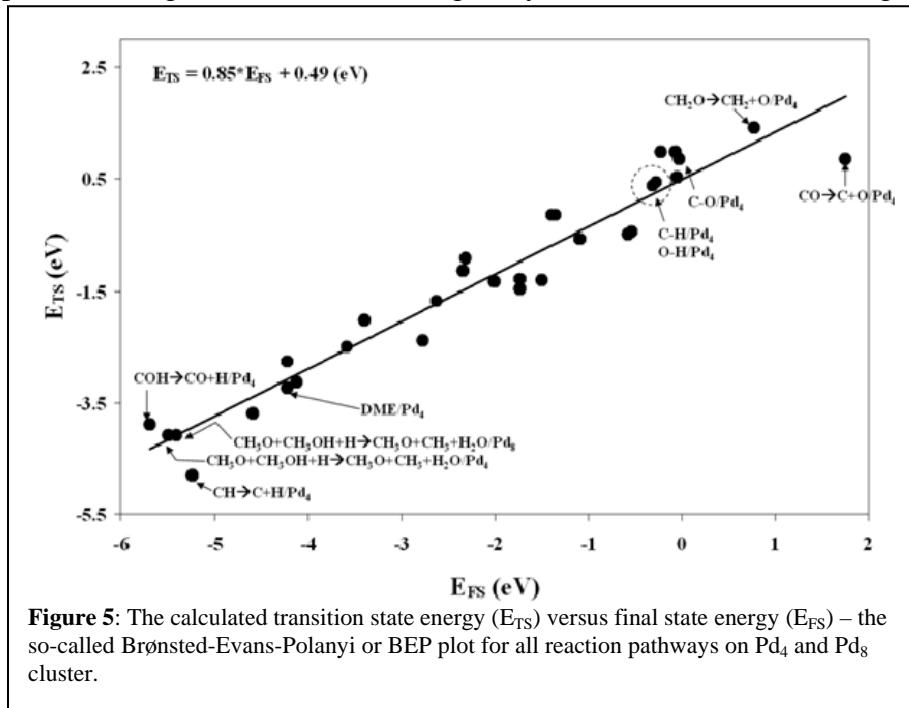


**Figure 5:** The calculated transition state energy ( $E_{TS}$ ) versus final state energy ( $E_{FS}$ ) – the so-called Brønsted-Evans-Polanyi or BEP plot for all reaction pathways on Pd<sub>4</sub> and Pd<sub>8</sub> cluster.

correlation has been done for subnanometer clusters.

### Future Plans

- Examine the influence of the ALD chemical precursor, reducing environment, and temperature on the Pd nanoparticle size and dispersion. We will use HAADF STEM as well as EXAFS to evaluate the ALD Pd nanoparticle size and dispersion on silica gel substrates that have been coated using ALD metal oxide support layers. We will also continue our investigation of the effect of ALD metal oxide overcoat layers on the Pd nanoparticle size, reactivity, and stability. Finally, we will measure the catalytic activity of these samples to determine the relationship between Pd nanoparticle size and environment on the conversion and selectivity of the catalyst.
- Conclude catalytic tests and GISAXS/TPRx tests of the existing size-selected catalysts on flat supports and define cluster compositions/sizes and support chemistry for the optimization of catalytic performance. Compare catalytic performance of nanolith-supported catalysts.
- Apply the recently developed combined GISAXS-GIXAS-TPRx for detailed understanding of the catalytic processes under realistic reaction conditions.
- Conclude the first set of systematic tests and identify catalyst/support composition for further optimization of nanocatalysts size and composition as well as support composition.
- Complete construction and commissioning of the new cluster beam synthesis apparatus.
- Complete work in progress to carry out a computational investigation on methanol decomposition on cobalt clusters. In this work we are calculating adsorption energies, geometries, reaction pathways and activation energy barriers for the different pathways. The results indicate that Co clusters are much more active for breaking C-O bonds in methanol than are the Pd clusters. The work on Pd clusters will be completed as part of this project. Further calculations on other clusters will depend on the findings of experimental studies in this project. We will also carry out some calculations on mixed clusters of Co and Pd to determine the effect on key pathways, as little work has been done on cluster alloys.
- Complete a computational investigation of the effect of the substrate on the Pd cluster results for methanol decomposition by carrying out calculations with Pd<sub>4</sub> on a  $\theta$ -Al<sub>2</sub>O<sub>3</sub> surface. The results of this study are showing that the substrate has little effect on the energetics of key reaction pathways. We will complete this work by considering the properties of Pd clusters on an amorphous Al<sub>2</sub>O<sub>3</sub> surface for which we have generated structures from molecular dynamics simulations and also investigating the catalytic properties of Co clusters on the  $\theta$  surface.

### Publications 2007-2009:

1. H. Feng, J. W. Elam, J. A. Libera, and P. C. Stair, Abstract submitted to: Atomic Layer Deposition 2009, Monterey, CA "Palladium Catalysts Synthesized Using Atomic Layer Deposition", March, 2009.
2. J. W. Elam, J. A. Libera, E. T. Huynh, H. Feng, and M. J. Pellin, "Atomic Layer Deposition of Aluminum Oxide in Nanoporous Silica Gel", *in preparation*, March 2009.
3. Mehmood, F.; Greeley, J.; Curtiss, L. A. Density functional studies of methanol decomposition on Pd clusters, *Journal of Physical Chemistry* March 2009, *in preparation*.
4. Mehmood, F.; Greeley, J.; Zapol, P., Curtiss, L. A., "Steps in hydrogen production from methanol on sub-nanometer palladium clusters," APS march 2009 meeting. Pittsburgh Pa
5. Greeley, J.; Mehmood, F.; Curtiss, L. A., "Trends in the Reactivity of CO and Light Oxygenates on Subnanometer Metal Clusters: A Density Functional Theory Study", NAM Meeting, June 2009, San Francisco.

**An *in situ* Electrode-Potential-Controlled Nuclear Magnetic Resonance Investigation of Sulfur-Poisoning Effect on Pt-Based Mono- and Bi-metallic Nanoscale Electrocatalysts**

Postdoc: Fatang Tan (partially supported)  
Students: Bingchen Du, Ceren Susut  
Contact: Georgetown University, 37<sup>th</sup> & O Streets, Washington, DC 20057;  
yyt@georgetown.edu

**Goal**

1. Advance significantly our fundamental understanding of sulfur poisoning of Pt-based mono- and bi-metallic nanoscale electrocatalysts through careful interrogation of long and short range electronic effects caused by the poisonous sulfur-metal bonding.
2. Investigate and establish correlations among the surface  $d$  band center, the frontier orbitals of the metal surface as represented by the surface local density of states at the Fermi level ( $E_f$  – LDOS), and the associated electrochemical reactivity.

**DOE Interest**

The prevailing sulfur poisoning of cathode and anode materials is a central issue that underlies the practical durability and performance of fuel cells and also determines the fuel specifications. Thus, achieving a mechanistic understanding of sulfur poisoning of Pt-based mono- and bi-metallic nanoscale materials that are widely used as cathode and anode in fuel cell applications is of both fundamental and practical importance. The project is using and developing further the surface  $^{195}\text{Pt}$  and  $^{13}\text{C}$  of chemisorbed  $^{13}\text{CO}$  as the key complementary pair of local probes of electrode-potential-controlled nuclear magnetic resonance (NMR) spectroscopy to investigate the local (surface) electronic alternations of the Pt-based electrocatalysts, in an unprecedented detailed fashion, as functions of sulfur coverage, electrode potential, alloying element (such as Ru/Rh, Sn/Pb, Au/Ag, or other elements), and surface coordination number (particle shape). The anticipated great stride brought to bear by this project on our fundamental understanding of the sulfur poisoning will facilitate the design and development of new impurity-resistant Pt-based electrocatalysts which will in turn contribute in a significant way to the development of more sustainable and reliable fuel cells.

**Recent Progress**

*Sulfur-Coverage Dependent Study of Pt Electrocatalytic Activity:* A continuous control of sulfur coverage on industrial Pt black was achieved by using open potential deposition in  $\text{Na}_2\text{S}$  solution. The resulting Pt nanoparticles (NPs) indicated sulfur coverage-dependent electrochemical characteristics in term of CO oxidation and methanol electro-oxidation. The sulfur adsorption changed the chemical/physical properties of the Pt surface, evidenced by the slight but clear peak shift of both CO oxidation and the reduction of Pt oxide towards high potential. On the other hand, unexpected high methanol electro-oxidation activities on the sulfur covered Pt surfaces were observed and need to be clarified in later research. The same sulfur adsorption procedure was successfully applied to deposit sulfur on shaped-controlled (octahedral/tetrahedral) nanoparticles and the preliminary results indicated that we could achieve a continuous control of sulfur coverage on these particles.

*Capping Polymer-Enhanced Electrocatalytic Activity on Pt Nanoparticles:* An exquisite control of shape and size of metal nanoparticles (NPs) is *essential* in achieving rational design of heterogeneous catalysts in general and electrocatalysts in particular. Polymers and organic

ligands such as poly(vinylpyrrolidone) (PVP) are crucial in this regard in the colloidal synthesis of metal NPs and are particularly indispensable in maintaining the post-synthesis stability of the shape and size of the metal NPs. However, in heterogeneous catalysis which includes fuel cell catalysis, the capping polymer is usually considered to hamper the catalytic activity therefore it is customary to remove it prior to catalysis usually at the expense of the well-defined shape and size. But in a recent study of the PVP effect on the catalytic activity of a well-known industrial electrocatalyst for fuel cell applications—the Johnson-Matthey Pt black, we discovered that the adsorbed PVP had the ability to enhance significantly the catalytic activity of the underlying Pt black towards *both* MeOH and formic acid (FA) electro-oxidation (EO) and the degree of the enhancement was tunable by varying the PVP content. These findings may open up a new paradigm of research in which the protecting/stabilizing organic ligands can now be incorporated as an advantageous part of a nanocatalytic system.

*Pt Coverage Controlled Ru@Pt NPs:* A one-pot ethylene glycol (EG) reduction based method was developed to prepare Pt-decorated Ru NPs and through which, Pt coverage was quantitatively controlled. The as-prepared Ru@Pt NPs indicated clearly Pt coverage-dependent electrocatalytic activities towards methanol electro-oxidation and oxidative removal of CO. The results showed that Pt atoms dispersed as submonolayer/islands on surface of the Ru NPs. When Pt coverage is within a range of ~30%–~40%, the Ru@Pt showed the highest activities. The synthesis has been successfully scaled up and preliminary results on  $^{195}\text{Pt}$  NMR of the Ru@Pt NPs have been obtained. Additionally, using such Ru@Pt NPs as starting materials, by controlling the sulfur coverage that has also been achieved in the preliminary work, Pt-sulfur interaction could be studied in a quantitative way.

*Pt Coverage Controlled Au@Pt NPs:* Au@Pt NPs of two spherical Au core size (6.25 nm and 17.5 nm respectively) and a total of 10 different Pt shell packing densities ranging between 0.53 to 3.4 have been synthesized and whose sizes and elemental atomic ratios were characterized respectively by transmission electron microscope and energy dispersive X-ray spectroscopy. Their electrocatalytic properties as functions of Pt shell packing density and Au core size have been investigated in terms of CO stripping, methanol oxidation reaction (MOR) and oxygen reduction reaction (ORR). All the Au@Pt NPs studied here showed a much-suppressed formation of Pt oxides that would imply an increased availability of surface sites for initial oxygen adsorption. However, inferior ORR activities as compared to those of commercial Pt black were observed instead, suggesting that  $\text{O}_2 + 2* \rightarrow 2\text{O}^*$  (where \* represents a surface site) was not the rate-limiting step on the Au@Pt NPs. All electrochemical properties measured on the Au@Pt samples, i.e., Pt oxides reduction, CO stripping, MOR and ORR, were much different from those of the commercial Johnson-Matthey Pt black but moved closer to them in a qualitatively similar fashion as the Pt packing density increased. Yet the recovering rate was substantially faster for the small than for the large Au core samples, of which the underlying mechanism still eludes us. Another recent development in the lab is the successful synthesis of shape-controlled Au@Pt NPs with perfect octahedral Au cores and homogeneous Pt shells whose thickness can be controlled. This controllability opens a variety of opportunities by which this project can be expanded.

### **Future Plans**

Follow the timelines outlined in the proposal:

**Year 1:** comparative electrode-potential-dependent  $^{195}\text{Pt}$  and  $^{13}\text{CO}$  NMR investigations of Pt black, PtRu (1:1) black, carbon supported Pt and PtRu(1:1) with and without sulfur adsorption



and deduction of the corresponding  $E_f$ -LDOS; correlations with catalytic activity analyzed and established; in situ capability of SEIR and Raman on Reinshaw spectrometer developed and deployed for the investigation of the above systems.

**Year 2:** comparative electrode-potential-dependent  $^{195}\text{Pt}/^{13}\text{C}$ O NMR, SEIR, and Raman investigations of Pt-based bimetallic systems Au/Pt vs Ag/Pt and Sn/Pt vs Pb/Pt with and without sulfur adsorption and deduction of the corresponding  $E_f$ -LDOS;  $^{109}\text{Ag}$ ,  $^{119}\text{Sn}$ , and  $^{207}\text{Pb}$  NMR developed and deployed; correlations with catalytic activity analyzed/established and possible remedies to the sulfur poisoning proposed; expand the work of Year 1 to particle size dependent regime.

**Year 3:** comparative electrode-potential-dependent  $^{195}\text{Pt}/^{13}\text{C}$ O NMR, SEIR, and Raman investigations of systems of different shape and core-shell structures with and without sulfur adsorption and deduction of the corresponding  $E_f$ -LDOS; correlations with catalytic activity analyzed/established; continuation of the work of Year 1 and 2.

### **Publications (2008 – 2009)**

1. Susut, C. and Tong, Y., "Capping Polymer-Enhanced Electrocatalytic Activity on Pt Nanoparticles". *Angew. Chem. Int. Ed.*, **2009**, submitted.
2. Hsu-Yao, T., Browne, K. P., Honesty, N., and Tong, Y., "Oxygen Electro-Reduction Reaction on Polyoxometalate-Stabilized Pt Nanoparticles". *Chem. Phys. Phys. Chem*, **2009**, in revisions.
3. Du, B., Zaluzhna, O., Susut, C., Kenyan, P. C., Lukac, P. J., and Tong, Y., "Electrocatalytic Properties of Au@Pt Nanoparticles: Effects of Pt Shell Packing Density and Au Core Size". *Phys. Chem.. Chem. Phys.*, **2009**, submitted.
4. Du, B. and Tong, Y., "A Volcano Curve: Methanol Electro-oxidation on Pt-decorated Ru Nanoparticles". *Phys. Chem. Chem. Phys.*, **2009**, revision submitted.
5. Susut, C., Chapman, G. B., Samjeské, G., Osawa, M., and Tong, Y. Y., "An Unexpected Enhancement in Methanol Electro-Oxidation on an Ensemble of Pt(111) Nanofacets: A Case of Nanoscale Single Crystal Ensemble Electrocatalysis ". *Chem. Phys. Phys. Chem*, **2008**, *10*, 3712-3721.

**Surface chemistry on base-metal oxide nanostructures: A model system approach**

Postdocs: Cheol-Woo Yi, Kumudu Mudiyansele  
Co-investigators: Ja Hun Kwak, Donghai Mei, Charles H.F. Peden  
Contacts: Pacific Northwest National Laboratory, 902 Battelle Blvd, MSIN:  
K8-87 –Richland, WA 99352; [janos.szanyi@pnl.gov](mailto:janos.szanyi@pnl.gov)

**Goal**

Understanding the fundamental aspects of NO<sub>x</sub> surface chemistry on base-metal oxide nanostructures supported on well-characterized metal oxide thin films and metal substrates.

**DOE Interest**

Beside the fundamental scientific importance of understanding the interactions of molecules with base-metal oxides, there are a number of practical reasons these studies support the mission of DOE. The results of these investigations help understanding how environmental pollutants (e.g. NO<sub>x</sub>) interact with oxide nanostructures. On the other hand, the recent advances in lean NO<sub>x</sub> technologies (in particular NO<sub>x</sub> storage/reduction (NSR)) allow the introduction of highly fuel efficient diesel and lean-burn gasoline engines. In order to maximize the efficiencies of these complicated catalyst systems the understanding of the chemistry on base-metal oxides is critical.

**Recent Progress****I. BaO/Al<sub>2</sub>O<sub>3</sub>/NiAl(110):**

*The Nature of Surface Nitrates:* In a combined experimental/theory study we unambiguously determined the nature of surface nitrates. The results of our experimental work on both model (i.e. single crystal-based) and high surface area BaO/Al<sub>2</sub>O<sub>3</sub> materials suggested the presence of two different types of nitrates, i.e., bulk and surface nitrates. Bulk nitrates were identified as nitrates that formed during the interaction of NO<sub>2</sub> with BaO clusters (the formation of bulk Ba(NO<sub>3</sub>)<sub>2</sub>). In this study we determined that surface Ba-nitrates were formed by the interaction of NO<sub>2</sub> with BaO “monomers” and “dimers” present on the alumina surface and strongly interact with pentacoordinate Al<sup>3+</sup> sites on the (100) facets of the γ-Al<sub>2</sub>O<sub>3</sub> surface. DFT calculations were carried out to determine the energetically most stable BaO structures on the γ-Al<sub>2</sub>O<sub>3</sub> surface, as well as the optimized nitrate structures formed by the reaction of NO<sub>2</sub> with BaO. The vibrational frequencies of surface as well as bulk nitrates predicted by the DFT calculations closely matched the ones determined in the experimental work.

*Adsorption of D<sub>2</sub>O:* The presence of water on oxide surfaces is well known to influence their surface chemistry. As a first step to understand the effect on water on the NO<sub>x</sub> chemistry on BaO-based model catalyst systems we investigated the adsorption/reaction of D<sub>2</sub>O on a thick BaO film supported on Al<sub>2</sub>O<sub>3</sub>/NiAl(110) using TPD and IRAS. Upon exposure of the BaO film to D<sub>2</sub>O at 300 K the formation of an amorphous Ba(OH)<sub>2</sub> was observed. At low H<sub>2</sub>O exposures this amorphous Ba(OH)<sub>2</sub> readily transformed into a crystalline α-Ba(OH)<sub>2</sub> at around 400 K. However, when the BaO film was exposed to excess D<sub>2</sub>O the thus formed amorphous Ba(OH)<sub>2</sub> went through a series of phase transformation during annealing: first crystalline β-Ba(OH)<sub>2</sub>D<sub>2</sub>O, then, upon loss of its hydrating D<sub>2</sub>O, β-Ba(OH)<sub>2</sub> and finally α-Ba(OH)<sub>2</sub> formed, before it decomposed to BaO.

**II. BaO/Pt(111):**

*NO oxidation on O/Pt(111):* Atomic oxygen adlayers with 0.25 and 0.75 ML coverages were prepared on Pt(111) by dissociative chemisorption of O<sub>2</sub> at 300 K and NO<sub>2</sub> at 400 K,

respectively. The well ordered p(2×2)-O layer, corresponding to  $\Theta_{\text{O}} = 0.25$  ML, does not react with NO to form NO<sub>2</sub> in the temperature range of 350 - 500 K, in contrast to CO oxidation which takes place readily at a sample temperature as low as 300 K. At  $\Theta_{\text{O}} = 0.75$  ML, the NO oxidation reaction is facile, and the formation of NO<sub>2</sub> is observed even at 150 K. However, the NO oxidation reaction completely stops as the atomic oxygen coverage drops below 0.28 ML, because all the weakly bound oxygen atoms available only at higher O coverages have been consumed.

*NO<sub>2</sub> adsorption on BaO/Pt(111)*: The interaction of NO<sub>2</sub> with BaO overlayers on Pt(111) at different coverages was studied. The adsorbed species formed were strongly dependent on the BaO coverage. At submonolayer BaO coverage NO<sub>x</sub> species formed on BaO, clean Pt(111) and at the BaO-Pt(111) interface. On thin BaO layers (~2MLE) nitrites formed first in the reaction of NO<sub>2</sub> with BaO, and then these nitrites were converted to nitrates. The interaction of NO<sub>2</sub> with a thick BaO layer (~20 MLE) was the same as we have shown for the BaO(>20 ML)/Al<sub>2</sub>O<sub>3</sub>/NiAl(110) system; i.e., first nitrite-nitrate ion pairs formed and then converted to Ba(NO<sub>3</sub>)<sub>2</sub>.

**III. Anchoring of catalytic phases to  $\gamma$ -Al<sub>2</sub>O<sub>3</sub>:** Ultrahigh magnetic field <sup>27</sup>Al solid state MAS-NMR and high resolution transmission electron microscopy, combined with high level DFT calculations were used to identify the anchoring sites of catalytically active phases (e.g. BaO and Pt) onto  $\gamma$ -Al<sub>2</sub>O<sub>3</sub>. The NMR results unambiguously showed that both BaO and Pt anchor to coordinatively unsaturated pentacoordinate Al<sup>3+</sup> sites on the  $\gamma$ -Al<sub>2</sub>O<sub>3</sub> surface. These sites are located on the (100) facets of the  $\gamma$ -Al<sub>2</sub>O<sub>3</sub> support, and readily form upon mild dehydroxylation conditions. At low loadings both BaO and Pt are atomically dispersed on this support, due to their specific interaction with the pentacoordinate Al<sup>3+</sup> sites.

#### **Future Plans**

*The effect of co-adsorbates on NO<sub>x</sub> chemistry on supported BaO*: Understand the effects of co-adsorbates (specifically H<sub>2</sub>O and CO<sub>2</sub>) on the NO<sub>x</sub> chemistry on supported BaO model NO<sub>x</sub> storage systems.

*Reduction mechanism of stored NO<sub>x</sub> on BaO/Pt(111) systems*: Determine the mechanism of NO<sub>x</sub> reduction on BaO/Pt(111) systems using CO and H<sub>2</sub> as reductants in a wide pressure (10<sup>-9</sup>-10<sup>1</sup> Torr) range using primarily IRAS.

#### **Publications (2007-2009)**

1. Kwak JH, JZ Hu, DH Kim, J Szanyi, and CHF Peden. "Penta-coordinated Al<sup>3+</sup> ions as preferential nucleation sites for BaO on  $\gamma$ -Al<sub>2</sub>O<sub>3</sub>: an ultra-high magnetic field <sup>27</sup>Al MAS NMR study." *Journal of Catalysis* **251**(2) 189 (2007).

2. Kwak JH, JZ Hu, AC Lukaski, DH Kim, J Szanyi, and CHF Peden, "The Role of Penta-Coordinated Al<sup>3+</sup> Ions in the High Temperature Phase Transformation of  $\gamma$ -Al<sub>2</sub>O<sub>3</sub>." *Journal of Physical Chemistry C* **112**(25) 9486 (2008).

3. Yi CW, JH Kwak, and J Szanyi, "The interaction of NO<sub>2</sub> with BaO: from cooperative adsorption to Ba(NO<sub>3</sub>)<sub>2</sub> formation." *Journal of Physical Chemistry C* **111**(42)15299 (2007).

4. Yi CW, JH Kwak, CHF Peden, CM Wang, and J Szanyi, "Understanding Practical Catalysts Using a Surface Science Approach: The Importance of Strong Interaction between BaO and Al<sub>2</sub>O<sub>3</sub> in NO<sub>x</sub> Storage Materials." *Journal of Physical Chemistry C* **111**(41)14942 (2007).

5. Yi CW, and J Szanyi. "D<sub>2</sub>O Adsorption on an Ultrathin Alumina Film on NiAl(110)." *Journal of Physical Chemistry C* **111**(47) 17597 (2007).
6. Yi CW, and Szanyi J, "Reaction of NO<sub>2</sub> with a pure, thick BaO film: the effect of temperature on the nature of NO<sub>x</sub> species formed", *Journal of Physical Chemistry C*, **113**(6) (2009) 2134.
7. Mei D, Ge Q, Kwak JH, Kim DH, Szanyi J, and Peden CHF, "Adsorption and Formation of BaO Overlayers on  $\gamma$ -Al<sub>2</sub>O<sub>3</sub> Surfaces", *Journal of Physical Chemistry C*, **112** (2008) 18050.
8. Kwak JH, Mei D, Yi CW, Kim DH, Peden CHF, Allard LF, and Szanyi J, "Understanding the Nature of Surface Nitrates in BaO/ $\gamma$ -Al<sub>2</sub>O<sub>3</sub> NO<sub>x</sub> Storage Materials: a combined experimental and theoretical study", *Journal of Catalysis*, **261** (2009) 21.
9. Yi CW, and Szanyi J, "BaO/Al<sub>2</sub>O<sub>3</sub>/NiAl(110) Model NO<sub>x</sub> Storage Materials: the effect of BaO film thickness on the amorphous-to-crystalline Ba(NO<sub>3</sub>)<sub>2</sub> phase transition", *Journal of Physical Chemistry C*, **113**(2) (2009) 716.
10. Mei D, Ge Q, Szanyi J and Peden CHF, "A First-principles Analysis of NO<sub>x</sub> Adsorption on Anhydrous  $\gamma$ -Al<sub>2</sub>O<sub>3</sub> Surfaces" *Journal of Physical Chemistry C*, DOI: 10.1021/jp8103563 (2009).
11. Mudiyansele K, Yi CW, and Szanyi J, "Oxygen coverage dependence of NO oxidation on Pt(111)", *Journal of Physical Chemistry C*, **113** (2009) 5766.

**Transformations of Organic Compounds via Homogeneous Catalysis & Heterogeneous Catalysis with Well-Defined Single Sites**

Postdoc: Pat Bazinet, Chris Bradley  
Students: Dan Ruddy, Jennifer McBee, Meredith McMurdo  
Collaborators: Alex Bell (LBNL), Heinz Frei (LBNL), Odile Eisenstein (U. Montpellier)  
Contact: T. Don Tilley, Division of Chemical Sciences, Lawrence Berkeley National Laboratory, Berkeley, CA 94720; phone: (510) 642-8939; Email: [tdtilley@berkeley.edu](mailto:tdtilley@berkeley.edu)

**Goal**

Activities in this program include the development and study of homogeneous and heterogeneous catalyst systems for selective transformations of organic compounds. Molecular-based, homogeneous catalysts are based on early or late transition metals, and are designed to provide novel bond activation pathways that may be incorporated into a catalytic cycle. Another goal of this project is to develop molecular chemistry that allows atomic-level and nanoscopic control over the structures of heterogeneous catalysts, and well-defined, single-site catalysts via chemical reactions on a surface. Such catalysts have been studied in selective hydrocarbon oxidations such as olefin epoxidation.

**DOE Interest**

This program is focused on the strategic design of novel catalysts of potential interest for the production of fuels and chemicals in an energy-efficient and environmentally acceptable fashion. Of particular interest is the development of structure-reactivity relationships via the controlled synthesis of catalytic centers, extensive characterization of catalyst structure, and evaluation of catalytic properties.

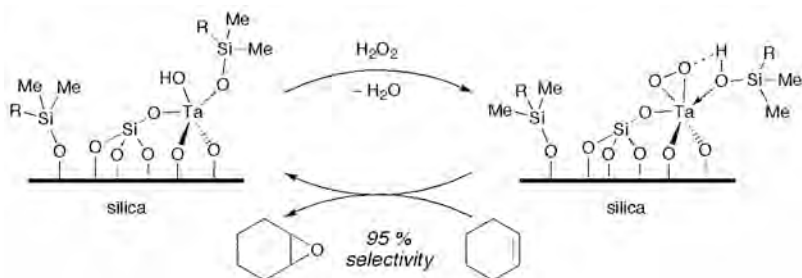
**Recent Progress**

*Homogeneous Catalysis:* Hydroaminations of norbornene with arylsulfonamides and weakly basic anilines were achieved using electrophilic Pt(II) bis(triflate) complexes of the type  $L_2Pt(OTf)_2$  ( $L_2 = tBu_2bpy, tBuC_6H_4N=C(CH_3)C(CH_3)=NC_6H_4tBu, (C_6H_5)_2PCH_2CH_2P(C_6H_5)_2, (C_6F_5)_2PCH_2CH_2P(C_6F_5)_2, S-BINAP$  [8]). Pseudo first order kinetics reveal little to no dependence of the reaction rate on the ancillary ligand. Mechanistic studies do not favor an olefin coordination mechanism but are instead consistent with a mechanism involving sulfonamide coordination and generation of an acidic proton that is transferred to the norbornene. It is postulated that the resulting norbornyl cation is then attacked by free sulfonamide, and loss of proton from this adduct completes the hydroamination. The platinum-sulfonamide complex readily undergoes deprotonation to give a  $\mu$ -amido platinum-bridged dimer that was isolated from the reaction solution. These studies also involve use of  $Me_3SiPh$  and  $Me_3SnPh$  as non-nucleophilic proton traps. Cleavage of the Ph-E bonds was used to detect the acidic, catalytically active species.

*Single-Site Selective Oxidation Catalysis:* For surface-bound catalytic centers, the chemical properties of the surface play an important role in determining catalyst activity and selectivity. For example, structural and electronic properties of the surface may

facilitate binding of the reactants, thereby promoting their interaction with the active sites. In addition, surface properties should influence the rate of product desorption, and such principles are well established in the mechanisms of enzyme catalysis. Thus, a general interest of our group is to investigate the role of surface functionalizations in promoting catalysis. In one aspect of this work, tantalum centers on the surface of an organically modified silica have been observed to exhibit high selectivities in the epoxidation of olefins with aqueous  $\text{H}_2\text{O}_2$  [1,6]. Modified Ta-SBA15 catalysts were prepared to give a hydrophobic surface and Ta-OSiMe<sub>2</sub>R functionalities. A product selectivity of >95% epoxide is observed for at least 6 h of reaction time versus 11% for the unmodified catalyst. Reactivity studies indicate that the Ta-OSiMe<sub>2</sub>R group plays an important role in determining this selectivity. DRUV-vis spectroscopy of the modified TaSBA15 materials after reaction with  $\text{H}_2\text{O}_2$  suggests that the key intermediate involved in oxygen transfer may be a Ta( $\eta^2\text{-O}_2$ ) species. The kinetic data are similar to that for epoxidations with  $\text{H}_2\text{O}_2$  catalyzed by the highly selective zeolite catalyst TS-1, and the mechanism proposed in Scheme 1 is supported by the observed kinetics.

**Scheme 1**



### Future Plans

The Pt-mediated proton transfer mechanism associated with hydroaminations by sulonamides may have broad implications for bond activation pathways in reactions catalyzed by electrophilic, late transition metal complexes. This possibility will be examined, starting with hydroarylations catalyzed by L<sub>2</sub>Pt(OTf)<sub>2</sub> complexes. Research with single-site oxidation catalysts will focus on attempts to more thoroughly characterize intermediates, for example by EXAFS. Additional mechanistic work involving *in situ* spectroscopic methods will address the formation, stability, and reactivity of the Ta(V)( $\eta^2\text{-O}_2$ ) intermediate. Efforts will also be directed toward identification of additional highly selective oxidations, for substrates such as arenes, alkynes, and carbonyl compounds.

### Publications (2007-2009)

1. D. A. Ruddy and T. D. Tilley, "Highly Selective Olefin Epoxidation with Aqueous  $\text{H}_2\text{O}_2$  over Surface-Modified TaSBA15 Prepared via the TMP Method" *Chem. Comm.* (2007) 3350.
2. A. Fischbach, P. R. Bazinet, R. Waterman, and T. D. Tilley, "1,2-Phosphinoboranes as Amphoteric Ligands in Nickel-Methyl Complexes" *Organometallics* **27** (2008) 1135.
3. P. Bazinet and T. D. Tilley, "Octa- and Nonamethylfluorenyl Complexes of Zr(II), Zr(IV), and Hf(IV). Investigation of Steric and Electronic Effects" *Organometallics* **27** (2008) 1267.
4. N. Barros, O. Eisenstein, L. Maron and T. D. Tilley, "DFT Investigation of the Catalytic Hydromethylation of  $\alpha$ -Olefins by Scandocenes. 2. Influence of the *ansa*

- Ligand on Propene and Isobutylene Hydromethylation" *Organometallics* **27** (2008) 2252.
5. D. A. Ruddy, R. L. Brutchey and T. D. Tilley, "The Influence of Surface Modification on the Epoxidation Selectivity and Mechanism of TiSBA15 and TaSBA15 Catalysts with Aqueous Hydrogen Peroxide" *Topics in Catalysis* **48** (2008) 99.
  6. D. A. Ruddy and T. D. Tilley, "Kinetics and Mechanism of Olefin Epoxidation with Aqueous H<sub>2</sub>O<sub>2</sub> and a Highly Selective Surface-Modified TaSBA15 Heterogeneous Catalyst" *J. Am. Chem. Soc.* **130** (2008) 11088.
  7. D. A. Ruddy, J. Jarupatrakorn, R. M. Rioux, J. T. Miller, J. L. McBee, M. J. McMurdo, K. A. Tupper and T. D. Tilley, "Site-Isolated Pt-SBA15 Materials from Tris(*tert*-butoxy)siloxy Complexes of Pt(II) and Pt(IV)" *Chem. Mater.* **20** (2008) 6517.
  8. J. L. McBee, A. T. Bell and T. D. Tilley, "Mechanistic Studies of Hydroamination of Norbornene with Electrophilic Platinum Complexes: The Role of Proton Transfer" *J. Am. Chem. Soc.* **130** (2008) 16562.
  9. C. A. Bradley, M. J. McMurdo, B. D. Yuhas and T. D. Tilley, "Functionalized Silicone Nanospheres: Synthesis, Transition Metal Immobilization, and Catalytic Applications" *Chem. Mater.* **21** (2009) 174.
  10. P. Bazinet and T. D. Tilley, "Octa- and Nonamethylfluorenyl Complexes of Zr(IV): Reactive Hydride Derivatives and Reversible Hydrogen Migration between the Metal and the Fluorenyl Ligand" *Organometallics*, in press.

**AN INTEGRATED APPROACH TOWARD RATIONAL NANOCATALYST DESIGN  
FOR HYDROGEN PRODUCTION**

Additional PIs: Douglas J. Buttrey and Jochen A. Lauterbach

Collaborator: J.G. Chen (Univ. of Delaware)

Students: Elizabeth D'Addio, Hua Yang, Rohit Vijay, Jonathan Sutton, Danielle Hansgen

Postdocs: Ayman Karim, Vinay Prasad

Undergraduate students: Jason Binz, Anabel Pineiro, Anshu Arya, Zack Ulissi, Parag Jalan

Contact information: Department of Chemical Engineering; University of Delaware; Newark, DE 19716; Phone number: 302-831-2830; Fax number: 302-831-2048; Email: vlachos@udel.edu

**Goal**

The overall objective of this grant is to develop a rational framework for the discovery of low cost, robust, and active nano-catalysts that will enable efficient hydrogen production from ammonia decomposition. Our approach integrates multiscale modeling, nano-catalyst synthesis, and nanoscale characterization assisted high throughput experimentation (HTE).

**Relation to the DOE/BES program**

This project directly addresses several of the long-term goals of the DOE/BES program. In particular, new nanoscale catalytic materials are synthesized, characterized and modeled for the production of hydrogen from ammonia and a computational framework is developed for efficient extraction of information from experimental data and for rational design of catalysts whose impact goes well beyond the proposed hydrogen production project.

**Progress Report**

The results of our previous high throughput screening experiments indicated that the presence of hollandite ( $\text{KRu}_4\text{O}_8$ ) structures on the surface of  $\text{Al}_2\text{O}_3$ -supported K-promoted Ru catalysts contributed to the high activity. By testing a variety of different alkali promoters, K was confirmed as the most active and the only promoter leading to hollandite nanowhiskers. One of our objectives was to synthesize a series of Ru catalysts with different K-loadings in order to optimize performance. A series of 4Ru/XK catalysts was synthesized using the  $\text{RuCl}_3$  precursor. The addition of any amount of K results in an increase in conversion compared to the unpromoted case. K loadings of 12% result in the greatest activity.

We have also undertaken the first systematic study of nanoparticle size effect on Ru activity and found that one can tune activity by up to orders of magnitude. We have combined for the first time microscopy, chemisorption, and EXAFS data to reconstruct the particle size and shape. DFT simulations and experimental data indicate that calcination leads to Ru flat oxide particles whose structure is retained upon reduction. First-principle microkinetic modeling has been found to quantitatively describe the activity and confirm the characterization results. The optimal nanoparticle size is very different from prior simplistic theoretical estimates due to important morphological support-nanoparticle effects we have discovered.

Finally, we have formulated a novel optimization framework that employs high throughput modeling and predicts ideal properties of a catalyst. Using DFT of surface alloys and the



optimization results, we have come up with 2 possible catalyst candidates for high activity in ammonia decomposition. We have subsequently synthesized single crystals and performed NH<sub>3</sub> TPD experiments. Our data show a phenomenal (the lowest temperature ever reported) activity of the new catalyst for ammonia dehydrogenation.

### **Publications Supported from this Grant**

1. V. Prasad and D.G. Vlachos, Multiscale model and informatics based optimal design of experiments: Application to the catalytic decomposition of ammonia on ruthenium. *Ind. Eng. Chem. Res.* **47**, 6555–6567 (2008).
2. D.G. Vlachos, A.B. Mhadeshwar, and N. Kaisare, Hierarchical multiscale model-based design of experiments, catalysts, and reactors for fuel processing. *Comput. Chem. Eng.* **30**, 1712-1724 (2006).
3. W. Pyrz, R. Vijay, J. Binz, J. Lauterbach, and D.J. Buttrely, Characterization of K-Promoted Ru Catalysts for Ammonia Decomposition Discovered Using High-Throughput Experimentation. *Topics Catal.* **50**(1-4), 180-191 (2008).
4. V. Prasad, A.M. Karim, Z. Ulissi, M. Zagrobelny, and D.G. Vlachos, High throughput multiscale modeling for design of experiments, catalysts, and reactors: Application to hydrogen production from ammonia. *Chem. Engng Sci.*, Accepted (2009).
5. D.G. Vlachos and S. Caratzoulas, The roles of catalysis and reaction engineering in overcoming the energy and the environment crisis. *Chem. Eng. Sci.*, accepted (2009).
7. A.M. Karim, V. Prasad, G. Mpourmpakis, W.W. Lonergan, A.I. Frenkel, J.G. Chen, and D.G. Vlachos, Correlating Particle Size and Shape of Supported Ru/ $\gamma$ -Al<sub>2</sub>O<sub>3</sub> with NH<sub>3</sub> Decomposition Activity, submitted (2009).
8. V. Prasad, A.M. Karim, A. Arya, and D.G. Vlachos, Assessment of overall rate expressions and multiscale, microkinetic model uniqueness via experimental data injection: Ammonia decomposition on Ru/ $\gamma$ -Al<sub>2</sub>O<sub>3</sub> for hydrogen production. *Ind. Eng. Chem. Res.*, Accepted (2009).

## Fundamental Studies of the Steam Reforming of Alcohols on Pd/ZnO and Co/ZnO Catalysts

Postdoc: Matthew Hyman  
Students: Ese Jeroro, Eddie Mortano  
Collaborators: Prof. Abhaya Datye (University of New Mexico), Dr. Yong Wang (PNNL)  
Contacts: University of Pennsylvania, Dept. of Chemical and Biomolecular Engineering,  
220 S. 33<sup>rd</sup> Street, Philadelphia, PA 19104-6393  
215-898-6318 [vohs@seas.upenn.edu](mailto:vohs@seas.upenn.edu)

### Goal

The goal of this project is to elucidate the relationships between the structure and reactivity of Pd/ZnO methanol and Co/ZnO ethanol steam reforming catalysts and to determine the origins of the unique reactivity of these catalytic systems. In addition to identifying the relevant reaction pathways and intermediates, the research program will determine how Zn alters the activity of Pd for the dehydrogenation of methanol and whether reactions on the ZnO support or at the PdZn-ZnO interface are important. For Co/ZnO the active phase of the catalyst will be determined (i.e. CoZn alloy, oxidized Co species, Co substituted into the ZnO lattice, etc.) and again the role of the support will be studied.

### DOE Interest

For H<sub>2</sub>-powered fuel cells to become a viable energy conversion technology highly efficient catalysts for the production of H<sub>2</sub> from renewable feedstocks, such as alcohols, are required. Our studies of the relationships between the structure and reactivity of novel methanol and ethanol reforming catalysts that consist of Pd or Co supported on ZnO will aid in the development of such catalysts. Our work is also providing valuable fundamental insight into the role of ligand and ensemble effects in alloy catalysts. This insight is useful in the design of catalyst for a wide range of industrially important chemical transformations of hydrocarbons.

### Recent Progress

Our approach in this project has been to study the reactivity of model catalysts consisting of Zn-modified Pd(111) surfaces and Pd thin films supported on ZnO single crystals. In previous years our studies of the Zn/Pd(111) system has shown that Zn atoms incorporated into the Pd(111) surface form ordered overlayers and have a dramatic affect on reactivity. Even small amounts of Zn (< 0.1 ML) were found to significantly destabilize the bonding of adsorbed CO, increase the activation energy for C-H bond cleavage in adsorbed methoxides, and stabilize adsorbed formaldehyde. The fact that these effects were observed for low Zn coverages suggests that the Zn atoms have relatively long range electronic effects on reactivity. In studies of Pd/ZnO(0001) catalysts we observed that incorporation of Zn into the Pd via reduction of the ZnO support was facile and occurred upon heating in vacuum. The reactivity trends for PdZn particles supported on ZnO(0001) were found to be consistent with those observed for Zn/Pd(111).

This year we have expanded our studies to include the reactivity of ethanol, acetaldehyde, and formic acid on of Zn/Pd(111). For comparison purposes we have also started to study Cu-

modified Pd(111) surfaces. Studies of the reactivity of Pd/ZnO(10-10) model catalysts have also been completed and we have recently commenced studies of the reactivity of alcohols on Co films supported on ZnO(0001). A brief descriptions of the results obtained in all of these areas are given below.

As noted above, our work with this Zn/Pd(111) model catalysts has focused on studying the effect of the added Zn on the reactivity of ethanol, acetaldehyde, and formic acid. TPD and HREELS results obtained in this study further demonstrate the dramatic effect that the incorporation of small amounts of Zn has on the reactivity of the Pd(111) surface towards alcohols and aldehydes. The addition of Zn was found to increase the barrier for C-H bond cleavage in adsorbed alkoxide and  $\eta^2$ -aldehyde intermediates. For Zn coverages below 0.1 ML this results in stabilization of adsorbed aldehydes which remain intact on the surface up to 300 K rather than undergoing decarbonylation to produce CO. The dehydrogenation activity is further decreased for higher Zn coverages producing surfaces that are nearly inactive for the decomposition of both alcohols and aldehydes. Zn incorporation also affects the barrier for C-H bond cleavage in adsorbed  $\eta^1$ -CH<sub>3</sub>CO intermediates. In this case decreasing the barrier and allowing the reaction to proceed at a lower temperature. The fact that these alterations in reactivity are observed for very low Zn coverages suggests that they are due to a ligand effect where the Zn atoms alter the electronic properties of nearby Pd sites.

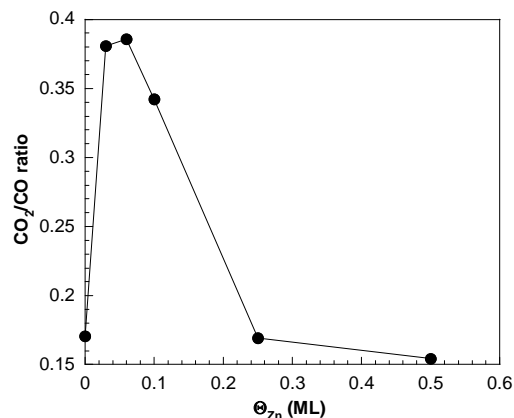


**Figure 1.** CO<sub>2</sub>/CO ratio as a function of Zn coverage on Pd(111) during formate decomposition as determined by TPD.

Based on the fact that the high selectivities for the production of H<sub>2</sub> and CO<sub>2</sub> during methanol steam reforming are not consistent with a reaction pathway that proceeds via CO as an intermediate, a pathway that proceeds via formate species has been proposed. In order to investigate this possibility we have studied the reaction of formic acid on Zn/Pd(111). Our results show that the added Zn increases the stability of formate species produced from adsorbed formic acid. As shown in Figure 1, at coverages < 0.1 ML, Zn addition also alters the selectivity of formate decomposition toward dehydrogenation to produce CO<sub>2</sub> and H<sub>2</sub> at the expense of dehydration to produce CO and H<sub>2</sub>O. The dramatic effect that small coverages of Zn have on reactivity is consistent with

those obtained in the reactions of alcohols and aldehydes on Zn-modified Pd(111) and suggests that alteration of the selectivity of for formate decomposition may be a key function of the Zn.

It is surprising that Zn appears to have long range electronic effects on the reactivity of Pd(111) since such effects would be expected to be localized to nearest neighbors. Another possible explanation for the apparent long-range effect is that they are caused by a lattice strain field around the incorporated Zn atoms. To investigate this possibility we have started to study Cu/Pd(111) surfaces. Since Cu and Zn have similar sizes their induced strain fields should be similar. Cu, however, was not found to form ordered overlayers on Pd(111) and acted merely to block adsorption sites as demonstrated by the CO TPD data for Zn/Pd(111) and Cu/Pd(111) in Figure 2. These results again point to electronic interactions being important for Zn.

We have also expanded the range of model catalysts to include Pd films on ZnO(10-10) and TPD studies of CO and methanol on Pd/ZnO(10-10) have been completed. These studies demonstrated that CO bonds more weakly on monolayer Pd films on ZnO(0001) compared to ZnO(10-10) suggesting that there is a stronger electronic interaction at the Pd-ZnO(0001) interface. TPD and XPS results also indicate that PdZn alloy formation is more facile on ZnO(0001) compared to ZnO(10-10). Large differences were observed in the CO yield during TPD from Pd/ZnO(0001) and Pd/ZnO(10-10) samples that were exposed to methanol and we have attributed this structure sensitivity to synergism between Pd and the ZnO(0001) substrate and the presence of sites at the Pd-ZnO(0001) interface that are highly active for methanol dehydrogenation. Comparisons to the reactivity of high surface area Pd/ZnO catalysts suggest that the observed differences in the reactivity of Pd/ZnO(0001) and Pd/ZnO(10-10) may play a role determining the reactivity of high surface area Pd/ZnO methanol steam reforming catalysts.

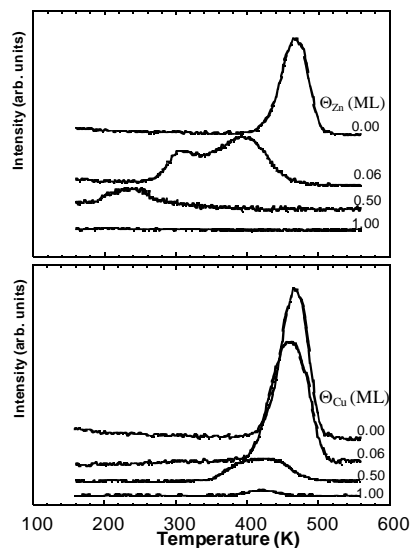


Fig. 2 CO TPD from Zn/Pd(111) and Cu/Pd(111).

### Future Plans

Our plan for the upcoming year is to complete the studies of the Cu/Pd(111) system. We believe that comparisons between Cu/Pd(111) and Zn/Pd(111) will provide valuable insights into the role of Zn in PdZn alloy reforming catalysts. We have also recently expanded our studies to include steam reforming of alcohols on Co/ZnO catalysts. In these studies we are following an experimental plan similar to that used for Pd/ZnO catalysts and are using both ZnO and cobalt single crystals as supports. We have recently started to characterize the structure of Co films supported on ZnO(0001). Our next step will be to use TPD to characterize the interaction of methanol and CO with the Co/ZnO(0001) model catalyst. Finally, we plan to initiate AFM studies of the structure of Pd and PdZn particles on ZnO(0001) and ZnO(10-10) surfaces.

### Publications (2007-2009)

1. E. Jerero, V. Lebarbier, A. Datye, Y. Wang and J. M. Vohs, "Interaction of CO with PdZn Alloys," *Surface Science*, **601** (2007) 5546-5554.
2. B. Halevi, J.M. Vohs, "Site Requirements for the Reactions of CH<sub>3</sub>SH and (CH<sub>3</sub>)<sub>2</sub>S<sub>2</sub> on ZnO(10-10)," *Surface Science*, **602** (2008) 198-204.
3. E. Jerero and J.M. Vohs, "Zn Modification of the Reactivity of Pd(111) Towards Methanol and Formaldehyde," *J. Am. Chem. Soc.*, **130** (2008) 10199-10207.
4. E. Jerero and J.M. Vohs, "Exploring the Role of Zn in PdZn Reforming Catalysts: Adsorption and Reaction of Ethanol and Acetaldehyde on Two-Dimensional PdZn Alloys," *J. Phys. Chem. C*, **113** (2009) 1486-1494.
5. M.P. Hyman, V.M. Lebarbier, Y. Wang, A.K. Datye, J.M. Vohs, "A Comparison of the Reactivity of Pd Supported on ZnO(10-10) and ZnO(0001)," *J. Phys. Chem. C*, under revision.
6. E. Jerero and J.M. Vohs, "Reaction of Formic Acid on Zn-modified Pd(111)," *Catt. Lett.*, submitted.

### Photooxidation of H<sub>2</sub>O and C<sub>3</sub> Hydrocarbons to H<sub>2</sub> Fuel and C<sub>3</sub>-Oxygenates with Molecular Designed Heterogeneous Nano-Photocatalysts

Students: C. Zhao (Chem), T. Kim (ChE), E.I. Ross-Medgaarden, E.L. Lee (ChE), K. Routray, (ChE), C. A. Roberts (ChE) S. P. Phivilay (ChE)  
Collaborators: Marco Daturi (ENSI Caen, France), Edmond Payen (ENSC-Lille, France), Guido Mul (TU Delft, The Netherlands), Alexander Puzov (ORNL)  
Contact: *Operando* Molecular Spectroscopy & Catalysis Laboratory,  
Chemical Eng. Department, Lehigh University, Bethlehem, PA 18015  
[iew0@lehigh.edu](mailto:iew0@lehigh.edu)

#### Goal

The goal of this study is to examine the photocatalysis of well-defined TiO<sub>2</sub> nanodomains supported on SiO<sub>2</sub> and to determine their structure-photocatalytic relationships. If possible, these findings will be extended to establish the scientific basis for the heterogeneous photocatalytic conversion of naturally abundant and inexpensive H<sub>2</sub>O to clean H<sub>2</sub> fuel and activated molecular O<sub>2</sub> for the selective oxidation of C<sub>3</sub> hydrocarbons.

#### DOE Interest

Understanding how catalytic structure relates to photocatalytic properties (photoluminescence, electron excitation, intermediate and product formation) in these catalysts of known structure will lead to more rapid development of improved photocatalysts for specific reactions. The progress in the fundamental understanding of photocatalysis has been extremely slow. One of the major reasons for this slow progress is the limited number of reported surface characterization studies of the bulk and supported mixed oxide photocatalyst systems, especially under *in situ* or during photocatalysis conditions, which can provide the desired molecular and electronic level insights

#### Recent Progress

The supported 1-60% TiO<sub>2</sub>/SiO<sub>2</sub> catalysts were synthesized by incipient wetness impregnation of Ti-isopropoxide into the SiO<sub>2</sub> support (Cab-O-Sil), with drying followed by calcination at 500 °C. The molecular and electronic structures of the TiO<sub>2</sub> nanodomains were determined with *in situ* Raman and UV-vis spectroscopy. The nature of the TiO<sub>2</sub> nanodomain was found to change in the following manner as a function of the titania loading: isolated site (1% TiO<sub>2</sub>/SiO<sub>2</sub>), polymeric chain (12% TiO<sub>2</sub>/SiO<sub>2</sub>), 2D sheets (20-40% TiO<sub>2</sub>/SiO<sub>2</sub>) and 3D nanoclusters (60% TiO<sub>2</sub>/SiO<sub>2</sub>). Catalytic active surface WO<sub>x</sub> and VO<sub>x</sub> species were subsequently impregnated onto the TiO<sub>2</sub>/SiO<sub>2</sub> in aqueous solutions of ammonium metatungstate, (NH<sub>4</sub>)<sub>10</sub>W<sub>12</sub>O<sub>41</sub>·5H<sub>2</sub>O and isopropanol solutions of vanadium triisopropoxide VO[CHO(CH<sub>3</sub>)<sub>2</sub>]<sub>3</sub>, respectively, to form supported WO<sub>3</sub>/TiO<sub>2</sub>/SiO<sub>2</sub> and V<sub>2</sub>O<sub>5</sub>/TiO<sub>2</sub>/SiO<sub>2</sub> multicentered catalysts. Studies were conducted using *in situ* photoluminescence (PL) spectroscopy to determine if the type of TiO<sub>2</sub> nanodomain present in the sample affects the emission spectrum. Samples were dehydrated under flowing 10% O<sub>2</sub> at 400 °C in order to avoid the quenching effect of

water on PL emission. Spectra were collected on a Jobin-Yvon Fluorolog system which also allowed collection of PL maps. Studies were also conducted *in situ* using a 76 MHz pulse tunable laser, tuned to 400 nm excitation, and a gated Picostar detector with time resolution in picoseconds. The same dehydration procedure was used and the lifetime of excited states of the various nanodomain containing samples was determined by changing the delay time of the detector.

The photocatalytic activity of the supported TiO<sub>2</sub>/SiO<sub>2</sub> catalysts was determined for H<sub>2</sub>O splitting under UV irradiation ( $\lambda > 290$  nm). The TOF for H<sub>2</sub> production was found to decrease by over an order of magnitude with increasing titania domain size. The anchoring of surface VO<sub>4</sub> species resulted in a ~9 fold increase in H<sub>2</sub> production and the anchoring of surface WO<sub>5</sub> species resulted in a ~14 fold increase in H<sub>2</sub> production.

The photoluminescence results reveal several main trends. The PL spectra show that as the percent loading of titania increases, the peak emission occurs at higher wavelength excitation, meaning those samples are more easily excited with lower energy irradiation. However, the excitation lifetime measurements indicate that the lower percent loading samples (those containing isolated TiO<sub>4</sub> sites) have slower decay rates, meaning there is a greater opportunity for reactions to occur. This finding offers an explanation for the observed higher production of H<sub>2</sub> during water splitting by the lower titania loading catalysts when normalized by exposed Ti site and the anchoring of surface VO<sub>4</sub> and WO<sub>5</sub> species leads to increased photocatalytic activity.

An *operando* DRIFTS with online MS spectroscopic propylene/O<sub>2</sub> photocatalytic investigation with supported TiO<sub>2</sub>/SiO<sub>2</sub> catalysts (details of this catalyst system are given below) was also initiated to examine how this oxidation reaction takes place when initiated by UV excitation at room temperature. The UV excitation resulted in the appearance of surface oxygenated intermediates in the IR spectrum with characteristic acetone-type C=O bonds. Simultaneously, propylene consumption was confirmed in the online mass spectrometer. Gas phase oxygenated products, however, did not appear in the MS. This implies that the majority of the formed oxygenates remained on the catalyst surface and did not desorb into the gas phase at this low reaction temperature. The negative photocatalytic experimental results with propylene/O<sub>2</sub> also lead to the abandonment of the more challenging study of the photocatalytic conversion of propylene/H<sub>2</sub>O mixtures. Thus, it was decided to focus the research program on photocatalytic splitting of naturally abundant H<sub>2</sub>O to non-carbon H<sub>2</sub> fuel since this photocatalytic reaction step is also prerequisite for all photocatalytic reactions involving transformation of carbon-containing molecules (e.g., CO<sub>2</sub>, CH<sub>4</sub>, C<sub>3</sub>, C<sub>3</sub><sup>-</sup>, etc.). It was also decided to employ well-defined supported TiO<sub>2</sub>/SiO<sub>2</sub> photocatalysts that would allow for the development of fundamental structure-photoactivity relationships.

### **Future Plans**

The research will extend its focus to both model supported oxide molecular structures and established photocatalytic bulk mixed oxides. The fundamental insights gained in the previous work will be investigated and applied to novel metal oxide materials that are currently producing the highest product yields for photocatalytic water-splitting. The use

of dopants and their effect on the lifetime of excited states will be investigated in an attempt to understand why certain synthesis techniques are successfully utilized.

### **Publications (2007-2009)**

1. T. Kim, A. Burrows, and I.E. Wachs, "Molecular/electronic structure–surface acidity relationships of model-supported tungsten oxide catalysts," *J. Catal.*, **246** (2007), 370-381.
2. M.J. Nash, S. Rykov, R.F. Lobo, D.J. Doren, and I.E. Wachs, "Photocatalytic Activity of Vanadium-Substituted ETS-10," *J. Phys. Chem. C* **111**, (2007), 7029-7037.
3. E. L. Lee and I.E. Wachs, "In Situ Spectroscopic Investigation of the Molecular and Electronic Structures of SiO<sub>2</sub> Supported Surface Metal Oxides," *J. Phys. Chem. C*, **111**, (2007), 14410-14425.
4. E.I. Ross-Medgaarden and I.E. Wachs, "Structural Determination of Bulk and Surface Tungsten Oxides with UV-vis Diffuse Reflectance Spectroscopy and Raman Spectroscopy," *J. Phys. Chem. C*, **111**, (2007), 15089-15099.
5. E. L. Lee and I.E. Wachs, "In Situ Raman Spectroscopy of SiO<sub>2</sub>-Supported Transition-Metal Oxide Catalysts: An Isotopic <sup>18</sup>O-<sup>16</sup>O Exchange Study," *J. Phys. Chem. C*, **112**, (2008), 6487-6498.
6. C. Zhao and I.E. Wachs, "An Operando Raman, IR and TPSR Spectroscopic Investigation of the Selective oxidation of propylene to acrolein over model supported vanadium oxide monolayer," *J. Phys. Chem. C* **112**, (2008), 11363-11372.
7. O. Guerrero-Perez, T. Kim, M. Banares, and I.E. Wachs, "Nature of Catalytic Active Sites for Sb-V-O Mixed Metal Oxides," *J. Phys. Chem. C*, **112**, (2008), 16858-16863.
8. E.L. Lee and I.E. Wachs, "Molecular Design and In Situ Spectroscopic Investigation of Multilayered Supported M<sub>1</sub>O<sub>x</sub>/M<sub>2</sub>O<sub>x</sub>/SiO<sub>2</sub> Catalysts," *J. Phys. Chem. C* **112**, (2008), 20418-20428.
9. T. Kim and I.E. Wachs, "CH<sub>3</sub>OH oxidation over well-defined supported V<sub>2</sub>O<sub>5</sub>/Al<sub>2</sub>O<sub>3</sub> catalysts: Influence of vanadium oxide loading and surface vanadium–oxygen functionalities," *J. Catal.*, **255**, (2008), 197-205.
10. K. Routray, L.E. Briand, and I.E. Wachs, "Is there a relationship between the M=O bond length (strength) of bulk mixed metal oxides and their catalytic activity?," *J. Catal.* **256**, (2008), 145-153.
11. C. Zhao and I.E. Wachs, "Selective oxidation of propylene over model supported V<sub>2</sub>O<sub>5</sub> catalysts: Influence of surface vanadia coverage and oxide support," *J. Catal.* **257**, (2008), 181-189.
12. E.L. Lee and I.E. Wachs, "Surface chemistry and reactivity of well-defined multilayered supported M<sub>1</sub>O<sub>x</sub>/M<sub>2</sub>O<sub>x</sub>/SiO<sub>2</sub> Catalysts," *J. Catal.* **258**, (2008). 103-110.
13. H.R.J. Veen, T. Kim, I.E. Wachs, and H.H. Brongersma, "Application of High Sensitivity Low Energy Ion Scattering (HS-LEIS) in Heterogeneous Catalysis," *Catal. Today* **140**, (2009), 197-201.
14. E.L. Lee and I.E. Wachs, "Use of Oxide Ligands in Designing Catalytic Active Sites," in *Design of Heterogeneous Catalysts: New Approaches Based on Synthesis*,

- Characterization and Modeling*, U. Ozkan, Ed., Wiley-VCH, Weinheim (2009) pp. 1-23.
15. I.E. Wachs and T. Kim, "Oxidation Reactions over Supported Metal Oxide Catalysts: Molecular/Electronic Structure-Activity/Selectivity Relationships," in *Metal Oxide Catalysis*, S.D. Jackson and J. Hargreaves, Eds., Wiley-VCH, Weinheim (2009) pp. 487-498.
  16. E.L. Lee and I.E. Wachs, Comparison of catalytic Active Sites Present in Supported  $\text{MO}_x/\text{SiO}_2$ ,  $\text{MO}_x/\text{AlO}_x/\text{SiO}_2$  and  $\text{MO}_x/\text{ZSM-5}$  Catalysts," in *Silica and Silicates in Modern Catalysis*, I. Halasz, Ed., Research Signpost (2009) pp. 1-48.



**Growth and reactivity of oxide phases on crystalline Pd and Pt surfaces**

Students: R. Bradley Shumbera, Heywood H. Kan, Can Hakanoglu, Austin Minter

Collaborators: Aravind Asthagiri (U. Florida)

Contact: Department of Chemical Engineering, University of Florida, Gainesville, FL 32611,  
Tel. 352-392-0869, [weaver@che.ufl.edu](mailto:weaver@che.ufl.edu)

**Goal**

The main goals of our project are to elucidate the mechanisms governing the oxidation of crystalline Pd and Pt surfaces, and to further the fundamental understanding of the reactivity of the resulting oxide phases.

**DOE Interest**

Understanding the growth and reactivity of oxide phases on late transition metal surfaces is critically important for rationally designing catalytic oxidation processes for oxygen-rich applications, including the catalytic combustion of natural gas, exhaust gas remediation in lean-burn diesel engines and the selective oxidation of organic compounds. Improving the efficiency of these catalytic processes would positively impact important technologies for energy conversion and utilization.

**Recent Progress**

*Oxidation of Pd(111)*. By using oxygen atom beams to prepare surface oxygen phases, we have been successful in broadly extending the range of oxygen concentrations that can be cleanly generated on Pt and Pd surfaces in ultrahigh vacuum (UHV). Over the past year, we conducted several investigations of the oxidation of Pd(111). Key findings of this work include identifying a precursor state that mediates bulk PdO formation on Pd(111), and characterizing the oxidation kinetics of this surface over a wide range of conditions. Our studies reveal that the precursor state has different properties from the surface and bulk oxides that develop on Pd(111). Specifically, the precursor state exhibits characteristics that are consistent with a distinct oxide phase that is present on the surface as small particles which become more stable during growth. We found that the kinetics for oxidation undergoes a transition with surface temperature and incident oxygen atom flux that is associated with the stability of the PdO precursor state.

We also discovered that a high-quality PdO(101) thin film can be grown on Pd(111) in UHV by oxidizing the metal at 500 K. This finding is significant since PdO is an excellent catalyst for the oxidation of alkanes under oxygen-rich conditions, but difficulties in preparing well-defined surfaces have hindered fundamental studies of PdO surface chemistry. As shown in Figure 1, the PdO(101) surface is characterized by adjacent rows of coordinatively unsaturated Pd and O atoms, which establish a uniquely reactive environment for several adsorbed species.

*Reactivity of a PdO(101) thin film.* We find that the PdO(101) film has a strong affinity toward several molecules important in the catalytic combustion of hydrocarbons, including O<sub>2</sub>, H<sub>2</sub>O, H<sub>2</sub> and alkanes. In particular, propane adsorbs into a strongly-bound molecular state on PdO(101) and undergoes facile C-H bond cleavage below 200 K. We have shown that the initial C-H bond cleavage of propane on PdO(101)

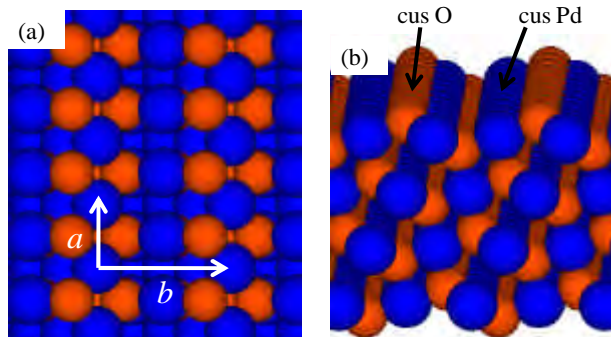


**Figure 1:** (a) Top and (b) side views of PdO(101) where the *a* and *b* directions in the top view depict the surface unit cell.

occurs by a precursor-mediated mechanism with a negative, apparent activation energy, and obtained evidence that the strong molecular-binding state serves as the precursor to the initial dissociation. We speculate that the strong molecular binding state results from a donor-acceptor interaction between a C-H bond(s) of the alkane molecule and a coordinatively unsaturated Pd atom. Experimental and computational studies of CH<sub>4</sub> and H<sub>2</sub> molecules adsorbed on PdO(101) support this interpretation. Current work is focusing on further characterizing molecularly adsorbed states and the reactivity of other alkanes on PdO(101).

### Future Plans

*Structural evolution of oxide phases.* Characterize the detailed structural changes that occur during the growth of bulk oxides on Pd and Pt surfaces as well as during oxide reduction by alkanes using *in situ* scanning tunneling microscopy.

*Alkane adsorption and activation on PdO(101).* Clarify the nature of strongly-bound molecular states of alkanes on PdO(101), and the role of the molecule-surface interaction in activating C-H bonds.

*Mechanisms for alkane oxidation on PdO(101).* Determine key steps involved in the complete oxidation of alkanes on PdO(101), and explore factors that control reaction selectivity.

*Computational studies of alkanes interactions with PdO(101).* Explore the mechanisms for the adsorption, activation and oxidation of alkanes on PdO(101) using computational methods, including density functional theory and kinetic Monte Carlo calculations. The computational effort will be directed by collaborator A. Asthagiri.

### Publications (2007-09)

1. “Facile C-H bond cleavage and deep oxidation of propane on a PdO(101) thin film”, J.F. Weaver, S.P. Devarajan and C. Hakanoglu, *J. Phys. Chem. C.*, submitted.

2. "Adsorption of water on a PdO(101) thin film: Evidence of an adsorbed HO-H<sub>2</sub>O complex", H.H. Kan, R.J. Colmyer, A. Asthagiri and J.F. Weaver", *J. Phys. Chem. C.* 113 (2009) 1495-1506.
3. "A PdO(101) thin film grown on Pd(111) in ultrahigh vacuum", H.H. Kan and J.F. Weaver, *Surf. Sci. Lett.* 602 (2008) L53-L57.
- "4. Molecular chemisorption of O<sub>2</sub> on a PdO(101) thin film on Pd(111)", J.A. Hinojosa Jr., H.H. Kan and J.F. Weaver, *J. Phys. Chem. C.* 112 (2008) 8324-8331.
5. "Adsorption and abstraction of oxygen atoms on Pd(111): Characterization of the precursor to PdO formation", H.H. Kan, R.B. Shumbera and J.F. Weaver, *Surf. Sci.* 602 (2008) 1337-1346.
6. "Temperature programmed reaction of CO adsorbed on oxygen-covered Pt(100): Reactivity of high-coverage oxygen phases", R.B. Shumbera, H.H. Kan and J.F. Weaver, *J. Phys. Chem. C.* 112 (2008) 4232-4241.
7. "Growth and properties of high-concentration phases of atomic oxygen on platinum single crystal surfaces", J.F. Weaver, R.B. Shumbera and H.H. Kan, *J. Phys.: Condensed Matter* 20 (2008) 184015.
8. "The transition from surface to bulk oxide growth on Pt(100): Precursor-mediated kinetics", R.B. Shumbera, H.H. Kan and J.F. Weaver, *Surf. Sci.* 601 (2007) 4809-4816.
9. "Hot precursor reactions during the collisions of gas-phase oxygen atoms with deuterium chemisorbed on Pt(100)", H.H. Kan, R.B. Shumbera and J.F. Weaver, *J. Chem. Phys.* 126 (2007) 134704:1-11.
10. "Oxidation of Pt(100)-hex-R0.7° by gas-phase oxygen atoms", R.B. Shumbera, H.H. Kan and J.F. Weaver, *Surf. Sci.* 601 (2007) 235-246.

KC0302010 (CO-019)

Jan Hrbek (BNL)  
James T. Muckerman (BNL)  
Jose A. Rodriguez (BNL)  
Michael G. White (BNL/SUNYSB)

## Catalysis on the Nanoscale: Preparation, Characterization and Reactivity of Metal-Based Nanostructures

Additional PI's: Ping Liu, Jon Hanson  
post docs (100%): YongMan Choi, Joon Park  
graduate students: M. Patterson, Y. Yang (Stony Brook University)

Chemistry Department  
Brookhaven National Laboratory  
Upton, NY 11973  
[hrbek@bnl.gov](mailto:hrbek@bnl.gov); [muckerma@bnl.gov](mailto:muckerma@bnl.gov); [rodriguez@bnl.gov](mailto:rodriguez@bnl.gov)

Department of Chemistry  
SUNY Stony Brook  
Stony Brook, NY 11794  
[mgwhite@bnl.gov](mailto:mgwhite@bnl.gov)

### Program Goals

The purpose of this project is to explore and manipulate the size, morphology and chemical environment of metal-containing nanoparticles with the goal of optimizing their reactivity with respect to elementary reactions that are of widespread interest in heterogeneous catalysis. The materials focus will be on nano-scaled molecular catalysts incorporating the early transition metals, e.g., carbides, sulfides and phosphides, which have promising catalytic properties and may offer significant advantages over more commonly used noble metals. The unique catalytic activity of Au nanoparticles supported on metal oxide and carbide surfaces is also being explored. Current methods being explored for nanoparticle preparation include reactive deposition onto metal and metal oxide substrates and deposition of size-selected clusters. Materials characterization and reactivity studies will make extensive use of NSLS beam line facilities for measurements of high-resolution core-level photoemission, near-edge x-ray adsorption spectroscopy and in situ x-ray diffraction (time-resolved) under reaction conditions. This project also emphasizes theory development for describing the structure and electronic properties of molecular nanomaterials and adapting quantal methodologies for exploring elementary surface reactions.

### Recent Progress

**Reactivity of size-selected  $\text{Mo}_x\text{S}_6$  nanoclusters:** Recent experiments have uncovered an unusual catalytic desulfurization reaction involving the  $\text{Mo}_6\text{S}_8$  cluster supported on the Au(111) surface. The  $\text{Mo}_6\text{S}_8$  cluster is well-known as the basic building block of the Chevrel phase of molybdenum sulfide with a unique cage-like structure in which the eight sulfur atoms are located in the triangular faces of a  $\text{Mo}_6$  octahedral core. Recent DFT calculations predict that  $\text{Mo}_6\text{S}_8$  cluster supported on Au(111) has five coordinatively unsaturated Mo atoms which can act as active sites for adsorbate binding and reaction (see Figure 1). The  $\text{Mo}_6\text{S}_8/\text{Au}(111)$  surface was prepared by size-selected deposition of the cluster cation onto the Au(111) surface at low energies (soft-landing). Thermal desorption studies show that the  $\text{Mo}_6\text{S}_8$  cluster can adsorb OCS molecularly as well as induce OCS

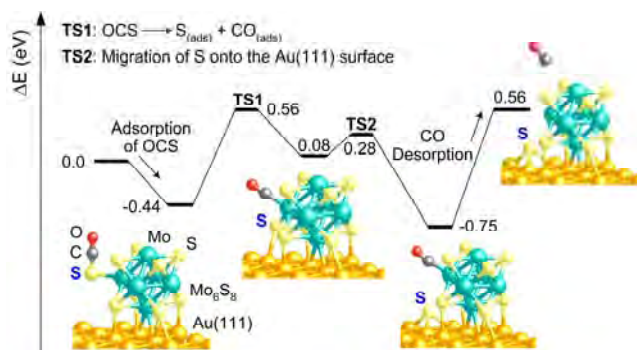
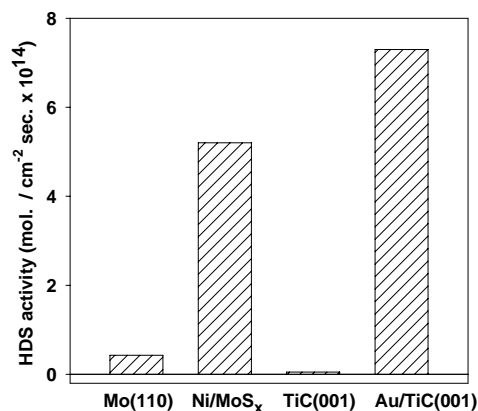


Figure 1. Potential energy profile for OCS/ $\text{Mo}_6\text{S}_8/\text{Au}(111)$

dissociation. Repeated cycles of OCS adsorption and reaction, however, did not result in a loss of activity suggesting that the S-atoms do not bind to the Mo-atom sites of the cluster. DFT calculations show that the lowest energy reaction path involves OCS adsorption and dissociation at a Mo-atom side site. The resulting S-atom does not stay bound to the cluster, but migrates to a three-fold hollow site on the Au(111) surface where it is most strongly bound. This mechanism frees the Mo-atom active sites for further reaction, in agreement with experiment. This reaction system highlights the unique interplay between the nanocatalyst particle and its support, and also represents a rare case in which both experiment and theory address precisely the same materials, i.e., cluster, substrate and reactant.

**Methanethiol chemistry on TiO<sub>2</sub>-supported Ni nanoparticles:** The thermal decomposition of methanethiol on Ni nanoparticles grown on TiO<sub>2</sub>(110) was studied by temperature programmed desorption (TPD), X-ray photoelectron spectroscopy (XPS) and low energy ion scattering (LEIS). On all of the Ni surfaces investigated, methane and hydrogen were observed as gaseous products, and the only sulfur-containing species that desorbs from the surface was methanethiol itself at low temperatures. The two pathways for methanethiol reaction were hydrodesulfurization to produce methane and nonselective decomposition, which leaves atomic carbon and sulfur on the surface. From high resolution XPS studies, methyl thiolate was identified as the surface intermediate for reaction on TiO<sub>2</sub> and all of the Ni surfaces investigated, similar to what is observed on single-crystal Ni surfaces. Based on the observed S(2p) binding energies, the binding sites for methyl thiolate are different for Ni nanoparticles deposited at 1 ML versus those at 2.5 ML and higher. No distinct changes in activity or selectivity were observed for the smaller Ni nanoparticles compared to the more film-like Ni surfaces other than what could be accounted for by changes in total surface area. Annealing the surfaces resulted in encapsulation of the Ni nanoparticles by reduced TiO<sub>x</sub> with a complete loss of methanethiol activity above 800 K.

**Dissociation of thiophene on Au/TiC(001): Effects of Au-C interactions and charge polarization:** High resolution photoemission and DFT calculations were used to study the interaction of thiophene with Au/TiC(001) surfaces. Thiophene is adsorbed weakly on TiC(001), desorbing at temperatures below 180 K. However, Au nanoparticles supported on a metal carbide substrate can exhibit extremely high desulfurization activity. In our DFT calculations, spontaneous dissociation was observed when thiophene was set in the interface of carbide and very small Au nanoparticles. Au and C sites work in a cooperative way during the cleavage of the S-C bonds, where Au binds S atoms and the hydrocarbon fragment sits at the carbide site. The polarization of charge induced by the Au-C interactions maximizes the flow of electrons from Au into the LUMO of the thiophene molecule, which helps the S-C bond breaking. Experimental tests showed that a TiC(001) surface with 0.2 ML of Au was more active for the hydrodesulfurization (HDS) of thiophene than conventional Ni/MoS<sub>x</sub> catalysts (see Figure 3). The Au clusters increase HDS activity by enhancing thiophene binding and H<sub>2</sub> dissociation which produces the H atoms necessary for the hydrogenolysis of C-S bonds and the removal of S.



**Figure 2:** Comparison of thiophene HDS activity for various surfaces

**Water-Gas Shift Activity of Au and Cu Nanoparticles supported on Molybdenum Oxides:** The water-gas shift (WGS, CO + H<sub>2</sub>O → H<sub>2</sub> + CO<sub>2</sub>) reaction was studied on a series of gold/molybdena and copper/molybdena surfaces. Films of MoO<sub>2</sub> were grown by exposing a Mo(110) substrate to NO<sub>2</sub> at 1000 K. Nanoparticles of Au and Cu were deposited on the oxide surfaces and their WGS activity was measured in a high pressure reaction cell. Although bulk metallic Au is inactive as a catalyst for

the WGS, Au nanoparticles supported on MoO<sub>2</sub> are a somewhat better catalyst than Cu nanoparticles. The WGS activity of the Au and Cu nanoparticles supported on MoO<sub>2</sub> is 5-8 times larger than that of Cu(100). The Cu/MoO<sub>2</sub> surfaces have a catalytic activity comparable to that of Cu/CeO<sub>2</sub>(111) surfaces and superior to that of Cu/ZnO(0001) surfaces. Post-reaction surface characterization indicates that the admetals in Au/MoO<sub>2</sub> and Cu/MoO<sub>2</sub> remain in a metallic state, while there is a minor MoO<sub>2</sub> → MoO<sub>3</sub> transformation. Formate- and/or carbonate-like species are present on the surface of the catalysts. DFT calculations indicate that the oxide support in Au/MoO<sub>2</sub> and Cu/MoO<sub>2</sub> is directly involved in the WGS process.

**Mechanistic study of water-gas shift reaction on Ni<sub>2</sub>P and Ti carbides:** We investigated the WGS reaction on the Ni<sub>2</sub>P(001) surface using a combination of experimental and theoretical methods. Our experimental measurements show that Ni<sub>2</sub>P(001) displays an activity larger than that of Ni(100) or even Cu(100), which is the best metal catalyst for the WGS process. The good behavior of Ni<sub>2</sub>P is associated with the Ni oxy-phosphides formed as a result of strong O↔P interactions (Figure 3). Under reaction conditions, most of the P sites of Ni<sub>2</sub>P(001) are covered with oxygen. The active sites of O/Ni<sub>2</sub>P(001) involve the combination of a metal and a light atom. The presence of O atoms helps to lower the barrier for water dissociation; and also deactivates the Ni sites in the surface to provide moderate bonding to the adsorbates. Our results imply that the high performances of catalysts in the WGS rely heavily on the cooperation between oxygen and metal centers with moderate activity.

DFT calculations were also used to study the molecular mechanism of the WGS water-gas shift reaction on three different catalyst models: the extended TiC(001) surface, the Ti<sub>8</sub>C<sub>12</sub> MetCar, and a Ti<sub>14</sub>C<sub>13</sub> nanoparticle (Figure 3). The catalytic activity was found to be highest for the TiC(001) surface, due to the overly strong adsorption of reactants and products on either Ti<sub>14</sub>C<sub>13</sub> or Ti<sub>8</sub>C<sub>12</sub>. The corresponding reaction energy profiles show that the redox mechanism is the preferred route for the nanoparticles, whereas the carboxyl formation route is preferred for the TiC(001) surface. The present study suggests that TiC and similar transition metal carbides may be good catalysts for the water-gas shift reaction and can be potential substitutes for current low-temperature catalysts. In addition, the results point to a possible tuning to control the particle size or rate of steps.

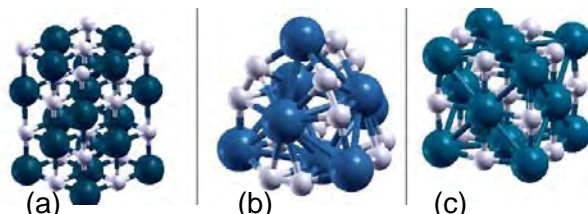


**Figure 3:** Optimized structures of a) TiC(001) surface unit cell; b) Ti<sub>8</sub>C<sub>12</sub> MetCar cluster and c) the Ti<sub>14</sub>C<sub>13</sub> nanocrystal (big blue: Ti; small white: C).

**Unusual structure and redox properties of ceria nanoparticles supported on TiO<sub>2</sub>(110):** Scanning tunneling microscopy, photoemission, and density-functional calculations were used to study the behavior of ceria nanoparticles deposited on a TiO<sub>2</sub>(110) surface. The titania substrate imposed non-typical coordination modes on the ceria nanoparticles. In the CeO<sub>x</sub>/TiO<sub>2</sub>(110) system, the Ce cations adopt an structural geometry and an oxidation state (+3) which are quite different from those seen in bulk ceria or for ceria nanoparticles deposited on metal substrates. The results of scanning tunneling microscopy show the formation of Ce<sub>2</sub>O<sub>3</sub> dimers which form small linear arrays on top of the TiO<sub>2</sub>(110) substrate (see Figure 5). An increase in the stability of the Ce<sup>3+</sup> oxidation state leads to an enhancement in the chemical and catalytic activity of the ceria nanoparticles. Thus, the exploration of mixed-metal oxides at the nanometer level may open new avenues for optimizing catalysts through stabilization of unconventional surface structures with special chemical activity.

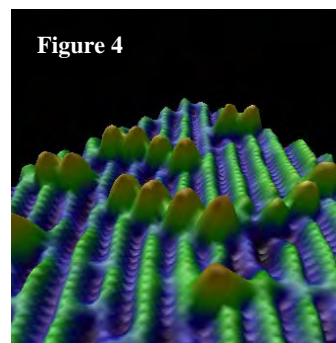


**Figure 4**

**Titanium Dioxide Nanocrystals Prepared on Au(111) by Reactive Layer-Assisted Deposition (Hrbek).** The nanocrystallite phases of  $\text{TiO}_2$  formed *via* reactive-layer-assisted deposition in ultrahigh vacuum were characterized by STM. The synthesis used reaction of a thin layer of water, on a Au(111) substrate at 130 K, with low-coverage vapor-deposited Ti. Large-scale ( $>20$  nm) patterns in the surface distribution of nanoparticles were observed with the characteristic length-scale of the pattern correlating with the thickness of the initial layer of  $\text{H}_2\text{O}$ . The phenomenon is explained as being due to the formation of droplets of liquid water at temperatures between 130 and 300 K. After the surface was annealed to 400 K, the individual titania nanoparticles formed by this process had diameters of 0.5-1 nm. When the surface was annealed to higher temperatures, nanoparticles coalesced and for annealing temperatures of 900 K compact nanocrystals formed with typical dimensions of 5-20 nm (see Figure 7). Three distinct classes of nanocrystallites were observed and their atomic structure and composition characterized.

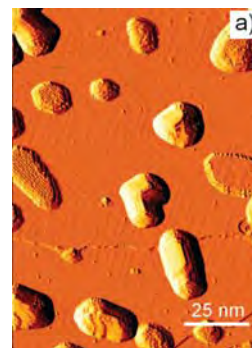


Figure 5

### Future

Future studies will continue to focus on the development and characterization of model nanocatalysts for heterogeneous catalysis applications such as desulfurization and the water-gas-shift reaction. In the area of desulfurization, we will extend our current size-selected deposition experiments of  $\text{Mo}_x\text{S}_y$  clusters to other sizes (structures) and stoichiometry as well as deposit them on oxide surfaces ( $\text{Al}_2\text{O}_3$ ,  $\text{SiO}_2$ ,  $\text{TiO}_2$ ) which are representative of non-reducible and reducible metal oxide surfaces typically used in catalysis applications. The oxide studies are particularly important as the binding of the  $\text{Mo}_x\text{S}_y$  clusters onto a metal oxide surface (Mo-O bonds) are expected to be very different than for the Au(111) surface (S-Au bonds). Desulfurization investigations will also include theoretical studies of deep-HDS on metal phosphides ( $\text{Ni}_2\text{P}$ ) surfaces to understand their high activity by exploring the adsorption and reaction of large molecules with imbedded sulfur atoms (dibenzothiophene). The recent finding of high  $\text{DeSO}_x$  activity for Au nanoparticles supported on a TiC(001) surface will be expanded to include other metal carbide supports (e.g., VC, ZrC, WC,  $\text{M}_x\text{C}$ ) to see if the unique electronic interactions found for Au/TiC are a general phenomena. Metal carbide surfaces and carbide supported Au nanoparticles will also be explored as low temperature water-gas-shift catalysts, as recent DFT calculations suggest that the barriers for rate-limiting reaction steps are smaller for TiC(001) than for Cu(111).

A new effort will be centered on alcohol reforming and synthesis as processes that can yield renewable sources of energy as hydrogen or as a liquid fuel, respectively. For reforming by partial oxidation or steam reforming, the catalysts must be efficient at C-C bond dissociation, CO oxidation and H-H association. For C2-C4 alcohol synthesis from syn gas ( $\text{H}_2 + \text{CO} + \text{CO}_2$ ), hydrogenation and C-C coupling are key elementary steps. The aims of this program are to evaluate the catalytic performance of nanocatalysts “designed” to meet the requirements for reforming or synthesis, and to perform fundamental studies to elucidate active sites and reaction intermediates. Potential catalyst materials include those that promote C-C bond formation (Rh), hydrogenation (Pt, Pd, Fe, Ni, metal sulfides) and CO oxidation (Au, Cu), many of which we have gained experience with in previous studies of hydrodesulfurization and the water gas shift reaction.

### Publications 2007-2009

1. “Water-Gas Shift Reaction on Cu and Au Nanoparticles Supported on CeO<sub>2</sub>(111) and ZnO(0001): Intrinsic Activity and Importance of Support Interactions,” J. A. Rodriguez, P. Liu, J. Hrbek, J. Evans, M. Pérez, *Angewandte Chemie*, International Edition **46**, 1329-1332 (2007).

2. “*In situ* Time-resolved Characterization of Novel Cu-MoO<sub>2</sub> Catalysts during the Water-Gas Shift Reaction,” W. Wen, J. Liu, M. G. White, N. Marinkovic, J. C. Hanson, J. A. Rodriguez, *Catal. Lett.*, 113, 1-7 (2007).
3. “STM and XPS study of growth of Ce on Au(111),” S. Ma, X. Y. Zhao, J. A. Rodriguez, J. Hrbek, *Journal of Physical Chemistry C* **111**, 3685-3691(2007).
4. “Reaction of Water with Ce-Au(111) and CeOx/Au(111) Surfaces: Photoemission and STM Studies,” X. Zhao, S. Ma, J. Hrbek, J. A. Rodriguez, *Surface Science* **601**, 2445-2452 (2007).
5. “Effects of hydrogen on the reactivity of O<sub>2</sub> towards gold nanoparticles and surfaces”, L. Barrio P. Liu, J.A. Rodriguez, J.M. Campos-Martin, J.L.G. Fierro, *Journal of Physical Chemistry C* 111 (2007) 19001-19008.
6. “Pd<sub>3</sub>Fe and Pt monolayer-modified Pd<sub>3</sub>Fe electrocatalysts for oxygen reduction,” M. Shao, K. Sasaki, P. Liu and R.R. Adzic, *Zeit. Phys. Chemie* **221**, 1175-1190 (2007).
7. “Gold Nanoparticles on Ceria: Importance of O vacancies in the Activation of Gold,” J. A. Rodriguez, X. Wang, P. Liu, W. Wen, J. C. Hanson, J. Hrbek, M. Pérez, J. Evans, *Topics in Catalysis* 44 (2007) 73-81.
8. “A systematic density functional study of molecular oxygen adsorption and dissociation on the (001) surface of group IV, V and VI transition metal carbides”, F. Viñes, C. Sousa, F. Illas, P. Liu and J. A. Rodriguez, *Journal of Physical Chemistry C* 111 (2007) 16982-16989.
9. “Electrodeposition of Pt onto RuO<sub>2</sub>(110) single-crystal surface”, M.B. Vukmirovic, P. Liu, J.T. Muckerman and R.R. Adzic, *Journal of Physical Chemistry C* 111 (2007) 15306-15311.
10. “Size-specific chemistry on bimetallic surfaces – a combined experimental and theoretical study”, M. Ruff, N. Takehiro, P. Liu, J.K. Nørskov and R.J. Behm, *ChemPhysChem* 8 (2007) 2068-2071.
11. “Hydrogen oxidation reaction on Pt in acidic media: adsorption isotherm and activation free energy,” J. X. Wang, T. E. Springer, P. Liu, M. Shao, R. R. Adzic, *Journal of Physical Chemistry C* 111 (2007) 12425-12433.
12. “Origin of enhanced activity in palladium alloy electrocatalysts for oxygen reduction reaction”, M. Shao, P. Liu and R.R. Adzic, *Journal of Physical chemistry B* 111 (2007) 6772-6775.
13. “Water-gas shift reaction on Cu and Au nanoparticles supported on CeO<sub>2</sub>(111) and ZnO(000 $\bar{1}$ ): intrinsic activity and importance of support interactions”, J. A. Rodriguez, P. Liu, J. Hrbek, J. Evans and M. Pérez, *Angewandte Chemie. International Edition* 46 (2007) 1329-1332.
14. “Density functional study of the adsorption of atomic oxygen on the (001) surface of early transition metal carbides”, F. Viñes, C. Sousa, F. Illas, P. Liu and J.A. Rodríguez, *Journal of Physical Chemistry C* 111 (2007) 1307-1314.
15. “A Scanning Tunneling Microscopy Study on the Effect of Post-Deposition Annealing of Copper Phthalocyanine Thin Films,” Manandhar, K.; Ellis, T.; Park, K.T.; Cai, T.; Song, Z.; Hrbek, J., *Surface Science*, 601, 17, 3623-3631 (2007).
16. “Photoemission and X-ray Absorption Spectroscopy Applied to Nanoparticle Activation,” Rodriguez, J.A., *Journal of Electron Spectroscopy and Related Phenomena*, 156-158, xxx, (2007).
17. “Water-Gas Shift Reaction on Inverse CeOx/Au(111) and TiOx/Au(111) Catalysts: Active Role of Oxide Nanoparticles,” Rodriguez, J.A.; Ma, S.; Liu, P.; Hrbek, J.; Evans, J.; Perez, M., *Science* 318, 1757-1760 (2007).
18. “Adsorption of Gold on TiC(001): Au-C Interactions and Charge Polarization,” Rodriguez, J.A.; Vines, F.; Illas, F.; Liu, P.; Takahashi, Y.; Nakamura, K., *Journal of Chemical Physics* 127, 211102 (2007).



19. "Structure-Activity Relationship in Nanostructured Copper-Ceria-Based Preferential CO Oxidation Catalysts," Gamarra, D., G. Munuera, A. Hungria, M. Fernandez-Garcia, J. Conesa, P. Midgley, X. Wang, J. Hanson, J. Rodriguez and A. Martinez-Arias, *J. Phys. Chem. C* **111**, 11026-11038 (2007).
20. "Ternary Pt/Rh/SnO<sub>2</sub> Electrocatalysts for Oxidizing Ethanol to CO<sub>2</sub>," A. Kowal, M. Li, M. Shao, K. Sasaki, M. B. Vukmirovic, J. Zhang, N. S. Marinkovic, P. Liu, A. Frenkel, and R. R. Adzic, *Nature Materials*, doi:10.1038/nmat2359.
21. "Dissociation of SO<sub>2</sub> on Au/TiC(001): Effects of Au↔C Interactions and Charge Polarization," J. A. Rodriguez, P. Liu, J. F. Viñes, F. Illas, Y. Takahashi and K. Nakamura, *Angew. Chemie. Int. Ed.* **47**, 6685-6689 (2008).
22. "Catalyst size matters: tuning the molecular mechanism of the water-gas-shift reaction on titanium carbide," F. Viñes, J.A. Rodriguez, P. Liu and F. Illas, *J. Catal.* **260**, 103-112 (2008).
23. "Formation of Pd/Au nanostructures from Pd nanowires via galvanic replacement reaction," X. Teng, Q. Wang, P. Liu, W. Han, A. I. Frenkel, W. Wen, N. Marinkovic, J. C. Hanson, J. A. Rodriguez, *J. Amer. Chem. Soc.* **130**, 1093-1101(2008).
24. "Characterization and Reactivity of the Mo<sub>4</sub>S<sub>6</sub><sup>+</sup> Cluster deposited on Au(111) by Size-Selected Deposition," J. M. Lightstone, M. Patterson, J. Lofaro, P. Liu and M. G. White, *J. Phys. Chem. C* **112**, 11495–11506 (2008)
25. "Structure of Molybdenum and Tungsten Sulfide M<sub>x</sub>S<sub>y</sub><sup>+</sup> Clusters: Experiment and DFT Calculations," M. Patterson, J. M. Lightstone, and M. G. White, *J. Phys. Chem. A*, **112**, 12011-12021 (2008).
26. "Adsorbate driven morphological changes of a gold surface at low temperatures," J. Hrbek, F. M. Hoffmann, J. B. Park, P. Liu, D. Satcchiola, Y. SooHoo, S. Ma, A. Nambu, J. A. Rodriguez and M. G. White, *J. Am. Chem. Soc.* **130**, 17272–17273 (2008).
27. "STM Study of the Growth of Cerium Oxide Nanoparticles on Au(111)", S. Ma, J.A. Rodriguez, and J. Hrbek, *Surf. Sci.* **602**, 3272-3278 (2008).
28. "Methanethiol Chemistry on TiO<sub>2</sub>-supported Ni Clusters", O. Ozturk, J.B. Park, T.J. Black, J.A. Rodriguez, J. Hrbek and D.A. Chen, *Surf. Sci.* **602**, 3077-3088 (2008).
29. "Theoretical Studies in Heterogeneous Catalysis: Towards a Rational Design of Novel Catalysts for Hydrodesulfurization and Hydrogen Production", J.A. Rodriguez and P. Liu, in *New Developments in Quantum Chemistry*, Transworld Research Network (2008), **invited book chapter**.
30. "STM Study of Titanium Dioxide Nanocrystals Prepared on Au(111) by Reactive Layer-Assisted Deposition," D. Potapenko, J. Hrbek and R. Osgood, *ASC Nano* **2**, 1353-1362 (2008)
31. "Heteroepitaxial Thin Film of Iron Phthalocyanine on Ag(111)," K. Manandhar, K.T. Park, S. Ma and J. Hrbek, *Surface Science*, doi:10.1016/j.susc.2008.12.031.
32. "Water-gas-shift reaction on a Ni<sub>2</sub>P(001) catalyst: Formation of oxy-phosphides and highly active reaction sites," P. Liu, J.A. Rodriguez, Y. Takahashi and K. Nakamura, *J. Catal.* **262** 294-303 (2009).
33. "High water-gas shift activity in TiO<sub>2</sub>(110) supported Cu and Au nanoparticles: role of the oxide and metal particle size", J.A. Rodriguez, J. Evans, J. Graciani, J. Park, P. Liu, J. Hrbek, J.F. Sanz, *Journal of Physical Chemistry C*, in press.
34. Dissociation of OCS on the Mo<sub>6</sub>S<sub>8</sub><sup>+</sup> Cluster Supported on Au(111), M. J. Patterson, Y. Choi, P. Liu, and M. G. White, *J. Am. Chem. Soc.* (submitted).

**DE-FG02-03ER15472 Francisco Zaera (University of California, Riverside) PI**  
**DE-FG02-03ER15472 David S. Sholl (Georgia Institute of Technology) Co-PI**  
**DE-FG02-03ER15472 Andrew J. Gellman (Carnegie Mellon University) Co-PI**  
**DE-FG02-03ER15472 Wilfred T. Tysoe (University of Wisconsin, Milwaukee) Co-PI**

***CATALYSIS SCIENCE INITIATIVE: Molecular Level Design of Chiral Heterogeneous Catalysts***

Additional PIs: L. Mueller (UCR), S. S. Perry (U. Houston), G. Zgrablich (U. San Luis), D. K. Saldin (UWM);

Post-docs: I. Lee (UCR), J. Kubota (UCR), L. Mink (UCR), D. Stacchiola (UWM);

Students: Z. Ma (UCR), R. A. Olsen (UCR), A. Agarwal (UCR), L. Burkholder (UWM), T. Zheng (UWM), J. D. Horvath (CMU), A. Koritnik (CMU), P. Kamakoti (CMU), R. B. Rankin (CMU), J. James (CMU)

Dept. Chemical Engineering Carnegie Mellon University Pittsburgh, PA 15213 ag4b@andrew.cmu.edu	School of Chemical & Biomolecular Engineering Georgia Institute of Technology Atlanta, GA, 30332-0100 david.sholl@chbe.gatech.edu	Dept Chemistry Univ. Wisconsin Milwaukee, WI 53211 wtt@uwm.edu	Dept. Chemistry Univ. California Riverside, CA 92521 zaera@ucr.edu
---	--	--	--

**Goals:**

The main goal of this project is to determine the mechanisms by which enantioselectivity can be bestowed on heterogeneous catalysts. Specifically, chirality is to be imparted to achiral surfaces either by exposing chiral planes or by using chiral modifiers.

**DOE Interest:**

Enantioselectivity is critical in the production of numerous fine chemicals for bioactive applications such as pharmaceuticals. Chiral heterogeneous catalysis has a number of attractive features to offer for its use in fine chemical synthesis, but has so far not been incorporated in any commercial process. This is mostly due to the difficulty in designing such processes without an understanding of the parameters that control chirality and enantioselectivity on surfaces. The basic knowledge generated from the studies being carried out by our research team is expected to advance the development of heterogeneous chiral catalysis, and in more general terms, selectivity in catalysis.

**Research Plan:**

The hypothesis underpinning our collaborative research effort is that there are three possible origins to chirality and enantioselectivity on catalytic metal surfaces:

- chirality arising from 1:1 interactions between the reactant and individual adsorbed chiral molecules, and
- chirality arising from adsorbates that form long-range chiral ensembles on the surface,
- natural chirality arising from the atomic structure of the metal surface,

Our collaborative program is aimed to understand the relative importance of each of these three mechanisms in enantiospecific adsorption and catalytic reactions.

## Recent Progress:

In order to understand the one-to-one modifier-reactant interaction mechanisms for imparting enantioselectivity, we have used infrared spectroscopy to characterize the adsorption of cinchonidine and other related modifiers on Pt surfaces from solution. Vibrational assignments for the cinchonidine were first made using a combination of experimental spectroscopic measurements and *ab initio* computational methods. It was found that the geometry of the cinchonidine modifier on Pt is very sensitive to its concentration in solution. At low and intermediate concentrations, the cinchonidine is adsorbed with the quinoline ring parallel to the surface; however, at high concentrations, the ring is tilted away from the surface. The optimum enantioselectivity occurs under conditions consistent with a modifier adsorption geometry having the quinoline ring parallel to the surface. The influence of dissolved gases on the adsorption of cinchonidine from  $\text{CCl}_4$  solutions onto polycrystalline Pt surfaces was characterized using FT-IRAS as well. Most of the gases studied, which included Ar,  $\text{N}_2$ ,  $\text{O}_2$ , air and  $\text{CO}_2$ , have no detectable influence on cinchonidine adsorption on Pt. On the other hand,  $\text{H}_2$  plays a unique role, initially accelerating the uptake kinetics of cinchonidine, but later displacing some of the adsorbed cinchonidine from the Pt surface.

The solvent was found to have a strong influence on the adsorption of cinchonidine on the catalyst surface. In particular, the polarity of the solvent was found to influence the kinetics of cinchonidine desorption into solution in a manner that correlated well with the solvent influence on the enantioselectivity of the cinchonidine modified Pt catalyst. Cinchonidine adsorbs irreversibly on Pt from non-polar solutions such as cyclohexane, but can be easily removed by more polar solvents such as  $\text{CH}_2\text{Cl}_2$ . The evolution of the adsorbed cinchonidine overlayer on Pt during flushing with different solvents is illustrated in Figure 1. The behavior observed in our studies correlates well with the solubility of cinchonidine in different solvents and with the activity and enantioselectivity of the cinchonidine/Pt catalyst for the Orito reaction in these solvents. In general, we have concluded that the enantioselective properties of the cinchonidine/Pt catalyst are defined by the adsorption of the chiral modifier, and that those in turn are influenced by details of the reaction system, such as the concentration of the modifier in solution, the type of solvent, and the nature of the gasses dissolved in the liquid phase.

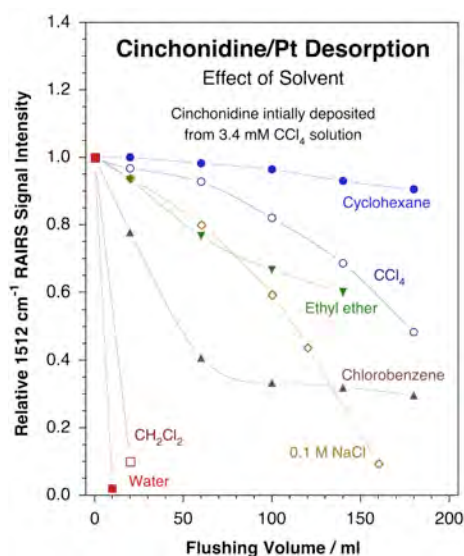


Figure 1. Desorption of adsorbed cinchonidine from a platinum surface into different solvents as a function of rinsing volume. In these experiments the cinchonidine was first adsorbed from a carbon tetrachloride-saturated solution, and then flushed with sequential 20 ml aliquots of the stated solvents. The coverage of the adsorbate remaining on the surface was determined in-situ by following the infrared absorption signal at  $1512\text{ cm}^{-1}$ , which corresponds to an in-plane deformation of the quinoline ring. The data show that the desorption kinetics are severely affected by the nature of the solvent, varying from fast desorption in water and dichloromethane to irreversible adsorption in cyclohexane and other alkanes. This trend correlates well with the chirality-imparting ability of cinchonidine for enantioselective hydrogenation reactions on platinum catalysts.

Having explored the effects of solution on cinchonidine adsorption on Pt, the next avenue of investigation was to understand the effects of the modifier's molecular structure on its

adsorption properties and on its ability to impart enantioselectivity to catalytic processes. A comparative study was carried out using cinchonidine, cinchonine, quinine, quinidine, and the dihydro analogs of those four molecules. Interesting trends in adsorption equilibria were observed, as illustrated by the data in Figure 2. The adsorption equilibrium constants ( $K_{\text{ads}}$ ) were found to follow the sequence cinchonine > quinidine > cinchonidine > quinine. Some of this ordering can be explained by differences in solubility, but quinidine displays a much larger  $K_{\text{ads}}$  than expected based on its large relative solubility; bonding to the surface must also play a role in determining the trends in  $K_{\text{ads}}$ .

Using FT-IRAS, it was determined that each of the cinchona alkaloids binds differently on Pt at saturation coverages; while the quinoline ring of cinchonidine tilts along its long axis to optimize  $\pi$ - $\pi$  intermolecular interactions, in cinchonine it tilts along the short axis and bonds through the lone electron pair of the nitrogen atom instead. Both quinine and quinidine exhibit additional bonding to the surface via the methoxy oxygen atom. Perhaps a more surprising result from this work is the fact that cinchonine displays a higher  $K_{\text{ads}}$  than cinchonidine, quinine or quinidine in spite of the fact that, according to previous work, it can be readily displaced from the surface by any of those other cinchona alkaloids. A full explanation of these observations requires consideration of the solvent interaction with the adsorbed species.

The differences observed among the different cinchona alkaloids, both in their adsorption properties and in their behavior in solution, were deemed to arise from intrinsic molecular properties associated with their structure: the relative solubilities of the different cinchona alkaloids remain approximately constant in different solvents. Correlations between the conformations of cinchona's and their chemical behavior have already been identified in a few cases, but not properly explained. Preliminary NMR and DFT data suggest that the most stable configuration of each molecule may be determined by the steric effects exerted by the peripheral functional groups (vinyl, methoxy) bonded to the quinuclidine and quinoline rings. This behavior may account for the reported differences in catalytic enantioselectivities observed when using cinchonidine and cinchonine as chiral modifiers. The role of these peripheral groups in defining the behavior of cinchona's in solution, their adsorption, and their ability to impart chirality in catalytic systems, is one of the directions of research proposed for the next funding period of this project. An improved understanding of this effect will lead to the preparation of specific new modifiers by changing their peripheral groups to tune their catalytic behavior.

In terms of the formation of chiral superstructures on the surface upon adsorption of chiral modifiers, we have shown that such a mechanism is indeed operative with a series of enantiopure compounds, including 2-butoxide, 2-methylbutanoic acid and (1-naphthyl)ethylamine (NEA) as well as a few aminoacids. Several metal surfaces have been used here, including those of Pd(111), Pt(111) and Cu(111) single crystals. The enantioselectivity of these systems has

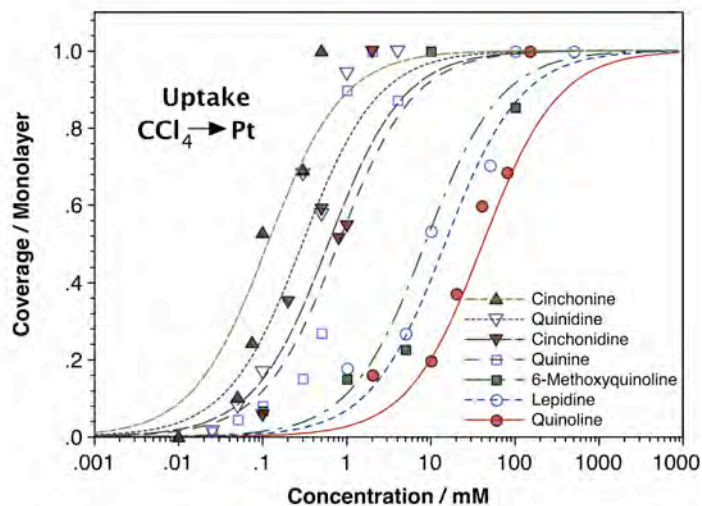


Figure 2. Adsorption isotherms for several cinchona and related compounds from solution onto a platinum surface, as determined by in-situ infrared spectroscopy detection.

been tested by using (R)- and (S)-propylene oxide as probes, by both quantifying their thermal desorption spectra and identifying the adsorbed species with infrared-absorption spectroscopy. In general, it has been observed that enantioselective adsorption on chirally templated surfaces is observed over a narrow range of 2-butoxide coverages near  $\theta_{2\text{-ButO}} \sim 1/2$ , where it shows a preference for the homochiral surfaces, that is, for surfaces covered with moieties of the same chirality as the chiral probe. This preference can reach enhancement ratios (ER) of about two. An example of the data obtained from these studies, in this case for the adsorption of (S)-NEA on Pt(111) probed with ethylene oxide, is provided in Figure 3. To note in that figure is the additional contribution from the energetics of the adsorption to the enantioselectivity of the surface. This places NEA as an intermediate case acting as both a 1:1 complex-forming modifier and a templating agent for chiral suprastructure formation.

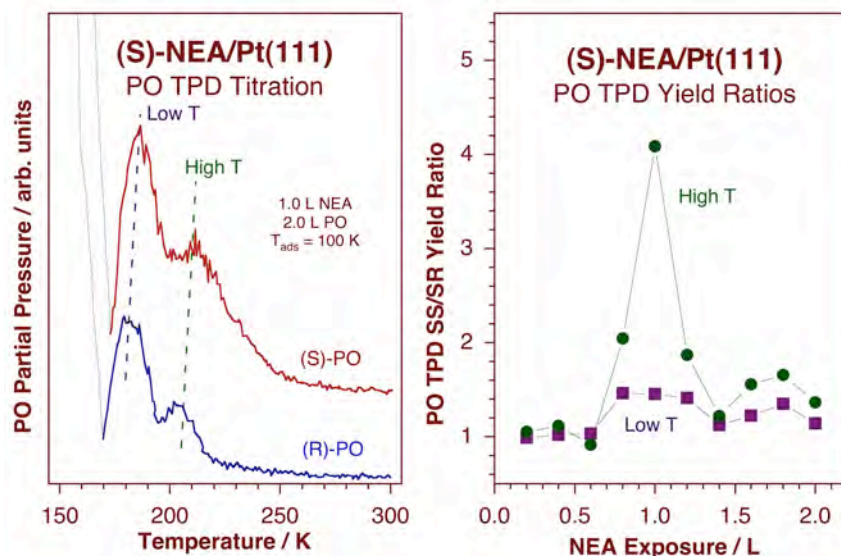


Figure 3. Left: TPD traces for the molecular desorption of (R)- and (S)-propylene oxide (PO) after saturation on a Pt(111) surface predosed with 1.0 L of (S)-(1-naphtyl)ethylamine (NEA). Two peaks are seen in each case, but with different yields and peak maxima due to the enantiopreference of adsorption for (S)-PO on the (S)-NEA templated surface. Right: Plot of the SS/SR yield ratios of (S)- vs. (R)-PO on (S)-NEA covered Pt(111) as a function of exposure of the latter. The contributions from the two TPD peaks were separated to highlight the fact that it is the high T peak the one responsible for the enantioselectivity. This example points to both energetic and entropic contributions to the chirality of the surface.

The effect reported here have proven quite general, except for the case of the adsorption of 2-methylbutanoic acid on Pd(111) (but not on Pt(111)). In order to try to understand this anomaly, the experimental work has been complemented with Density Functional Theory (DFT) calculations. Specifically, since density functional theory calculations show that 2-butoxy and 2-methylbutanoate species exhibit identical chiral footprints, the loss of enantioselectivity of the 2-methylbutanoate species on Pd(111) has been explained by the freer rotation of the 2-butyl species in 2-methylbutanoate compared to 2-butoxy species. In order to test this hypothesis, a methyl group was replaced by an  $\text{NH}_2$ - group, which should bond to the surface to inhibit azimuthal rotation. A series of experiment to measure the chemisorptive enantioselectivity of (R)- or (S)-PO on surfaces modified by 2-aminobutanoic acid, where the PO coverages were measured using beams of propylene oxide by the King and Wells method, revealed that the enantioselectivity was restored. In this case, the variation in enantioselectivity varied as a function of 2-aminobutanoate coverage, also reaching a maximum at  $\sim 50\%$  of saturation as found above for 2-butoxide species, and reaching a maximum enhancement ratio of  $1.7 \pm 0.1$ .

Experiments were carried out for a number of amino acids to gauge the effect of altering the aminoacid functional group. It was found that there is a slight decrease in ER from  $2.0 \pm 0.2$  to  $1.6 \pm 0.1$  in going from alanine, to 2-aminobutanoic acid to norvaline, where the function group varies in the homologous series, methyl, ethyl to propyl. This implies that the size of the chiral “pocket” is not strongly affected by the length of the alkyl group. Aminoacids with branched side groups (valine and leucine) resulted in a complete loss in enantioselectivity, presumably due to steric hindrance by the bulky, branched side chains preventing the aminoacids from approaching sufficiently close to properly define a chiral pocket. Isoleucine, where branching occurs at the second carbon, exhibits intermediate enantioselectivity ( $ER = 1.3 \pm 0.1$ ).

Further work has proceeded to determine the structure of aminoacids on Pd(111) and to measure their thermal stability, reaction pathways and chemisorptive enantioselectivity. Low-energy electron diffraction (LEED) intensity versus beam energy (I/E) experiments are being used to measure the structure of amino acids. Initial experiments were carried out using a conventional LEED system with an incident electron beam current of  $\sim 1 \mu\text{A}$ . It was however found that aminoacids on Pd(111) are extremely susceptible to damage in the electron beam and completely decompose before an I/E curve could be collected. In order to circumvent this problem, data were collected for glycine and alanine using a system in which the incident beam current is  $\sim 200 \text{ fA}$ , thus allowing LEED I/E curves to be collected for an electron exposure much lower than the adsorbate coverage, thereby obviating electron beam decomposition problems. Aminoacid surface structures were calculated using density functional theory (DFT) to compare with the measured LEED I/E data.

Additional X-ray photoelectron spectroscopy (XPS) shows that aminoacids adsorb on Pd(111) in both their zwitterionic ( $\sim 70\text{-}80\%$ ) and anionic forms ( $20\text{-}30\%$ ), where the ratio of each depends only slightly on coverage. Glycine, alanine and proline each thermally decompose at slightly above 300 K by scission of the C-C bond in the aminoacid framework, and evolve CO and  $\text{CO}_2$  originating from the carboxylate group. A small amount of the amine is found to desorb, with the amine depending on the nature of the side group in the aminoacid. The majority, however, decomposes to form HCN. These results confirm that the chemisorptive enantioselectivity measurements made above for propylene oxide on various aminoacids were carried out for surfaces covered by a mixture of zwitterionic and anionic forms. The chemisorptive enantioselectivity of propylene oxide was also measured on aminoacid-covered surfaces by monitoring the propylene oxide coverage by TPD, and yielded ER values in good agreement with those found above when using the King and Wells method. Lastly, experiments were carried out to examine the selectivity of  $\beta$ -hydride elimination of (R)- or (S)-2-butoxide species compared to rehydrogenation to yield 2-butanol in the presence of (R)- or (S)-propylene oxide. In this case, propylene oxide acts as the chiral modifier rather than the probe. It was found that, at least on Pd(111), the surface 2-butoxy hydrogenation and  $\beta$ -hydrogenation reactions are enantioselective, with the yield of 2-butanol due to 2-butoxide rehydrogenation increasing when co-adsorbed with propylene oxide of the same chirality. Thus, such experiments should allow us to explore not only how chiral pockets affect the adsorption of chiral molecules but also their subsequent surface reactivity.

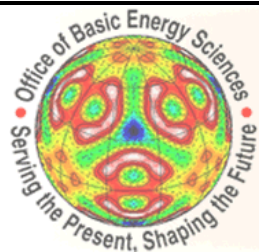
Finally, in terms of naturally chiral surfaces, our most recent work has extended the past research to studies of reactivity on these surfaces. Using chiral 2-bromobutane, it was possible to create chiral 2-butyl groups on naturally chiral Cu surfaces, and to show that the kinetics of their  $\beta$ -hydride elimination is enantioselective. The next step will be to investigate the possibility of imprinting chirality on achiral surfaces by using chiral adsorbate agents.

## Recent Publications:

1. F. Gao, Z. Li, Y. Wang, L. Burkholder, W.T. Tysoe, Chemistry of Glycine on Pd(111): Temperature-programmed Desorption and X-ray Photoelectron Spectroscopic Study, *J. Phys. Chem. C.*, **111**, 9981 (2007).
2. F. Gao, Z. Li, Y. Wang, L. Burkholder, W.T. Tysoe, Chemistry of Alanine on Pd(111): Temperature-programmed Desorption and X-ray Photoelectron Spectroscopic Study, *Surf. Sci.*, **601**, 3276 (2007).
3. F. Gao, Y. Wang, L. Burkholder, W.T. Tysoe, Chemistry of L-Proline on Pd(111): Temperature-programmed Desorption and X-ray Photoelectron Spectroscopic Study, *Surf. Sci.*, **601**, 3579 (2007).
4. F. Gao, Y. Wang, L. Burkholder, W. T. Tysoe, Enantioselective Chemisorption of Propylene Oxide on a 2-Butanol-Modified Pd(111) Surface: The Role of Hydrogen-Bonding Interactions, *J. Am. Chem. Soc.*, **129**, 15240 (2007).
5. Z. Ma, I. Lee, F. Zaera, Factors Controlling Adsorption Equilibria from Solution onto Solid Surfaces: The Uptake of Cinchona Alkaloids onto Platinum Surfaces, *J. Am. Chem. Soc.*, **129(51)**, 16083-16090 (2007).
6. Y. Huang, A. J. Gellman, Enantiospecific adsorption of (R)-3-methylcyclohexanone on naturally chiral Cu(531)R&S surfaces, *Catal. Lett.*, **125**, 177-182 (2008).
7. J. N. James, D. S. Sholl, Theoretical studies of chiral adsorption on solid surfaces, *Curr. Op. Colloid Interface Sci.*, **13**, 60-64 (2008).
8. J. N. James, D. S. Sholl, Density Functional Theory studies of dehydrogenated and zwitterionic glycine and alanine on Pd and Cu surfaces, *J. Mol. Catal. A*, **281**, 44-48 (2008).
9. F. Gao, Y. Wang, Z. Li, O. Furlong, W.T. Tysoe, Enantioselective Reactions on a Au/Pd(111) Surface Alloy with Co-adsorbed Chiral 2-Butanol and Propylene Oxide, *J. Phys. Chem. C.*, **112**, 3362 (2008).
10. F. Gao, Y. Wang, W.T. Tysoe, Enantioselective Chemisorption and Reactions on Model Chirally Modified Surfaces: 2-Butanol on L-Proline Templated Pd(111) Surfaces, *J. Phys. Chem. C.*, **112**, 6145 (2008).
11. F. Gao, Y. Wang, L. Burkholder, C. Hirschmugl, D. K. Saldin, H. C. Poon, D. Sholl, J. James, W. T. Tysoe, The Structure and Reactivity of 2-butanol on Pd(111), *Surf. Sci.*, **602**, 2264-2270 (2008).
12. L. Mink, Z. Ma, R. A. Olsen, J. N. James, D. S. Sholl, L. J. Mueller, F. Zaera, The Physico-Chemical Properties of Cinchona Alkaloids Responsible for their Unique Performance in Chiral Catalysis, *Top. Catal.*, **48(1-4)**, 120-127 (2008).
13. F. Zaera, Chiral Modification of Solid Surfaces: A Molecular Level View (Centennial Feature Article), *J. Phys. Chem. C*, **112(42)**, 16196-16203 (2008).
14. I. Lee, Z. Ma, S. Kaneko, F. Zaera, 1-(1-Naphthyl)Ethylamine Adsorption on Platinum Surfaces: On the Mechanism of Chiral Modification in Catalysis, *J. Am. Chem. Soc.*, **130(44)**, 14597-14604 (2008).
15. Z. Ma, F. Zaera, Chiral Modification of Catalytic Surfaces, in *Design of Heterogeneous Catalysts: New Approaches based on Synthesis, Characterization, and Modelling*, edited by U.S. Ozkan, Wiley-VCH, Weinheim, pp 113-140 (2009).

# Participant List

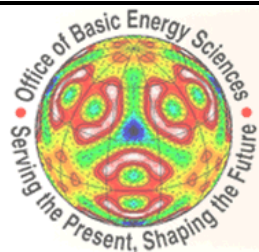




# Announcing the 2009 DOE/BES Catalysis Sciences Meeting

Sponsored by the U.S. Department of Energy, Office of Basic Energy Sciences

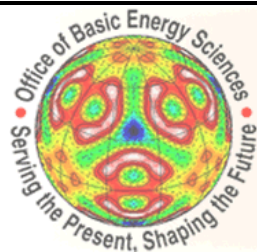
Name	Affiliation	Email
Radoslav Adzic	Brookhaven National Laboratory	adzic@bnl.gov
Eric Altman	Yale University	eric.altman@yale.edu
Frances Arnold	Caltech	frances@cheme.caltech.edu
Aravind Asthagiri	University of Florida	aasthagiri@che.ufl.edu
David Avnir	Hebrew University	david@chem.ch.huji.ac.il
Perla Balbuena	Texas A&M University	balbuena@tamu.edu
Xiaoguang Bao	Ohio State University	xibao@chemistry.ohio-state.edu
Craig Barnes	University of Tennessee	cebarnes@utk.edu
Ludwig Bartels	University of California at Riverside	bartels@ucr.edu
Alexis Bell	University of California, Berkeley	bell@cchem.berkeley.edu
Carol Bessel	National Science Foundation	cbessel@nsf.gov
Elizabeth Biddinger	The Ohio State University	Biddinger.12@osu.edu
Janet Blumel	Texas A&M University	blumel@tamu.edu
Suzanne Blum	University of California at Irvine	blums@uci.edu
Jeff Brinker	University of New Mexico/Sandia National Labs	cjbrink@sandia.gov
Richard Brutchey	University of Southern California	brutchey@usc.edu
Archibald Buchanan, III	Oak Ridge National Laboratory	buchananac@ornl.gov
Emilio Bunel	Argonne National Laboratory	ebunel@anl.gov
Nicholas Camillone	Brookhaven National Laboratory	nicholas@bnl.gov
Charles Campbell	University of Washington	campbell@chem.washington.edu
Jingguang Chen	University of Delaware	jpgchen@udel.edu
Peng Chen	Cornell University	pc252@cornell.edu
Bradley Chmelka	University of California, Santa Barbara	bradc@engineering.ucsb.edu
William Curtis Conner	University of Massachusetts	wconner@ecs.umass.edu
David Cox	Virginia Tech	dfcox@vt.edu
Richard Crooks	University of Texas at Austin	crooks@cm.utexas.edu
Larry Curtiss	Argonne National Laboratory	curtiss@anl.gov
Sheng Dai	Oak Ridge National Laboratory	dais@ornl.gov
Abhaya Datye	University of New Mexico	datye@unm.edu
Robert Davis	University of Virginia	rjd4f@virginia.edu
William Delgass	Purdue University	delgass@ecn.purdue.edu
Ulrike Diebold	Tulane University	diebold@tulane.edu
David Dixon	University of Alabama	dadixon@bama.ua.edu
Zdenek Dohnalek	Pacific Northwest National Laboratory	Zdenek.Dohnalek@pnl.gov
Bingchen Du	Georgetown University	bd52@georgetown.edu
Michel Dupuis	Pacific Northwest National Laboratory	donna.sturdevant@pnl.gov
Jonah Erlebacher	Johns Hopkins University	jonah.erlebacher@jhu.edu
Richard Finke	Colorado State University	rfinke@lamar.colostate.edu



Announcing the  
**2009 DOE/BES  
 Catalysis Sciences Meeting**

Sponsored by the U.S. Department of Energy, Office of Basic Energy Sciences

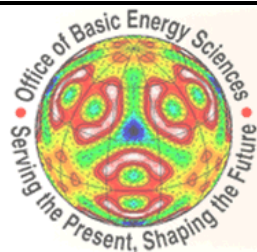
Name	Affiliation	Email
Maria Flytzani-Stephanopoulos	Tufts University	mflytzan@tufts.edu
Heinz Frei	Lawrence Berkeley National Laboratory	HMFrei@lbl.gov
Anatoly Frenkel	Yeshiva University	anatoly.frenkel@yu.edu
Cynthia Friend	Harvard University	cfriend@deas.harvard.edu
Bruce Garrett	Pacific Northwest National Laboratory	bruce.garrett@pnl.gov
Bruce Gates	University of California, Davis	bcgates@ucdavis.edu
Andrew Gellman	Carnegie Mellon University	gellman@cmu.edu
David Goodman	Texas A & M University	goodman@mail.chem.tamu.edu
Raymond Gorte	University of Pennsylvania	gorte@seas.upenn.edu
Robert Grubbs	California Institute of Technology	rhg@caltech.edu
Vadim Guliant	University of Cincinnati	vguliant@alpha.che.uc.edu
Gary Haller	Yale University	gary.haller@yale.edu
Robert Hamers	University of Wisconsin	rjhamers@wisc.edu
Jonathan Hanson	Brookhaven National Laboratory	hanson1@bnl.gov
Alexander Harris	Brookhaven National Laboratory	alexh@bnl.gov
Tony Heinz	Columbia University	tony.heinz@columbia.edu
Michael Henderson	Pacific Northwest National Laboratory	ma.henderson@pnl.gov
Graeme Henkelman	The University of Texas at Austin	henkelman@mail.utexas.edu
Craig Hill	Emory University	lchauvi@emory.edu
Jan Hrbek	Brookhaven National Laboratory	hrbek@bnl.gov
Thomas Jaramillo	Stanford University	jaramillo@stanford.edu
Jim Haw	University of Southern California	jhaw@usc.edu
Duane Johnson	University of Illinois Urbana-Champaign	duanej@illinois.edu
Christopher Jones	Georgia Institute of Technology	chris.jones@chbe.gatech.edu
Alexander Katz	University of California, Berkeley	askatz@berkeley.edu
John Kitchin	Carnegie Mellon University	jkitchin@andrew.cmu.edu
Harold Kung	Northwestern University	hkung@northwestern.edu
Victor Lin	Iowa State University/Ames Laboratory	vsylin@iastate.edu
Suljo Linic	University of Michigan	linic@umich.edu
Meilin Liu	Georgia Institute of Technology	meilin.liu@mse.gatech.edu
Ping Liu	Brookhaven National Laboratory	pingliu3@bnl.gov
Raul Lobo	University of Delaware	lobo@udel.edu
Diane Marceau	Department of Energy	diane.marceau@science.doe.gov
Tobin Marks	Northwestern University	t-marks@northwestern.edu
Christopher Marshall	Argonne National Laboratory	marshall@anl.gov
Paul Maupin	DOE -Office of Science	paul.maupin@science.doe.gov
Manos Mavrikakis	University of Wisconsin - Madison	manos@engr.wisc.edu
Eric McFarland	University of California, Santa Barbara	mcfar@engineering.ucsb.edu



Announcing the  
**2009 DOE/BES  
 Catalysis Sciences Meeting**

Sponsored by the U.S. Department of Energy, Office of Basic Energy Sciences

Name	Affiliation	Email
Michael McKittrick	University at Buffalo	mm355@buffalo.edu
John Miller	U.S. Department of Energy	john.miller@science.doe.gov
Raul Miranda	U.S. Department of Energy	raul.miranda@science.doe.gov
Charles Mullins	University of Texas at Austin	mullins@che.utexas.edu
David Mullins	Oak Ridge National Laboratory	mullinsdr@ornl.gov
Djamaladdin Musaev	Emory University	dmusaev@emory.edu
Matthew Neurock	University of Virginia	mn4n@virginia.edu
SonBinh Nguyen	Northwestern University	stn@northwestern.edu
Jens K. Norskov	Technical University of Denmark	norskov@fysik.dtu.dk
Justin Notestein	Northwestern University	j-notestein@northwestern.edu
Ralph Nuzzo	University of Illinois	r-nuzzo@illinois.edu
Stephen O'Brien	Columbia University	so188@columbia.edu
Steve Overbury	Oak Ridge National Laboratory	overburysh@ornl.gov
Umit Ozkan	The Ohio State University	ozkan.1@osu.edu
Stewart Parker	STFC Rutherford Appleton Laboratory	stewart.parker@stfc.ac.uk
Charles Peden	Pacific Northwest National Laboratory	chuck.peden@pnl.gov
Baron Peters	University of California, Santa Barbara	baronp@engineering.ucsb.edu
Phillip F. Britt	Oak Ridge National Laboratory	brittpf@ornl.gov
Marek Pruski	Ames Laboratory	mpruski@iastate.edu
Talat Rahman	University of Central Florida	talat@physics.ucf.edu
Andrew Rappe	University of Pennsylvania	rappe@sas.upenn.edu
Fabio Ribeiro	Purdue University	fabio@purdue.edu
Robert Rioux	Pennsylvania State University	rioux@enr.psu.edu
Jose Rodriguez	Brookhaven National Laboratory	rodriguez@bnl.gov
Eric Rohlifing	U.S. Department of Energy	eric.rohlifing@science.doe.gov
Beatriz Roldan Cuenya	University of Central Florida	roldan@physics.ucf.edu
Roger Rousseau	Pacific Northwest National Laboratory	donna.sturdevant@pnl.gov
Ryong Ryoo	Center for Functional Nanomaterials	rryo@kaist.ac.kr
Aaron Sadow	Ames Lab/Iowa State	sadow@iastate.edu
Lanny Schmidt	University of Minnesota	schmidt@cems.umn.edu
William Schneider	University of Notre Dame	wschneider@nd.edu
Udo Schwarz	Yale University	udo.schwarz@yale.edu
Susannah Scott	University of California, Santa Barbara	sscott@engineering.ucsb.edu
Annabella Selloni	Princeton University	aselloni@princeton.edu
Jorge Seminario	Texas A&M University	seminario@tamu.edu
David Sherrill	Georgia Institute of Technology	sherrill@gatech.edu
Gabor Somorjai	Lawrence Berkeley National Laboratory	Somorjai@berkeley.edu
Peter Stair	Northwestern University, Argonne National Lab	pstair@northwestern.edu



Announcing the  
**2009 DOE/BES  
Catalysis Sciences Meeting**

Sponsored by the U.S. Department of Energy, Office of Basic Energy Sciences

Name	Affiliation	Email
Andreas Stierle	MPI für Metallforschung	stierle@mf.mpg.de
Steve Suib	University of Connecticut	Steven.Suib@uconn.edu
Ceren Susut	Georgetown University	cs345@georgetown.edu
Janos Szanyi	Pacific Northwest National Laboratory	janos.szanyi@pnl.gov
David Thorn	Los Alamos National Laboratory	dthorn@lanl.gov
Don Tilley	Lawrence Berkeley National Laboratory	tdtilley@berkeley.edu
Wilfred Tysoe	University of Wisconsin, Milwaukee	wtt@uwm.edu
Stefan Vajda	Argonne National Laboratory	vajda@anl.gov
Jeroen A. van Bokhoven	ETH Zurich	j.a.vanbokhoven@chem.ethz.ch
Dion Vlachos	University of Delaware	vlachos@udel.edu
John Vohs	University of Pennsylvania	vohs@seas.upenn.edu
Dieter von Deak	Ohio State University	vondeak.2@osu.edu
Miomir Vukmirovic	Brookhaven National Laboratory	miomir@bnl.gov
Israel Wachs	Lehigh University	iew0@lehigh.edu
Jia Wang	Brookhaven National Laboratory	jia@bnl.gov
Lin-Lin Wang	University of Illinois at Urbana-Champaign	llw@illinois.edu
Jason Weaver	University of Florida	weaver@che.ufl.edu
Marcus Weck	New York University	marcus.weck@nyu.edu
Michael White	Brookhaven National Laboratory, Stony Brook University	mgwhite@bnl.gov
Zili Wu	Oak Ridge National Laboratory	wuz1@ornl.gov
Judith Yang	University of Pittsburgh	judyang@pitt.edu
Weitao Yang	Duke University	TheoryOffice@chem.duke.edu
Francisco Zaera	University of California	zaera@ucr.edu

# Author Index

Abbott, J. ....	11	Bell, A. T. ....	53
Abernathy, H. ....	193	Bergman, R. ....	14
Abruña, H. ....	20	Besson, C. ....	14
Abu-Omar, M. ....	96	Beste, A. ....	231
Adhikari, B. ....	46	Bhopana, B. ....	197
Adzic, R. R. ....	20, 29, 75, 150	Biddinger, E. J. ....	39
Agarwal, A. ....	323	Binz, J. ....	251, 305
Agarwal, V. ....	79	Blau, G. E. ....	96
Aguilar-Guerrero, V. ....	127	Blinn, K. ....	193
Ahn, C. H. ....	42, 265	Bluemel, J. ....	56
Aindow, M. ....	8	Blum, S. A. ....	57
Albers, B. ....	265	Bollman, L. ....	96
Alcántara Ortigoza, M. ....	150	Boothroyd, A. ....	42
Alivisatos, P. ....	272	Borisevich, A. ....	231
Allard, L. ....	116, 231	Bosco, J. ....	75
Allotta, P. ....	281	Boucher, M. ....	116
Alonso, J. ....	26	Bradley, C. ....	302
Altman, E. I. ....	42, 265	Bram, A. ....	123
Ando, Y. ....	20	Bray, J. ....	262
Andreasen, A. ....	69	Bredas, J. L. ....	193
Arey, B. W. ....	63	Brinker, C. J. ....	59
Arnold, F. H. ....	2	Broadbelt, L. ....	284
Aronson, M. ....	93	Bromberg, M. ....	225
Arya, A. ....	305	Bronkema, J. ....	53
Asthagiri, A. R. ....	45, 314	Brooks, J. D. ....	82
Auerbach, S. M. ....	79	Brus, L. E. ....	150
Avnir D. ....	1	Brutchey, R. L. ....	62
Axnanda, S. ....	131	Buchbinder, A. ....	284
Baca, E. ....	87	Burghaus, U. ....	63
Baca, L. ....	87	Burgos, J. C. ....	49
Baik, J. H. ....	251	Burkholder, L. ....	323
Bakac, A. ....	187	Burton, P. ....	87
Baker, T. A. ....	124	Buttrey, D. J. ....	29, 110, 139, 305
Bakhtmutsky, K. ....	136	Cai, Y. ....	187
Balbuena, P. B. ....	46, 49, 271	Cai, Yun ....	20
Balonek, C. ....	259	Callejas-Tovar, R. ....	46
Bao, X. ....	39	Cameron, L. ....	69
Bare, S. R. ....	75	Camillone, N. ....	66
Barke, I. ....	26	Campbell, C. T. ....	69
Barnes, C. E. ....	11	Cao, J. ....	96
Barrio, L. ....	145, 252	Cao, R. ....	215
Barteau, M. ....	29, 72, 110	Carino, E. ....	29
Bartels, L. ....	52	Carr, R. ....	237
Bäumer, M. ....	124	Caruthers, J. M. ....	96
Baykara, M. ....	265	Chambers, S. A. ....	156
Bazinet, P. ....	302	Chan, S.-W. ....	116
Bedzyk, M. ....	284	Chaterjee, A. ....	221
Behafarid, F. ....	36	Chattopadhyay, S. ....	268
Bell, A. ....	302	Chen, C. ....	8

Chen, H.-T. ....	187	Dmowski, W. ....	231
Chen, J. G. ....	29, 72, 75, 110, 305	Dobley, A. ....	8
Chen, L. ....	284	Dohnalek, Z. ....	4, 212, 237
Chen, M. ....	146	Dong, Y. ....	82
Chen, N. ....	11	Doren, D. ....	197
Chen, P. ....	78	Downing, C. ....	184, 284
Chen, T.-L. ....	231	Dozol, H. ....	268
Chen, W.-F. ....	20	Du, B. ....	296
Cheng, H. ....	102	Dumesic, J. A. ....	29, 72, 110
Cheng, Z. ....	52, 150	Dunlop, S. ....	96
Chheda, J. ....	110	Dunphy, D. ....	59
Chmelka, B. F. ....	268	Dupuis, M. ....	156
Choi, Y. M. ....	193, 317	Durand, J. ....	8
Christensen, S. ....	284	Egami, T. ....	231
Christopher, P. ....	32	Eichhorn, B. ....	29
Chung, P.-W. ....	187	Eisenstein O. ....	302
Chupas, P. ....	290	Elam, J. ....	26, 86, 205, 284, 290
Clark, J. ....	231	Eldrich, G. ....	11
Colby, J. ....	259	Ellis, D. ....	284
Collins, S. ....	200	Enterkin, J. ....	284
Conant, T. ....	87	Eom, D. ....	150
Conner, W. C. ....	79	Erlebacher, J. ....	113
Coons, T. ....	8	Ertl, G. ....	150, 247
Corma, A. ....	127	Espinal, A. ....	8
Cox, D. F. ....	82	Estrella, M. ....	145
Craciun, R. ....	105, 237	Evans, J. W. ....	187
Crisostomo, V. ....	8	Fahmy, T. ....	142
Crooks, R. M. ....	29, 85	Fan, H.-Y. ....	237
Croy, J. R. ....	36	Farmer, J. ....	69
Curtiss, L. ....	26, 86, 284, 290	Felberg, L. E. ....	224
D'Addio, E. ....	305	Feng, H. ....	284, 290
Dai, S. ....	139, 231	Feng, Z. ....	284
Danon, A. ....	284	Ferreira, G. ....	116
Daturi, M. ....	310	Ferrin, P. ....	29
Datye, A. ....	87, 110, 307	Fingland, B. R. ....	248
Davis, R. J. ....	93, 110, 169	Finke, R. G. ....	14
Deguns, E. ....	268	Finney, E. E. ....	14
DelFerro, M. ....	200	Flynn, G. W. ....	116, 150
Delgass, W. N. ....	96, 262	Flytzani-Stephanopoulos, M. ....	116
Dellamorte, J. ....	29	Fornasiero, P. ....	136
Deng, W. ....	205	Foster, A. ....	265
Deng, X. ....	124	Fragala I. ....	200
Deskins, N. A. ....	156	Fraille-Rodriguez, A. ....	26
Di Valentin, C. ....	102	Frei, H. ....	122, 272, 302
Diebold, U. ....	102	Frenkel, A. I. ....	8, 75, 116, 123, 225
Dimitrijevic, N. ....	284	Frenkel, E. ....	75
Ding, Y. ....	8	Freund, H. ....	69
DiSalvo, F. ....	20	Friend, C. M. ....	124
Dixon, D. A. ....	105, 146, 156, 237	Frueh, S. ....	8

Gadzikwa, T. ....	284	Hawkins, J. M. ....	45
Galloway, J. ....	184	He, Y. ....	102
Gao, F. ....	131	Head-Gordon, M. ....	53
Gao, W. ....	124	Heinz, T. F. ....	52, 150, 247
Gates, B. C. ....	127, 146	Henderson, M. A. ....	156
Geiger, F. ....	284	Henkelman, G. ....	31, 69, 212
Geletti, Y. ....	215	Henrich, V. E. ....	42, 265
Gellman, A. J. ....	130, 323	Herman, I. ....	116, 150
Getman, R. ....	262	Herron, J. ....	29
Getsoian, A. ....	53	Hersam, M. ....	284
Gharibeh, M. ....	79	Hill, C. L. ....	215
Ghilarducci, J. M. ....	179	Hillesheim, D. A. ....	215
Gibbs, G. V. ....	82	Hilliard, C. ....	56
Gill, C. ....	169	Hirunsit, P. ....	46
Gist, N. ....	105, 237	Hisamoto, M. ....	268
Gittleston, F. ....	116	Hone, J. ....	150
Gómez-Gualdrón, D. ....	49	Hong, S. ....	52, 150, 247
Gong, J. ....	212	Horowitz, E. ....	75
Gong, K. ....	20	Horvath, J. D. ....	323
Goodman, D. W. ....	131	Hou, Y. ....	215
Gordon, M. S. ....	187	Hrbek, J. ....	75, 145, 162, 252, 317
Gordon, W. ....	231	Hu, B. ....	8
Gorte, R. ....	136	Hu, J. ....	237
Govindasamy, A. ....	139	Hu, Z. ....	208
Goyal, P. ....	169	Huang, Y. ....	187
Graciani, J. ....	196, 252	Huang, L. ....	150
Graham, C. ....	14	Huang, W. ....	29
Gray, K. ....	284	Huber, G. W. ....	79
Greeley, J. ....	26, 86, 290	Huchon, C. ....	52, 150
Grey, C. P. ....	79	Hulbert, S. L. ....	75
Grubbs, R. H. ....	18	Humbert, M. ....	72
Guenther, J. ....	56	Hupp, J. ....	284
Guliants, V. V. ....	139	Hybertsen, M. ....	150
Guy, K. ....	225	Hyman, M. ....	307
Hadjiivanov, K. ....	127	Idriss, H. ....	156
Hagaman, E. W. ....	11, 231	Iglesia, E. ....	179, 237
Hakanoglu, C. ....	314	Inoglu, N. ....	182
Halevi, B. ....	87	Iyer, A. ....	8
Hall, A. ....	247	Jacobi, K. ....	247
Haller, G. L. ....	142	Jacobson, P. ....	102
Hamers, R. J. ....	6	Jain, S. ....	169
Hammer, B. ....	26	Jakobi, K. ....	150
Hammond, K. D. ....	79	Jalan, P. ....	305
Hansgen, D. ....	29, 305	James, J. ....	323
Hanson, J. ....	8, 75, 116, 136, 145, 162, 252, 317	Jaramillo, T. F. ....	168
Hao, Y. ....	127	Jerero, E. ....	87, 307
Harrison, R. J. ....	231	Jia, Z. ....	150
Haubrich, J. ....	124	Jiang, D. ....	231
Haw, J. F. ....	146	Jiang, Y.-B. ....	59



Jiao, J. ....	11	Kung, H. H. ....	184, 284
Jin, L. ....	8	Kung, M. ....	184, 284
Johnson, D. ....	123, 225	Kunkes, E. ....	110
Jones, C. W. ....	169	Kuttiyel, K. ....	20
Jones, M. ....	96	Kuznetsov, A. ....	215
Joyce, A. ....	146	Kwak, J. H. ....	237, 299
Kadossov, E. ....	63	Lahr, D. ....	93
Kaledin, A. ....	215	Langell, M. A. ....	156
Kalid, S. ....	116	Lauterbach, J. ....	29, 305
Kamakoti, P. ....	323	Lazarus, L. L. ....	62
Kan, H. H. ....	314	Le, D. T. ....	52, 150, 247
Kao, C.-C. ....	75	Lebarbier, V. ....	87
Karan, H. ....	20	Lee, B. ....	26
Karim, A. ....	305	Lee, E. L. ....	310
Karp, E. ....	69	Lee, I. ....	323
Kas, J. ....	123	Lee, J. K. ....	184
Katz, A. ....	179	Lee, M.-Y. ....	268
Kay, B. D. ....	212, 237	Lee, Sungchul ....	142
Kelly, T. ....	72	Lee, Sungsik ....	205, 290
Kelly, T. G. ....	146	Lee, S. ....	26
Kent, P. ....	221	Lei, Y. ....	26
Kerney, R. ....	208	Li, G. ....	284
Key, R. ....	169	Li, L. ....	123, 225
Kim, C.-Y. ....	284	Li, Meijun ....	231
Kim, D. H. ....	52, 150	Li, Meng.....	20
Kim, D. J. ....	156	Li, Min ....	42
Kim, H.-S. ....	284, 290	Li, S. ....	105, 237
Kim, T. ....	310	Li, S.-C. ....	102
Kim, T.-W. ....	187	Li, W. ....	8
Kim, Y. K. ....	237	Liang, A. J. ....	127, 146
Kitchin, J. ....	182	Liang, C. ....	11
Kleibert, A. ....	26	Liang, T. ....	284
Klie, R. F. ....	42	Lim, S.-G. ....	57
Knapke, D. S. ....	39	Lin, M. C. ....	193
Knözinger, H. ....	127	Lin, V. S.-Y. ....	187, 258
Koel, B. ....	20	Lin, X. ....	284
Koirala, S. ....	46	Linic, S. ....	32
Kona, J. ....	8	Liu, J. ....	237
Korinda, A. W. ....	224	Liu, M. ....	193
Koritnik, A. ....	323	Liu, P. ....	20, 72, 162, 196, 252, 317
Korovchenko, P. ....	139	Liu, X. ....	124
Kosuda, K. ....	284	Liu, Z. ....	110
Kowal, A. ....	20	Lobo, R. F. ....	29, 197
Kozlowski, J. ....	93	Lobo-Lapidus, R. J. ....	146
Krishnamurthy, B. ....	96	Long, R. T. ....	105, 237
Krishnamurthy, G. ....	96	López, M. ....	26
Kromer, B. ....	96	Lu, J. ....	281
Kropf, A. J. ....	200, 248	Lucas, T. ....	197
Kubota, J. ....	323	Ludovice, P. ....	169

Lundwall, M. ....	131	Ming, L. ....	63
Luo, M. M. ....	52, 150	Mink, L. ....	323
Luo, Z. ....	215	Minter, A. ....	314
Luthman, K. ....	39	Missaghi, M. ....	184, 284
Lynch, M. ....	193	Molina, L. ....	26
Lyubinetzky, I. ....	156	Mondloch, J. E. ....	14
Ma, Y. ....	46	Morey, A. ....	8
Ma, Zhen ....	231	Morlanes-Sanchez, N. ....	224
Ma, Z. ....	323	Morokuma, K. ....	215
Macchioni, A. ....	200	Mortano, E. ....	307
Macht, J. ....	237	Moses, A. ....	268
Madhavan, N. ....	169	Mostafa, S. ....	36
Madix, R. J. ....	124	Mucherie, S. ....	26
Maity, N. ....	179	Muckerman, J. T. ....	252, 317
Malecky, R. ....	284	Mudiyanselage, K. ....	299
Malik, T. ....	96	Mueller, L. ....	323
Manna, K. ....	258	Mul, G. ....	310
Manz, T. ....	96	Mullins, C. B. ....	212
Marinkovic, N. ....	75	Mullins, D. R. ....	8, 75, 139, 231
Marks, L. ....	284	Mun, B. S. ....	248
Marks, T. J. ....	200, 284	Murray, C. ....	150
Marshall, C. ....	26, 86, 200, 205, 284, 290	Musaev, D. G. ....	215
Martinez de la Hoz, J. ....	46	Myers, S. V. ....	85
Mashayekhi, N. ....	284	Naghipour, A. ....	56
Mathur, A. ....	113	Nambu, A. ....	162
Matolin, V. ....	69	Nare, D. ....	259
Matthey, J. ....	221	Nelson, R. ....	268
Mavrikakis, M. ....	20, 29, 69, 110	Neumark, G. ....	150
Mayes, R. ....	11	Neurock, M. ....	72, 221
McAfee, M. ....	146	Nickias, P. ....	200
McBee, J. ....	302	Nilekar, A. ....	29
McClure, S. ....	131	Njuyen, S. ....	284
McFarland, E. ....	208	Norman, A. ....	169
McKittrick, M. W. ....	211	Nørskov, J. K. ....	19
McMurdo, M. ....	302	Notestein, J. M. ....	224, 284
Medvedev, G. ....	96	Novstrup, K. ....	96
Mehmood, F. ....	26, 86, 290	Nuckolls, C. ....	150
Mei, D. ....	299	Nuzzo, R. G. ....	123, 225
Meiwes-Broer, K.-H. ....	26	O'Brien, S. ....	247
Meka, S. ....	271	O'Halloran, K. ....	215
Menning, C. ....	72	Ogino, I. ....	127
Metiu, H. ....	208	Olsen, R. A. ....	323
Meyer, R. ....	26	Onishi, H. ....	156
Michael, B. ....	259	Opembe, N. ....	8
Midkiff, S. P. ....	96	Orcun, S. ....	96
Miller, J. T. ....	110, 200, 248, 284	Ostojic, G. ....	284
Miller, S. ....	182	Ott, L. S. ....	14
Mims, C. ....	69	Overbury, S. H. ....	75, 116, 139, 231
Min, B. K. ....	124	Ozkan, U. S. ....	39

Özkar, S. ....	14	Ratts, J. ....	96
Pacchioni, G. ....	102	Redfern, P. ....	26
Paiz, J. ....	87	Rehr, J. ....	123, 225
Pala, R. ....	208	Rei, C. ....	208
Pang, J. ....	59	Resasco, D. E. ....	49
Park, J. ....	317	Ribeiro, F. H. ....	96, 248, 262
Park, J.-N. ....	208	Richardson, J. ....	169
Parker, S. F. ....	5	Rim, K. T. ....	116
Patterson, M. ....	317	Rioux, R. M. ....	251
Paul, M. ....	221	Roberts, C. A. ....	310
Pawin, G. ....	52, 150	Rodriguez, B. ....	200
Payen, E. ....	310	Rodriguez, J. A. ...	75, 116, 145, 162, 196, 252, 317
Peden, C. H. F. ....	69, 237, 299	Roldan Cuenya, B. ....	36
Pellin, M. ....	26, 284	Rondinone, A. J. ....	139
Pennycook, S. J. ....	231	Ross-Medgaarden, E. I. ....	310
Perera, M. ....	56	Rosso, K. M. ....	156
Peretich, M. ....	11	Rousseau, R. ....	237
Perry, S. S. ....	323	Routray, K. ....	310
Peters, B. ....	246, 268	Ruddy, D. ....	302
Petersen, E. ....	87	Ryan, P. ....	284
Petkov, V. ....	225	Ryoo, R. ....	7
Pfefferle, L. ....	142	Sachtler, W. ....	284
Phivilay, S. P. ....	310	Sadow, A. D. ....	187, 258
Picone, D. ....	105, 146, 237	Salazar, P. ....	271
Pineiro, A. ....	305	Saldin, D. K. ....	323
Pinon, V. ....	169	Salmeron, M. ....	272
Poepelmeier, K. ....	284	Saltsburg, H. ....	116
Polenova, T. ....	197	Sanchez, S. ....	123, 225
Prakash J. ....	20	Sasaki K. ....	20
Prasad, V. ....	305	Sauter, D. ....	281
Prieto-Centurion, D. ....	224	Savara, A. ....	284
Pruski, M. ....	187	Schauermann, S. ....	69
Puretzky, A. ....	310	Schlögl (Schloegl), R. ....	26, 87
Pushkarev, V. ....	130	Schmidt, H. ....	197
Pyrz, W. ....	29	Schmidt, L. D. ....	259
Quezada, B. ....	284	Schneider, W. F. ....	248, 262
Quigley, J. ....	75	Schoenfeldt, N. J. ....	224
Quiñonero, D. ....	215	Schwartz, V. ....	139, 231
Raab, C. ....	268	Schwarz, U. D. ....	265
Rabuffetti, F. ....	284	Schwendemann, T. ....	42, 265
Rahman, T. S. ....	20, 52, 247	Scott, S. L. ....	246, 268
Raitano, J. ....	116	Sears, J. ....	169
Rajh, T. ....	284	Segal, R. ....	75
Ramirez-Caballero, G. ....	46	Seifert, S. ....	26
Ramsahye, N. ....	268	Sell, K. ....	26
Rankin, R. B. ....	323	Sellers, J. ....	69
Rapp, J. L. ....	187	Selloni, A. ....	102
Rappe, A. M. ....	30	Seminario, J. M. ....	46, 271
Rashkeev, S. ....	231	Senanayake, S. ....	231, 252

Setthapun, S. ....	284, 290	Swann, A. ....	169
Sfeir, M. ....	150	Switzer, J. ....	96
Shafai, G. ....	150	Szanyi, J. ....	299
Shaffer, C. ....	96	Taha, Z. ....	268
Shah, P. ....	136	Tai, J. ....	93
Shapley, J. ....	225	Takatani, T. ....	169
Shayib, R. ....	268	Tan, F. ....	296
She, X. ....	237	Tang, W. ....	208
Shehab, A. ....	96	Teng, X. ....	225
Shekhar, M. ....	96	Tenne, R. ....	63
Sherrill, D. ....	169	Teschner, D. ....	26
Shiels, R. ....	169	Thibodaux, M. ....	69
Shiju, N. R. ....	139	Thompsett, D. ....	221
Sholl, D. S. ....	323	Thomson, K. T. ....	96
Shultz, A. ....	284	Tilley, T. D. ....	302
Shumbera, R. B. ....	314	Tilocca, A. ....	102
Si, R. ....	116	Tompsett, G. A. ....	79
Simonetti, D. ....	110	Tong, Y. Y. ....	296
Sithambaram, S. ....	8	Toste, F. D. ....	272
Sivasankar, N. ....	122	Travia, N. ....	96
Small, M. ....	123	Turro, N. ....	150, 247
Small, M. ....	225	Tysoe, W. T. ....	323
Smeltz, A. D. ....	248	Ulissi, Z. ....	305
Snurr, R. ....	284	Uzun, A. ....	146
Snyder, J. ....	113	Vajda, S. ....	26, 86, 205, 248, 290
Soares, R. ....	110	Van Bokhoven, J. A. ....	3
Solovyov, A. ....	179	Van Duyne, R. ....	284
Somorjai, G. A. ....	272, 278	Vaz, C. A. F. ....	42, 265
Song, J. ....	215	Venkatasubbaiah, K. ....	169
Sotelo, J. ....	46	Venkatasubramanian, V. ....	96
Sotelo-Campos, J. M. ....	271	Vijay, R. ....	305
Stacchiola, D. ....	162	Vila, F. ....	123
Stach, E. ....	248	Vining, W. ....	53
Stair, P. C. ....	86, 281, 284, 290	Vlachos, D. G. ....	29, 305
Stamatis, S. ....	96	Vohs, J. M. ....	87, 136, 307
Stegemann, C. ....	69	Von Deak, D. ....	39
Stephenson, N. ....	53	Von Oeynhausen, V. ....	26
Stewart, S. M. ....	246, 268	Vukmirovic, M. ....	20
Stierle, A. ....	35, 102	Wachs, I. E. ....	310
Stocchiola, D. ....	323	Wang, C. ....	142
Strunk, J. ....	53	Wang, D. ....	237
Stuchinskaya, T. ....	237	Wang, F. ....	150
Suib, S. L. ....	8	Wang, H. ....	96, 262
Sun, D. ....	52, 150	Wang, J. ....	20
Sung, C.-Y. ....	284	Wang, L.-L. ....	123, 225
Susut, C. ....	296	Wang, L.-S. ....	105, 237
Sutter, E. ....	20	Wang, Q. ....	123, 225
Sutter, P. ....	66	Wang, T.-H. ....	146
Sutton, J. ....	305	Wang, W. ....	116

Wang, X. ....	142	Yang, J. ....	123, 225
Wang, X.-Q. ....	145	Yang, Lei ....	193
Wang, Yilin ....	131	Yang, Liu ....	197
Wang, Yong (at PNNL). ....	87, 237, 307	Yang, P. ....	272
Wang, Yong (at UC-Irvine). ....	57	Yang, W. ....	27
Wang, Z. ....	131	Yang, Y. ....	317
Watzky, M. A. ....	14	Yi, C.-W. ....	299
Weaver, J. F. ....	45, 314	Yi, N. ....	116
Weberski, M. ....	200	Yin, M. ....	247
Weck, M. ....	169	Yin, S. ....	284
Wegener, S. ....	200, 284	Yin, X. ....	237
Weimer, A. W. ....	139	Young, P. D. ....	224
Weir, Michael G. ....	29, 85	Zaera, F. ....	323
Weitz, E. ....	284	Zapol, P. ....	26, 86, 284
Wen, W. ....	145, 162	Zehr, R. T. ....	156
Wenzel, T. ....	200	Zemlyanov, D. ....	248
Werth, C. ....	225	Zgrablich, G. ....	323
West, R. ....	29	Zhai, H.-J. ....	105, 237
White, B. ....	247	Zhai, Y. ....	116
White, J. M. ....	156, 212, 237	Zhang, L. ....	116
White, M. G. ....	252, 317	Zhang, Y. ....	8
Wiench, J. W. ....	187	Zhang, Zhongfan ....	225
Williams, D. ....	96	Zhang, Z. ....	237
Williams, L. ....	200	Zhao, C. ....	310
Willis, W. S. ....	8	Zhao, J. ....	49
Winans, R. ....	26, 290	Zheng, T. ....	323
Wise, A. ....	59	Zheng, X. ....	169
Wittstock, A. ....	124	Zhou, G. ....	145
Wong, K. L. ....	150	Zhou, H. ....	150
Woo, J. ....	139	Zhou, J. ....	231
Wormsbecher, R. ....	268	Zhou, W.-P. ....	20
Wu, C. ....	262	Zhou, Z. ....	131
Wu, C.-W. ....	187	Zhu, J. ....	69
Wu, Z. ....	11, 231	Zhu, K. ....	237
Wyrick, J. ....	52, 150	Zhu, X. ....	169
Xi, Y. ....	93	Zhu, Y. ....	150
Xin, H. ....	32	Zielasek, V. ....	124
Xing, Y. ....	8	Zones, S. ....	268
Xing, Yangchuan. ....	20	Zygmunt, S. ....	284
Xiong, S. ....	59		
Xu, B. ....	124		
Xu, F. ....	130		
Xu, L. ....	8		
Xu, Y. ....	139, 231, 262		
Yan, K. ....	258		
Yan, T. ....	212		
Yan, Z. ....	131		
Yang, F. ....	252		
Yang, H. ....	305		

## DOE Catalysis Contractors' Meeting, May 31-June 3, 2009

### Summary of Meeting Participant Discussions (by Susannah Scott and David Dixon)

*Two general areas were chosen for particular discussion: catalyst synthesis and catalysis theory. These discussions can be used for information supplementing the presentation abstracts and for guidance on the future needs perceived by the community represented at this meeting.*

#### **I - Summary of the discussion of new directions/needs in catalyst synthesis and characterization**

*Questions were posed by the discussion leaders (Susannah Scott and Tobin Marks)*

*1) Are there generalizable synthetic principles for the synthesis of nanostructured materials/catalysts over multiple length scales? Can theory make a contribution to catalyst synthesis efforts?*

The use of theory to predict, or even rationalize, synthesis (e.g. pathway prediction and discovery), is a very challenging goal. Nucleation is a key problem that requires more theoretical/computational effort, perhaps building on the efforts in gas phase aerosols. A key challenge for theory is the ability to do multiscale modeling so as to develop predictive models for synthesis over multiple length scales.

An extremely important use of computation in the support of catalyst synthesis and characterization is the prediction of spectroscopic signatures from first principles, facilitating the identification of transient, low abundance, or otherwise difficult to isolate species. This has recently become feasible and reliable, especially for vibrational spectroscopy, nmr, epr, and UV-Vis.

There is a need to develop computational and database approaches to analyze spectroscopic signals (e.g., IR, NMR, mass spectroscopy) which could be used to identify new compounds for which experimental reference data does not yet exist.

Theory could shed light on questions about mobility/viscosity in confined spaces (e.g., water in zeolites or nanotubes).

*2) How can we build more robustness into nanomaterials, or can we design catalysts that can repair themselves to restore their activity?*

No specific response was received. This point is valid and still open for input.

*3) Does the method of "directed evolution" have an analog in non-biological catalyst discovery, or in the development of complementary enzymes/chemical tandem systems?*

Phages are known to direct the assembly of metal clusters and films using peptide displays on their surfaces. This could be used to create libraries of nanoparticle catalysts for screening. For examples, see the links at [http://en.wikiversity.org/wiki/Materials\\_Science\\_and\\_Engineering/Phage\\_Display\\_and\\_Materials\\_Science](http://en.wikiversity.org/wiki/Materials_Science_and_Engineering/Phage_Display_and_Materials_Science)

*4) Do we need more methods for studying dynamic structures under catalytically relevant conditions?*

High spatial and temporal resolution in catalysis on individual nanoparticles will be enabled by new synchrotron capabilities, such as the high brilliance of NSLS2. New experiments will need to be designed to take advantage of its beam spot sizes in the range 10 nm – 50  $\mu$ m. There will also be opportunities in surface science with ultrafast lasers using pulsed X-ray sources at synchrotrons. Combinations of characterization techniques are being used to provide simultaneous information on different aspects of reacting systems, e.g., IR/EXAFS with sub-second time resolution.

There is a need to extend time-resolved IR from gas-solid systems to liquid-solid interfaces, e.g., using ATR crystals. This will enable the study of reactions involving condensed phases, particularly with biomass targets.

There are also opportunities in the ability to correlate vibrations with catalyst dynamics. A combination of ultrahigh spatial resolution and time-resolution is likely to prove useful; there are new developments in tip-enhanced Raman and IR microscopy which enable single molecule spectroscopy (for example, the work of Martin Raschke at University of Washington).

More sharing of DOE-funded special equipment at universities, along the lines of the DOE user facilities like the EMSL and the Nanocenters, could put cutting-edge equipment in the hands of more users.

*5) How can we make homogeneous catalysts more like heterogeneous catalysts (e.g., in robustness)? How can we make heterogeneous catalysts more like homogeneous catalysts (e.g., in the atomic level of structural control and uniformity)?*

The expanded use of homogeneous (chemical and enzyme) catalysts and homogeneous catalysis principles in the design of heterogeneous catalysts requires that we find ways to reduce operating temperatures (e.g., below 200 °C) to be compatible with thermally fragile ligands. To make heterogeneous catalysts more like homogeneous catalysts, we should aspire to assemble catalyst structures unit-by-unit, as in peptide assembly,

There is a need for more work on controlled synthesis of active sites containing numbers of metal atoms intermediate between atomically-dispersed and metallic particles (i.e., in the  $M_2$ - $M_{500}$  range). There is a need to better understand the participation of catalyst supports, for example, the distribution and reactivity of surface hydroxyl groups. This is a

perfect size range for testing theoretical methods as well as one can often tackle the electronic structure of this size of metal particle today or using emerging computer architectures and computational approaches.

There is a need for more measurement and understanding of the physical and thermodynamic properties (such as electron affinities, ionization potentials, enthalpies of formation and adsorption, 2D phase diagrams) of small metal clusters.

*6) What are the opportunities for new catalytic reaction types (e.g. C-H functionalization, C-O bond cleavage, in processing of biomass)?*

A new class of reactions we should study is depolymerization (e.g., of natural polymers).

*7) What are the opportunities for new catalyst supports, and what applications could these supports enable?*

There is great need for more work at the catalysis/electrocatalysis interface, for example, the study of surfaces under applied potential.

The use of supports as ligands for homogeneous catalysts has not been widely-explored.

*8) How can we expand the catalytic applications of non-precious metals?*

No specific response was received. This point is valid and still open for input.

*9) What types of information about catalysts would we like to have that we cannot currently get? Can we make a “movie” of a catalytic reaction?*

Single molecule spectroscopy studies of reacting catalysts are becoming possible and are likely to be important in elucidating the relationships between the structures of individual catalyst particles/sites and their reactivity. Pump-probe experiments involving single molecules could be extended to surface chemistry, to explore the behavior of molecules on single crystal surfaces, or individual nanoparticles.

The emerging use of in situ XRD on single nanoparticles is particularly complementary to the spectroscopy effort, as is environmental TEM for imaging particle dynamics in response to reaction conditions. Developments in aberration corrected electron microscopy potentially will play an important role. Four-dimensional (4D) ultrafast electron microscopy and diffraction such as the work of A. Zewail at Caltech can also play a role in improving our understanding of the relationship between structure and dynamics.

*10) What new synthetic techniques can we explore/exploit for catalysts?*

The use of combinatorial synthesis techniques (templating agents, synthesis conditions) was recommended to explore new microporous structures. Based on the computational



predictions of Mike Deem, there are  $10^6$  possible zeolite structures, of which only ~200 have been synthesized and <10 are in commercial use. The potential utility of metal-organic frameworks (such as those made recently by Jeff Long) in catalysis could also be explored using combinatorial techniques. The use of microwave heating to speed nucleation and foster more uniform crystal sizes should be explored. Microwaves may also speed epitaxial growth. The input of theory is needed to relate pore structure to activity.

There is a need to better match synthetic targets with their catalytic applications. This requires more communication between the synthesis and catalysis communities.

## **II - Summary of the discussion of new directions/needs in catalysis theory, modeling and simulation**

*Questions were posed by the discussion leaders (Matthew Neurock and David Dixon)*

- 1) *What are the current capabilities of computational catalysis?*
  - (a) Prediction of structure and electronic properties (charges, orbital energies, d-bands); (b) prediction of spectral properties: vibrational, electronic (UV-vis), nmr, epr, etc. for aid in the identification of species (better developed and more reliable for molecules than for extended surfaces); (c) prediction of energetics: reaction equilibria, effects of substitution, stability of substituents, stability of intermediates, bond energies, stability of metal surfaces and alloys; (d) Rates of reactions: qualitative and quantitative; (e) Elucidation of mechanism and mechanism development; (f) Initial stages of catalyst design; (g) Incorporation of environmental effects: solvents, nanostructures, tethering to a surface (iust beginning)
- 2) *What are some of the current needs and challenges?*
  - (a) In order for quantitative predictions of kinetics and reactivity, we need improved ab initio methods, improved exchange-correlation functionals for DFT including non-bonded interactions, improved techniques for excited states and reactivity on excited states, improved transition state search strategies, especially for solids and in solution, improved theories for reaction kinetics, new tools for the reliable prediction of excited states and bad gaps, and new tools to deal with entropy and preexponential factors in complex systems. An electronic structure method that may prove useful is quantum Monte Carlo which scales well on massively parallel computers. This has been implemented for molecular systems but is not widely available if at all for solids and surfaces.
  - (b) Realistic models of the reaction environment are required for reliable predictions. Improved methods are needed to predict the influence of structure, morphology, support, coverage, medium, composition, etc. on reactivity.

- (c) It is important to simulate catalytic performance under working conditions. Examples include: modeling adsorption/diffusion/reaction in microporous systems, and simulating myriad of competing kinetic processes on metals and oxides. An example of the latter is the use of Kinetic Monte Carlo.
  - (d) How do we follow the dynamic structural changes in the catalyst as well as in the reaction medium that occur under working conditions?
- 3) *How do we predict the conversion of non-conventional resources into fuels and feedstocks for industry?*
- (a) The solution of this issue presents many new challenges for computational approaches. These include complex multicomponent feedstocks with, for example, 100,000 different molecules and their myriad of reaction paths.
  - (b) How do we deal with complex media including an aqueous phase with contaminants, mixed phases, or ionic liquids?
- 4) *How do we deal with photo- and electro-catalytic conversion, which require the simulation of electron transfer, excited states, and the influence of potential and solution?*
- (a) These issues will require quantum dynamical effects as well as the electronic structure issues. How important are quantum effects in proton/hydrogen transfer reactions?
- 5) *What are best approaches to catalyst design?*
- (a) What are the roles of design vs. screening? How do we turn data into knowledge? How do we broadly implement catalyst informatics? An issue raised by all was the development of data bases that contain computational results in terms of electronic structure and structure results, energetics, thermodynamics, kinetics, and reaction paths that can be made broadly available to improve mechanism development and the search for new reaction processes.
- 6) *How do we improve the accuracy of our models which is just as important as accuracy in the simulation?*
- (a) Issues to be addressed include interactions of the catalyst with the support, the role of defect sites, stress/strain, particle size and morphology, coverage, promoters, poisons, the role of solvent and interfaces in liquids, and electric fields.
- 7) *A grand challenge for catalyst design is the determination of the following sequence: Synthesis → structure → function. How can we make this happen?*
- (a) In order to address the first step we need to be able to predict collective phenomena in multicomponent systems. We need to be able to predict reaction in

solution which is currently very difficult especially for the pre-exponential factor (the “entropy” issue). We need to be able to predict nucleation phenomena, precipitation kinetics, particle growth, and particle solubility. We need to develop a new theory for self assembly.

- (b) We need to simulate beyond just performance of single steps. How do we predict *operando* catalyst stability, lifetime, and durability?
- (c) How can we develop general scaling laws?

A general issue raised by the group was the development and ease of use of codes, especially for solid state calculations. A proposal was made to nucleate a larger effort in code development by following the European model. What was suggested that the code developers form a group that would work closely together and develop one or two high performance, user friendly codes with broad capabilities. This is especially needed for the solid state. This has already occurred with the molecular codes, although continued efforts are needed here even to take advantage of DOE’s largest computers.

---